"Catalytic synthesis of P-chiral supramolecular phosphines, their self-assembled metal complexes and implication in asymmetric catalysis"

Thesis submitted to AcSIR

For the Award of the Degree of

DOCTOR OF PHILOSOPHY

In

CHEMICAL SCIENCES

BY

Vijaykumar Shivaji Koshti
(Registration Number: 10CC12A26016)

Under the guidance of
Dr. Samir H. Chikkali

Polymer Science and Engineering Division
CSIR-National Chemical Laboratory
Pune - 411008, India.

April 2018

Dedicated to

My Parents and Teachers

6th April, 2018

Dr. Samir H. Chikkali
Senior Scientist and Assistant Professor
Polymer Science and Engineering Division
CSIR-National Chemical Laboratory
Dr. Homi Bhabha Road, Pashan, Pune-411008,
Maharashtra, India. Tel.: 020-2590-3145
E-mail: s.chikkali@ncl.res.in

Ph.D. Thesis Certificate

This is to certify that the work incorporated in this Ph.D. thesis entitled **"Catalytic synthesis of P-chiral supramolecular phosphines, their self-assembled metal complexes and implication in asymmetric catalysis"** submitted by **Mr. Vijaykumar Shivaji Koshti (Registration No. 10CC12A26016)** to Academy of Scientific and Innovative Research (AcSIR) in fulfilment of the requirements for the award of the Degree of Doctor of Philosophy, embodies original research work under my supervision. I further certify that this work has not been submitted to any other University or Institution in part or full for the award of any degree or diploma. Research material obtained from other sources has been duly acknowledged in the thesis. Any text, illustration, table etc., used in the thesis from other sources, have been duly cited and acknowledged.

Mr. Vijaykumar Shivaji Koshti

(Research Student)

Dr. Samir H. Chikkali

(Research Supervisor)

Declaration by the Candidate

I hereby declare that the original research work embodied in this thesis entitled **"Catalytic synthesis of P-chiral supramolecular phosphines, their self-assembled metal complexes and implication in asymmetric catalysis"** submitted to Academy of Scientific and Innovative Research (AcSIR) for the award of degree of Doctor of Philosophy (Ph. D.). This is the outcome of experimental investigations carried out by me under the supervision of **Dr. Samir H. Chikkali**, Senior Scientist, Polymer Science and Engineering Division, CSIR-National Chemical Laboratory, Pune. I affirm that the work incorporated is original and has not been submitted to any other academy or institute for the award of any degree or diploma.

April 2018

Polymer Science and Engineering Division

CSIR-National Chemical Laboratory   **Vijaykumar Shivaji Koshti**

Pune-411008   **(Research Fellow)**

This thesis represents the amalgamation of my work with the good and bad moments in the past five years in Polymer Science and Engineering (PSE) Division, CSIR-NCL. Dozens of people have helped and taught me immensely in life as well as during my Ph. D. stint, I would like to take this as an opportunity to thank all those people.

First of all, I would like to express my enormous gratitude to my research supervisor **Dr. Samir H. Chikkali** for his cherished guidance, understanding and patience which added considerably to my graduate experience. I am thankful to him for giving me freedom at work place and make my dream. I must also mention that he has had so much patience during my PhD work. My sincere regards and reverence for him will remain forever. The disciplines whatever he taught me, I will follow them throughout my life.

It is really a great help and guidance rendered by Dr. Rajesh Gonnade, Dr. Nitin Patil and Dr. P. R. Rajamohanan, their group. Without their help it would be an incomplete research. I express my gratitude to all of them.

Dr. Prakash P. Wadgaonkar, for his advice, guidance, supports and encouragements during every stage of this research work.

I also thank Head of the PSE Division, Dr. Ulhas K. Kharul and the former Head of the PSE Division, Dr. Ashish Lele and also the Director of NCL for providing infrastructural facilities. I am also thankful to UGC, New Delhi for the financial assistance in the form of fellowship.

I gratefully acknowledge the valuable suggestions and timely help of DAC committee, Dr. Benudhar Punji, Dr. Darbha Srinivas, Dr. Ekambaram Balaraman and Dr. Sayam Sengupta suggestions offered during assessments and other presentations are also gratefully acknowledged.

My sincere thanks to the people in various parts of the institute and SAC office staff for their cooperation. I would also like to acknowledge all the staff members of X-ray single crystal analysis, HPLC, IR, NMR, Mass spectroscopy, Microanalysis, Library, Administration and technical divisions of NCL for their assistance during the course of my work.

I would like to offer thanks to my friends and beloved seniors Dr. Prakash Chavan, Dr. Santosh Chavan, Dr. Suleman Inamdar, Dr. Kishor Harale, Dr. Pradip Pachpule, Dr. Manoj Mane, Dr. Majid Tamboli, Dr. Sachin Bhojgude, Dr. Shekhar Shinde, Dr. Shrikant Khake, Dr. Rohan Erande, Dr. Prakash Sultane, Dr. Vaijinath Mane, Dr. Mubarak Shaikh and Dr. Nagesh kolhe for their love and affection.

I would like to thank all my colleagues for always maintaining cheerful and healthy work environment inside as well as outside the Lab. My special thanks to Dr. Ketan Patel, Dr. Dipa Mandal, Dr. Shrikant Khake, Shahaji Gaikwad, Satej Deshmukh, Nilesh Mote, Vineeta Soni, Hanuman Pandiri, Bahushaheb Rajput, Ulhas

Patel, Swechchhha Pandey, Dilip Pandey, Ravi Gote, Rahul Jagtap, Dnyneshor Bodake, Anirban Sen, Rohit kumar, Amol Chandanshive and Dipesh Sharma whom I shared my most precious moments during my PhD.

I would like to thank all my collaborator colleagues Nilesh, Ravi, Anirban and Amol for their valuable time and cooperation.

No words will be sufficient to express my thanks to my friends Madhukar, Digambar, Tushar, Dinesh, Amol, Pradip, Aslam, Gorak, Mahendra, Popat, Ravi, Kailash, Balasaheb, Manik, Yogesh, Shridhar, Samir, Arun, Pravin, Bhagyashree, Pradnya, Megha, Suwarna, and Ashwini for the cherished friendships and creating such wonderful atmosphere around me with their support outside the lab. I also extend my gratitude to all my friends of Mi-Marathi group of CSIR-NCL for their help and exquisite moments. I also thank my friends, Prabhakar, Trimbak, Nilesh, Nagesh and Kundan in IISER Pune.

I especially thanks to Sandip Agalave and Sanjay Koshti who stood up behind me throughout my Ph.D career and became my strong moral support.

I would further like to thank my college friends – Nilesh, Anil, Datta, Faiyaj, Ganesh, Shomeshower, Shripad, Krashana, Khandu, Prashant and Machinchra for always being there for me.

I also like to thanks my School friends – Naushad, Dipak, Nilesh, Avinash, Balashaheb, and Manoj.

My family is always source of inspiration and great moral support for me in perceiving my education, I am thankful to God for having me such a supportive family. The words are insufficient to express my gratitude towards my family. I take this opportunity to express gratitude to my parents, Shanta and Shivaji Koshti for their tons of love, sacrifice, blessings, unconditional support and encouragement. I express my deep and paramount gratitude to my brother Sanjay and sister-in-law Shital. Without their constant support and encouragement, I could not stand with this dissertation. I like to thank my younger sisters, Mrs. Ujjawala Narkhedkar and Sukshala Waste. I also like to thanks my brother-in-low Kailash Narkhedkar and Tukaram Waste. I am lucky to have lovely niece and nephew Sushant, Shlok, Ajay, Sanika, Sanket and Avanti. I always enjoy their company even at short stays at home. I would also like to show my deep gratitude to Snehal, Rahul, Suhas, and Ashwin and my relatives.

At last but not the least, I thank whole heartedly, the omnipotent God, the illimitable superior spirit, for the strength and determination to put my chin up when faced with hardships in life.

Vijaykumar Shivaji Koshti

Ac_2O	Acidic anhydride
$AlCl_3$	Aluminum chloride
A-T	Adenine-Thymine
aq	Aqueous
BF_4	TetrafluoroborateBn
BH_3	Borane
BINOL	1,1'-Bi-2-naphthol
BiPhePhos	6,6′-[(3,3′-Di-tert-butyl-5,5′-dimethoxy-1,1′-biphenyl-2,2′diyl)bis(oxy)]bis(dibenzo[d,f][1,3,2]dioxaphosphepin)
CCDC	Cambridge Crystallographic Data Centre
C-chiral	Chirality on the carbon
$CDCl_3$	Deuterated chloroform
CD_3CN	Deuterated acetonitrile
cm	Centimeter
conv	Conversion
CSD	Cambridge Structural Database
d	Doublet
Da	Dalton
DABCO	1,4-diazabicyclo[2.2.2]octane
DCC	N,N'-Dicyclohexylcarbodiimide
DCM	Dichloromethane
DEPT	Distortionless enhancement by polarization transfer
DFT	Density functional theory
DMAE	Dimethylethanolamine
DMAP	4-Dimethylaminopyridine
DMF	Dimethylformamide
DMSO	Dimethyl sulfoxide
DNA	Deoxyribonucleic acid
Dppp	1,3-Bis(diphenylphosphino)propane
DSC	Differential scanning calorimeter

ee	Enantiomeric excess
eq.	Equivalent
ESI-MS	Electro-Spray Ionization Mass-Spectroscopic
Et_2O	Diethylether
EtOH	Ethanol
EtOAc	Ethyl acetate
Et_3N	Triethyl amine
etc	et cetera
Fig.	Figure
FTIR	Fourier-transform infrared spectroscopy
g	Grams
GC	Gas chromatography
HCl	Hydrochloric acid
hr	Hour/s
HPLC	High performance liquid chromatography
Hz	Hertz
*i*Pr2NEt	N-ethyl-N-isopropylpropan-2-amine
IPA	Isopropyl alcohol
K_2CO_3	Potassium carbonate
K_2HPO_4	Dipotassium phosphate
KH_2PO_4	Monopotassium phosphate
KO*t*Bu	Potassium *tert*-Butoxide
$KPPh_2$	Potassium diphenyl phosphine
$LiAlH_4$	Lithium aluminium hydride
LiOH	Lithium hydroxide
LN2	Liquid nitrogen
m	Multiplet
M^+	Molecular ion
Me_2NPCl_2	1,1-dichloro-N,N-dimethylphosphanamine
MeOH	Methanol
MeONa	Sodium metoxide

MeOTf	Methyl trifluoromethanesulfonate
mg	Milligrams
$MgSO_4$	Magnesium sulfate
MHz	Megahertz
min	Minutes
ml	Milliliter
mmol	Millimole
MP	Melting point
NaOAc	Sodium acetate
$NaOSiMe_3$	Sodium trimethylsilanolate
n-BuLi	*n*-Butyllithium
Na_2SO_4	Sodium sulfate
$NaHCO_3$	Sodium bicarbonate
NEt_3	Triethyl amine
NH_3	Ammonia
NMR	Nuclear Magnetic Resonance
P-chiral	Chirality on the phosphorous
$Pd(dba)_2$	Bis(dibenzylideneacetone)palladium(0)
PhI	Phenyl iodide
PPh_3	Triphenylphosphine
Py	Pyridine
q	Quartet
Rh	Rhodium
RT(rt)	Room temperature
Rt	Retention time
R_f	Retention factor
s	Singlet
(*S*,*S*)-Me-DuPHOS	(+)-1,2-Bis[(2S,5S)-2,5dimethylpholano] Benzene
(S,S)Me-FerroLANE	1,1′-Bis[(2S,5S)-2,5-dimethylpholano] ferrocene

t	Triplet
TBAB	Tetrabutylammonium bromide
TBAF	Tetra-n-butyl ammonium fluoride
t-Bu-Xantphos	9,9-Dimethyl-4,5-bis(di-tert-butylphosphino) xanthene
TMEDA	Tetramethylethylenediamine
THF	Tetrahydrofuran
TLC	Thin layer chromatography

GENERAL REMARKS

- Solution NMR spectra were recorded on a Bruker Avance 200, 400 and 500 MHz instruments at 298 K unless mentioned otherwise. Chemical shifts are referenced to external reference TMS (^{1}H and ^{13}C) or 85% H_3PO_4 (Ξ = 40.480747 MHz, ^{31}P).

- Enantiomeric excess of the P-stereogenic phosphines was determined by chiral HPLC on an Agilent Technologies 1260 Infinity instrument with Chiralpak IA-IF column (20 cm).

- The single crystal data was collected using Bruker SMART APEX II single crystal X-ray CCD diffractometer with graphite-monochromatised (Mo-kα = 0.71073 A^o) radiation.

- Mass spectra were recorded on Thermo scientific Q-Exactive mass spectrometer, with Hypersil gold C18 column 150 x 4.6 mm diameter 8 µm particle size mobile phase used is 90% methanol + 10 % water + 0.1 % formic acid.

- Optical rotations were measured with a JASCO DIP 370 digital polarimeter.

- All reactions are monitored by Thin Layer Chromatography (TLC) carried out on 0.25 mm E-Merck silica gel plates (60F–254) with UV light and I_2.

- All reactions were carried out under argon atmosphere with dry, freshly distilled solvents under anhydrous conditions unless otherwise specified. Yields refer to chromatographically and spectroscopically homogeneous materials unless otherwise stated.

- All evaporations were carried out under reduced pressure on high vacuum pump and rotary evaporator below 50 °C unless otherwise specified.

- Neutral alumina and silica gel (60-120) mesh were used for column chromatography.

- **Each chapter has different compound numbers and reference numbers.**

Synopsis

Catalytic synthesis of P-chiral supramolecular phosphines, their self-assembled metal complexes and implication in asymmetric catalysis

	Synopsis of the Thesis to be submitted to the Academy of Scientific and Innovative Research for Award of the Degree of Doctor of Philosophy in Chemistry
Name of the Candidate	Vijaykumar Shivaji Koshti
Degree Enrolment No. & Date	Ph. D in Chemical Sciences (10CC12A26016); August 2012
Title of the Thesis	**Catalytic synthesis of P-chiral supramolecular phosphines, their self-assembled metal complexes and implication in asymmetric catalysis**
Research Supervisor	Dr. Samir Chikkali

The thesis titled "Catalytic synthesis of P-chiral supramolecular phosphines, their self-assembled metal complexes and implication in asymmetric catalysis" is divided into six different chapters. Chapter-1 deals with the detailed literature survey on the chiral supramolecular phosphine ligands and their self-assembled metal complexes. Various chiral supramolecular phosphine ligand and their self-assembled metal complexes used in asymmetric catalysis such as hydrogenation and hydroformylation will be discussed.[1] Synthetic aspects of all these chiral supramolecular phosphine ligands will be highlighted.[2] In addition to this, on the basis of backbone chirality, the chiral supramolecular phosphine ligands have been subdivided into two parts, 1) C-chiral backbone supramolecular phosphines, and 2) Axially chiral supramolecular phosphines. Chapter-2 deals with the synthesis and characterization of (Me-Duphos)-Pd complexes and their application towards the enantioselective synthesis of P-chiral supramolecular phosphine. Chapter-3 describes the Pd-catalyzed synthesis of a library of P-chiral supramolecular phosphine ligands under mild conditions *via* enhancing the rate of P-C coupling reaction through rational catalyst selection. The nickel catalyzed synthesis of P-chiral supramolecular phosphine ligands is illustrated in Chapter-4. Chapter-5 deals with the implication of P-chiral supramolecular phosphine ligands and their self-assembled metal complexes in asymmetric hydrogenation. Chapter-6 concludes the work and provides future direction.

Chapter 2. Highly enantioselective Pd-catalyzed synthesis of P-stereogenic supramolecular phosphines

Bidentate Phosphine ligands play a crucial role in transition metal catalysis but the synthesis of such bidentate phosphine ligand very tedious and time consuming. To overcome this hurdle one step synthesis of the supramolecular phosphine ligands that can mimic bidentate ligand through hydrogen bonding interaction between two supramolecular phosphine ligands.[2] In this chapter, synthesis of iodophenyl urea as hydrogen bonding motif, synthesis of palladium catalysts and their implication in the synthesis of P-chiral supramolecular phosphine ligands (Scheme 1) is presented.[3] This reaction proceeds *via* path-I which was confirmed by ^{31}P NMR spectroscopy. The library of enantiopure P-chiral supramolecular phosphines was synthesized and their characterisation is reported.
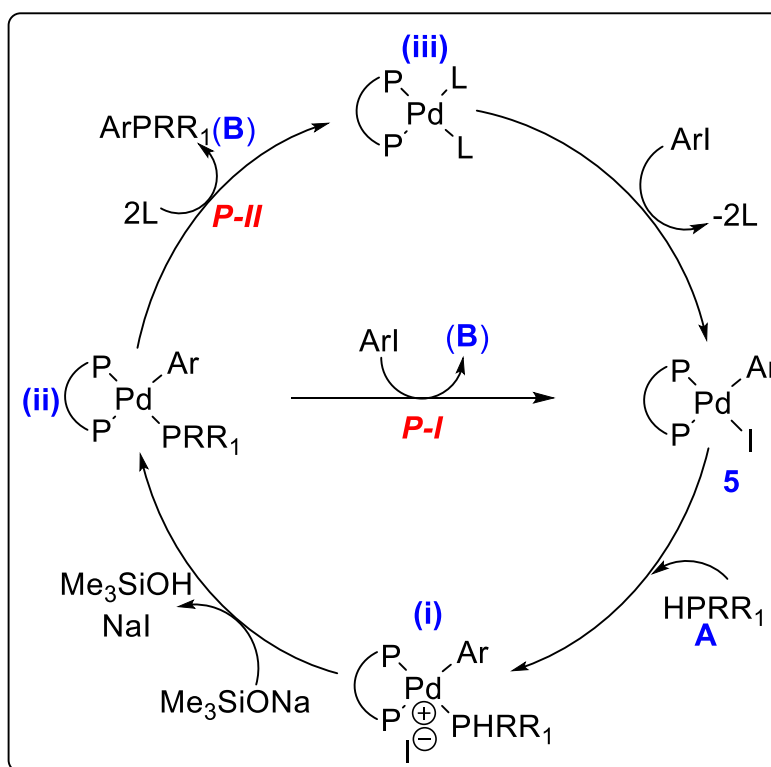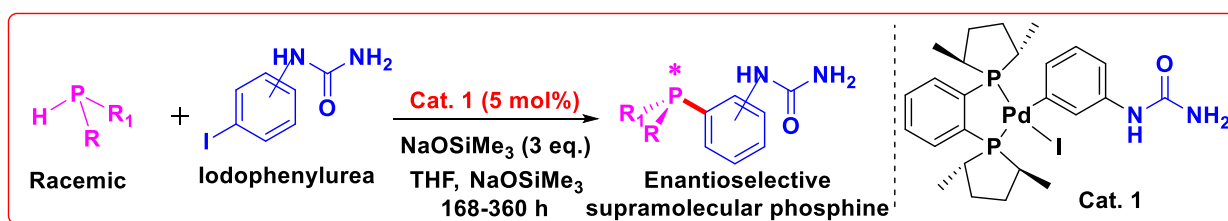
Scheme 1. Pd-catalyzed enantioselective synthesis of P-chiral supramolecular phosphines and their mechanistic study.

Chapter 3. Enhancing the rate of enantioselective P-C coupling reaction through rational catalyst selection

In this chapter, development of the Pd- catalyst to decrease the reaction time and improve the yield and enantiomeric excess is described. The Pd-catalyst **2** is used in a P-C bond formation reaction with the different derivatives of *N*-substituted iodophenyl urea as hydrogen bonding motif [4] and different secondary racemic phosphine (Scheme 2). This reaction was found to be faster and completes in 18 hours with 58 %ee and 99% yield. Following this a library of enantiopure P-chiral supramolecular phosphine was synthesized and their characterisation has been presented.
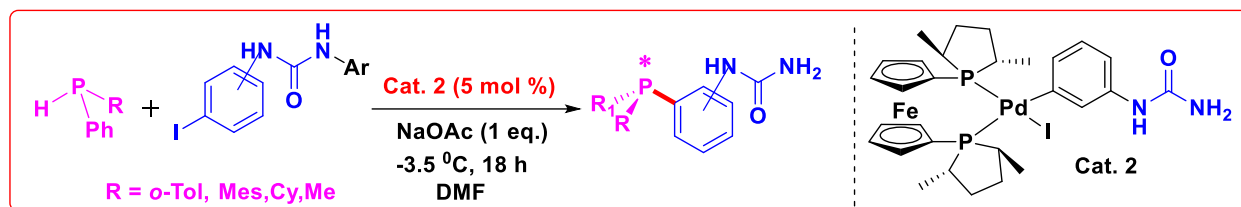
Scheme 2. Pd-catalyzed enantioselective synthesis of P-chiral supramolecular phosphines.

Chapter 4. Ni-catalyzed enantioselective synthesis of P-stereogenic (supramolecular) phosphines

Literature reports Palladium and Platinum catalyzed P-C bond formation but those metals are expensive and rare. This chapter illustrates the synthesis of a nickel catalysts and their implication in P-C bond coupling reaction.[5] Ni-catalyst was used in P-C bond formation reaction under mild reaction condition. The urea functional group change the activity of Ni-catalyst and due to that undesired product formation was observed.
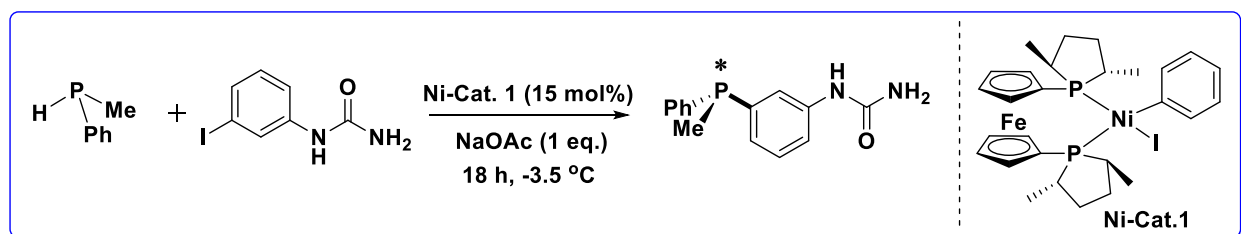
Scheme 3. Ni-catalyzed enantioselective synthesis of P-chiral (supramolecular) phosphines.

Chapter 5. Ligand-directed enantioselectivity: Understanding the role of secondary interaction in asymmetric hydrogenation

P-stereogenic supramolecular phosphine and their self-assembled Rh-complex were used in asymmetric hydrogenation which produce an excellent ee 99%. To establish the nature of hydrogen bonding in the self-assembled Rh-complex NMR experiments were performed at different concentration and temperature. It was observed that at different concentration and temperature the chemical shift of NH and NH_2 protons in P-stereogenic supramolecular phosphine changes. With increasing concentration of ligand, the value of NH and NH_2 peaks shifted down the field. Along the same line, with decreasing temperature, the value of NH and NH_2 peaks of ligand shifted downfield. In contrast, this kind of phenomenon was not observed in the self-assembled Rh-complex. These experiments confirm the existence of strong hydrogen bonding interaction in the self-assembled Rh-complex. In the stoichiometric experiment of self-assembled Rh-complex with *N*-acetyldehydrophenylalanine (S2), the NH_2 protons were found to shift downfield as compared to the self-assembled Rh-complex NH_2 protons. These observations confirm that there is a hydrogen bonding interaction between complex and substrate. To further attest this hypothesis, deuterium exchange experiments were conducted, which confirmed hydrogen bonding interaction in between complex and substrate. The presence of this interaction could be one parameter that leads to high ee.
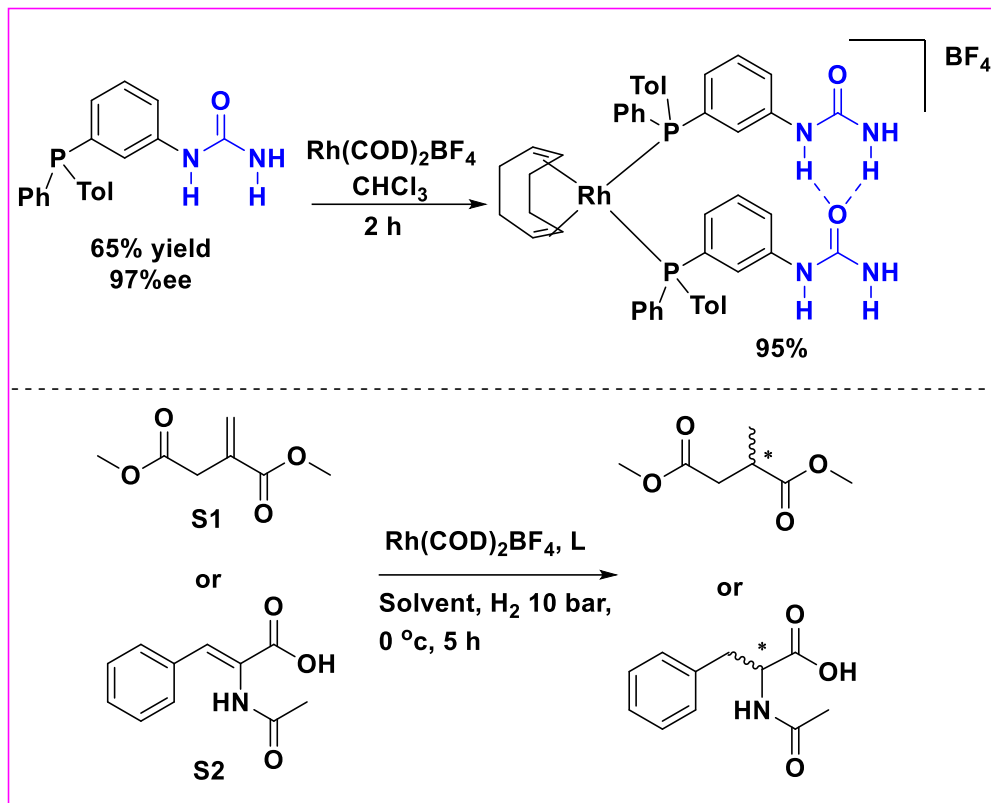
Scheme 4. Asymmetric hydrogenation by using self assembled Rh-complex.

Chapter 6. Conclusions and outlook

This work summarizes the synthesis of P-chiral supramolecular phosphine ligands with excellent yield and 97% ee. The idea is to use two structurally less complex monodentate ligands, which are held together through non-covalent attractive interactions and imitate a bidentate ligand at the catalytically active metal center. There are ligand–ligand interactions, which can be weak like van der Waals, π-π stacking, charge-transfer, and dipole–dipole interactions to hydrogen bonding and even stronger coordinative interactions.[6] This concept has been applied in the generation of the first bidentate ligand libraries based on self-assembly through hydrogen bonding. The self-assembled complexes catalyze asymmetric hydrogenation of alkenes to highly enantioselective product.

The work described in this thesis contributes to the continuing trend of merging classical disciplines namely supramolecular phosphines and P-chiral (chirality on phosphorous) phosphines. This asymmetric synthesis of P-chiral supramolecular phosphine ligands helps to surpass limitations of bidentate phosphine ligands and greatly expands the freedom of designing

transition metal catalyst. Finally, improving systems discovered in the laboratory and incorporating them into applications is the ultimate driving-force for organometallic chemistry advances.

References

(1) a) R. R. Noyori, *Asymmetric Catalysis in Organic Synthesis*; Wiley-Interscience: New York, 1994; (b) W. S. Knowles, In *Asymmetric Catalysis on Industrial Scale, Challenges, Approaches, and Solutions*; H. U. Blaser and E. Schmidt, Eds.; Wiley-VCH: Weinheim, Germany, 2004; pp23−38.

(2) a) P. R. Breuil, F. W. Patureau and J. N. H. Reek. *Angew. Chem. Int. Ed.,* 2009, **48**, 2162 –2165; b) I. Usui, S. Schmidt, M. Keller and B. Breit. *Org. Lett.,* 2008 **10**, 1207-1210; c) P. Li, X. Hu, X. Dong and X. Zhang. *Chem. Commun.*, 2016, **52**, 11677-11680.

(3) a) V. S. Koshti, S. R. Gaikwad and S. H. Chikkali, *Coord. Chem. Rev*., 2014, **265**, 52−73. b) V. S. Koshti, N. R. Mote, and S. H. Chikkali, *Organometallics,* 2015, **34**, 4802-4805.

(4) V. S. Koshti, S. H. Thorat, R. P. Gote, S. H. Chikkali and R. G. Gonnade, *CrystEngComm,* 2016, **18**, 7078-7094.

(5) T. J. Brunker, N. F. Blank, J. R. Moncarz, C. Scriban, B. J. Anderson, D. S. Glueck, L. N. Zakharov, J. A. Golen, R. D. Sommer, C. D. Incarvito, and A. L. Rheingold., *Organometallics,* 2005, **24***, 2730-2746.

(6) V. W. Yam, X. Lu and C. Ko, *Angew. Chem. Int. Ed.,* 2003, **42**, 3385-3388.

TABLE OF CONTENTS

Chapter 1. Supramolecular phosphine ligands in homogenous catalysis: A general introduction

Chapter 2. Highly enantioselective Pd-catalyzed synthesis of P-stereogenic supramolecular phosphines

Chapter 3. Enhancing the rate of enantioselective P-C coupling reaction through rational catalyst selection

Chapter 4. Ni-catalyzed enantioselective synthesis of P-stereogenic (supramolecular) phosphines

Chapter 5. Self-assembly of P-chiral supramolecular phosphine on rhodium and a direct evidence for Rh-catalyst-substrate interaction in asymmetric hydrogenation

Chapter 6. Summary and Outlook

Appendix 1. The impact of modular substitution on crystal packing: The tale of two urea's

Chapter 1

Supramolecular phosphine ligands in homogenous catalysis: A general introduction

1.1 Abstract

Notable advance and current progressive developments in the synthesis of supramolecular phosphine ligands and their catalytic implication are summarized in this chapter. The concept is to use two structurally less complex monodentate ligands, which are held together through non-covalent attractive interactions and imitate a bidentate ligand at the catalytically active metal center. There are ligand-ligand interactions, which can be weak like van der Waals, π-π stacking, charge-transfer, and dipole-dipole interactions to hydrogen bonding and even stronger coordinative interactions. Irrespective of the strength of the hydrogen bonding interaction, the specific formation of homo- and hetero-dimeric ligands requires two different sets of monodentate ligands with complementary binding sites. The binding sites in supramolecular phosphine ligands are phosphorous atoms because phosphorous ligands are well-known ligands in metal catalyst due to its electronic and coordination properties. The hydrogen bonding motif contains hydrogen donor and hydrogen acceptor incorporated in phosphorus ligand. These ligands are applied in the generation of the self-assembled metal complex and this supramolecular phosphine ligand can mimic bidentate phosphine ligands due to hydrogen bonding interaction in between them in the self-assembled metal complex. This field covers the principles of supramolecular phosphine chemistry, supramolecular chiral chemistry, supramolecular P-stereogenic chemistry, coordination chemistry, and catalysis for the generation of ligand libraries for homogeneous catalysis.
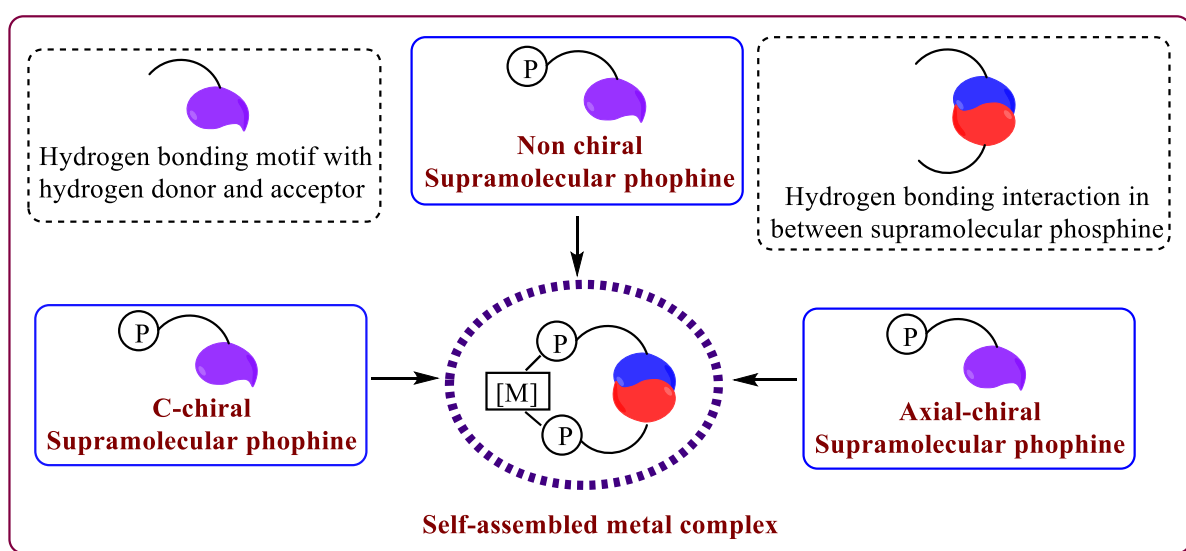
1.1. Introduction

The reactivity and selectivity of a metal catalyzed transformation can be tuned by tweaking the ligands; among which phosphine ligands play a prominent role. Last few decades have witnessed a tremendous increase in a number of phosphine ligands that have been designed with a purpose. While significant progress has been made in finding new ligand motifs, fundamental understanding of the role of ligand and selectivity remains a significant challenge. Monodentate phosphine ligands were the first ligands used in homogeneous catalysis, however, these provide active metal center during the catalytic reaction.[1] The field of phosphine ligands has been developed based on electronic, steric, and chelating factors (like bidentate, tridentate, tetradentate ligands, etc.) (Figure 1).[2] The chelating ability of bidentate ligands can lead to highly active metal center. However, synthesis of bidentate ligands generally requires a number of synthetic steps compared to the synthesis of monodentate ligands.

The dominance of bidentate ligands has been now challenged by supramolecular monodentate ligands that mimic bidentate ligands when mixed with metal precursor. There are various non-covalent interactions such as van-der Waals interactions, π-π stacking, cation–π interactions, charge-transfer interactions, electrostatic interactions, hydrogen bonding, and coordinative interactions. Thus, moving from a metal complex having two truly monodentate ligands with no attractive interaction between them, to a metal complex with a bidentate ligand having two covalently connected binding sites, there is a continuum of arrangements consisting of two donor ligands and a metal center that emulate chelation through non-covalent attractive ligand-ligand interactions. A differentiation within this continuum may be made according to the strength and nature of the attractive ligand-ligand interaction. As depicted in Figure 1, the supramolecular motifs attract each other and these attractive interactions between the two-monodentate ligands enforce pseudo-bidentate character to these monodentate ligands (Fig. 1).[2,3] In particular, supramolecular phosphine ligands have emerged as a most suitable candidate for various organometallic transformations.

Thus, herein discussed the synthesis of supramolecular phosphine ligands and metal catalyst and implications in catalysis. The introduction of each supramolecular phosphine ligands covered into three part; 1) to categorize the supramolecular phosphine ligands, 2) to summarize the synthetic aspects of supramolecular phosphine ligands and 3) to highlight the significance of these ligands in homogeneous catalysis.
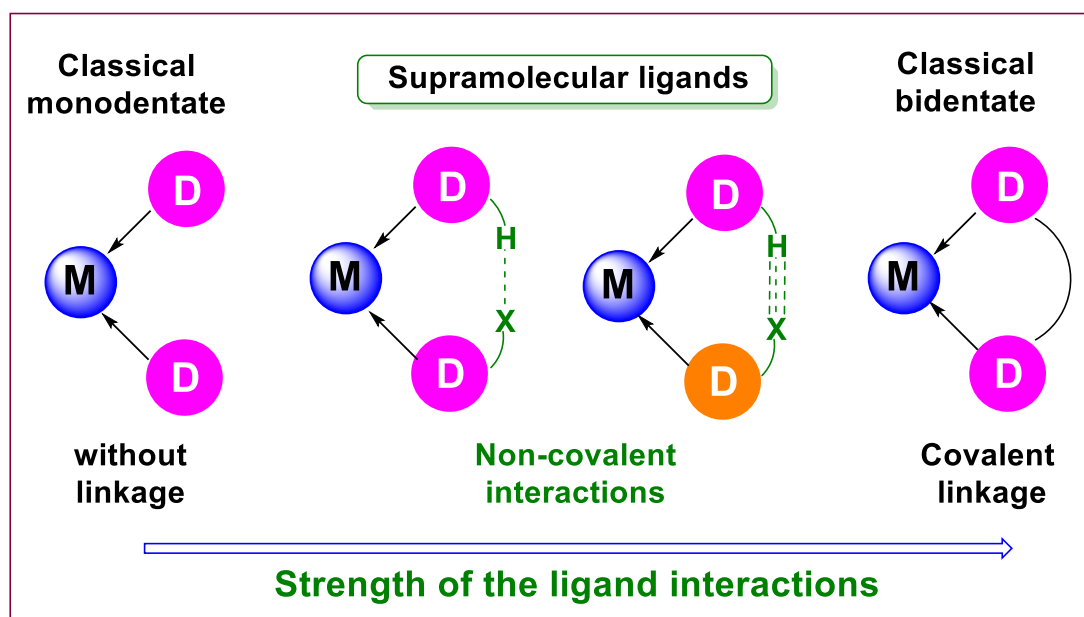
Figure 1: Conceptual representation of monodentate, supramolecular ligands and classical bidentate ligands.

1.2. Supramolecular phosphine ligands

The supramolecular phosphine ligands can be broadly classified in to; 1) Non-chiral supramolecular phosphines, 2) Supramolecular phosphines with backbone chirality, and 3) P-stereogenic supramolecular phosphine ligands (Fig. 2). The phosphine ligands with backbone chirality can be sub-divided into two categories, a) C-chiral supramolecular phosphine ligands, and b) Axially chiral supramolecular phosphine ligands.
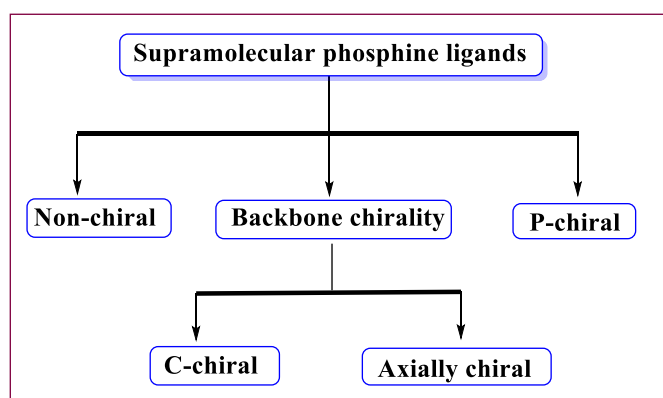
Figure 2: General classification of supramolecular phosphine ligands.

1.2.1. Non-chiral supramolecular phosphine ligands

In 2003 B. Breit and co-workers reported in situ generation of bidentate ligand based on the self-assembly of a monodentate ligand in the coordination sphere of a platinum metal center in the *cis*-[PtCl$_2$(6-DPPon)$_2$] (**6**) through hydrogen bonding. The 2-pyridone (6-DPPon)

(**5A**)/2-hydroxypyridine (6-DPPon) (**5B**) tautomer system dimerizes in aprotic solvents to form predominantly the symmetrical pyridone dimer **5** through hydrogen bonding. These ligands were synthesized using 2,6-dichloro-pyridine (**1**) and Potassium *tert*-Butoxide to obtain **2**. Then, compound **2** was treated with PPh$_3$ in presence of sodium in liquid ammonia to generate compound **3**; which after hydrolysis produced pure **4** (Scheme 1). The electronic properties of "P (phosphorous)" were tuned with a range of electron withdrawing groups at *para* position (Scheme 1, top).[4]
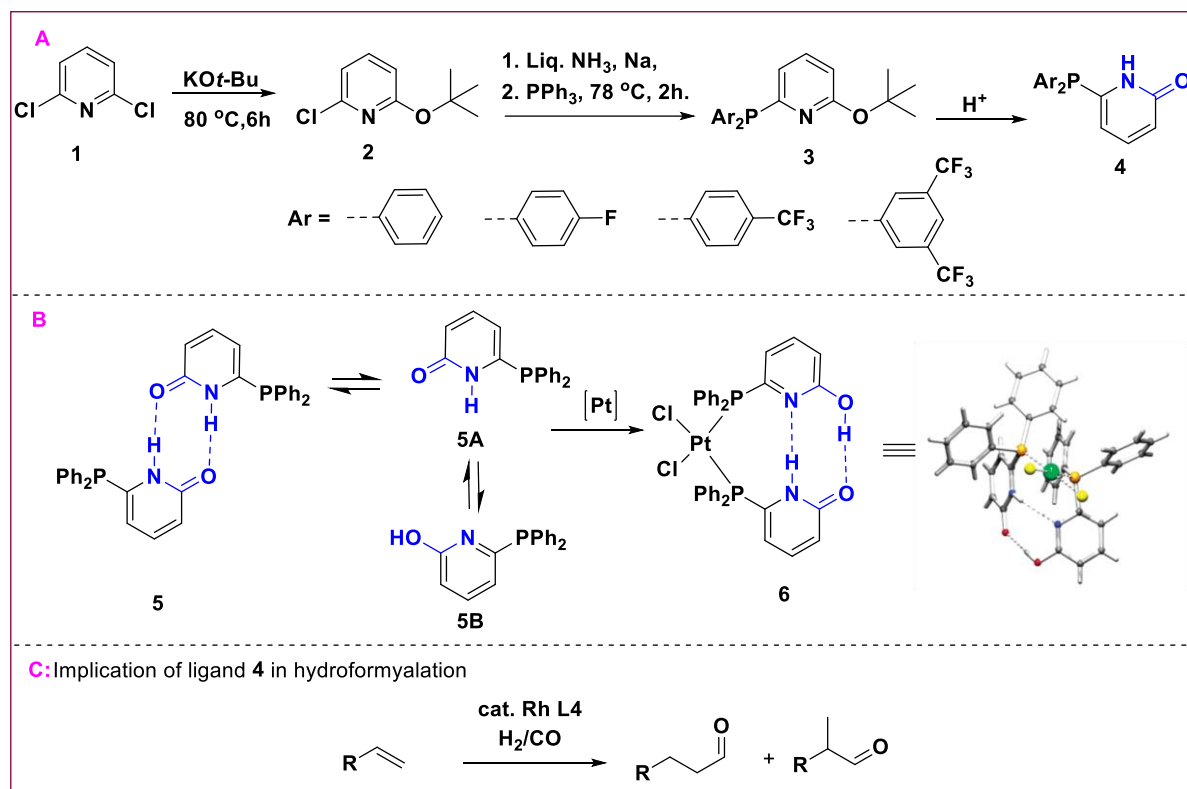
Scheme 1: Synthesis of 6-diphenylphosphanyl-2-pyridone (6-DPPon) **4** (A), hydrogen bonding study of **5** and X-ray structure of cis-[PtCl$_2$(6-DPPon)$_2$] **6** (B), regioselective hydroformylation of terminal alkenes with the Rhodium/6-DPPon (**4**) Catalyst (C).

Complex **6** was synthesized by mixing 2 equivalent of 6-DPPon (**4**) with [PtCl$_2$(1,5-COD)]. Ligand **4** induced bidentate binding mode was confirmed by single crystal X-ray diffraction of **6**. Ligand **4** with [Rh(COD)$_2$BF$_4$] in presence of H$_2$/CO gas was used for hydroformylation of various terminal olefins (Scheme 1, bottom)[5]. This self-assembled metal catalyst yields highly active as well as highly regioselective product compared to monodentate biphenyl phosphine and bidentate *t*-Bu-Xantphos, and BiPhePhos derived catalysts.[6,7]

Hetero non-covalent interactions have been well known in DNA bases like hydrogen bonding between Adenine (A) and Thymine (T). Based on this concept, a supramolecular phosphine ligand with A-T base pair as a hydrogen bonding unit was designed (Fig. 3).[8]

1) NH$_4$OH, 190 ^{o}C, 5 h; 2) pivaloylchloride, NEt$_3$, CH$_2$Cl$_2$, 0 ^{o}C to RT; 3) *n*-BuLi (2 equiv), THF, 100 ^{o}C, then ClPR$_2$,100 ^{o}C to RT; 4) KO*t*-Bu (1.1 equiv), toluene, 80 ^{o}C, 1 h; 5) *n*-BuLi (1 equiv.), THF, 100 ^{o}C, then ClPR$_2$, 100 ^{o}C to RT, then H$_2$O (1 equiv)and formic acid excess (50-75%).
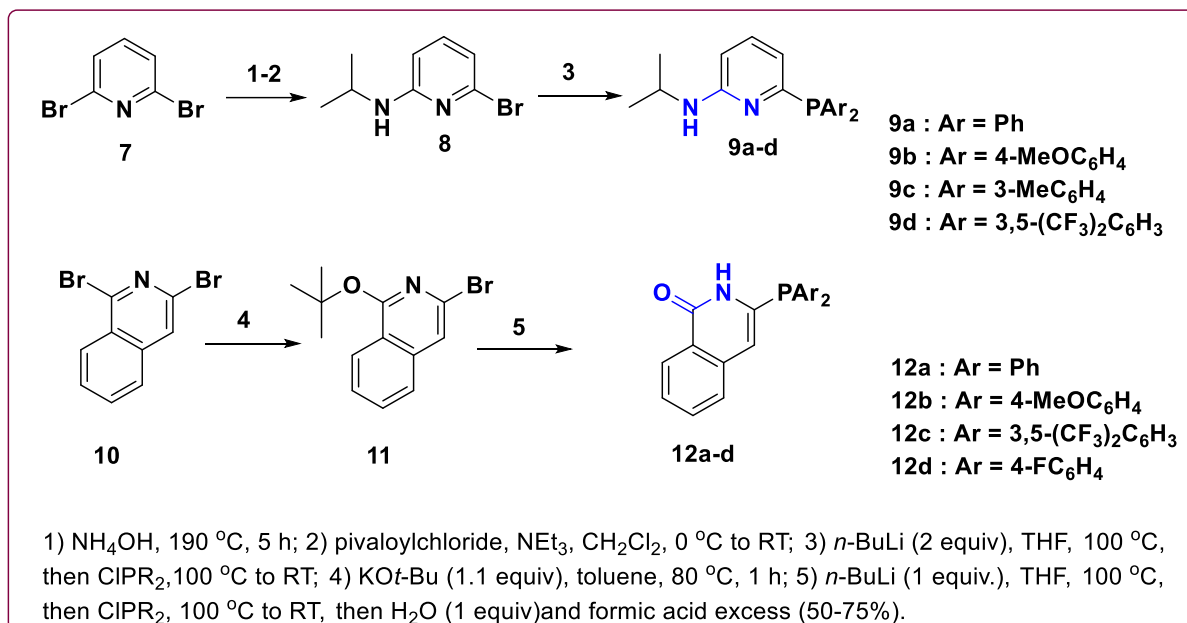
Scheme 1.2: Synthesis of monodentate aminopyridinylphosphines **9** and isoquinolones **12**.

Important interatomic distances [A^o] and angles [^{o}]: Pt-P1 2.2486(5), Pt-P22.2437(5), NH···N 2.932(2), O···HN 2.977(2); P1-Pt-P2 102.896(18), NH···N, 163(2) O···H-N 172(2). Green Pt, yellow Cl, orange P, blue N, red O.
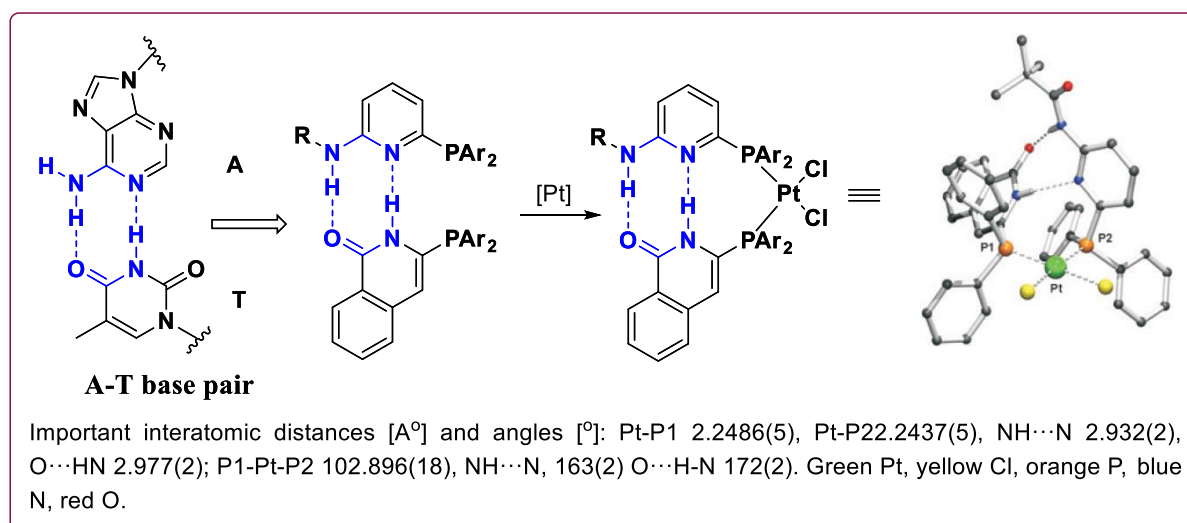
Figure 3: a) An A-T base-pair model as a platform for the self-assembly of monomeric to mixed bidentate ligands. b) X-ray structure of [cis-**9a**, **12a**-PtCl$_2$] in the solid state.

The required substituted aminopyridine phosphine ligand **9** (Scheme 2) was prepared from commercially available chemicals such as 2,6-dibromopyridine (**7**) in presence of aqueous ammonia and protected amine to give compound **8** (Scheme 2). Then **8** was treated with diaryl phosphine chloride in presence of *t*-BuLi at -100 ^{o}C to obtain compound **10**. The isoquinolone based ligand precursor **11** was synthesized using 1,3-dibromoisoquinoline (**10**) and 1 eq. of potassium *tert*-butoxide. Compound **11** was treated with diaryl phosphine chloride in presence of *t*-BuLi at -100 ^{o}C to give compound **12** (Scheme 2).[9]

Heterodimeric phosphine ligand complexes were found to be superior to homodimeric phosphine ligand complexes. This concept was practically demonstrated by employing these

ligands in hydroformylation reaction of terminal alkenes[10] and terminal alkyls including high enantioselectivity (99:1). The reason for high ee's could be the strong hydrogen bonding in heterodimeric phosphine ligand-metal complex as compared to homodimeric complexes (Fig. 1 and 4).
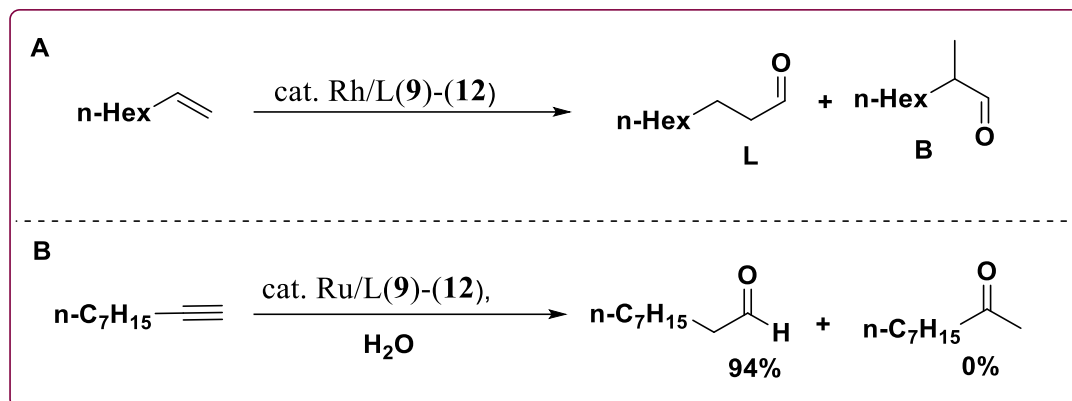
Figure 4: Hydroformylation of terminal olefin (A) and terminal alkyls (B).

In 2007 B. Breit and co-worker reported new supramolecular phosphine ligand library where in the 2-hydroxy pyridine group was replaced by 2-amine heteroaromatic ring. These ligands with palladium were successfully used in alkylation of indoles by allylic alcohol[11] and in Ni-catalyzed hydrocyanation.[12]

Supramolecular phosphine ligands *N*-(6-(diphenylphosphanyl)pyridin-2-yl)-2,2,2-trifluoroacetamide (**15**)**,** *N*-(3-(diphenylphosphanyl)isoquinolin-1-yl)pivalamide (**18**)**,** *N*-(2-(diphenylphosphanyl)thiazol-4-yl)pivalamide (**21**) and *N*-(2-(diphenylphosphanyl)thiazol-4-yl)-2,2,2-trifluoroacetamide (**24**) were synthesized using commercially available amine heterocycles 6-bromopyridin-2-amine (**13**), 3-bromoisoquinolin-1-amine (**16**), 2-bromothiazol-4-amine (**19**) and 2-bromothiazol-4-amine (**22**) respectively, which upon treatment with acidic anhydride or acid chloride produced amide functionalized products *N*-(6-bromopyridin-2-yl)-2,2,2-trifluoroacetamide (**14**), *N*-(3-bromoisoquinolin-1-yl)pivalamide (**17**), *N*-(2-bromothiazol-4-yl)pivalamide (**20**) and *N*-(2-bromothiazol-4-yl)-2,2,2-trifluoroacetamide (**23**) respectively (Scheme 1.3). The P-C bond was formed upon lithiation and chlorodiphenylphosphine treatment to give **15**, **18**, **21** and **24**. Ligand 2-(diphenylphosphanyl)-1*H*-pyrrolo[2,3-b]pyridine (**27**) was synthesized using commercially available compound 1-(phenylsulfonyl)-1*H*-pyrrolo[2,3-b]pyridine (**25**). Treatment of **25** with LDA (Lithium diisopropylamide) at 0 ºC, followed by addition of chlorodiphenyl phosphine generated phosphine 2-(diphenylphosphanyl)-1-(phenylsulfonyl)-1*H*-pyrrolo[2,3-b]pyridine

(**26**). TBAF (Tetra-*n*-butyl ammonium fluoride) deprotonation of **26** led to ligand **27** (Scheme 3).[13]
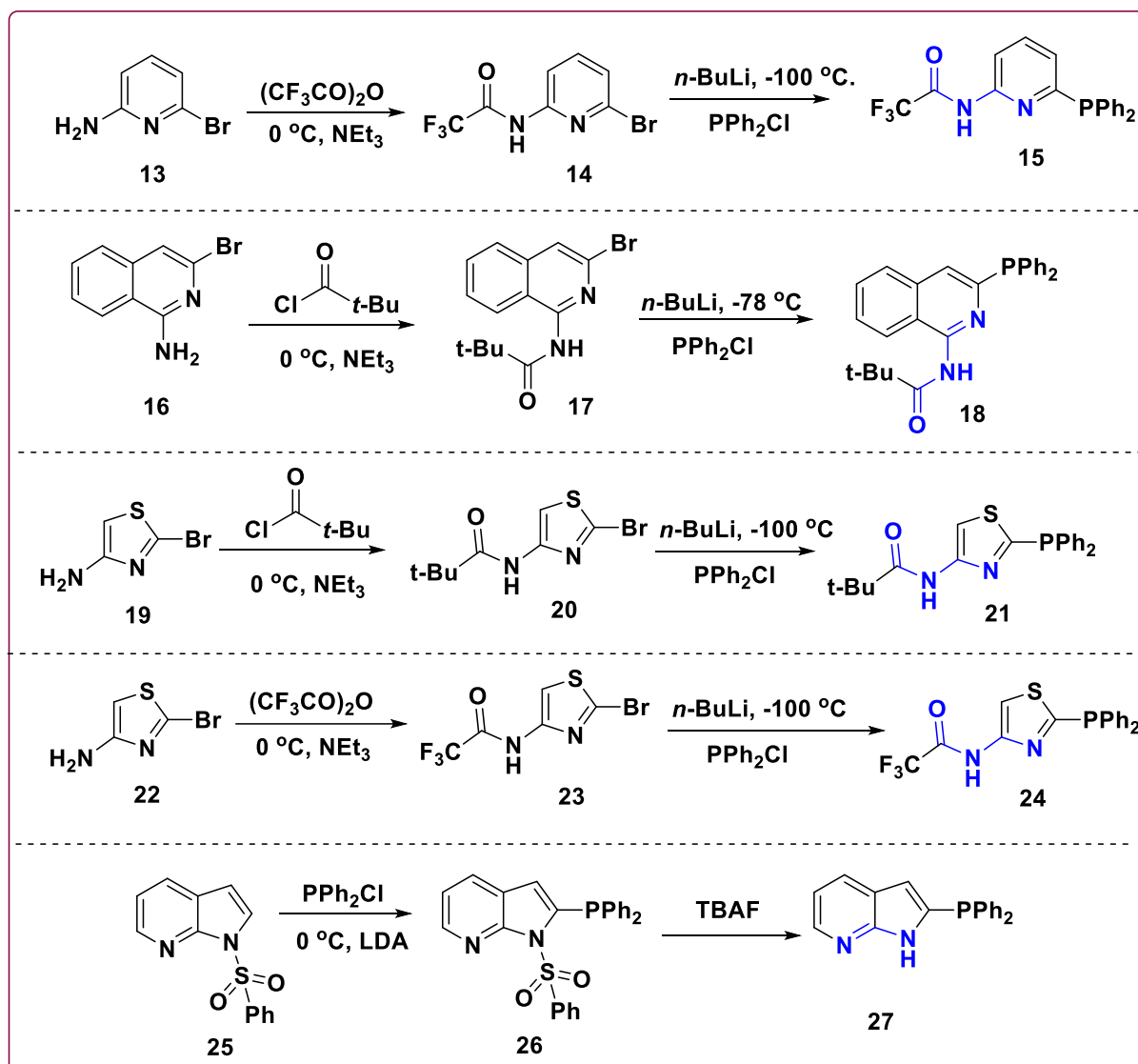
Scheme 3: Synthesis of supramolecular monodentate phosphine ligands.

In 2008, B. Breit and co-workers reported supramolecular phosphine ligands with Rh-metal which was used for decarboxylation of *α,β*-unsaturated carboxylic acids followed by hydroformylation. Synthesis of ligands *N*-carbamimidoyl-6-(diphenylphosphanyl)picolinamide (**31**), *N*-carbamimidoyl-3-(diphenylphosphanyl)benzamide (**32**) and 6-(diphenylphosphanyl)-*N*-(6-methylpyridin-2-yl)picolinamide (**33**) was started with 2,6 dibromopyridine or 2,6 dibromophenyl (**28**), which after lithiation and chlorodiphenyl phosphine treatment gave 2-bromo-6-(diphenylphosphanyl)pyridine (**29**). The carboxylic acid

functional group was introduced in the next step to give 6-(diphenylphosphanyl)picolinic acid (**30**). The acid was treated with various amines to generate **31**, **32**, and **33** (Scheme 4).[14]
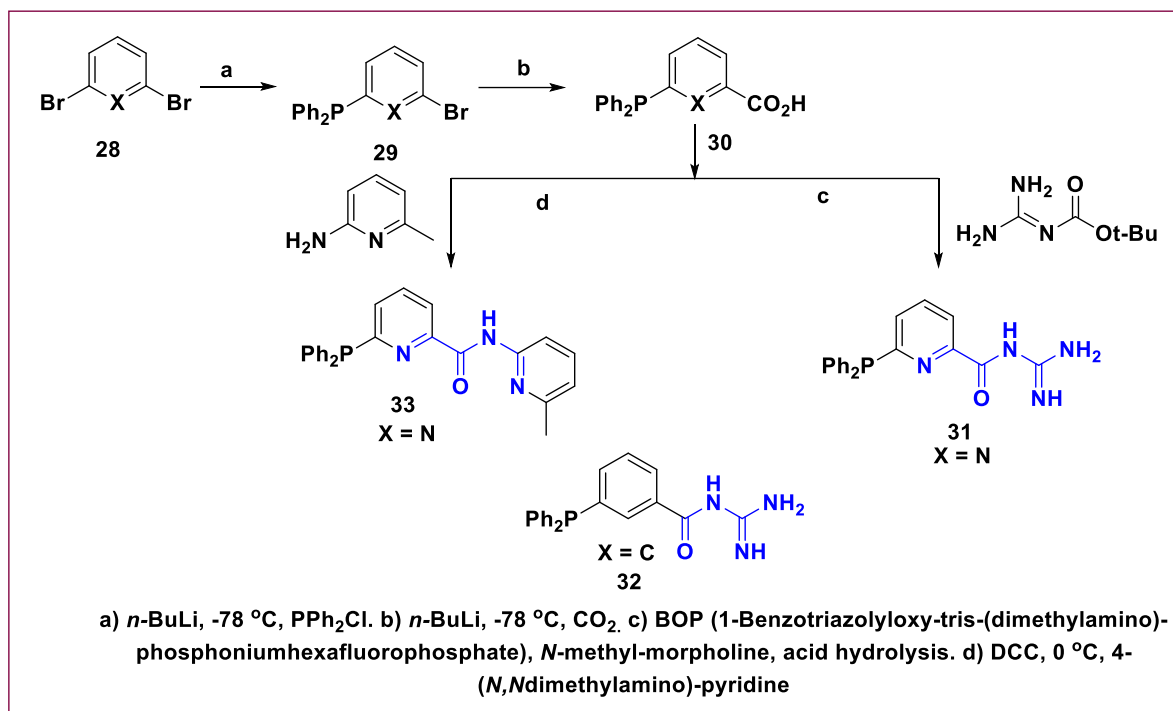
Scheme 4: Synthesis of supramolecular monodentate phosphine ligands.
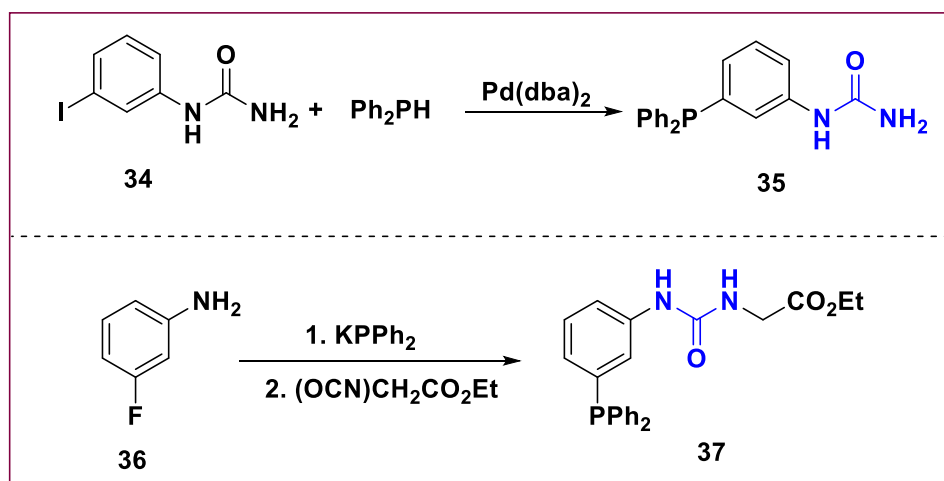
Scheme 5: Synthesis of supramolecular monodentate phosphine ligands.

In a parallel, Reek and co-worker investigated "Ureaphos" ligands (Scheme 5). Ureaphos ligands with appropriate metal (in this case Rh) were found to be highly active and selective in asymmetric hydrogenation. Synthesis of such type of phosphine ligands was achieved using diphenyl phosphine and 3-iodophenylurea (**34**) in presence of [Pd(dba)$_2$] catalyst to give 1-(3-(diphenylphosphanyl)phenyl)urea (**35**) (Scheme 5).[15]

Synthesis of ligand **37** was started with the 3-flouroaniline (**36**) and potassium diphenyl phosphine to give urea functionalized compound ethyl ((3-(diphenylphosphanyl)phenyl)carbamoyl)glycinate (**37**) (Scheme 5).[16]

1.3. Supramolecular phosphine ligands with chiral backbone

P-chiral ligands were the first ligands employed in asymmetric homogeneous catalysis. However, use of phosphorous ligands with back-bone chirality supplanted the application of P-chiral ligands. Supramolecular phosphine ligands can be broadly classified into a) C-chiral, b) P-chiral. The C-chiral phosphines can be further classified into i) Supramolecular phosphine with the C-chiral center and ii) Axially chiral supramolecular phosphine ligands.

1.3.1. Supramolecular phosphine ligands with the C-chiral center

The performance of self-assembled metal catalysts depends upon the environment around hydrogen bonding motif and it can affect the catalytic reaction. Supramolecular C-chiral phosphine ligands were treated with metal to generate chiral catalyst that induced high enantioselectivities in a catalytic reaction. In 2007, B. Breit and A. Borner introduced sterically demanding C-chiral supramolecular ligands (Scheme 6).[17]

Compound 6-((2R,5R)-2,5-dimethylphospholan-1-yl)pyridin-2(1H)-one (**44**) was prepared from 2,6-dibromopyridine (**38**). Nucleophilic substitution of **38** using potassium *tert*-butoxide gave compound 2-bromo-6-(*tert*-butoxy)pyridine (**39**). Lithiation of compound **39** with the help of *n*-BuLi and addition of chlorodiaminophosphine produced compound 1-(6-(*tert*-butoxy)pyridin-2-yl)-*N,N,N',N'*-tetraethylphosphanediamine (**40**). Then the two P-N bonds were replaced by two P-O bonds with the help of ethanol to give compound diethyl (6-(*tert*-butoxy)pyridin-2-yl)phosphonite (**41**). These two P-O bonds were reduced by LiAlH$_4$ to give primary phosphine 2-(*tert*-butoxy)-6-phosphanylpyridine (**42**). This compound was cyclized with 2,5 protected hexane diols to give compound **44** followed by acid hydrolysis. Thus the desired ligand **44** was synthesized using a multistep synthetic approach.

Even more tedious and time consuming synthesis was reported for ligand 6-((2R,5R)-2,5-diphenylphospholan-1-yl)pyridin-2(1H)-one (**56**). First the dichlorophosphine compound was cyclized with diene to yield (2R,5S)-1-(dimethylamino)-2,5-diphenyl-2,5-dihydrophosphole 1-oxide (**46**). After that reduction of double bond with Pd/C to generate (1S,2R,5S)-1-(dimethylamino)-2,5-diphenylphospholane 1-oxide (**47**) and after that acid hydrolysis led to the generation of racemic phosphoric acid (2S,5S)-1-hydroxy-2,5-

diphenylphospholane 1-oxide (**48**) and (2*R*,5*R*)-1-hydroxy-2,5-diphenylphospholane 1-oxide (**49**). After optical resolution one isomer was separated, this isomer (2*R*,5*R*)-2,5-diphenylphospholane 1-oxide (**50**) was treated with compound 2-(*tert*-butoxy)-6-iodopyridine (**53**) in presence of palladium catalyst to give phosphine oxide product (2*R*,5*R*)-1-(6-(*tert*-butoxy)pyridin-2-yl)-2,5-diphenylphospholane 1-oxide (**54**). The P=O bond of **54** was reduced by LiAlH$_4$ followed by protection and deprotection steps to obtain pure **56**.
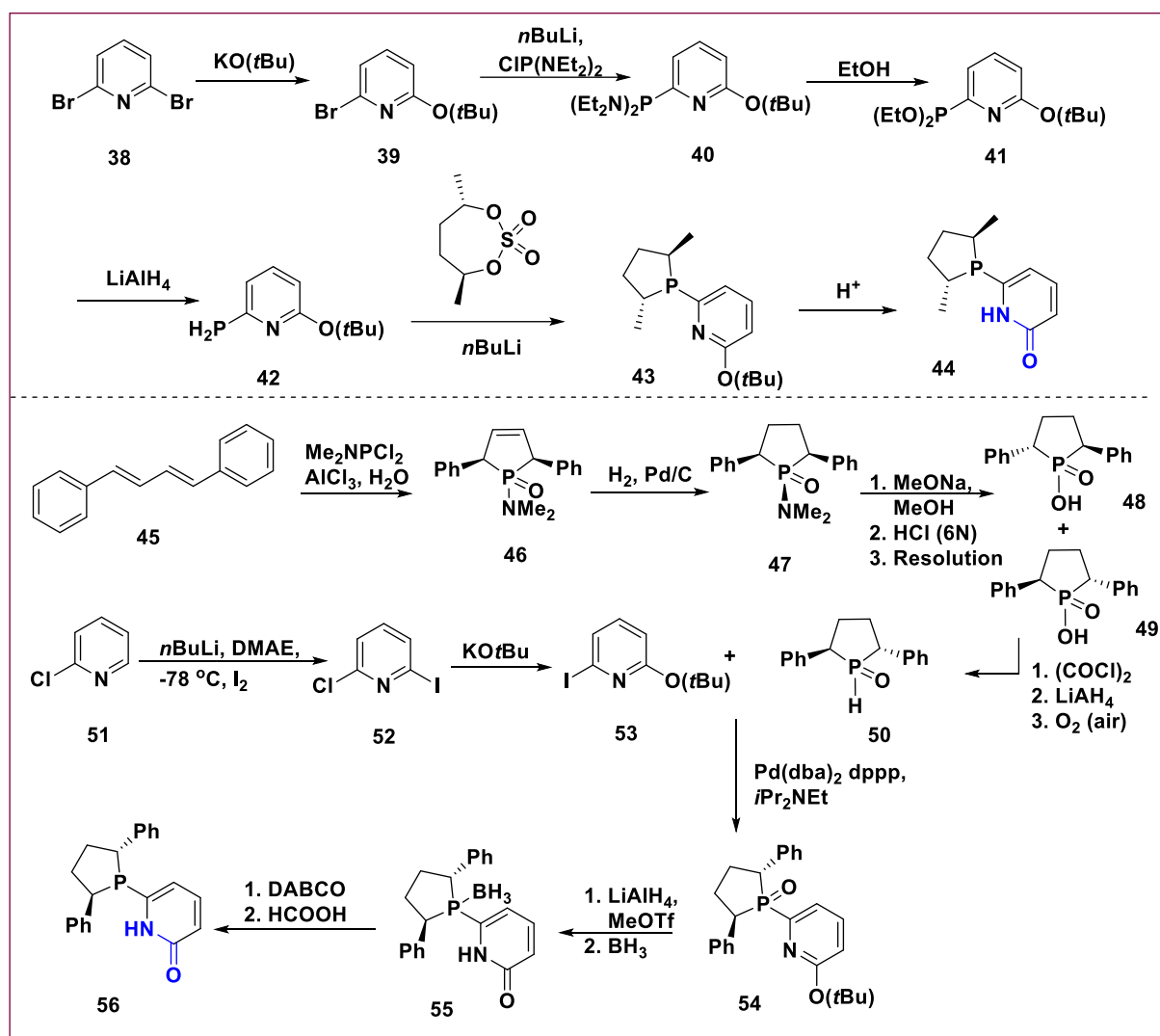
Scheme 6: Synthesis of C-chiral supramolecular phosphine ligands.
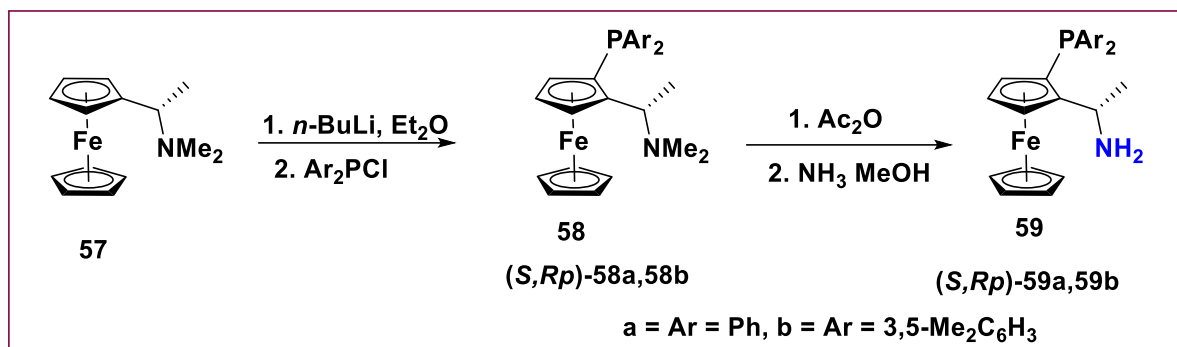
Scheme 7: Synthesis of C-chiral and axial chiral supramolecular phosphine ligands.

Supramolecular phosphine ligand consisting of C-chirality and axial chirality (in the same ligand motif) in presence of Gold was used in 3+2 cycloadditions reaction. The (1*S*)-1-(2-(diphenylphosphanyl)ferrocene)ethan-1-amine (**59a**) and (1*S*)-1-(2-(bis(3,5-dimethylphenyl)phosphanyl)ferrocene)ethan-1-amine (**59b**) ligand was synthesized in two steps. The synthesis was started with commercially available (*S*)-*N*,*N*-Dimethyl-1-ferrocenylethylamine (**57**). Compound **57** was treated with *n*-BuLi and diaryl chlorophosphine to (1*S*)-1-(2-(diphenylphosphanyl)ferrocene)-*N*,*N*-dimethylethan-1-amine (**58a**) and (1*S*)-1-(2-(bis(3,5-dimethylphenyl)phosphanyl)ferrocene)-*N*,*N*-dimethylethan-1-amine (**58b**) were obtained. After primary amine compound **59a** and **59b** was deprotected followed by acidic anhydride ammonia treatment (Scheme 7).[18]

In 2013, L. Bouteiller and co-worker synthesized a library of supramolecular phosphine ligands with three hydrogen bonding sites in a single ligand structure and studied their application in the asymmetric hydrogenation reaction. Synthesis of such types of ligands was started with 3-(diphenylphosphanyl)aniline (**60**). Condensation of appropriate amount of benzene-1,3,5-tricarbonyl trichloride **61** with **60** and octan-2-amine (**62**) produced the desired supramolecular phosphine ligand N^1-(3-(diphenylphosphanyl)phenyl)-N^3,N^5-di(octan-2-yl)benzene-1,3,5-tricarboxamide (**63**). Synthesis of ligand N^1-(3-(diphenylphosphanyl)phenyl)-N^3,N^5-diethyl-N^3,N^5-di((*S*)-octan-2-yl)benzene-1,3,5-tricarboxamide (**66**) was started with trimethyl benzene-1,3,5-tricarboxylate (**64**) in presence of oxalyl chloride and *N*-ethyl-1-(*S*)-methyl-heptylamine to give methyl 3,5-bis(ethyl((*S*)-octan-2-yl)carbamoyl)benzoate (**65**). Then, **65** in the presence of LiOH and 3-diphenylphosphine aniline produced the desired supramolecular phosphine ligands **66** (Scheme 8).[19]
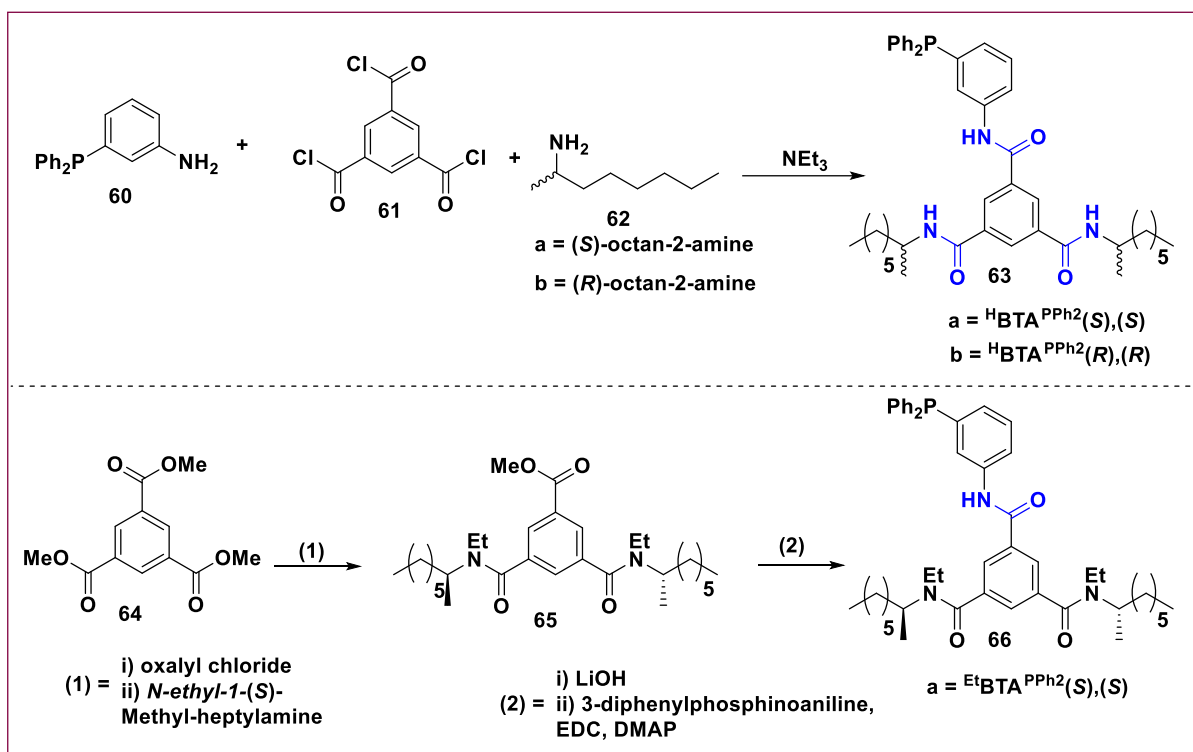
Scheme 8: Synthesis of C-chiral supramolecular phosphine ligands.

1.3.2. Axially chiral supramolecular phosphines
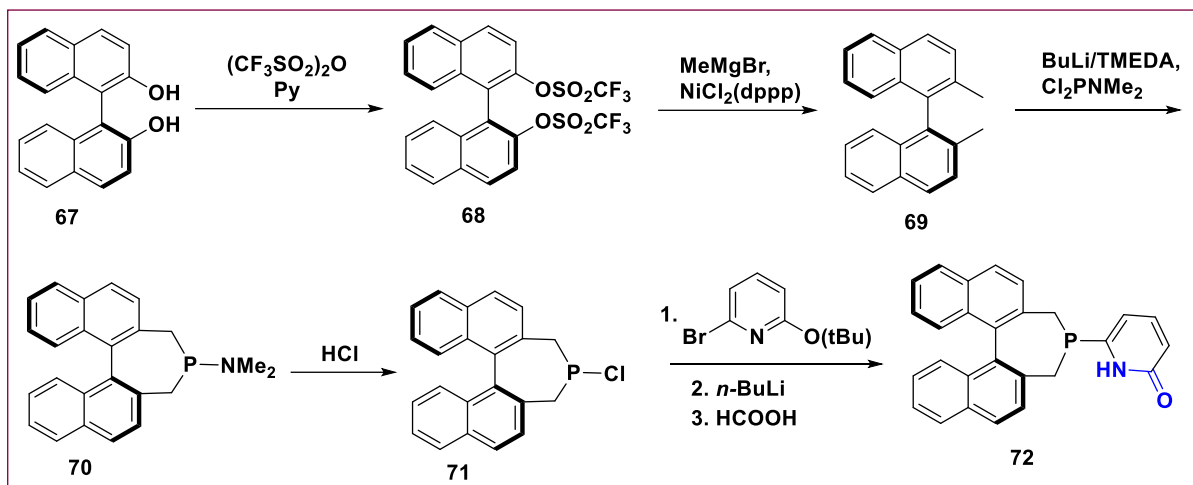
Scheme 9: Synthesis of axially chiral supramolecular phosphine ligands.

Synthesis of axially chiral supramolecular phosphines is rarely attempted. In 2007, Breit and Borner reported the synthesis of 6-((11bS)-3,5-dihydro-4H-dinaphtho[2,1-c:1',2'-e]phosphepin-4-yl)pyridin-2(1H)-one (**72**). Treatment of BINOL (**67**) with anhydrous sulphuric acid followed by methylation of (S)-[1,1'-binaphthalene]-2,2'-diyl bis(trifluoromethanesulfonate) (**68**) produced the intermediate (S)-2,2'-dimethyl-1,1'-binaphthalene (**69**). Lithiation of **69** followed by addition of dichloroaminophosphine led to

(11b*S*)-*N*,*N*-dimethyl-3,5-dihydro-4*H*-dinaphtho[2,1-c:1',2'-e]phosphepin-4-amine (**70**). Nucleophilic displacement with 2-Bromo substituted pyridine gave desired ligand **72** after acid hydrolysis (Scheme 9).[15,17]

1.4. P-stereogenic phosphine ligands

P-stereogenic phosphines are generally prepared using a stoichiometric amount of chiral auxiliaries or by the tedious resolution processes. It is, therefore, necessary to develop more efficient and practical methodologies for the synthesis of P-stereogenic phosphine ligands.

1.4.1. P-Stereogenic phosphine ligands

Asymmetric synthesis of P-stereogenic phosphines was recently developed using metal catalyzed asymmetric transformation such as asymmetric hydrophosphination.[20] Phosphines are known to invert very easily, losing chirality at ambient conditions. Hence, synthesis of P-stereogenic phosphines is a very challenging task. The first metal-catalyzed synthesis of P-stereogenic phosphine was reported by D. S. Glueck and co-worker.[21] Synthesis of P-stereogenic phosphine **74** was achieved by treating racemic methyl(2,4,6-triisopropylphenyl)phosphane **73** with phenyl iodide in presence of a Pd-catalyst. Initial enantioselectivity was very low. However, the highest ee of 78% was achieved at +4 °C, although at the cost of very low conversion (Scheme 10).
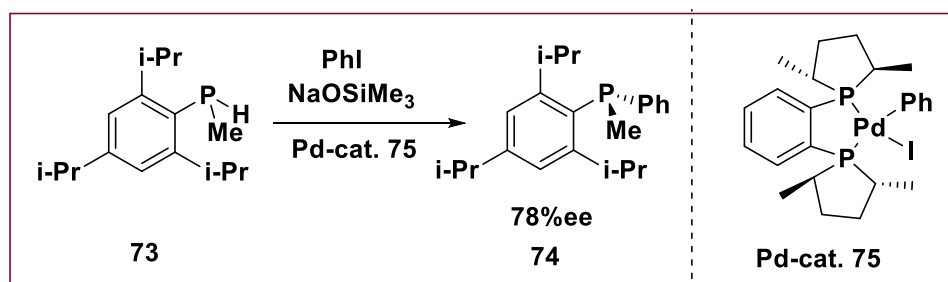
Scheme 10: Synthesis of P-stereogenic phosphine ligands.

In a catalytic strategy, Leung and co-worker recently reported hydrophosphination of enones, in presence of catalytic amount of a palladacycle. P-stereogenic phosphine **78** was synthesized from a racemic secondary phosphine with *α,β* unsaturated ketone in presence of chiral palladacycle to give P-stereogenic phosphine **78** with 82 % ee (Scheme 11).
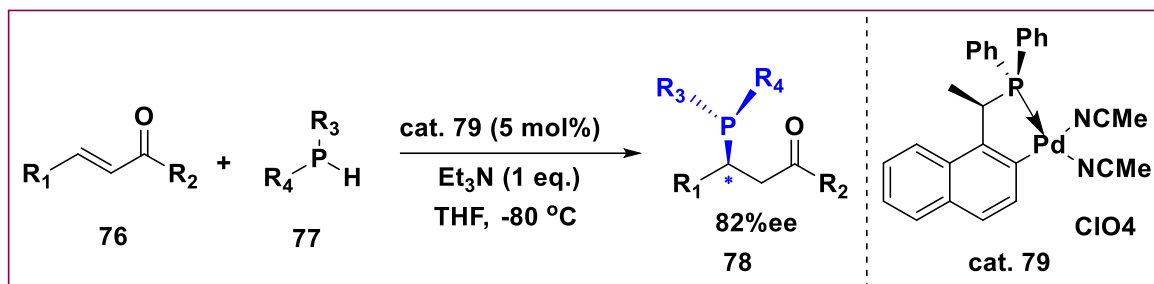
Scheme 11: Synthesis of P-stereogenic phosphine ligands.
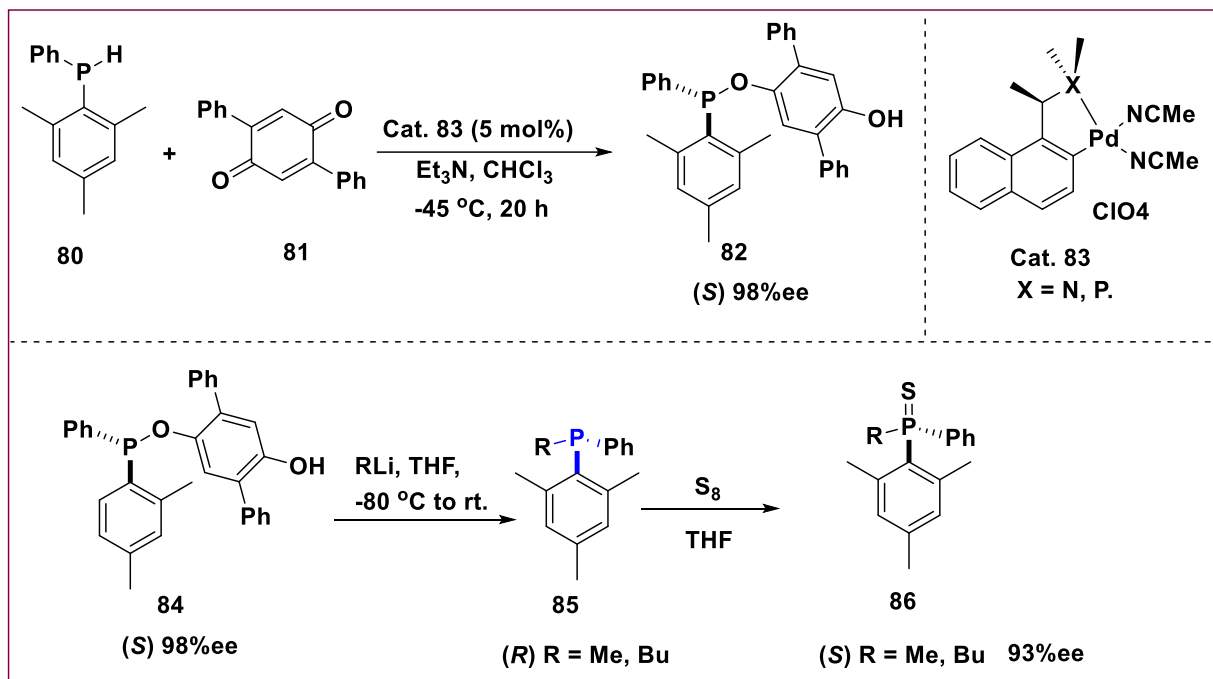
Scheme 12: Synthesis of P-stereogenic phosphine ligands.

In 2014 Tamio Hayashi and co-worker[22] reported synthesis of P-stereogenic phosphine from racemic secondary mistyle(phenyl)phosphine (**80**) with 2,5-Diphenyl-1,4-benzoquinone (**81**) in presence of chiral nitrogen or phosphorus ligated palladium catalyst to give 5'-((mesityl(phenyl)phosphanyl)oxy)-[1,1':4',1''-terphenyl]-2'-ol (**82**). The nucleophilic addition of butyl or methyl lithium on compound **82** followed by chiral inversion led to P-chiral sulfur protected product **86** (Scheme 12). Thus, mainly strategies have been developed for the synthesizing P-stereogenic phosphine ligands.[23] However, the highest enantioselective in a direct synthesis so far has been limited to only 82%.

1.4.2. P-stereogenic supramolecular phosphine ligands

As noted in the introduction, supramolecular phosphine ligands play a crucial role in homogeneous catalysis. However, there is hardly one example of P-stereogenic supramolecular phosphine ligand to date. The only example of P-stereogenic supramolecular phosphine was

reported by B. Breit and co-worker in 2006.[24] The synthesis of P-stereogenic phosphine ligand library was started with *N*-(6-bromopyridin-2-yl)pivalamide (**87**) and racemic chlorophosphine **88** in presence of *n*-BuLi at -100 ℃ to give racemic supramolecular phosphine compound **89**. Then the two isomers were separated by preparative HPLC. This P-stereogenic supramolecular phosphine ligand in combination with another supramolecular phosphonite ligand and rhodium metal were used in asymmetric hydrogenation reaction (Scheme 13).
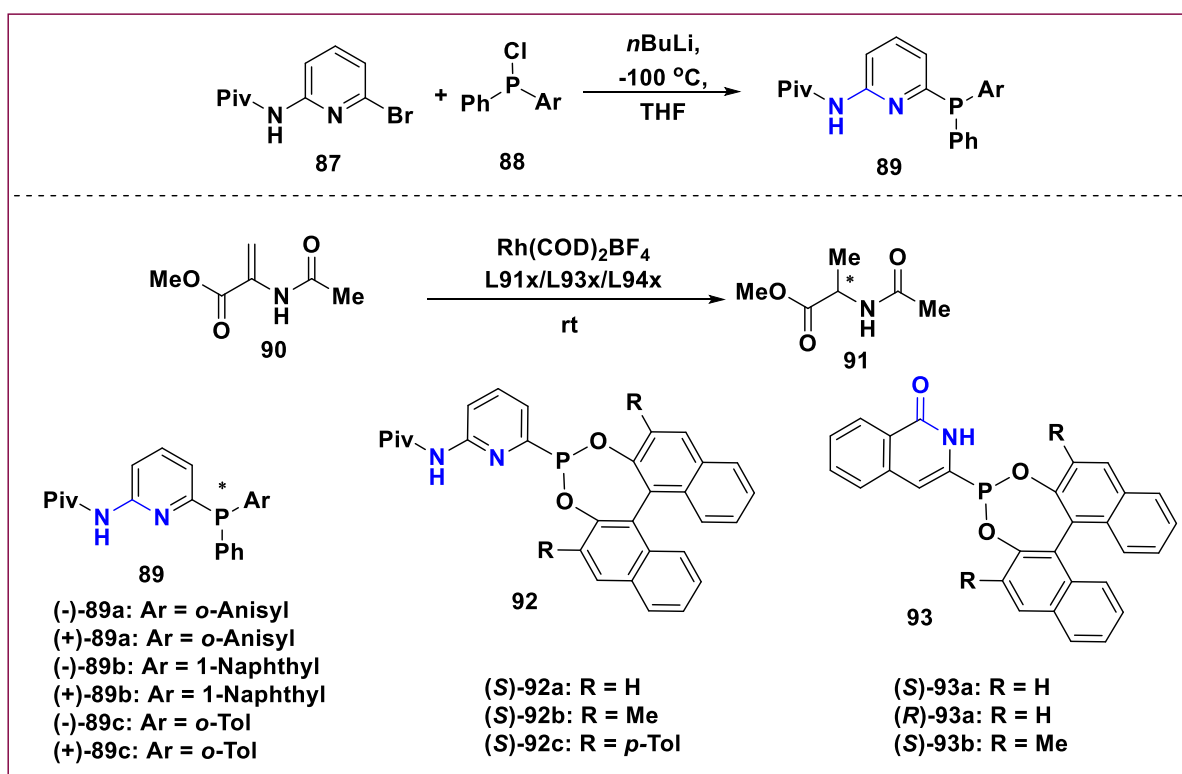
Scheme 13: Synthesis of P-stereogenic supramolecular phosphine ligands and their application in metal-catalyzed asymmetric hydrogenation.

1.5. Conclusion

This chapter summarizes recent developments in the synthesis of supramolecular phosphine ligands, in which the synthesis of chelating ligands has been simplified significantly. The concept is to use two structurally less complex monodentate ligands, which are held together through non-covalent attractive interactions and imitate a bidentate ligand at the catalytically active metal center. There are ligand-ligand interactions, which can be weak like van-der Waals, π-π stacking, charge-transfer, and dipole-dipole interactions to hydrogen bonding and even stronger coordinative interactions.[25] Irrespective of the strength of the interaction, the specific formation of heterodimeric ligands requires two different sets of monodentate ligands with complementary binding sites. This concept has been applied in the

generation of the first bidentate ligand libraries based on self-assembly, either through hydrogen bonding or coordinative interactions, and has resulted in the identification of excellent catalysts for regioselective of hydroformylation and asymmetric allylic alkylation. This field covers the principles of supramolecular phosphine chemistry, supramolecular chiral chemistry, supramolecular P-stereogenic chemistry, coordination chemistry, and catalysis for the generation of ligand libraries for homogeneous catalysis.

Thus far, only one example of P-stereogenic supramolecular phosphine has been reported. However, this P-stereogenic supramolecular phosphine was obtained from HPLC separation of a racemic P-stereogenic supramolecular phosphine. To the best of our knowledge, catalytic asymmetric synthesis of P-stereogenic supramolecular phosphine has not been reported. Therefore, new strategies to develop a catalytic process for the synthesis of P-stereogenic supramolecular phosphine will be highly desirable.

1.6. References

1.   Borner, A. Phosphorus Ligands in Asymmetric Catalysis; WILY-VCH Verlag GmbH and Co. KGaA, Weinheim 2008, 1.

2.   Breit, B. *Angew. Chem. Int. Ed.,* 2005, **44**, 6816-6825.

3.   M. Raynal, P. Ballester, A. Vidal-Ferran and P. W. N. M. van Leeuwen, *Chem. Soc. Rev.,* 2014, **43**, 1660-1733.

4.   B. Breit and W. Seiche, *J. Am. Chem. Soc.,* 2003, **125**, 6608-6609.

5.   W. Seiche, A. Schuschkowski and B. Breit, *Adv. Synth. Catal.,* 2005, **347**, 1488-1494.

6.   V. Agabekov, W. Seiche and B. Breit, *Chem. Sci.,* 2013, **4**, 2418-2422.

7.   U. Gellrich, W. Seiche, M. Keller and B. Breit, *Angew. Chem. Int. Ed.,* 2012, **51**, 11033-11038.

8.   J. Wieland, and B. Breit, *Nat. Chem.,* 2010, **2**, 832-837.

9.   B. Breit and W. Seiche, *Angew. Chem. Int. Ed.,* 2005, **44**, 1640-1643.

10.   F. Chevallier and B. Breit, *Angew. Chem. Int. Ed.,* 2006, **45**, 1599-1602.

11.   I. Usui, S. Schmidt, M. Keller and B. Breit, *Org. Lett*., 2008, **10**, 1207-1210.

12.   M. de Greef and B. Breit, *Angew. Chem. Int. Ed.,* **2009**, *48*, 551-554.

13.   T. Šmejkal and B. Breit, *Angew. Chem. Int. Ed*., 2008, **47**, 3946-3949.

14.   T. Šmejkal and B. Breit, *Angew. Chem. Int. Ed.,* 2008, **47**, 311-315.

15.   A. J. Sandee, A. M. van der Burg and J. N. H. Reek, *Chem. Commun*., 2007, 864-866.

16.   P. A. R. Breuil, F. W. Patureau and J. N. H. Reek, *Angew. Chem. Int. Ed*., 2009, **48**, 2162-2165.

17.   M. N. Birkholz, N. V. Dubrovina, H. Jiao, D. Michalik, J. Holz, R. Paciello, B. Breit and A. Börner, *Chem. Eur. J*., 2007, **13**, 5896-5907.

18.   W. Zeng, G. Chen, Y. Zhou and Y. X. Li, *J. Am. Chem. Soc.,* **2007**, *129*, 750-751.

19.   M. Raynal, F. Portier, P. W. N. M. van Leeuwen and L. Bouteiller, *J. Am. Chem. Soc.,* 2013, **135**, 17687-17690.

20.   D. S. Glueck, *Chem. Eur. J.,* 2008, **14***, 7108-7117.

21.   J. R. Moncarz, N. F. Laritcheva and D. S. Glueck, *J. Am. Chem. Soc.,* 2002, **124**, 13356-13357.

22.   M. Weis, C. Waloch, W. Seiche and B. Breit, *J. Am. Chem. Soc.,* 2006, **128**, 4188-4189.

23.   Y. Huang, S. A. Pullarkat, Y. Li and P. Leung, *Inorg. Chem.,* 2012, **51**, 2533- 2540.

24.   Y. Huang, Y. Li, P. Leung and T. Hayashi, *J. Am. Chem. Soc.,* 2014, **136**, 4865-4868.

25.   V. W. Yam, X. Lu and C. Ko, *Angew. Chem. Int. Ed.,* 2003, **42**, 3385-3388.

Chapter 2

Highly enantioselective Pd-catalyzed synthesis of P-stereogenic supramolecular phosphines

2.1. Abstract

Metal catalyzed asymmetric addition of a secondary phosphine to an aryl-halide is one of the most efficient and reliable approaches for the construction of enantiopure carbon-phosphorus bonds. An isolated Pd(II) complex (**2.5**) catalyzes the carbon-phosphorus coupling reaction between *o*-tolyl(phenyl)phosphine (**2.1a**) and 3-iodophenylurea (**2.2b**), which proceeds with an unprecedented enantiomeric excess (ee) of 97%. The generality of the strategy has been demonstrated by preparing a small library of a new class of P-stereogenic phosphines with in-built hydrogen bonding motif for the first time. The P-stereogenic phosphine self-assemble on metal template via deliberately installed hydrogen-bonding motifs and mimic the bidentate ligand coordination. Interestingly, when employed in asymmetric hydrogenation, the supramolecular phosphine [1-(3-(phenyl(o-tolyl)phosphanyl)phenyl)urea] (**2.6b**) produced corresponding hydrogenated product with the highest enantiomeric excess of 99% along with excellent conversion, demonstrating the potential of these enantio-enriched P-stereogenic supramolecular phosphines in asymmetric catalysis.
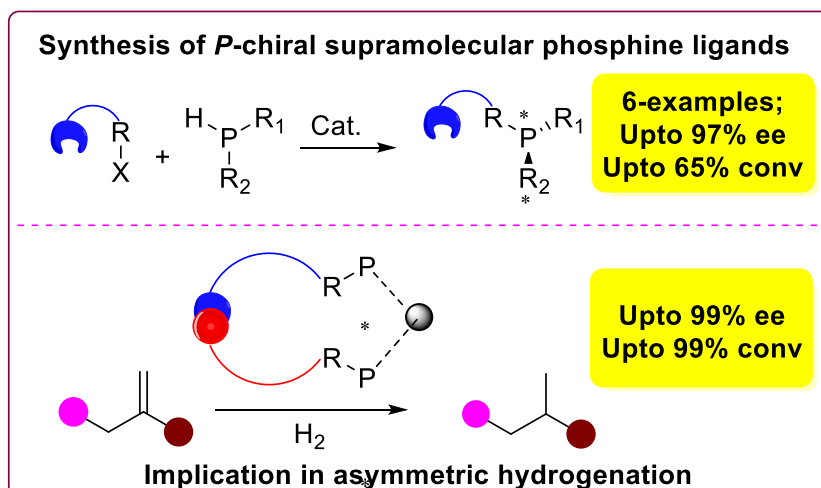
Synthesis of *P*-chiral supramolecular phosphine ligands

6-examples;
Upto 97% ee
Upto 65% conv

Upto 99% ee
Upto 99% conv

Implication in asymmetric hydrogenation

2.2. Introduction

Metal catalyzed asymmetric synthesis depends on chiral ligands, among which phosphines play a prominent role.[1] Although P-chiral phosphines were the first chiral ligands applied in homogeneous catalysis[2,3] they have been supplanted by phosphines having chirality on the backbone and the development of P-chiral phosphines has been incredibly slow.[4] This is most likely due to the difficulty of synthesis of P-chiral compounds which are traditionally generated with stoichiometric amount of chiral auxiliary or through resolution techniques.[5] A paradigm shift could be achieved if enantiopure P-stereogenic ligands could be catalytically prepared. Although highly desirable, the transition metal catalyzed synthesis of P-stereogenic ligands is still in its infancy,[6] and only a handful of ligands with enantioselectivities up to 88%[6c] have been synthesized using this concept. Furthermore, to the best of our knowledge there are no reports on the catalytic synthesis of enantiopure P-stereogenic ligands equipped with additional supramolecular bonding motif.

In spite of the increasing knowledge of homogeneous catalysis, current discovery and designing of an efficient and selective catalyst still relies on tedious and time consuming, trial and error methodology.[7] To shorten the time needed to identify a suitable catalyst, combinatorial screening techniques have been devised. However, these techniques still make use of covalently synthesized ligands. To address this synthetic bottleneck, strategies based on the formation of bidentate ligands held together by non-covalent interactions have recently emerged (Fig. 2.1).[8] Thus, catalytic synthesis of P-stereogenic supramolecular phosphines will significantly increase the chemical space within which an optimal ligand set can be identified. However, currently there is no precedent in literature on catalytic synthesis of enantiopure P-stereogenic supramolecular phosphines, although supramolecular phosphines (C-chiral or achiral) have found wide range of applications in industrially important transformations such as hydrogenation,[9] hydroformylation,[10] hydrocyanation[11] and hydrosilylation.[12]
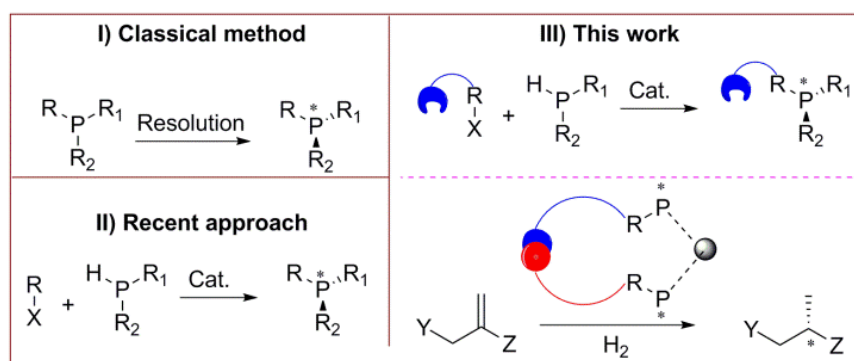
Figure 2.1: Synthesis of p-stereogenic phosphines; I) Classical method, II) Recent approach and, III) This work.

Here in we disclose the first example of a highly enantio-selective C-P coupling (asymmetric phosphination) reaction that generates enantio-enriched P-stereogenic supramolecular phosphine. The generality of the strategy is demonstrated by preparing a small library of enantio-enriched P-stereogenic supramolecular phosphines. Furthermore, self-assembly of these P-stereogenic supramolecular phosphines and implication in asymmetric hydrogenation is reported.

P-stereogenic phosphines have attracted significant attention in recent years and various synthetic methodologies have been deployed in the last decade.[13] We anticipated that a palladium catalyzed C-P coupling reaction between a racemic phosphine and aryl-halide equipped with urea would produce the desired P-stereogenic supramolecular phosphine. Figure 2.1, depicts, I) classical synthesis of P-chiral phosphines, II) recent catalytic approach and, III) our strategy.

2.3. Results and discussion
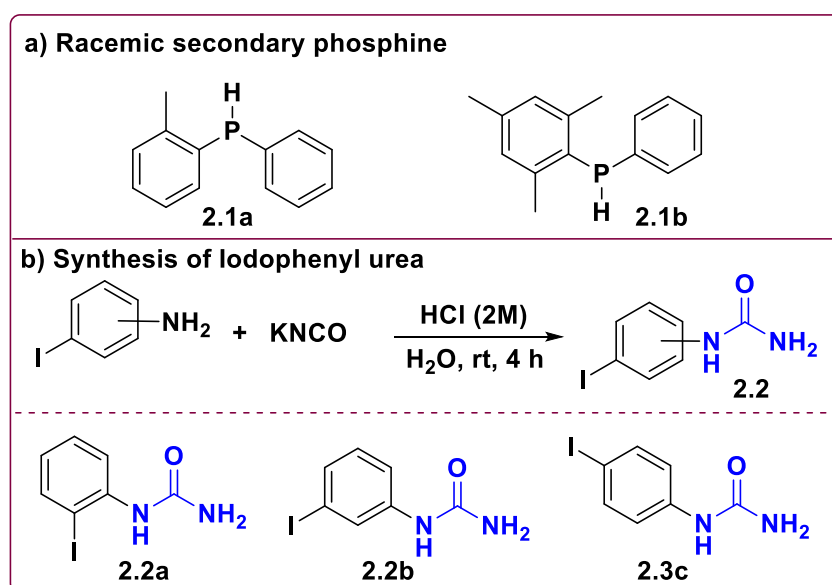
Scheme 2.1: a) Racemic secondary phosphine, b) Synthesis of iodophenyl urea **2.2**.

In our pursuit to realize the synthesis of enantio-enriched P-stereogenic supramolecular phosphine, we set out to prepare the three components of the phosphination reaction. Phenyl(o-tolyl)phosphine (**2.1a**) and mesityl(phenyl)phosphine (**2.1b**) were prepared using literature protocols (Scheme. 2.1, top).[14] Whereas, the hydrogen bonding motifs, 2-iodophenylurea (**2.2a**), 3-iodophenylurea (**2.2b**) and, 4-iodophenylurea (**2.2c**), were synthesized using modified literature methods (Scheme. 2.1, bottom).[15] The third component, palladium catalyst, was prepared in a two-step synthetic protocol. A stoichiometric reaction between 3-iodophenylurea

(**2.2b**), [Pd(dba)$_2$] and tetramethylethylenediamine (TMEDA) produced the anticipated pre-catalyst [Pd(tmeda)(3-phenylurea)(I)] (**2.3**) in good yield (63%) (Scheme 2.2). The existence of **2.3** was unambiguously ascertained using a combination of analytical and spectroscopic methods. Electro-Spray Ionization Mass-Spectroscopic (ESI-MS) analysis revealed a pseudo-molecular ion peak at m/z = 357.09 [M-I]$^+$ confirming the presence of **2.3** (Fig. 2.3). The spectroscopic results were further corroborated by single crystal X-ray diffraction. Complex **2.3** crystallizes in monoclinic crystal system with P$_1$ space group (Table 2.1). The geometry around palladium is distorted square-planar with regular bond angles and bond lengths.
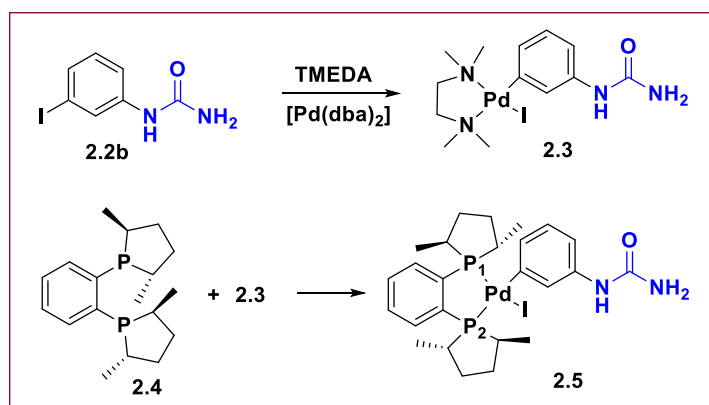
Scheme 2.2: Synthesis of palladium complex **2.5**.
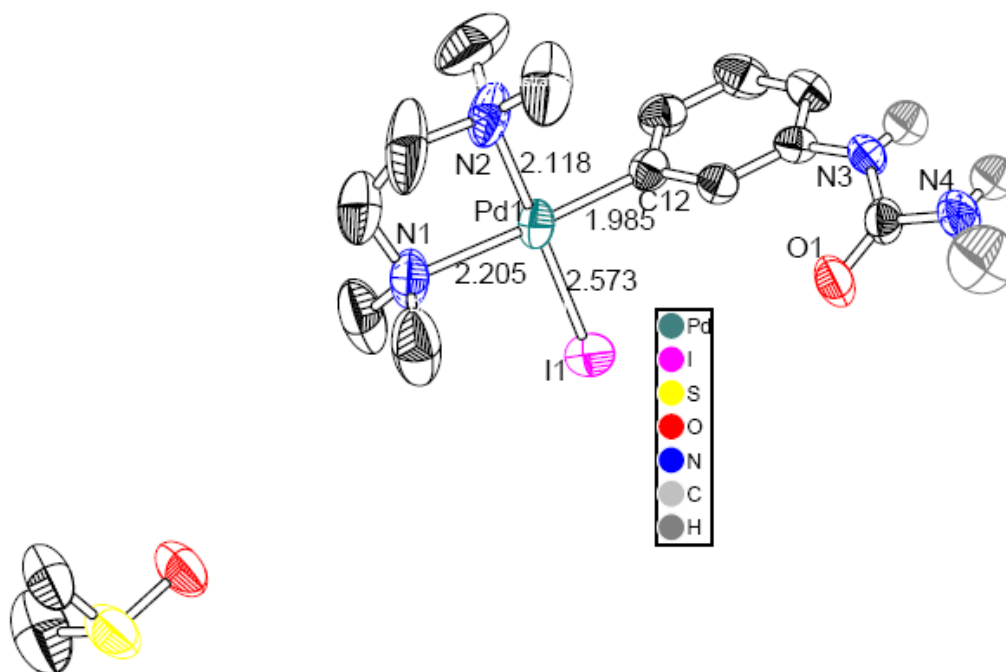
Figure 2.2: Molecular structure of complex **2.3**; solvent molecules (except DMSO) and *H*-atoms (except *N-H*) are omitted for clarity; thermal ellipsoids are drawn at 50% probability level.

Table 2.1: Crystal data and structural refinement parameters for complex **2.3** (**CCDC: 1046371**)

Formula sum	C$_{13}$ H$_{23}$ I N$_4$ O Pd-DMSO

Formula weight	562.78 g/mol
Crystal system	monoclinic
Space-group	P1 21/c 1 (14)
Cell parameters	a=15.7782(4) Å b=8.3688(2) Å c=17.7446(4) Å
	β=110.066(2)°
Cell ratio	a/b=1.8854 b/c=0.4716 c/a=1.1246
Cell volume	2200.85(9) Å^3
Z	4
Calc. density	1.6983 g/cm^3
RAll	0.0657
Pearson code	*mP212*

A notable difference is a short N_2-Pd bond of 2.118 Å; compared to N_1-Pd bond distance of 2.205 Å. This difference can be attributed to the *trans*-effect imparted by iodide (Fig. 2.2).[16] Addition of (+)-1,2-Bis[(2*S*,5*S*)-2,5-dimethylpholano]benzene ((*S*,*S*)-Me-DuPHOS) to complex **2.3** in acetonitrile (CH_3CN) at room temperature and tracking the reaction progress by ^{31}P NMR indicated completion of the reaction within 2 hours.[17] After 2 hours, volatiles were evaporated under reduced pressure to obtain gray colored residue, which after *n*-hexane washing produced pure complex **2.5** (Scheme 2.2). ^{31}P NMR of the isolated compound displayed a doublet-of-doublet due to the magnetically non-equivalent phosphorus centers. The doublet at 69.4 ($^2J_{P1P2}$ = 25 Hz) can be assigned to P_1 and the second doublet at 65.1 ppm ($^2J_{P1P2}$ = 25 Hz) can be readily assigned to P_2 (Scheme 2.2, Fig. 2.4). ESI-MS analysis revealed a pseudo-molecular ion peak at m/z = 547.12 [M-I]$^+$ confirming the presence of anticipated complex **2.5** (Fig. 2.5).[15,18] After having established the existence of complex **2.5**; we set out to evaluate the performance of **2.5** in catalytic asymmetric C-P coupling (phosphination) reaction. A general phosphination reaction leading to P-stereogenic supramolecular phosphine is depicted in Scheme 2.3 and Table 2.2 summarizes the most important findings. THF was found to be the solvent of choice as it provided optimal solubility for all the reaction components.
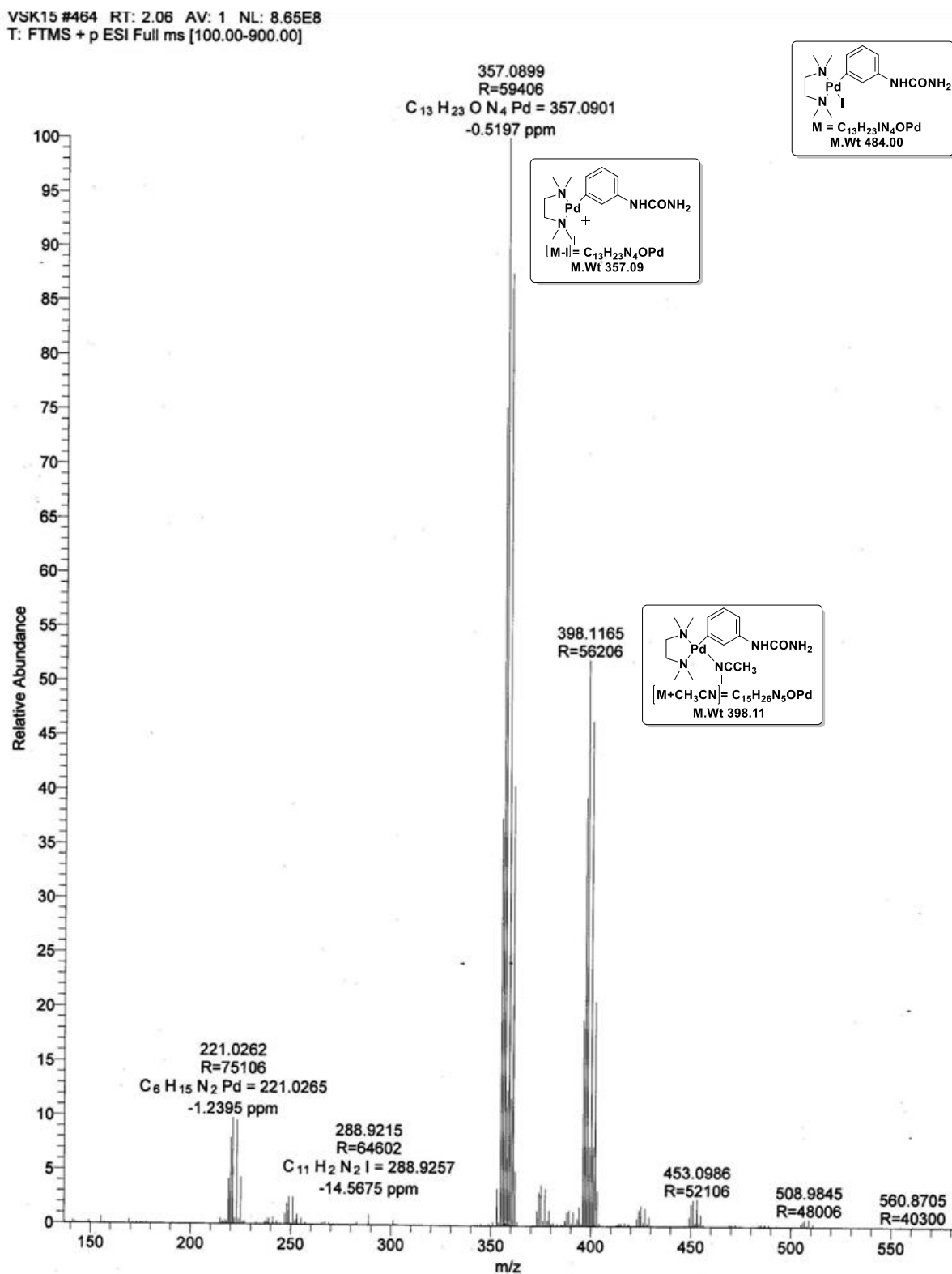
Figure 2.3: ESI-MS (+ve mode) spectrum of complex **2.3**.
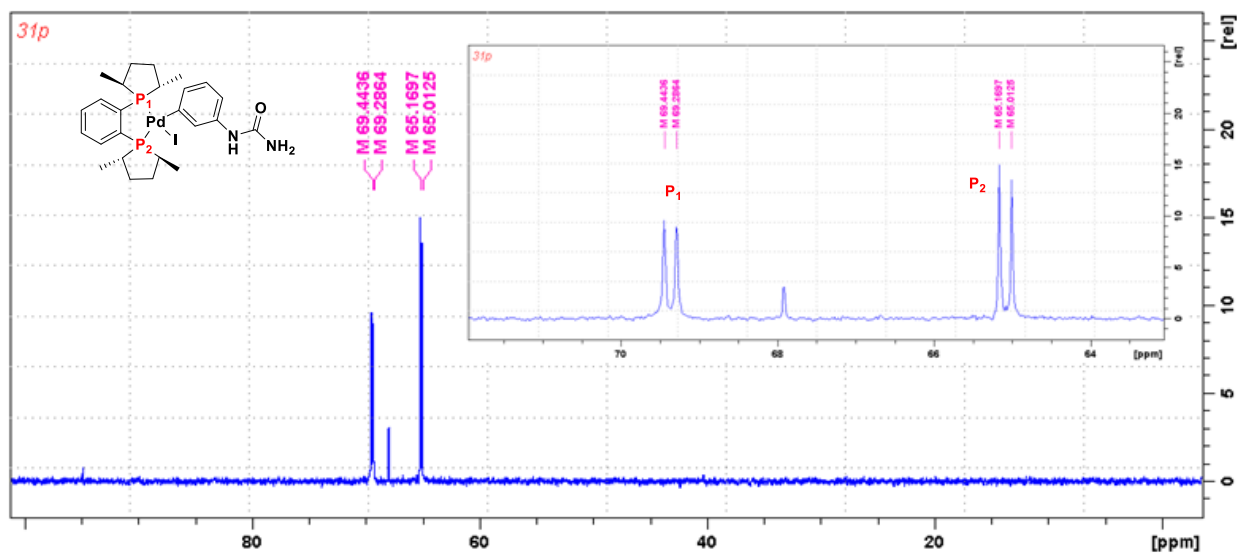
Figure 2.4: ^{31}P NMR spectrum of complex **2.5** in CD$_3$CN.
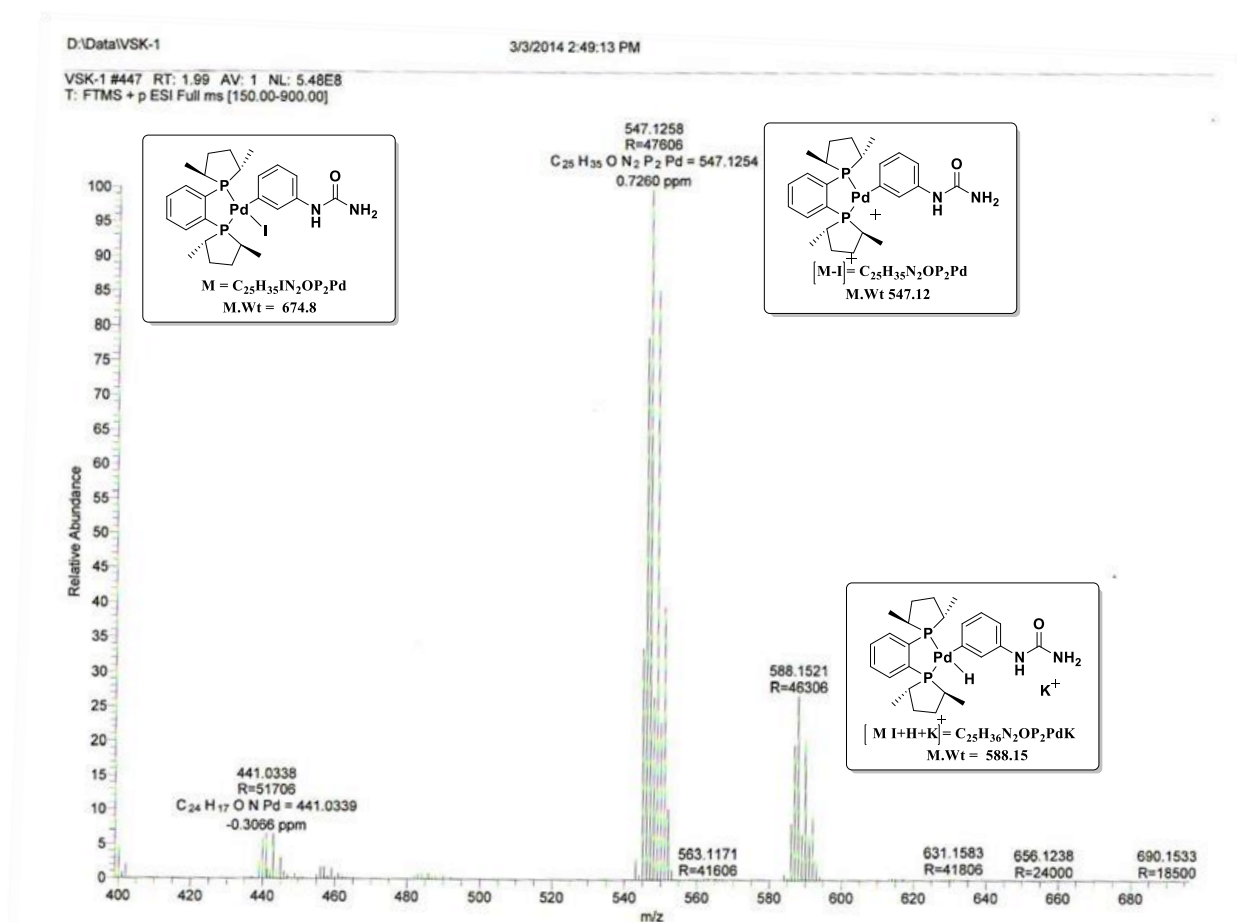
Figure 2.5: ESI-MS (+ve) spectrum of complex **2.5** in acetonitrile.
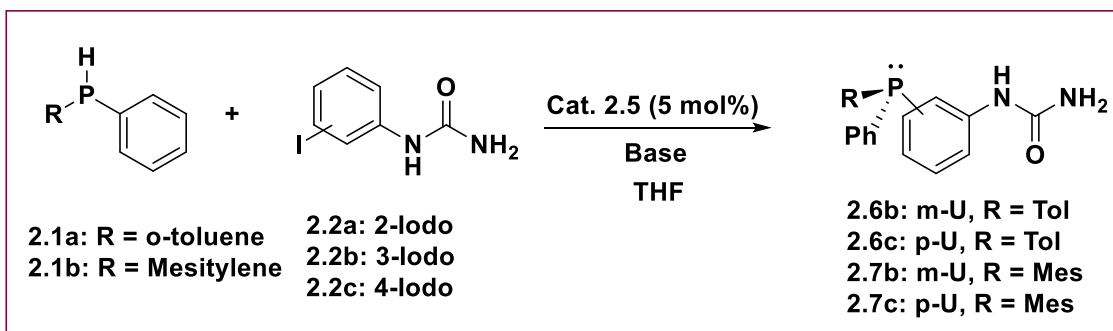
Scheme 2.3: Catalytic synthesis of enantio-enriched P-stereogenic supramolecular phosphine (**2.6a-c** and **2.7a-c**).

Table 2.2: Palladium catalyzed asymmetric phosphination of racemic phosphines with phenyl-urea.[a]

Run	Product[b]	Temp (°C)	Time (h)	Conv.%[c]	% ee[d]
1	2.6b (1)	RT	24	~8	ND
2	2.6b (2)	RT	24	31	ND
3	2.6b (3)	RT	24	>99	00
4	2.6b (3)	20	144	22	46
5	2.6b (3)	0	72	7	83
6[e]	2.6b (3)	0	360	>99	79(-)
7[e]	2.6b (3)	-5[f]	168	65	97(-)
8	2.6c (3)	RT	60	>99	4
9	2.6c (3)	0	432	50	11
10	2.6c (3)	-5[e,f]	144	25	40
11	2.7b (3)	RT	64	>99	ND
12	2.7b (3)	0	152	42	11
13	2.7b (3)	-5[e,f]	168	42	11
14	2.7c (3)	0	168	25	11
15	2.7c (3)	-5[e,f]	168	38	11

[a] Conditions: Catalyst = 0.005 mmol, **2.1a** = 0.1 mmol, **2.2a** = 0.1 mmol, total 1 ml THF, RT = room temperature; [b] Equivalent of NaOSiMe3; [c] Determined by ^{31}P NMR; [d] Determined by chiral HPLC after protection of **2.6/2.7** by sulfur; [e] 15 mol% catalyst loading; [f] +/-5°C; ND: Not determined.
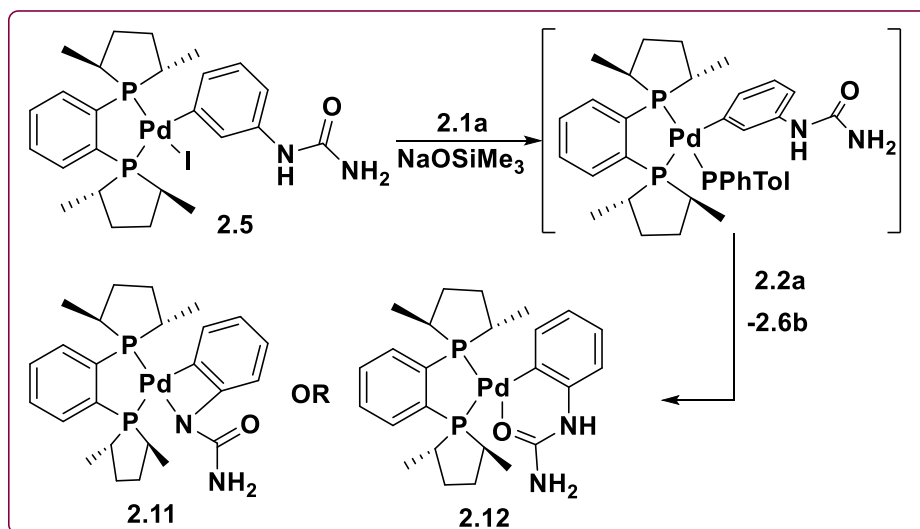
Scheme 2.4: Proposed formation of N-H addition (**2.11**) or C=O chelation (**2.12**) products.

Surprisingly, complex **2.5** failed to catalyze the reaction between **2.1a** and **2.2a**.[19] In our pursuit to understand the failure, we performed stoichiometric reaction; which suggested C=O chelation and suppression of C-P coupling (Scheme 2.4). Phosphination of **2.1a** with **2.2a** was attempted, however without any success. All our attempts to catalyze this reaction failed. In our pursuit to understand the failures, we performed stoichiometric reaction between **2.5**, **2.1a** and **2.2a**. The progress of the reaction was monitored using ^{31}P NMR. The time resolved spectra is depicted in Figure 2.6, which displayed only oxidation product of **2.1a** and **2.6b**. The starting urea **2.2a** can potentially generate either C=O chelation or N-H addition (Fig. 2.7) products **2.11** or **2.12** respectively in presence of a base. Formation of compound **2.11** is most unlikely as 4-membered palladium-rings are highly strained and mostly unstable. Therefore, it is most likely that compound **2.12** is generated under these conditions. Indeed, FT-IR Fourier-transform infrared spectroscopy spectrum of the above reaction mixture (after extraction) displayed a C=O stretching band at 1598 cm^{-1} (Fig. 2.7). A similar C=O band is reported for a cationic urea palladacycle.[27] Formation of such intermediate most likely blocks the vacant site on the metal and suppresses the desired phosphination reaction. These species were observed and further identification by ^{31}P NMR and IR. Based on these investigations we anticipated that installing the urea group away from the metal center might overcome C=O chelation and might catalyze the phosphination.
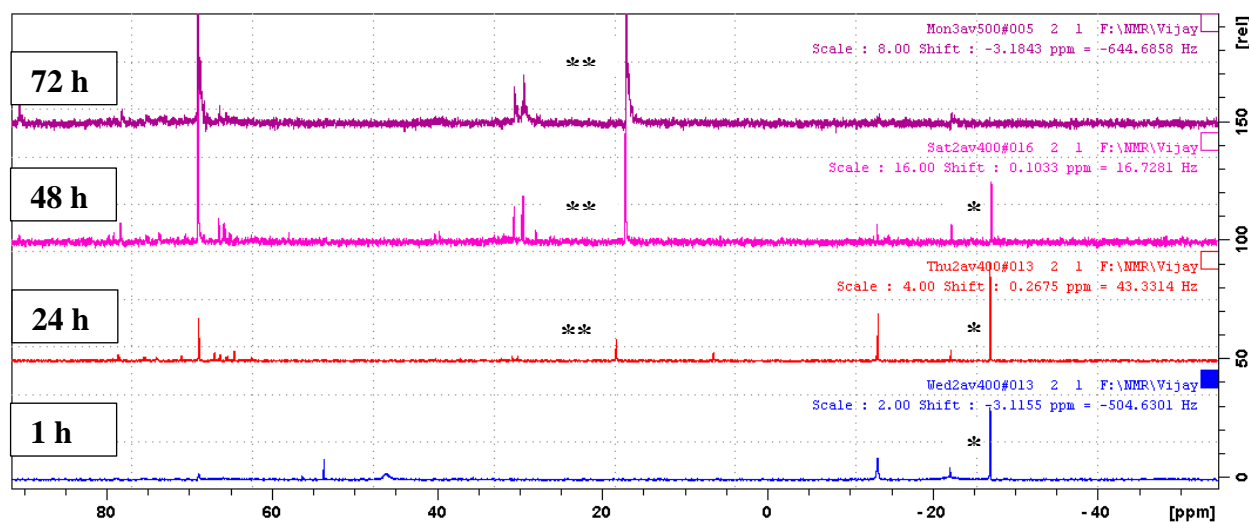
Figure 2.6: ^{31}P NMR spectra of a stoichiometric reaction between **2.5**, **2.1a** and **2.2a** (* = 2.1a, **= 2.1a oxidized).
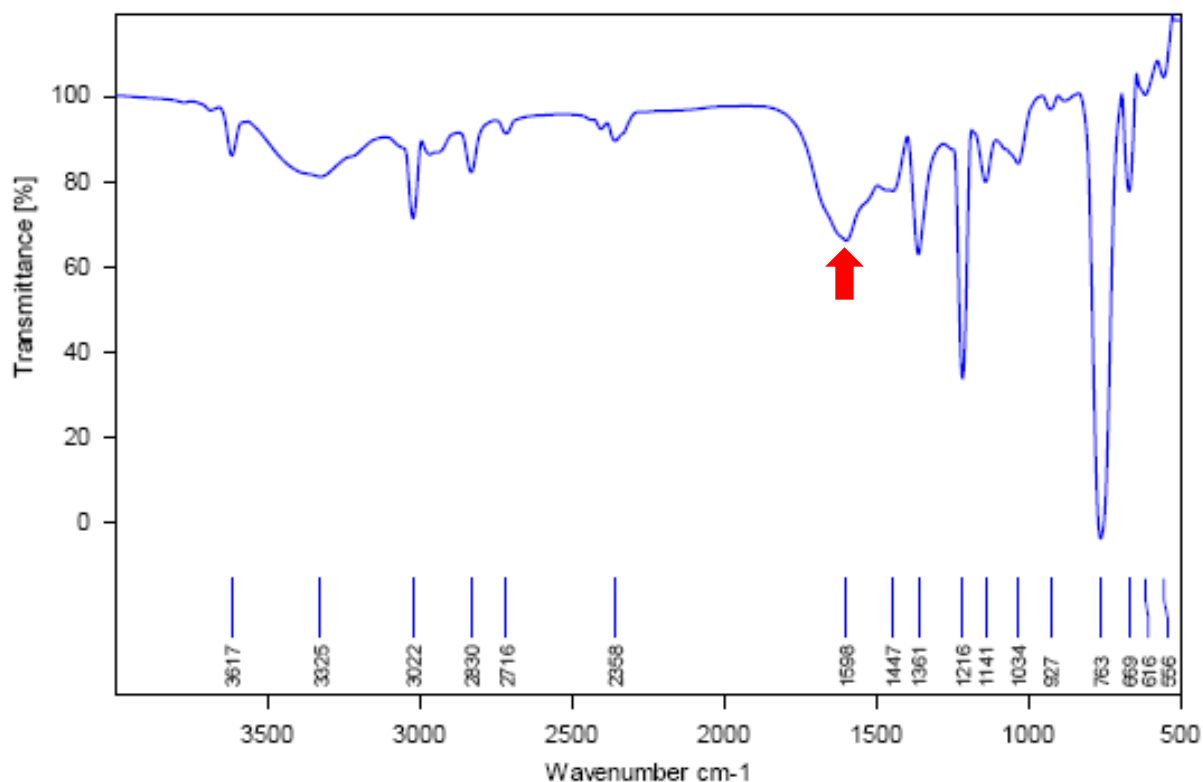
Figure 2.7: IR spectrum of a stoichiometric reaction between **2.5**, **2.1a** and **2.2a** after extracting **2.6b**.

Indeed, initial catalyst optimization studies using **2.2b** indicated completion of the reaction within 12 hours. The effect of catalyst loading on conversion was investigated and the optimal catalyst loading was found to be 5 mol%. Effect of various bases was investigated and sodium trimethylsilanolate (NaOSiMe$_3$) outperformed the other common bases (Table 2.3). Increasing the amount of base from 1-3 equivalents progressively led to better conversions (Table 2.1, run 1 to 3);[20] but only racemic product was observed. Decreasing the reaction temperature pointed at a much better stereo-control. Performing the reaction at 20 °C resulted into a moderate enantiomeric excess of 46% with a lower conversion of 22%. Decreasing the temperature further to 0 °C resulted in 83% enantiomeric excess (run 5). Prolonged reaction

Table 2.3: Asymmetric phosphination of racemic phenyl(o-tolyl)phosphine (**2.1a**) with 3-iodophenylurea (**2.2b**).[a]

Ex. No.	Base	Equivalent (mmol)	Condition	Time (hr)	Conversion (%)[b]	ee (%)[c]
1	NEt$_3$	3 (0.3)	RT	24	>99	-
2	NaOSiMe$_3$	3 (0.3)	RT	24	>99	0.0
3	NaOSiMe$_3$	3 (0.3)	20°C	144	22	46
4	NaOSiMe$_3$	3 (0.3)	0°C	72	7	83
5	NaOSiMe$_3$	3 (0.3)	0°C[d]	360	>99	79

| 6 | NaOSiMe$_3$ | 3 (0.3) | -5°C^e | 168 | 65 | 97 |

a: Catalyst (**2.5**)-5 mol%; THF- 0.5-1 ml, phenyl(o-tolyl)phosphine (**2.1a**): 0.1 mmol, 3-iodophenylurea (**2.2b**): 0.1 mmol.; RT = room temperature. b: Conversion was determined by ^{31}P NMR spectroscopy. C: Enantiomeric excess was determined after sulfur protection by using chiral HPLC. d: 15 mol% catalyst loading; e: 15 mol% catalyst loading and, the temperature variation was +/-5°C.

time at 15 mol% catalyst loading increased the conversion to **2.6b** (>99) without significantly affect the selectivity (run 6). To our delight, performing the reaction at -5 °C produced **2.6b** with an unprecedented enantiomeric excess of 97% (run 7) along with significant (65%) conversion. To the best of our knowledge, the enantiomeric excess of 97% reported for **2.6b** is the highest ever reported in any asymmetric phosphination/hydrophosphination reaction. The **2.6** and **2.7** were protected by sulfur (S$_8$) powder at reaction temperature to avoid the phosphine inversion during enantiomeric excess measurement (Scheme 2.5). The enantiomeric excess was measured by High Pressure Liquid Chromatography (HPLC) using Daicel Chiralpak-IA and Daicel Chiralpak-IB column. The compound **2.8b** and **2.8c** were resolved in HPLC at Hexane:2-PrOH (90:10) solvent combination on Daicel Chiralpak-IA column (Fig 2.10 and 2.13 respectively). Compound **2.9b** was resolved in HPLC at Hexane:2-PrOH (90:10) solvent combination on Daicel Chiralpak-IB column (Fig.2.15). Compound **2.9c** was resolved in HPLC at Hexane:EtOH (93:07) solvent combination on Daicel Chiralpak-IA column (Fig. 2.17).
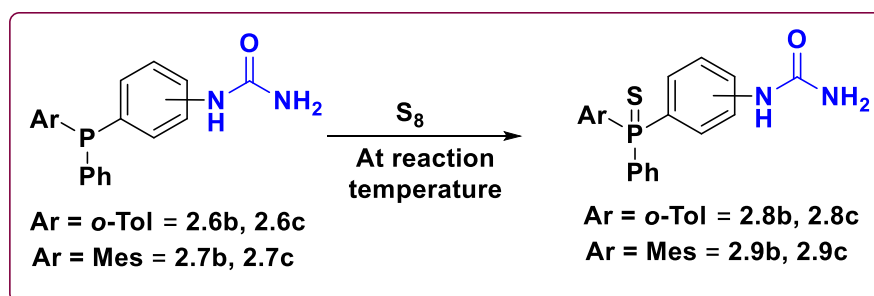
Scheme 2.5: Protection of p-stereogenic supramolecular phosphine (**2.6a-c** and **2.7a-c**) by Sulfur (S$_8$).

Motivated by the excellent performance of catalyst **2.5**, we further expanded the substrate scope and phosphination of **2.1a** with 4-iodophenyurea (**2.2c**) was attempted. Only 40% ee could be obtained using **2.5**, even after extensive screening of various reaction parameters (run 8 to 10). We then explored the scope of phosphine and performance of **2.5** in the phosphination of **2.2b** and **2.2c** with mesitylphenyphosphine (**2.1b**) was evaluated. The mesitylphenyphosphine (**2.1b**) smoothly reacts with 3-iodophenylurea (**2.2b**) under the optimized conditions to produce the corresponding phosphines in good yields and decent enantiomeric excess (4-11%) (run 11 to 13). Similar reactivity was witnessed with 4-iodophenylurea (**2.2c**) and decent ee's (11%) were recorded (run 15). In combination of **2.1b** with **2.2b** and **2.2c** less enantiomeric excess was observed (Table 2.4).

Table 2.4: Asymmetric phosphination of racemic phenyl(mesityl)phosphine (**2.1b**) with 3-iodophenylurea (**2.2b**).[a]

Ex. No.	Base	Equivalent (mmol)	Temp (°C)	Time (hr.)	Conversion (%)[b]	ee (%)[c]
1	NEt₃	1 (0.1)	RT	192	5.3	-
2	NEt₃	3 (0.3)	RT	192	75	-
3	NEt₃	5 (0.5)	RT	192	83	-
4	NaOSiMe₃	3 (0.3)	RT	60	>99	-
5	NaOSiMe₃	3 (0.3)	0	152	25	11
6 [d]	NaOSiMe₃	3 (0.3)	-5	168	38	11

a: Catalyst (**2.5**)-5 mol%; THF- 0.5-1 ml, phenyl(mesityl)phosphine (**2.1b**): 0.1 mmol, 3-iodophenylurea (**2.2b**): 0.1 mmol. RT = room temperature. b: Conversion was determined by ³¹P NMR spectroscopy. C: Enantiomeric excess was determined by using chiral HPLC. d: 15 mol% catalyst loading.

In our quest to understand the mechanism of C-P coupling reaction, we investigated the reactivity of catalyst **2.5** in a stoichiometric NMR tube reaction. Complex **2.5** was dissolved in THF-d₈ and 1 equiv. of **2.1a** (Scheme 2.6) was added to the NMR tube. Apart from the Pd-Me-DuPHOS resonances, the ³¹P NMR spectrum of this mixture displayed a broad singlet at -49.4 ppm that can be easily assigned to free phosphine **2.1a**. (Fig. 2.8-1 blue color spectrum). After addition of stiometric base (NaOSiMe₃), an immediate change was apparent, the free phosphine disappeared and a new resonance at -23.9 ppm was observed (Fig. 2.8-2 red-color spectrum). This new signal most likely originates from an intermediate species **(ii)** (Scheme 2.6). Simultaneously, a clear shift in the ³¹P resonance of the (*S,S*)-Me-DuPHOS phosphorus atoms was spotted. Thus, the Pd-complex signals at 65.9 & 61.9 ppm were shifted to 52.3 ppm and 44.6 ppm. Although presence of intermediate **(i)** could not be detected, broad NMR signals suggest an equilibrium process (Scheme 2.6). The changes in the spectrum were recorded after 20, 40 minutes (Fig. 2.8-3 & 4; pink, and violet-color spectrum). After addition of base the broad resonance at -23.9 ppm disappeared and a sharp product (**2.6b**) resonance was detected after 40 minutes. Similar changes were recorded in case of (*S,S*)-Me-DuPHOS phosphorus atoms. After 40 minutes **2.2b** was added to above NMR tube and spectrum was recorded at an interval of 0 and 72 hours. The peak at 44.6 ppm disappeared and complex **2.5** peaks reappeared (Fig. 2.8-5; yellow color spectrum). Thus, room temperature investigations indicated formation of **(ii)** (only limited information could be obtained) but no information could be obtained about existence of intermediate **(i)** (Scheme 2.6).
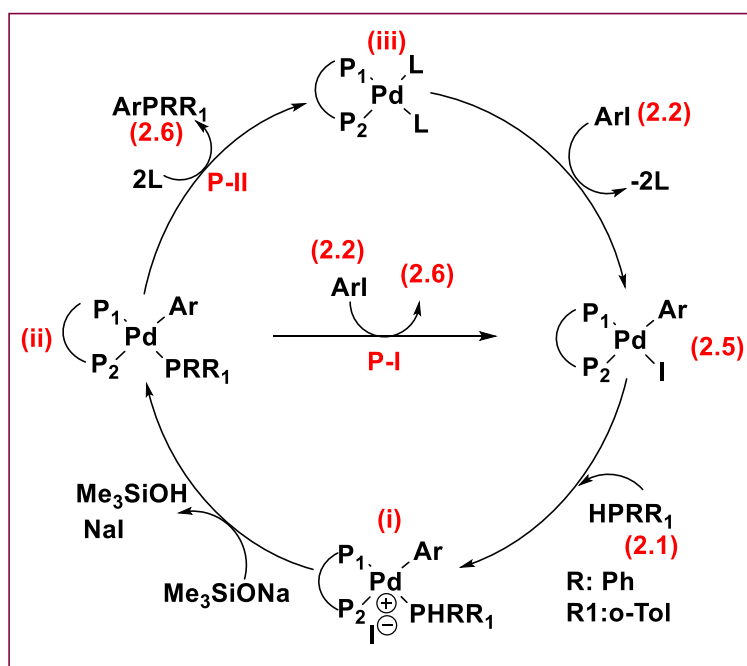
Scheme 2.6: Proposed mechanism for the phosphination reaction.
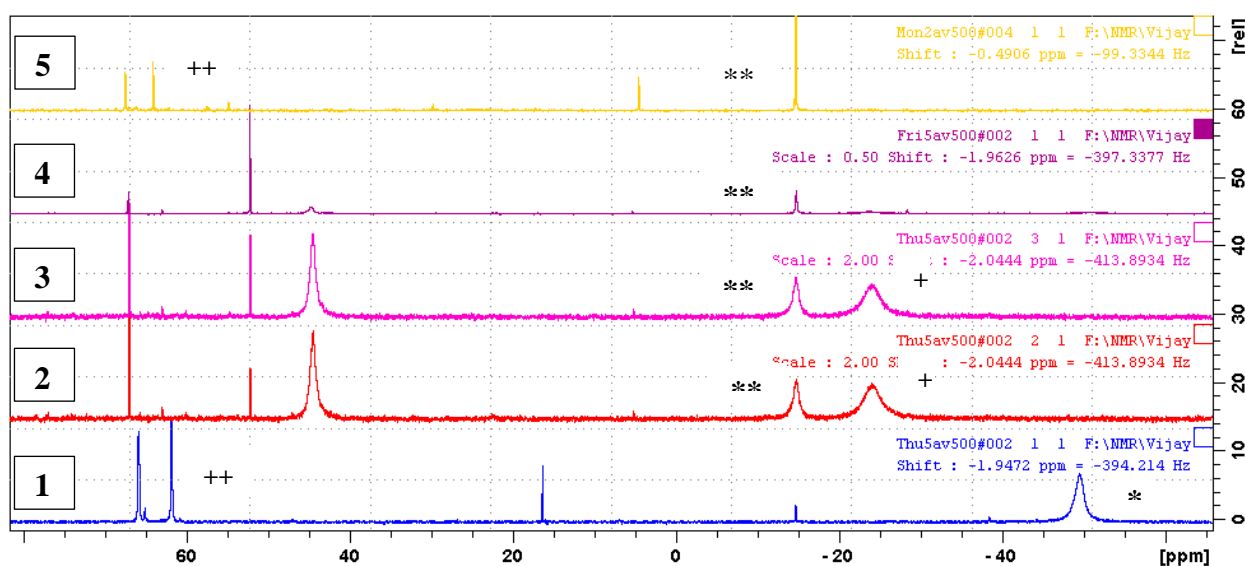
Figure 2.8: Stacked ^{31}P NMR spectra of *in-situ* generated intermediates in a stoichiometric C-P coupling reaction (1: before addition of NaOSiMe$_3$, 2: immediately after addition of base, 3&4: after 20 and 40 minutes of addition of base, 5: after 72 hours of addition of **2.2b**) (* = **2.1a**, + = Intermediate, ** = **2.6b**, ++ = **2.5**).

In our quest to pin-down the underlying intermediates, low temperature NMR experiments were performed and Figure 2.9 depicts the stacked spectra. A room temperature NMR of a mixture of tolylphenylphosphine **2.1a** (3 mg, 0.0148 mmol) and palladium complex**2.5** (10 mg, 0.0148 mmol) displayed a broad ^{31}P NMR resonance at -49.5 ppm (free phosphine **2.1a**) (Fig. 2.9-1, bottom). Cooling down the same NMR tube to -40 °C revealed broad doublet centered at -22.2 ppm with a $^2J_{\text{P-P}}$ = 353 Hz (Fig. 2.9-3; pink color spectrum).
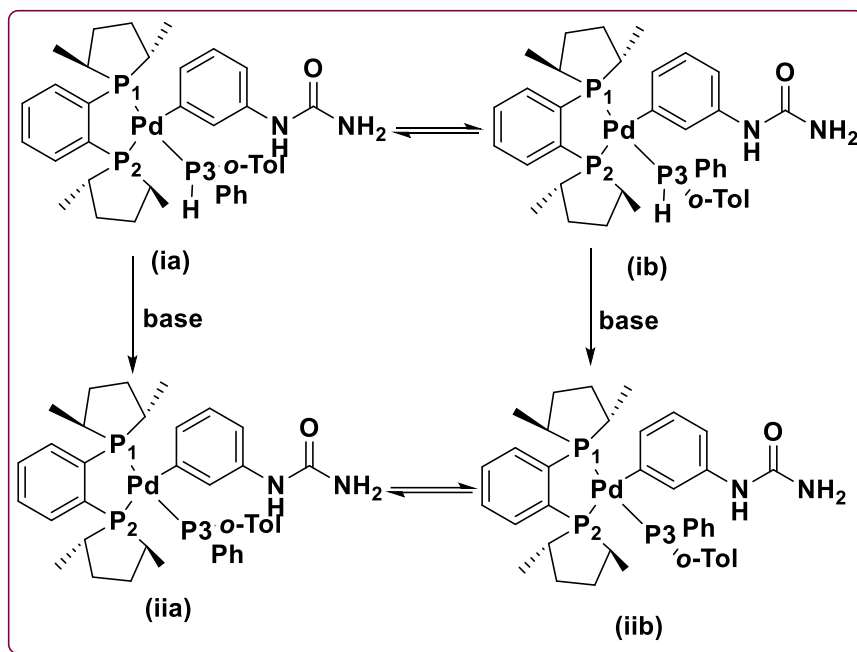
Scheme 2.7: The equilibrium between different isomers of (**i**) and (**ii**).

We tentatively assign this resonance to species (**i**) which displayed an equilibrium between (**ia**) and (**ib**) at low temperature (Scheme 2.7). Similar observations have been previously reported by Glueck et al.[6a] In a separate NMR tube, the THF-d_8 solution of **2.1a** (3 mg, 0.0148 mmol) and **2.5** (10 mg, 0.0148 mmol) was frozen to -195 °C (LN$_2$) and base (NaOSiMe$_3$, 0.044 mmol) was added to the mixture. The NMR tube was quickly transferred to the spectrometer and was slowly warmed to -40 °C (from -195 °C), and ^{31}P NMR spectrum was recorded (Fig. 2.9-4; violet color spectrum). The low temperature spectrum revealed two doublet-of-doublets at -18.3 (dd, $^2J_{\text{P-P}}$ = 40 Hz, 106 Hz) and -26.1 ppm (dd, $^2J_{\text{P-P}}$ = 56 Hz, 117 Hz) that can be assigned to the phosphido-intermediate (**ii**) which again displays an equilibrium between isomers (**iia**) and (**iib**) (Scheme 2.7). It is most likely that the two isomers exchange very fast on the NMR time scale at room temperature and only a coalesced average broad signal was detected at room temperature (Fig. 2.9-2; red color spectrum). Thus, the two intermediates (**i**) and (**ii**) could be detected at low temperature and these NMR observations support the proposed mechanism in Scheme 2.6. The NMR findings are summarized in Table 2.5. These resonances can be attributed to the phosphido-Pd intermediate (**ii**) (**iia** $\rightleftharpoons$ **iib**; scheme 2.7). These spectroscopic evidences suggest that path **P-I** is more likely than **P-II** (Scheme 2.6).[22]
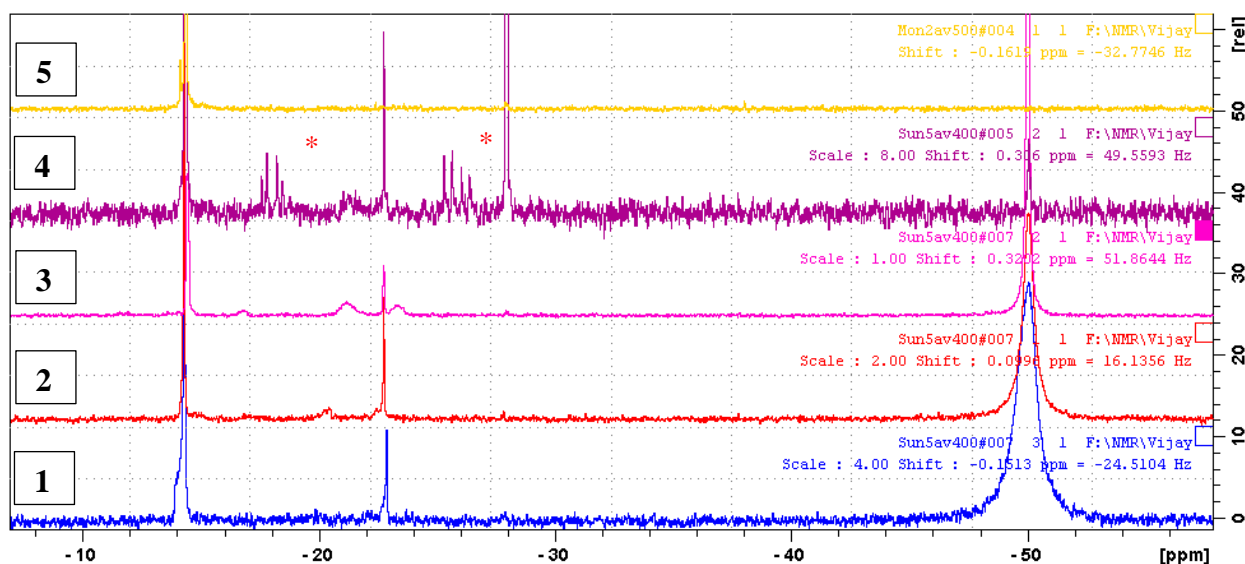
Figure 2.9: Stacked ^{31}P NMR spectra of *in-situ* generated intermediates in a C-P coupling reaction (1: before addition of NaOSiMe$_3$ at room temperature, 2: at -15°C, 3: at -40 °C, 4: after addition of NaOSiMe$_3$, at -40 °C, 5: at room temperature; * = could not be assigned).

Table 2.5: ^{31}P NMR shifts for (**i**) and (**ii**)

Intermediates	**δ P1**	**δ P2**	**δ P3**	**J$_{12}$ (Hz)**	**J$_{13}$ (Hz)**	**J$_{23}$ (Hz)**
(**i**)	65.1	61.9	-26.1	26	106	40
(**ii**)	52.3	44.6	-18.3	-	117	56

   The thus prepared P-stereogenic supramolecular phosphines were found to self-assemble on a metal template to produce self-assembled metal complexes (such as **2.10**). Multinuclear NMR and IR spectroscopy indicates existence of hydrogen bonding interactions. Such metal complexes have been found to catalyze asymmetric reactions (hydrogenation, hydroformylation etc.) of range of olefins.[23] The performance of supramolecular phosphine ligand **2.6b** with highest ee of 97% was evaluated in asymmetric hydrogenation of dimethyl-itaconate (**S1**) and *N*-acetyldehydrophenylalanine (**S2**) (detailed explanation is provided in chapter **5**). Preliminary asymmetric hydrogenation of dimethyl-itaconate at 0 °C revealed modest enantiomeric excess of 32%. Interestingly, testing **2.6b** in the asymmetric hydrogenation of (**S2**) led to a preliminary ee of 67% at room temperature within 5 hours. Performing the reaction at 0 °C revealed 99% ee, importantly, along with 91% isolated yields, within 5 hours.[24] Changing solvent did not affect the selectivity and 98% enantiomeric excess could be recorded in THF. Thus, asymmetric hydrogenation of (**S2**) was apply catalyzed by **2.6b** in presence of [Rh(COD)$_2$BF$_4$] (1 mol%) leading to excellent (99%) enantiomeric excess along with 91% conversion.
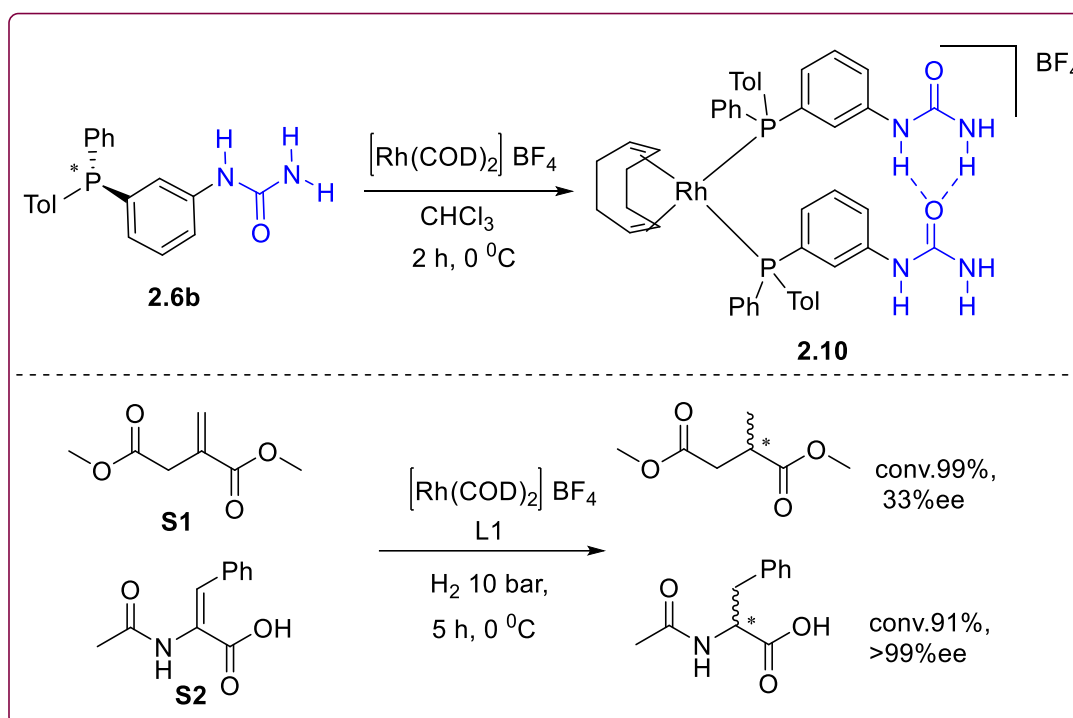
Scheme 2.8: Synthesis of self-assembled Rh-complex (C1) (top) and asymmetric hydrogenation (bottom).

2.4. Conclusion

In summary, we report catalytic asymmetric synthesis of a new class of P-stereogenic supramolecular phosphines for the first time. An isolated Pd-Me-DuPHOS complex **2.5** catalyzes phosphination of urea substituted aryl-halides and secondary phosphines to produce the corresponding C-P coupling products.[25] Judicious selection of substrate and tuning of reaction parameters led to an unprecedented enantioselectivity of 97% in **2.6b**; along with significant conversion (65%). Preliminary mechanistic investigations failed to spot Pd(0)-species **(iii)**; whereas spectroscopic observation of a phosphido-intermediate **(ii)** suggest that the phosphination reaction most likely proceeds via path **P-I**. Moreover, the thus prepared enantio-enriched P-stereogenic supramolecular phosphines self-assemble upon simple mixing with [Rh(COD)$_2$BF$_4$]. When employed in asymmetric hydrogenation of (**S2**), **2.6b** displayed an excellent enantiomeric excess of 99%, along with 91% conversion (detailed in chapter 4). These findings demonstrate the potential of P-stereogenic supramolecular phosphines in asymmetric catalysis. We are currently exploring the synthesis library of iodophenyl urea where *N*-substituted electron withdrawing and electron donating group thus preparation of library of P-stereogenic supramolecular phosphines in asymmetric catalysis (detailed discussion in chapter 3).

2.5. Experimental section

2.5.1. General methods and materials

All manipulations were carried out under an inert atmosphere using standard Schlenk line techniques or m-Braun glove box. Solvents were dried by standard procedures unless otherwise mentioned.[26] Toluene was distilled from sodium, diethyl ether and THF from sodium/benzophenone under argon atmosphere. Acetonitrile and methylene chloride were distilled on calcium-hydride. Hydrogen gas was supplied by Ms. Vadilal Chemicals Ltd., Pune, India. NaOSiMe$_3$, (*S, S*)-Me-DuPHOS, Mesitylbromide, Sulfur powder and [Rh(COD)$_2$BF$_4$] were purchased from Sigma-Aldrich and [Pd(dba)$_2$], 3-Iodoaniline and dichlorophenylphosphine were purchased from Alfa-Aesar. All other reagents/chemicals, solvents were purchased from local suppliers (Spectrochem Pvt. Ltd.; Avra Synthesis Pvt. Ltd.; Thomas Baker Pvt. Ltd. etc). 3-Iodophenyl urea (**2.2b**),[9] Phenyl(o-tolyl)phosphine/ mesityl(phenyl)phosphine(**2.1a**)[14] were prepared employing known procedures.

Solution NMR spectra were recorded on a Bruker Avance 200, 400 and 500 MHz instruments at 298 K unless mentioned otherwise. Chemical shifts are referenced to external reference TMS (^{1}H and ^{13}C) or 85% H$_3$PO$_4$ (Ξ = 40.480747 MHz, ^{31}P). Coupling constants are given as absolute values. Multiplicities are given as follows s: singlet, d: doublet, t: triplet, m: multiplet, quat: quaternary carbon. FT-IR spectra were recorded on a Bruker α-T spectrophotometer in the range of 4000-400 cm^{-1}. Mass spectra were recorded on Thermo scientific Q-Exactive mass spectrometer, with Hypersil gold C18 column 150 x 4.6 mm diameter 8 µm particle size mobile phase used is 90% methanol + 10 % water + 0.1 % formic acid. Enantiomeric excess of the P-stereogenic phosphines was determined by chiral HPLC on an Agilent Technologies 1260 Infinity instrument with Chiralpak IA column (20 cm) and Chiralpak IB column (20 cm). Specific optical rotations were measured on a Jasco P-1020 polarimeter at 298 K temperature and was measured in Model CGS-100 cylindrical glass cell (3.5 mm ID x 100 mm) in CHCl$_3$. The single crystal data was collected using Bruker SMART APEX II single crystal X-ray CCD diffractometer with graphite-monochromatised (Mo-kα = 0.71073 A°) radiation.

2.5.2. Synthesis of [Pd(tmeda)(3-phenylurea)(I)] complex (2.3)

To a stirred suspension of [Pd(dba)$_2$] (1 g, 1.74 mmol) in toluene (20 mL) was added TMEDA (0.36 mL, 2.23 mmol) and m-iodophenylurea (0.46 gm, 1.74 mmol) under argon. The reaction mixture was heated to 55 °C, at which point it turned green (approximately after 5 h) and solid material was settled down. The reaction mixture was cooled to room temperature and filtered to obtained solid material. The solid compound was washed with toluene (20 ml × 3) and dried in vacuum to yield an air sensitive greenish-gray solid in 63% yield (0.532 gm, 1.09 mmol). Recrystallization from DMSO/THF afforded yellow crystals suitable for single crystal X-ray measurement. In the solid state, complex 2.3 cocrystallizes with 1 molecule of Dimethyl sulfoxide (DMSO).
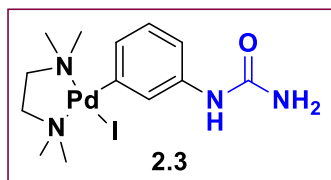
^{1}H NMR (500 MHz, DMSO-d$_6$, 298 K) δ = 8.11 (s, ^{1}H, N*H*), 7.09 (s, ^{1}H, Ar), 6.80 (d, J_{H-H} = 7.2 Hz, 1H, Ar), 6.68 (m, 2H, Ar), 5.66 (s, 2H, N*H$_2$*), 2.78 (d, J_{H-H} = 23 Hz, 2H, C*H$_2$*), 2.61 (s, 2H, C*H$_2$*), 2.55 (s, 6H, C*H$_3$*), 2.30 (s, 3H, C*H$_3$*), 2.22 (s, 3H, C*H$_3$*). **^{13}C NMR** (125 MHz, DMSO-d$_6$, 298 K) δ = 156.0 (s, *C*O), 146.4 (s, Ar, quat.), 137.3 (s, Ar, quat.), 129.8 (s, Ar, *C*H), 125.2 (s, Ar, *C*H), 112.2 (s, Ar, *C*H), 61.4 (s, CH$_2$), 57.4 (s, *C*H$_2$), 49.5 (m, *C*H$_3$). **ESI-MS** (+ve) (Cal. For C$_{13}$H$_{23}$IN$_4$OPd) m/z = 357.09 [M-I]$^+$, 398.11 [M-I+CH$_3$CN]$^+$.

2.5.3. Synthesis of [Pd-(MeDuphos)(*m*-phenylurea)(I)] complex (2.5)

A solution of [Pd-(TMEDA)(m-phenylurea)(I)] complex (2.3) (158 mg, 0.326 mmol) in acetonitrile (20 mL) and (S,S)-Me-DuPhos (100 mg, 0.326 mmol) was stirred at room temperature and the reaction progress was monitored by ^{31}P NMR spectroscopy. The reaction was completed in 2 h. After completion of reaction volatiles were evaporated to obtain gray solid material. The solid was washed with *n*-hexane (10 mL x 3 times) to yield the desired palladium complex in 65% yield (0.143 mg, 0.211 mmol).
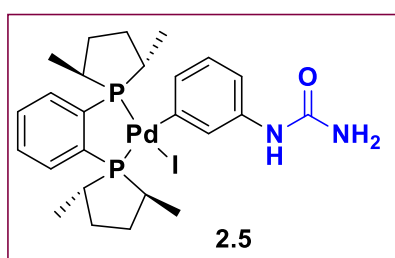
^{1}H NMR (500 MHz, CD$_3$CN, 298 K) δ = 7.87 (s, 1H, N*H*), 7.78 (s, 1H, Ar), 7.68 (m, 2H, Ar), 7.36 (s, 1H, Ar), 7.22-7.01 (m, 2H, Ar), 6.95 (s, 2H, Ar), 4.84 (s, 2H, N*H$_2$*), 3.58 (m, 1H, C*H*), 3.16 (m, 1H, C*H*), 2.79-2.46 (m, 4H, C*H$_2$*), 2.41-2.13 (m, 4H, C*H$_2$*), 2.09-1.99 (m, 2H, C*H*), 1.48 (dd, J_{H-H} = 6.9, 18.6 Hz, 3H, C*H$_3$*), 1.29 (dd, J_{H-H} = 6.9, 19.0 Hz, 3H, C*H$_3$*), 0.90 (dd, J_{H-H} = 2.0, 7.4 Hz, 3H, C*H$_3$*), 0.86 (d, J_{H-H} = 7.4, 3H, C*H$_3$*). **^{13}C NMR** (125 MHz, DMSO-d$_6$, 298 K) δ = 156.2 (s, *C*O), 142.4 (t, J_{C-P} = 36 Hz, Ar, quat), 141.1 (t, J_{C-P} = 29 Hz, Ar, quat),

138.2 (m, Ar, quat), 133.6 (d, J_{C-P} = 14.2 Hz, Ar, *C*H), 133.2 (d, J_{C-P} = 15.3 Hz, Ar, *C*H), 131.7 (s, Ar, *C*H), 125.8 (s, Ar, *C*H), 112.5 (s, Ar, *C*H), 45.2 (s, *C*H), 42.2 (d, J_{C-P} = 29 Hz, *C*H), 41.1 (d, J_{C-P} = 21 Hz, *C*H), 36.6 (s, *C*H), 36.4 (s, *C*H$_2$), 35.9 (s, *C*H$_2$), 35.5 (s, *C*H$_2$), 34.8 (d, J_{C-P} = 3 Hz, *C*H$_2$), 17.0 (d, $^2J_{C-P}$ = 12 Hz, *C*H$_3$), 15.2 (d, $^2J_{C-P}$ = 7.7 Hz, *C*H$_3$), 14.2 (d, $^2J_{C-P}$ = 17 Hz, *C*H$_3$). **^{31}P NMR** (500 MHz, CD$_3$CN, 298 K) δ = 65.09 (d, $^2J_{P-P}$ = 25 Hz, 1P$_{P2}$), 69.36 (d, $^2J_{P-P}$ = 25 Hz, 1P$_{P1}$). **IR** (cm^{-1}): 3461 (NH$_2$), 3319 (NH$_2$), 3184 (NH), 1672 (C=O). **ESI-MS** (+ve) (Cal. For C$_{25}$H$_{35}$IN$_2$OP$_2$Pd) m/z = 547.12 [M-I]$^+$, 588.15 [M-I+H+K]$^+$.

2.5.4. Synthesis of P-stereogenic supramolecular phosphines (2.6-2.7)

2.5.4.1. General procedure for phosphination reaction

A sample vial was loaded with catalyst 2.5, iodophenylurea 2.2, racemic secondary phosphine 2.1, and desired quantity of THF in a glove box. The content of the sample vial was transferred to a Schlenk tube. The vial was rinsed with additional THF which was added to the Schlenk tube. The screw capped Schlenk tube was taken out and after the standard vacuum-argon cycle NaOSiMe$_3$ was added to the reaction mixture. The reaction mixture was stirred at appropriate temperature and for desired time. The progress of the reaction was monitored by ^{31}P NMR spectroscopy.

2.5.4.2. 1-(3-(phenyl(o-tolyl)phosphanyl)phenyl)urea (2.6b)

A sample vial was loaded with [Pd(OAc)$_2$] (4.5 mg, 0.005 mol), 3-iodophenylurea (**2.2b**) (22.6 mg, 0.1 mmol), phenyl(o-tolyl)phosphine (**2.1a**) (20 mg, 0.1 mmol) and 0.2 ml of

2.6b

THF in a glove box. The content of the sample vial was transferred to a Schlenk tube. The vial was rinsed with additional THF (0.3 mL) which was added to the Schlenk tube. The screw capped Schlenk tube was taken out and appropriate temperature was attained. After the standard vacuum-argon

cycle NaOSiMe$_3$ (0.3 mL of a 1.0 M THF solution, 1 mmol) was added to the reaction mixture. The progress of the reaction was monitored by ^{31}P NMR spectroscopy. After completion of the reaction, the content was treated with degassed water (which was pre-cooled at appropriate temperature) and extracted with ethyl acetate (10 mL × 3) (which was pre-cooled at appropriate temperature). The combined organic layer was dried on MgSO$_4$ for 2 hours at suitable temperature and the volatiles were evaporated under reduced pressure. The crude reaction mixture was purified by silica gel column chromatography using 70:30 mixture of DCM:ethyl

acetate. The desired product **2.6b** was isolated as a yellow solid in good to excellent conversion (reported in Table 2.2).

¹H NMR (500 MHz, CDCl₃, 298 K) δ = 7.42 (d, $J_{\text{H-H}}$ = 7.8 Hz, 1H, N*H*), 7.33-7.26 (m, 3H, Ar) 7.25-7.12 (m, 6H, Ar), 7.03 (t, $J_{\text{H-H}}$ = 7.0 Hz, 2H, Ar), 6.93 (t, $J_{\text{H-H}}$ = 7 Hz, 1H, Ar), 6.80-6.68 (m, 1H, Ar), 4.79 (s, 2H, N*H₂*), 2.35 (s, 3H, C*H₃*). **¹³C NMR** (125 MHz, CDCl₃, 298 K) δ = 156.7 (s, *C*O), 142.3 (d, $J_{\text{C-P}}$ = 24.25 Hz, Ar, quat.), 138.9 (d, $J_{\text{C-P}}$ = 8.08 Hz, Ar, quat.), 137.9- (d, $J_{\text{C-P}}$ = 11.02 Hz, Ar, quat.), 136.1 (d, $J_{\text{C-P}}$ = 9.55 Hz, Ar, quat.), 135.8 (d, $J_{\text{C-P}}$ = 11.76 Hz, Ar, quat.), 134.1 (d, $J_{\text{C-P}}$ = 20.98 Hz, Ar, *C*H), 130.3 (d, $J_{\text{C-P}}$ = 4.3 Hz, Ar, *C*H), 132.8 (s, Ar, *C*H), 129.5 (d, $J_{\text{C-P}}$ = 7.6 Hz, Ar, *C*H), 128.9 (d, $J_{\text{C-P}}$ = 7.08 Hz, Ar, *C*H), 129.4 (s, Ar, *C*H), 128.7 (d, $J_{\text{C-P}}$ = 6.7 Hz, Ar, *C*H), 126.5 (s, Ar, *C*H), 125.7 (d, $J_{\text{C-P}}$ = 21.27 Hz, Ar, *C*H), 121.3 (s, Ar, *C*H), 21.2 (d, $J_{\text{C-P}}$ = 20.98 Hz, *C*H₃). **³¹P NMR** (500 MHz, CDCl₃, 298 K) δ = -13.0 (s). **IR** (cm⁻¹): 3500 (NH₂), 3342 (NH₂), 3202 (NH), 1670 (C=O). **ESI-MS** (+ve) (Cal. For C₂₀H₁₉N₂OP) m/z = 335.13 [M+H]⁺, 357.11 [M+Na]⁺.

2.5.4.3. 1-(3-(phenyl(o-tolyl)phosphorothioyl)phenyl)urea (2.8b)
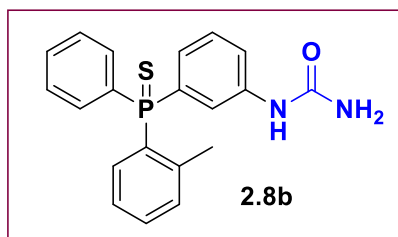
The phosphine **2.6b** (0.1 mmol) was prepared as described in section 2.5.4.2 and was *in-situ* protected without isolation. Thus, after completion of the reaction, excess Sulfur powder (S₈) (9.6 mg, 0.3 mmol) was added to the reaction mixture at 0 °C and the mixture was stirred for one hour followed by warming up to room temperature. Above mixture was then treated with degassed water and was extracted with ethyl acetate (3 × 10 mL). The combined organic layer was dried on MgSO4 for 2 hours and the volatiles were evaporated under reduced pressure. The crude 2.8b was purified by silica gel column chromatography using 80:20 mixture of DCM:Ethyl acetate. The desired product was isolated as a yellowish solid in 87% yield (32 mg, 0.087 mmol).

³¹P NMR (500 MHz, CDCl₃, 298 K) δ = 42.3 (s, P). **HPLC:** Daicel Chiralpak-IA, 1 mL/min, 10:90 (2-PrOH:Hexane), (*R*) Rt_1 = 15.4 min; (*S*) Rt_2 = 16.7 min. ee = 83%. $[\alpha]^{25}_{\lambda}$: -23 (579) (*c* 0.25, CHCl₃).

VWD: Signal A, 254 nm Results

Retention Time	Area	Area %
15.483	105878219	49.72
16.733	107069205	50.28

Totals		
	212947424	100.00

Figure. **2.10.** HPLC chromatogram of racemic 1-(3-(phenyl(*o*-tolyl)phosphorothioyl)phenyl)urea **2.8b**.
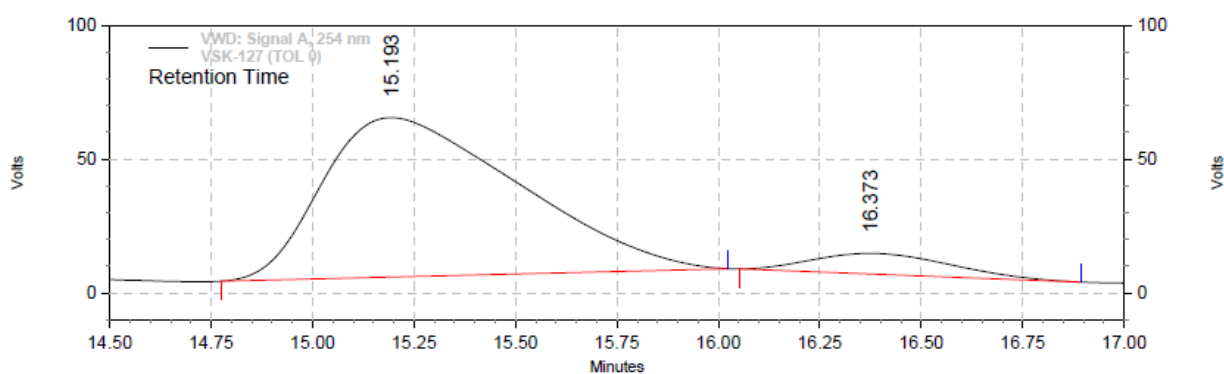
VWD: Signal A, 254 nm
Results

Pk #	Retention Time	Area	Area %
1	15.193	33604696	91.60
2	16.373	3080984	8.40

Totals		
	36685680	100.00

Figure 2.11. HPLC chromatogram of *p*-stereogenic 1-(3-(phenyl(*o*-tolyl)phosphorothioyl)phenyl)urea **6b** (at. 0ºC).

VWD: Signal A, 254 nm Results		
Retention Time	Area	Area %
15.503	8476393	98.31
16.510	145956	1.69
Totals		
	8622349	100.00

Figure 2.12. HPLC chromatogram of *p*-stereogenic 1-(3-(phenyl(*o*-tolyl)phosphorothioyl)phenyl)urea **6b** (at. -5°C).

2.5.4.4. 1-(4-(phenyl(o-tolyl)phosphanyl)phenyl)urea (2.6c)

A sample vial was loaded with [Pd(OAc)$_2$] (4.5 mg, 0.005 mol), 4-iodophenylurea (**2.2c**) (22.6 mg, 0.1 mmol), phenyl(o-tolyl)phosphine (**2.1a**) (20 mg, 0.1 mmol) and 0.2 ml of
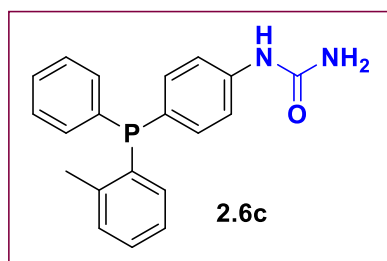
THF in a glove box. The content of the sample vial was transferred to a Schlenk tube. The vial was rinsed with additional THF (0.3 mL) which was added to the Schlenk tube. The screw capped Schlenk tube was taken out and appropriate temperature was attained. After the standard vacuum-argon cycle NaOSiMe$_3$ (0.3 mL [1.0 M THF solution], 1 mmol) was added to the reaction mixture. The progress of the reaction was monitored by ^{31}P NMR spectroscopy. After completion of the reaction, the content was treated with degassed water (which was pre-cooled at appropriate temperature) and extracted with ethyl acetate (10 mL × 3) (which was pre-cooled at appropriate temperature). The combined organic layer was dried on MgSO$_4$ for 2 hours at suitable temperature and the volatiles were evaporated under reduced pressure. The crude reaction mixture was purified by silica gel column chromatography using 75:25 mixture of DCM:ethyl acetate. The desired product **2.6c** was isolated as a yellow solid in 89% yield (30 mg, 0.089 mmol).

¹H NMR (500 MHz, CDCl₃, 298 K) δ = 7.52 (s, 1H, N*H*), 7.41 (s, 1H, Ar), 7.34-7.13 (m, 8H, Ar), 7.06 (s, 2H, Ar), 6.94-6.91 (m, 1H, Ar), 6.76 (s, 1H, Ar), 4.93 (s, 2H, N*H₂*), 2.36 (s, 3H, CH₃). **¹³C NMR** (125 MHz, CDCl₃, 298 K) δ = 157.1 (s, *C*O), 142.4 (d, J_{C-P} = 25 Hz, Ar, quat.), 139.1 (s, Ar, quat.), 137.7 (d, J_{C-P} = 12 Hz, Ar, quat.), 136.2 (d, J_{C-P} = 10 Hz, Ar, quat.), 135.9 (d, J_{C-P} = 12 Hz, Ar, quat.), 134.2 (d, J_{C-P} = 20 Hz, Ar, *C*H), 132.9 (s, Ar, *C*H), 130.3 (d, J_{C-P} = 5 Hz, Ar, *C*H), 129.6 (d, J_{C-P} = 8 Hz, Ar, *C*H), 129.4 (s, Ar, *C*H), 129.0 (d, J_{C-P} = 6 Hz, Ar, *C*H), 128.8 (d, J_{C-P} = 7 Hz, Ar, *C*H), 126.2 (s, Ar, *C*H), 125.5 (d, J_{C-P} = 19 Hz, Ar, *C*H), 121.2 (s, Ar, *C*H), 21.4 (d, J_{C-P} = 21 Hz, *C*H₃). **³¹P NMR** (500 MHz, CDCl₃, 298 K) δ = -13.8 (s). **IR** (cm⁻¹): 3684 (NH₂), 3433 (NH₂), 3337 (NH), 1667 (C=O), 1586 (C-N_I), 1528 (C-N_II). **ESI-MS** (+ve) (Cal. For C₂₀H₁₉N₂OP) m/z = 335.13 [M+H]⁺, 357.11 [M+Na]⁺.
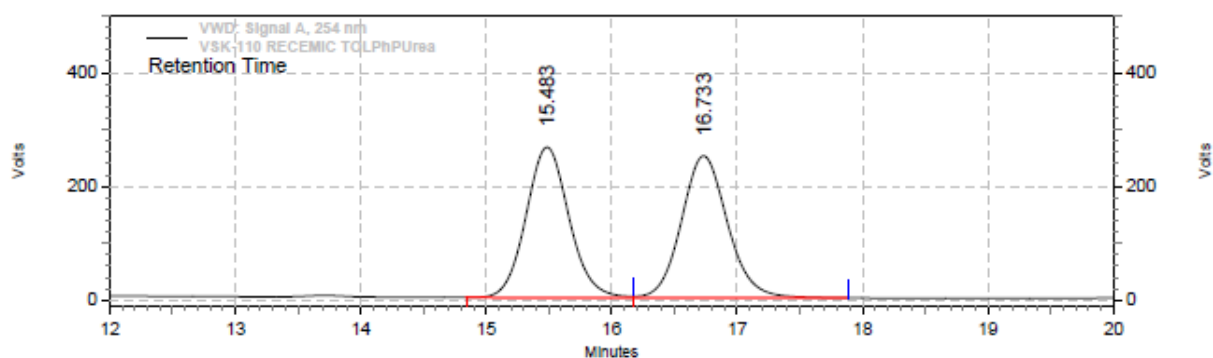
2.5.4.5. 1-(4-(phenyl(o-tolyl)phosphorothioyl)phenyl)urea (2.8c)

The phosphine **2.6c** (0.1 mmol) was prepared as described in section 2.5.4.4 and was *in-situ* protected without isolation. Thus, after completion of the reaction, excess sulfur powder (S₈) (9.6 mg, 0.3 mmol) was added to the reaction mixture at suitable temperature and the mixture was stirred for one hour followed by warming up to room temperature. Above mixture
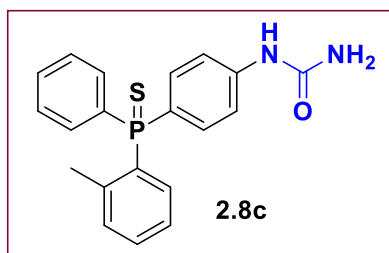
was then treated with degassed water and was extracted with ethyl acetate (3 ×10 mL) at appropriate temperature. The combined organic layer was dried on MgSO₄ for 2 hours and the volatiles were evaporated under reduced pressure. The crude **2.8c** was purified by silica gel column chromatography using 80:20 mixture of DCM:Ethyl acetate. The desired product was isolated as a yellowish solid in 87% yield (32 mg, 0.087 mmol).

³¹P NMR (500 MHz, CDCl₃, 298 K) δ = 39.4 (s, P). **HPLC:** Daicel Chiralpak IA, 1 mL/min, 90:10 (Hexane:2-PrOH), Rt_1 = 42.8 min; Rt_2 = 47.8 min. ee = 40%. [α]²⁵_λ: -22 (583) (*c* 0.25, CHCl₃).

VWD: Signal A, 254 nm Results

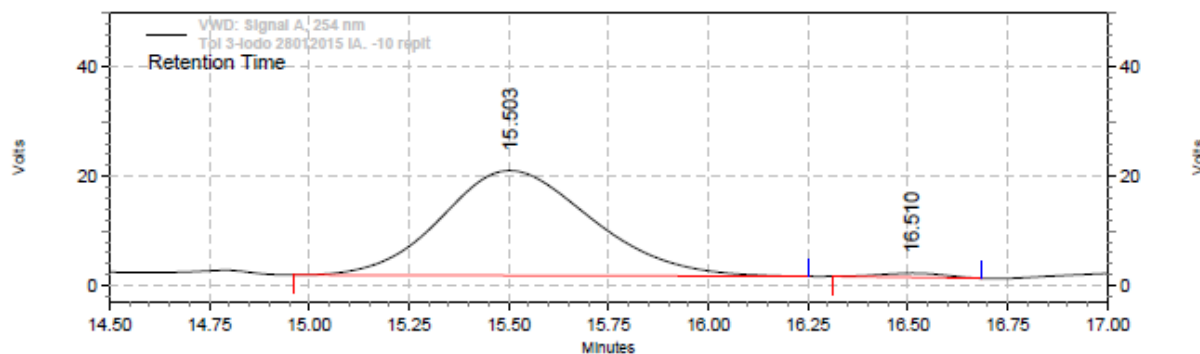| Retention Time	Area	Area %
40.827	190173406	50.40
45.040	187159257	49.60
Totals	377332663	100.00

Figure 2.13. HPLC chromatogram of racemic 1-(3-(phenyl(*o* tolyl)phosphorothioyl)phenyl)urea **2.8c**.
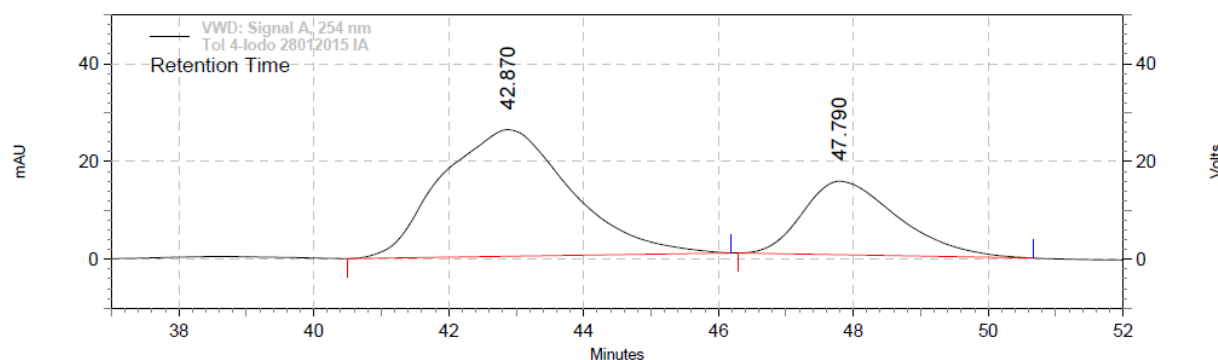
VWD: Signal A, 254 nm Results

Retention Time	Area	Area %
42.870	57889506	70.15
47.790	24638647	29.85
Totals	82528153	100.00

Figure 2.14. HPLC chromatogram of *p*-stereogenic 1-(3-(phenyl(*o*-tolyl)phosphorothioyl)phenyl)urea **2.8c** (at - 5°C).

2.5.4.6. 1-(3-(mesityl(phenyl)phosphanyl)phenyl)urea (2.7b)

A sample vial was loaded with [Pd(OAc)$_2$] (4.5 mg, 0.005 mol), 3-iodophenylurea (**2.2b**) (22.6 mg, 0.1 mmol), mesityl(phenyl)phosphine (**2.1b**) (22 mg, 0.1 mmol) and 0.2 ml of


THF in a glove box. The content of the sample was transferred to a Schlenk tube. The vial was rinsed with additional THF (0.3 mL) which was added to the Schlenk tube. The screw capped Schlenk tube was taken out and appropriate temperature was attained. After the standard vacuum-argon cycle NaOSiMe$_3$ (0.3 mL of a 1.0 M THF solution, 0.3 mmol) was added to the reaction mixture. The progress of the reaction was monitored by ^{31}P NMR spectroscopy. After completion of the reaction, the content was treated with degassed water (which was pre-cooled at appropriate temperature) and extracted with ethyl acetate (10 mL × 3) (which was pre-cooled at appropriate temperature). The combined

organic layer was dried on MgSO$_4$ for 2 hours and the volatiles were evaporated under reduced pressure. Crude compound **2.7b** was purified by silica gel column chromatography using 80:20 mixture of DCM:ethyl acetate. The desired product was isolated as a yellowish solid in 82% yield (29 mg, 0.082 mmol).

^{1}H NMR (500 MHz, CDCl$_3$, 298 K) δ = 7.39-7.20 (m, 7H, N*H*, Ar, C*H*), 7.06 (m, 2H, Ar, C*H*), 6.89 (s, 2H, Ar, C*H*), 6.67 (s, 1H, Ar, C*H*), 4.67 (s, 2H, N*H*$_2$), 2.28 (s, 3H, C*H*$_3$), 2.16 (s, 6H, C*H*$_3$). **^{13}C NMR** (125 MHz, CDCl$_3$, 298 K) δ = 156.6 (s, *C*O), 145.8 (s, Ar, quat), 145.7 (s, Ar, quat.), 140.5 (s, Ar, quat.), 138.6 (s, Ar, quat.), 136.1 (s, Ar, quat.), 131.9 (d, J_{C-P} = 18 Hz, Ar, *C*H), 130.2 (d, J_{C-P} = 5 Hz, Ar, *C*H), 129.6 (d, J_{C-P} = 6 Hz, Ar, *C*H), 128.7 (d, J_{C-P} = 5 Hz, Ar, *C*H), 127.9 (s, Ar, quat.), 127.8 (s, Ar, *C*H), 127.6 (d, J_{C-P} = 19 Hz, Ar, *C*H), 123.9 (d, J_{C-P} = 21 Hz, Ar, *C*H), 120.8 (s, Ar, *C*H), 23.9 (d, J_{C-P} = 19 Hz, *C*H$_3$), 21.3 (s, *C*H$_3$), **^{31}P NMR** (500 MHz, CDCl$_3$, 298 K) δ = -16.3 (s). **IR** (cm^{-1}): 3453 (NH$_2$), 3361 (NH$_2$), 3200 (NH), 1725 (C=O). **ESI-MS** (+ve) (Cal. For C$_{22}$H$_{23}$N$_2$OP) m/z = 363.16 [M+H]$^+$.
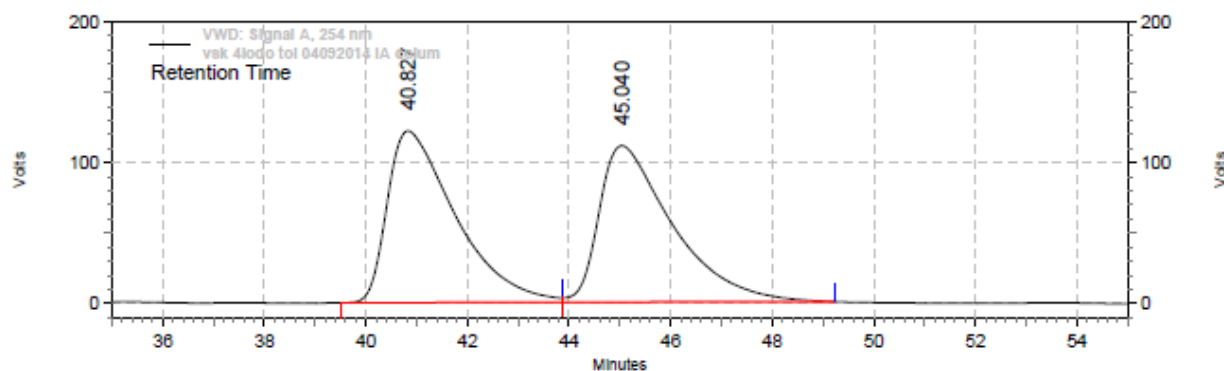
2.5.4.7. 1-(3-(mesityl(phenyl)phosphorothioyl)phenyl)urea (2.9b)

2.9b
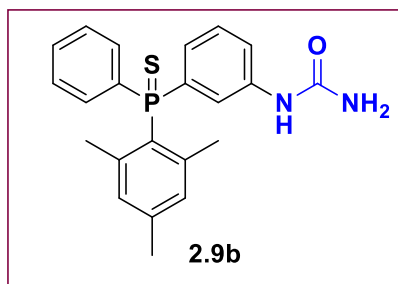
The phosphine **2.7b** (0.1 mmol) was prepared as described in section 2.5.4.6 and was *in-situ* protected without isolation. Thus, after completion of the reaction, excess of sulfur powder (S$_8$) (9.6 mg, 0.3 mmol) was added to the reaction mixture at suitable temperature and the mixture was stirred for one hour followed by warming up to room temperature. Above mixture was then treated with degassed water and was extracted with ethyl acetate (3 × 10 mL). The combined organic layer was dried on MgSO$_4$ for 2 hours and the volatiles were evaporated under reduced pressure. The crude **2.9b** was purified by silica gel column chromatography using 80:20 mixture of DCM:Ethyl acetate. The desired product was isolated as a yellowish solid in 77% yield (30 mg, 0.077 mmol).

^{31}P NMR (500 MHz, CDCl$_3$, 298 K) δ = 36.4 (s, P). **HPLC:** Daicel Chiralpak IB, 1 mL/min, 90:10 (Hexane: 2-PrOH), Rt_1 = 26.5 min; Rt_2 = 29.7 min. ee = 11%. [α]$^{25}_{\lambda}$: -20 (589) (*c* 0.25, CHCl$_3$).
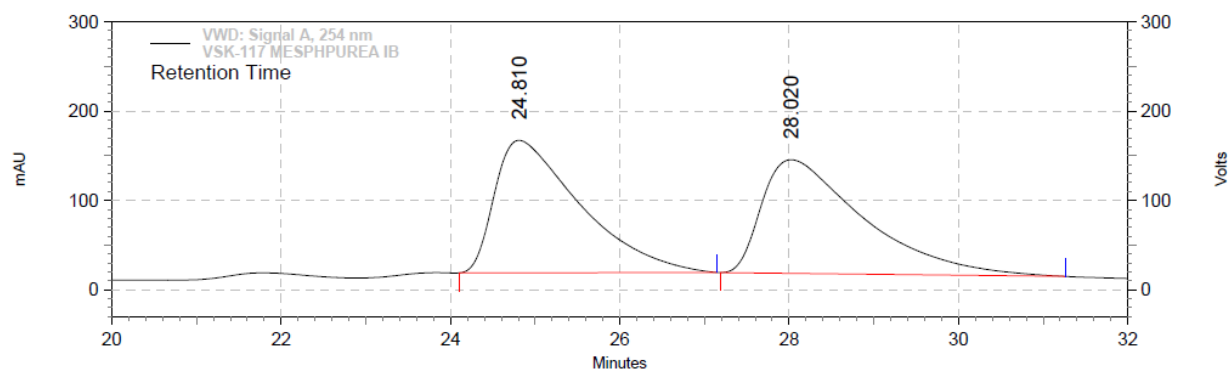
VWD: Signal A, 254 nm
Results

Pk #	Retention Time	Area	Area %
1	26.993	169587458	52.80
2	30.127	151585922	47.20
Totals		321173380	100.00

Figure 2.15. HPLC chromatogram of *racemic* 1-(3-(mesityl (phenyl) phosphorothioyl) phenyl) urea **2.9b**.
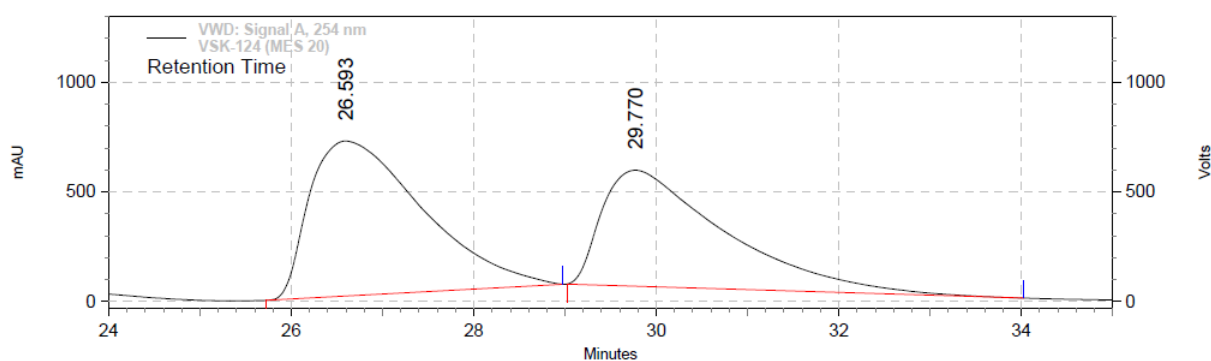
VWD: Signal A, 254 nm
Results

Pk #	Retention Time	Area	Area %
1	26.593	1020523330	55.09
2	29.770	831979977	44.91
Totals		1852503307	100.00

Figure 2.16. HPLC chromatogram of enantio-enriched 1-(3-(mesityl (phenyl) phosphorothioyl) phenyl) urea **2.9b**.

2.5.4.8. 1-(4-(mesityl(phenyl)phosphanyl)phenyl)urea (2.7c)

A sample vial was loaded with [Pd(OAc)$_2$] (4.5 mg, 0.005 mol), 4-iodophenylurea (**2.2c**) (22.6 mg, 0.1 mmol), mesityl(phenyl)phosphine (**2.1b**) (22 mg, 0.1 mmol) and 0.2 ml of THF in a glove box. The content of the sample was transferred to a Schlenk tube. The vial was rinsed with additional THF (0.3 mL) which was added to the Schlenk tube. The screw capped Schlenk tube was taken out and appropriate temperature was attained. After the standard vacuum-argon cycle NaOSiMe$_3$ (0.3 mL of a 1.0 M THF solution, 0.3 mmol) was added to the reaction mixture. The progress of the reaction was monitored by ^{31}P NMR spectroscopy. After completion of the reaction, the content was treated with degassed water (which was pre-cooled at appropriate temperature) and extracted with ethyl acetate (3 × 10 mL) (which was pre-cooled at appropriate temperature). The combined organic layer was dried on MgSO$_4$ for 2 hours and the volatiles were evaporated under reduced pressure. Crude compound **2.7c** was purified by silica gel column chromatography using 80:20 mixture of DCM:ethyl acetate. The desired product was isolated as a yellowish solid in 69% yield (25 mg, 0.069 mmol).
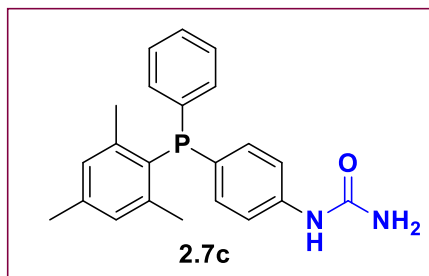
^{1}H NMR (500 MHz, CDCl$_3$, 298 K) δ = 8.55 (s, 1H, N*H*), 7.34 (d, *J*$_{H-H}$ = 8 Hz, 2H, Ar, C*H*), 7.30-7.20 (m, 5H, Ar, C*H*), 7.16 (t, *J*$_{H-H}$ = 8 Hz, 2H, Ar, C*H*), 6.86 (s, 2H, Ar, C*H*), 5.35 (s, 2H, N*H*$_2$), 2.25 (s, 3H, C*H*$_3$), 2.11 (s, 6H, C*H*$_3$). **^{13}C NMR** (125 MHz, CDCl$_3$, 298 K) δ = 157.2 (s, *C*O) 145.4 (s, Ar, quat.), 145.2 (s, Ar, quat.), 141.2 (s, Ar, quat.), 140.4 (s, Ar, quat.), 133.1 (d, *J*$_{C-P}$ = 20 Hz, Ar, *C*H), 131.8 (d, *J*$_{C-P}$ = 17 Hz, Ar, *C*H), 130.4 (d, *J*$_{C-P}$ = 5 Hz, Ar, *C*H), 128.6 (d, *J*$_{C-P}$ = 7 Hz, Ar, *C*H), 128.7 (s, Ar, quat.), 119.8 (d, *J*$_{C-P}$ = 8 Hz, Ar, *C*H), 23.7 (d, *J*$_{C-P}$ = 16 Hz, *C*H$_3$), 21.3 (s, *C*H$_3$). **^{31}P NMR** (500 MHz, CDCl$_3$, 298 K) δ = -17.0 (s). **IR** (cm^{-1}): 3683 (NH$_2$), 3503 (NH$_2$), 3342 (NH), 1682 (C=O). **ESI-MS** (+ve) (Cal. For C$_{22}$H$_{23}$N$_2$OP) m/z = 363.16 [M+H]$^+$.

2.5.4.9. 1-(4-(mesityl(phenyl)phosphorothioyl)phenyl)urea (2.9c)

The phosphine **2.7c** (0.1 mmol) was prepared as described in section 2.5.4.8 and was *in-situ* protected without isolation. Thus, after completion of the reaction, excess of sulfur powder (S_8) (9.6 mg, 0.3 mmol) was added to the reaction mixture at suitable temperature and the mixture was stirred for one hour followed by warming up to room temperature. Above mixture was then treated with degassed water and was extracted with ethyl acetate (3 ×10 mL). The combined organic layer was dried on $MgSO_4$ for 2 hours and the volatiles were evaporated under reduced pressure. The crude **2.9c** was purified by silica gel column chromatography using 80:20 mixture of DCM:Ethyl acetate. The desired product was isolated as a yellowish solid in 77% yield (30 mg, 0.077 mmol).
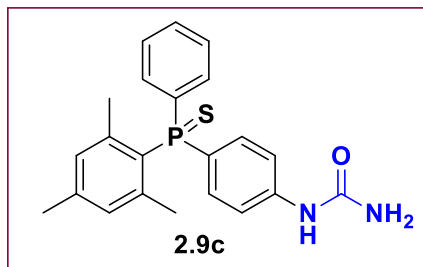
31P NMR (500 MHz, CDCl$_3$, 298 K) δ = 35.7 (s, P). **HPLC:** Daicel Chiralpak IA, 1 mL/min, 93:7 (Hexane:EtOH), Rt_1 = 47.2 min; Rt_2 = 51.7 min. ee = 11%. [α]$^{25}_\lambda$: -22 (589) (*c* 0.25, CHCl$_3$).
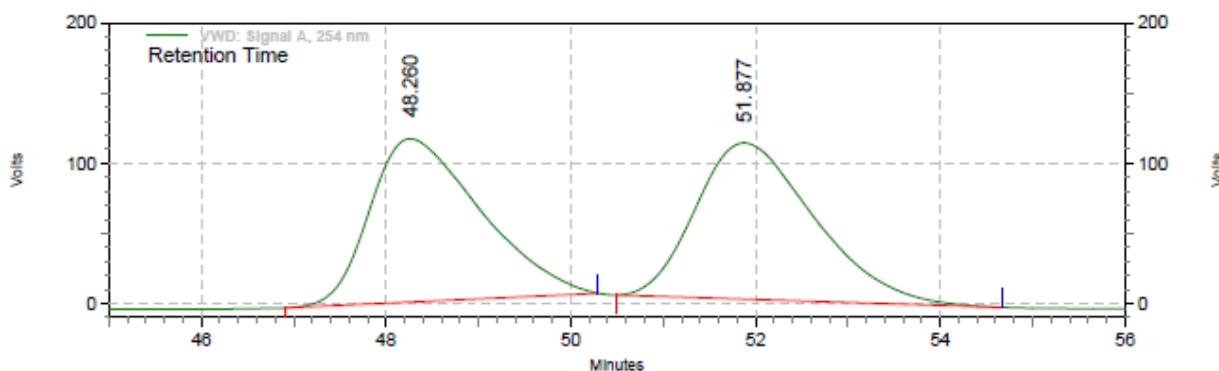
VWD: Signal A,
254 nm Results

Retention Time	Area	Area %	Height	Height %
48.260	162069631	49.28	1951975	51.12
51.877	166838683	50.72	1866166	48.88
Totals	328908314	100.00	3818141	100.00

Figure 2.17. HPLC chromatogram of *racemic* 1-(3-(mesityl (phenyl) phosphorothioyl) phenyl) urea **2.9c**.
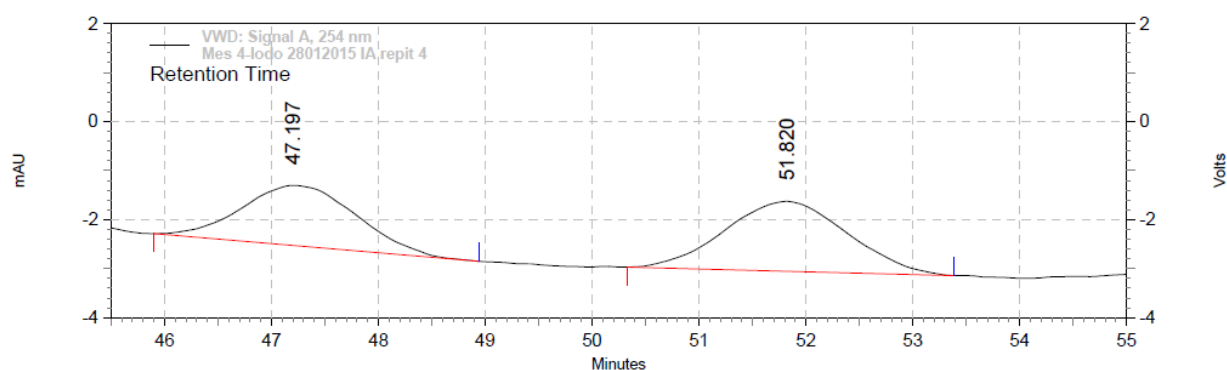
| VWD: Signal A, 254 nm Results | | |
Retention Time	Area	Area %
47.197	1542010	44.83
51.820	1897910	55.17
Totals		
	3439920	100.00

Figure 2.18. HPLC chromatogram of enantio-enriched 1-(3-(mesityl (phenyl) phosphorothioyl) phenyl) urea **2.9c**.

2.5.5. Synthesis of racemic protected (S) phosphines (2.8b, 2.8c, 2.9b and 2.9c)

2.5.5.1. General procedure for the synthesis of racemic phosphines (2.6b, 2.6c, 2.7b and 2.7c)

A 3-iodophenylurea (**2.2b** and **2.2c**) (0.17gm, 0.64 mmol) was dissolved in THF (1.5 ml)/DMF (0.5 ml) (3:1) mixture, followed by addition of triethylamine (0.18 ml, 1.29 mmol) and secondary phosphine **2.1a** (0.13 gm, 0.64 mmol) or **2.1b** (0.15 gm, 0.64 mmol). After stirring for few minutes, [Pd(OAc)$_2$] (0.5 mol %) was added and the mixture was refluxed overnight at 68 °C. After completion of the reaction the volatiles were evaporated and the residue was suspended in degassed water. The desired product was extracted in ethyl acetate to obtain a crude mixture. The solvent was stripped-off. The crude mixture was dissolved in DCM and filtered over a plug of silica. The plug was washed with DCM until the impurities were eluted, and then the expected product was pushed through with ethyl acetate. After evaporation of the solvent the product was obtained as a pale yellow solid which was analyzed by a combination of spectroscopic and analytical tools. The spectral and analytical data for **2.6b**, **2.6c**, **2.7b** and **2.7c** was found to be similar to those reported in sections, 2.5.4.2, 2.5.4.4, 2.5.4.6 and 2.5.4.8 respectively.

2.5.5.2. General procedure for the synthesis of racemic protected (S) phosphines (2.8b, 2.8c, 2.9b and 2.9c)

Above phosphine (**2.6b, 2.6c**, **2.7b**, and **2.7c**) (1 mmol) and excess of sulfur powder (2-3 mmol) was dissolved in THF (10 mL) in the Schlenk flask. The mixture was stirred for one hour at room temperature and volatiles were evaporated. This was followed by addition of degassed water to the residue and the desired product was extracted with ethyl acetate. The crude compound was loaded on a silica column and was washed with DCM, followed by elution with ethyl acetate. The resultant anticipated product (**2.8b**, **2.8c**, **2.9b** and **2.9c**) was isolated in ca. 60-80% yield. The spectroscopic and analytical data was found to be same as that of (**2.8b, 2.8c, 2.9b** and **2.9c**) reported under sections, 2.5.4.3, 2.5.4.5, 2.5.4.7 and 2.5.4.9 respectively.

2.5.6. Mechanistic investigations

In our pursuit to understand the mechanism, we monitored the progress of phosphination in a stoichiometric NMR tube reaction. Addition of one equivalent of tolylphenylphosphine **2.1a** (3 mg, 0.0148 mmol) to palladium complex **2.5** (10 mg, 0.0148 mmol) resulted in a broad ^{31}P NMR resonance at -49.4 ppm that could be assigned to free phosphine **2.1a** (Fig. 2.8-1 blue color spectrum). After addition of base (NaOSiMe$_3$, 0.044 mmol), an immediate change was apparent, the free phosphine disappeared and a new resonance at -23.9 ppm was observed (Fig. 2.8-2 red-color spectrum). This new signal most likely originates from an intermediate species (**ii**) (Scheme 2.6)

In our quest to pin-down the underlying intermediates, low temperature NMR experiments were performed and Figure 2.9 depicts the stacked spectra. A room temperature NMR of a mixture of tolylphenylphosphine **2.1a** (3 mg, 0.0148 mmol) and palladium complex **2.5** (10 mg, 0.0148 mmol) displayed a broad ^{31}P NMR resonance at -49.5 ppm (free phosphine **2.1a**) (Fig. 2.9-1, bottom). Cooling down the same NMR tube to -40 °C revealed broad doublet centered at -22.2 ppm with a $^2J_{\text{P-P}}$ = 353 Hz (Fig. 2.9-3; pink color spectrum). We tentatively assign this resonance to species (**i**) which displayed an equilibrium between (**ia**) and (**ib**) at low temperature (Scheme 2.7). Similar observations have been previously reported by Glueck et al.[6a] In a separate NMR tube, the THF-d$_8$ solution of **2.1a** (3 mg, 0.0148 mmol) and **2.5** (10 mg, 0.0148 mmol) was frozen to -195 °C (LN$_2$) and base (NaOSiMe$_3$, 0.044 mmol) was added to the mixture. The NMR tube was quickly transferred to the spectrometer and was slowly warmed to -40 °C (from -195 °C), and ^{31}P NMR spectrum was recorded (Fig. 2.9-4; violet color spectrum). The low temperature spectrum revealed two doublet-of-doublets at -18.3 (dd, $^2J_{\text{P-P}}$

= 40 Hz, 106 Hz) and -26.1 ppm (dd, $^2J_{P\text{-}P}$ = 56 Hz, 117 Hz) that can be assigned to the phosphido-intermediate **(ii)** which again displays an equilibrium between isomers **(iia)** and **(iib)** (Scheme 2.7). It is most likely that the two isomers exchange very fast on the NMR time scale at room temperature and only a coalesced average broad signal was detected at room temperature (Fig. 2.8-2; red color spectrum). Thus, the two intermediates **(i)** and **(ii)** could be detected at low temperature and these NMR observations support the proposed mechanism in Scheme 2.6. The NMR findings are summarized in Table 2.5.

2.5.7. Self-assembly of P-stereogenic phosphine (2.6b)

2.5.7.1. Self-assembly of P-stereogenic phosphine (2.6b) on rhodium (2.10)
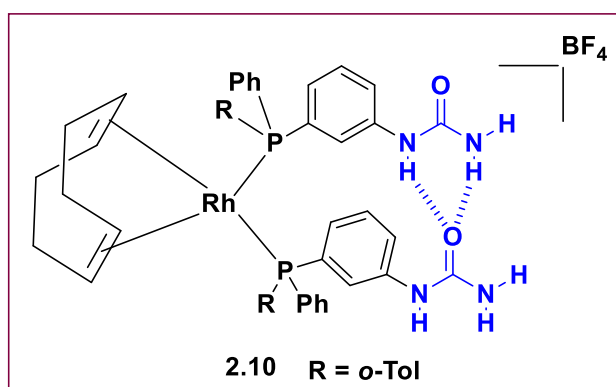
The supramolecular phosphine (**2.6b**) (0.0308 mmol, 2.2 eq.) and [Rh(COD)₂BF₄] (0.014 mmol, 1.0 eq.) were placed in a dry sample vial under argon atmosphere. DCM (1 mL) was added leading to a transparent solution. The mixture was stirred for 1 hour at room temperature. After that volatiles were evaporated and the dark-red solid compound was dried under vacuum for 4 h at room temperature. The resultant material was isolated in near quantitative yields and was analysed by spectroscopic techniques. Observation of a ^{31}P NMR resonance at 21.0 ppm clearly suggested the phosphine coordination and formation of Rhodium complex (Fig. 2.34). However, the proton NMR was very broad (due to counter anion BF₄) and reliable information could not be retrieved (Fig. 2.35). The existence of hydrogen bonding was attested by the change in CO stretching frequencies from 1669 (free **2.6b**) to 1683 cm^{-1} (Fig. 2.36 and 2.37). Although the shift is very small, similar shifts have been accounted for hydrogen bonding interactions.[9] Given the interference of BF₄ anion in proton NMR, we attempted the self-assembly of **2.6b** on a palladium template and the details are reported in the following (2.5.7.2) section.

2.5.7.2. Self-assembly of P-stereogenic phosphine (2.6b) on Palladium (2.11)

The supramolecular phosphine (**2.6b**) (2 mmol, 2 eq.) and [Pd(COD)Cl$_2$] (1 mmol) were placed in a dry sample vial under argon atmosphere. DCM (5 mL) was added leading to a transparent solution. The mixture was stirred for 1 h at room temperature. After that volatiles were evaporated and the yellow solid compound was dried under vacuum for 4 h at room temperature. The resultant material was isolated in near quantitative yields and was analysed by spectroscopic techniques. Observation of a ^{31}P NMR resonance at 18.5 ppm clearly suggested the phosphine coordination and formation of palladium complex (Fig. 2.38). The down field shift of the NH protons in **2.11** as compared to the free ligand **2.6b** may be attributed to hydrogen bonding (Fig. 2.42), although NH shift is very sensitive to various parameter.
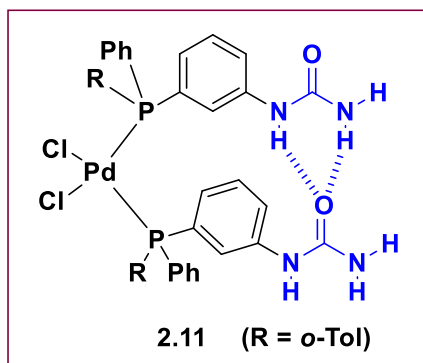
^{1}H NMR (500 MHz, DMF-d$_7$, 298 K) δ = 8.95 (s, 2H, N*H*), 7.94 (s, 2H, Ar) 7.84 (s, 4H, Ar), 7.71-7.69 (m, 2H, Ar), 7.63-7.48 (m, 6H, Ar), 7.46-7.31 (m, 8H, Ar), 7.19 (t, $J_{\text{H-H}}$ = 7.6 Hz, 2H, Ar), 6.97 (s, 2H, Ar), 5.98 (s, 4H, N*H$_2$*), 2.73 (s, 3H, C*H$_3$*), 2.72 (s, 3H, C*H$_3$*). **^{13}C NMR** (125 MHz, DMSO-d$_6$, 298 K) δ = 155.8 (s, *C*O), 141.4 (s, Ar, quat.), 140.5 (s, Ar, quat.), 135.5 (s, Ar, *C*H), 134.6 (d, $J_{\text{C-P}}$ = 11 Hz, Ar, *C*H), 132.3 (s, Ar, *C*H), 131.1 (m, Ar, *C*H), 130.9 (s, Ar, *C*H), 130.7 (s, Ar, *C*H), 130.6 (s, Ar, *C*H), 129.5 (s, Ar, quat), 129.3 (s, Ar, quat), 129.1 (s, Ar, quat.), 128.6 (s, Ar, *C*H), 128.4 (m, Ar, *C*H), 128.2 (m, Ar, *C*H), 127.9 (m, Ar, *C*H), 125.5 (s, Ar, *C*H), 123.9 (m, Ar, *C*H), 120.2 (s, Ar, *C*H), 120.0 (s, Ar, *C*H), 23.0 (t, $J_{\text{C-P}}$ = 5 Hz, *C*H$_3$), **^{31}P NMR** (500 MHz, DMSO-d$_6$, 298 K) δ = 18.5 (d, $J_{\text{P-P}}$ = 11.6 Hz, P). **IR** (cm^{-1}): 3313 (NH$_2$), 3326 (NH$_2$), 3201 (NH), 1663 (C=O).

2.6 Characterization of compounds
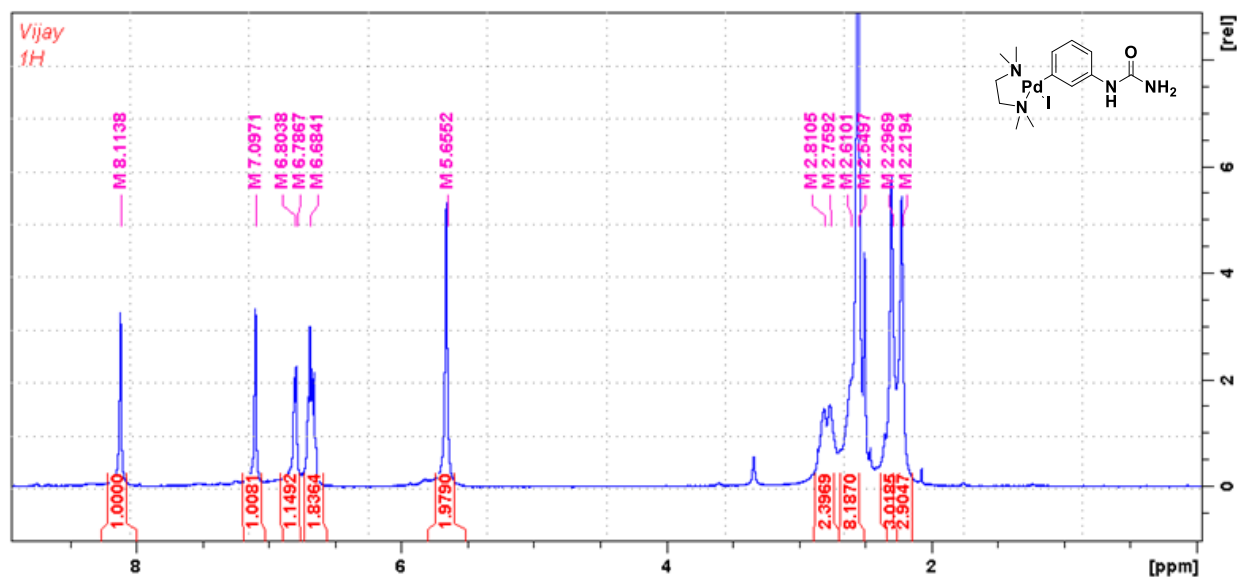
Figure 2.19: ^{1}H NMR (in DMSO-d[6]) spectrum of complex **2.3**.
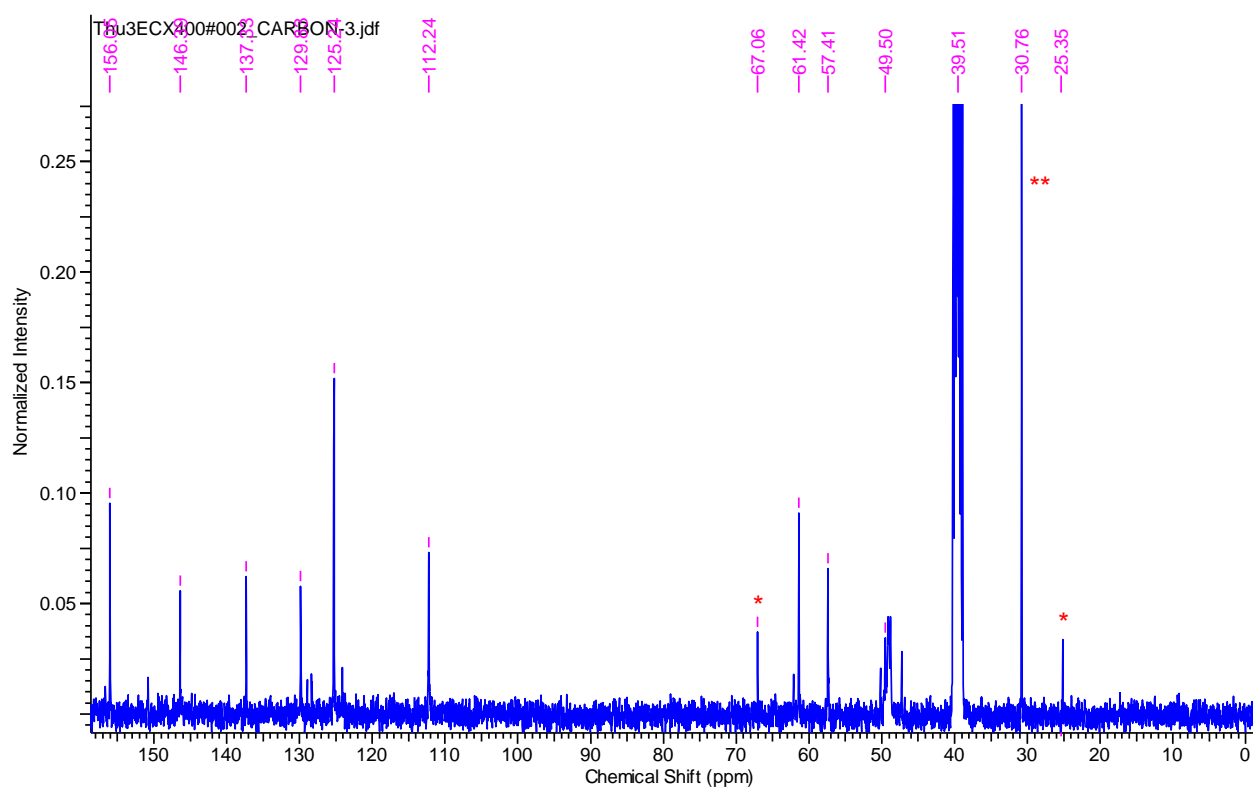
Figure 2.20: ^{13}C NMR (in DMSO-d[6]) spectrum of complex 2.3 (*= THF, ** = Acetone).
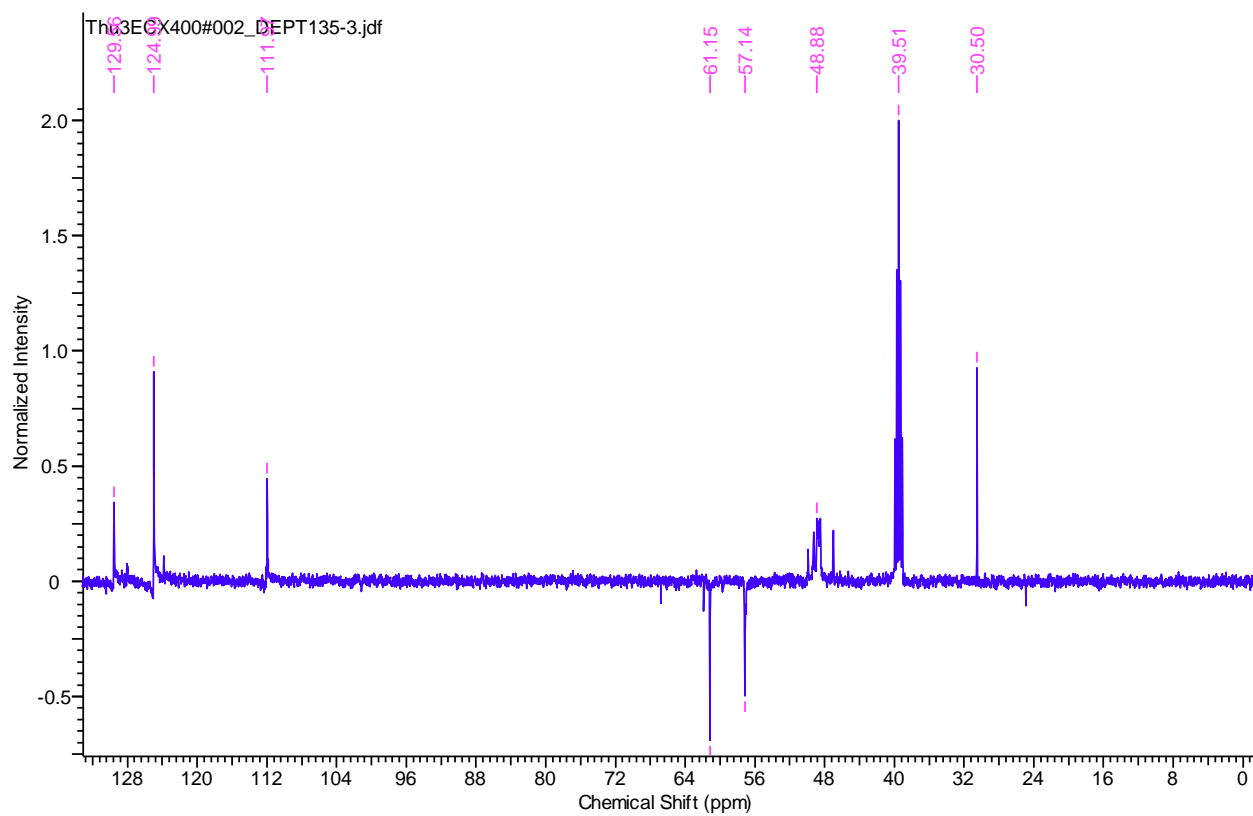
Figure 2.21: DEPT spectrum of complex **2.3** in DMSO-d$_6$ at 298K.
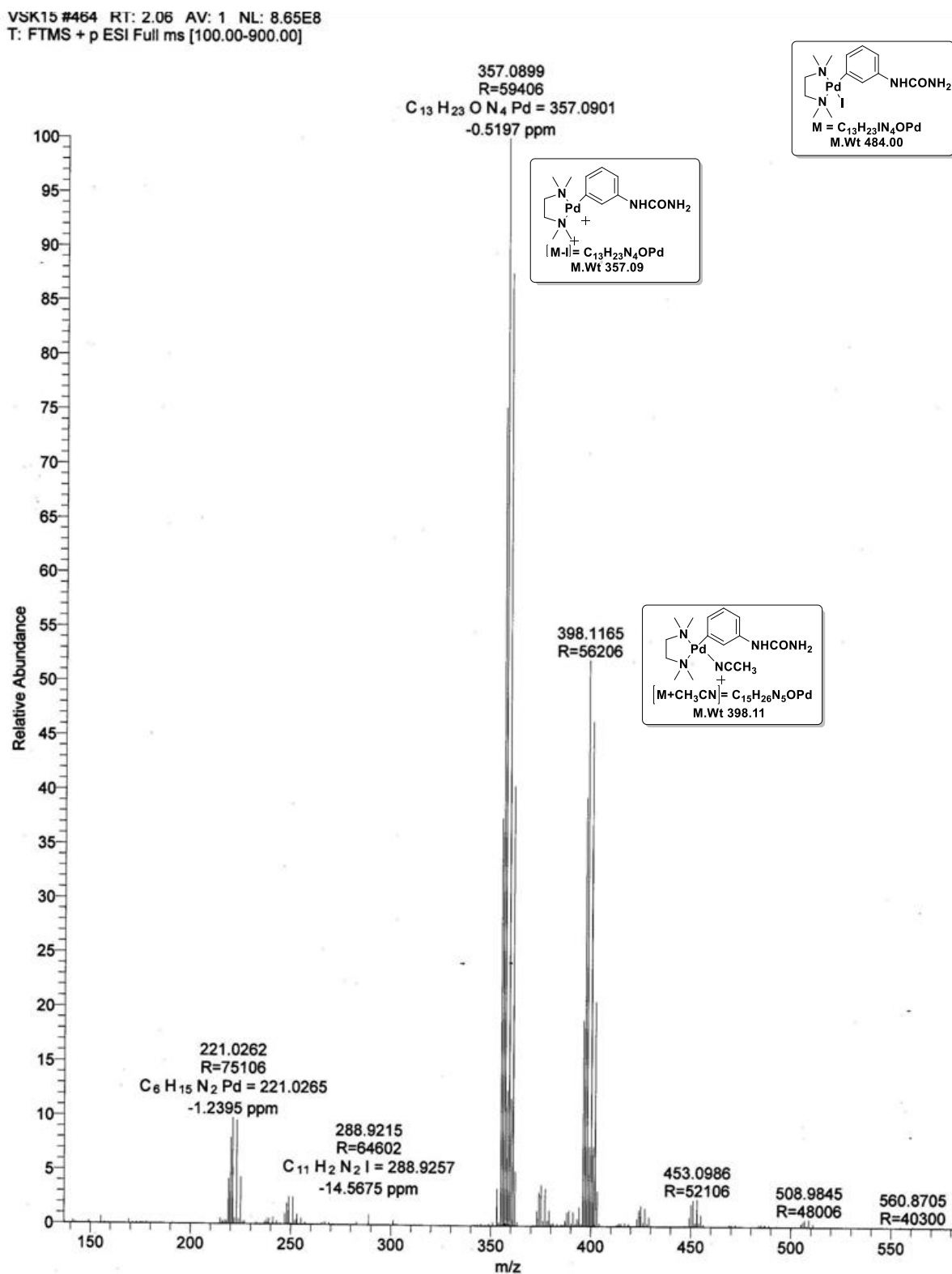
Figure 2.22: ESI-MS (+ve mode) spectrum of complex **2.3**.
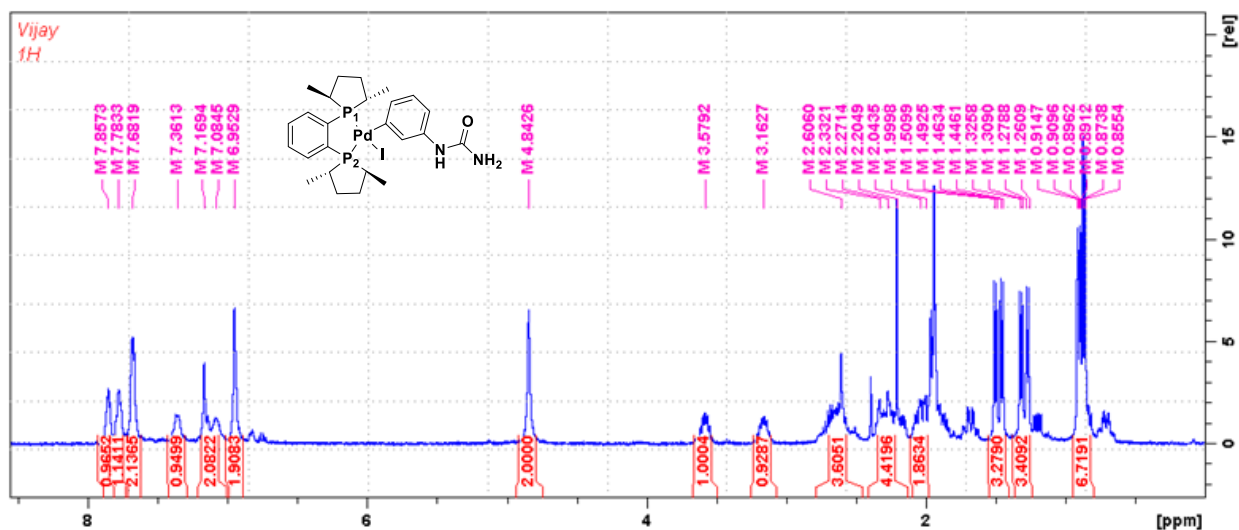
Figure 2.23: ¹H NMR spectrum of complex **2.5** in CD₃CN.
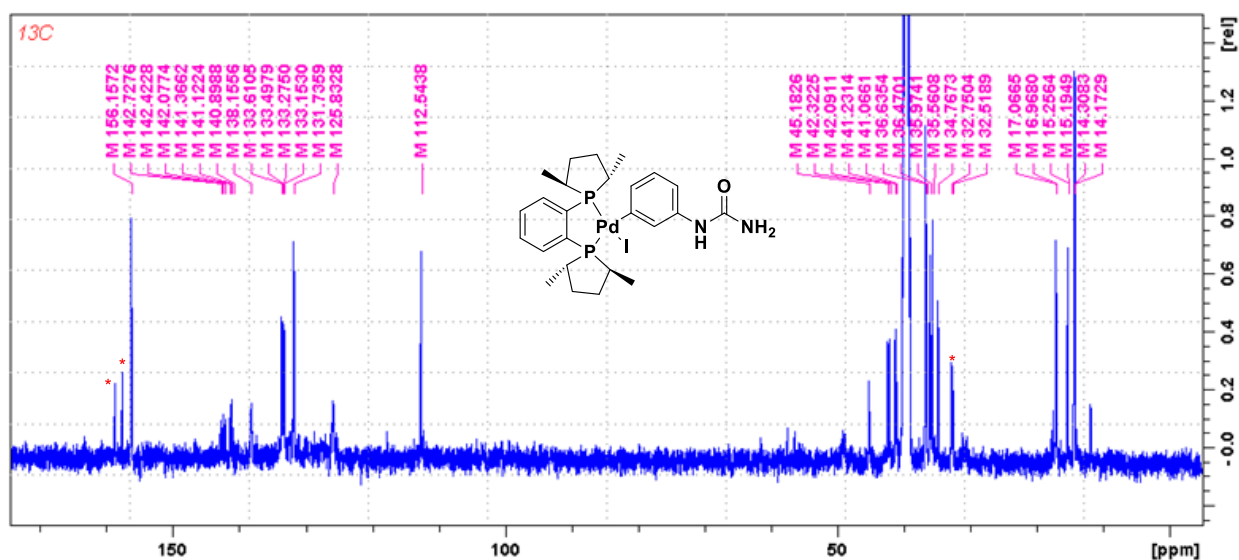
Figure 2.24: ¹³C NMR (in DMSO-d₆) spectrum of complex **2.5** (* = DMF).
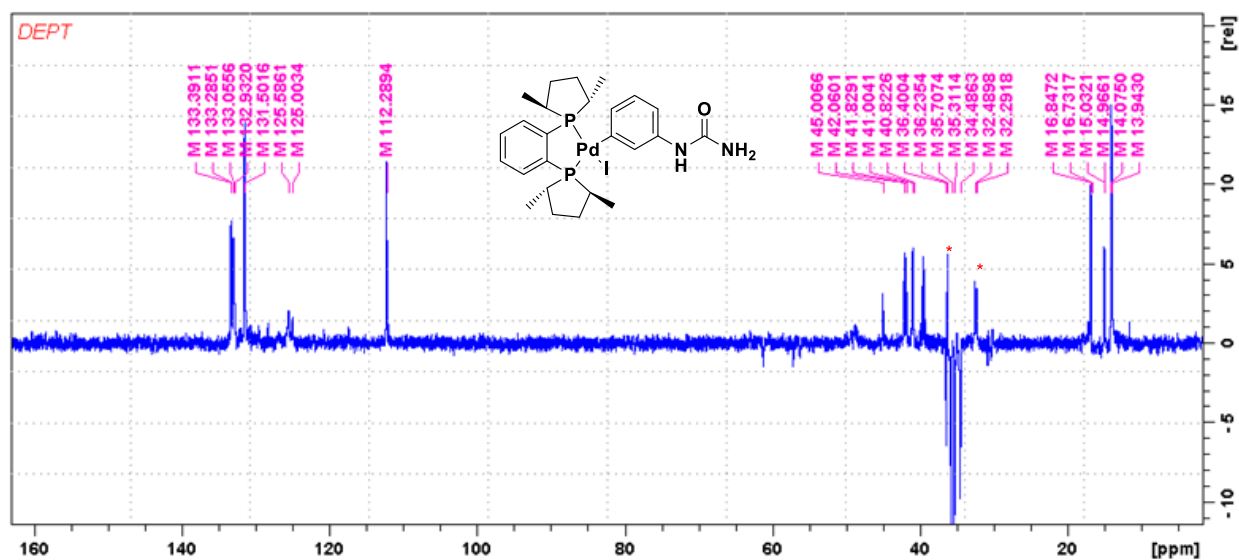
Figure 2.25: DEPT NMR (in DMSO-d₆) spectrum of complex **2.5** (* = DMF).
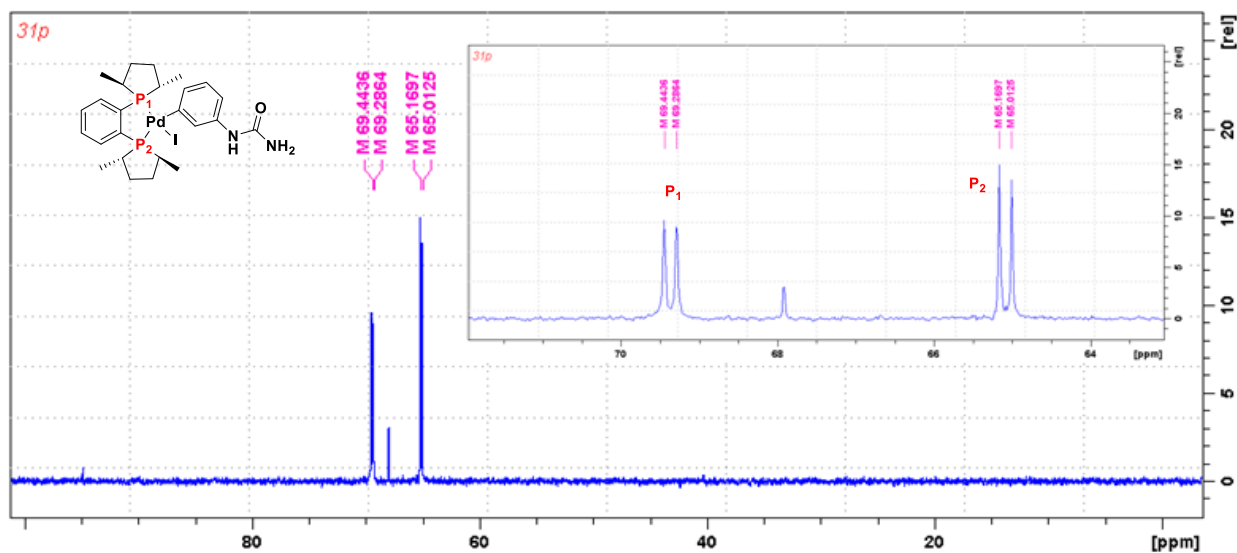
Figure 2.26: ^{31}P NMR spectrum of complex **2.5** in CD$_3$CN.
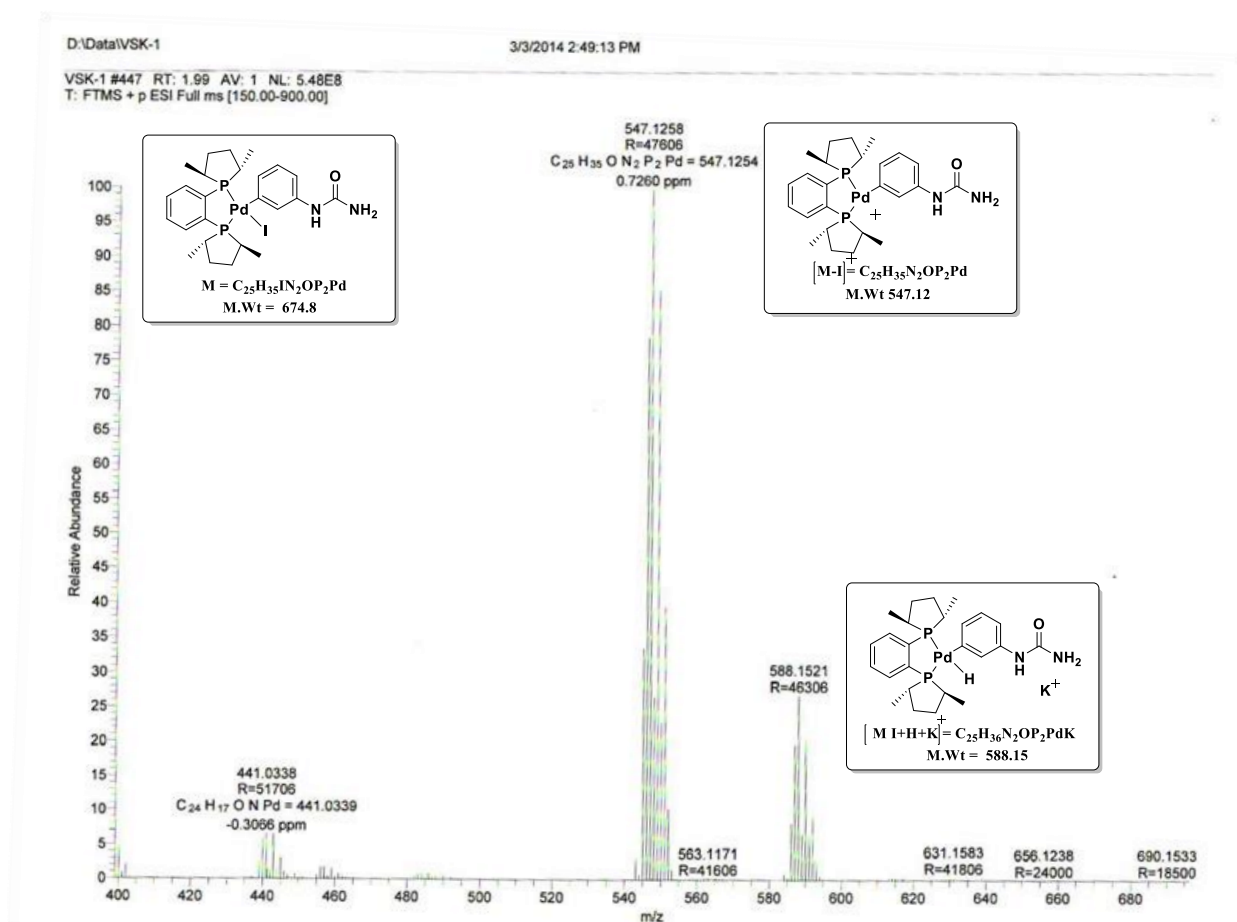
Figure 2.27: ESI-MS (+ve) spectrum of complex 2.5 in acetonitrile.
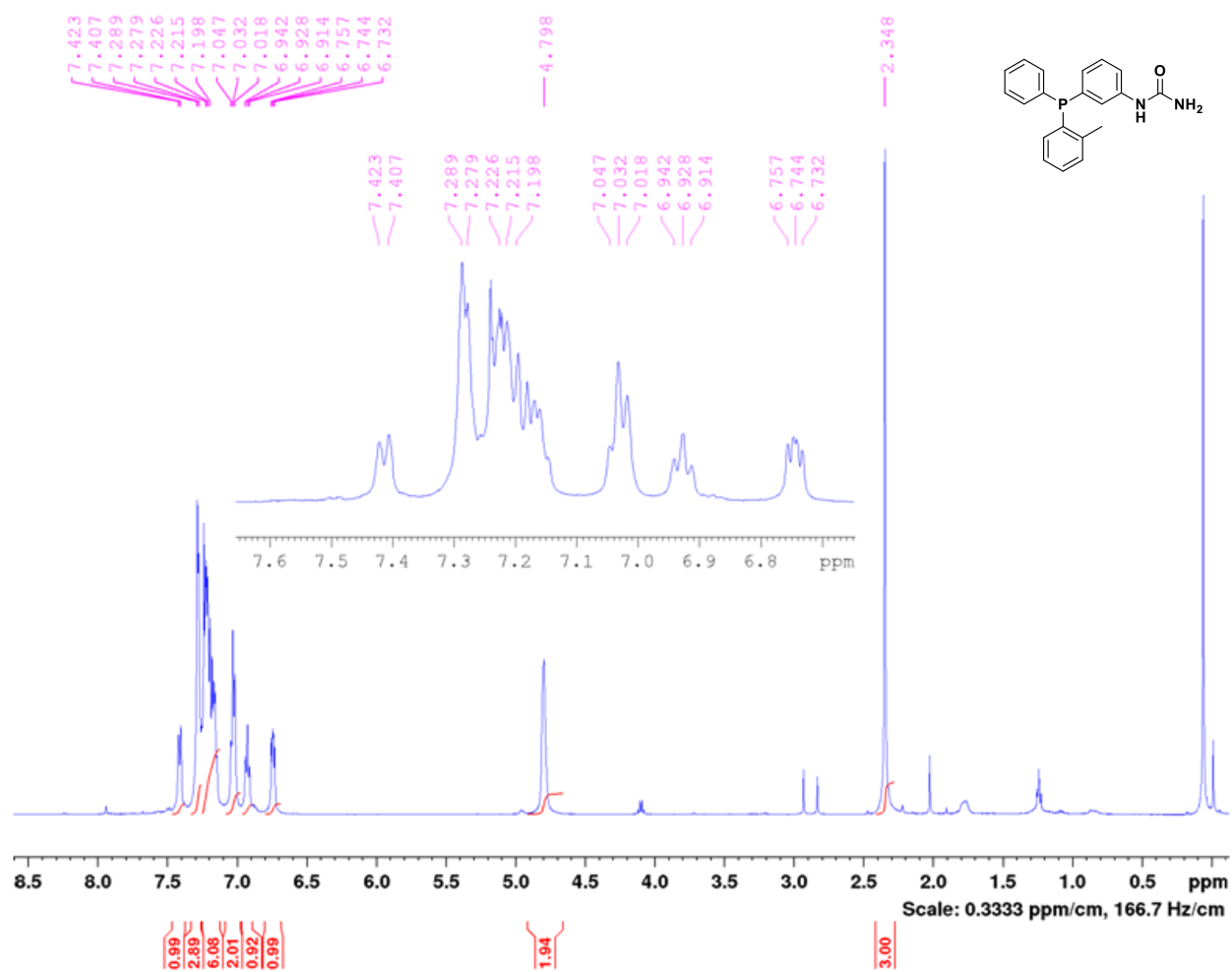
Figure 2.28: ^{1}H NMR spectrum of 1-(3-(phenyl(o-tolyl)phosphanyl)phenyl)urea (**2.6b**) in CDCl$_3$.
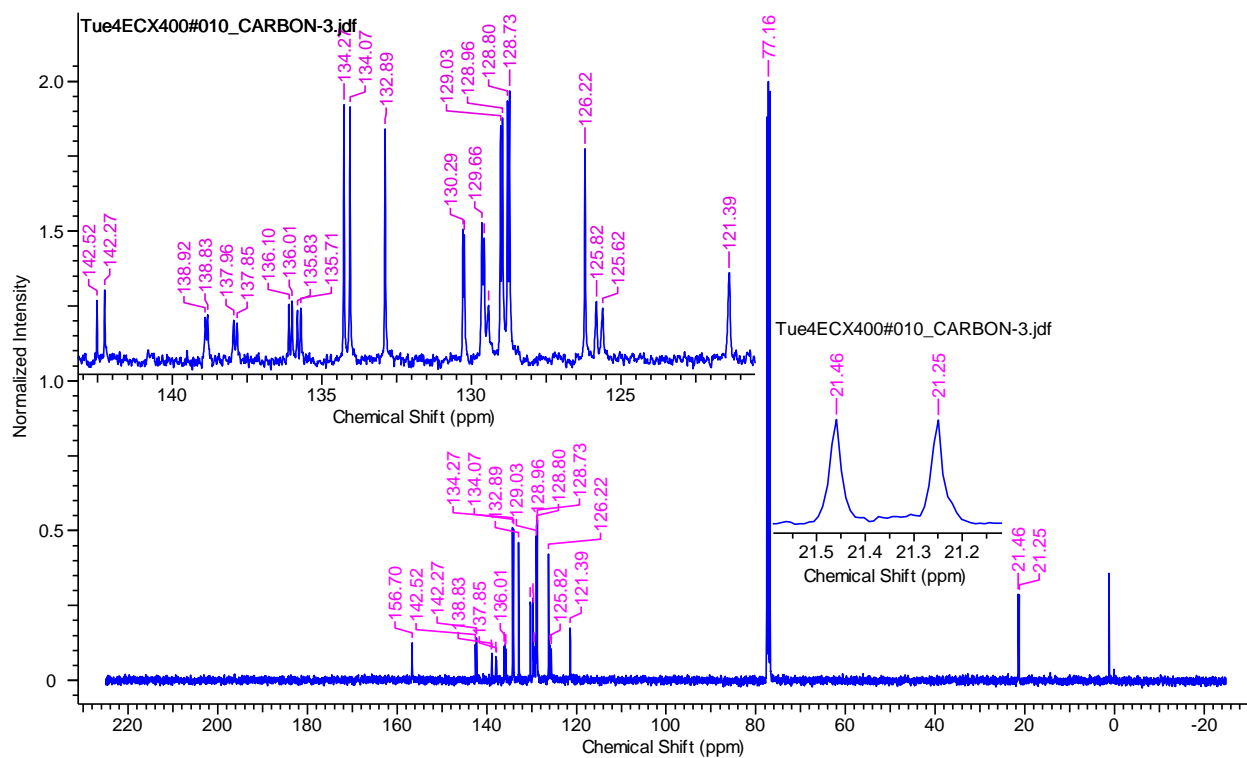
Figure 2.29: ^{13}C NMR spectrum of 1-(3-(phenyl(o-tolyl)phosphanyl)phenyl)urea (**2.6b**) in CDCl$_3$.
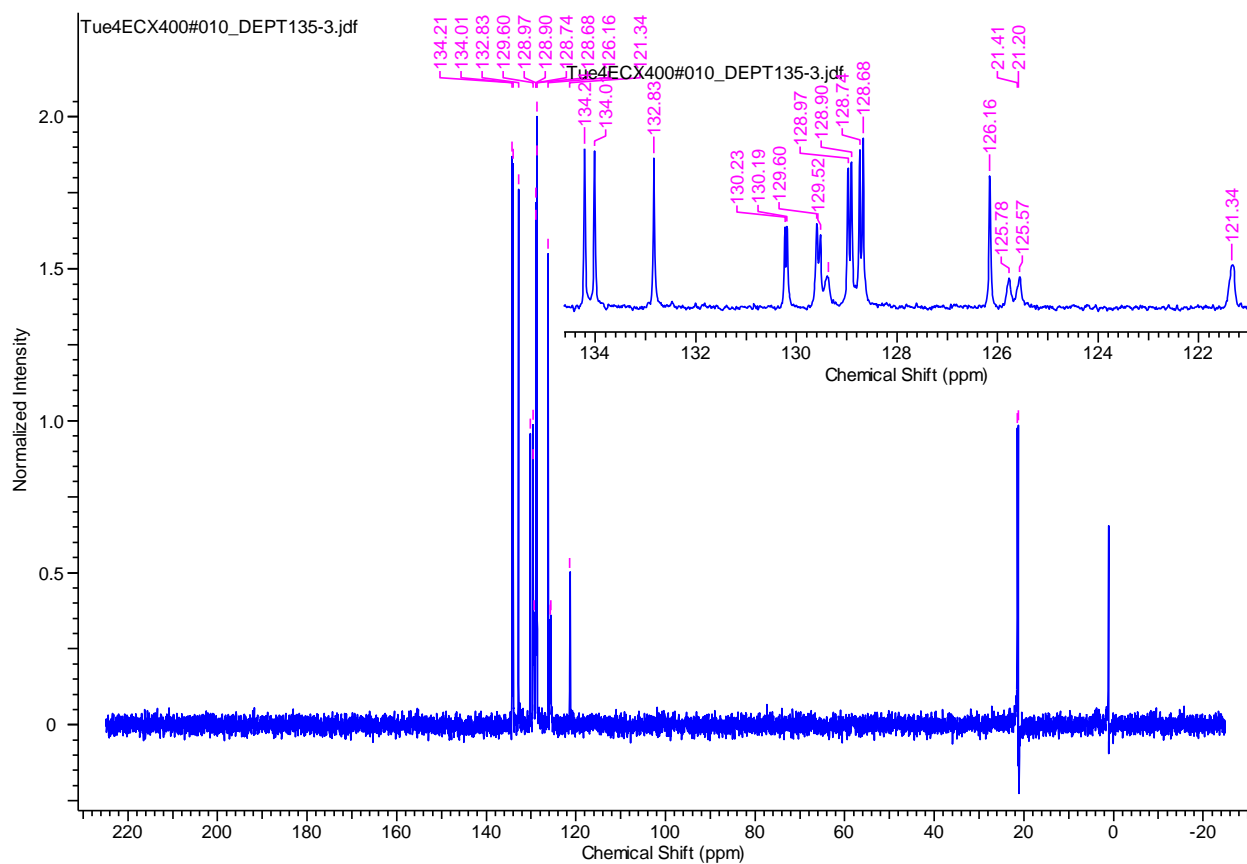
Figure 2.30: DEPT spectrum of 1-(3-(phenyl(o-tolyl)phosphanyl)phenyl)urea (**2.6b**) in CDCl$_3$.
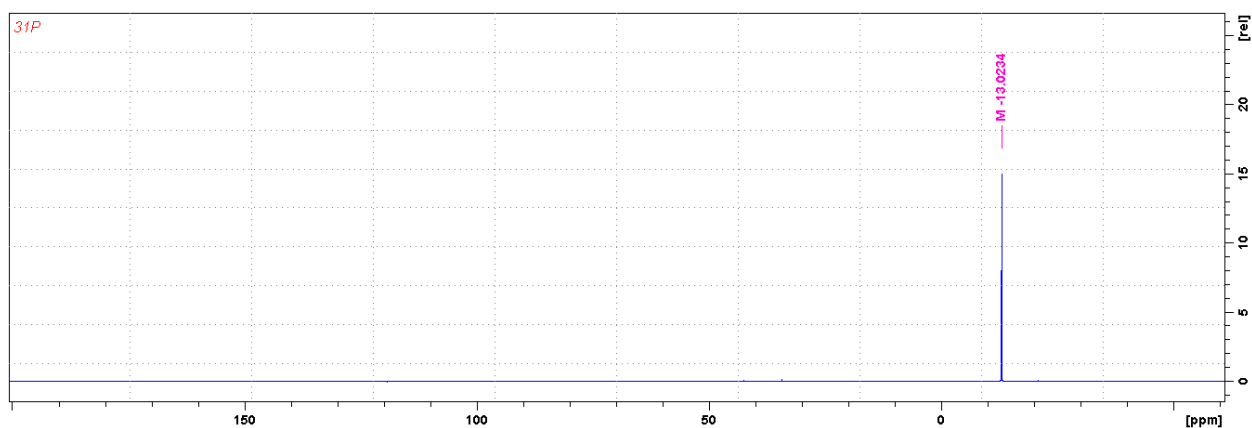
Figure 2.31: ^{31}P NMR spectrum of 1-(3-(phenyl(o-tolyl)phosphanyl)phenyl)urea (**2.6b**) in CDCl$_3$.
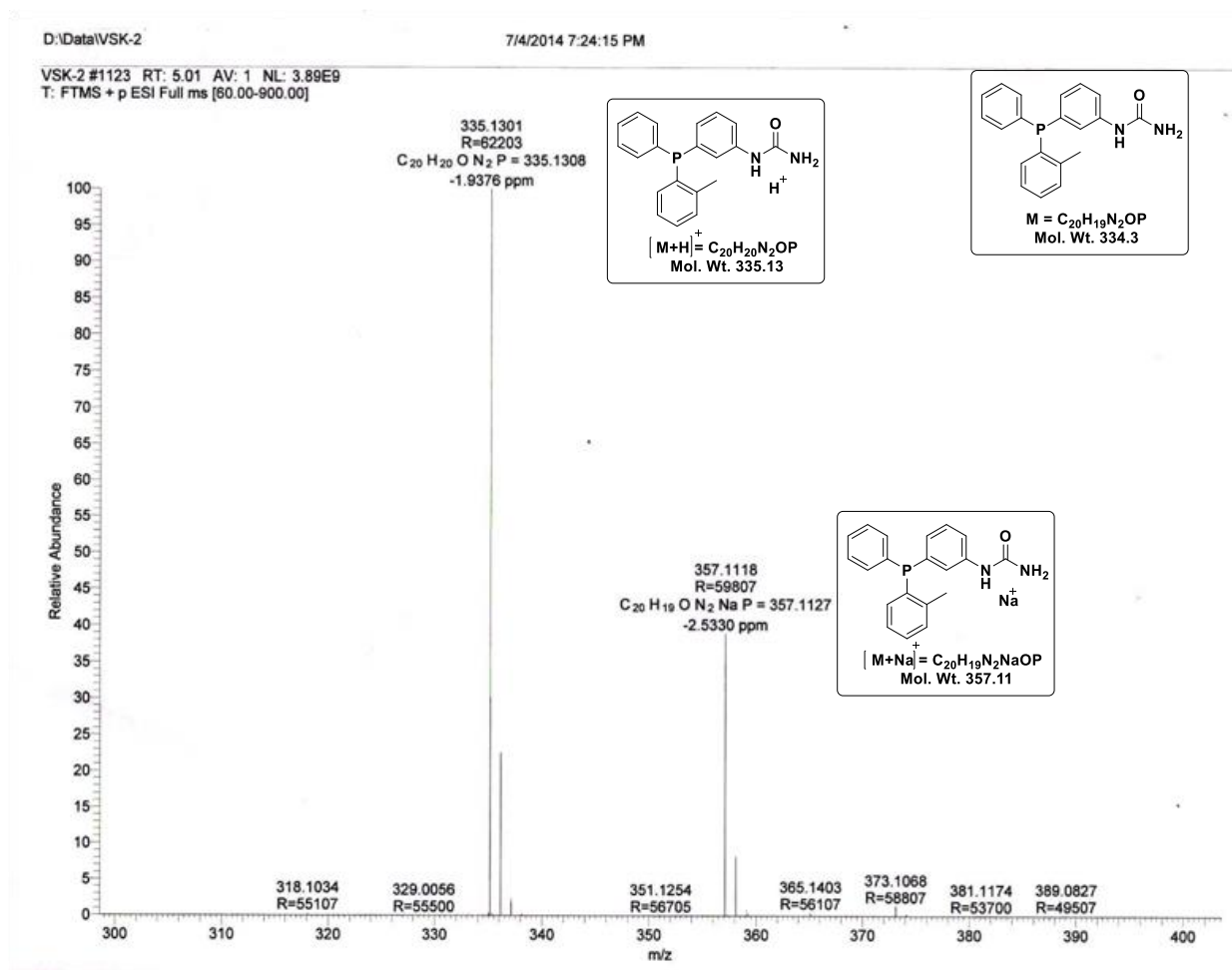
Figure 2.32: ESI-MS (+ve) spectrum of **2.6b** in methanol.
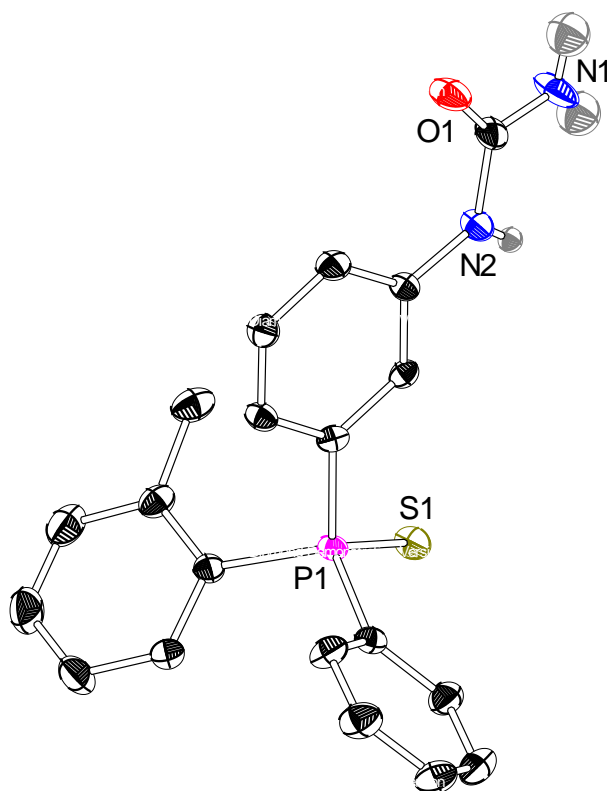
Figure 2.33: Molecular structure of **2.8b**; thermal ellipsoids are drawn at 50% probability level, solvent molecules and H-atoms (except urea) are omitted for clarity.

Table 2.6: Crystal data and structural refinement parameters for **2.8b** (**CCDC: 1046370**).

Formula sum	$C_{21}H_{21}Cl_2N_2OPS$
Formula weight	451.33 g/mol
Crystal system	monoclinic
Space-group	P 1 21/n 1 (14)
Cell parameters	a=15.1568(3) Å b=9.2688(2) Å c=15.4616(4) Å β=99.887(1)°
Cell ratio	a/b=1.6352 b/c=0.5995 c/a=1.0201
Cell volume	2139.87(8) Å^3
Z	4
Calc. density	1.40085 g/cm^3
RAll	0.0704
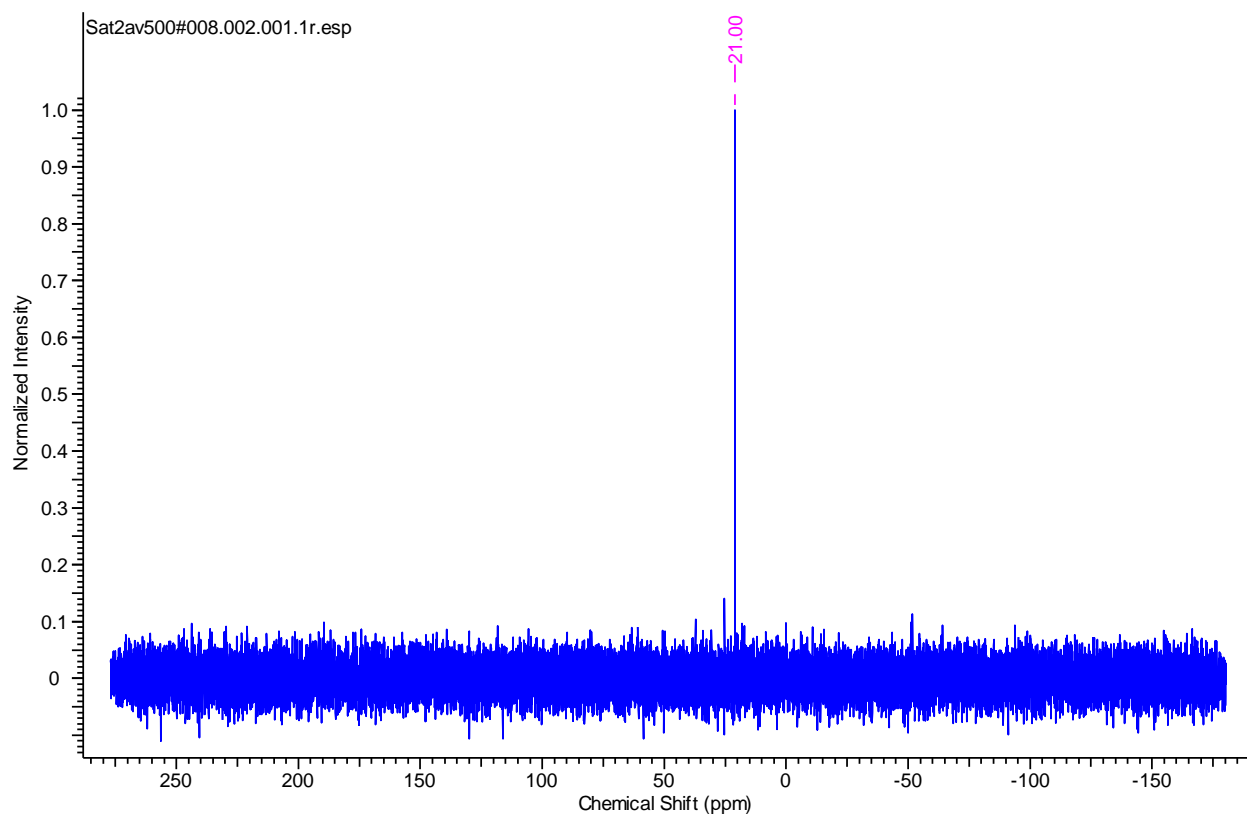
Figure 2.34: ^{31}P NMR spectrum of the self-assembled complex **2.10** in CDCl$_3$.
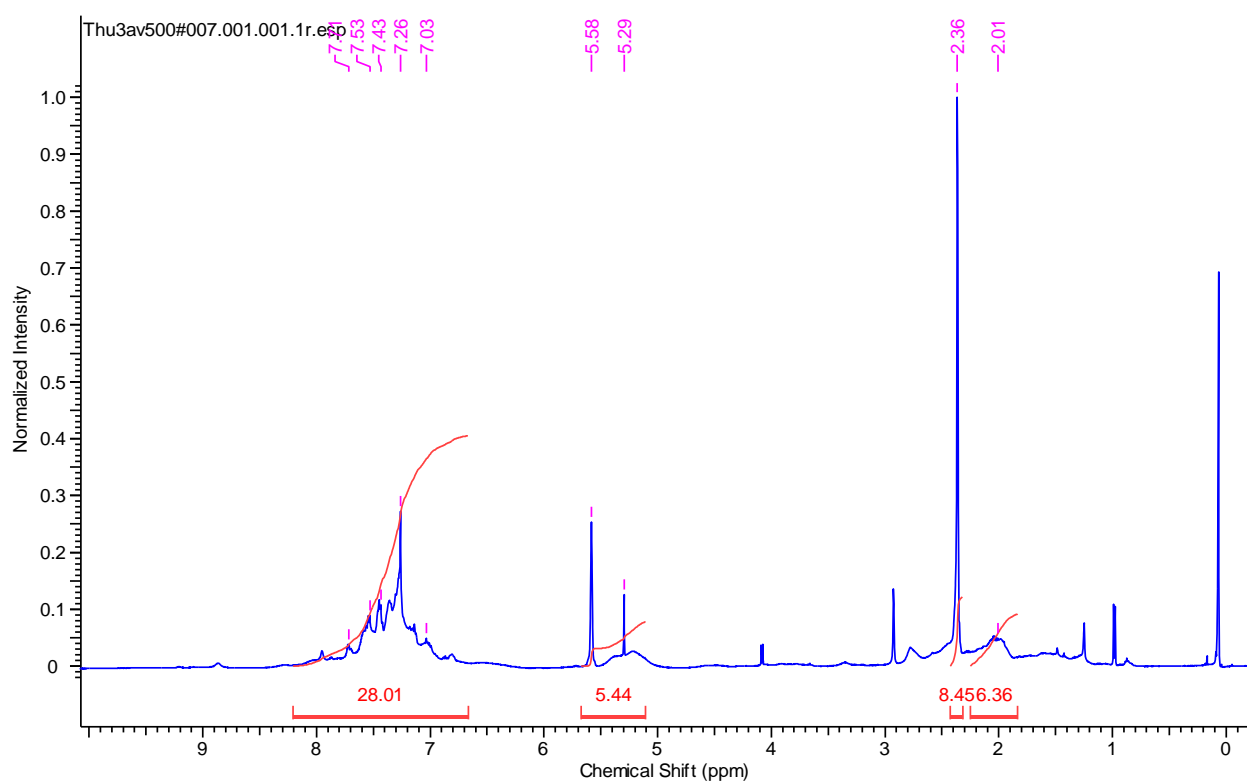
Figure 2.35: ^{1}H NMR spectrum of the self-assembled complex **2.10** in CDCl$_3$.
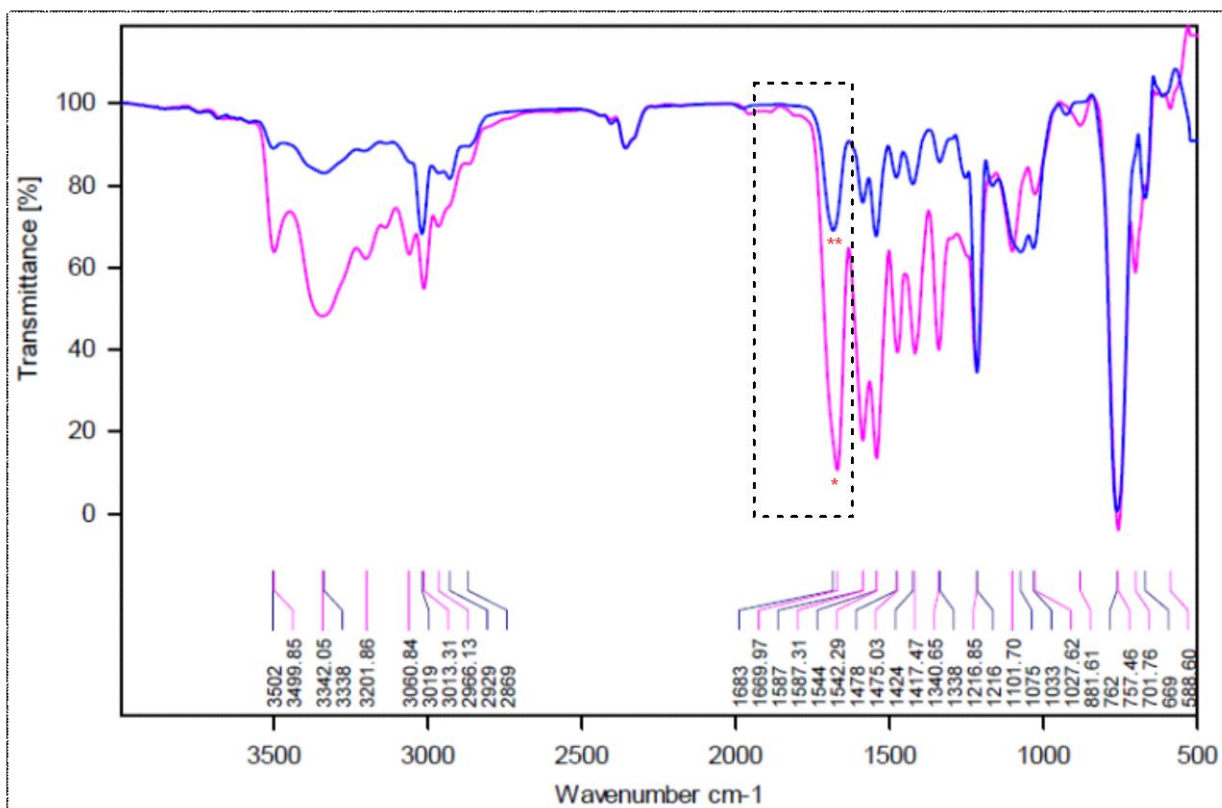
Figure 2.36: IR spectrum of the self-assembled Rh-complex 2.10 (**blue) and ligand 2.6b (*pink).
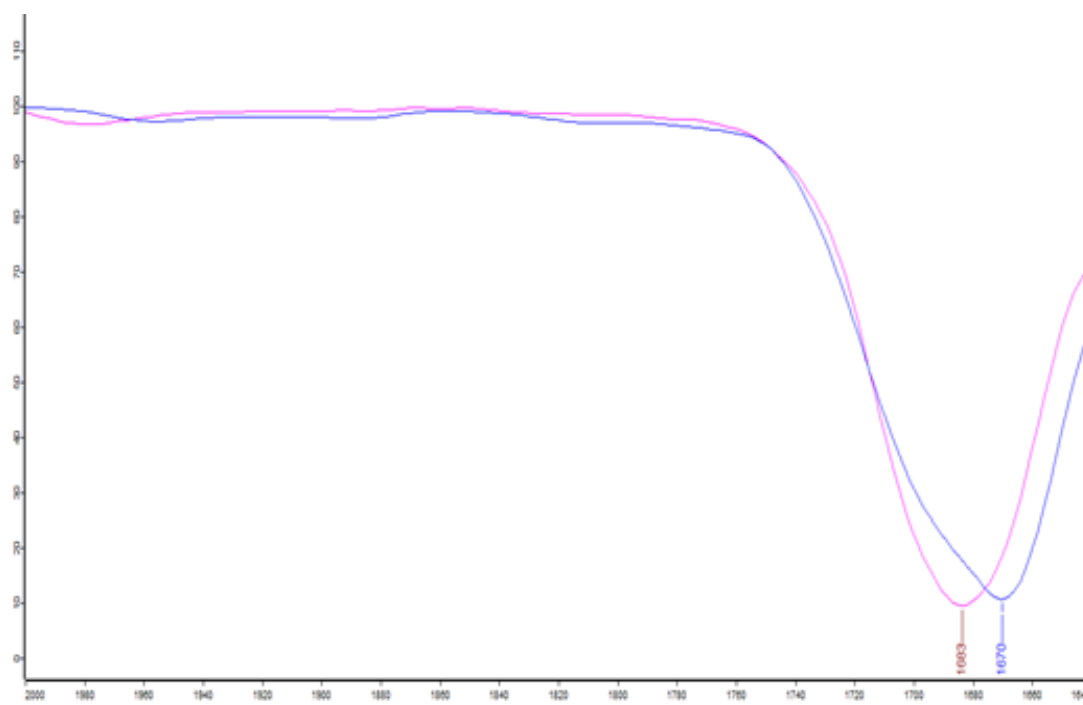
Figure 2.37: Zoomed Infrared spectrum of the self-assembly 2.10 (pink) and free 2.6b (blue) displaying the C=O stretching bands.
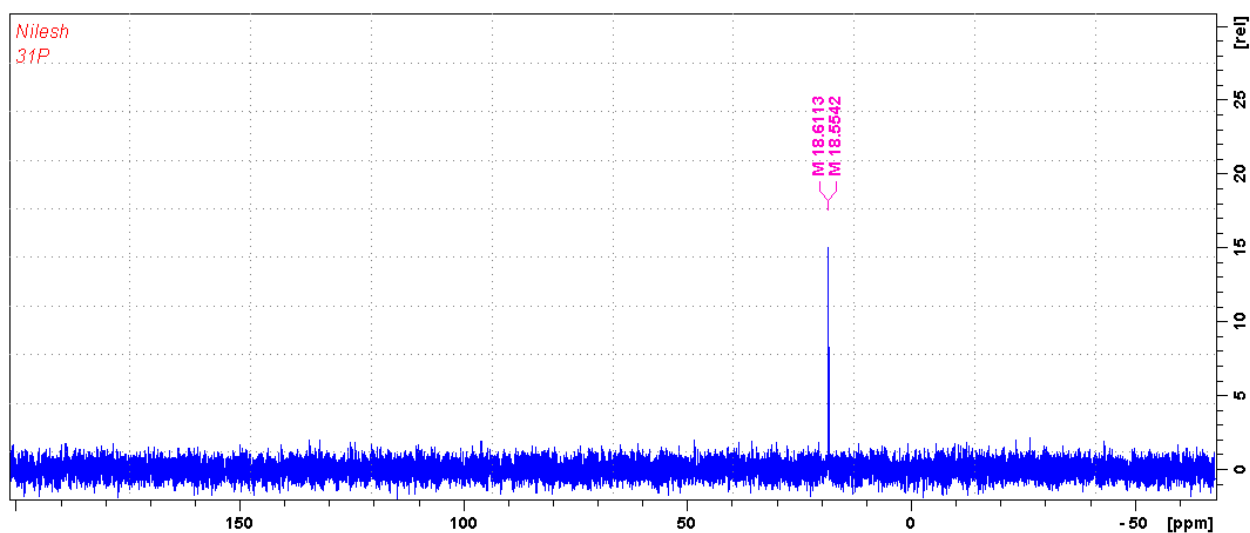
Figure 2.38: ^{31}P NMR spectrum of the self-assembled complex **2.11** in DMSO-d_6.
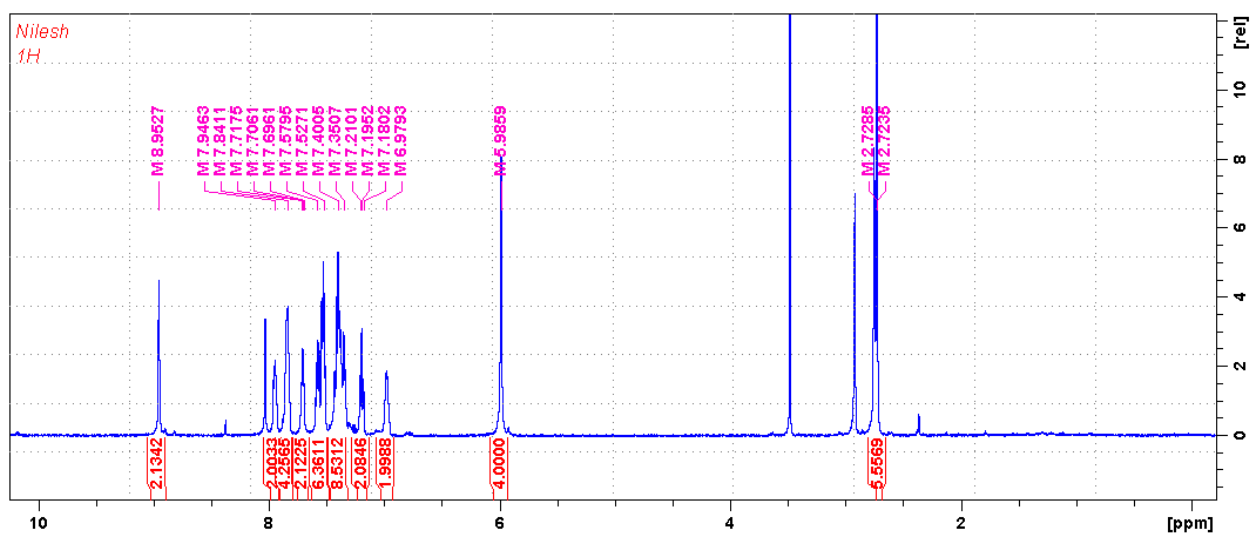
Figure 2.39: ^{1}H NMR spectrum of the self-assembled complex **2.11** in DMSO-d6.
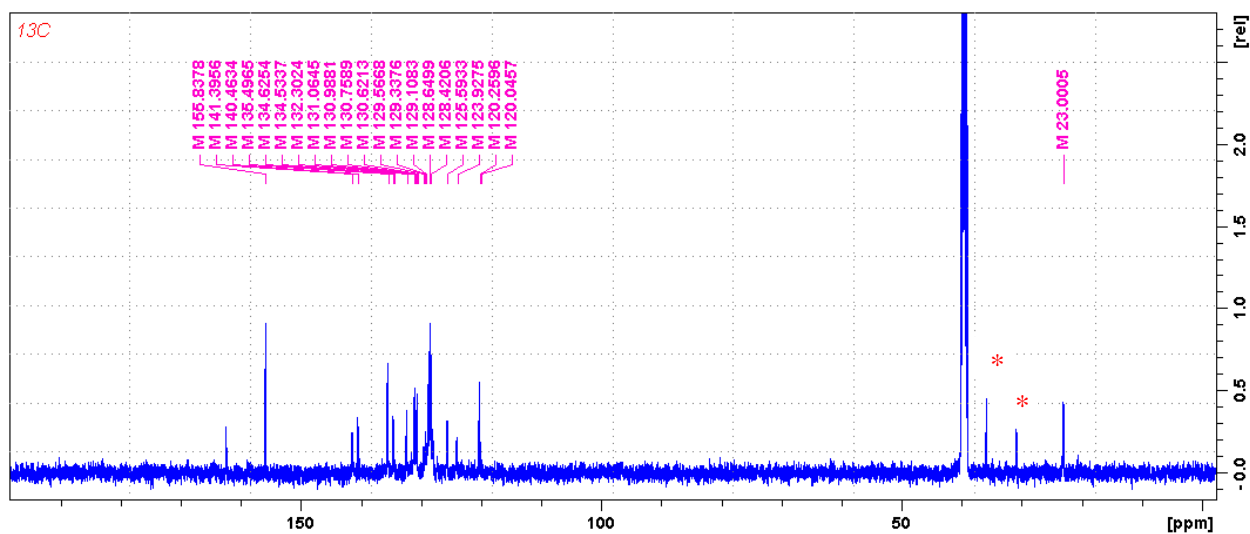
Figure 2.40: ^{13}C NMR spectrum of the self-assembled complex **2.11** in DMSO-d_6 (* DMF).
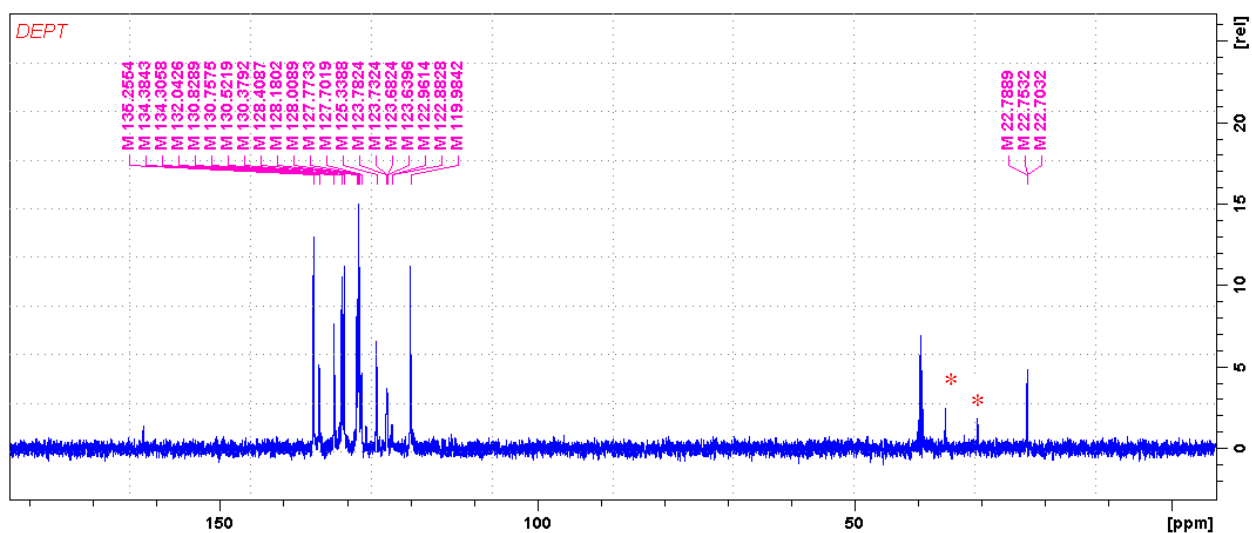
Figure 2.41: ^{13}C NMR (DEPT) spectrum of the self-assembled complex **2.11** in DMSO-d_6 (* DMF).
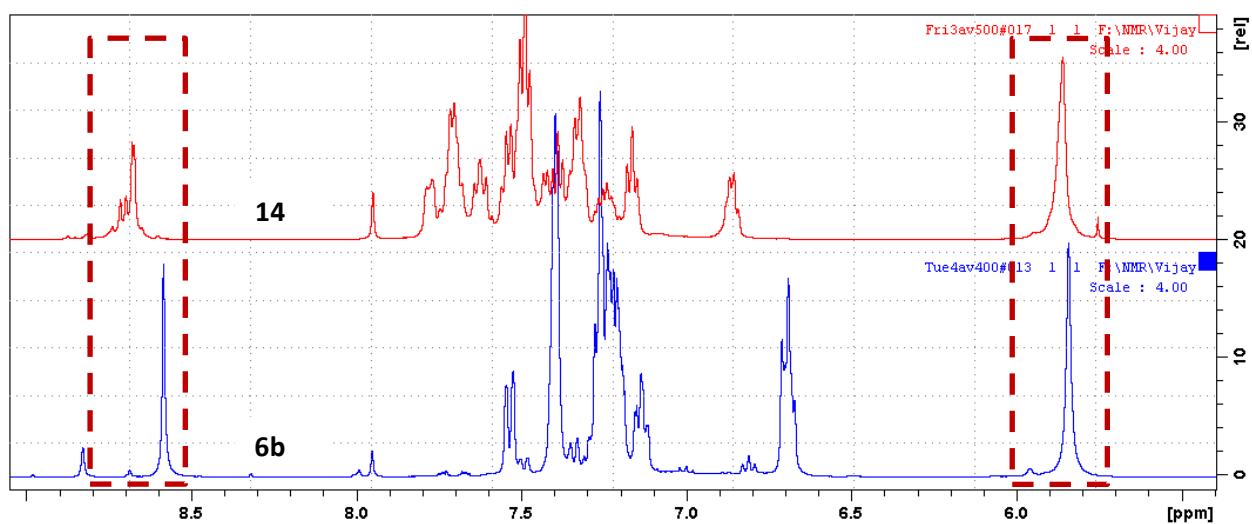
Figure 2.42: Stacked ^1H NMR of **2.6b** (blue curve: bottom) and self-assembled Pd-complex **2.11** (red curve: top) in DMSO-d_6, displaying the N$\underline{H}$ shift.

2.7.   References

(1)   a) R. R. Noyori, *Asymmetric Catalysis in Organic Synthesis,* Wiley-Interscience, New York, 1994; b) W. S. Knowles, *Asymmetric Catalysis on Industrial Scale, Challenges, Approaches, and Solutions (Eds.: H. U. Blaser and E. Schmidt),* Wiley-VCH, Weinheim, 2004, pp 23-38.

(2)   T.Ohkuma, M. Kitamura and R. Noyori, *Catalytic Asymmetric Synthesis*, Wiley-VCH, New York, 1993.

(3)   The p-stereogenic phosphines earned Prof. Knowles the 2001 Nobel Prize, for more details see: a) B. D. Vineyard, W. S. Knowles, M. J. Sabacky, G. L. Bachmann and D. J. Weinkauff, *J. Am. Chem. Soc.,* 1977, **99**, 5946-5952; b) W. S. Knowles, *Angew. Chem. Int. Ed.,* 2002, **41**, 1998-2007 and the references there in.

(4)   A. Grabulosa, J. Granell and G. Muller, *Coord. Chem. Rev.,* 2007, **251,** 25-90.

(5)   Chiral auxiliary based synthesis of p-chiral phosphines is the most established method to prepare p-chiral phosphines on larger scale; for the synthesis, see: a) K. M. Pietrusiewicz and M. Zablocka, *Chem. Rev.,* 1994, **94**, 1375-1411; b) W. Tang, and X. Zhang, *Chem. Rev*., 2003, **103**, 3029-3070; c) J. Bayardon and S. Juge, *Phosphorus (III) Ligands in Homogeneous Catalysis: Design and Synthesis (Eds.: P. C. J. Kamer and P. W. N. M. van Leeuwen)*, Jon Wiley & Sons Ltd., 2012, pp 335; d) T. Imamoto, K. Tamura, Z. Zhang, Y. Horiuchi, M. Sugiya, K. Yoshida, A. Yanagisawa and A. D. Gridnev, *J. Am. Chem. Soc.,* 2012, **134**, 1754-1769; e) T. Imamoto, Y. Saitoh, A. Koide, T. Ogura and K. Yoshida, *Angew. Chem. Int. Ed.,* 2007, **46**, 8636-8639; f) A. Karim, A. Mortreux, F. Petit, G. Buono, V. Peiffer and C. Siv, *J. Organomet. Chem.,* 1986, **317**, 93-104.

(6)   a) J. R. Moncarz, M. F. Laritcheva and D. S. Glueck, *J. Am. Chem. Soc.,* 2002, **124**, 13356-13357; b) J. R. Moncarz, T. J. Brunker, J. C. Jewett, M. Orchowski and D. S. Glueck, *Organometallics,* 2003, **22**, 3205-3221; c) N. F. Blank, J. R. Moncarz, T. J. Brunker, C. Scriban, B. J. Anderson, O. Amir, D. S. Glueck, L. N. Zakharov, J. A. Golen, C. D. Incarvito and A. L. Rheingold, *J. Am. Chem. Soc.,* 2007, **129**, 6847-6858; d) N. F. Blank, K. C. McBroom, D. S. Glueck, W. S. Kassel and A. L. Rheingold, *Organometallics,* 2006, **25**, 1742-1748; e) D. Julienne, O. Delacroix, J. F. Lohier, J. S. de Oliveira-Santos and A. C. Gaumont, *Eur. J. Inorg. Chem.,* 2011, **16**, 2489-2498; (f) D. S. Glueck, *Chem. Eur. J.,* 2008, **14**, 7108-7117.

(7)   a) P. Y. Renard, P. Vayron and C. Mioskowski, *Org. Lett.,* 2003, **5**, 1661-1664; b) J. M. Tackas, D. S. Reddy, S. A. Moteki, D. Wu and H. Palencia, *J. Am. Chem. Soc*., 2004, **126**, 4494-4495.

(8)   For reviews on supramolecular catalysis, see: a) P. Dydio and J. N. H. Reek, *Chem. Sci.,* 2014, **5**, 2135-2145; b) T. Besset, R.Gramage-Doria and J. N. H. Reek, *Angew. Chem. Int. Ed.,* 2013, **52**, 8795-8797; c) A. J. Sandee and J. N. H. Reek, *Dalton Trans.,* 2006, 3385-3391; d) B. Breit, *Angew. Chem. Int. Ed.,* 2005, **44**, 6816-6825; e) M. J. Wilkinson, P. W. N. M. van Leeuwen and J. N. H. Reek, *Org. Biomol. Chem.,* 2005, **3**, 2371-2383.

(9)   a) P. A. R. Breuil, F. W.Patureau and J. N. H. Reek, *Angew. Chem. Int. Ed.,* 2009, **48**, 2162-2165; b) M. T. Reetz and S. R. Waldvogel, *Angew. Chem. Int. Ed.,* 1997, **36**, 865-867.

(10)   a) For supramolecular phosphines in hydroformylation, see: a) T. Besset, D. W. Norman and J. N. H. Reek, *Adv. Synth. Catal.,* 2013*,* **355***,* 348-352; b) P. Dydio, R. J. Detz and J. N. H. Reek, *J. Am. Chem. Soc.,* 2013, **135**, 10817-10828; c) D. Fuchs, G. Rousseau, L. Diab, U. Gellrich, and B. Breit, *Angew. Chem. Int. Ed.,* 2012, **51**, 2178-2182; d) U. Gellrich, W. Seiche, M. Keller and B. Breit, *Angew. Chem. Int. Ed.,* 2012, **51**, 11033-11038; e) P. Dydio, C. Rubay, T. Gadzikwa, M. Lutz and J. N. H. Reek, *J. Am. Chem. Soc.,* 2011,

133, 17176-17179. For supramolecular phosphorus ligands in hydroformylation see: a) P. Dydio and J. N. H. Reek, *Angew. Chem. Int. Ed.,* 2013, **52**, 3878-3882; b) T. Gadzikwa, R. Bellini, H. L. Dekker and J. N. H. Reek, *J. Am. Chem. Soc.,* 2012, **134**, 2860-2863; c) R. Bellini, S. H. Chikkali, G. Berthon-Gelloz and J. N. H. Reek, *Angew. Chem. Int. Ed.,* 2011, **50**, 7342-7345.

(11) M. de Greef and B. Breit, *Angew. Chem. Int. Ed.,* 2009, **48**, 551-554.

(12) a) D. Anselmo, R. Gramage-Doria, T. Besset, M. V. Escarcega-Bobadilla, G. Salassa, E. C. Escudero-Adan, B. M. Martinez, E. Martin, J. N. H. Reek and A. W. Kleij, *Dalton Trans.,* 2013, **42**, 7595-7603; b) L. Leclercq and A. R. Schmitzer, *Organometallics,* 2010, **29**, 3442-3449.

(13) a) V. S. Koshti, S. R. Gaikwad, and S. H. Chikkali *Coord. Chem. Rev.,* 2014, **265**, 52-73; b) S. A. Pullarkat and P. H. Leung, *Topics in Organomet. Chem.,* 2013, **43**, 145-166; c) J. S. Harvey and V. Gouverneur, *Chem. Commun.,* 2010, **46**, 7477-7485; d) V. S. Chan, M. Chiu, R. G. Bergman and F. D. Toste, *J. Am. Chem. Soc.,* 2009, **131**, 6021-6032; e) J. S. Harvey, S. J. Malcolmson, K. S. Dunne, S. J. Meek, A. L. Thompson, R. R. Schrock, A. H. Hoveyda and V. Gouverneur, *Angew. Chem. Int. Ed.,* 2009, **48**, 762-766; f) Q. Xu, C. Q. Zhao and L. B. Han, *J. Am. Chem. Soc.,* 2008, **130**, 12648-12655; g) N. Vinokurov, K. M. Pietrusiewicz, S. Frynas, M. Wiebcke and H. Butenschoen, *Chem. Commun.,* 2008, 5408-5410; h) B. J. Anderson, M. A. Guino-o, D. S. Glueck, J. A. Jolen, A. G. DiPasquale, L. M. Liable-Sands and A. L. Rheingold, *Org. Lett.,* 2008, **10**, 4425-4428; i) V. S. Chan, I. C. Stewart, R. G. Bergman and F. D. Toste, *J. Am. Chem. Soc.,* 2006, **128**, 2786-2787.

(14) See supporting information of the following article: Y. Huang, Y. Li, P. H. Leung and T. Hayashi, *J. Am. Chem. Soc.,* 2014, **136**, 4865-4868.

(15) Synthesis of 3-iodophenylurea (**2.2b**) has been reported, see ref. 9a. A modified protocol has been developed for the synthesis of **2.2b** and **2.2c**.

(16) The choice of a ligand is a very crucial parameter in asymmetric phosphination, as the substrate (secondary phosphine) and the product can potentially coordinate to the metal center and displace the ligand. Our ligand choice is based on the following criteria: a) Ligand should resist displacement from the metal; b) The ligand to metal coordination should be robust (preferably more than monodentate) and; c) Donor atoms on the ligand should be electron rich.

(17) The desired complex **2.5** was found to be unstable in solution over extended period of time. However, it is stable in solid state over months and do not decompose. Our attempts to crystalize **2.5** failed and only the undesired di-iodo-complex could be isolated.

(18) Phosphination with ortho-substituted aryl compounds has been reported by Glueck et al see ref. **2.6b**. However, in our case, ortho-substituted iodophenylurea failed to provide the anticipated coupling product.

(19) It is most likely that the urea protons interact with base and might consume 2 equivalent of base per urea group.

(20) Similar ^{31}P chemical shifts and mechanism was presented by Glueck et al see: a) J. R. Moncarz, T. J. Brunker, D. S. Glueck, R. D. Sommer and A. L. Rheingold, *J. Am. Chem. Soc.,* 2003, **125**, 1180-1181; b)

(21) Although the existence of species (**iii**) cannot be completely ruled out, no evidence supporting the existence of (**iii**) could be obtained.

(22) a) J. Wieland and B. Breit, *Nat. Chem.,* 2010, **2**, 832-837; b) J. Meeuwissen and J. N. H. Reek, *Nat. Chem.,* 2010, **2**, 615-621; c) J. Meeuwissen, R. J. Detz, A. J. Sandee, B. De Bruin and J. N. H. Reek, *Dalton Trans.,*

2010, **39**, 1929-1931; d) A. C. Laungani and B. Breit, *Chem. Commun.* 2008, 844-846; e) M. N. Brikholz, N. V. Dubrovina, H. Jiao, D. Michalik, J. Holz, R. Paciello, B. Breit and A. Borner*, Chem. Eur. J.,* 2007, **13**, 5896-5907; f) M. Weis, C. Waloch, W. Seiche and B. Breit, *J. Am. Chem. Soc.,* 2006, **128**, 4188-4189.

(23) Asymmetric hydrogenation of *N*-acetyldehydrophenylalanine has been reported earlier, see the following reference: D. R. Boyd, M. Bell, K. S. Dunne, B. Kelly, P. J. Stevenson, J. F. Malone and C. A. R. Allen, *Org. Biomol. Chem.,* 2012, **10**, 1388-1395.

(24) For palladium catalyzed C-P coupling (without enantio-selection) reactions see: L. Bonnafoux, R. Gramage- Doria, F. Colobert and F. R. Leroux, *Chem. Eur. J.,* 2011, **17**, 11008-11016.

(25) D. D. Perrin, W. L. Armarego and L. F. Willfred, *Purification of Laboratory Chemicals*, Pergamon, Oxford, 1988.

(26) See compound **2.1d** in: D. M. Nickerson and A. E. Mattson, *Chem. Eur. J.,* 2012, **18**, 8310-8314.

Chapter 3

Enhancing the rate of enantioselective P-C coupling reaction through rational catalyst selection

3.1. Abstract

Rational designing and synthesis of the Pd- catalyst to reduce the reaction time, improve the yield and enantiomeric excess in a P-C coupling reaction is described. The new Pd-catalyst has been developed in such way that, it will improve the rate of oxidative step as well as the rate of reductive elimination step. Synthesis of [Pd-((*S,S*)Me-FerroLANE)(*m*-phenylurea)(I)] complex (**Cat.2**) from *(S,S)*Me-FerroLANE and [Pd-(TMEDA)(*m*-phenylurea)(I)] in acetonitrile solvent is presented. The choice of (*(S,S)*Me-FerroLANE) bidentate ligand is based on the fact that the ferrocene moiety provides electrons to Pd-metal center to improve the rate of oxidative steps whereas the *bite* angle in **Cat.2** accelerates the reductive elimination step. Reaction conditions have been optimized for the synthesis of P-chiral supramolecular phosphine using **Cat.2**. Syntheses of P-chiral supramolecular phosphines using iodophenyl ureas (**3.2a-3.2l**) and different secondary phosphines (**3.1a-3.1c**) in presence of **Cat. 2** has been evaluated. The current **Cat.2** was found to be faster than **Cat.1** and the P-C coupling reaction was complete within 18 hours with 61% ee and >99% yield. The 1-(3-methoxyphenyl)-3-(3-(methyl(phenyl)phosphanyl)phenyl)urea **3.5h** and 1-(3-(mesityl(phenyl)phosphanyl)phenyl)-3-(3-methoxyphenyl)urea (**3.5v**) revealed the highest enantiomeric excess of 61% along with the excellent conversion of 99%. Following this strategy, a library of enantiopure P-chiral supramolecular phosphines has been synthesized.
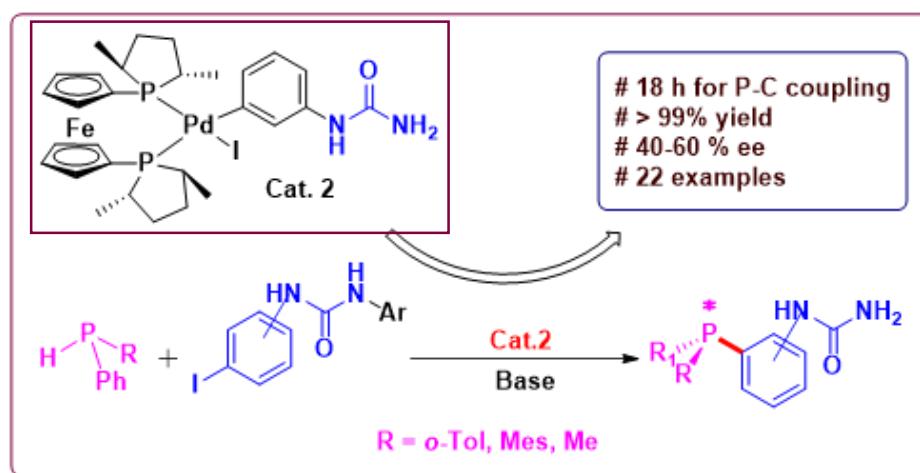
3.2. Introduction

Ligands create certain regulated microenvironment around the metal center in the metal catalysts. The microenvironment plays a very important role in metal-catalyzed asymmetric reactions and might yield highly enantiopure compounds in an asymmetric transformation.[1,2] Depending on the requirements of a reaction, people have been designing metal catalysts using monodentate, bidentate, and tridentate chiral phosphine ligand.[3] The bidentate phosphine ligands have a chelating ability which can create specific *bite* angle that might engage the space around metal center. Therefore, such metal catalyst might yield better regioselectivity in hydrogenation and hydroformylation reactions.[4,5] Thus, last decades have witnessed designing, synthesis, and application of bidentate phosphine ligands in catalytic organic transformations.[6] Although bidentate phosphine ligands are important in metal catalysis, but the synthesis of bidentate phosphines requires more number of steps for their synthesis.[7] To overcome this hurdle, *Reek*[8] and *Breit*[9] developed one-two step synthesis of monodentate phosphine ligands appended with hydrogen bonding motifs and such ligands are called as "supramolecular phosphine ligands". These monodentate phosphine ligands can mimic bidentate ligand in presence of metal due to hydrogen bonding interaction in between two monodentate supramolecular phosphine ligands.[8,9] The c-chiral and axially chiral backbone supramolecular phosphine ligands with metal provide excellent activity in hydrogenation,[10] hydroformylation,[11] hydrocyanation,[12] and hydrosilylation[13] reactions. However, phosphorous is the coordinating atom to the metal which is the actual reaction center in metal-catalyzed reactions.[14] As stated by Noble laureate Prof. W. S. Knowles, "*The asymmetry would have to be directly on the phosphorus. That is where the action is.*" Therefore, synthesis of ligands with chirality on phosphorus would be highly desirable.

The inversion of phosphorous lone pair leads to loss of chirality in P-chiral phosphine compounds and due to this, the synthesis of P-chiral phosphine compounds is a challenging task.[15] To address this challenge, synthesis of P-chiral phosphine compounds by protecting the phosphorous lone pair, by chiral auxiliary method, and by using chiral metal catalysts with racemic phosphine has been attempted.[16] Asymmetric metal catalyzed phosphination is well known with palladium,[17] platinum,[18] and ruthenium[19] metals in presence of different types of bidentate chiral phosphine ligands. Gluck and co-workers established that Pd-catalyst can be used for enantio-pure phosphination reaction in combination with (*S,S*)Me-DUPHOS ligand (Fig. 3.1).[20] In their attempts to synthesize enantiopure P-chiral phosphines, Glueck and co-workers achieved 88 % ee, which is the highest reported enantiomeric excess for any P-chiral

phosphine.[20c] To the best of our knowledge, there are no such reports on P-chiral supramolecular phosphines where P-chiral phosphine ligands have been appended with hydrogen bonding motif. As presented in chapter 2, we have been able to achieve 97% ee in the Pd-catalysed synthesis of P-chiral supramolecular phosphine.[21] However, the reaction took a very long time for reasonable conversion and the yields were limited.
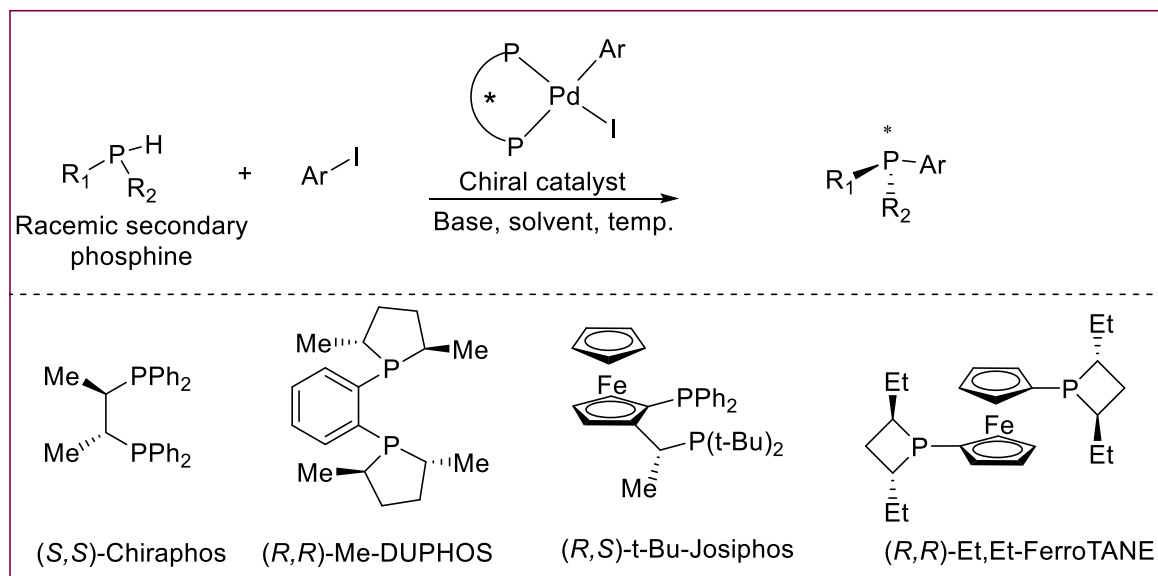
Figure 3.1. Asymmetric phosphination (top) and a small library of bis-phosphorous ligands for asymmetric phosphination.

Here in this chapter, we report rational designing, synthesis and application of a novel catalyst for enhanced yields in a short period of time. A detailed explanation of how chiral bidentate ligands and their chiral Pd-catalysts play a game changing role in asymmetric phosphination will be presented. Synthesis of a large library of P-chiral supramolecular phosphine ligands and their characterization is also described.

3.3. Results and discussion

In the previous chapter on Pd-catalyzed (**Cat.1**) (Scheme 3.2) synthesis of P-chiral supramolecular phosphine, it was noted that the reaction is very sluggision (Fig. 3. 2a, top). For example, **Cat.1** required 180 h to 360 h to obtain reasonable conversion. There could be two reasons for slow reaction, i) Pd-metal center is not sufficiently electron rich for oxidation step (Fig. 3.2b, left). ii) **Cat.1** is less bulky and offers acute *bite* angle which might be responsible for slow reductive elimination reaction (Fig. 3.2b, left and 3.2c).[20f, 22] Therefore, synthesis of a catalyst that can address the above two limitations would be highly desirable. Following rational was applied to select a better catalyst. 1) Electron-rich ligand, 2) the ligand should offer

wide *bite* angle, 3) the ligand should be able to offer steric bulk around metal center, and 4) it should not easily de-coordinate from metal center. Based on these requirments we selected (S,S)Me-Ferro-LANE as the ligand which meets the above strigent criteria. The new catalyst thus is [Pd-((*S,S*)Me-FerroLANE)(*m*-phenylurea)(I)] complex **Cat.2** with electron-rich ferrocene backbone and offers ~100° *bite* angle (Fig. 3.2d, left).[22]
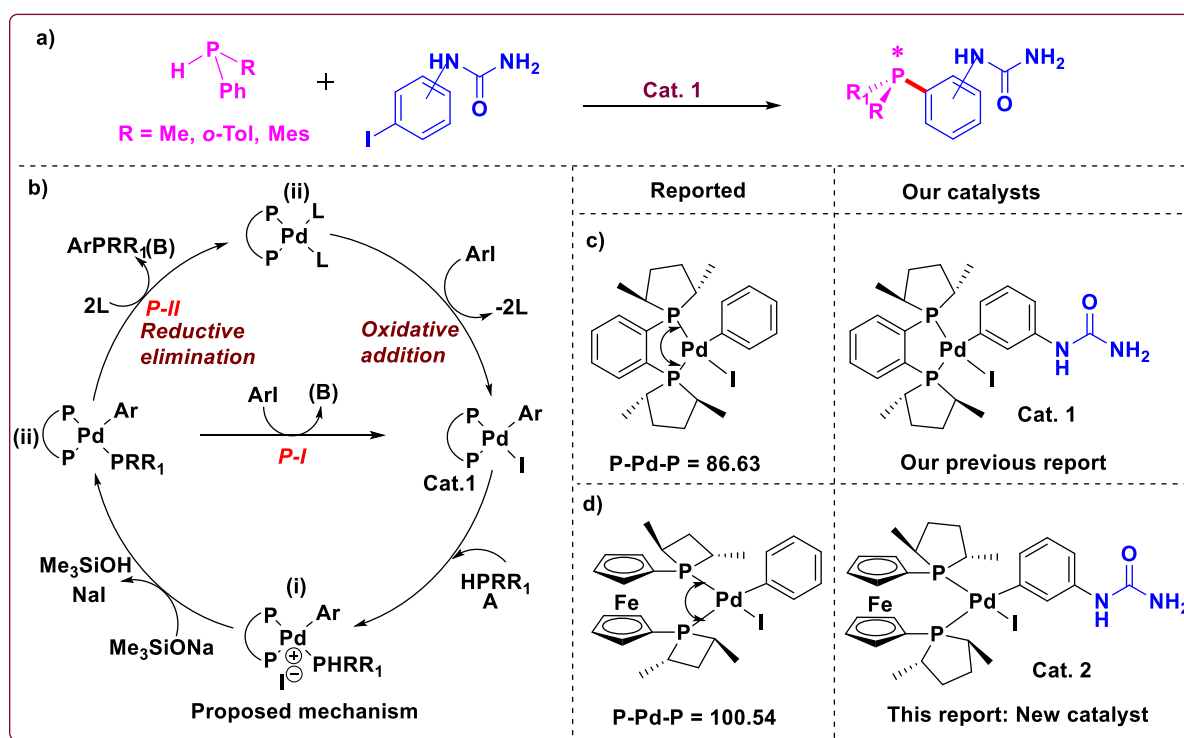
Figure 3.2. a) Synthesis of supramolecular phosphine ligand, b) Proposed mechanism for the synthesis of supramolecular phosphine ligand, c) Reported catalyst, d) New catalyst.

As depicted in Fig.3.2a, the synthesis of enantio-enriched P-stereogenic supramolecular phosphine requires three components, i) racemic secondary phosphine, ii) iodophenylurea (*N*-substituted derivative) (hydrogen bonding motif), and iii) chiral Pd-catalyst. The phosphine components were prepared using literature protocols.[23] Whereas, a library of hydrogen bonding motifs, **3.2a** to **3.2l** (12 derivatives) was synthesized using modified literature methods.[24] These iodo-compounds were characterized by NMR, Mass, FTIR and single crystal XRD methods (see appendix chapter for details) (Fig. 3.3). The third component, a palladium catalyst, was prepared in a two-step synthetic protocol. A stoichiometric reaction between 3-iodophenylurea (**3.2a**), [Pd(dba)₂] and tetramethylethylenediamine (TMEDA) produced the anticipated pre-catalyst [Pd(TMEDA)(3-phenylurea)(I)] (**3.3**) in good 63% yield (Scheme 3.1). The existence

of complex **3.3** was unambiguously ascertained using a combination of analytical and
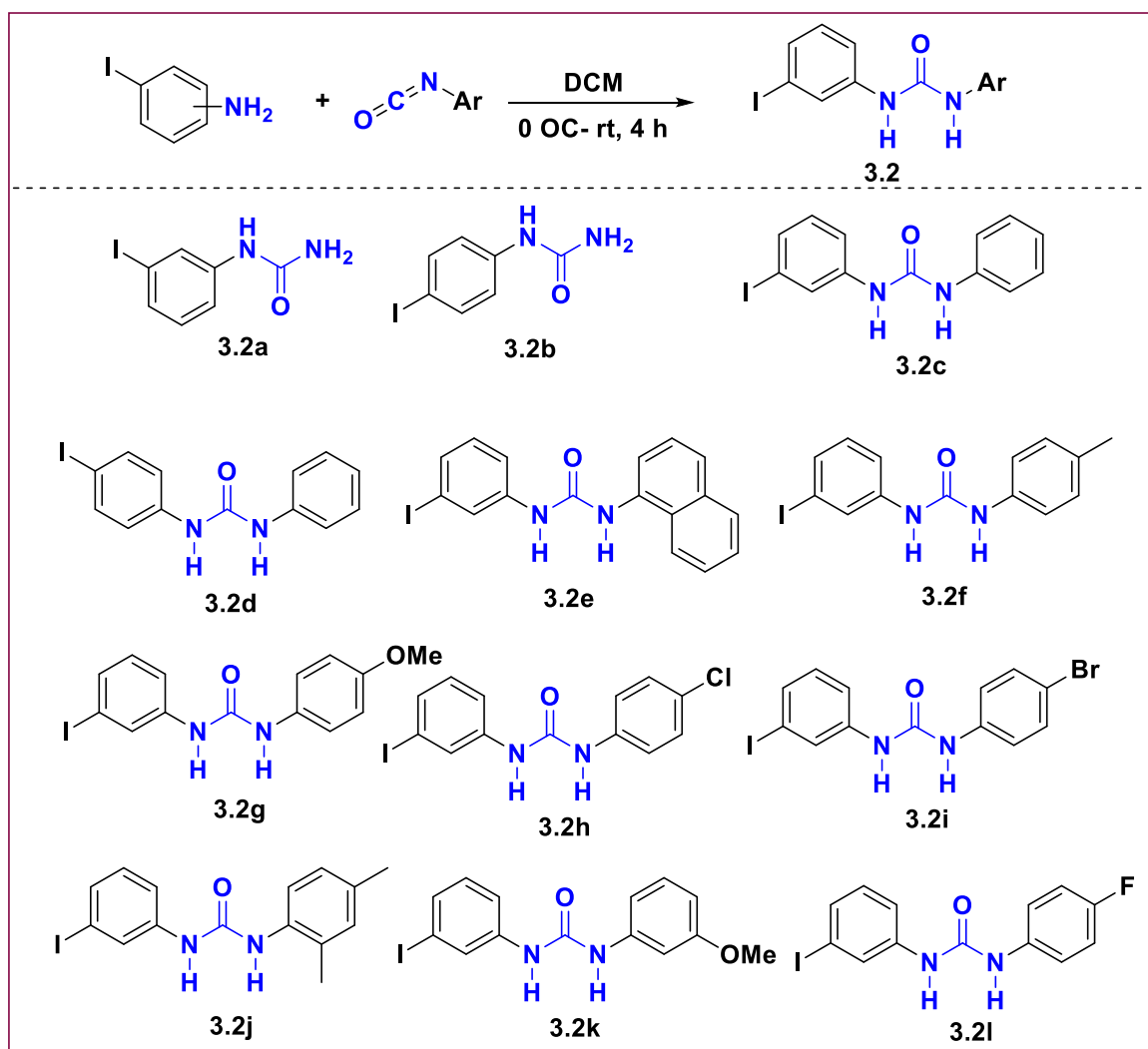
Figure3.3. Synthesis of Iodophenylurea and their derivatives (**3.2a to 3.2l**).

spectroscopic methods.[21] Addition of (*S,S*)Me-FerroLANE **3.4** to complex **3.3** in acetonitrile (CH₃CN) at room temperature and tracking the reaction progress by ^{31}P NMR indicated completion of the reaction within 1 hour. After 1 hour, volatiles was evaporated under reduced pressure to obtain a dark-gray color residue, which after *n*-hexane washing produced pure complex **Cat.2**. ^{31}P NMR of the isolated compound displayed a doublet-of-doublet due to the magnetically non-equivalent phosphorus nuclei (Fig.3.4). The doublet-of-doublet at 40.2 ($^2J_{\text{P-P}}$ = 23 Hz) can be assigned to P_1 and the second doublet-of-doublet 23.5 ppm ($^2J_{\text{P-P}}$ = 23 Hz)[22] can be readily assigned to P_2 (Scheme 3.1). Electro-Spray Ionization Mass-Spectroscopic (ESI-MS) analysis of **Cat.2** revealed a pseudo-molecular ion peak at m/z = 789.70 [M-Li]$^+$ confirming the presence of anticipated **Cat.2** (see in Fig. 3.5). After having established the existence of **Cat.2** we set out to evaluate the performance of **Cat.2** in catalytic asymmetric C-P coupling (phosphination) reaction. A general phosphination reaction leading to P-stereogenic

supramolecular phosphine is depicted in Scheme 3.2 and reaction screening is summarized in Table 3.1.
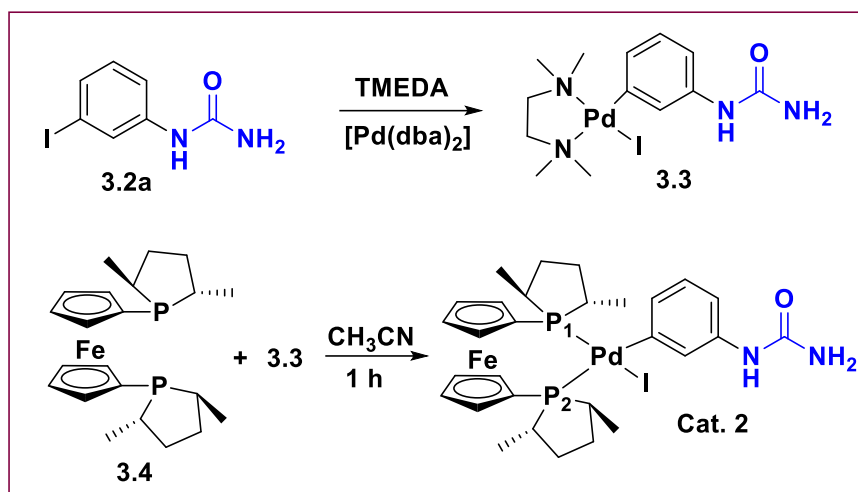
Scheme 3.1. Synthesis of [Pd-((*S*,*S*)Me-FerroLANE)(*m*-phenylurea)(I)] complex (**Cat.2**).
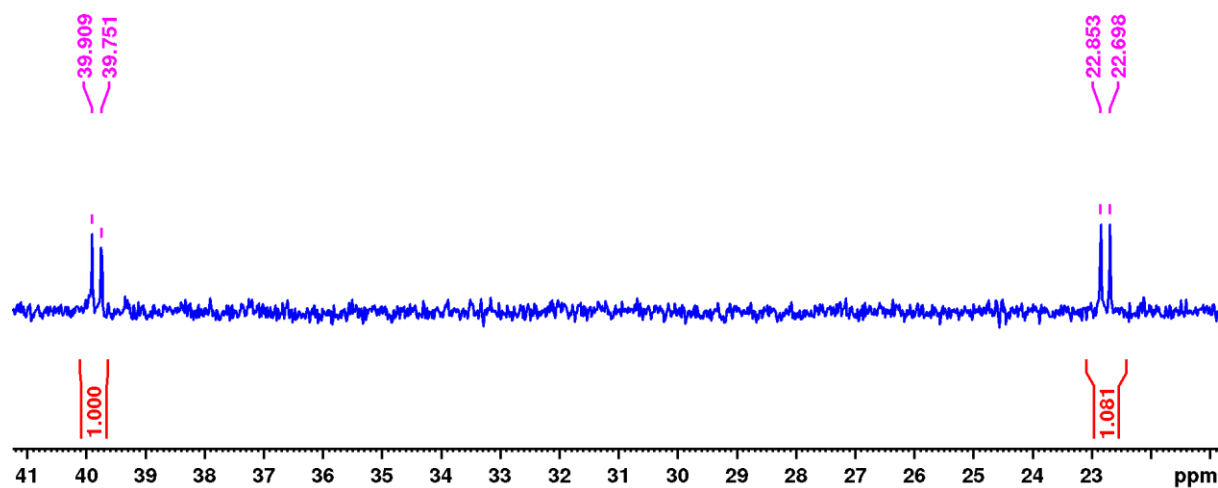
Figure. 3.4. ^{31}P NMR spectrum of **Cat.2** in DMSO-d[6].
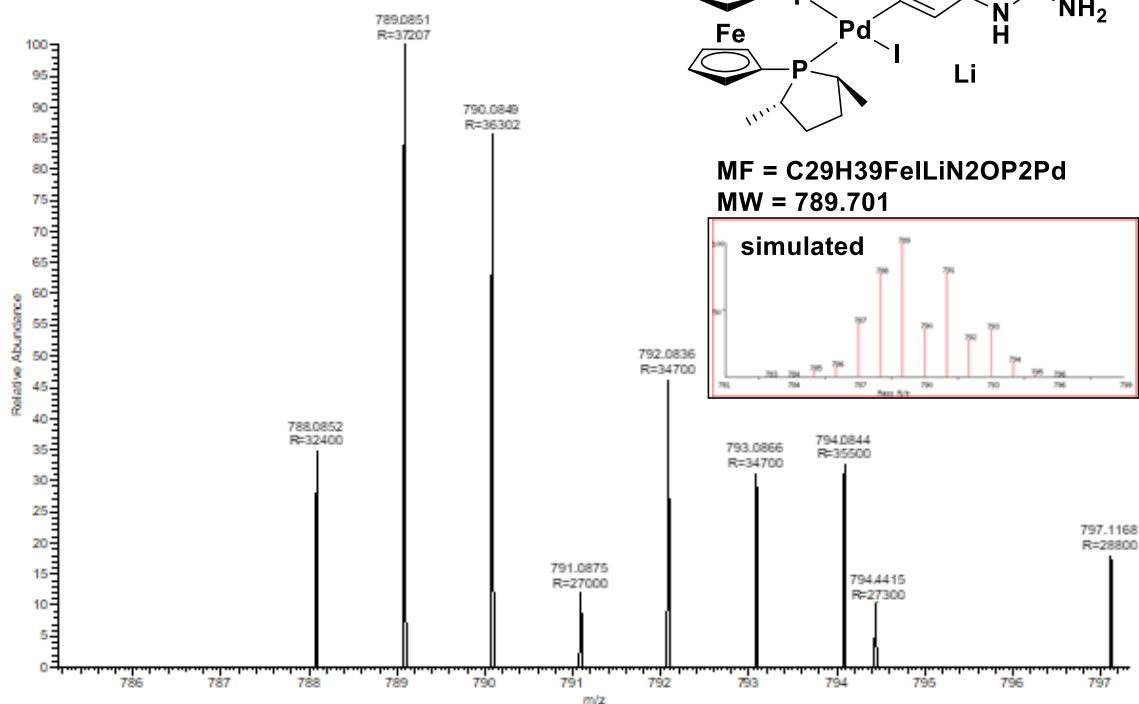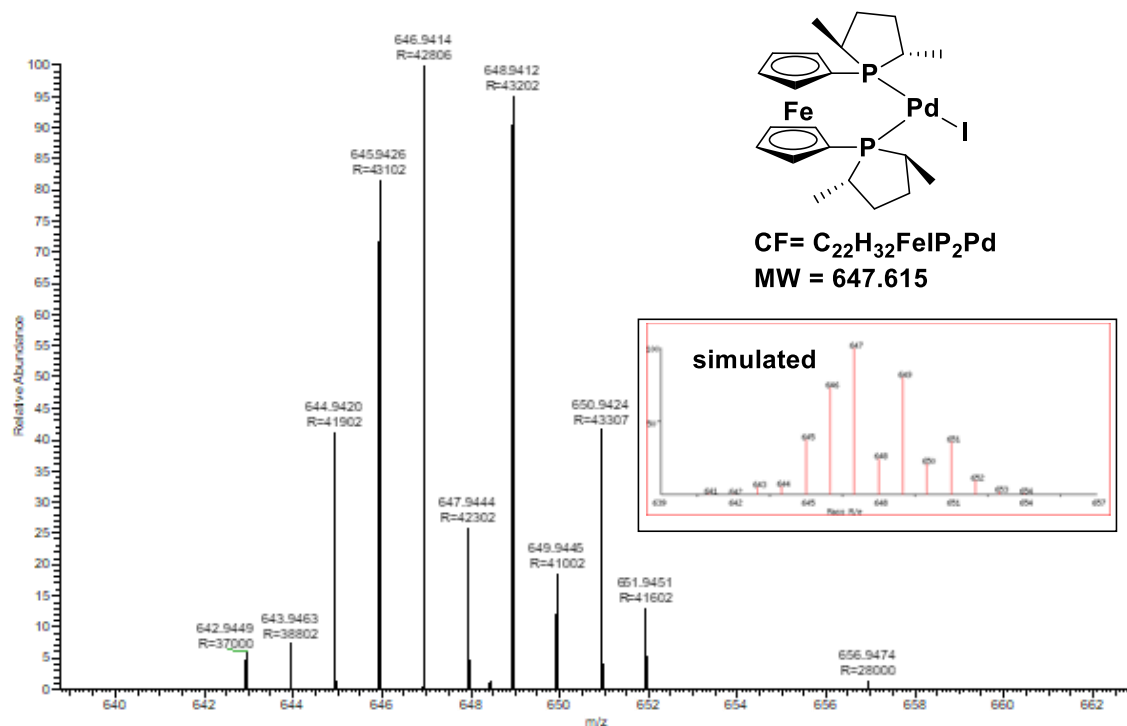
Figure 3.5. ESI-MS (+ve) spectra of [Pd-((*S,S*)Me-FerroLANE)(*m*-phenylurea)(I)] (**Cat.2**).
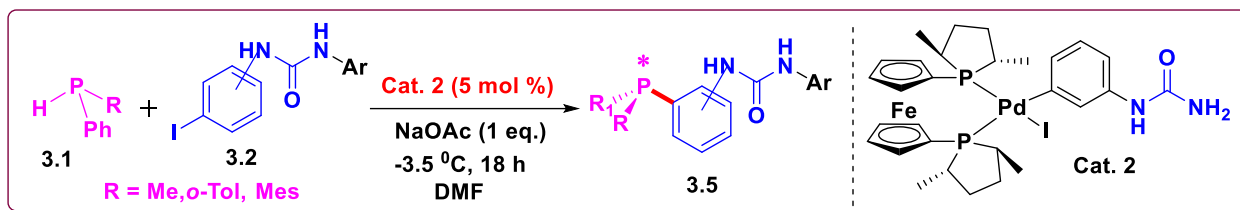
Scheme 3.2: Pd-catalyzed (**Cat.2**) enantioselective synthesis of P-chiral supramolecular phosphines **3.5a-v**.

Table 3.1: Palladium-catalyzed asymmetric phosphination.[a]

Sr. No.	R	Base	Reaction Condition	Time (h)	Conv. (%)[b]	ee (%)[c]
1[d]	Me	NaOSiMe₃	THF	48	10	0
2	Me	NaOSiMe₃	THF	48	>99	33
3[e]	Me	NaOSiMe₃	THF	36	>99	33
4	Me	NEt₃	THF	36	39	31
6	Me	Piperidine	THF	36	49	35
7	Me	Morpholine	THF	36	46	36
8	Me	DABCO	THF	36	46	37
9	Me	N-Me- Morpholine	THF	36	46	39
10	Me	K₃PO₄	THF	36	34	40
11	Me	K₂HPO₄	THF	36	46	41
12	Me	KH₂PO₄	THF	36	46	37
13	Me	K₂CO₃	THF	36	42	32
14	Me	NaOAc	THF	36	45	41
15	Me	NaOTFA	THF	36	46	40
16	Me	KOtBu	THF	36	54	26
17[f]	Me	NaOAc	THF	48	20	45
18[f]	Tol	NaOAc	THF	48	21	26
19	Me	NaOAc	DMF:THF	18	>99	41
20	Me	NaOAc	DMSO:THF	18	>99	51
21	**Me**	**NaOAc**	**DMF**	**18**	**>99**	**50**
22	**Tol**	**NaOAc**	**DMF**	**18**	**>99**	**47**
23	**Mes**	**NaOAc**	**DMF**	**18**	**>99**	**50**

[a] Conditions: **Cat.2** = 0.005 mmol, **3.1a** = 0.1 mmol, **3.2a** = 0.1 mmol, base = 0.3 mmol, at -3.5 °C; [b] Determined by ^{31}P NMR; [c] Determined by chiral HPLC after protection by sulfur; [d] **Cat. 1** = 0.015 mmol; [e] 3-iodoaniline instead of **3.2a**; [f] -20 °C.

The **Cat.2** was found to be highly active in the asymmetric phosphine leading to >99% conversion (run 2), as compared to only 10% conversion by **Cat.1** (run 1). These results indicate that **Cat.2** accelerates the rate of oxidative addition and rate of reductive elimination (Fig 3.2d). Although **Cat.2** provided high conversion in asymmetric phosphination the enantiomeric excess was only 33%. When 3-iodoaniline was utilized (instead of **3.2a**) in catalytic asymmetric phosphination in presence of **Cat. 2** similar enantiomeric excess of 33% was observed (run 3). This observation suggests that urea motif does not really affect the enantiomeric excess. In our attempts to identify suitable base, various organic bases such as sodium silonate (NaOAc), triethyl amine (NEt$_3$), piperidine, morpholine, diazabicyclo-octane (DABCO) were screened (Table 3.1, run 3-9). Among these, *N*-Me morpholine yielded the best ee of 39%, along with 46% conversion. The soft and mild inorganic bases (run 10-16) were also evaluated in catalytic asymmetric phosphination reaction. Among these K$_2$HPO$_4$ (run 11) and NaOAc (run 14) delivered 41% ee. Use of K$_2$HPO$_4$ led to oxidation of racemic phosphines (**3.1a-c**).[25] Among the screened inorganic bases, sodium acetate was found to yield 41% ee. Performing asymmetric phosphination at a lower temperature (-20 ^{0}C) using NaOAc led to improved ee of 45 %, but at the cost of lower conversion (Table 3.1, run 17). To evaluate the effect of solubility of inorganic bases on asymmetric phosphination various solvents were screened. Indeed, a polar solvent such DMF and DMSO (which can solubilize NaOAc) proved to be highly efficient and an excellent conversion of >99 % was observed within 18 hours. Along the same line, **3.1b** and **3.1c** yielded ee's of 47 and 50 % respectively with full conversion (Table 3.1, runs 22, 23). Thus, the standard reaction conditions are; **Cat.2** (5mol %), DMF solvent, -3.5 °C temperature, NaOAc base, and 18 hours reaction time. A library of P-chiral supramolecular phosphine **3.5a-v** was developed (Fig. 3.6) using these standard reaction conditions. The identity of these compounds has been fully established and the details have been presented in the experimental section. The enantiomeric excess was determined by using chiral HPLC. Before HPLC measurement the P-chiral supramolecular phosphine was protected by sulfur powder at an appropriate temperature to avoid the phosphine inversion. The position of urea functional group (*meta* and *para* with respect to phosphorous) and electron donation as well as withdrawing functional group on *N*-Phenyl ring will effect on enantiomeric excess. Effect of the position of urea functional group when at *meta* and *para* was observed in compound **3.5a** and **3.5b.** The conversion of **3.5a** and **3.5b** was same observed in both reactions but a change in ee's 50% and 35% respectively. But when compared the *meta* and *para* position
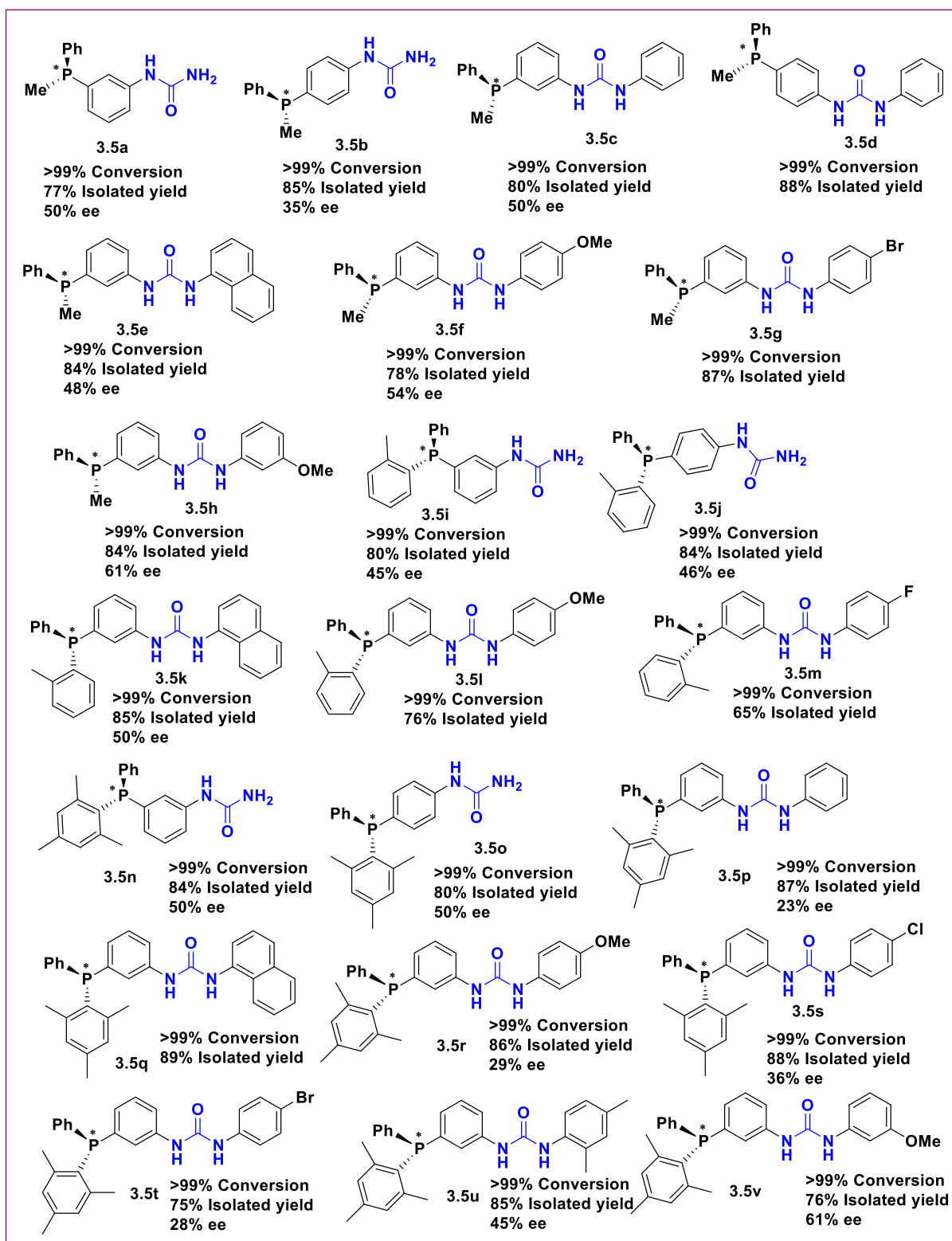
Figure. 3.6. A library of P-chiral supramolecular phosphine.

of urea function group in the compound **3.5i** and **3.5j** with **3.5n** and **3.5o** respectively, then small changes were observed in ee 45%, 46%, 50%, and 50% respectively. A similar observation in the *N*-substituted Phenyl urea **3.5c** was 50%. A small increase in enantiomeric excess 48% and 50%, when the *N*-substituted naphthalene in the **3.5e** and **3.5k**. The small

increases in ee when electron donating group present on *N*-substituted phenyl ring at the *para* position with respect to urea. In the compound **3.5f**, **3.5i**, and **3.5r** the -OMe functional group present at the *para* position with respect to urea function group then the ee was 54%, 50%, and 29% respectively. When the bromide present at *N*-substituted phenyl ring then enantiomeric excess decreases which was observed in the compound **3.5t** with 28%. A similar observation was observed in the compound **3.5s** have chloride at *N*-substituted phenyl ring with 36% ee. If the -OMe group present at *meta* position of *N*-substituted phenyl ring then enantiomeric excess was increased in **3.5h** (61% ee) and **3.5v** (61% ee). The reason could be electronic factor of methoxy whish is attached to *N*-substituted phenyl ring in **3.5h** and **3.5v**. If the methyl group present at *ortho* and *para* position of *N*-substituted phenyl ring then enantiomeric excess was decreases in **3.5u** (45% ee).

3.4. Conclusions

Synthesis of [Pd-((*S*,*S*)Me-FerroLANE)(*m*-phenylurea)(I)] complex (**Cat.2**) from *(S)*Me-FerroLANE and [Pd-(TMEDA)(*m*-phenylurea)(I)] precursor has bee achieved. Two doublets in ^{31}P NMR and 1-2D NMR data suggested the formation of **Cat.2** which was isolated in 65% yield. Indeed the rationally designed **Cat. 2** was found to accelerate the reaction to completion within 18 hours. It is most likely that the electron-rich nature and wide *bite* angle offered by (*S*,*S*)Me-FerroLANE is responsible for the improved performance of **Cat. 2**. The thus obtained **Cat. 2** was screened to optimize reaction conditions for a P-C coupling reaction. Sodium acetate in polar solvents (DMF, DMSO) was found to be the optimal combination. A P-C coupling reaction was typically carried out at -3.5 °C for 18 hours. A library of 22 P-chiral supramolecular phosphine ligands was synthesized using **Cat. 2**. The 1-(3-methoxyphenyl)-3-(3-(methyl(phenyl)phosphanyl)phenyl)urea **3.5h** and 1-(3-(mesityl(phenyl)phosphanyl)phenyl)-3-(3-methoxyphenyl)urea (**3.5v**) revealed the highest enantiomeric excess of 61% along with the excellent conversion of 99%.

3.5. Experimental section

3.5.1. General methods and materials

All manipulations were carried out under an inert atmosphere using standard Schlenk line techniques or m-Braun glove box. Solvents were dried by standard procedures unless otherwise mentioned.[26] Toluene was distilled from sodium, diethyl ether, and THF from sodium/benzophenone under argon atmosphere. Acetonitrile, DMF, DMSO, and methylene

chloride were distilled on calcium-hydride. NaOSiMe$_3$, DABCO, N-Me-Morpholine, NaOTf, KOtBu, (*S*,*S*)-Me-DuPHOS, (*S*,*S*)Me-FerroLANE, mesitylbromide, sulfur powder, [Pd(dba)$_2$], were purchased from Sigma-Aldrich and 3-iodoaniline, 2-bromotoluene, dichlorophenylphosphine were purchased from Alfa-Aesar. All other reagents/chemicals, solvents were purchased from local suppliers (Spectrochem Pvt. Ltd.; Avra Synthesis Pvt. Ltd.; Thomas Baker Pvt. Ltd. etc). Iodophenyl urea (**3.2a-3.2l**),[24] [Pd-(TMEDA)(m-phenylurea)(I)] complex (**3.3**)[21] Methyl(phenyl)phosphine(**3.1a**),[23] Phenyl(*o*-tolyl)phosphine(**3.1b**),[23] mesityl(phenyl)phosphine(**3.1c**)[23] were prepared by following known procedures.

Solution NMR spectra were recorded on a Bruker Avance 200, 400 and 500 MHz instruments at 298 K unless mentioned otherwise. Chemical shifts are referenced to external reference TMS (^{1}H and ^{13}C) or 85% H$_3$PO$_4$ (Ξ = 40.480747 MHz, ^{31}P). Coupling constants are given as absolute values. Multiplicities are given as follows s: singlet, d: doublet, t: triplet, m: multiplet, Mass spectra were recorded on Thermo Scientific Q-Exactive mass spectrometer, with Hypersil gold C18 column 150 x 4.6 mm diameter 8 µm particle size mobile phase used is 90% methanol + 10% water + 0.1% formic acid. The enantiomeric excess of the P-stereogenic phosphines was determined by chiral HPLC on an Agilent Technologies 1260 Infinity instrument with Chiralpak IA column (20 cm), Chiralpak IB column (20 cm), Chiralpak IC column (20 cm), and Chiralpak IF column (20 cm).

3.5.2. Synthesis of [Pd-((*S*,*S*)Me-FerroLANE)(*m*-phenylurea)(I)] complex (Cat.2)
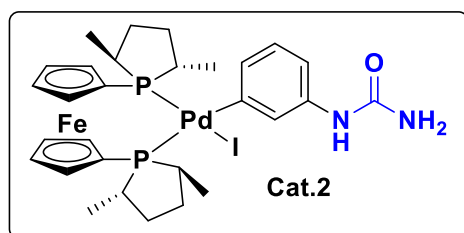
A solution of [Pd-(TMEDA)(m-phenylurea)(I)] complex (**3.3**) (0.326 mmol) in

acetonitrile (20 mL) and (*S*,*S*)Me-FerroLANE (0.326 mmol) was stirred at room temperature and the reaction progress was monitored by ^{31}P NMR spectroscopy. The reaction was completed in 2 h. After completion of the reaction volatiles were evaporated to obtain dark gray solid material. The solid was washed with n-hexane (10 mL x 3 times) to yield the desired palladium complex in 65% yield (0.211 mmol).

^{1}H NMR (500 MHz, DMSO-d$_6$, 298 K): δ = 8.22 (d, J_{H-H} = 10.1 Hz, 1H, N*H*), 7.32 (d, J_{H-H} = 7.1 Hz, 1H, Ar), 7.07-7.02 (m, 1H, Ar), 6.86-6.78 (m, 2H, Ar), 5.68 (s, 1H, N*H*$_2$), 5.61 (s, 1H, N*H*$_2$), 3.58 (m, 1H, C*H*), 4.69 (d, J_{H-H} = 8.9 Hz, 1H, Ar-Fr), 4.65 (s, 1H, Ar-Fr), 4.51 (s, 2H, Ar-Fr), 4.46 (s, 2H, Ar-Fr), 4.38 (s, 1H, Ar-Fr), 4.29 (d, J_{H-H} = 15.9 Hz, 1H, Ar-Fr),

2.22-2.18 (m, 3H, C*H₃*), 1.92-1.76 (m, 8H, C*H*, C*H₂*), 1.56-1.52 (m, 2H, C*H₂*), 1.26-1.15 (m, 3H, C*H₃*), 0.99-0.98 (m, 2H, C*H₂*), 0.81 (q, J_{H-H} = 7.40, 6.60 Hz, 3H, C*H₃*), 0.42 (td, J_{H-H} = 18.23, 7.53 Hz, 3H, C*H₃*). **³¹P NMR** (500 MHz, DMSO-d₆, 298 K): δ = 39.82 (d, J_{P-P} = 31.9 Hz, 1P$_{P2}$), 22.77 (J_{P-P} = 31.4 Hz 1P$_{P1}$). **¹³C NMR** (125 MHz, DMSO-d₆, 298 K): δ = 155.9 (s, *C*O), 139.4 (d, J_{C-P} = 10.7 Hz, Ar, quat), 138.8 (d, J_{C-P} = 9.2 Hz, Ar, quat), 129.7 (d, J_{C-P} = 235.8 Hz, Ar, *C*H), 127.2 (d, J_{C-P} = 9.5 Hz, Ar, *C*H), 125.1 (d, J_{C-P} = 222.3 Hz, Ar, *C*H), 122.1 (s, Ar, *C*H), 76.4 (q, J_{C-P} = 14.5, 6.1 Hz, Fr, *C*H), 74.3 (d, J_{C-P} = 24.8 Hz, Fr, *C*H), 72.7 (d, J_{C-P} = 12.2 Hz, Fr, *C*H), 72.4 (s, Fr, *C*H), 72.40(s, Fr, *C*H), 71.7 (s, Fr, *C*H), 68.6 (d, J_{C-P} = 24.8 Hz, Fr, *C*H), 37.3 (d, J_{C-P} = 20.1 Hz, *C*H), 35.9 (s, *C*H), 35.7 (s, *C*H₂), 35.6 (s, *C*H₂), 35.3 (s, *C*H₂), 34.5 (d, J_{C-P} = 45.4 Hz, *C*H), 33.3 (d, J_{C-P} = 23.1 Hz, *C*H₃), 33.4 (s, *C*H₂), 21.1 (q, J_{C-P} = 10.6, 2.0 Hz, *C*H₃), 20.3 (q, J_{C-P} = 10.9, 18.6 Hz, *C*H₃), 14.0 (d, J_{C-P} = 17.1 Hz, *C*H₃), 13.8 (d, J_{C-P} = 43.2 Hz, *C*H₃). **ESI-MS** (+ve): (Cal. For C₂₉H₃₉FeILiN2OPd) m/z = 789.70 [M+Li]⁺, 647.61 [M-3-phenylurea]⁺.

3.5.3. Synthesis of P-stereogenic supramolecular phosphines (3.5)

3.5.3.1. General procedure for phosphination reaction

A Schenk tube was loaded with catalyst **Cat.2**, iodophenylurea **3.2a-l**, racemic secondary phosphine **3.1a-c** in a glove box. The screw capped Schlenk tube was taken out and after the standard vacuum-argon cycle, NaOAc and 1 ml of DMF were added to the reaction mixture under positive argon flow. The reaction mixture was stirred at appropriate temperature and for desired time. The progress of the reaction was monitored by ³¹P NMR spectroscopy.

3.5.3.2. *Racemic* 1-(3-(methyl(phenyl)phosphorothioyl)phenyl)urea (3.5a)

A 1-(3-iodophenyl)urea (**3.2a**) (0.40 mmol) was dissolved in 2 ml of THF, which was followed
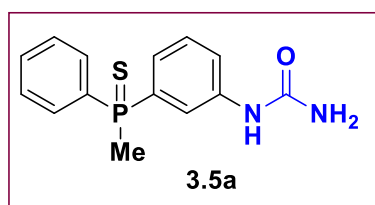
by addition of triethylamine (0.80 mmol) and methyl(phenyl)phosphine **3.1a** (0.40 mmol). After stirring for few minutes, [Pd(OAc)₂] (0.5 mol %) was added and the mixture was refluxed overnight at 68 °C. After completion of the reaction, excess Sulfur powder (S₈) (3 eq.) was added to the reaction mixture at same temperature and the mixture was stirred for one hour. Thus, above mixture was then treated with degassed water and was extracted with ethyl acetate (3 × 10 mL). The combined organic layer was dried on MgSO₄ for 2 hours and the volatiles were evaporated under reduced

pressure. The crude **3.5a** was purified by silica gel column chromatography using 80:20 mixture of DCM:Ethyl acetate. The desired product was isolated as a yellowish solid in 77% yield (90 mg, 0.36 mmol).

¹H NMR (500 MHz, CDCl₃, 298 K): δ = 7.83.7.79 (m, 3H, Ar), 7.63 (s, 1H, N*H*), 7.53.7.47 (m, 4H, Ar), 7.35-7.33 (m, 2H, Ar), 5.20-4.81 (m, 2H, N*H₂*), 2.27 (d, J_{H-P} =13.15 Hz, 3H, CH₃).

³¹P NMR (500 MHz, CDCl₃, 298 K): δ = 37.34. **ESI-MS** = (+ve): (Cal. For $C_{14}H_{16}N_2OPS$) m/z = 291.07 $[M+H]^+$.

3.5.3.3. *Chiral* **1-(3-(methyl(phenyl)phosphorothioyl)phenyl)urea (3.5a)**

A Schlenk tube was loaded with catalyst **Cat.2** (0.005 mmol), 3-iodophenylurea (**3.2a**) (0.1 mmol), methyl(phenyl)phosphine (**3.1a**) (0.1 mmol) in a glove box. The screw capped Schlenk

tube was taken out and appropriate temperature was attained. After the standard vacuum-argon cycle NaOAc and 1 ml of DMF were added to the reaction mixture. The progress of the reaction was monitored by ³¹P NMR spectroscopy. After completion of the reaction, the Sulphur powder was added in reaction mixture at same temperature and stirred it for half an hour. The content was treated with degassed water (which was pre-cooled at appropriate temperature) and extracted with ethyl acetate (10 mL × 3) (which was pre-cooled at appropriate temperature). The combined organic layer was dried on MgSO₄ for half hours at suitable temperature and the volatiles were evaporated under reduced pressure. The crude mixture was dissolved in DCM and filtered over a plug of silica. The plug was washed with DCM until the impurities were eluted, and then the expected product was pushed through with ethyl acetate. After evaporation of the solvent the product was obtained as a pale yellow solid **3.5a** which was analyzed by a combination of spectroscopic and analytical tools.

³¹P NMR (500 MHz, CDCl₃, 298 K) δ = 37.34 (s, P). **HPLC:** Daicel Chiralpak-IF, 1 mL/min, 10:90 (2-PrOH:Hexane), Rt_1 = 36.3 min; Rt_2 = 40.5 min. ee = 50%.

VSK-541 #274 RT: 1.22 AV: 1 NL: 3.72E7
T: FTMS + p ESI Full ms [100.0000-1500.0000]

Figure 3.7. ESI-MS (+ve) spectrum of 1-(3-(methyl(phenyl)phosphorothioyl)phenyl)urea (**3.5a**).

VWD: Signal A, 254 nm Results

Retention Time	Area	Area %
33.050	196419930	50.86
37.050	189797204	49.14
Totals	386217134	100.00

Figure. **3.8.** HPLC chromatogram of racemic 1-(3-(methyl(phenyl)phosphorothioyl)phenyl)urea (**3.5a**).

VWD: Signal A, 254 nm Results

Retention Time	Area	Area %
36.393	333681101	75.31
40.560	109395630	24.69

Totals		
	443076731	100.00

Figure 3.9. HPLC chromatogram of chiral 1-(3-(methyl(phenyl)phosphorothioyl)phenyl)urea (**3.5a**).

3.5.3.4. *Racemic* 1-(4-(methyl(phenyl)phosphorothioyl)phenyl)urea (3.5b)

A 1-(4-iodophenyl)urea (**3.2b**) (1.00 mmol) was dissolved in 3 ml of THF, followed by
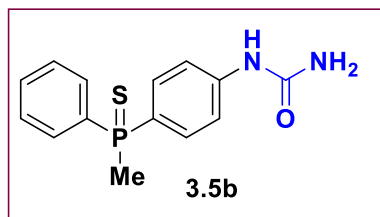
addition of triethylamine (2.00 mmol) and methyl(phenyl)phosphine **3.1a** (1.00 mmol). After stirring for 10 minutes, [Pd(OAc)$_2$] (0.5 mol %) was added and the mixture was refluxed overnight at 68 °C. After completion of the reaction, excess Sulfur powder (S$_8$) (3 eq.) was added to the reaction mixture at same temperature and the mixture was stirred for one hour. After this, the above mixture was then treated with degassed water and was extracted with ethyl acetate (3 × 10 mL). The combined organic layer was dried on MgSO$_4$ for 2 hours and the volati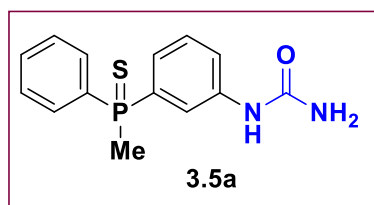les were evaporated under reduced pressure. The crude **3.5b** was purified by silica gel column chromatography using 80:20 mixture of DCM:Ethyl acetate. The desired product was isolated as a yellowish solid in 85% yield (250 mg, 0.86 mmol).

^{1}H NMR (500 MHz, CDCl$_3$, 298 K): δ = 7.84-7.69 (m, 3H, Ar), 7.50-7.32 (m, 5H, Ar), 7.07-6.95 (s, 1H, Ar), 6.58 (s, 1H, N*H*), 4.76 (s, 1H, N*H*), 2.19 (s, 3H, CH$_3$). **^{31}P NMR** (500 MHz, CDCl$_3$, 298 K): δ = 36.17. **ESI-MS** = (+ve): (Cal. For C$_{14}$H$_{16}$N$_2$OPS) m/z = 291.07 [M+H]$^+$.

3.5.3.5. *Chiral* **1-(4-(methyl(phenyl)phosphorothioyl)phenyl)urea (3.5b)**
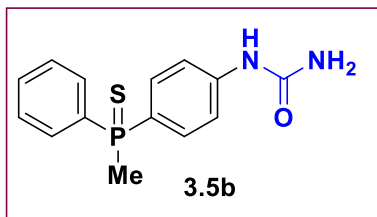
A Schlenk tube was loaded with catalyst **Cat.2** (0.005 mmol), 4-iodophenylurea (**3.2b**) (0.1 mmol), methyl(phenyl)phosphine (**3.1a**) (0.1 mmol) in a glove box. The screw capped Schlenk tube was taken out and appropriate temperature was attained. After the standard vacuum-argon cycle, NaOAc and 1 ml of DMF were added to the reaction mixture. The progress of the reaction was monitored by ^{31}P NMR spectroscopy. After completion of the reaction, the Sulphur powder was added in reaction mixture at same temperature and stirred it for half an hour. The content was treated with degassed water (which was pre-cooled at appropriate temperature) and extracted with ethyl acetate (10 mL × 3) (which was pre-cooled at appropriate temperature). The combined organic layer was dried on MgSO$_4$ for half hours at suitable temperature and the volatiles were evaporated under reduced pressure. The plug was washed with DCM until the impurities were eluted, and then the expected product was pushed through with ethyl acetate. After evaporation of the solvent the product was obtained as a pale yellow solid **3.5b** which was analyzed by a combination of spectroscopic and analytical tools.

^{31}**P NMR** (500 MHz, CDCl$_3$, 298 K): δ = 37.34 (s, P). **HPLC:** Daicel Chiralpak-IF, 0.7 mL/min, 06:94 (2-PrOH:Hexane), Rt_1 = 30.2 min; Rt_2 = 52.0 min. ee = 35%.

VSK-541-A #269 RT: 1.20 AV: 1 NL: 6.83E7
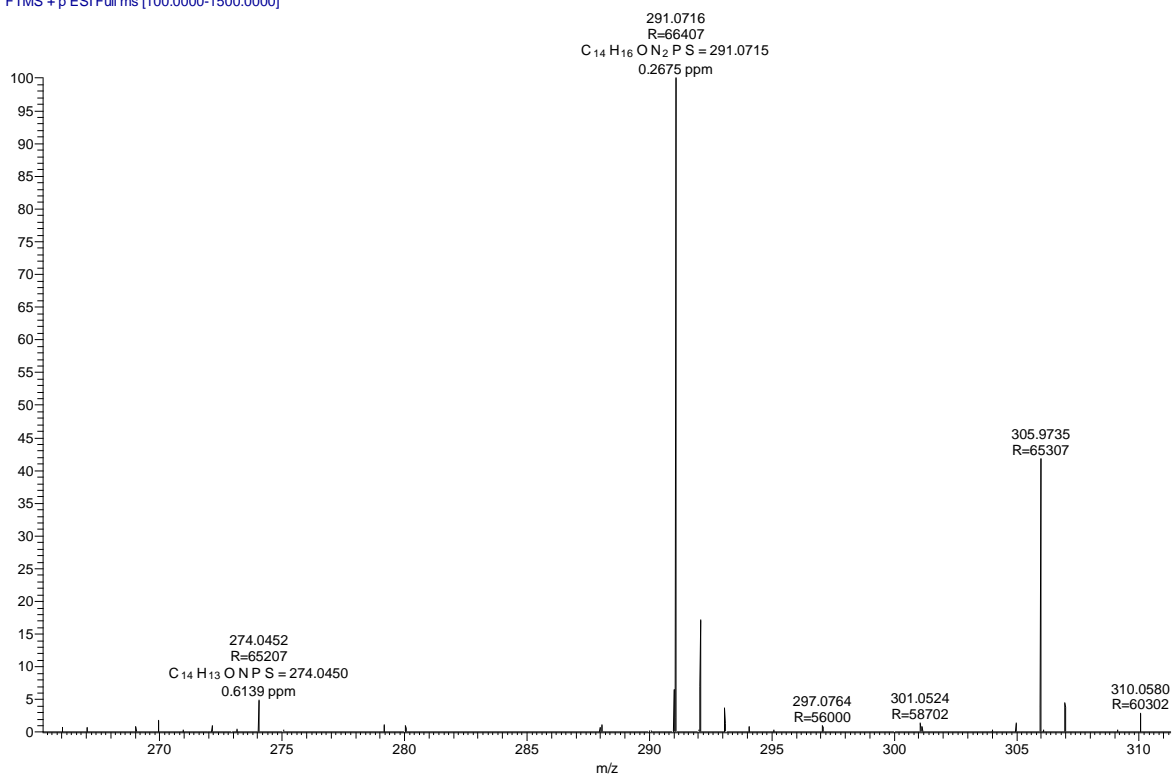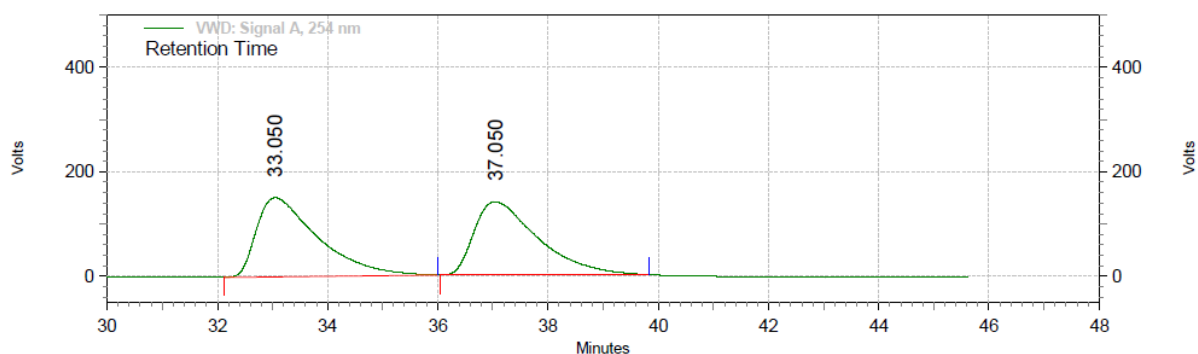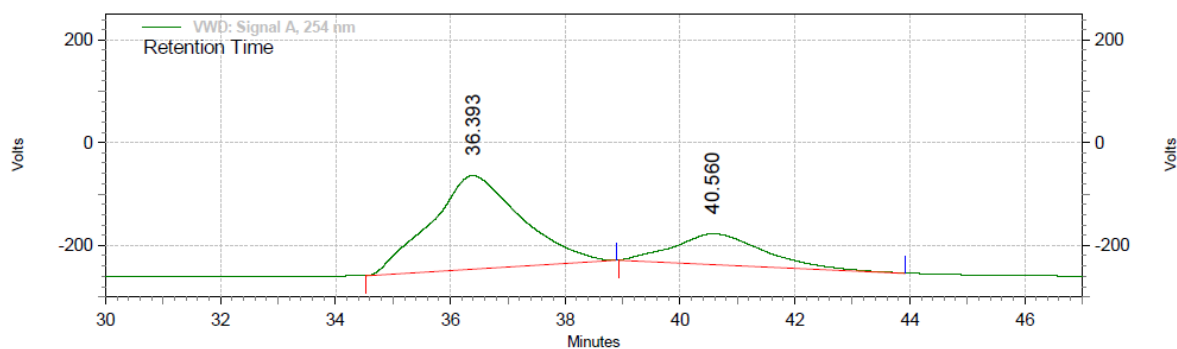T: FTMS + p ESI Full ms [100.0000-1500.0000]

Figure 3.10. ESI-MS (+ve) spectrum of 1-(4-(methyl(phenyl)phosphorothioyl)phenyl)urea (**3.5b**).

VWD: Signal A, 254 nm Results

Retention Time	Area	Area %
30.333	3912015846	54.75
50.647	3233693718	45.25

Totals		
	7145709564	100.00

Figure 3.11. HPLC chromatogram of racemic 1-(4-(methyl(phenyl)phosphorothioyl)phenyl)urea (**3.5b**).

VWD: Signal A, 254 nm Results

Retention Time	Area	Area %
30.283	317450749	67.37
52.063	153747474	32.63

Totals		
	471198223	100.00

Figure 3.12. HPLC chromatogram of chiral 1-(4-(methyl(phenyl)phosphorothioyl)phenyl)urea (**3.5b**).

3.5.3.6. *Racemic* 1-(3-(methyl(phenyl)phosphorothioyl)phenyl)-3-phenylurea (3.5c)

A 1-(3-iodophenyl)-3-phenylurea (**3.2c**) (0.05 mmol) was dissolved in 2 ml of THF, followed

by addition of triethylamine (0.10 mmol) and methyl(phenyl)phosphine **3.1a** (0.05 mmol). After stirring for 10 minutes, [Pd(OAc)$_2$] (0.5 mol %) was added and the mixture was refluxed overnight at 68 °C. After completion

of the reaction, excess Sulfur powder (S$_8$) (3 eq.) was added to the reaction mixture at same temperature and the mixture was stirred for one hour. After this, the above mixture was then treated with degassed water and was extracted with ethyl acetate (3 × 10 mL). The combined organic layer was dried on MgSO$_4$ for 2 hours and the volatiles were evaporated under reduced pressure. The crude **3.5c** was purified by silica gel column chromatography using 80:20 mixture of DCM:Ethyl acetate. The desired product was isolated as a yellowish solid in 80% yield (82 mg, 0.04 mmol).

^{1}H NMR (500 MHz, CDCl$_3$, 298 K): δ = 7.87 - 7.85 (m, 2H, Ar), 7.78 (q, J_{H-H} =7.4, 5.8 Hz, 2H, Ar), 7.73 (s, 1H, N*H*), 7.48 (t, J_{H-H} =7.4 Hz, 1H, Ar), 7.44-7.39 (m, 3H, Ar), 7.29 (s, 1H, Ar), 7.28 (s, 1H, N*H*), 7.24-7.15 (m, 4H, Ar), 7.01 (t, J_{H-H} = 7.28 Hz, 1H, Ar), 2.23 (d, $_{JH-P}$ =13.24 Hz, 3H, CH$_3$). **^{31}P NMR** (500 MHz, CDCl$_3$, 298 K): δ = 37.06. **^{13}C NMR** (125 MHz, CDCl$_3$, 298 K): δ = 152.9 (s, Ar, *C*O), 139.5 (d, J_{C-P} = 15.5 Hz, Ar, quat.), 138.1 (s, Ar, quat.), 133.8 (d, J_{C-P} = 82.7 Hz, Ar, quat.), 132.3 (d, J_{C-P} = 83.1 Hz, Ar, quat.), 131.8 (s, Ar, *C*H), 130.9 (d, J_{C-P} = 10.9 Hz, Ar, *C*H), 129.3 (d, J_{C-P} = 13.9 Hz, Ar, *C*H), 129.0 (s, Ar, *C*H), 128.6 (d, J_{C-P} = 12.4 Hz, Ar, *C*H), 124.3 (d, J_{C-P} = 10.2 Hz, Ar, *C*H), 123.4 (s, Ar, *C*H), 122.4 (s, Ar, *C*H), 120.8 (d, J_{C-P} = 12.8 Hz, Ar, *C*H), 119.8 (s, Ar, *C*H), 21.1 (d, J_{C-P} = 59.7 Hz, CH$_3$). **ESI-MS** (+ve): (Cal. For C$_{20}$H$_{19}$N$_2$OP) m/z = 334.12 [M]$^+$.

3.5.3.7. *Chiral* 1-(3-(methyl(phenyl)phosphorothioyl)phenyl)-3-phenylurea (3.5c)

A Schlenk tube was loaded with catalyst **Cat.2** (0.005 mmol), 1-(3-iodophenyl)-3-

phenylurea (**3.2c**) (0.1 mmol), methyl(phenyl)phosphine (**3.1a**) (0.1 mmol) in a glove box. The screw capped Schlenk tube was taken out and appropriate temperature was attained. After the standard vacuum-argon cycle,

NaOAc and 1 ml of DMF were added to the reaction mixture. The progress of the reaction was monitored by ^{31}P NMR spectroscopy. After completion of the reaction, Sulphur powder was added to reaction mixture at same temperature and the mixture was stirred for half an hour. The
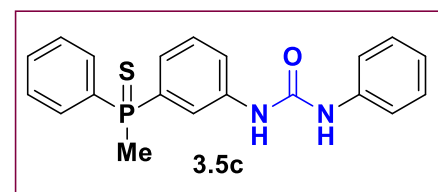
content was treated with degassed water (which was pre-cooled at appropriate temperature) and extracted with ethyl acetate (10 mL × 3) (which was pre-cooled at appropriate temperature). The combined organic layer was dried on $MgSO_4$ for half hours at suitable temperature and the volatiles were evaporated under reduced pressure. The plug was washed with DCM until the impurities were eluted, and then the expected product was pushed through with ethyl acetate. After evaporation of the solvent the product was obtained as a pale yellow solid **3.5c** which was analyzed by a combination of spectroscopic and analytical tools.

^{31}**P NMR** (500 MHz, CDCl$_3$, 298 K): δ = 37.06 (s, P). **HPLC:** Daicel Chiralpak-IC, 1 mL/min, 10:90 (2-PrOH:Hexane), Rt_1 = 26.6 min; Rt_2 = 37.8 min. ee = 50%.
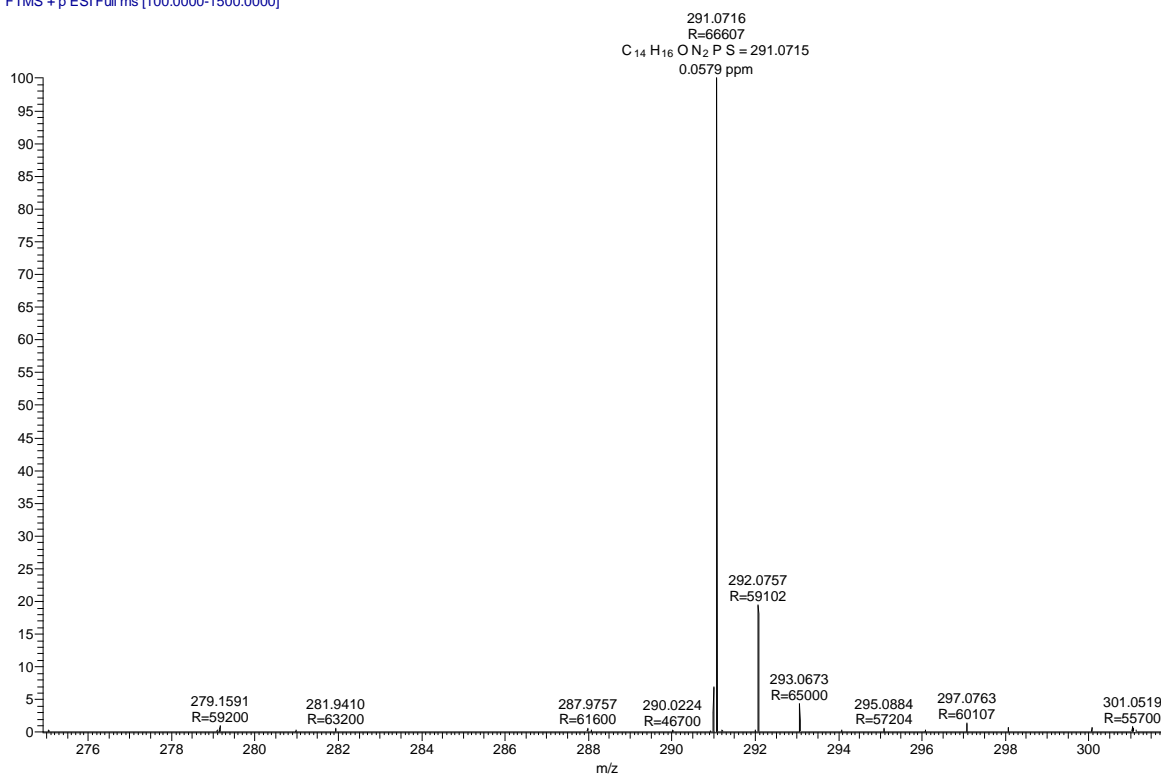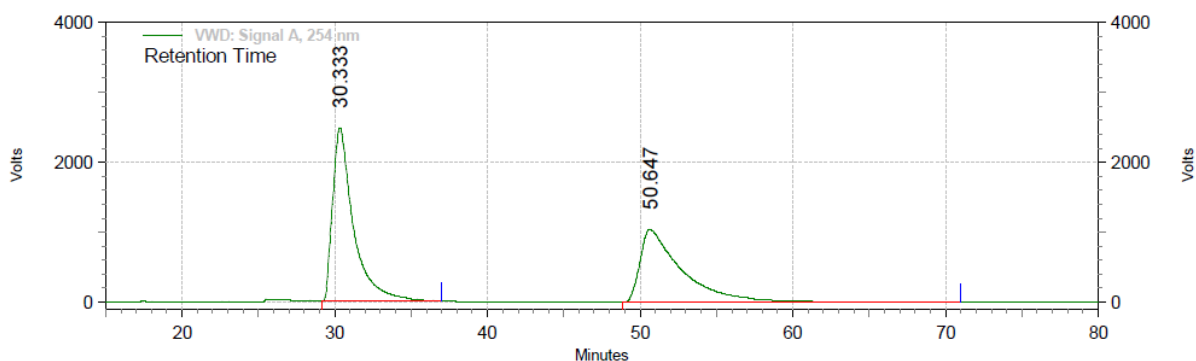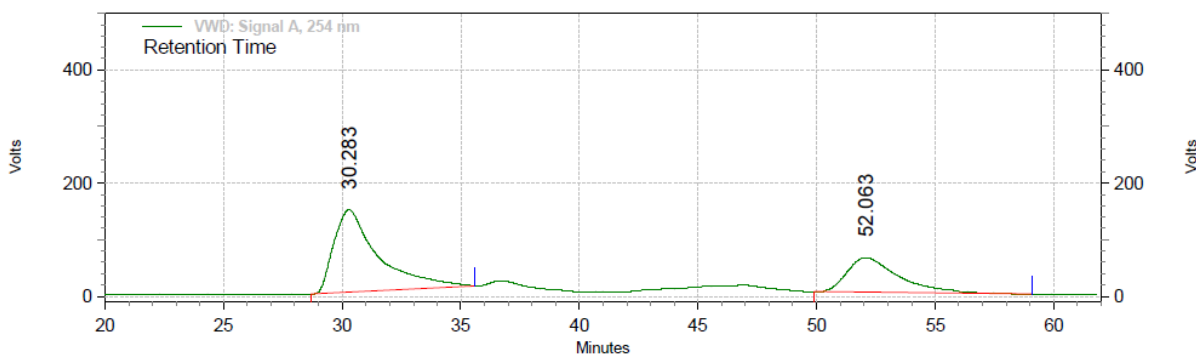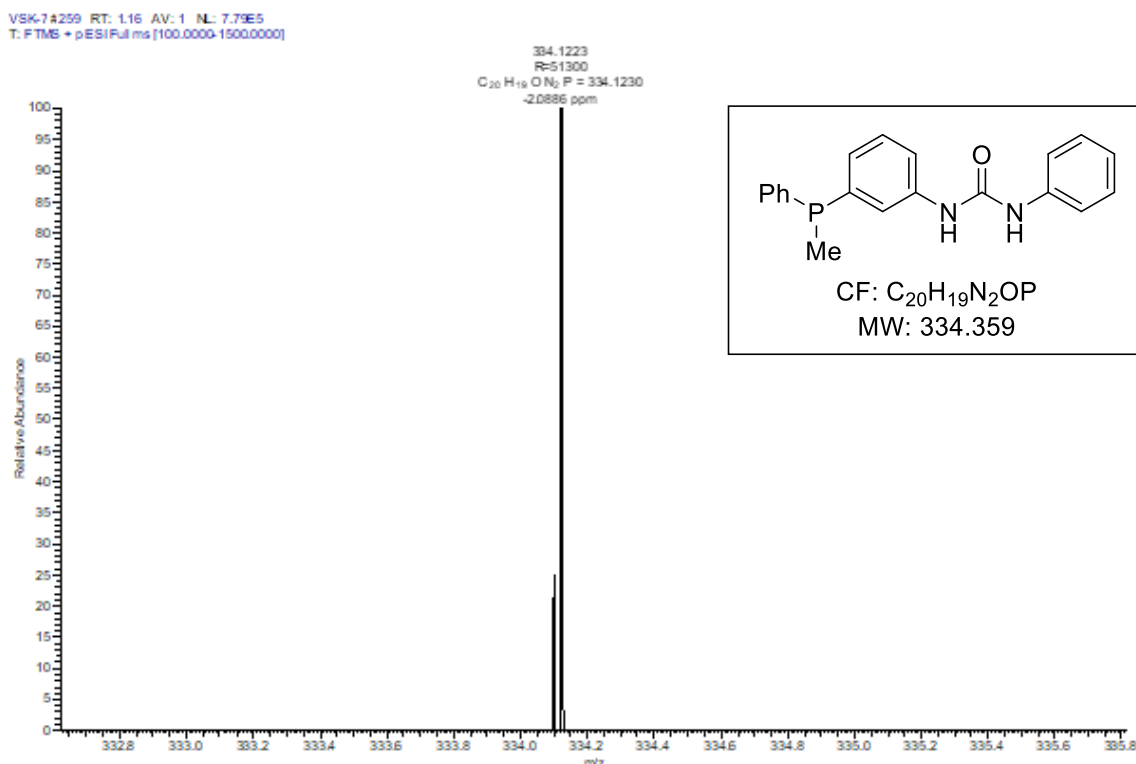

Figure 3.13. ESI-MS (+ve) spectrum of 1-(3-(methyl(phenyl)phosphorothioyl)phenyl)-3-phenylurea (**3.5c**).
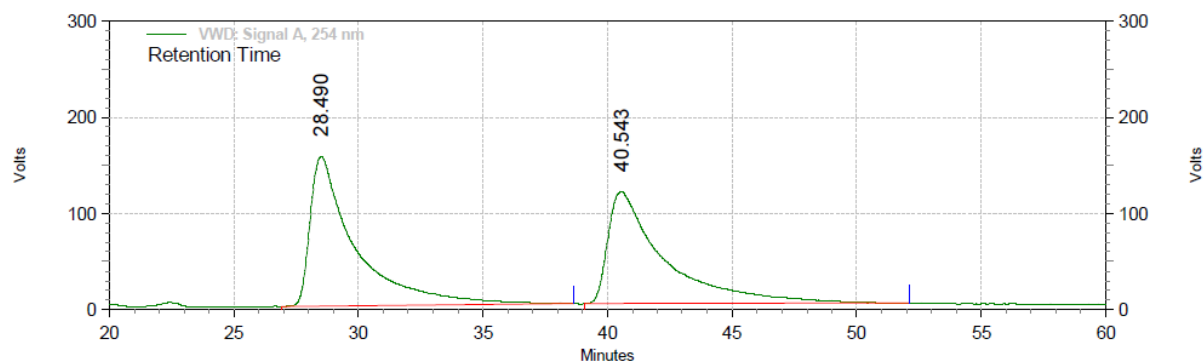
VWD: Signal A, 254 nm Results

Retention Time	Area	Area %
28.490	330097343	51.75
40.543	307751440	48.25

Totals		
	637848783	100.00

Figure 3.14. HPLC chromatogram of racemic 1-(3-(methyl(phenyl)phosphorothioyl)phenyl)-3-phenylurea (**3.5c**).
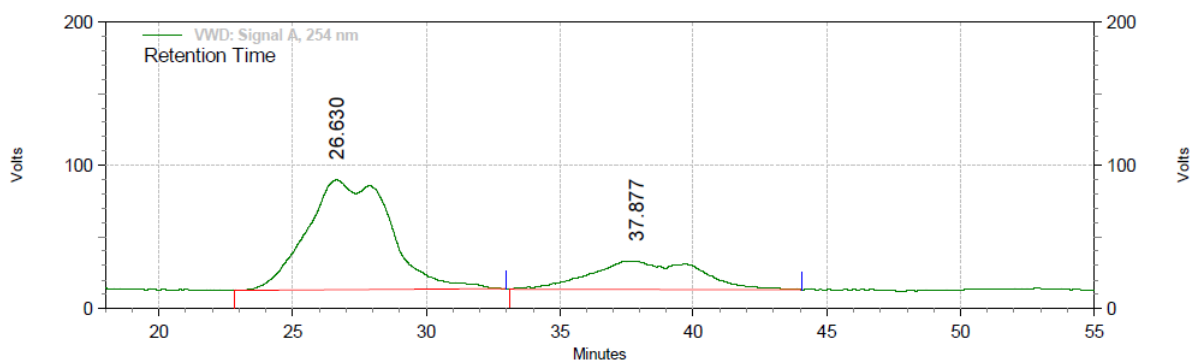
VWD: Signal A, 254 nm Results

Retention Time	Area	Area %
26.630	280830094	75.06
37.877	93290828	24.94

Totals		
	374120922	100.00

Figure 3.15. HPLC chromatogram of chiral 1-(3-(methyl(phenyl)phosphorothioyl)phenyl)-3-phenylurea (**3.5c**).

3.5.3.8. *Racemic* 1-(4-(methyl(phenyl)phosphorothioyl)phenyl)-3-phenylurea (3.5d)

A 1-(4-iodophenyl)-3-phenylurea (**3.2d**) (0.80 mmol) was dissolved in 3 ml of THF, followed by addition of triethylamine (1.60 mmol) and methyl(phenyl)phosphine **3.1a** (0.80 mmol). After stirring for 10 minutes, [Pd(OAc)$_2$] (0.5 mol %) was added and the mixture was refluxed overnight at 68 °C. After completion of the reaction, excess Sulfur powder (S$_8$) (3 eq.) was added to the reaction
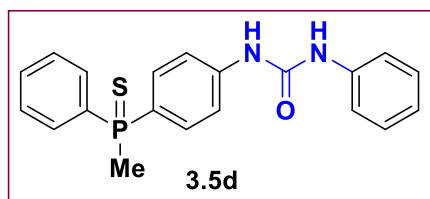
mixture at same temperature and the mixture was stirred for one hour. After this, the above mixture was then treated with degassed water and was extracted with ethyl acetate (3×10 mL). The combined organic layer was dried on $MgSO_4$ for 2 hours and the volatiles were evaporated under reduced pressure. The crude **3.5d** was purified by silica gel column chromatography using 15:85 mixture of DCM:Ethyl acetate. The desired product was isolated as a yellowish solid in 88% yield (256 mg, 0.20 mmol).

¹H NMR (500 MHz, CDCl₃, 298 K): δ = 7.91 (d, J_{H-H} = 10.6 Hz, 2H, Ar), 7.76 (q, J_{H-H} = 13.5, 7.5 Hz, 2H, Ar), 7.49-7.37 (m, 7H, Ar), 7.28-7.23 (m, 4H, Ar, N*H*), 7.04 (t, J_{H-H} = 7.26 Hz, 1H, Ar), 2.21 (d, J_{H-P} =13.12 Hz, 3H, CH₃). **³¹P NMR** (500 MHz, CDCl₃, 298 K): δ = 36.46. **¹³C NMR** (125 MHz, CDCl₃, 298 K): δ = 152.6 (s, Ar, *C*O), 142.1 (s, Ar, quat.), 138.1 (s, Ar, quat.), 132.9 (s, Ar, quat.), 132.1 (s, Ar, quat.), 131.8 (s, Ar, *C*H), 131.3 (d, J_{C-P} = 11.6 Hz, Ar, *C*H), 130.9 (d, J_{C-P} = 11.0 Hz, Ar, *C*H), 129.0 (s, Ar, *C*H), 128.7 (d, J_{C-P} = 12.5 Hz, Ar, *C*H), 123.5 (s, Ar, *C*H), 119.8 (s, Ar, quat.), 119.0 (d, J_{C-P} = 12.9 Hz, Ar, *C*H), 21.4 (d, J_{C-P} = 59.8 Hz, *C*H₃). **ESI-MS** (+ve): (Cal. For $C_{20}H_{19}N_2OP$) m/z = 334.12 [M]⁺.

3.5.3.9. *Chiral* 1-(4-(methyl(phenyl)phosphorothioyl)phenyl)-3-phenylurea (3.5d)
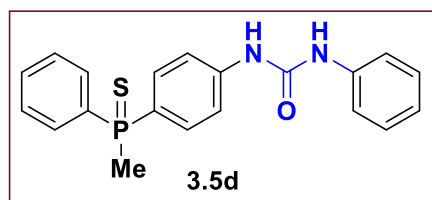
A Schlenk tube was loaded with catalyst **Cat.2** (0.005 mmol), 1-(4-iodophenyl)-3-phenylurea (**3.2d**) (0.1 mmol), methyl(phenyl)phosphine (**3.1a**) (0.1 mmol) in a glove box. The screw capped Schlenk tube was taken out and appropriate temperature was attained. After the standard vacuum-argon cycle NaOAc and 1 ml of DMF were added to the reaction mixture. The progress of the reaction was monitored by ³¹P NMR spectroscopy. After completion of the reaction, Sulphur powder was added to the reaction mixture at same temperature and stirred for half an hour. The content was treated with degassed water (which was pre-cooled at appropriate temperature) and extracted with ethyl acetate (10 mL × 3) (which was pre-cooled at appropriate temperature). The combined organic layer was dried on $MgSO_4$ for half hours at suitable temperature and the volatiles were evaporated under reduced pressure. The plug was washed with DCM until the impurities were eluted, and then the expected product was pushed through with ethyl acetate. After evaporation of the solvent the product was obtained as a pale yellow solid **3.5d** which was analyzed by a combination of spectroscopic and analytical tools.

³¹P NMR (500 MHz, CDCl₃, 298 K): δ = 36.46 (s, P).
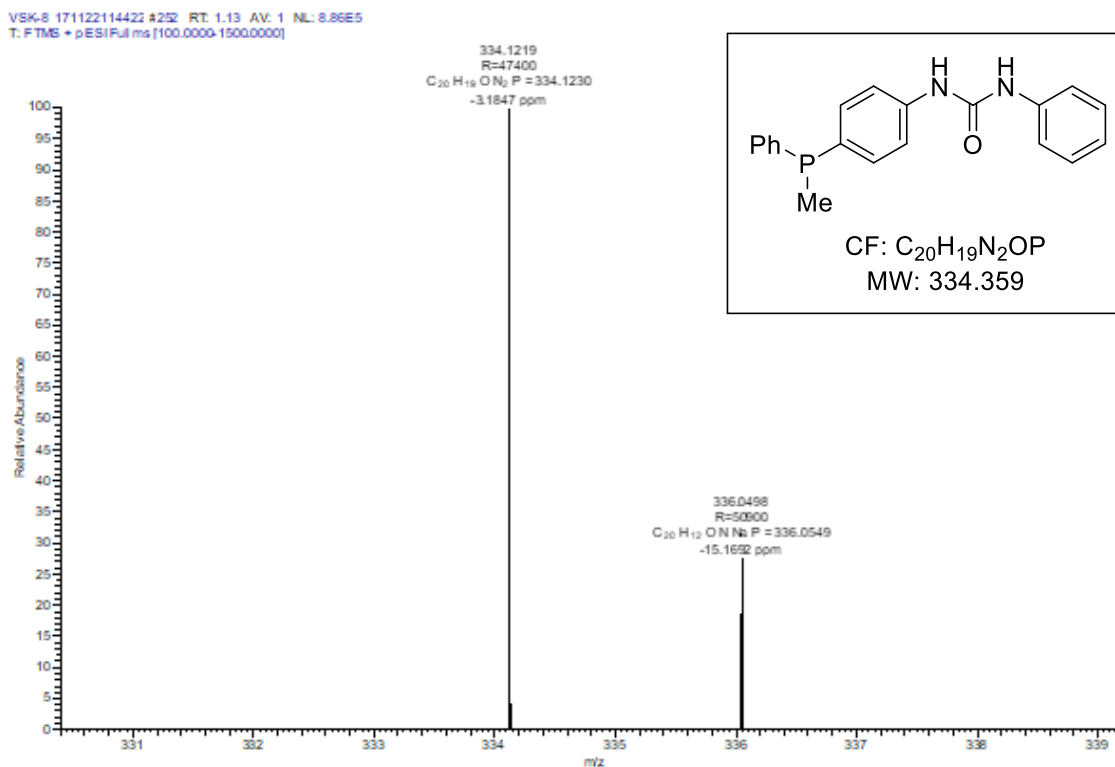
Figure 3.16. ESI-MS (+ve) spectrum of 1-(4-(methyl(phenyl)phosphorothioyl)phenyl)-3-phenylurea (**3.5d**).

3.5.3.10. *Racemic* 1-(3-(methyl(phenyl)phosphorothioyl)phenyl)-3-(naphthalen-1-yl)urea (3.5e)

A 1-(3-iodophenyl)-3-(naphthalen-1-yl)urea (**3.2e**) (0.81 mmol) was dissolved in 3 ml of THF, which was followed by addition of triethylamine (1.62 mmol) and secondary phosphine **3**.**1a** (0.81 mmol). After stirring for 10 minutes, [Pd(OAc)$_2$] (0.5 mol %) was added and the mixture was refluxed overnight at 68 °C. After completion of the reaction, excess Sulfur powder (S$_8$) (3 eq.) was added to the reaction mixture at same temperature and the mixture was stirred for one hour. After this, the above mixture was then treated with degassed water and was extracted with ethyl acetate (3 × 10 mL). The combined organic layer was dried on MgSO$_4$ for 2 hours and the volatiles were evaporated under reduced pressure. The crude **3.5e** was purified by silica gel column chromatography using 90:10 mixture of DCM:Ethyl acetate. The desired product was isolated as a yellowish solid in 84% yield (28 mg, 0.067 mmol).
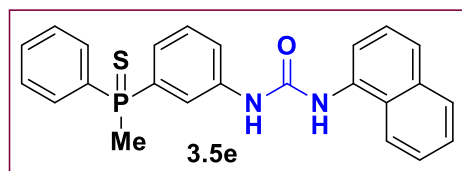
¹H NMR (500 MHz, CDCl$_3$, 298 K): δ = 7.90-7.70 (m, 6H, Ar), 7.60 (d, J_{H-H} = 7.2 Hz, 2H, Ar), 7.52 (s, 1H, N*H*), 7.45-7.39 (m, 3H, Ar), 7.35-7.18 (m, 6H, Ar), 2.18 (d, J_{H-P} = 13.12 Hz, 3H, CH$_3$). **³¹P NMR** (500 MHz, CDCl$_3$, 298 K): δ = 36.60. **¹³C NMR** (125 MHz, CDCl$_3$, 298

K): δ = 154.1 (s, Ar, *C*O), 139.3 (d, J_{C-P} = 14.9 Hz, Ar, quat.), 134.3 (d, J_{C-P} = 25.2 Hz, Ar, quat.), 133.7 (s, Ar, quat.), 133.2 (s, Ar, quat), 132.6 (s, Ar, quat), 1.32.4 (s, Ar, quat), 131.5 4 (s, Ar, quat), 1.30.7 (d, J_{C-P} = 10.2 Hz, Ar, *C*H), 129.3 (d, J_{C-P} = 13.4 Hz, Ar, *C*H), 128.6 (d, J_{C-P} = 12.4 Hz, Ar, *C*H), 128.4 (s, Ar, *C*H), 126.3 (s, Ar, *C*H), 126.1 (s, Ar, *C*H), 125.9 (s, Ar, *C*H), 125.6 (s, Ar, *C*H), 124.6 (d, J_{C-P} = 10.3 Hz, Ar, *C*H), 122.5 (s, Ar, *C*H), 122.4 (s, Ar, *C*H), 121.7 (s, Ar, *C*H), 121.3 (s, Ar, *C*H), 121.2 (s, Ar, *C*H), 21.2 (d, J_{C-P} = 59.9 Hz, *C*H$_3$).
ESI-MS (+ve): (Cal. For $C_{24}H_{21}N_2OPS$) m/z = 417.11 [M+H]$^+$, 439.10 [M+Na]$^+$.

3.5.3.11. *Chiral* 1-(3-(methyl(phenyl)phosphorothioyl)phenyl)-3-(naphthalen-1-yl)urea (3.5e)

A Schlenk tube was loaded with catalyst **Cat.2** (0.005 mmol), 1-(3-iodophenyl)-3-(naphthalen-1-yl)urea (**3.2e**) (0.1 mmol), methyl(phenyl)phosphine (**3.1a**) (0.1 mmol) in a glove box. The screw capped Schlenk tube was taken out and appropriate temperature was attained. After the standard vacuum-argon cycle NaOAc and 1 ml of DMF were added to the reaction mixture. The progress of the reaction was monitored by ^{31}P NMR spectroscopy. After completion of the reaction, Sulphur powder was added to the reaction mixture at same temperature and the mixture was stirred for half an hour. The content was treated with degassed water (which was pre-cooled at appropriate temperature) and extracted with ethyl acetate (10 mL × 3) (which was pre-cooled at appropriate temperature). The combined organic layer was dried on MgSO$_4$ for half hour at suitable temperature and the volatiles were evaporated under reduced pressure. The plug was washed with DCM until the impurities were eluted, and then the expected product was pushed through with ethyl acetate. After evaporation of the solvent the product was obtained as a pale yellow solid **3.5e** which was analyzed by a combination of spectroscopic and analytical tools.

^{31}**P NMR** (500 MHz, CDCl$_3$, 298 K): δ = 36.6 (s, P). **HPLC:** Daicel Chiralpak-IF, 1 mL/min, 10:90 (2-PrOH:Hexane), Rt_1 = 37.7 min; Rt_2 = 46.7 min. ee = 48%.

VSK-3_180206182727 #268 RT: 1.19 AV: 1 NL: 1.16E8
T: FTMS + p ESI Full ms [100.0000-1500.0000]
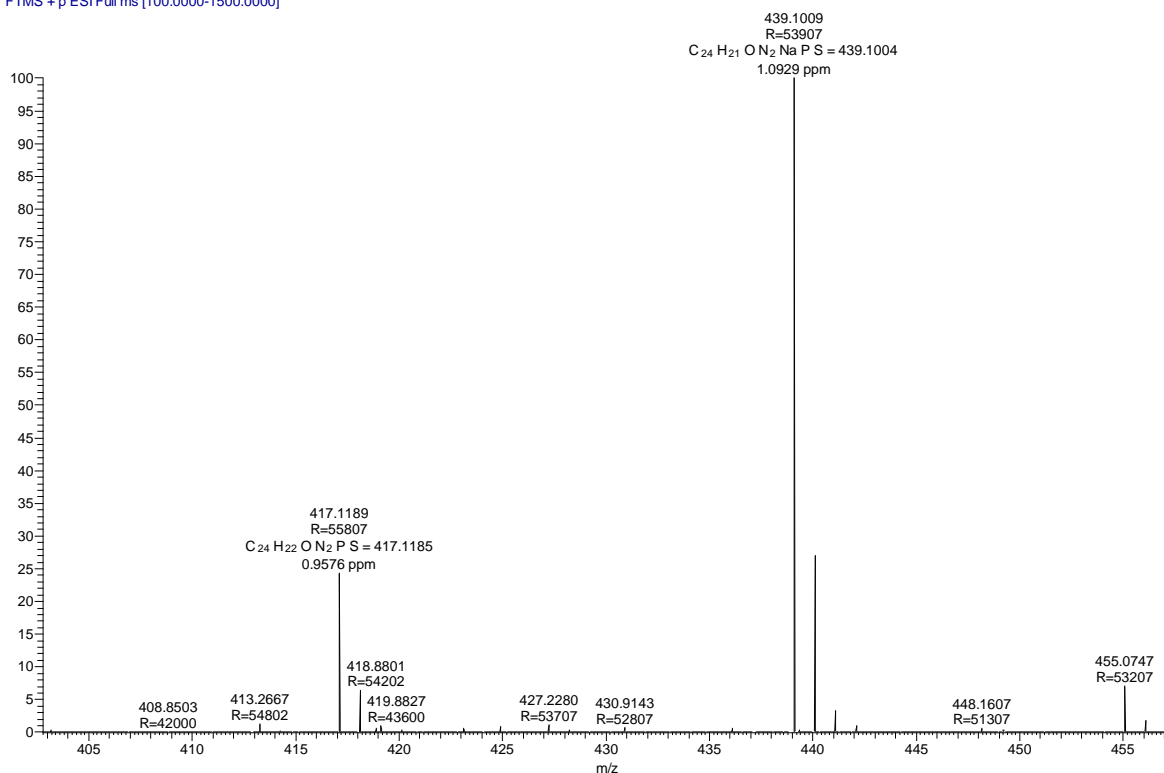
Figure 3.17. ESI-MS (+ve) spectrum of 1-(3-(methyl(phenyl)phosphorothioyl)phenyl)-3-(naphthalen-1-yl)urea (**3.5e**).
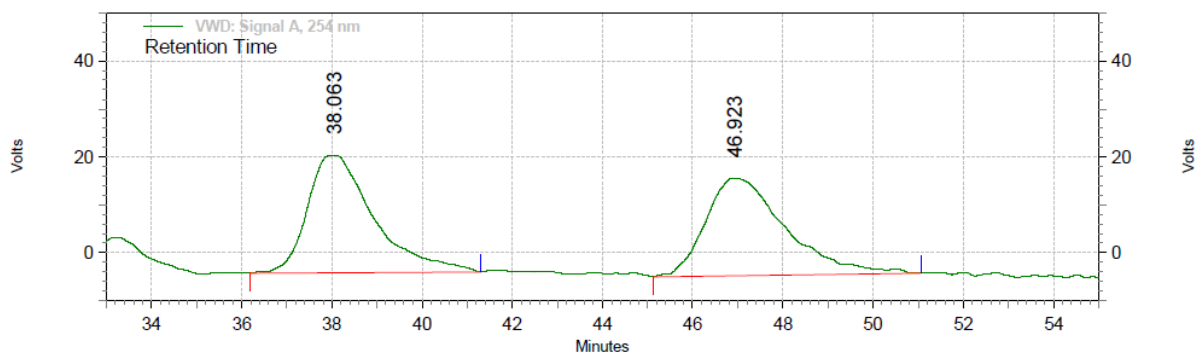
VWD: Signal A, 254 nm Results

Retention Time	Area	Area %
38.063	41962275	50.00
46.923	41969233	50.00

Totals		
	83931508	100.00

Figure 3.18. HPLC chromatogram of racemic 1-(3-(methyl(phenyl)phosphorothioyl)phenyl)-3-(naphthalen-1-yl)urea (**3.5e**).
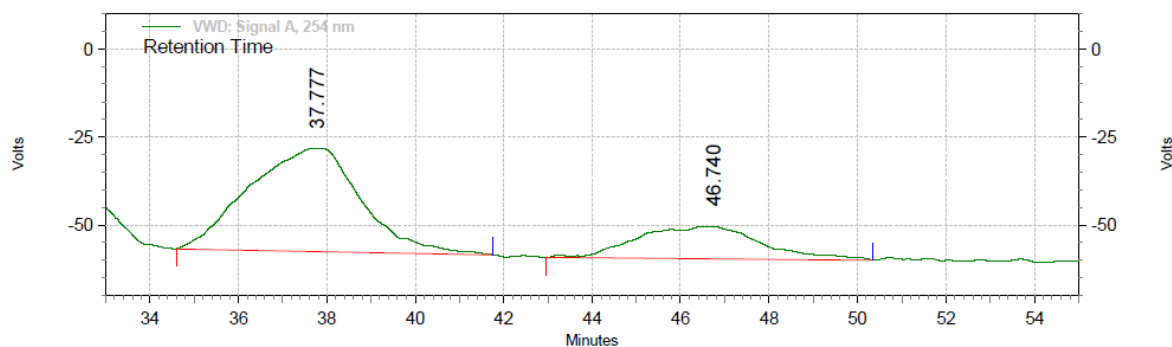
Figure 3.19. HPLC chromatogram of chiral 1-(3-(methyl(phenyl)phosphorothioyl)phenyl)-3-(naphthalen-1-yl)urea (**3.5e**).

3.5.3.12. *Racemic* 1-(4-methoxyphenyl)-3-(3-(methyl(phenyl)phosphorothioyl)phenyl) urea (3.5f)

A 1-(3-iodophenyl)-3-(4-methoxyphenyl)urea (**3.2g**) (1.00 mmol) was dissolved in 4 ml of
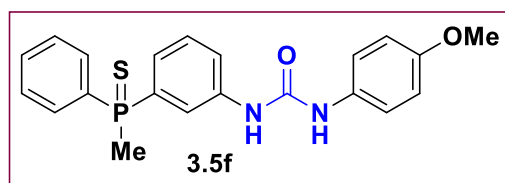
THF, which was followed by addition of triethylamine (2.00 mmol) and methyl(phenyl)phosphine **3.1a** (1.00 mmol). After stirring for 10 minutes, [Pd(OAc)$_2$] (0.5 mol %) was add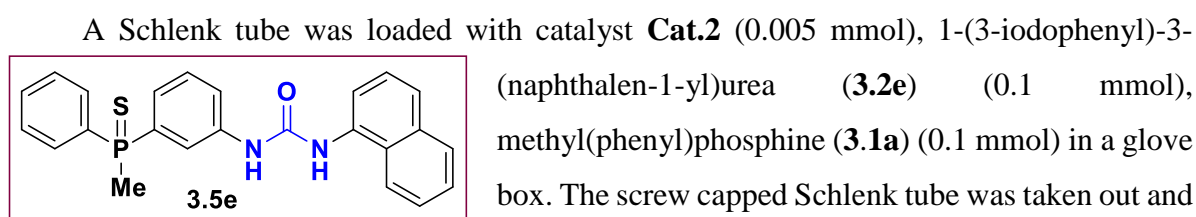ed and the mixture was refluxed overnight at 68 °C. After completion of the reaction, excess Sulfur powder (S$_8$) (3 eq.) was added to the reaction mixture at same temperature and the mixture was stirred for one hour. After this, the above mixture was then treated with degassed water and was extracted with ethyl acetate (3 × 10 mL). The combined organic layer was dried on MgSO$_4$ for 2 hours and the volatiles were evaporated under reduced pressure. The crude **3.5f** was purified by silica gel column chromatography using 90:10 mixture of DCM:Ethyl acetate. The desired product was isolated as a yellow-white color solid in 78% yield (270 mg, 0.068 mmol).

^{1}H NMR (500 MHz, CDCl$_3$, 298 K): δ = 7.82-7.77 (m, 4H, Ar), 7.66 (d, J_{H-H} = 8.3 Hz, 1H, Ar), 7.49 (d, J_{H-H} = 7.1 Hz, 2H, Ar), 7.45-7.42 (m, 2H, Ar), 7.24-7.21 (m, 1H, Ar), 7.17-7.12 (m, 2H, Ar), 7.06 (m, 1H, N*H*), 6.83 (d, J_{H-H} = 7.9 Hz, 1H, Ar), 6.58 (d, J_{H-H} = 8.2 Hz, 1H, Ar), 3.74 (s, 3H, OCH$_3$), 2.24 (d, J$_{H-P}$ = 13 Hz, 3H, CH$_3$). **^{31}P NMR** (500 MHz, CDCl$_3$, 298 K): δ

= 37.12. **^{13}C NMR** (125 MHz, CDCl$_3$, 298 K): δ = 160.2 (s, Ar, *C*-OMe), 152.6 (s, Ar, *C*O), 139.5 (s, Ar, quat.), 139.4 (d, J_{C-P} = 15.2 Hz, Ar, quat.), 133.7 (d, J_{C-P} = 82.1 Hz, Ar, quat.), 132.2 (d, J_{C-P} = 83.2 Hz, Ar, quat.), 131.8 (d, J_{C-P} = 2.9 Hz, Ar, *C*H), 131.6 (d, J_{C-P} = 2.9 Hz, Ar, *C*H), 130.8 (d, J_{C-P} = 10.8 Hz, Ar, *C*H), 130.4 (d, J_{C-P} = 10.3 Hz, Ar, *C*H), 129.7 (s, Ar, *C*H), 129.4 (d, J_{C-P} = 13.7 Hz, Ar, *C*H), 128.7 (d, J_{C-P} = 12.5 Hz, Ar, *C*H), 124.2 (d, J_{C-P} = 10.3 Hz, Ar, *C*H), 122.4 (s, Ar, *C*H), 120.7 (d, J_{C-P} = 12.9 Hz, Ar, *C*H), 111.9 (s, Ar, *C*H), 109.1 (s, Ar, *C*H), 105.5 (s, Ar, *C*H), 21.1 (d, J_{C-P} = 59.7 Hz, *C*H$_3$). **ESI-MS** (+ve): (Cal. For C$_{21}$H$_{21}$N$_2$O$_2$PS) m/z = 397.11 [M-H]$^+$, 419.09 [M-Na]$^+$.

3.5.3.13. *Chiral* 1-(4-methoxyphenyl)-3-(3-(methyl(phenyl)phosphorothioyl)phenyl)urea (3.5f)

A Schlenk tube was loaded with catalyst **Cat.2** (0.005 mmol), 1-(3-iodophenyl)-3-(4-

methoxyphenyl)urea (**3.2g**) (0.1 mmol), and methyl(phenyl)phosphine (**3.1a**) (0.1 mmol) in a glove box. The screw capped Schlenk tube was taken out and appropriate temperature was attained. After the standard vacuum-argon cycle NaOAc and 1 ml DMF were added to the reaction mixture. The progress of the reaction was monitored by ^{31}P NMR spectroscopy. After completion of the reaction, the Sulphur powder was added in reaction mixture at same temperature and stirred it for half an hour. The content was treated with degassed water (which was pre-cooled at appropriate temperature) and extracted with ethyl acetate (10 mL × 3) (which was pre-cooled at appropriate temperature). The plug was washed with DCM until the impurities were eluted, and then the expected product was pushed through with ethyl acetate. After evaporation of the solvent the product was obtained as a pale yellow solid **3.5f** which was analyzed by a combination of spectroscopic and analytical tools.

^{31}P NMR (500 MHz, CDCl$_3$, 298 K): δ = 37.12 (s, P). **HPLC:** Daicel Chiralpak-IF, 1 mL/min, 10:90 (2-PrOH:Hexane), Rt_1 = 54.8 min; Rt_2 = 59.7 min. ee = 54%.
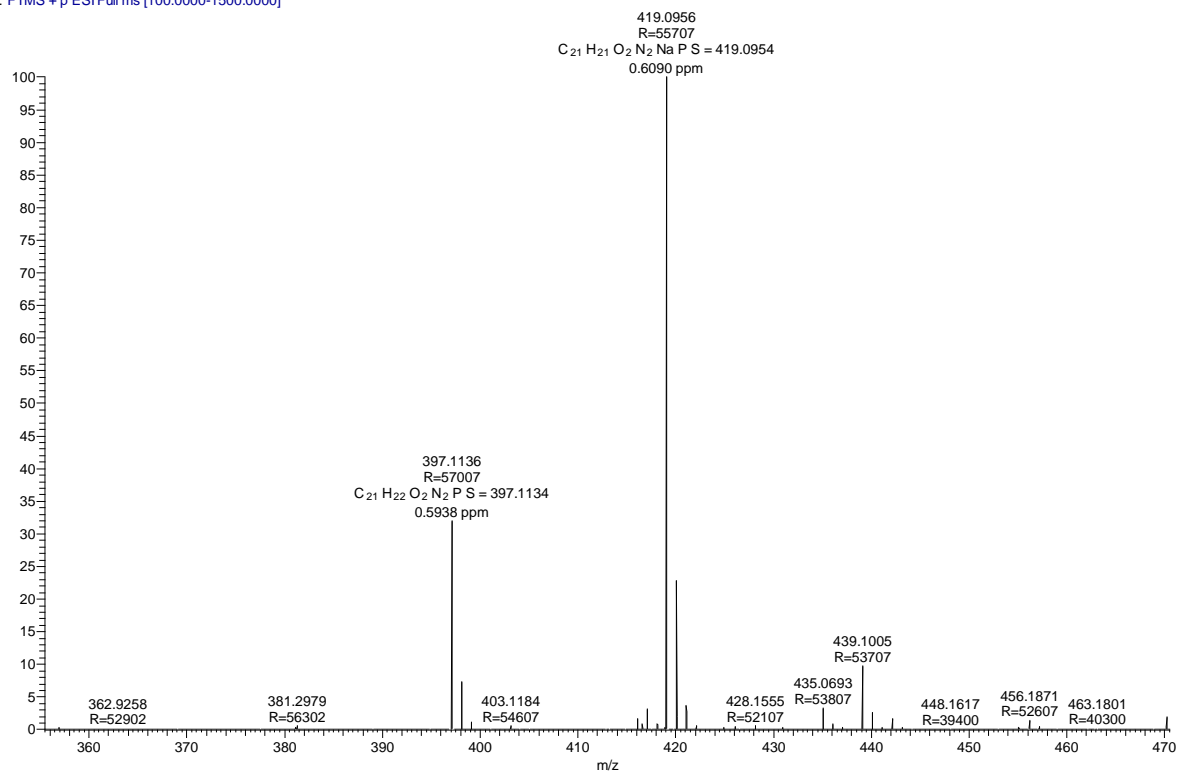
Figure 3.20. ESI-MS (+ve) spectrum of 1-(4-methoxyphenyl)-3-(3-(methyl(phenyl)phosphorothioyl)phenyl) urea (**3.5f**).
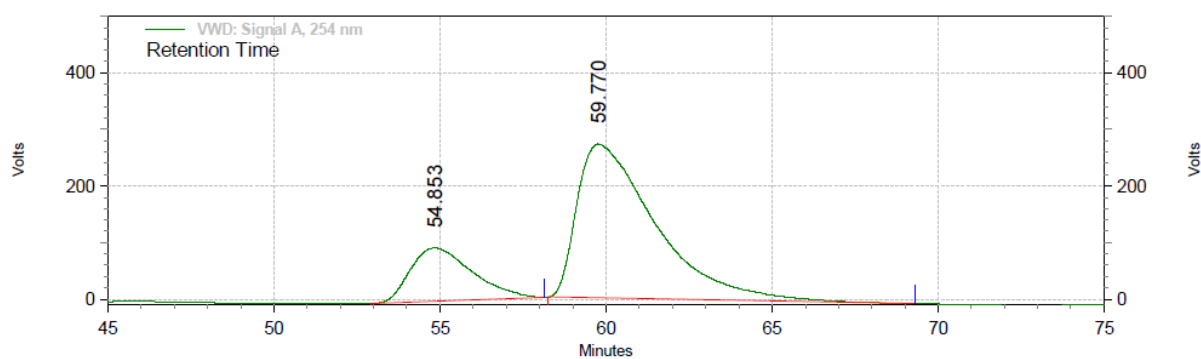
VWD: Signal A, 254 nm Results

Retention Time	Area	Area %
54.853	203296266	21.36
59.770	748326409	78.64
Totals	951622675	100.00

Figure 3.21. HPLC chromatogram of chiral 1-(4-methoxyphenyl)-3-(3-(methyl(phenyl)phosphorothioyl)phenyl) urea (**3.5f**).

3.5.3.14. *Racemic* 1-(4-bromophenyl)-3-(3-(methyl(phenyl)phosphorothioyl)phenyl)urea (3.5g)
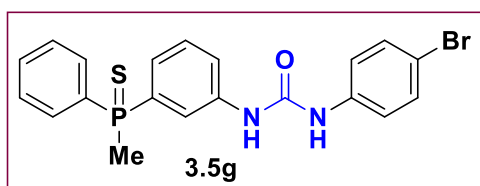
A 1-(4-bromophenyl)-3-(3-iodophenyl)urea (**3.2i**) (0.80 mmol) was dissolved in 3 ml of THF, which was followed by addition of triethylamine (1.60 mmol) and methyl(phenyl)phosphine **3.1a** (0.80 mmol). After stirring for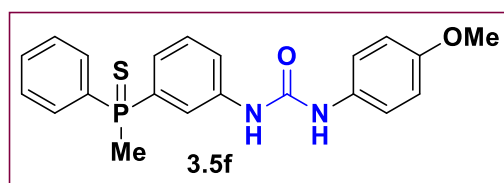 10 minutes, [Pd(OAc)$_2$] (0.5 mol %) was added and the mixture was refluxed overnight at 68 °C. After completion of the reaction, excess Sulfur powder (S$_8$) (3 eq.) was added to the reaction mixture at same temperature and the mixture was stirred for one hour. After this, the above mixture was then treated with degassed water and was extracted with ethyl acetate (3 × 10 mL). The combined organic layer was dried on MgSO$_4$ for 2 hours and the volatiles were evaporated under reduced pressure. The crude **3.5g** was purified by silica gel column chromatography using 80:20 mixture of DCM:Ethyl acetate. The desired product was isolated as a brownish yellow solid in 87% yield (315 mg, 0.75 mmol).

^{1}H NMR (500 MHz, CDCl$_3$, 298 K): δ = 7.91-7.87 (m, 1H, Ar), 7.82-7.69 (m, 4H, Ar and N*H*), 7.52-7.44 (m, 4H, Ar and N*H*), 7.33 (d, J_{H-H} = 8.64 Hz, 2H, Ar), 7.21 (d, J_{H-H} = 8.76 Hz, 3H, Ar), 7.05 (q, J_{H-H} = 12.66, 7.70 Hz, 1H, Ar), 2.26 (d, J$_{H-P}$ =13.12 Hz, 3H, CH$_3$). **^{31}P NMR** (500 MHz, CDCl$_3$, 298 K): δ = 37.39. **^{13}C NMR** (125 MHz, CDCl$_3$, 298 K): δ = 154.3 (s, Ar, *C*O), 139.5 (d, J_{C-P} = 15.3 Hz, Ar, quat.), 137.5 (s, Ar, quat.), 134.0 (s, Ar, quat.), 133.3 (s, Ar, quat.), 132.0 (s, Ar, *C*H), 131.8 (s, Ar, *C*H), 130.9 (d, J_{C-P} = 10.9 Hz, Ar, *C*H), 129.5 (d, J_{C-P} = 13.7 Hz, Ar, *C*H), 128.8 (d, J_{C-P} = 12.5 Hz, Ar, *C*H), 124.1 (d, J_{C-P} = 10.1 Hz, Ar, *C*H), 122.3 (s, Ar, *C*H), 120.9 (s, Ar, *C*H), 21.1 (d, J_{C-P} = 59.9 Hz, *C*H$_3$). **ESI-MS** (+ve): (Cal. For C$_{20}$H$_{18}$N$_2$OBrPS) m/z = 466.99 [M-Na]$^+$

3.5.3.15. *Chiral* 1-(4-bromophenyl)-3-(3-(methyl(phenyl)phosphorothioyl)phenyl)urea (3.5g)

A Schlenk tube was loaded with catalyst **Cat.2** (0.005 mmol), 1-(4-bromophenyl)-3-(3-iodophenyl)urea (**3.2i**) (0.1 mmol), and methyl(phenyl)phosphine (**3.1a**) (0.1 mmol) in a glove box. The screw capped Schlenk tube was taken out and appropriate temperature was attained. After the standard vacuum-argon cycle, NaOAc and 1 ml DMF were added to the reaction mixture. The progress of the reaction was monitored by ^{31}P NMR spectroscopy. After completion of the

reaction, the Sulphur powder was added to the reaction mixture at same temperature and the reaction mixture was stirred for half an hour. The content was treated with degassed water (which was pre-cooled at appropriate temperature) and extracted with ethyl acetate (10 mL × 3) (which was pre-cooled at appropriate temperature). The combined organic layer was dried on MgSO₄ for half hour at suitable temperature and the volatiles were evaporated under reduced pressure. The plug was washed with DCM until the impurities were eluted, and then the expected product was pushed through with ethyl acetate. After evaporation of the solvent the product was obtained as a pale yellow solid **3.5f** which was analyzed by a combination of spectroscopic and analytical tools.

^{31}**P NMR** (500 MHz, CDCl₃, 298 K) δ = 37.12 (s, P). **HPLC:** Daicel Chiralpak-IA, 1 mL/min, 10:90 (2-PrOH:Hexane), Rt_1 = 57.3 min; Rt_2 = 69.6 min.
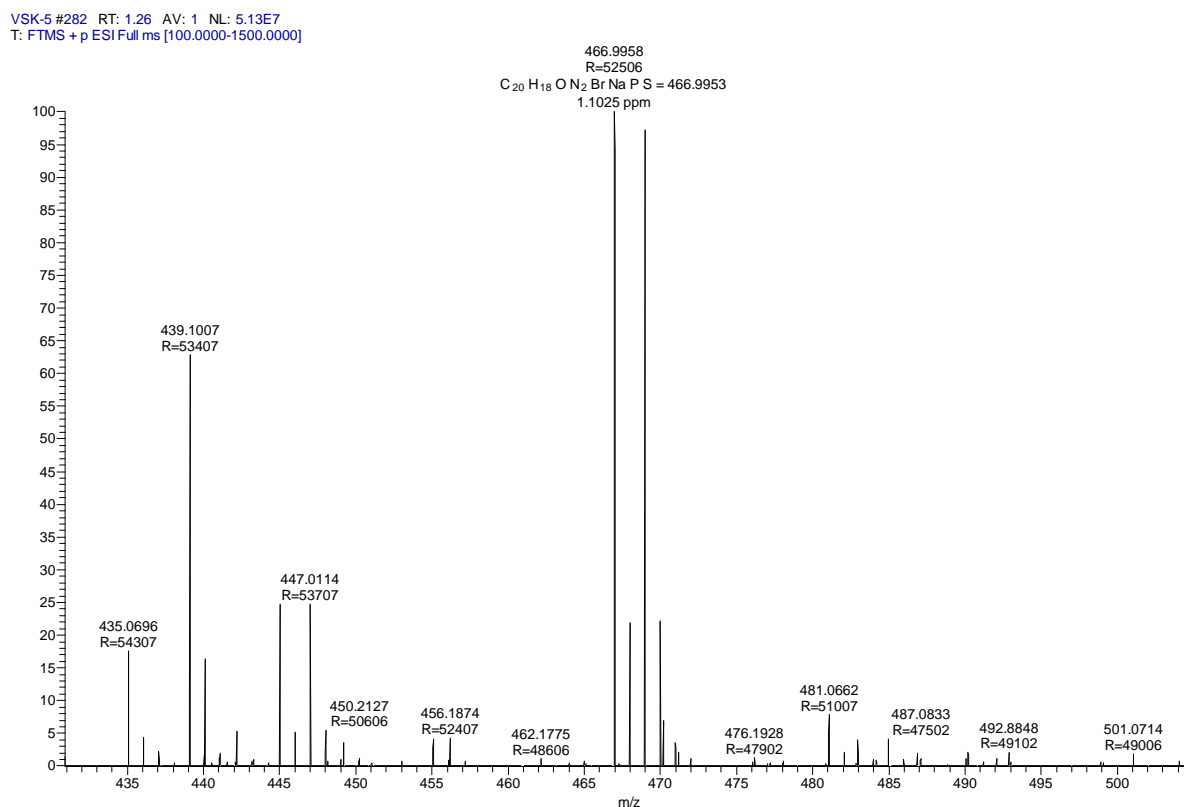
Figure 3.22. ESI-MS (+ve) spectrum of 1-(4-bromophenyl)-3-(3-(methyl(phenyl)phosphorothioyl)phenyl) urea (**3.5g**).
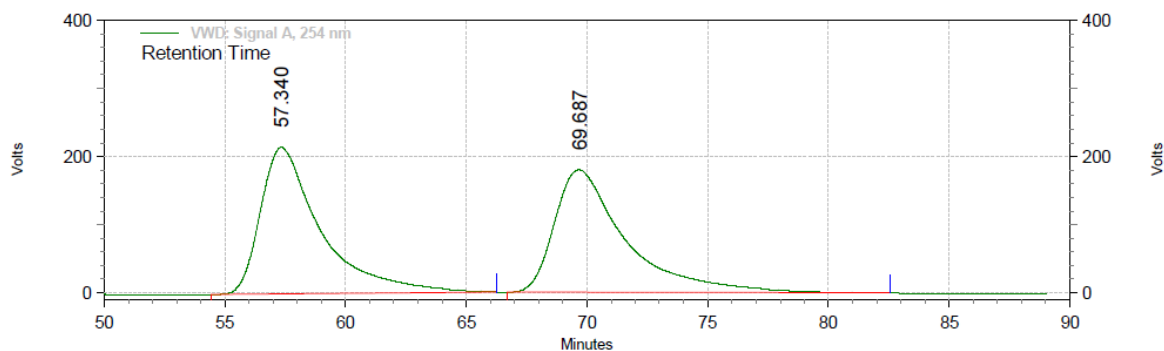
Figure 3.23. HPLC chromatogram of racemic 1-(4-bromophenyl)-3-(3-(methyl(phenyl)phosphorothioyl)phenyl) urea (**3.5g**).
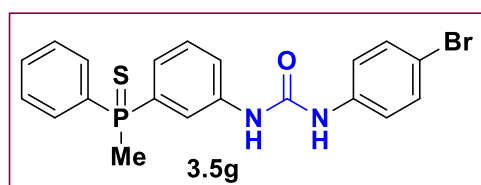
3.5.3.16. *Racemic* 1-(3-methoxyphenyl)-3-(3-(methyl(phenyl)phosphorothioyl)phenyl) urea (3.5h)

A 1-(3-iodophenyl)-3-(3-methoxyphenyl)urea (**3.2k**) (0.81mmol) was dissolved in 2 ml of THF, which was followed by addition of triethylamine (1.62 mmol) and secondary phosphine **3.1a** (0.81mmol). After stirring for 10 minutes, [Pd(OAc)$_2$] (0.5 mol %) was added and the mixture was refluxed overnight at 68 °C. After completion of the reaction, excess Sulfur powder (S$_8$) (3 eq.) was added to the reaction mixture at same temperature and the mixture was stirred for one hour. After this, the above mixture was then treated with degassed water and was extracted with ethyl acetate (3 × 10 mL). The combined organic layer was dried on MgSO$_4$ for 2 hours and the volatiles were evaporated under reduced pressure. The crude **3.5h** was purified by silica gel column chromatography using 90:10 mixture of DCM:Ethyl acetate. The desired product was isolated as a whitish yellow solid in 84% yield (270 mg, 0.68 mmol).

¹H NMR (500 MHz, CDCl$_3$, 298 K): δ = 7.82-7.76 (m, 4H, Ar), 7.69 (s, 1H N*H*), 7.48-7.43 (m, 4H, Ar), 7.24-7.20 (m, 1H, Ar), 7.16-7.11 (m, 2H, Ar), 7.06 (s, 1H N*H*), 6.82 (d, $J_{H\text{-}H}$ = 7.8 Hz, 1H, Ar), 6.58 (d, $J_{H\text{-}H}$ = 7.8 Hz, 1H, Ar), 3.74 (s, 3H, OCH$_3$), 2.24 (d, $J_{H\text{-}P}$ = 13.10 Hz, 3H, CH$_3$). **³¹P NMR** (500 MHz, CDCl$_3$, 298 K): δ = 37.12. **¹³C NMR** (125 MHz, CDCl$_3$, 298 K):

δ = 160.2 (s, Ar, *C*O), 152.6 (s, Ar, quat.), 139.4 (d, J_{C-P} = 15.3 Hz, Ar, quat.), 134.1 (s, Ar, quat.), 133.4 (s, Ar, quat.), 132.6 (s, Ar, quat.), 131.8 (s, Ar, *C*H), 130.8 (d, J_{C-P} = 10.8 Hz, Ar, *C*H), 129.7 (s, Ar, *C*H), 129.4 (d, J_{C-P} = 13.8 Hz, Ar, *C*H), 128.7 (d, J_{C-P} = 12.5 Hz, Ar, *C*H), 124.2 (d, J_{C-P} = 10.3 Hz, Ar, *C*H), 122.4 (s, Ar, *C*H), 120.8 (d, J_{C-P} = 12.9 Hz, Ar, *C*H), 111.9 (s, Ar, *C*H), 109.1 (s, Ar, *C*H), 105.0 (s, Ar, *C*H), 55.2 (s, O*C*H), 21.1 (d, J_{C-P} = 59.9 Hz, *C*H$_3$). **ESI-MS** (+ve): (Cal. For $C_{21}H_{21}N_2O_2PS$) m/z = 397.11 [M-H]$^+$, 419.09 [M-Na]$^+$.

3.5.3.17. Chiral 1-(3-methoxyphenyl)-3-(3-(methyl(phenyl)phosphorothioyl)phenyl)urea (3.5h)

A Schlenk tube was loaded with catalyst **Cat.2** (0.005 mmol), 1-(3-iodophenyl)-3-(3-

methoxyphenyl)urea (**3.2k**) (0.1 mmol), and methyl(phenyl)phosphine (**3.1a**) (0.1 mmol) in a glove box. The screw capped Schlenk tube was taken out and appropriate temperature was attained. After the standard vacuum-argon cycle, NaOAc and 1 ml DMF were added to the reaction mixture. The progress of the reaction was monitored by ^{31}P NMR spectroscopy. After completion of the reaction, Sulphur powder was added in reaction mixture at same temperature and the reaction mixture was stirred for half an hour. The content was treated with degassed water (which was pre-cooled at appropriate temperature) and extracted with ethyl acetate (10 mL × 3) (which was pre-cooled at appropriate temperature). The combined organic layer was dried on MgSO$_4$ for half hour at suitable temperature and the volatiles were evaporated under reduced pressure. The plug was washed with DCM until the impurities were eluted, and then the expected product was pushed through with ethyl acetate. After evaporation of the solvent the product was obtained as a pale yellow solid **3.5f** which was analyzed by a combination of spectroscopic and analytical tools.

^{31}**P NMR** (500 MHz, CDCl$_3$, 298 K): δ = 37.12 (s, P). **HPLC:** Daicel Chiralpak-IF, 1 mL/min, 07:93 (2-PrOH:Hexane), Rt_1 = 70.0 min; Rt_2 = 75.0 min. ee = 61%.
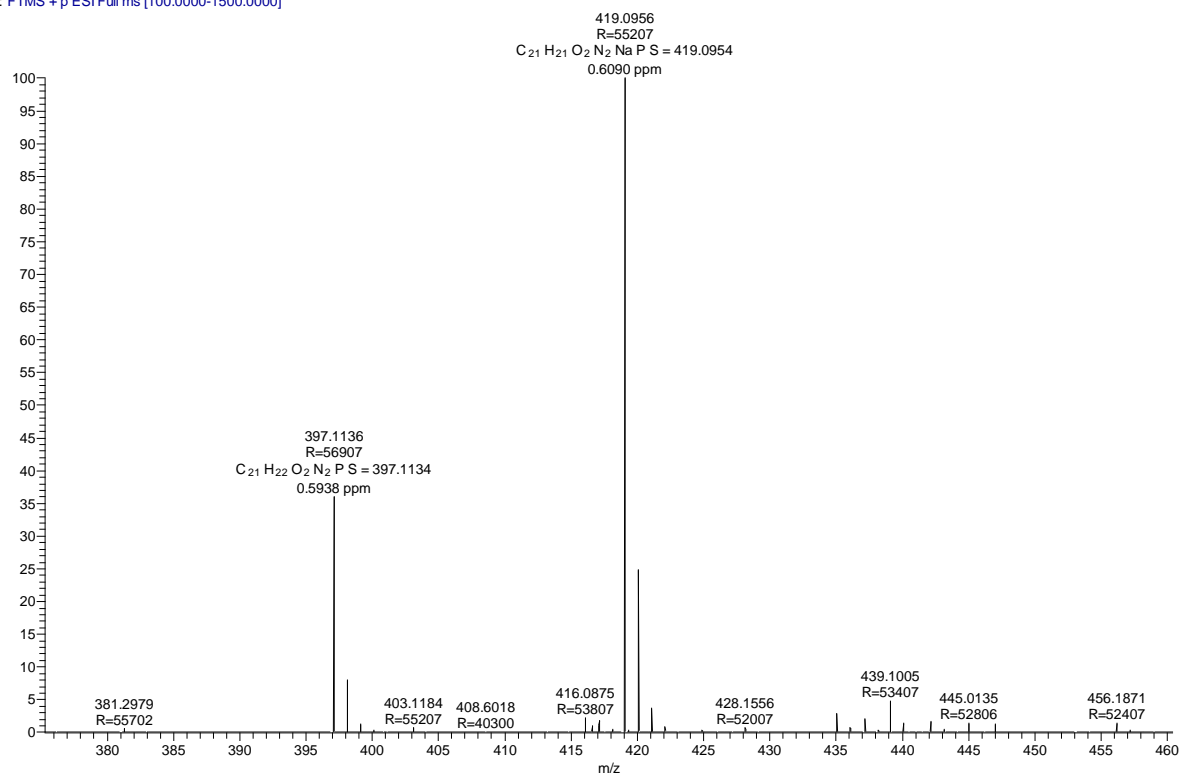
Figure 3.24. ESI-MS (+ve) spectrum of 1-(3-methoxyphenyl)-3-(3-(methyl(phenyl)phosphorothioyl)phenyl) urea (**3.5h**).
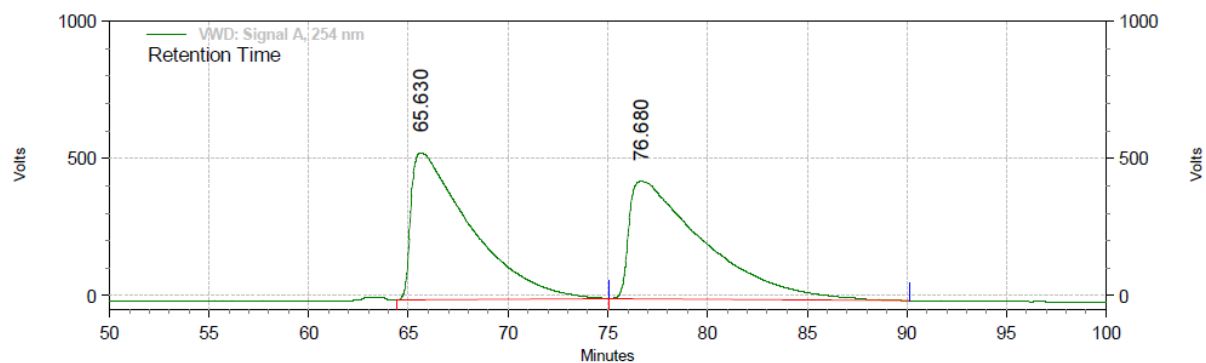
VWD: Signal A, 254 nm Results

Retention Time	Area	Area %
65.630	1858826615	49.88
76.680	1867424321	50.12

Totals		
	3726250936	100.00

Figure 3.25. HPLC chromatogram of racemic 1-(3-methoxyphenyl)-3-(3-(methyl(phenyl)phosphorothioyl) phenyl)urea (**3.5h**).
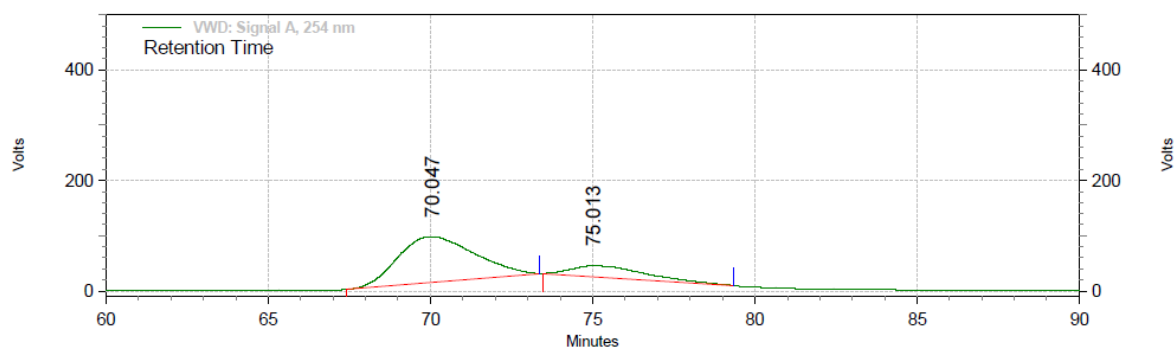
VWD: Signal A, 254 nm Results		
Retention Time	Area	Area %
70.047	225967070	80.84
75.013	53566074	19.16
Totals		
	279533144	100.00

Figure 3.26. HPLC chromatogram of chiral 1-(4-bromophenyl)-3-(3-(methyl(phenyl)phosphorothioyl)phenyl) urea (**3.5g**).

3.5.3.18. 1-(3-(phenyl(*o*-tolyl)phosphine)phenyl)urea (3.5i)
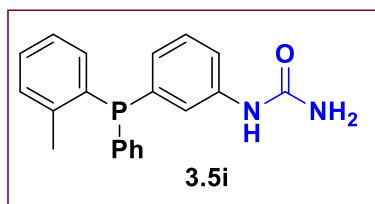
For characterization see chapter 2 (section 2.5.4.2)

HPLC: Daicel Chiralpak-IF, 0.7 mL/min, 06:94 (2-PrOH:Hexane), Rt_1 = 69.1 min; Rt_2 = 75.4 min. ee = 45%.
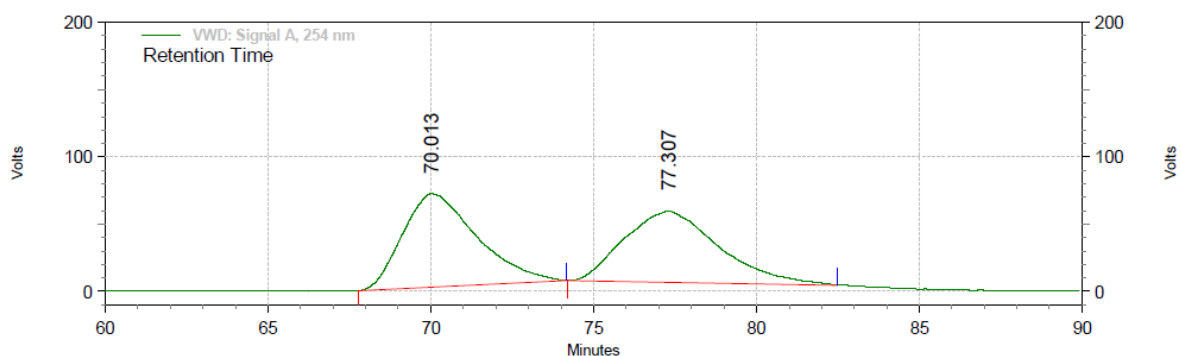
VWD: Signal A, 254 nm Results		
Retention Time	Area	Area %
70.013	183978627	50.76
77.307	178492353	49.24
Totals		
	362470980	100.00

Figure 3.27. HPLC chromatogram of racemic 1-(3-(phenyl(*o*-tolyl)phosphine)phenyl)urea (**3.5i**).
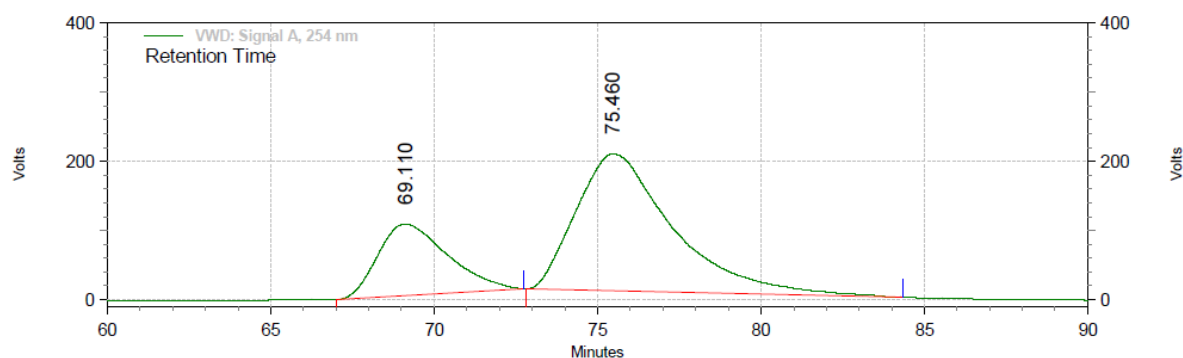
VWD: Signal A, 254 nm Results

Retention Time	Area	Area %
69.110	256056935	27.36
75.460	679934549	72.64

Totals		
	935991484	100.00

Figure 3.28. HPLC chromatogram of chiral 1-(3-(phenyl(*o*-tolyl)phosphine)phenyl)urea (**3.5i**).

3.5.3.19. 1-(4-(phenyl(*o*-tolyl)phosphanyl)phenyl)urea (3.5j)
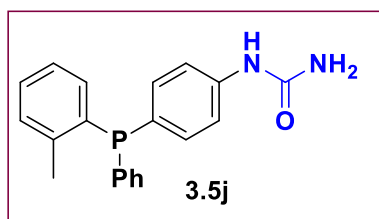
For characterization see chapter 2 (section 2.5.4.4)

HPLC: Daicel Chiralpak-IA, 1 mL/min, 10:94 (2-PrOH:Hexane), Rt_1 = 38.4 min; Rt_2 = 43.0 min. ee = 46%.
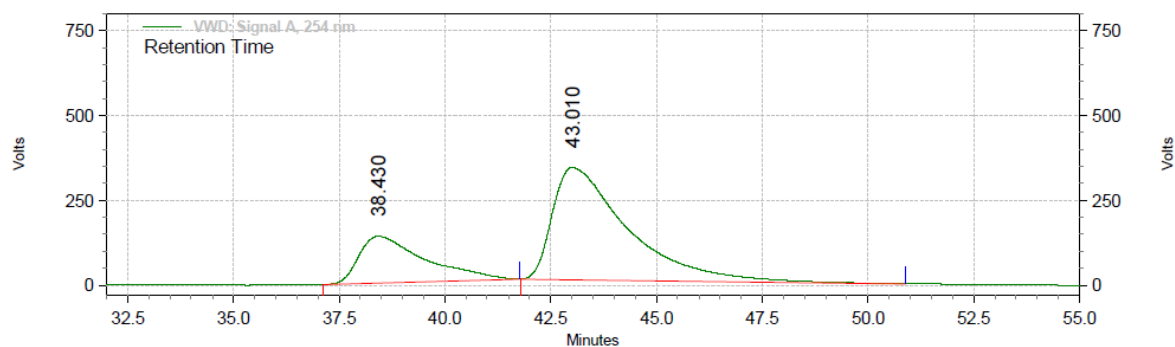
VWD: Signal A, 254 nm Results

Retention Time	Area	Area %
38.430	250784280	26.75
43.010	686816648	73.25

Totals		
	937600928	100.00

Figure 3.29. HPLC chromatogram of chiral 1-(4-(phenyl(*o*-tolyl)phosphanyl)phenyl)urea (**3.5j**).

3.5.3.20. *Racemic* 1-(naphthalen-1-yl)-3-(3-(phenyl(o-tolyl)phosphorothioyl)phenyl)urea (3.5k)

A 1-(3-iodophenyl)-3-(naphthalen-1-yl)urea (**3.2e**) (0.50 mmol) was dissolved in 2 ml of THF, which was followed by addition of triethylamine (1.00 mmol) and phenyl(o-tolyl)phosphine **3.1b** (0.50 mmol). After stirring for 10 minutes, [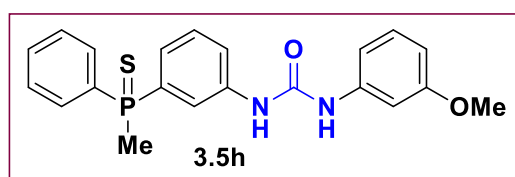Pd(OAc)$_2$] (0.5 mol %) was added and the mixture was refluxed overnight at 68 °C. After completion of the reaction, excess Sulfur powder (S$_8$) (3 eq.) was added to the reaction mixture at same temperature and the mixture was stirred for one hour. After this, the above mixture was then treated with degassed water and was extracted with ethyl acetate (3 × 10 mL). The combined organic layer was dried on MgSO$_4$ for 2 hours and the volatiles were evaporated under reduced pressure. The crude **3.5k** was purified by silica gel column chromatography using 85:15 mixture of DCM:Ethyl acetate. The desired product was isolated as a yellowish solid in 85% yield (210 mg, 0.042 mmol).
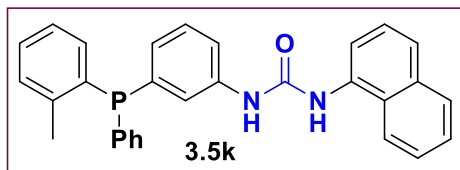
^{1}H NMR (500 MHz, CDCl$_3$, 298 K): δ = 7.69-7.58 (m, 1H, Ar), 7.54-7.48 (m, 2H, Ar), 7.33 (d, J_{H-H} = 4.6 Hz, 3H, Ar), 7.30-7.28 (m, 2H, Ar), 7.26 (s, 1H, Ar), 7.25 (s, 1H, Ar), 7.22-7.19 (m, 3H, Ar), 7.09 (d, J_{H-H} = 7.2 Hz, 1H, Ar), 7.06 (s, 1H, Ar), 6.94 (t, J_{H-H} = 8.5 Hz, 5H, Ar), 6.78 (q, J_{H-H} = 7.2, 4.6 Hz, 2H, Ar), 2.38 (s, 3H, CH$_3$). **^{31}P NMR** (500 MHz, CDCl$_3$, 298 K): δ = -13.45. **^{13}C NMR** (125 MHz, CDCl$_3$, 298 K): δ = 152.2 (s, Ar, *C*O), 142.3 (s, Ar, quat.), 141.2 (s, Ar, quat.), 138.3 (s, Ar, quat.), 137.8 (s, Ar, quat.), 134.0 (d, J_{C-P} = 19.9 Hz, Ar, *C*H), 133.7 (s, Ar, quat.), 132.7 (s, Ar, *C*H), 130.1 (d, J_{C-P} = 5 Hz, Ar, *C*H), 129.5 (d, J_{C-P} = 7.6 Hz, Ar, *C*H), 129.3 (d, J_{C-P} = 16.2 Hz, Ar, *C*H), 129.2 (s, Ar, quat.), 129.0 (s, Ar, quat.), 128.8 (d, J_{C-P} = 7.1 Hz, Ar, *C*H), 128.5 (d, J_{C-P} = 7.1 Hz, Ar, *C*H), 126.0 (s, Ar, *C*H), 125.6 (s, Ar, *C*H), 125.4 (s, Ar, *C*H), 122.8 (d, J_{C-P} = 8 Hz, Ar, *C*H), 121.1 (s, Ar, *C*H), 115.8 (s, Ar, *C*H), 115.6 (s, Ar, *C*H), 21.1 (d, J_{C-P} = 21.9 Hz, CH$_3$). **ESI-MS** (+ve): (Cal. For C$_{30}$H$_{26}$N$_2$OP) m/z = 461.17 [M+H]$^+$.

3.5.3.21. *Chiral* 1-(naphthalen-1-yl)-3-(3-(phenyl(o-tolyl)phosphanyl)phenyl)urea (3.5k)
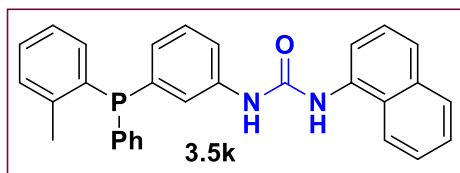
A Schlenk tube was loaded with catalyst **Cat.2** (0.005 mmol), 1-(3-iodophenyl)-3-(naphthalen-1-yl)urea (**3.2e**) (0.1 mmol), and phenyl(*o*-tolyl)phosphine (**3.1b**) (0.1 mmol) in a glove box. The screw capped Schlenk tube was taken out and appropriate temperature was attained. After the standard vacuum-argon cycle, NaOAc and 1

ml DMF were added to the reaction mixture. The progress of the reaction was monitored by ^{31}P NMR spectroscopy. After completion of the reaction, Sulphur powder was added to the reaction mixture at same temperature and the reaction mixture was stirred for half an hour. The content was treated with degassed water (which was pre-cooled at appropriate temperature) and extracted with ethyl acetate (10 mL × 3) (which was pre-cooled at appropriate temperature). The combined organic layer was dried on MgSO$_4$ for half hour at suitable temperature and the volatiles were evaporated under reduced pressure. The plug was washed with DCM until the impurities were eluted, and then the expected product was pushed through with ethyl acetate. After evaporation of the solvent the product was obtained as a pale yellow solid **3.5k** which was analyzed by a combination of spectroscopic and analytical tools.

^{31}**P NMR** (500 MHz, CDCl$_3$, 298 K): δ = 37.12 (s, P). **HPLC:** Daicel Chiralpak-IA, 0.7 mL/min, 07:93 (2-PrOH:Hexane), Rt_1 = 50.3 min; Rt_2 = 57.7 min. ee = 50%.
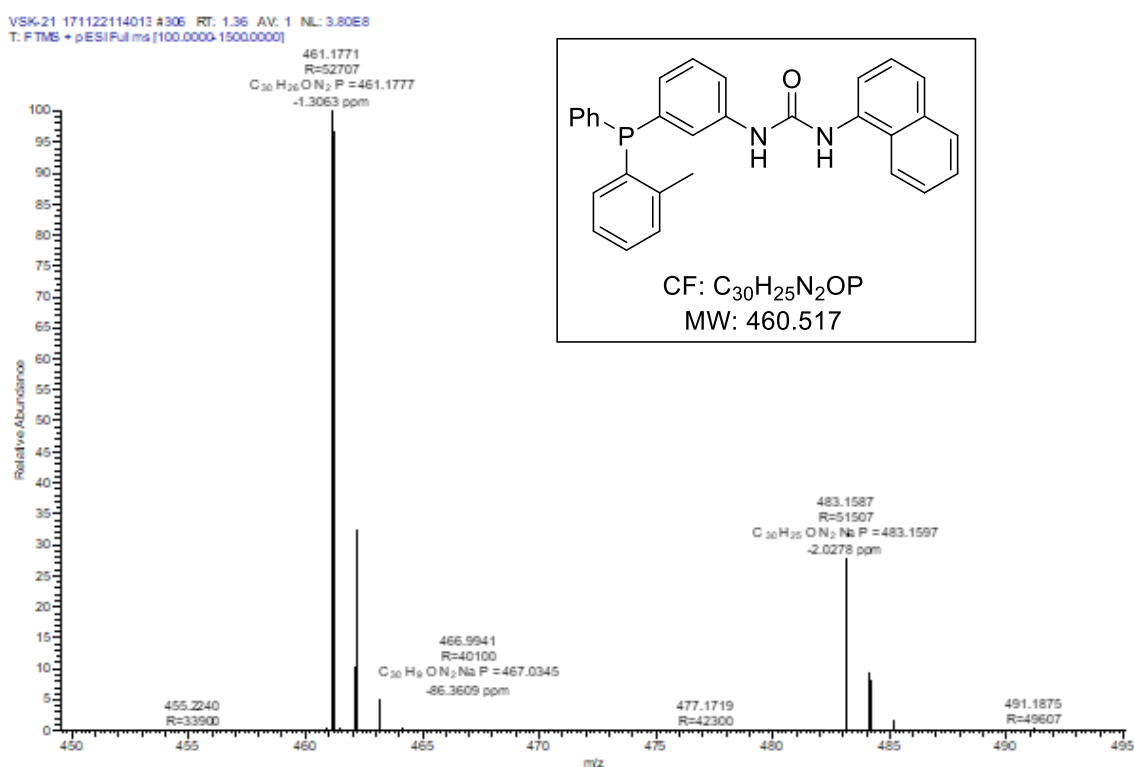
Figure 3.30. ESI-MS (+ve) spectrum of 1-(naphthalen-1-yl)-3-(3-(phenyl(o-tolyl)phosphorothioyl)phenyl)urea (**3.5k**).
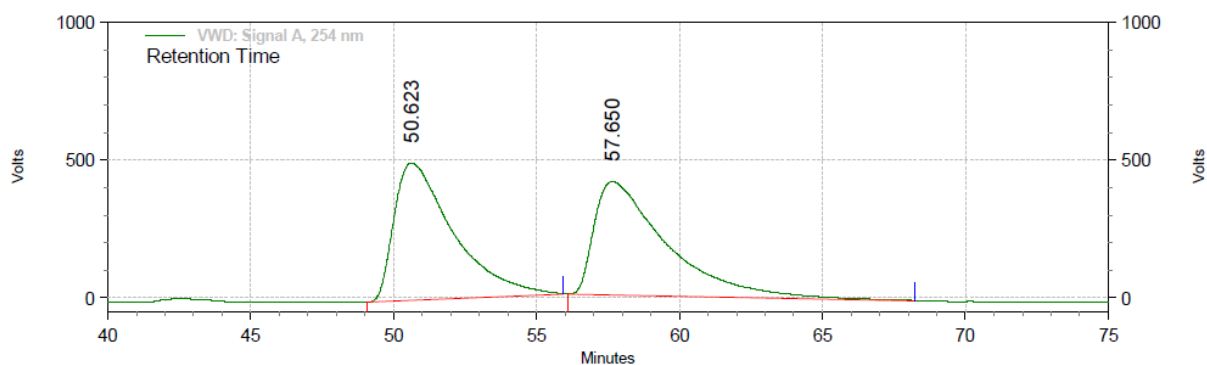
VWD: Signal A, 254 nm Results

Retention Time	Area	Area %
50.623	1193306150	49.77
57.650	1204549234	50.23

Totals		
	2397855384	100.00

Figure 3.31. HPLC chromatogram of racemic 1-(naphthalen-1-yl)-3-(3-(phenyl(o-tolyl)phosphorothioyl)phenyl) urea (**3.5k**).
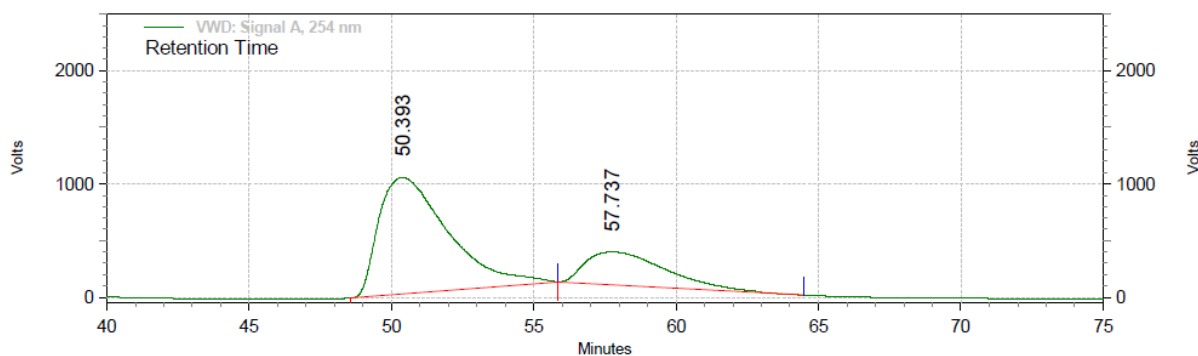
VWD: Signal A, 254 nm Results

Retention Time	Area	Area %
50.393	2913613550	75.28
57.737	956531028	24.72

Totals		
	3870144578	100.00

Figure 3.32. HPLC chromatogram of chiral 1-(naphthalen-1-yl)-3-(3-(phenyl(o-tolyl)phosphorothioyl)phenyl) urea (**3.5k**)

3.5.3.22. *Racemic* 1-(4-methoxyphenyl)-3-(3-(phenyl(o-tolyl)phosphorothioyl)phenyl) urea (3.5l)

A 1-(3-iodophenyl)-3-(4-methoxyphenyl)urea (**3.2g**) (0.5 mmol) was dissolved in 2 ml of THF, which was followed by addition of triethylamine (1.00 mmol) and phenyl(o-tolyl)phosphine **3.1b** (0.5 mmol. After stirring for 10 minutes, [Pd(OAc)$_2$] (0.5 mol %) was added and the mixture was refluxed overnight at 68 °C. After completion of the reaction, excess Sulfur powder (S$_8$) (3 eq.) was added to the reaction mixture at same temperature and the mixture was stirred for one hour. After this the above mixture was then treated with degassed water and was extracted with ethyl acetate (3 × 10 mL). The combined organic layer was dried on MgSO$_4$ for 2 hours and the volatiles were evaporated under reduced pressure. The crude **3.5l** was purified by silica gel column chromatography using 90:10 mixture of DCM:Ethyl acetate. The desired product was isolated as a yellowish solid in 76% yield (180 mg, 0.038 mmol).
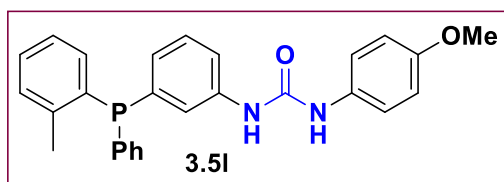
^{1}H NMR (500 MHz, CDCl$_3$, 298 K): δ = 7.51 (d, J_{H-H} = 8.0 Hz, 1H, Ar), 7.31-7.30 (m, 3H, Ar), 7.26-7.17 (m, 5H, Ar), 7.12-7.04 (m, 5H, Ar/N*H*), 6.96 (s, 1H, N*H*), 6.93 (t, J_{H-H} = 7.25 Hz, 1H, Ar), 6.77 (dd, J_{H-H} = 11.85, 2.2 Hz, 1H, Ar), 6.71 (d, J_{H-H} = 7.85, 2.2 Hz, 1H, Ar), 6.59 (dd, J_{H-H} = 8.17, 1.5 Hz, 1H, Ar), 3.71 (s, 3H, OCH$_3$), 2.37 (s, 3H, CH$_3$). **^{31}P NMR** (500 MHz, CDCl$_3$, 298 K): δ = -13.06 **^{13}C NMR** (125 MHz, CDCl$_3$, 298 K): δ = 160.2 (s, Ar, *C*-OMe), 153.2 (s, Ar, *C*O), 142.1 (d, J_{C-P} = 25 Hz, Ar, quat.), 139.0 (s, Ar, quat.), 138.3 (d, J_{C-P} = 8.6 Hz, Ar, quat.), 137.5 (s, Ar, quat.), 135.8 (d, J_{C-P} = 10.2 Hz, Ar, quat.), 135.6 (d, J_{C-P} = 11.9 Hz, Ar, quat.), 134.0 (s, Ar, *C*H), 133.9 (s, Ar, *C*H), 132.7 (s, Ar, *C*H), 130.0 (d, J_{C-P} = 4.5 Hz, Ar, *C*H), 129.8 (s, Ar, *C*H), 129.4 (d, J_{C-P} = 6.4 Hz, Ar, *C*H), 129.2 (s, Ar, *C*H), 129.6 (s, Ar, *C*H), 128.7 (d, J_{C-P} = 7.8 Hz, Ar, *C*H), 128.5 (d, J_{C-P} = 7 Hz, Ar, *C*H), 126.0 (s, Ar, *C*H), 125.4 (s, Ar, *C*H), 125.2 (s, Ar, *C*H), 120.9 (s, Ar, *C*H), 112.9 (s, Ar, *C*H), 109.8 (s, Ar, *C*H), 106.5 (s, Ar, *C*H), 55.2 (s, Ar, OCH$_3$), 21.1 (d, J_{C-P} = 21 Hz, CH$_3$). **ESI-MS** (+ve): (Cal. For C$_{30}$H$_{26}$N$_2$O$_2$P) m/z = 441.17 [M+H]$^+$, 463.15 [M+Na]$^+$.

3.5.3.23. *Chiral* 1-(4-methoxyphenyl)-3-(3-(phenyl(*o*-tolyl)phosphanyl)phenyl)urea (3.5l)
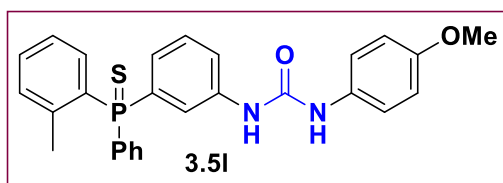
A Schlenk tube was loaded with catalyst **Cat.2** (0.005 mmol), 1-(3-iodophenyl)-3-(4-methoxyphenyl)urea (**3.2g**) (0.1 mmol), and phenyl(*o*-tolyl)phosphine (**3.1b**) (0.1 mmol) in a glove box. The screw capped Schlenk tube was taken out and appropriate temperature was attained. After the standard vacuum-argon cycle, NaOAc and 1 ml DMF were added to the reaction mixture. The progress of the reaction was monitored by ^{31}P NMR spectroscopy. After completion of the reaction, Sulphur powder was added to the reaction mixture at same temperature and stirred it for half an hour. The content was treated with degassed water (which was pre-cooled at appropriate temperature) and extracted with ethyl acetate (10 mL × 3) (which was pre-cooled at appropriate temperature). The combined organic layer was dried on MgSO$_4$ for half hour at suitable temperature and the volatiles were evaporated under reduced pressure. The plug was washed with DCM until the impurities were eluted, and then the expected product was pushed through with ethyl acetate. After evaporation of the solvent the product was obtained as a pale yellow solid **3.5l** which was analyzed by a combination of spectroscopic and analytical tools.

^{31}**P NMR** (500 MHz, CDCl$_3$, 298 K): δ = 37.12 (s, P).

Figure 3.33. ESI-MS (+ve) spectrum of 1-(4-methoxyphenyl)-3-(3-(phenyl(o-tolyl)phosphorothioyl)phenyl) urea (**3.5l**).

3.5.3.24. *Racemic* 1-(4-fluorophenyl)-3-(3-(phenyl(o-tolyl)phosphorothioyl)phenyl)urea (3.5m)

A 1-(4-fluorophenyl)-3-(3-iodophenyl)urea (**3.2i**) (0.50mmol) was dissolved in 2 ml THF, which was followed by addition of triethylamine (1.00 mmol) and phenyl(o-tolyl)phosphine **3.1b** (0.50 mmol). After stirring for 10 minutes, [Pd(OAc)$_2$] (0.5 mol %) was added and the mixture was refluxed overnight at 68 °C. After this, the above mixture was then treated with degassed water and was extracted with ethyl acetate (3 × 10 mL). The combined organic layer was dried on MgSO$_4$ for 2 hours and the volatiles were evaporated under reduced pressure. The crude **3.5m** was purified by silica gel column chromatography using 80:20 mixture of DCM:Ethyl acetate. The desired product was isolated as a yellowish solid in 65% yield (180 mg, 0.039 mmol).
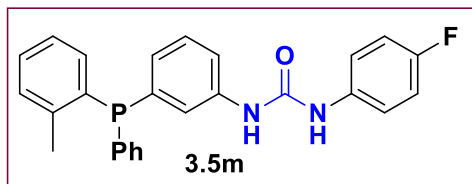
^{1}H NMR (500 MHz, CDCl$_3$, 298 K): δ = 7.53 (d, J_{H-H} = 7.6 Hz, 1H, Ar), 7.34 (s, 3H, Ar), 7.28-7.25 (m, 4H, Ar), 7.21 (s, 3H, Ar), 7.08 (t, J_{H-H} = 8.8 Hz, 2H, Ar), 6.96 (s, 3H, Ar/N*H*), 6.83-6.79 (m, 3H, Ar/N*H*), 2.39 (s, 3H, CH$_3$). **^{31}P NMR** (500 MHz, CDCl$_3$, 298 K): δ = -13.02. **^{13}C NMR** (125 MHz, CDCl$_3$, 298 K): δ = 153.2 (s, Ar, *C*O), 142.3 (s, Ar, quat.), 141.3 (s, Ar, quat.), 138.3 (d, J_{C-P} = 8.3 Hz, Ar, quat.), 137.8 (d, J_{C-P} = 10.6 Hz, Ar, quat.), 135.8 (d, J_{C-P} = 9.8 Hz, Ar, quat.), 135.6 (d, J_{C-P} = 12 Hz, Ar, quat.), 134.1 (s, Ar, *C*H), 133.9 (s, Ar, *C*H), 133.6 (s, Ar, quat.), 132.7 (s, Ar, *C*H), 130.1 (d, J_{C-P} = 4 Hz, Ar, *C*H), 129.6 (s, Ar, *C*H), 129.5 (s, Ar, *C*H), 129.3 (s, Ar, *C*H), 128.8 (d, J_{C-P} = 6.8 Hz, Ar, *C*H), 128.6 (d, J_{C-P} = 7 Hz, Ar, *C*H), 126.0 (s, Ar, *C*H), 125.7 (s, Ar, *C*H), 125.4 (s, Ar, *C*H), 123.0 (s, Ar, *C*H), 122.9 (s, Ar, *C*H), 121.2 (s, Ar, *C*H), 115.9 (s, Ar, *C*H), 115.7 (s, Ar, *C*H), 21.2 (d, J_{C-P} = 23.6 Hz, *C*H$_3$). **ESI-MS** (+ve): (Cal. For C$_{26}$H$_{23}$N$_2$OFPS) m/z = 461.12 [M+H]$^+$.

3.5.3.25. *Chiral* 1-(4-fluorophenyl)-3-(3-(phenyl(*o*-tolyl)phosphanyl)phenyl)urea (3.5m)

A Schlenk tube was loaded with catalyst **Cat.2** (0.005 mmol), 1-(4-fluorophenyl)-3-(3-iodophenyl)urea (**3.2l**) (0.1 mmol), and phenyl(*o*-tolyl)phosphine (**3.1b**) (0.1 mmol) in a glove box. The screw capped Schlenk tube was taken out and appropriate temperature was attained. After the standard vacuum-argon cycle, NaOAc and 1 ml of DMF were added to the reaction mixture.

The progress of the reaction was monitored by ^{31}P NMR spectroscopy. After completion of the reaction, Sulphur powder was added to the reaction mixture at same temperature and the reaction mixture was stirred for half an hour. The content was treated with degassed water (which was pre-cooled at appropriate temperature) and extracted with ethyl acetate (10 mL × 3) (which was pre-cooled at appropriate temperature). The combined organic layer was dried on $MgSO_4$ for half hours at suitable temperature and the volatiles were evaporated under reduced pressure. The plug was washed with DCM until the impurities were eluted, and then the expected product was pushed through with ethyl acetate. After evaporation of the solvent the product was obtained as a pale yellow solid **3.5m** which was analyzed by a combination of spectroscopic and analytical tools.

[31]**P NMR** (500 MHz, CDCl₃, 298 K) δ = 36.11 (s, P).
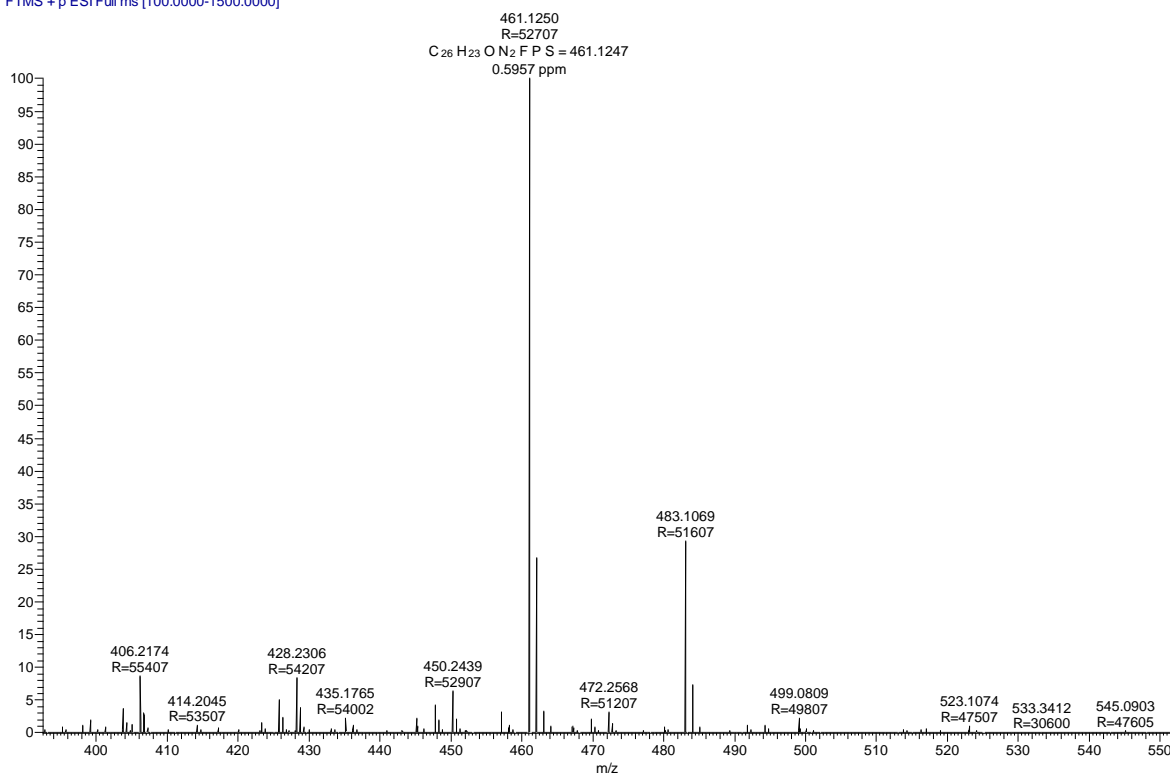
Figure 3.34. ESI-MS (+ve) spectrum of 1-(4-fluorophenyl)-3-(3-(phenyl(*o*-tolyl)phosphanyl)phenyl)urea (3.5m).

3.5.3.26. 1-(3-(mesityl(phenyl)phosphanyl)phenyl)urea (3.5n)
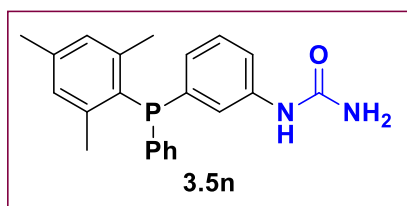
For characterization see chapter 2 (section 2.5.4.6)

HPLC: Daicel Chiralpak IB, 1 mL/min, 10:90 (2-PrOH:Hexane), $Rt_1 = 24.3$ min; $Rt_2 = 27.3$ min. ee = 50%.
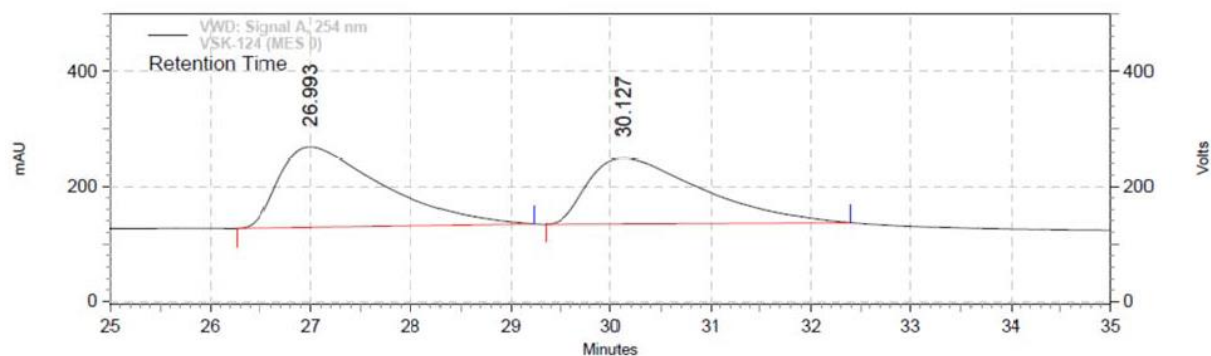
VWD: Signal A, 254 nm Results

Retention Time	Area	Area %
26.993	169587458	52.80
30.127	151585922	47.20

Totals		
	321173380	100.00

Figure 3.35. HPLC chromatogram of racemic 1-(3-(mesityl(phenyl)phosphanyl)phenyl)urea (**3.5n**).
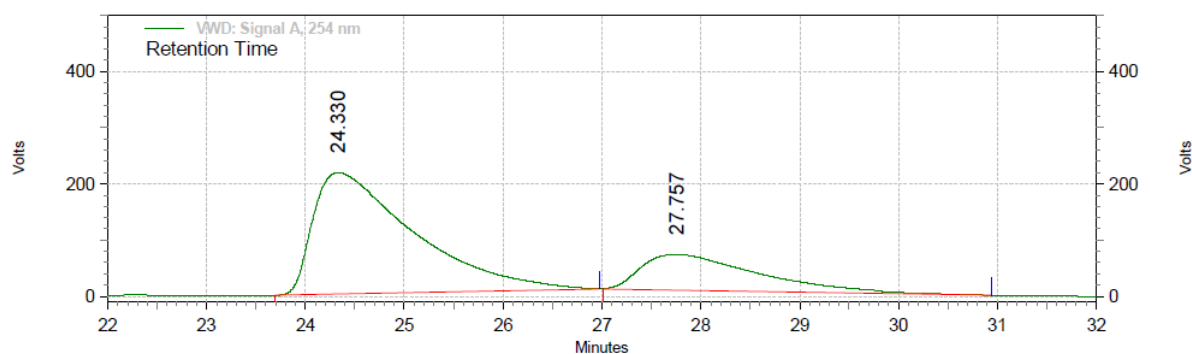
VWD: Signal A, 254 nm Results

Retention Time	Area	Area %
24.330	255330025	74.71
27.757	86427739	25.29

Totals		
	341757764	100.00

Figure 3.36. HPLC chromatogram of chiral 1-(3-(mesityl(phenyl)phosphanyl)phenyl)urea (**3.5n**).

3.5.3.27. 1-(4-(mesityl(phenyl)phosphanyl)phenyl)urea (3.5o)
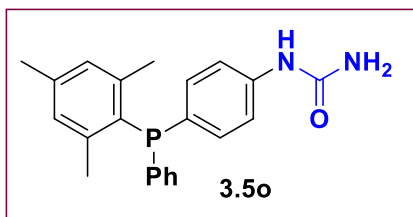
For characterization see chapter 2 (section 2.5.4.8)

HPLC: Daicel Chiralpak IA, 1 mL/min, 93:7 (Hexane:EtOH), Rt_1 = 48.2 min; Rt_2 = 51.7 min. ee = 50%.
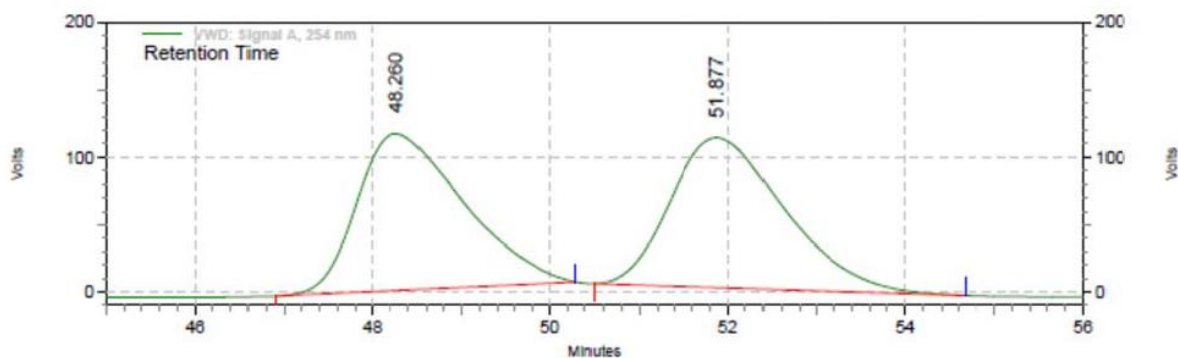
VWD: Signal A,
254 nm Results

Retention Time	Area	Area %	Height	Height %
48.260	162069631	49.28	1951975	51.12
51.877	166838683	50.72	1866166	48.88

Totals				
	328908314	100.00	3818141	100.00

Figure 3.37. HPLC chromatogram of racemic 1-(4-(mesityl(phenyl)phosphanyl)phenyl)urea (**3.5o**).

3.5.3.28. *Racemic* 1-(3-(mesityl(phenyl)phosphorothioyl)phenyl)-3-phenylurea (3.5p)

A 1-(3-iodophenyl)-3-phenylurea (**3.2c**) (4.38 mmol) was dissolved in 15 ml of THF, which
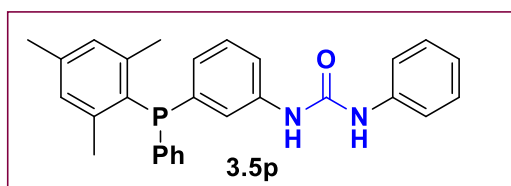
was followed by addition of triethylamine (8.76 mmol) and mesityl(phenyl)phosphine **3.1c** (4.38 mmol). After stirring for 10 minutes, [Pd(OAc)₂] (0.5 mol %) was added and the mixture was

refluxed overnight at 68 °C. Thus, after above mixture was then treated with degassed water and was extracted with ethyl acetate (3 × 10 mL). The combined organic layer was dried on MgSO₄ for 2 hours and the volatiles were evaporated under reduced pressure. The crude **3.5p** was purified by silica gel column chromatography using 80:20 mixture of DCM:Ethyl acetate. The desired product was isolated as a yellowish solid in 87% yield (1.8 mg, 3.8 mmol).

¹H NMR (500 MHz, CDCl$_3$, 298 K): δ = 7.35-7.31 (m, 3H, Ar), 7.28-7.18 (m, 9H, Ar), 7.15 (s, 1H, N*H*), 7.13 (s, 1H, N*H*), 7.05-7.02 (m, 2H, Ar), 6.89 (d, $J_{H\text{-}H}$ = 2.28 Hz, 2H, Ar), 2.28 (s, 3H, CH$_3$), 2.18 (s, 6H, CH$_3$). **³¹P NMR** (500 MHz, CDCl$_3$, 298 K): δ = -16.23. **¹³C NMR** (125 MHz, CDCl$_3$, 298 K): δ = 154.0 (s, Ar, *C*O), 145.3 (d, $J_{C\text{-}P}$ = 16.2 Hz, Ar, quat.), 139.9 (s, Ar, quat.), 138.4 (s, Ar, quat.), 138.0 (s, Ar, quat.), 137.8 (d, $J_{C\text{-}P}$ = 14.9 Hz, Ar, quat.), 136.2 (d, $J_{C\text{-}P}$ = 11.3 Hz, Ar, quat.), 131.6 (d, $J_{C\text{-}P}$ = 18.2 Hz, Ar, *C*H), 129.9 (d, $J_{C\text{-}P}$ = 4 Hz, Ar, *C*H), 129.1 (s, Ar, *C*H), 128.8 (s, Ar, *C*H), 128.7 (s, Ar, quat.), 128.3 (d, $J_{C\text{-}P}$ = 5.34 Hz, Ar, *C*H), 128.0 (d, $J_{C\text{-}P}$ = 15.0 Hz, Ar, quat.), 127.5 (s, Ar, *C*H), 126.4 (d, $J_{C\text{-}P}$ = 16.12 Hz, Ar, *C*H), 123.4 (s, Ar, *C*H), 123.1 (d, $J_{C\text{-}P}$ = 121.7 Hz, Ar, *C*H), 120.5 (s, Ar, *C*H), 119.6 (s, Ar, *C*H), 23.8 (s, *C*H$_3$), 23.6 (s, *C*H$_3$), 21.1 (s, *C*H$_3$). **ESI-MS** (+ve): (Cal. For C$_{28}$H$_{27}$N$_2$OP) m/z = 439.19 [M+H]$^+$.

3.5.3.29. *Chiral* 1-(3-(mesityl(phenyl)phosphanyl)phenyl)-3-phenylurea (3.5p)

A Schlenk tube was loaded with catalyst **Cat.2** (0.005 mmol), 1-(3-iodophenyl)-3-

phenylurea (**3.2c**) (0.1 mmol), and mesityl(phenyl)phosphine (**3.1c**) (0.1 mmol) in a glove box. The screw capped Schlenk tube was taken out and appropriate temperature was attained. After the standard vacuum-argon cycle, NaOAc and 1 ml DMF were added to the reaction mixture. The progress of the reaction was monitored by ³¹P NMR spectroscopy. After completion of the reaction, Sulphur powder was added in reaction mixture at same temperature and stirred it for half an hour. The content was treated with degassed water (which was pre-cooled at appropriate temperature) and extracted with ethyl acetate (10 mL × 3) (which was pre-cooled at appropriate temperature). The combined organic layer was dried on MgSO$_4$ for half hour at suitable temperature and the volatiles were evaporated under reduced pressure. The plug was washed with DCM until the impurities were eluted, and then the expected product was pushed through with ethyl acetate. After evaporation of the solvent the product was obtained as a pale yellow solid **3.5p** which was analyzed by a combination of spectroscopic and analytical tools.

³¹P NMR (500 MHz, CDCl$_3$, 298 K) δ = 36.11 (s, P). **HPLC:** Daicel Chiralpak-IB, 1 mL/min, 02:98 (2-PrOH:Hexane), Rt_1 = 60.5 min; Rt_2 = 74.9 min. ee = 23%.

Figure 3.38. ESI-MS (+ve) spectrum of 1-(3-(mesityl(phenyl)phosphanyl)phenyl)-3-phenylurea (**3.5p**).

VWD: Signal A, 254 nm Results

Retention Time	Area	Area %
58.123	4973179473	50.19
72.257	4935236337	49.81

Totals		
	9908415810	100.00

Figure 3.39. HPLC chromatogram of racemic 1-(3-(mesityl(phenyl)phosphanyl)phenyl)-3-phenylurea (**3.5p**).

VWD: Signal A, 254 nm Results

Retention Time	Area	Area %
60.543	123227280	61.41
74.963	77424422	38.59

Totals		
	200651702	100.00

Figure 3.40. HPLC chromatogram of chiral 1-(3-(mesityl(phenyl)phosphanyl)phenyl)-3-phenylurea (**3.5p**).

3.5.3.30. *Racemic* 1-(3-(mesityl(phenyl)phosphanyl)phenyl)-3-(naphthalen-1-yl)urea (3.5q)

A 1-(3-iodophenyl)-3-(naphthalen-1-yl)urea (**3.2e**) (0.438 mmol) was dissolved in 2 ml of
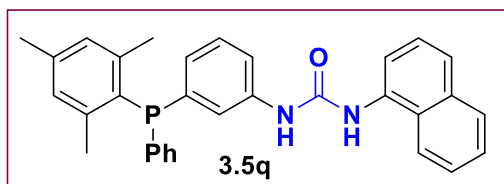
THF, which was followed by addition of triethylamine (0.876 mmol) and mesityl(phenyl)phosphine **3.1c** (0.438 mmol. After stirring for 10 minutes, [Pd(OAc)$_2$] (0.5 mol %) was added and the mixture was refluxed overnight at 68 °C. After this, the above mixture was then treated with degassed water and was extracted with ethyl acetate (3 × 10 mL). The combined organic layer was dried on MgSO$_4$ for 2 hours and the volatiles were evaporated under reduced pressure. The crude **3.5q** was purified by silica gel column chromatography using 80:20 mixture of DCM:Ethyl acetate. The desired product was isolated as a yellowish solid in 89% yield (205 mg, 0.39 mmol).

¹H NMR (500 MHz, CDCl$_3$, 298 K): δ = 7.71 (d, J_{H-H} = 7.6 Hz, 2H, Ar), 7.52 (d, J_{H-H} = 7.95 Hz, 1H, Ar), 7.44 (d, J_{H-H} = 6.45 Hz, 2H, Ar), 7.34-7.29 (m, 4H, Ar), 7.25-7.10 (m, 8H, Ar), 6.96 (t, J_{H-H} = 6.5 Hz, 1H, Ar), 6.83 (s, 2H, N*H*), 2.21 (s, 3H, CH$_3$), 2.15 (s, 6H, CH$_3$). **³¹P NMR** (500 MHz, CDCl$_3$, 298 K): δ = -16.15. **¹³C NMR** (125 MHz, CDCl$_3$, 298 K): δ = 154.4 (s, Ar, *C*O), 145.4 (d, J_{C-P} = 16.2 Hz, Ar, quat.), 140.0 (s, Ar, quat.), 138.5 (s, Ar, quat.), 137.8 (d, J_{C-P} = 14.0 Hz, Ar, quat.), 136.3 (s, Ar, quat.), 134.2 (s, Ar, quat.), 132.6 (s, Ar, quat.), 131.5

(d, J_{C-P} = 18.2 Hz, Ar, CH), 129.9 (d, J_{C-P} = 4.1 Hz, Ar, CH), 129.0 (s, Ar, CH), 128.7 (s, Ar, quat.), 128.3 (s, Ar, CH), 128.0 (s, Ar, quat.), 127.4 (s, Ar, CH), 126.5 (s, Ar, CH), 126.3 (s, Ar, CH), 126.1 (s, Ar, CH), 125.6 (s, Ar, CH), 122.8 (d, J_{C-P} = 7.8 Hz, Ar, CH), 122.2 (s, Ar, CH), 126.6 (s, Ar, CH), 119.5 (s, Ar, CH), 23.7 (s, CH$_3$), 23.6 (s, CH$_3$), 21.0 (s, CH$_3$).

3.5.3.31. *Chiarl* 1-(3-(mesityl(phenyl)phosphanyl)phenyl)-3-(naphthalen-1-yl)urea (3.5q)
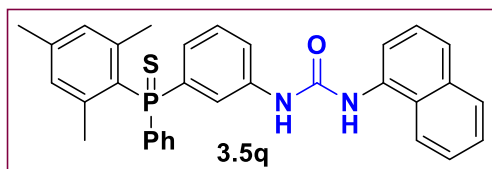
A Schlenk tube was loaded with catalyst **Cat.2** (0.005 mmol), 1-(3-iodophenyl)-3-(naphthalen-1-yl)urea (**3.2e**) (0.1 mmol), and mesityl(phenyl)phosphine (**3.1c**) (0.1 mmol) in a glove box. The screw capped Schlenk tube was taken out and appropriate temperature was attained. After the standard vacuum-argon cycle, NaOAc and 1 ml DMF were added to the reaction mixture. The progress of the reaction was monitored by ^{31}P NMR spectroscopy. After completion of the reaction, Sulphur powder was added to the reaction mixture at same temperature and the mixture was stirred for half an hour. The content was treated with degassed water (which was pre-cooled at appropriate temperature) and extracted with ethyl acetate (10 mL × 3) (which was pre-cooled at appropriate temperature). The combined organic layer was dried on MgSO$_4$ for half hour at suitable temperature and the volatiles were evaporated under reduced pressure. The plug was washed with DCM until the impurities were eluted, and then the expected product was pushed through with ethyl acetate. After evaporation of the solvent the product was obtained as a pale yellow solid **3.5q** which was analyzed by a combination of spectroscopic and analytical tools.

^{31}**P NMR** (500 MHz, CDCl$_3$, 298 K): δ = 37.23 (s, P).

3.5.3.32. *Racemic* 1-(3-(mesityl(phenyl)phosphanyl)phenyl)-3-(4-methoxyphenyl)urea (3.5r)

A 1-(3-iodophenyl)-3-(4-methoxyphenyl)urea (**3.2g**) (0.438mmol) was dissolved in 2 ml of
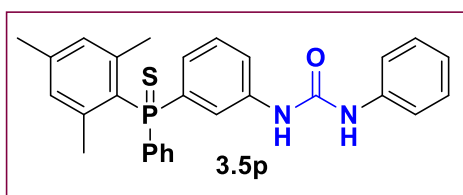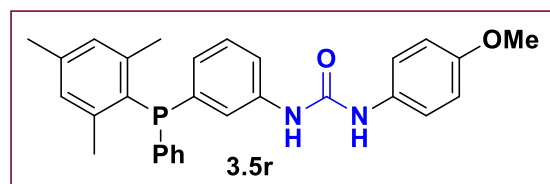

THF, which was followed by addition of triethylamine (0.876 mmol) and mesityl(phenyl)phosphine **3.1c** (0.438 mmol). After stirring for 10 minutes, [Pd(OAc)$_2$] (0.5 mol %) was added and the mixture was refluxed overnight at 68 °C. After this, the above mixture was then treated with degassed water and was extracted with ethyl acetate (3 × 10 mL). The combined organic layer was dried on MgSO$_4$ for 2 hours and the volatiles were evaporated under reduced pressure. The crude **3.5r** was purified by silica gel column chromatography

using 80:20 mixture of DCM:Ethyl acetate. The desired product was isolated as a yellowish solid in 86% yield (19 mg, 0.37 mmol).

^{1}H NMR (500 MHz, CDCl$_3$, 298 K): δ = 7.41 (d, J_{H-H} = 7.3 Hz, 1H, Ar), 7.34-7.29 (m, 4H, Ar), 7.27-7.23 (m, 2H, Ar), 7.19-7.15 (m, 3H, Ar), 7.03 (t, J_{H-H} = 7 Hz, 1H, Ar), 6.90 (s, 2H, Ar), 6.83 (d, J_{H-H} = 8.9 Hz, 2H, Ar), 6.77 (s, 1H, N*H*), 6.60 (s, 1H, N*H*), 3.78 (s, 3H, OCH$_3$), 2.29 (s, 3H, CH$_3$), 2.19 (s, 6H, CH$_3$). **^{31}P NMR** (500 MHz, CDCl$_3$, 298 K): δ = -16.11. **^{13}C NMR** (125 MHz, CDCl$_3$, 298 K): δ = 156.4 (s, Ar, *C*-OMe), 154.1 (s, Ar, *C*O), 145.4 (s, Ar, quat.), 145.3 (s, Ar, quat.), 131.7 (s, Ar, quat.), 131.5 (s, Ar, quat.), 131.4 (s, Ar, quat.), 131.3 (s, Ar, quat.), 130.7 (s, Ar, *C*H), 130.1 (s, Ar, *C*H), 129.1 (d, J_{C-P} = 5 Hz, Ar, *C*H), 128.9 (d, J_{C-P} = 6.7 Hz, Ar, *C*H), 128.4 (d, J_{C-P} = 6.7 Hz, Ar, *C*H), 127.9 (s, Ar, *C*H), 126.3 (s, Ar, *C*H), 126.2 (s, Ar, *C*H), 123.5 (s, Ar, *C*H), 122.9 (s, Ar, *C*H), 122.7 (d, J_{C-P} = 8.5 Hz, Ar, *C*H), 121.5 (s, Ar, *C*H), 119.9 (s, Ar, *C*H), 114.2 (s, Ar, *C*H), 114.0 (d, J_{C-P} = 6.1 Hz, Ar, *C*H), 55.4 (s, Ar, O*C*H$_3$), 23.8 (s, *C*H$_3$), 23.4 (s, *C*H$_3$), 21.1 (s, *C*H$_3$). **ESI-MS** (+ve): (Cal. For C$_{29}$H$_{30}$N$_2$O$_2$P) m/z = 469.16 [M+H]$^+$.

3.5.3.33. *Chiral* 1-(3-(mesityl(phenyl)phosphanyl)phenyl)-3-(4-methoxyphenyl)urea (3.5r)

A Schlenk tube was loaded with catalyst **Cat.2** (0.005 mmol), 1-(3-iodophenyl)-3-(4-methoxyphenyl)urea (**3.2g**) (0.1 mmol), and mesityl(phenyl)phosphine (**3.1c**) (0.1 mmol) in a glove box. The screw capped Schlenk tube was taken out and appropriate temperature was attained. After the standard vacuum-argon cycle, NaOAc and 1 ml DMF were added to the reaction mixture. The progress of the reaction was monitored by ^{31}P NMR spectroscopy. After completion of the reaction, Sulphur powder was added to the reaction mixture at same temperature and the reaction mixture was stirred for half an hour. The content was treated with degassed water (which was pre-cooled at appropriate temperature) and extracted with ethyl acetate (10 mL × 3) (which was pre-cooled at appropriate temperature). The combined organic layer was dried on MgSO$_4$ for half hour at suitable temperature and the volatiles were evaporated under reduced pressure. The plug was washed with DCM until the impurities were eluted, and then the expected product was pushed through with ethyl acetate. After evaporation of the solvent the product was obtained as a pale yellow solid **3.5r** which was analyzed by a combination of spectroscopic and analytical tools.

^{31}**P NMR** (500 MHz, CDCl$_3$, 298 K) δ = 35.12 (s, P). **HPLC:** Daicel Chiralpak-IF, 1 mL/min, 07:93 (2-PrOH:Hexane), Rt_1 = 58.9 min; Rt_2 = 64.3 min. ee = 29%.
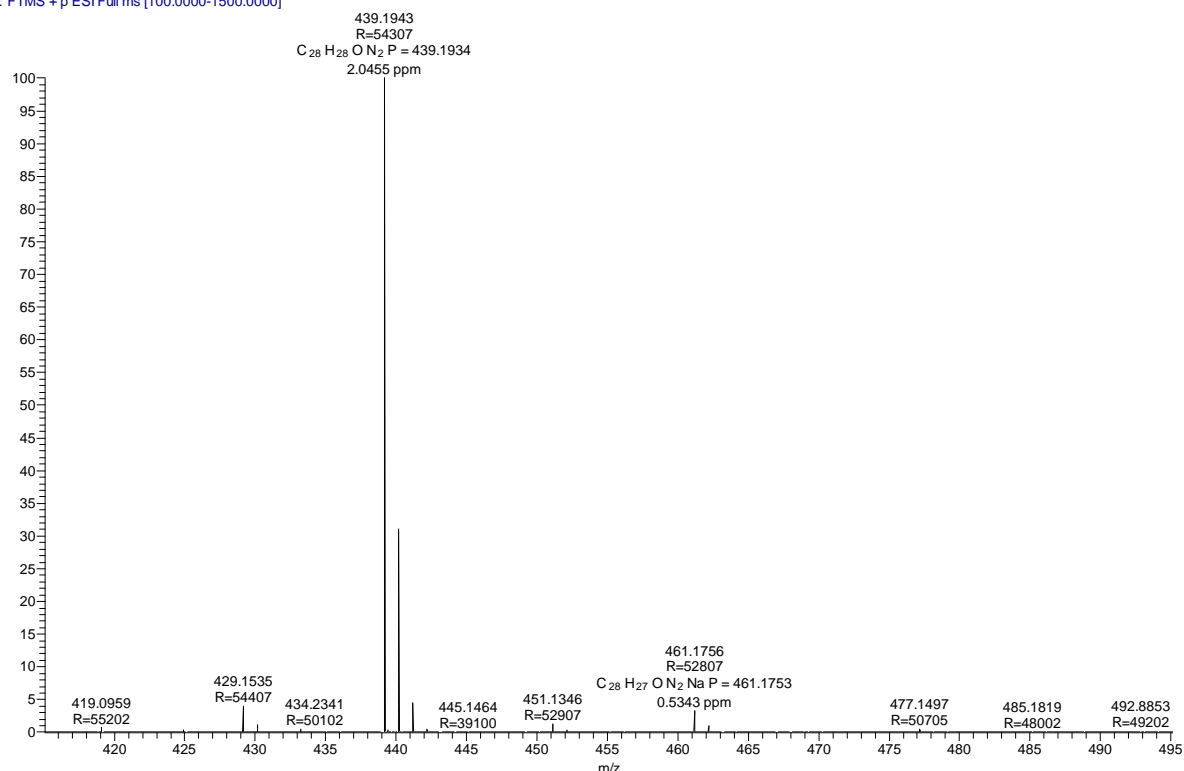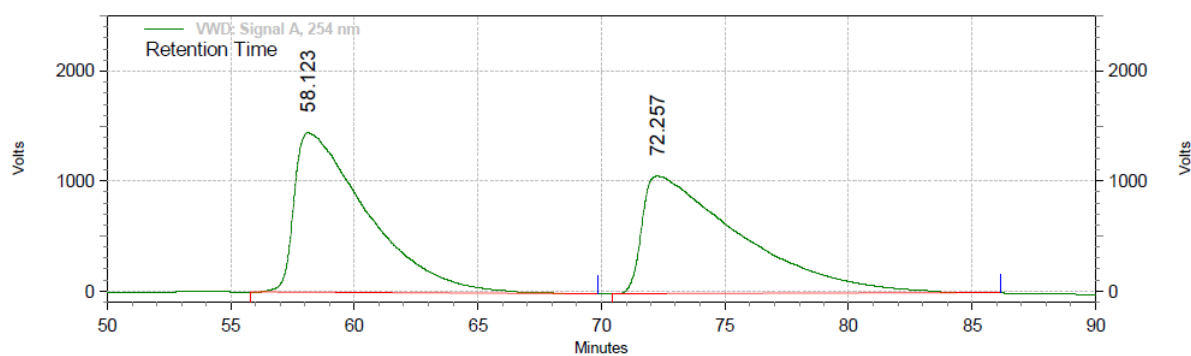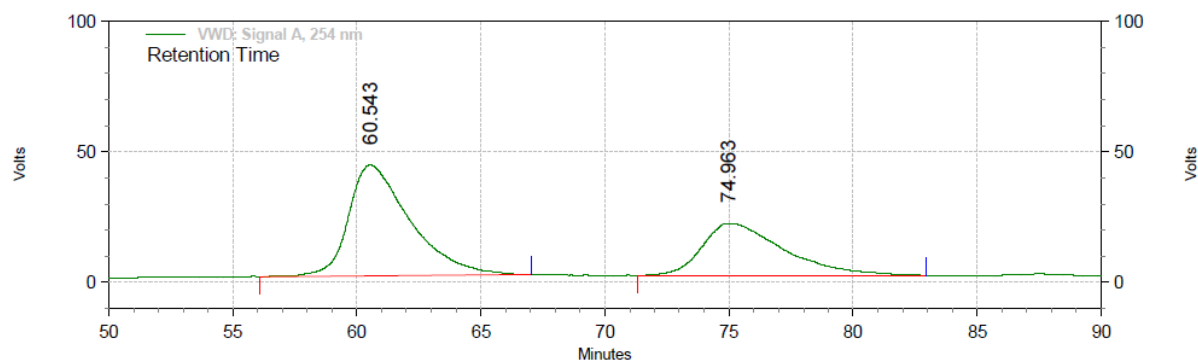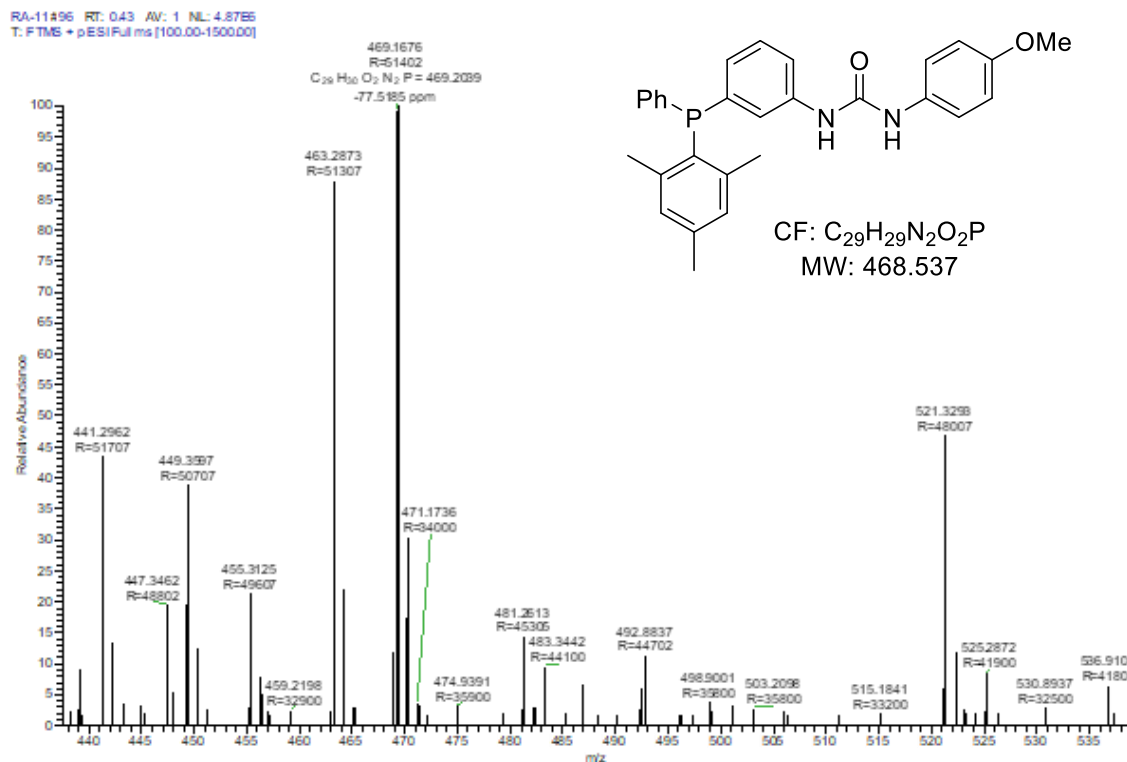

Figure 3.41. ESI-MS (+ve) spectrum of 1-(3-(mesityl(phenyl)phosphanyl)phenyl)-3-(4-methoxyphenyl)urea (**3.5r**).
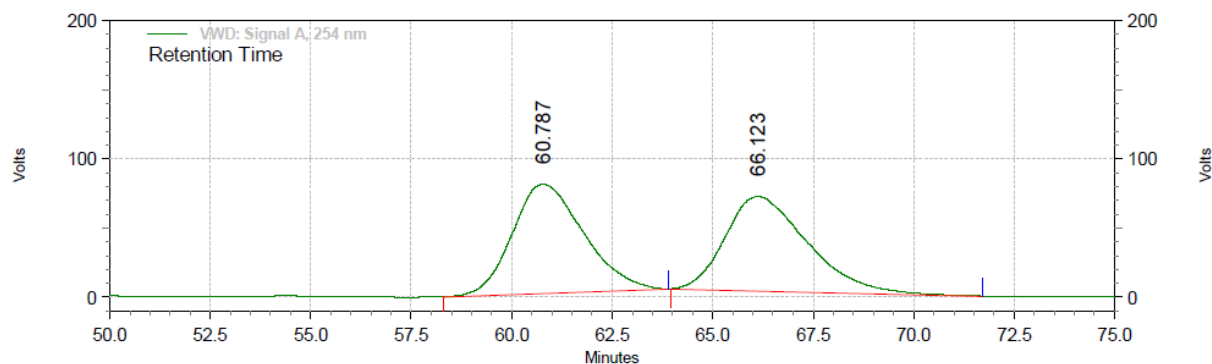
VWD: Signal A, 254 nm Results

Retention Time	Area	Area %
60.787	163714448	50.14
66.123	162773534	49.86

Totals		
	326487982	100.00

Figure 3.42. HPLC chromatogram of racemic 1-(3-(mesityl(phenyl)phosphanyl)phenyl)-3-(4-methoxyphenyl) urea (**3.5r**).
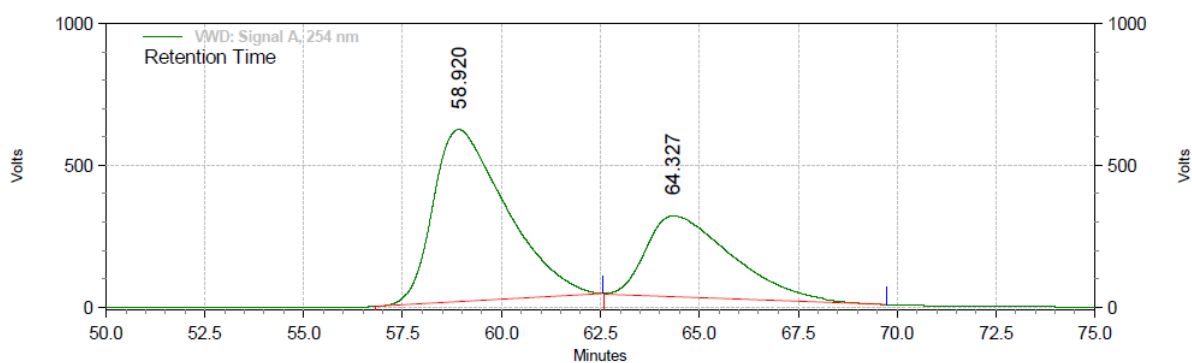
VWD: Signal A, 254 nm Results

Retention Time	Area	Area %
58.920	1312242477	64.53
64.327	721156749	35.47

Totals		
	2033399226	100.00

Figure 3.43. HPLC chromatogram of chiral 1-(3-(mesityl(phenyl)phosphanyl)phenyl)-3-(4-methoxyphenyl)urea (**3.5r**).

3.5.3.34. *Racemic* 1-(4-chlorophenyl)-3-(3-(phenyl(o-tolyl)phosphorothioyl)phenyl)urea (3.5s)

A 1-(4-chlorophenyl)-3-(3-iodophenyl)urea (**3.2h**) (0.438 mmol) was dissolved in 2 ml of THF, which was followed by addition of triethylamine (0.876 mmol) and mesityl(phenyl)phosphine **3.1c** (0.438 mmol). After stirring for 10 minutes, [Pd(OAc)$_2$] (0.5 mol %) was added and the mixture was refluxed overnight at 68 °C. After this, the above mixture was then treated with degassed water and was extracted with ethyl acetate (3 × 10 mL). The combined organic layer was dried on MgSO$_4$ for 2 hours and the volatiles were evaporated under reduced pressure. The crude **3.5s** was purified by silica gel column chromatography using 80:20 mixture of DCM:Ethyl acetate. The desired product was isolated as a yellowish solid in 88% yield (195 mg, 0.38 mmol).
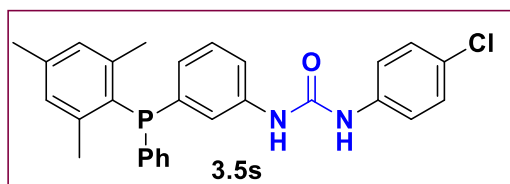
^{1}**H NMR** (500 MHz, CDCl$_3$, 298 K): δ = 7.33-7.23 (m, 6H, Ar), 7.21-7.17 (m, 3H, Ar), 7.13-7.10 (m, 5H, Ar), 7.06 (t, J_{H-H} = 6.7 Hz, 1H, Ar), 6.89 (s, 2H, N*H*), 2.28 (s, 3H, CH$_3$), 2.17 (s, 6H, CH$_3$). ^{31}**P NMR** (500 MHz, CDCl$_3$, 298 K): δ = -16.18. ^{13}**C NMR** (125 MHz, CDCl$_3$, 298 K): δ = 153.5 (s, Ar, *C*O), 145.5 (s, Ar, quat.), 145.2 (s, Ar, quat.), 140.1 (s, Ar, quat.), 138.0 (d, J_{C-P} = 6.6 Hz, Ar, quat.), 136.5 (s, Ar, quat.), 136.0 (s, Ar, quat.), 131.7 (s, Ar, *C*H), 131.3

(s, Ar, *C*H), 129.9 (d, J_{C-P} = 4.3 Hz, Ar, *C*H), 129.1 (d, J_{C-P} = 4 Hz, Ar, *C*H), 128.8 (s, Ar, *C*H), 128.6 (s, Ar, quat.), 128.4 (d, J_{C-P} = 4.4 Hz, Ar, *C*H), 127.5 (s, Ar, *C*H), 127.1 (s, Ar, *C*H), 126.7 (s, Ar, *C*H), 123.6 (d, J_{C-P} = 20.7 Hz, Ar, *C*H), 121.5 (s, Ar, *C*H), 120.0 (s, Ar, *C*H), 23.8 (s, *C*H_3), 23.5 (s, *C*H_3), 21.0 (s, *C*H_3). **ESI-MS** (+ve): (Cal. For $C_{28}H_{26}N_2OClP$) m/z = 473.15 [M+H]$^+$.

3.5.3.35. *Chiral* 1-(4-chlorophenyl)-3-(3-(mesityl(phenyl)phosphanyl)phenyl)urea (3.5s)
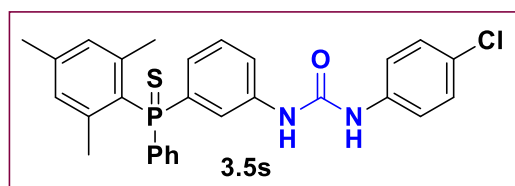
A Schlenk tube was loaded with catalyst **Cat.2** (0.005 mmol), 1-(4-chlorophenyl)-3-(3-iodophenyl)urea (**3.2h**) (0.1 mmol), and mesityl(phenyl)phosphine (**3.1c**) (0.1 mmol) in a glove box. The screw capped Schlenk tube was taken out and appropriate temperature was attained. After the standard vacuum-argon cycle, NaOAc and 1 ml DMF were added to the reaction mixture. The progress of the reaction was monitored by ^{31}P NMR spectroscopy. After completion of the reaction, Sulphur powder was added to the reaction mixture at same temperature and the reaction mixture was stirred for half an hour. The content was treated with degassed water (which was pre-cooled at appropriate temperature) and extracted with ethyl acetate (10 mL × 3) (which was pre-cooled at appropriate temperature). The combined organic layer was dried on MgSO_4 for half hour at suitable temperature and the volatiles were evaporated under reduced pressure. The plug was washed with DCM until the impurities were eluted, and then the expected product was pushed through with ethyl acetate. After evaporation of the solvent the product was obtained as a pale yellow solid **3.5s** which was analyzed by a combination of spectroscopic and analytical tools.

^{31}**P NMR** (500 MHz, CDCl_3, 298 K) δ = 36.11 (s, P). **HPLC:** Daicel Chiralpak-IF, 1 mL/min, 07:93 (2-PrOH:Hexane), Rt_1 = 21.9 min; Rt_2 = 25.5 min. ee = 36%.
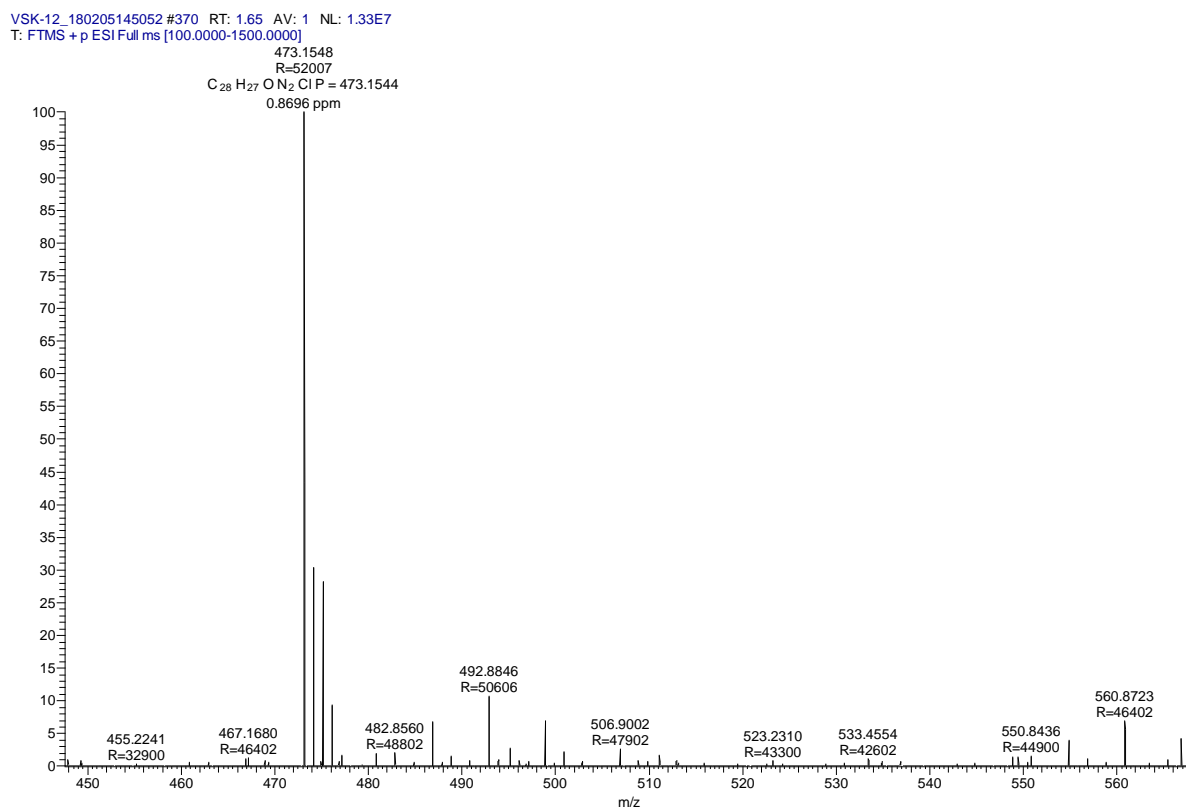
Figure 3.44. ESI-MS (+ve) spectrum of 1-(4-chlorophenyl)-3-(3-(phenyl(o-tolyl)phosphorothioyl)phenyl)urea (**3.5s**).
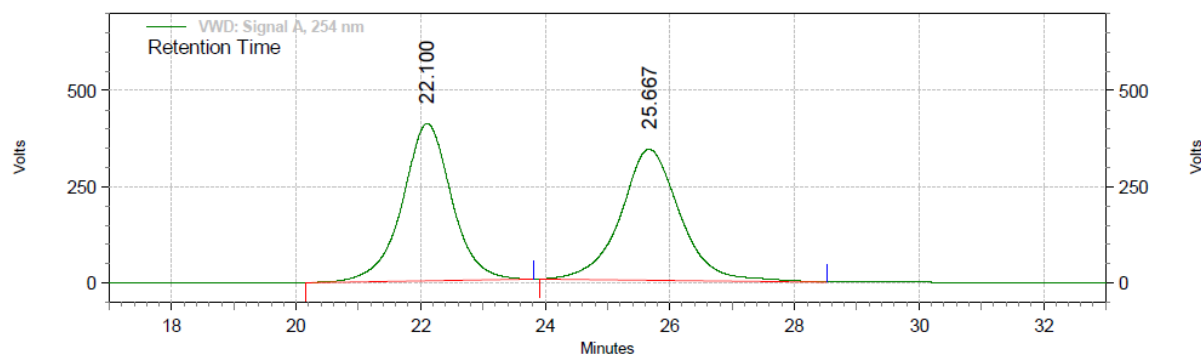
VWD: Signal A, 254 nm Results

Retention Time	Area	Area %
22.100	377222430	49.96
25.667	377852008	50.04

Totals		
	755074438	100.00

Figure 3.45. HPLC chromatogram of racemic 1-(4-chlorophenyl)-3-(3-(phenyl(o-tolyl)phosphorothioyl)phenyl) urea (**3.5s**).
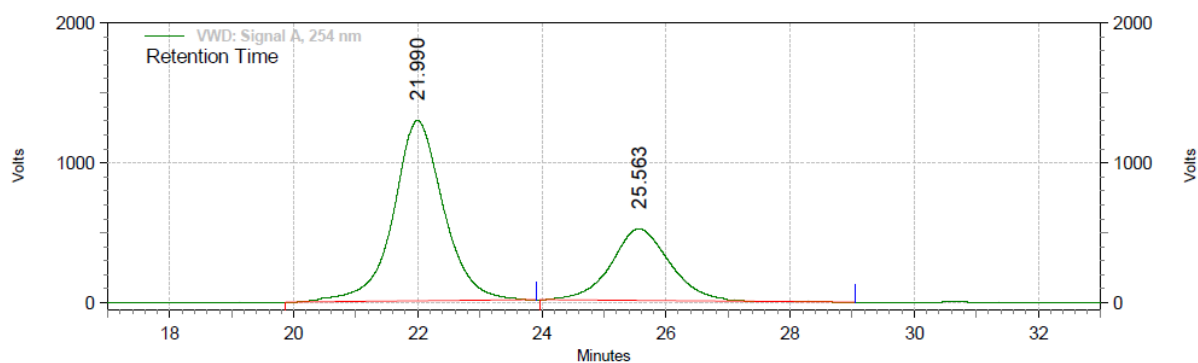
VWD: Signal A, 254 nm Results

Retention Time	Area	Area %
21.990	1210563355	68.09
25.563	567419846	31.91

Totals		
	1777983201	100.00

Figure 3.46. HPLC chromatogram of chiral 1-(4-chlorophenyl)-3-(3-(phenyl(o-tolyl)phosphorothioyl)phenyl) urea (**3.5s**).

3.5.3.36. *Racemic* 1-(4-bromophenyl)-3-(3-(mesityl(phenyl)phosphanyl)phenyl)urea (3.5t)

A 1-(4-bromophenyl)-3-(3-iodophenyl)urea (**3.2i**) (0.438 mmol) was dissolved in 2 ml of THF,
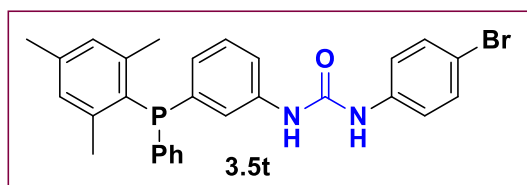
which was followed by addition of triethylamine (0.876 mmol) and mesityl(phenyl)phosphine **3.1c** (0.438 mmol). After stirring for 10 minutes, [Pd(OAc)$_2$] (0.5 mol %) was added and the mixture was refluxed overnight at 68 °C. After this, the above mixture was then treated with degassed water and was extracted with ethyl acetate (3 × 10 mL). The combined organic layer was dried on MgSO$_4$ for 2 hours and the volatiles were evaporated under reduced pressure. The crude **3.5t** was purified by silica gel column chromatography using 80:20 mixture of DCM:Ethyl acetate. The desired product was isolated as a brownish yellow solid in 75% yield (18 mg, 0.32 mmol).

¹H NMR (500 MHz, CDCl$_3$, 298 K): δ = 7.62-7.43 (m, 1H, Ar), 7.33-7.30 (m, 4H, Ar), 7.28-7.22 (m, 4H, Ar), 7.19 (s, 1H, Ar), 7.17 (s, 1H, Ar), 7.10 (d, J_{H-H} = 7.5 Hz, 3H, Ar), 7.06 (t, J_{H-H} = 7.6 Hz, 1H, Ar), 6.89 (s, 2H, NH), 2.28 (s, 3H, CH$_3$), 2.18 (s, 6H, CH$_3$). **³¹P NMR** (500 MHz, CDCl$_3$, 298 K): δ = -16.19. **¹³C NMR** (125 MHz, CDCl$_3$, 298 K): δ = 153.4 (s, Ar, CO), 145.5 (s, Ar, quat.), 145.3 (s, Ar, quat.), 140.1 (s, Ar, quat.), 138.6 (s, Ar, quat.), 138.4 (s, Ar, quat.), 137.9 (d, J_{C-P} = 6.8 Hz, Ar, quat.), 136.6 (s, Ar, quat.), 135.9 (d, J_{C-P} = 13.9 Hz, Ar,

quat.), 131.6 (s, Ar, *C*H), 131.4 (s, Ar, *C*H), 129.9 (d, J_{C-P} = 4.4 Hz, Ar, *C*H), 129.2 (d, J_{C-P} = 5.4 Hz, Ar, *C*H), 128.9 (s, Ar, *C*H), 128.6 (s, Ar, *C*H), 128.3 (d, J_{C-P} = 5.3 Hz, Ar, *C*H), 127.8 (d, J_{C-P} = 14 Hz, Ar, quat.), 127.5 (s, Ar, *C*H), 127.1 (s, Ar, *C*H), 126.9 (s, Ar, *C*H), 123.5 (s, Ar, *C*H), 123.3 (s, Ar, *C*H), 121.4 (s, Ar, *C*H), 121.1 (s, Ar, *C*H), 120.1 (s, Ar, *C*H), 23.7 (s, *C*H$_3$), 23.6 (s, *C*H$_3$), 21.0 (s, *C*H$_3$). **ESI-MS** (+ve): (Cal. For $C_{28}H_{26}N_2OBrP$) m/z = 517.10 [M+H]$^+$.

3.5.3.37. *Chiral* 1-(4-bromophenyl)-3-(3-(mesityl(phenyl)phosphanyl)phenyl)urea (3.5t)

A Schlenk tube was loaded with catalyst **Cat.2** (0.005 mmol), 1-(4-bromophenyl)-3-(3-

iodophenyl)urea (**3.2i**) (0.1 mmol), and mesityl(phenyl)phosphine (**3.1c**) (0.1 mmol) in a glove box. The screw capped Schlenk tube was taken out and appropriate temperature was attained. After the standard vacuum-argon cycle, NaOAc and 1 ml DMF were added to the reaction mixture. The progress of the reaction was monitored by ^{31}P NMR spectroscopy. After completion of the reaction, Sulphur powder was added to the reaction mixture at same temperature and the reaction mixture was stirred for half an hour. The content was treated with degassed water (which was pre-cooled at appropriate temperature) and extracted with ethyl acetate (10 mL × 3) (which was pre-cooled at appropriate temperature). The combined organic layer was dried on MgSO$_4$ for half hour at suitable temperature and the volatiles were evaporated under reduced pressure. The plug was washed with DCM until the impurities were eluted, and then the expected product was pushed through with ethyl acetate. After evaporation of the solvent the product was obtained as a pale yellow solid **3.5t** which was analyzed by a combination of spectroscopic and analytical tools.

^{31}**P NMR** (500 MHz, CDCl$_3$, 298 K) δ = 36.11 (s, P). **HPLC:** Daicel Chiralpak-IF, 1 mL/min, 10:90 (2-PrOH:Hexane), Rt_1 = 16.1 min; Rt_2 = 18.8 min. ee = 28%.
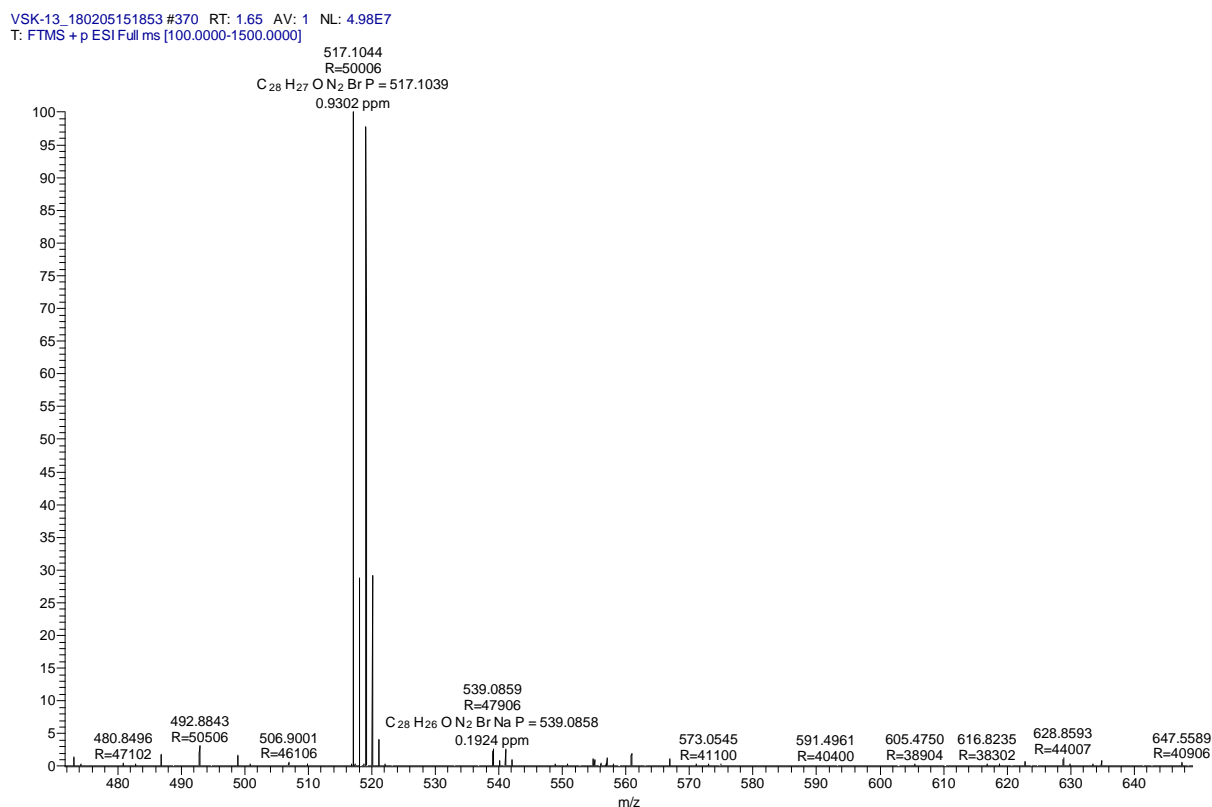
Figure 3.47. ESI-MS (+ve) spectrum of 1-(4-bromophenyl)-3-(3-(mesityl(phenyl)phosphanyl)phenyl)urea (**3.5t**).
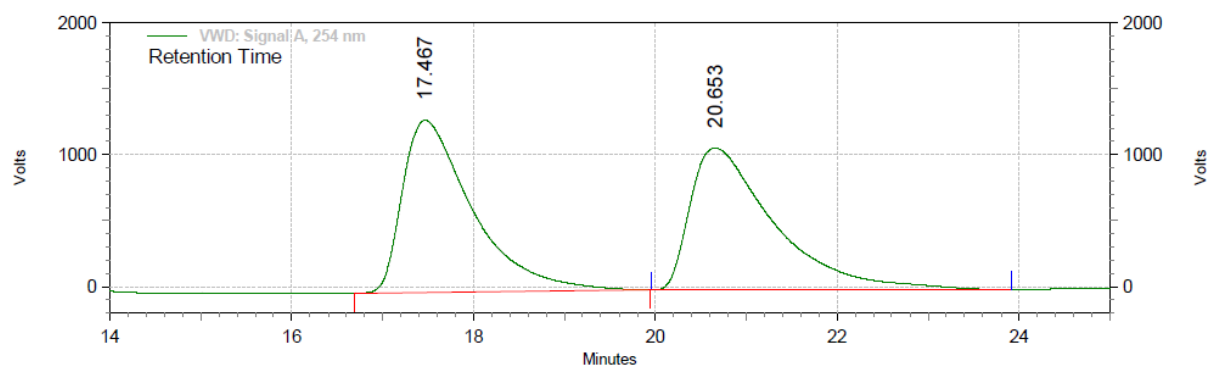
VWD: Signal A, 254 nm Results

Retention Time	Area	Area %
17.467	1169796123	50.34
20.653	1153807020	49.66

Totals		
	2323603143	100.00

Figure 3.48. HPLC chromatogram of racemic 1-(4-bromophenyl)-3-(3-(mesityl(phenyl)phosphanyl)phenyl)urea (**3.5t**).
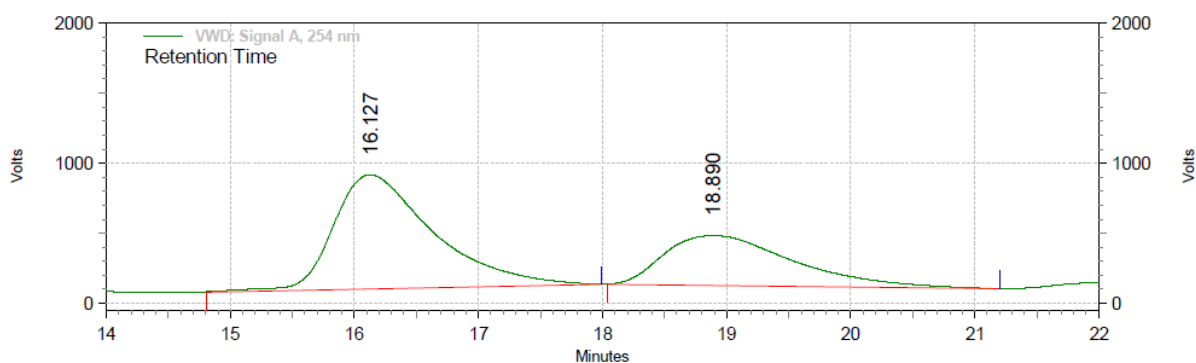
Figure 3.49. HPLC chromatogram of chiral 1-(4-bromophenyl)-3-(3-(mesityl(phenyl)phosphanyl)phenyl)urea (**3.5t**).

3.5.3.38. *Racemic* 1-(2,4-dimethylphenyl)-3-(3-(mesityl(phenyl)phosphanyl)phenyl)urea (3.5u)

A 1-(2,4-dimethylphenyl)-3-(3-iodophenyl)urea (**3.2j**) (0.43 mmol) was dissolved in 2 ml of THF, which was followed by addition of triethylamine (0.86 mmol) and mesityl(phenyl)phosphine **3.1c** (0.43 mmol). After stirring for 10 minutes, [Pd(OAc)$_2$] (0.5 mol %) was added and the mixture was refluxed overnight at 68 °C. After completion of the reaction, excess Sulfur powder (S$_8$) (3 eq.) was added to the reaction mixture at same temperature and the mixture was stirred for one hour. After this, the above mixture was then treated with degassed water and was extracted with ethyl acetate (3 × 10 mL). The combined organic layer was dried on MgSO$_4$ for 2 hours and the volatiles were evaporated under reduced pressure. The crude **3.5u** was purified by silica gel column chromatography using 90:10 mixture of DCM:Ethyl acetate. The desired product was isolated as a whitish yellow solid in 85% yield (186 mg, 0.085 mmol).
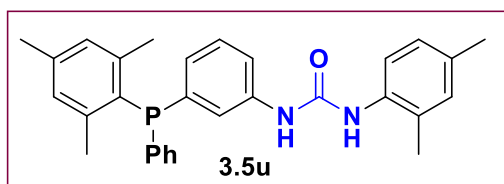
^{1}H NMR (500 MHz, CDCl$_3$, 298 K): δ = 7.42 (d, J_{H-H} = 7.9 Hz, 1H, Ar), 7.32-7.15 (m, 7H, Ar), 7.10 (d, J_{H-H} = 7.5 Hz, 1H, Ar), 6.98 (s, 1H, Ar), 6.88 (s, 2H, Ar), 6.90 (s, 2H, Ar), 6.68 (s, 1H, Ar), 6.33 (s, 1H, Ar), 2.29 (s, 6H, CH$_3$), 2.18 (s, 6H, CH$_3$), 2.15 (s, 3H, CH$_3$). **^{31}P NMR** (500 MHz, CDCl$_3$, 298 K): δ = -16.28. **^{13}C NMR** (125 MHz, CDCl$_3$, 298 K): δ = 154.0 (s, Ar,

*C*O), 145.5 (d, $J_{\text{C-P}}$ = 16.2 Hz, Ar, quat.), 140.0 (s, Ar, quat.), 138.4 (s, Ar, quat.), 138.3 (s, Ar, quat.), 138.0 (s, Ar, quat.), 137.9 (s, Ar, quat.), 136.2 (s, Ar, quat.), 136.0 (s, Ar, quat.), 132.8 (s, Ar, quat.), 132.6 (s, Ar, quat.), 131.7 (s, Ar, *C*H), 131.5 (s, Ar, *C*H), 129.9 (d, $J_{\text{C-P}}$ = 4.2 Hz, Ar, *C*H), 129.1 (d, $J_{\text{C-P}}$ = 5.1 Hz, Ar, *C*H), 128.3 (d, $J_{\text{C-P}}$ = 5.4 Hz, Ar, *C*H), 127.6 (s, Ar, *C*H), 127.5 (s, Ar, *C*H), 126.7 (s, Ar, *C*H), 126.5 (s, Ar, *C*H), 125.7 (s, Ar, *C*H), 123.2 (s, Ar, *C*H), 122.9 (s, Ar, *C*H), 119.8 (s, Ar, *C*H), 23.7 (s, Ar, *C*H$_3$), 23.5 (s, *C*H$_3$), 21.0 (s, *C*H$_3$), 20.8 (s, *C*H$_3$) 17.7 (s, Ar, *C*H$_3$). **ESI-MS** (+ve): (Cal. For $C_{30}H_{31}N_2OP$) m/z = 467.22 $[M+H]^+$.

3.5.3.39. *Chiral* 1-(2,4-dimethylphenyl)-3-(3-(mesityl(phenyl)phosphanyl)phenyl)urea (3.5u)

A Schlenk tube was loaded with catalyst **Cat.2** (0.005 mmol), 1-(2,4-dimethylphenyl)-3-(3-iodophenyl)urea (**3.2j**) (0.1 mmol), and mesityl(phenyl)phosphine (**3.1c**) (0.1 mmol) in a glove box. The screw capped Schlenk tube was taken out and appropriate temperature was attained.
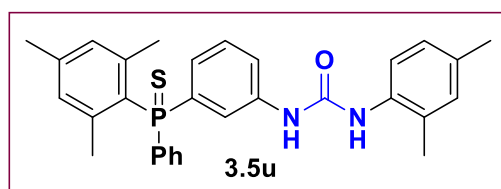
After the standard vacuum-argon cycle, NaOAc and 1 ml DMF were added to the reaction mixture. The progress of the reaction was monitored by ^{31}P NMR spectroscopy. After completion of the reaction, Sulphur powder was added to the reaction mixture at same temperature and the reaction mixture was stirred for half an hour. The content was treated with degassed water (which was pre-cooled at appropriate temperature) and extracted with ethyl acetate (10 mL × 3) (which was pre-cooled at appropriate temperature). The combined organic layer was dried on MgSO$_4$ for half hour at suitable temperature and the volatiles were evaporated under reduced pressure. The plug was washed with DCM until the impurities were eluted, and then the expected product was pushed through with ethyl acetate. After evaporation of the solvent the product was obtained as a pale yellow solid **3.5u** which was analyzed by a combination of spectroscopic and analytical tools.

^{31}**P NMR** (500 MHz, CDCl$_3$, 298 K) δ = 37.12 (s, P). **HPLC:** Daicel Chiralpak-IF, 1 mL/min, 10:90 (2-PrOH:Hexane), Rt_1 = 24.6 min; Rt_2 = 27.5 min. ee = 45%.

VSK-14 #366 RT: 1.63 AV: 1 NL: 8.48E5
T: FTMS + p ESI Full ms [100.0000-1500.0000]
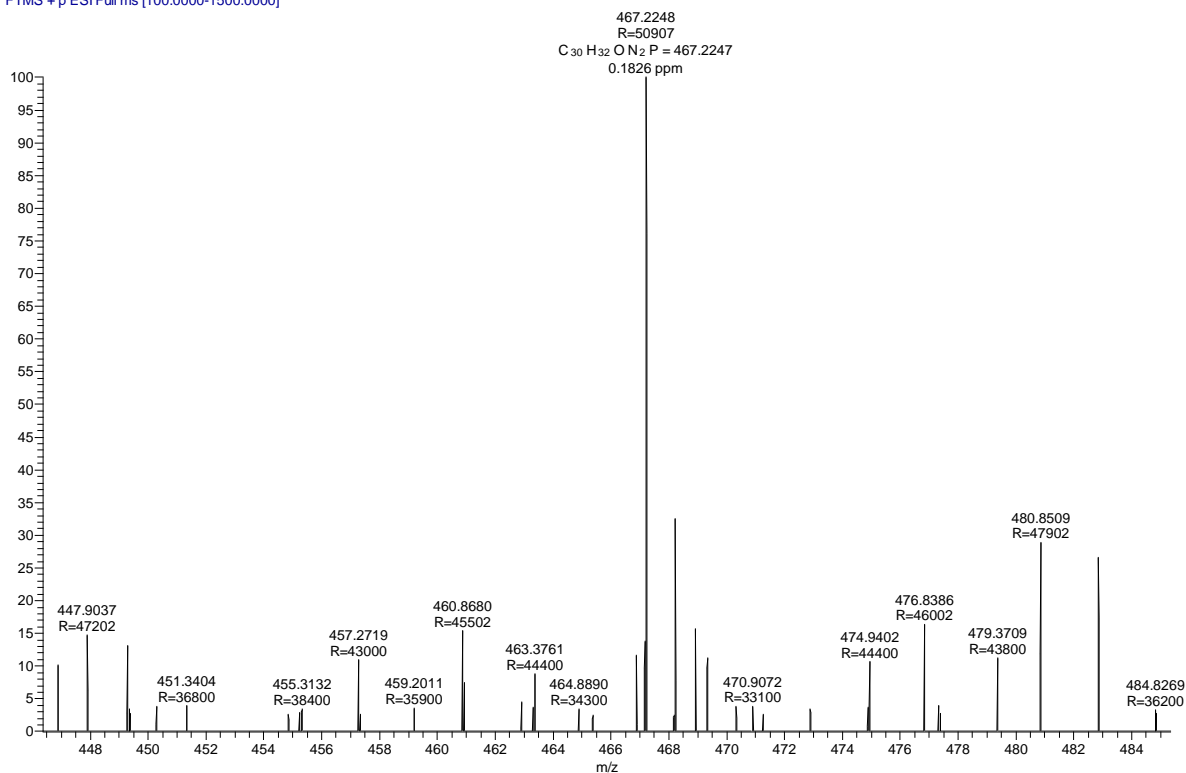
Figure 3.50. ESI-MS (+ve) spectrum of 1-(2,4-dimethylphenyl)-3-(3-(mesityl(phenyl)phosphanyl)phenyl)urea (**3.5u**).
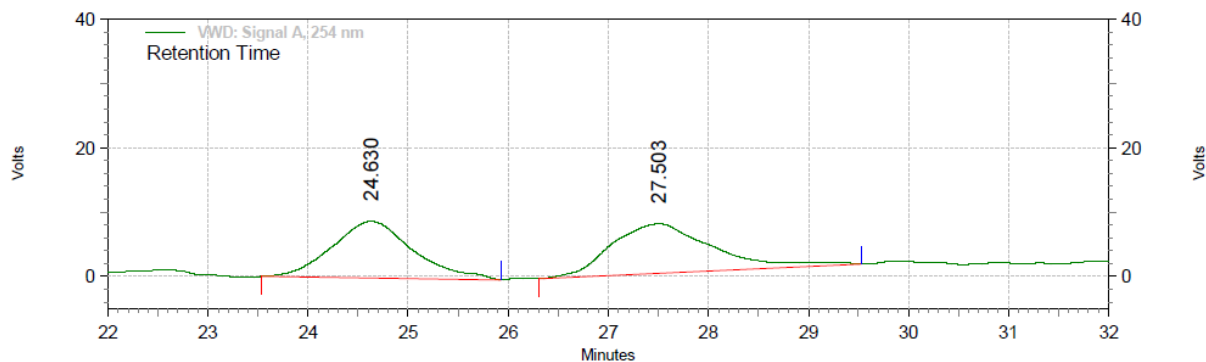
VWD: Signal A, 254 nm Results

Retention Time	Area	Area %
24.630	8287778	47.92
27.503	9008523	52.08

Totals		
	17296301	100.00

Figure 3.51. HPLC chromatogram of racemic 1-(2,4-dimethylphenyl)-3-(3-(mesityl(phenyl)phosphanyl)phenyl) urea (**3.5u**).
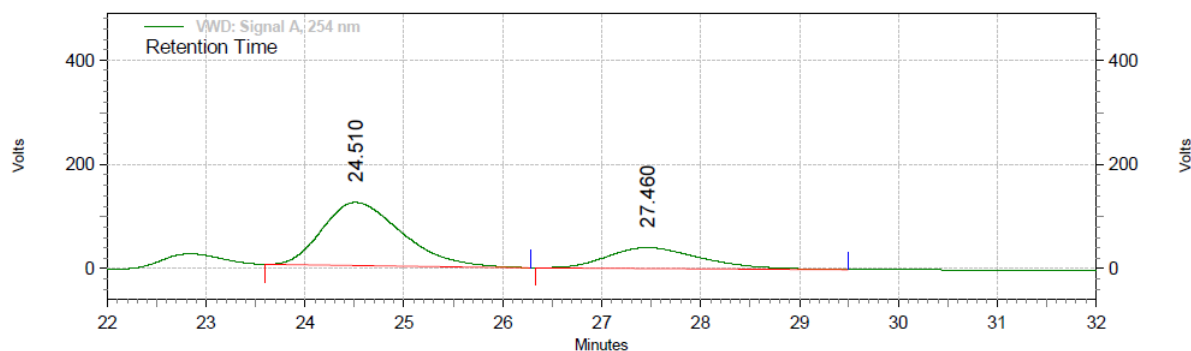
VWD: Signal A, 254 nm Results		
Retention Time	Area	Area %
24.510	113996697	72.48
27.460	43286288	27.52

Totals	
157282985	100.00

Figure 3.52. HPLC chromatogram of chiral 1-(2,4-dimethylphenyl)-3-(3-(mesityl(phenyl)phosphanyl)phenyl) urea (**3.5u**).

3.5.3.40. *Racemic* 1-(3-(mesityl(phenyl)phosphorothioyl)phenyl)-3-(3-methoxyphenyl) urea (3.5v)

A 1-(3-iodophenyl)-3-(3-methoxyphenyl)urea (**3.2k**) (0.43 mmol) was dissolved in 2 ml of
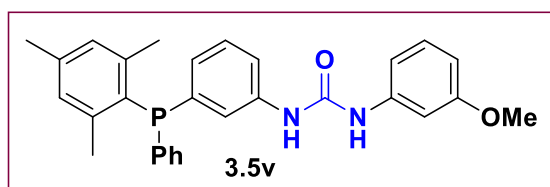
THF, which was followed by addition of triethylamine (0.86 mmol) and mesityl(phenyl)phosphine **3.1c** (0.43 mmol). After stirring for 10 minutes, [Pd(OAc)$_2$] (0.5 mol %) was added and the mixture was refluxed overnight at 68 °C. Thus, after above mixture was then treated with degassed water and was extracted with ethyl acetate (3 × 10 mL). The combined organic layer was dried on MgSO$_4$ for 2 hours and the volatiles were evaporated under reduced pressure. The crude **3.5v** was purified by silica gel column chromatography using 80:20 mixture of DCM:Ethyl acetate. The desired product was isolated as a yellowish solid in 76% yield (86 mg, 0.36 mmol).

^{1}H NMR (500 MHz, CDCl$_3$, 298 K): δ = 7.36-7.28 (m, 4H, Ar), 7.26-7.23 (m, 2H, Ar), 7.22-7.18 (m, 3H, Ar), 7.15 (s, 1H, N*H*), 7.10 (t, J_{H-H} = 8.9 Hz, 1H, Ar), 7.03 (t, J_{H-H} = 6.9 Hz, 1H, Ar), 6.97 (s, 1H, N*H*), 6.88 (s, 2H, Ar), 6.71 (d, J_{H-H} = 7.8 Hz, 1H, Ar), 6.58 (d, J_{H-H} = 8.1 Hz, 1H, Ar), 3.70 (s, 3H, OCH$_3$), 2.27 (s, 3H, CH$_3$), 2.17 (s, 6H, CH$_3$). **^{31}P NMR** (500 MHz, CDCl$_3$, 298 K): δ = -16.17. **^{13}C NMR** (125 MHz, CDCl$_3$, 298 K): δ = 160.2 (s, Ar, *C*-OMe), 153.3 (s, Ar, *C*O), 145.4 (d, J_{C-P} = 16 Hz, Ar, quat.), 140.1 (s, Ar, quat.), 139.1 (s, Ar, quat.), 138.3 (d,

$J_{\text{C-P}}$ = 8 Hz, Ar, quat.), 136.0 (d, $J_{\text{C-P}}$ = 13.8 Hz, Ar, quat.), 131.6 (s, Ar, *C*H), 131.5 (s, Ar, *C*H), 131.4 (s, Ar, *C*H), 129.9 (s, Ar, *C*H), 129.7 (d, $J_{\text{C-P}}$ = 20.6 Hz, Ar, *C*H), 129.2 (d, $J_{\text{C-P}}$ = 5.4 Hz, Ar, *C*H), 128.3 (d, $J_{\text{C-P}}$ = 5.4 Hz, Ar, *C*H), 127.8 (s, Ar, *C*H), 126.9 (s, Ar, *C*H), 126.7 (s, Ar, *C*H), 126.8 (s, Ar, *C*H), 123.2 (s, Ar, *C*H), 123.1 (s, Ar, *C*H), 120.0 (s, Ar, *C*H), 112.8 (s, Ar, *C*H), 109.6 (s, Ar, *C*H), 106.3 (s, Ar, *C*H), 122.2 (s, Ar, *C*H), 55.1 (s, Ar, O*C*H$_3$), 23.7 (s, *C*H$_3$), 23.6 (s, *C*H$_3$), 21.0 (s, *C*H$_3$). **ESI-MS** (+ve): (Cal. For $C_{29}H_{30}N_2O_2P$) m/z = 469.16 [M+H]$^+$.

3.5.3.41. *Chiral* 1-(3-(mesityl(phenyl)phosphanyl)phenyl)-3-(3-methoxyphenyl)urea (3.5v)

A Schlenk tube was loaded with catalyst **Cat.2** (0.005 mmol), 1-(3-iodophenyl)-3-(3-methoxyphenyl)urea (**3.2k**) (0.1 mmol), and mesityl(phenyl)phosphine (**3.1c**) (0.1 mmol) in a glove box. The screw capped Schlenk tube was taken out and appropriate temperature was attained. After the standard vacuum-argon cycle, NaOAc and 1 ml DMF were added to the reaction mixture. The progress of the reaction was monitored by ^{31}P NMR spectroscopy. After completion of the reaction, Sulphur powder was added in reaction mixture at same temperature and stirred it for half an hour. The content was treated with degassed water (which was pre-cooled at appropriate temperature) and extracted with ethyl acetate (10 mL × 3) (which was pre-cooled at appropriate temperature). The combined organic layer was dried on MgSO$_4$ for half hour at suitable temperature and the volatiles were evaporated under reduced pressure. The plug was washed with DCM until the impurities were eluted, and then the expected product was pushed through with ethyl acetate. After evaporation of the solvent the product was obtained as a pale yellow solid **3.5v** which was analyzed by a combination of spectroscopic and analytical tools.

^{31}**P NMR** (500 MHz, CDCl$_3$, 298 K) δ = 37.12 (s, P). **HPLC:** Daicel Chiralpak-IF, 1 mL/min, 07:93 (2-PrOH:Hexane), Rt_1 = 68.5 min; Rt_2 = 73.5 min. ee = 61%.

R-14 #195 RT: 0.87 AV: 1 NL: 1.48E9
T: FTMS + p ESI Full ms [100.00-1500.00]

469.2043
R=52507
$C_{29} H_{30} O_2 N_2 P = 469.2039$
0.7971 ppm

453.1710
R=45200
$C_{28} H_{26} O_2 N_2 P = 453.1726$
-3.7108 ppm

463.3029
R=42600

485.1989
R=50300
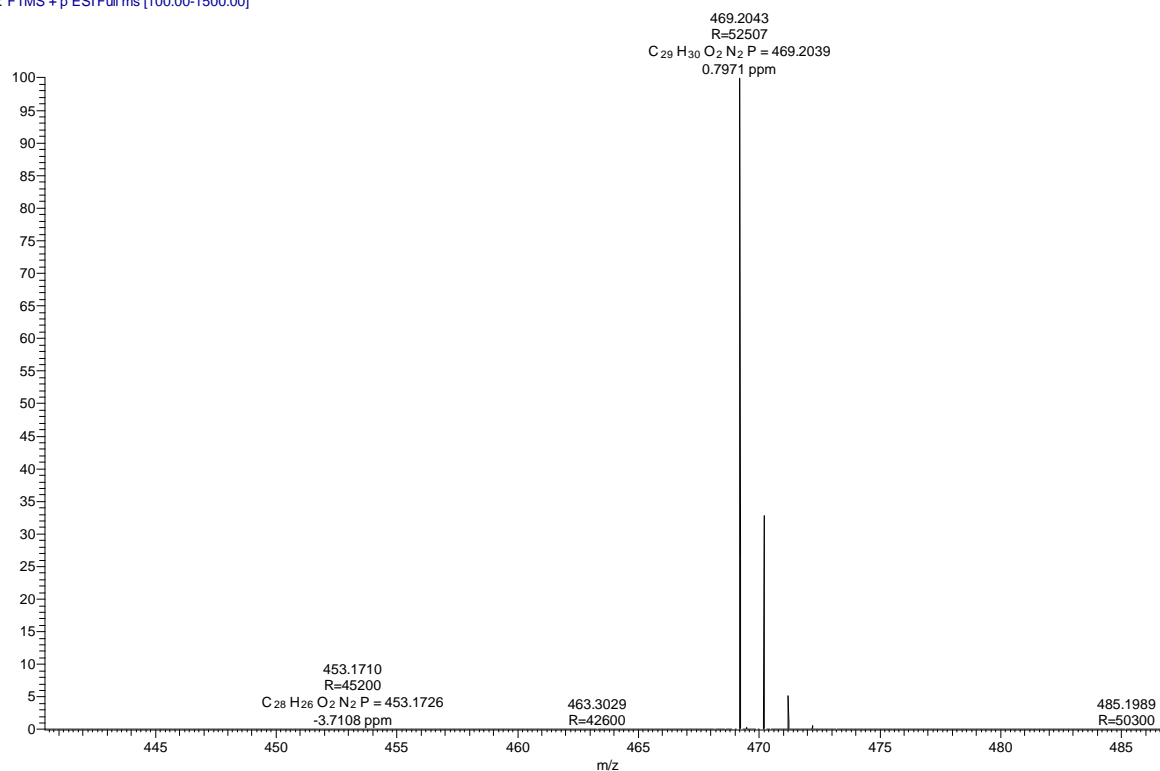
Figure 3.53. ESI-MS (+ve) spectrum of 1-(3-(mesityl(phenyl)phosphanyl)phenyl)-3-(3-methoxyphenyl)urea (**3.5v**).
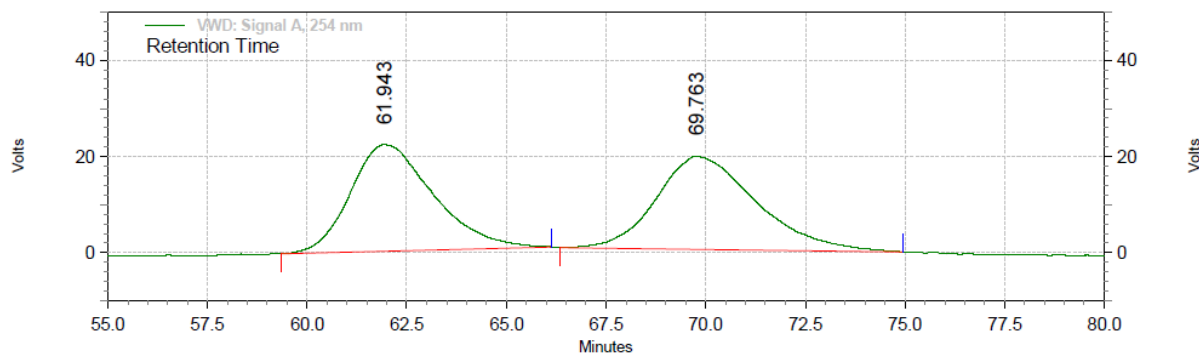
VWD: Signal A, 254 nm Results

Retention Time	Area	Area %
61.943	53931256	48.82
69.763	56532866	51.18
Totals	110464122	100.00

Figure 3.53. HPLC chromatogram of racemic 1-(3-(mesityl(phenyl)phosphanyl)phenyl)-3-(3-methoxyphenyl) urea (**3.5v**).
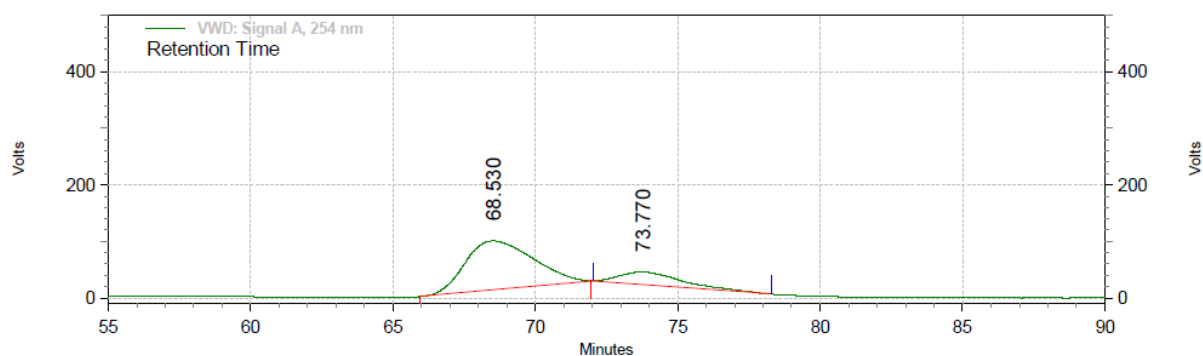
VWD: Signal A, 254 nm Results

Retention Time	Area	Area %
68.530	238982429	81.08
73.770	55782825	18.92
Totals	294765254	100.00

Figure 3.54. HPLC chromatogram of chiral 1-(3-(mesityl(phenyl)phosphanyl)phenyl)-3-(3-methoxyphenyl)urea (**3.5v**).

3.6. Characterization of compounds
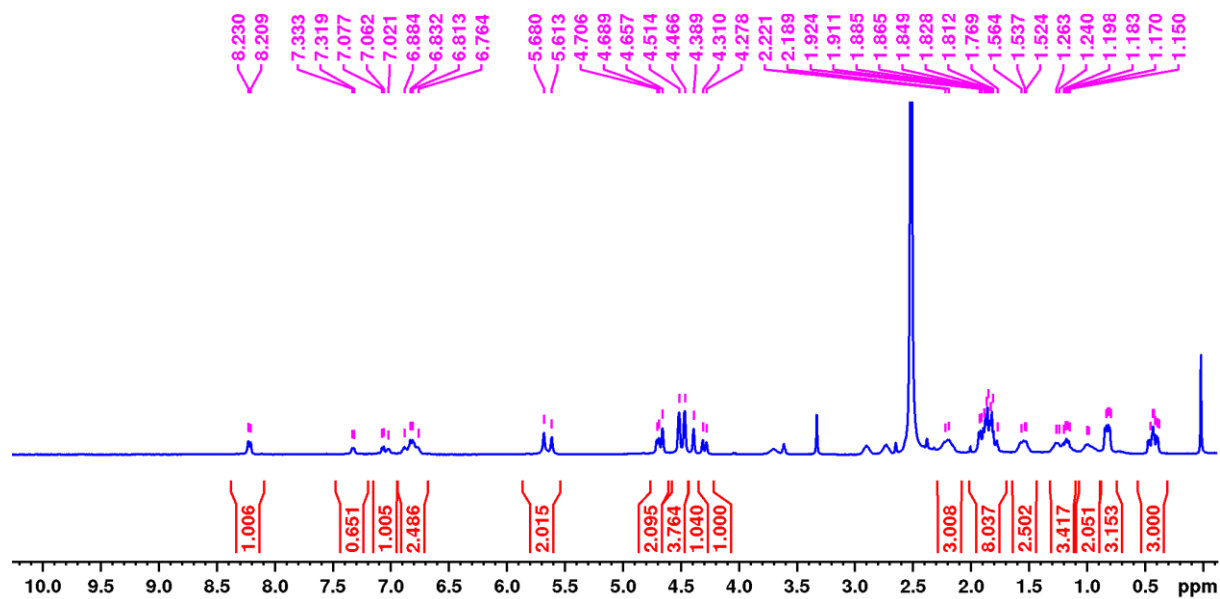
Figure 3.56. ^{1}H NMR spectrum of **Cat.2** in DMSO-d$_6$.
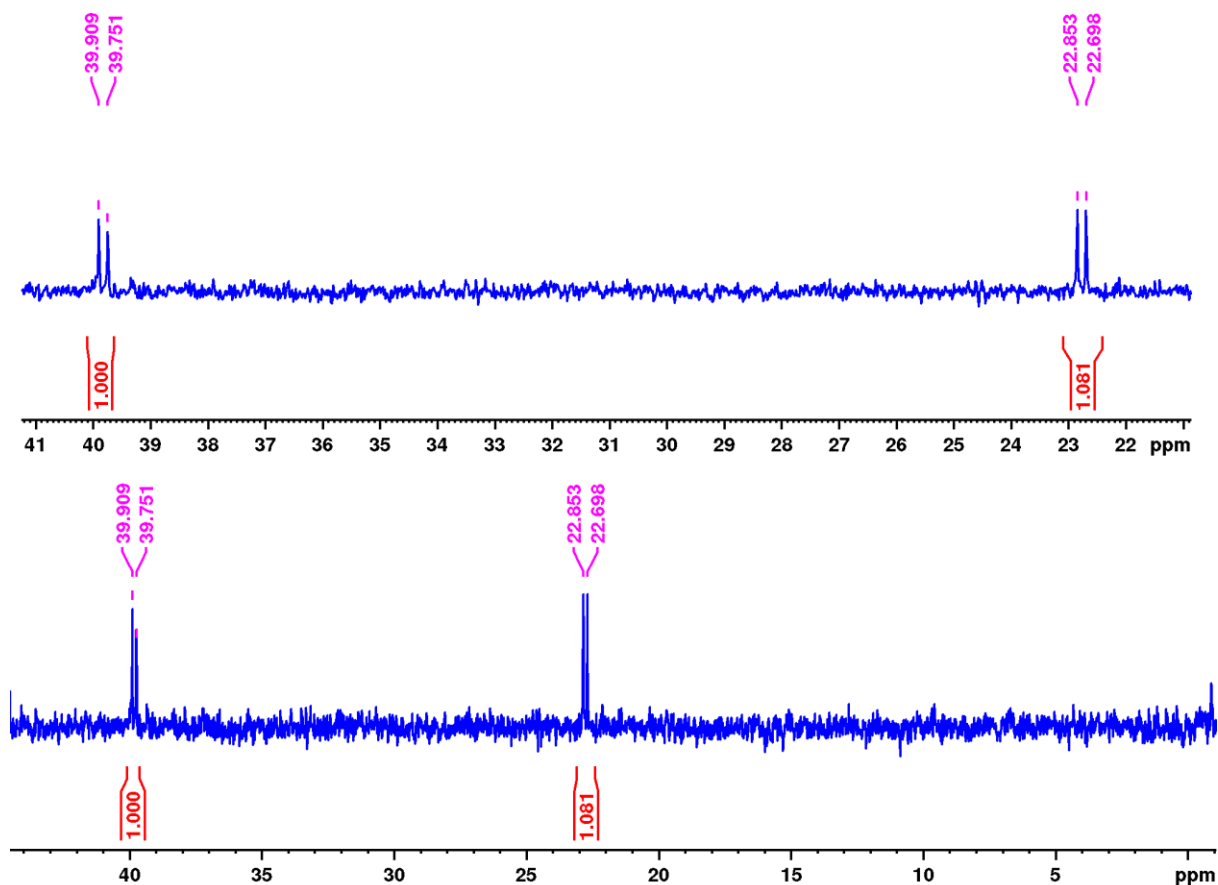
Figure 3.57. ³¹P NMR spectra of **Cat.2** in DMSO-d₆.
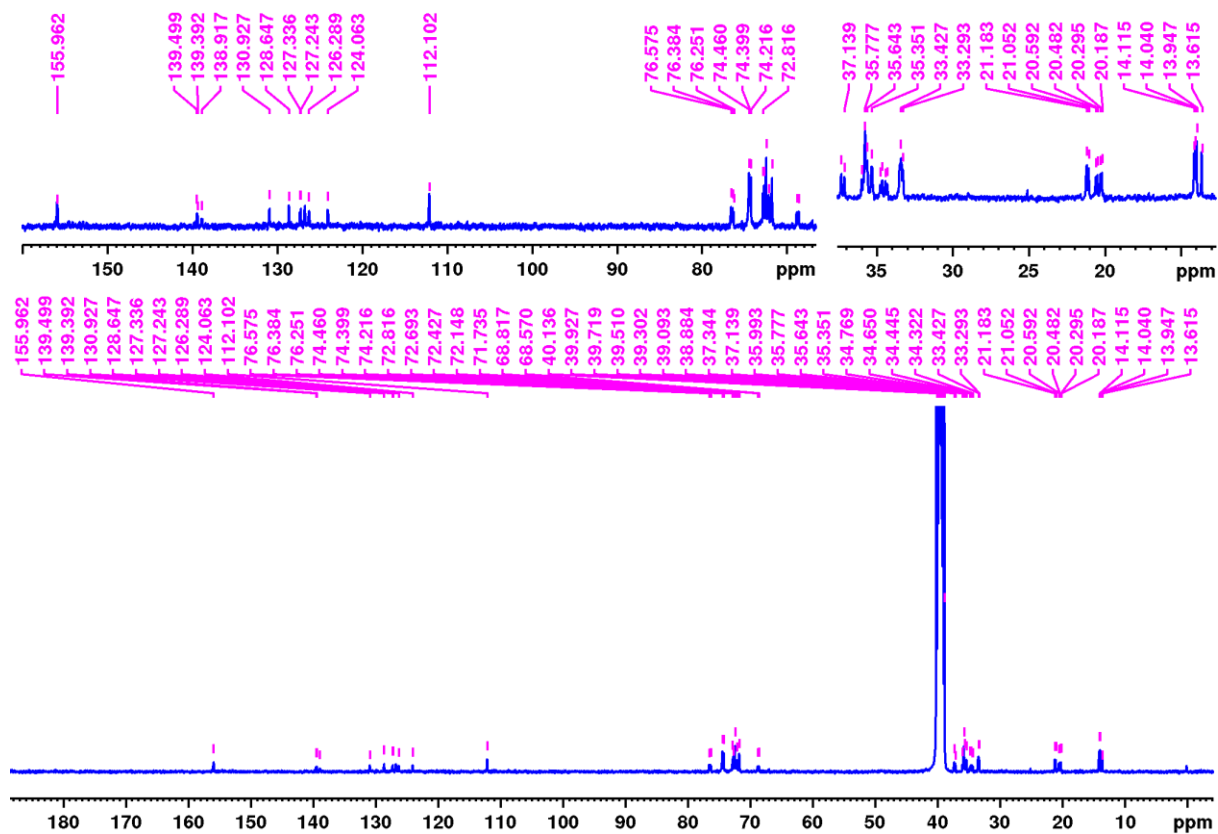
Figure 3.58. ¹³C NMR spectra of **Cat.2** in DMSO-d₆.
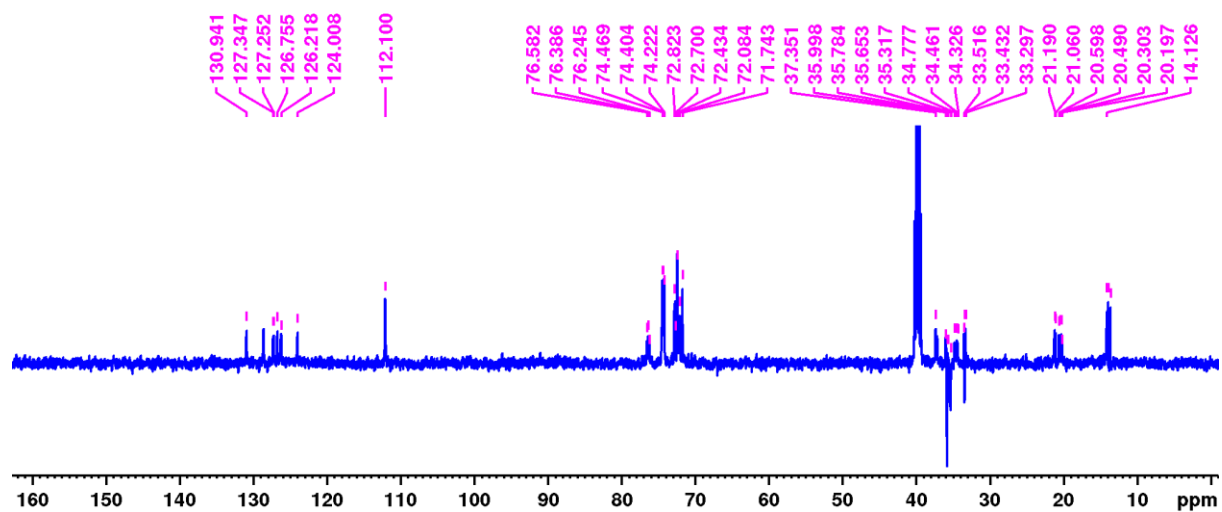
Figure 3.59. ^{13}C (DEPT) NMR spectrum of **Cat.2** in DMSO-d_6.
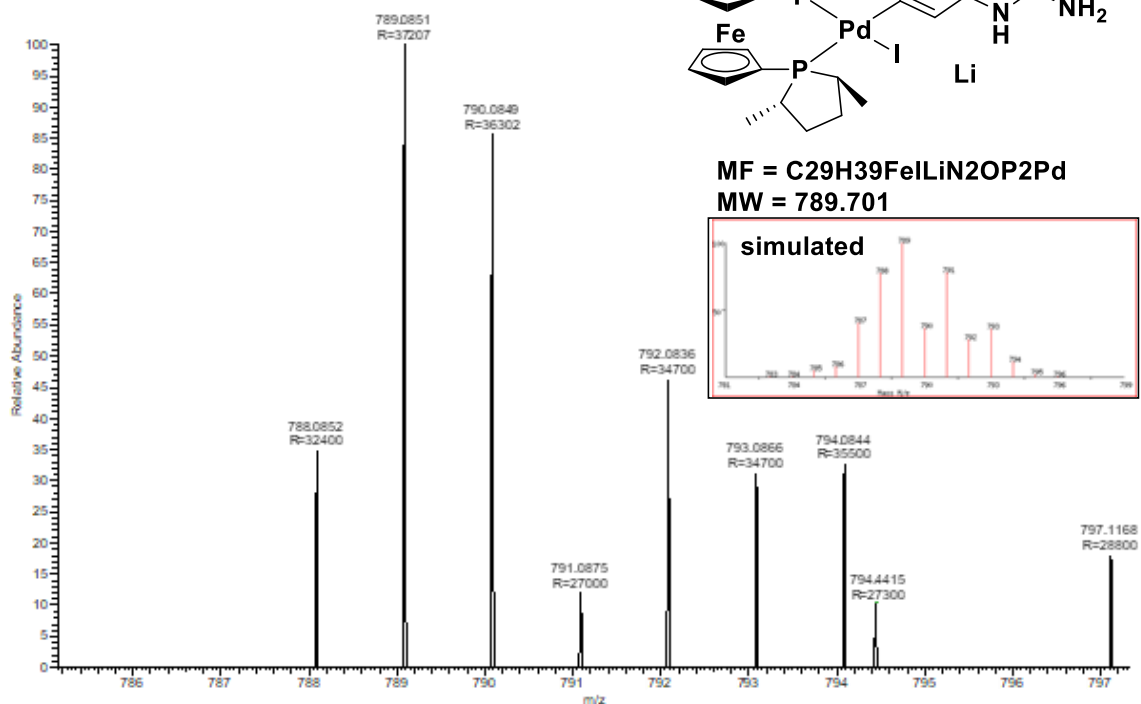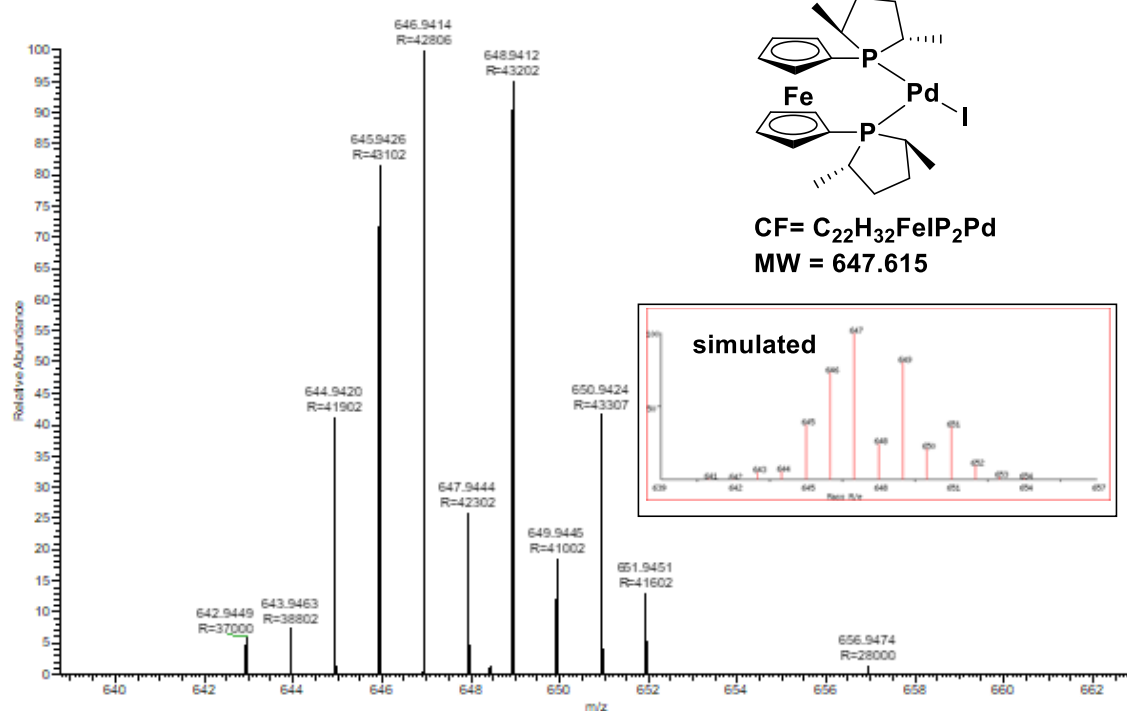
Figure 3.60. ESI-MS (+ve) spectra of **Cat.2**.
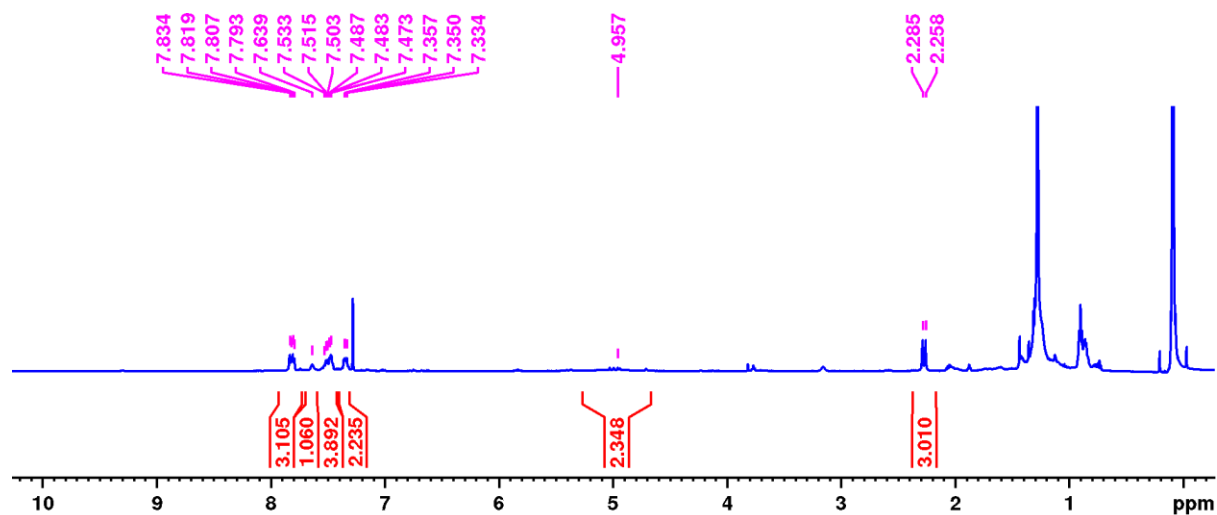
Figure 3.61. ^{1}H NMR spectrum 1-(3-(methyl(phenyl)phosphorothioyl)phenyl)urea (**3.5a**)
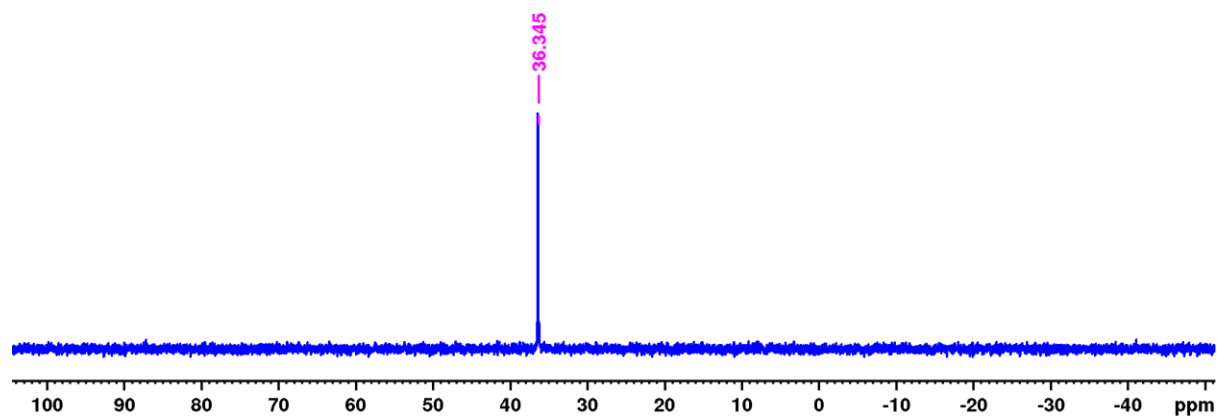
Figure 3.62. ^{31}P NMR spectrum 1-(3-(methyl(phenyl)phosphorothioyl)phenyl)urea (**3.5a**)
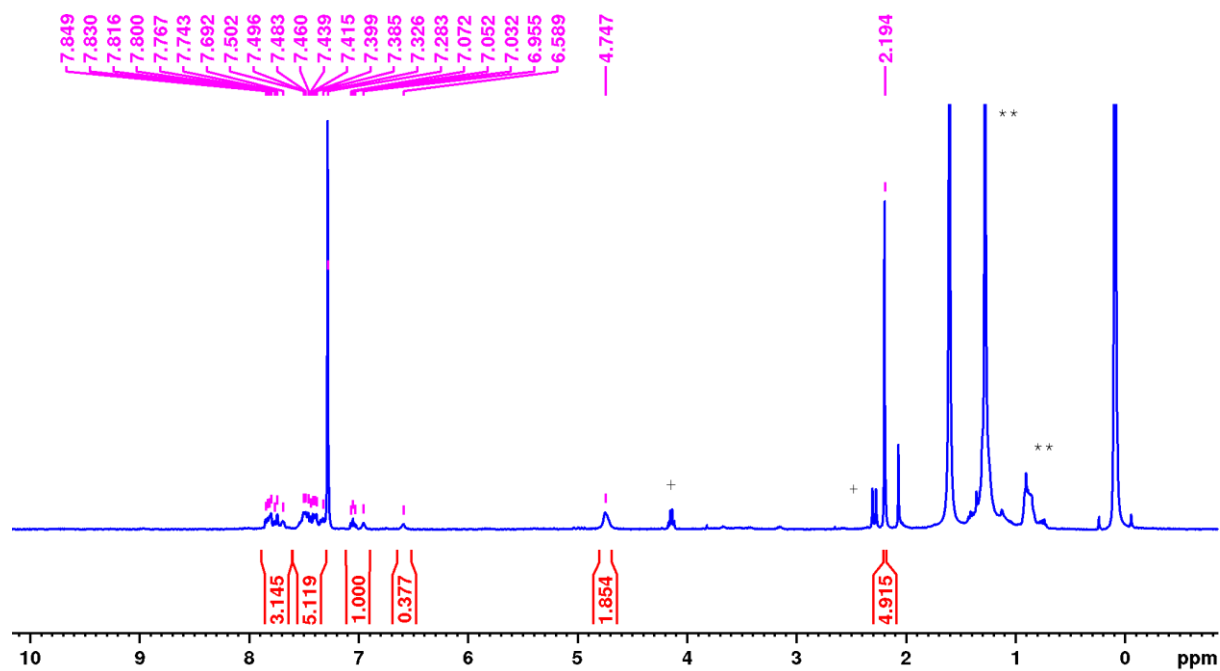
Figure 3.63. ^{1}H NMR spectrum 1-(4-(methyl(phenyl)phosphorothioyl)phenyl)urea (**3.5b**)
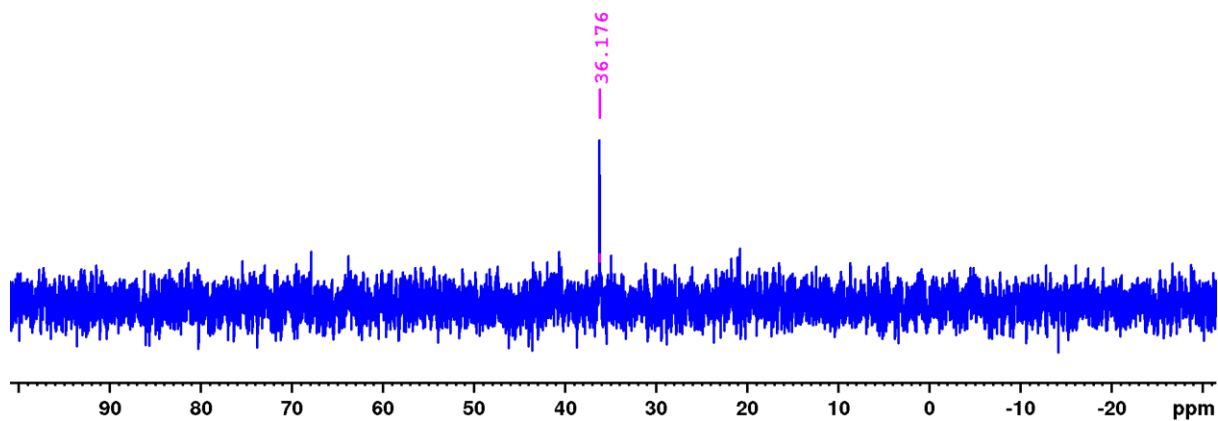
Figure 3.64. ^{31}P NMR spectrum 1-(4-(methyl(phenyl)phosphorothioyl)phenyl)urea (**3.5b**)
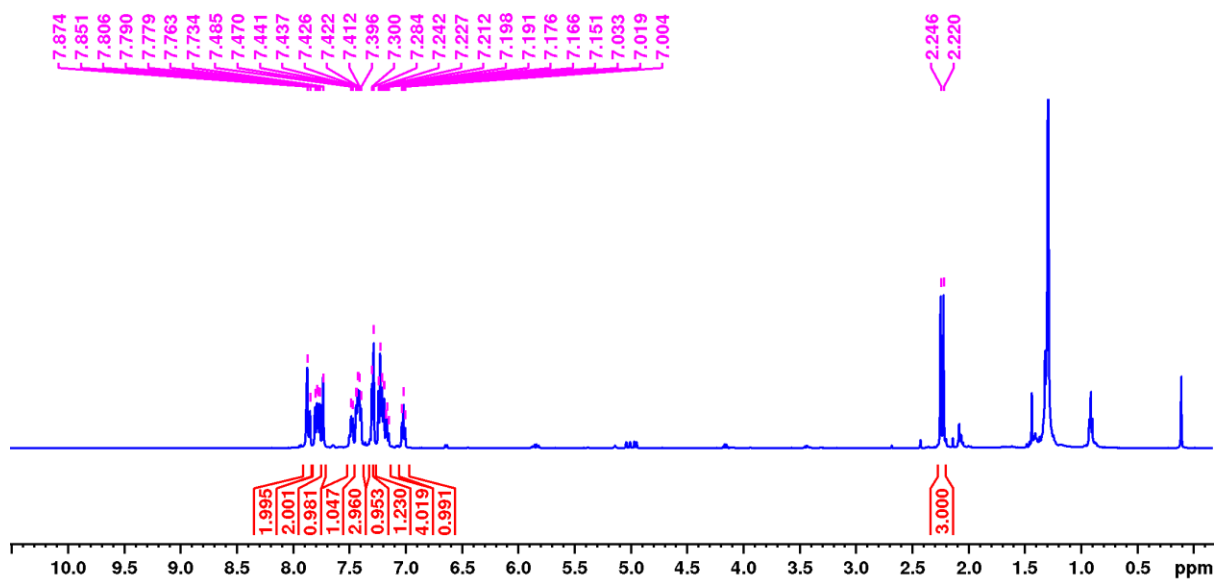
Figure. 3.65. ^{1}H NMR spectrum 1-(3-(methyl(phenyl)phosphorothioyl)phenyl)-3-phenylurea (**3.5c**).in CDCl₃.
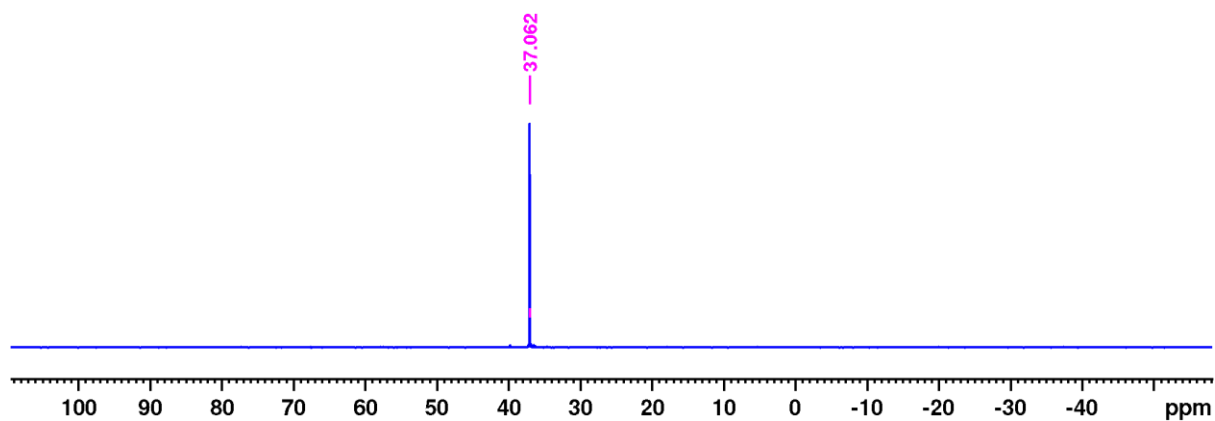
Figure. 3.66. ^{31}P NMR spectrum of 1-(3-(methyl(phenyl)phosphorothioyl)phenyl)-3-phenylurea (**3.5c**).in CDCl₃.
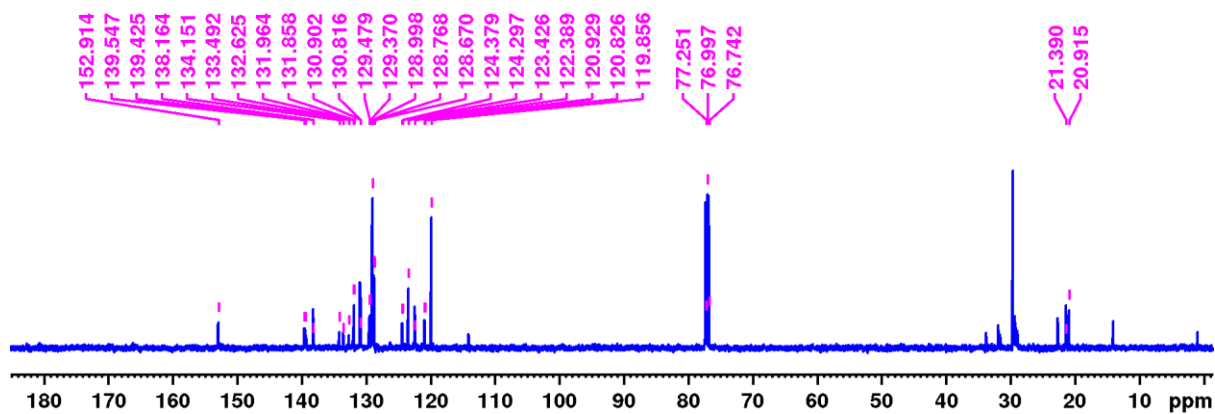
Figure 3.67. ^{13}C NMR spectrum of 1-(3-(methyl(phenyl)phosphorothioyl)phenyl)-3-phenylurea (**3.5c**).in CDCl$_3$.
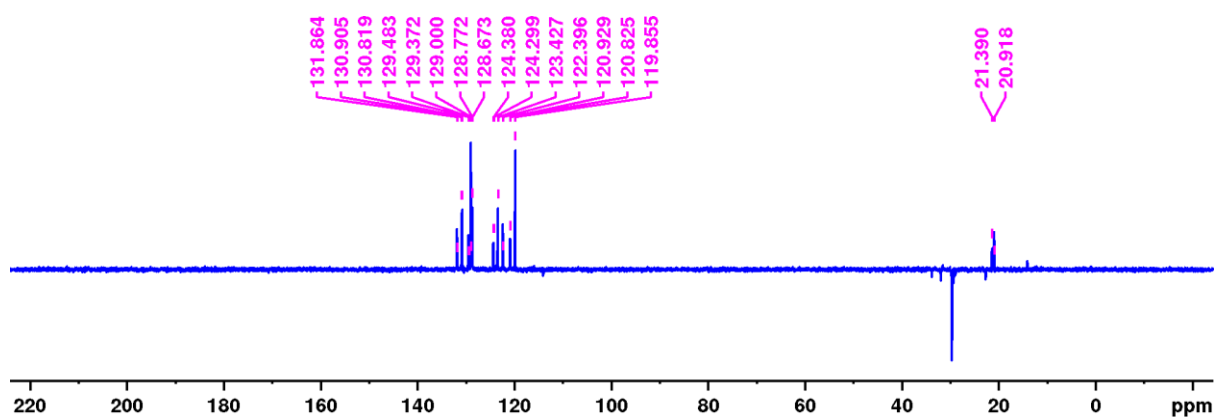
Figure 3.68. ^{13}C (DEPT) NMR spectrum of 1-(3-(methyl(phenyl)phosphorothioyl)phenyl)-3-phenylurea (**3.5c**).in CDCl$_3$.
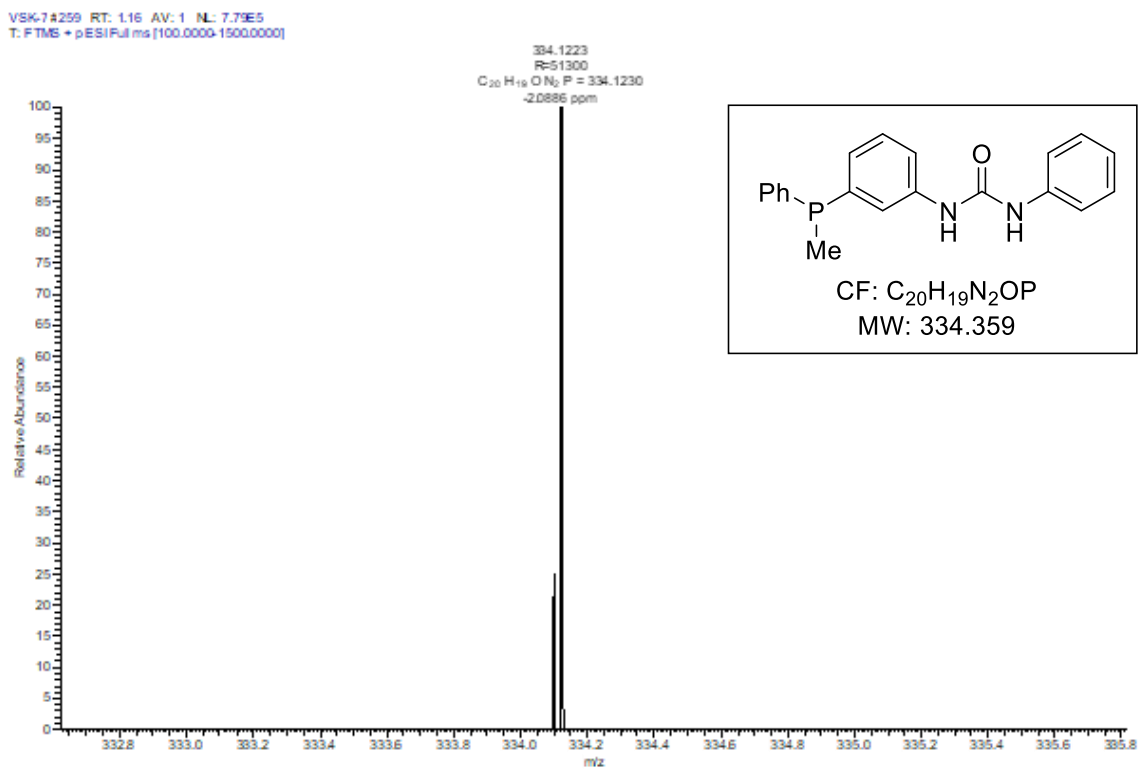
Fig. 3.67. ESI-MS (+ve) spectrum of 1-(3-(methyl(phenyl)phosphorothioyl)phenyl)-3-phenylurea (**3.5c**).

3.7. References

1. *Phosphorus Ligands in Asymmetric Catalysis*; A. Börner, Ed.; Wiley-VCH: Weinheim, 2008; Vols. *I−III*.

2. a) R. R. Noyori, *Asymmetric Catalysis in Organic Synthesis,* Wiley-Interscience, New York, 1994; b) W. S. Knowles, *Asymmetric Catalysis on Industrial Scale, Challenges, Approaches, and Solutions (Eds.: H. U. Blaser and E.Schmidt),* Wiley-VCH, Weinheim, 2004, pp 23-38.

3. L. M. Pignolet, *Homogeneous Catalysis with Metal Phosphine Complexes,* Springer US, 1983.

4. *P. W. N. M*. Leeuwen*,* P. C. J. Kamer, J. N. H. Reek and P. Dierkes, *Chem. Rev.,* 2000, **100**, 2741–2770.

5. S. H. Chikkali, J. I. van der Vlugt and J. N. H. Reek, *Coord. Chem. Rev*., 2014, **262**, 1-15.

6. a) M. L. Clarke and J. J. R. Frew, *Ligand Electronic Effects in Homogeneous Catalysis using Transition Metal Complexes of Phosphine Ligands: (Eds.*: *I. J. S. Fairlamb and J. M. Lynam,), Organomet. Chem.,* 2009, **35***,* pp 19-46.; b) L. A. Adrio and K. K. Hii, *Application of phosphine ligands in organic synthesis: (Eds.*: *I. J. S. Fairlamb and J. M. Lynam), Organomet. Chem.,* 2009, **35***,* pp 62-62.

7. J. Bayardon and S. Juge, *Phosphorus (III) Ligands in Homogeneous Catalysis: Design and Synthesis (Eds.: P. C. J. Kamer and P. W. N. M. van Leeuwen)*, Jon Wiley & Sons Ltd., 2012, pp 335.

8. P. A. R. Breuil, F. W. Patureau and J. N. H. Reek, *Angew. Chem. Int. Ed.,* 2009, **48**, 2162-2165.

9. B. Breit and W. Seiche, *J. Am. Chem. Soc.,* 2003, **125**, 6608-6609.

10. M. T. Reetz and S. R. Waldvogel, *Angew. Chem. Int. Ed.,* 1997, **36**, 865-867.

11. a) For supramolecular phosphines ligands in hydroformylation and hydroformylation, see: a) T. Besset, D. W. Norman and J. N. H. Reek, *Adv. Synth. Catal.,* 2013*,* **355***,* 348-352; b) P. Dydio, R. J. Detz and J. N. H. Reek, *J. Am. Chem. Soc.,* 2013, **135**, 10817-10828; c) D. Fuchs, G. Rousseau, L. Diab, U. Gellrich and B. Breit, *Angew. Chem. Int. Ed.,* 2012, **51**, 2178-2182; d) U. Gellrich, W. Seiche, M. Keller and B. Breit, *Angew. Chem. Int. Ed.,* 2012, **51**, 11033-11038; e) P. Dydio, C. Rubay, T. Gadzikwa, M. Lutz and J. N. H. Reek, *J. Am. Chem. Soc.,* 2011, **133**, 17176-17179, f) P. Dydio and J. N. H. Reek, *Angew. Chem. Int. Ed.,* 2013, **52**, 3878-3882; g) T. Gadzikwa, R. Bellini, H. L. Dekker and J. N. H. Reek, *J. Am. Chem. Soc.,* 2012, **134**, 2860-2863; h) R. Bellini, S. H. Chikkali, G. Berthon-Gelloz and J. N. H. Reek, *Angew. Chem. Int. Ed.,* 2011, **50**, 7342-7345.

12. M. de Greef and B. Breit, *Angew. Chem. Int. Ed.,* 2009, **48**, 551-554.

13. a) D. Anselmo, R. Gramage-Doria, T. Besset, M. V. Escarcega-Bobadilla, G. Salassa, E. C. Escudero-Adan, B. M. Martinez, E. Martin, J. N. H. Reek and A. W. Kleij, *Dalton Trans.,* 2013, **42**, 7595-7603; b) L. Leclercq and A. R. Schmitzer, *Organometallics*, 2010, **29**, 3442-3449.

14. The p-stereogenic phosphines earned Prof. Knowles the 2001 Nobel Prize, for more details see: a) B. D. Vineyard, W. S. Knowles, M. J. Sabacky, G. L. Bachmann and D. J. Weinkauff, *J. Am. Chem. Soc.,* 1977, **99**, 5946-5952; b) W. S. Knowles, *Angew. Chem. Int. Ed.,* 2002, **41**, 1998-2007; c) D. S. Glueck, *Synlett,* 2007, **17**, 2627–2634 and the references there in.

15. a) S. Jugé, *Phosphorus, Sulfur Silicon* 2008, **183**, 233; b) A. Grabulosa, J. Granell and G. Muller, *Coord. Chem. Rev.,* 2007, **251**, 25; c) T. Ohkuma, M. Kitamura, R. Noyori, *Catalytic Asymmetric Synthesis*, Wiley-VCH, New York, 1993.

16. Chiral auxiliary based synthesis of p-chiral phosphines is the most established method to prepare p-chiral phosphines on larger scale; for the synthesis, see: a) K. M. Pietrusiewicz and M. Zablocka, *Chem. Rev.,*

1994, **94**, 1375-1411; b) W. Tang and X. Zhang, *Chem. Rev*., 2003, **103**, 3029-3070; c) T. Imamoto, K. Tamura, Z. Zhang, Y. Horiuchi, M. Sugiya, K. Yoshida, A. Yanagisawa and A. D. Gridnev, *J. Am. Chem. Soc.,* 2012, **134**, 1754-1769; d) T. Imamoto, Y. Saitoh, A. Koide, T. Ogura and K. Yoshida, *Angew. Chem. Int. Ed.,* 2007, **46**, 8636-8639; e) A. Karim, A. Mortreux, F. Petit, G. Buono, V. Peiffer and C. Siv, *J. Organomet. Chem.,* 1986, **317**, 93-104.

17. J. R. Moncarz, M. F. Laritcheva and D. S. Glueck, *J.Am.Chem.Soc.,* 2002, **124**, 13356−13357.

18. C. Scriban and D. S. Glueck, *J. Am. Chem. Soc*., 2006, **128**, 2788.

19. V. S. Chan, I. C. Stewart, R. G. Bergman and F. D. Toste, *J. Am. Chem. Soc*., 2006, **128**, 2786.

20. a) J. R. Moncarz, M. F. Laritcheva and D. S. Glueck, *J. Am. Chem. Soc.,* 2002, **124**, 13356-13357; b) J. R. Moncarz, T. J. Brunker, J. C. Jewett, M. Orchowski, D. S. Glueck, *Organometallics,* 2003, **22**, 3205-3221; c) N. F. Blank, J. R. Moncarz, T. J. Brunker, C. Scriban, B. J. Anderson, O. Amir, D. S. Glueck, L. N. Zakharov, J. A. Golen, C. D. Incarvito and A. L. Rheingold, *J. Am. Chem. Soc.,* 2007, **129**, 6847-6858; d) N. F. Blank, K. C. McBroom, D. S. Glueck, W. S. Kassel and A. L. Rheingold, *Organometallics,* 2006, **25**, 1742-1748; e) D. Julienne, O. Delacroix, J. F. Lohier, J. S. de Oliveira-Santos and A. C. Gaumont, *Eur. J. Inorg. Chem.,* 2011, **16**, 2489-2498; (f) D. S. Glueck, *Chem. Eur. J.,* 2008, **14**, 7108-7117.

21. V. S. Koshti, N. R. Mote, R.G. Gonnade and S. Chikkali, *Organometallics*, 2015, **34**, 4802-4805.

22. T. J. B runker, N. F. Blank, J. R. Moncarz, C. Scriban, B. J. Anderson, D. S. Glueck, L. N. Zakharov, J. A. Golen, R. D. Sommer, C. D. Incarvito and A. L. Rheingold, *Organometallics,* 2005, **24**, 2730-2746.

23. Y. Huang, Y. Li, P. H. Leung and T. Hayashi, *J. Am. Chem. Soc.,* 2014, **136**, 4865-4868.

24. Synthesis of 3-iodophenylurea (**3.2a**) has been reported, see ref. 8. A modified protocol has been developed for the synthesis of **3.2b** and **3.2l**; V. S. Koshti, S. H. Thorat, R. P. Gote, S. H. Chikkali and R. G. Gonnade, *CrystEngComm*, 2016, **18**, 7078-7094.

25. **3.1a-c** are moisture and oxygen sensitive. K_2HPO_4 act as base as well as oxidizing agent and it can oxidize one of coupling partner (**3.1a-c**).

26. D. D. Perrin, W. L. Armarego and L. F. Willfred, Purification of Laboratory Chemicals, Pergamon, Oxford, 1988.

Chapter 4

Ni-catalyzed enantioselective synthesis of P-stereogenic (supramolecular) phosphines

4.1. Abstract

This chapter illustrates the synthesis of nickel catalysts and their implication in P-C bond forming reactions. [Ni-((*S,S*)Me-FerroLANE)(phenyl)(I)] (**Ni-Cat.1**) complex has been synthesized by mixing *(S,S)*Me-FerroLANE with [(diphenylphosphanyl)nickel(phenyl)(I)] in good yields. Treatment of racemic methyl(phenyl)phosphine (**4.1**) with 1-iodo-3-methylbenzene (**4.2b**) in presence **Ni-Cat.1** yields methyl(phenyl)(*m*-tolyl)phosphine (**4.3b**) in 99%. The scope of the reaction was extended and a small library of the phosphine compounds such as methyl(phenyl)(*o*-tolyl)phosphine (**4.3a**) and methyl(phenyl)(*p*-tolyl)phosphine (**4.3c**) was prepared. When **Ni-Cat.1** was employed in a P-C coupling reaction between methyl(phenyl)phosphine (**4.1**) and 1-(3-iodophenyl)urea (**4.2d**) the corresponding P-chiral supramolecular phosphine was obtained with excellent enantiomeric excess (99.4% ee) and moderate conversion 51%.
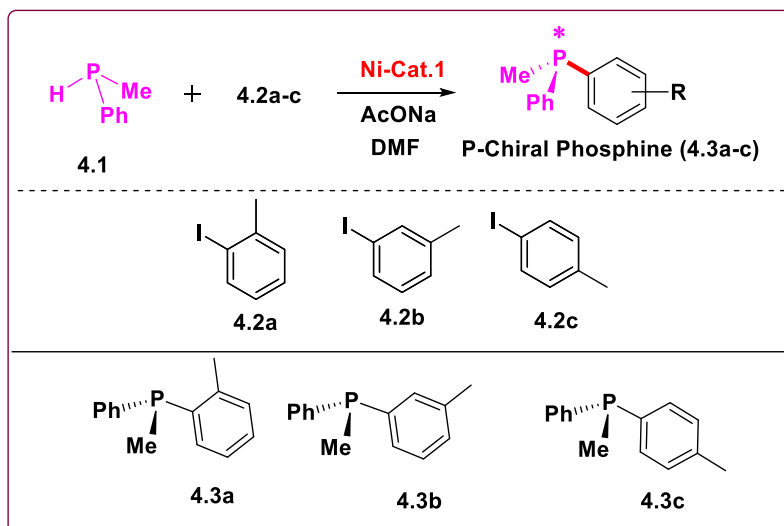
4.2. Introduction

In metal catalyzed reactions ligand plays a prominent role as it tailors the electronic and steric properties of the catalyst. The activity of metal catalyst not only depends on the metal center of the catalyst but also on the ligand.[1,2] After understanding the importance of ligand in metal catalysis, different types of ligands were developed based on the requirement of organic transformation. Thus, various ligands such as monodentate, bidentate, tridentate phosphine ligands have been developed.[3] The bidentate phosphine ligand can chelate to create specific *bite* angle that might engage the space around metal center. Therefore, such metal catalyst might yield better regioselectivity in hydrogenation and hydroformylation reactions.[4,5] Thus, the last decade witnessed a flood of literature on designing, synthesis, and application of bidentate phosphine ligands in catalytic organic transformations.[6] Although bidentate phosphine ligands are important in metal catalysis. However, the synthesis of bidentate phosphine ligands requires a number of steps and is a tedious, labor-intensive work.[7] To overcome this bottle-neck, Reek[8] and Breit[9] introduced monodentate phosphine ligands having hydrogen bonding motif which are known as supramolecular phosphine ligands. These ligands can mimic a bidentate ligand by hydrogen bonding interaction. The self-assembled metal catalysts of these supramolecular ligands are known to display excellent activity in hydrogenation[10] and hydroformylation[11] reactions.
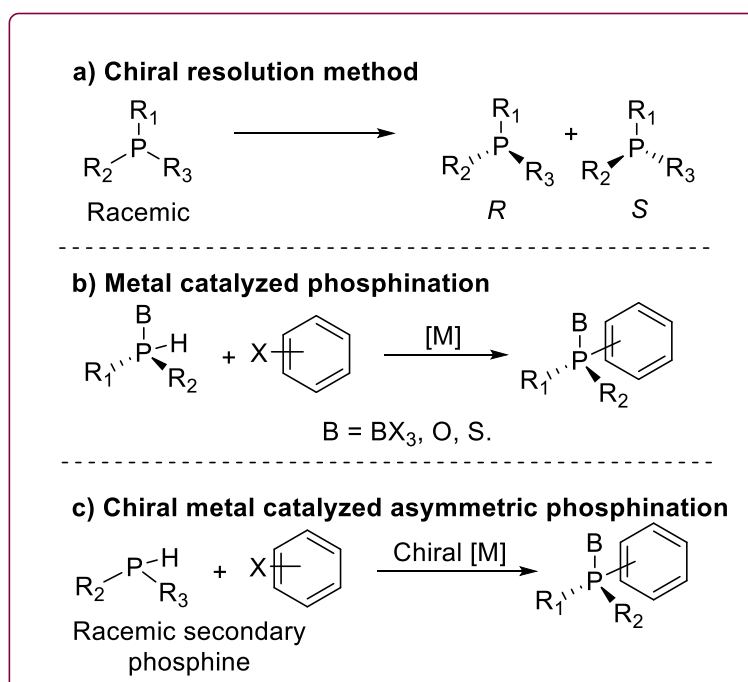
Figure 4.1: State-of-the-art in the synthesis of P-chiral phosphine; chiral resolution (a), Metal catalyzed phosphination (b) and Chiral metal catalyzed asymmetric phosphination (c).

P-chiral phosphines are important ligands for asymmetric catalysis. To explore this concept, different methods for the synthesis of the P-chiral phosphine compounds have been developed.[12] Synthesis of P-chiral compounds is highly challenging for two reasons; a) the phosphorus atom carries a lone pair which readily inverts at room temperature and loses the chirality, b) the phosphine compounds are extremely sensitive to air and moisture posing a handling challenge.[13] To overcome these challenges phosphorous lone pair is protected with an aryl halide in presence of a metal catalyst (Fig. 4.1, b).[14] Catalytic P-C bond forming reactions are well established with Pd,[15] Pt,[16] and Ru[17] metal catalyst with secondary racemic phosphine and aryl halide (Fig. 4.1, c).

Inspired by our previous findings,[18] in this chapter we present the synthesis of chiral Ni-catalysts and their implication in the synthesis of P-chiral (supramolecular) phosphine ligands. We have designed the new metal catalyst where the cheaper and more earth abundant nickel metal is employed which makes P-C bond coupling reaction a sustainable process as compared to precious and rare Pd,[15] and Pt,[16] metal.

4.3. Result and discussion

In metal catalyzed reactions, oxidative addition and reductive elimination govern the reaction time. Palladium is known to undergo oxidation step much faster than the nickel.[19] To overcome this limitation, we have designed the nickel catalyst in which the metal center is electron rich and may increase the rate of oxidative addition step. The bulk around the metal center can influence the rate of reductive elimination step. While designing a new catalyst the steric parameters have to be taken into account. Nickel catalyst has been prepared in a two-step synthetic protocol.[20] A stoichiometric reaction between iodobenzene and [tetrakis(triphenylphosphine)Ni(0)] produced the anticipated pre-catalyst [(di(triphenylphosphine)nickel(phenyl)(I)] in good yield of 65% (Scheme 4.1). The existence of complex [(di(triphenylphosphine)nickel(phenyl)(I)] was unambiguously ascertained using a combination of analytical and spectroscopic methods which exactly match with reported data.[20] **Ni-Cat.1** was synthesized by the addition of (*S,S*)Me-FerroLANE to [(di(triphenylphosphine)nickel(phenyl)(I)] precursor in THF at room temperature and the reaction progress was monitored by ^{31}P NMR spectroscopy. The ^{31}P NMR indicated completion of the reaction within 1 hour (Fig.4.2). After 1 hour, volatiles was evaporated under reduced pressure to obtain a violet-brown color residue, which after *n*-hexane washing produced pure complex **Ni-Cat.1** with 65% yield. The **Ni-Cat.1** was confirmed by ^{1}H NMR (Fig. 4.25) and ^{13}C NMR spectroscopy (Fig. 4.27). Electro-Spray Ionization Mass-

Spectroscopic (ESI-MS) analysis of **Ni-Cat.1** revealed a pseudo-molecular ion peak at m/z = 678.67 [M+H]$^+$, 599.06 [M-Ph]$^+$confirming the presence of anticipated **Ni-Cat.1** (Fig. 4.3).
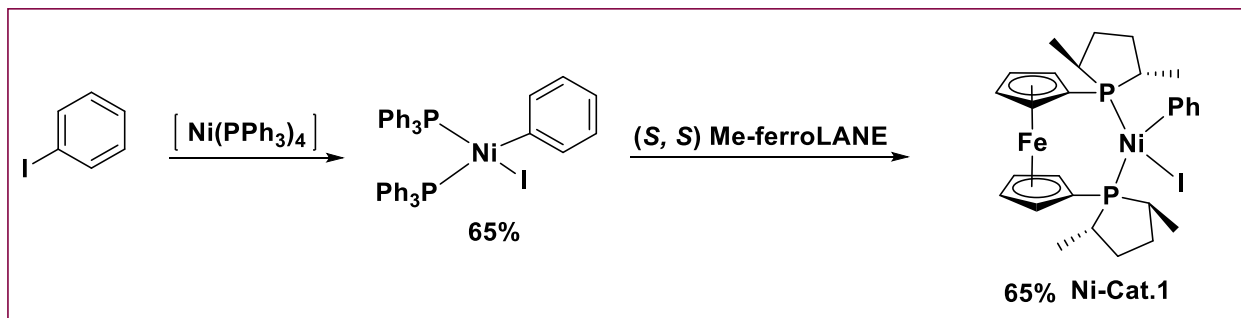
Scheme 4.1: Synthesis of chiral [Ni-((*S*,*S*)Me-FerroLANE)(phenyl)(I)] complex (**Ni-Cat.1**).
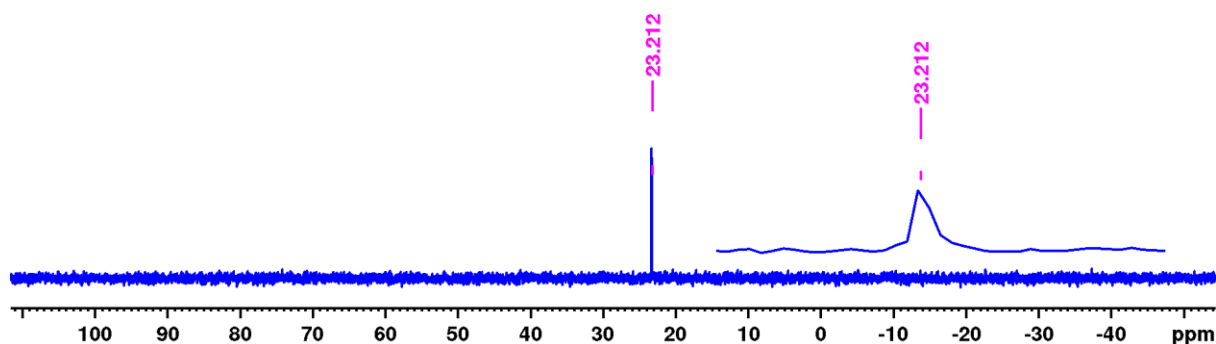
Figure 4.2: ^{31}P NMR spectrum of [Ni-((*S*,*S*)Me-FerroLANE)(phenyl)(I)] complex (**Ni-Cat.1**) in a DMSO-d$_6$.

VSK-NI-A #220 RT: 0.98 AV: 1 NL: 4.77E5
T: FTMS + p ESI Full ms [100.0000-1500.0000]

CF = C$_{28}$H$_{38}$FeINiP$_2$
MW = 678.002
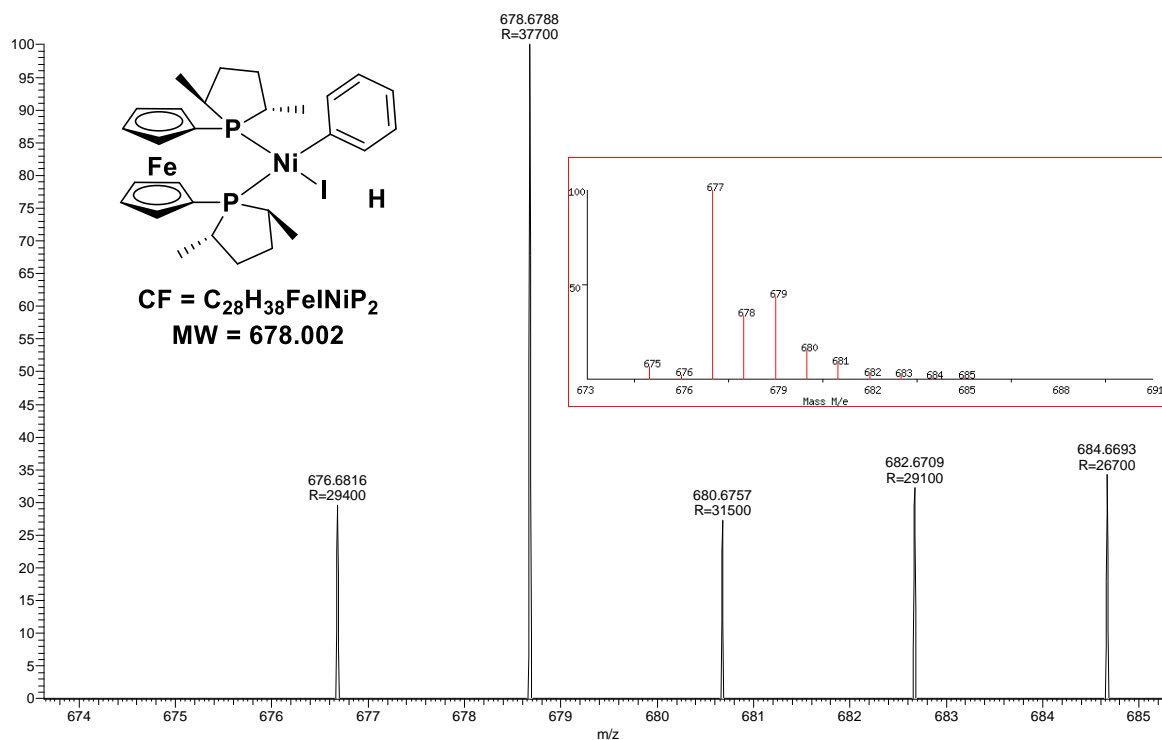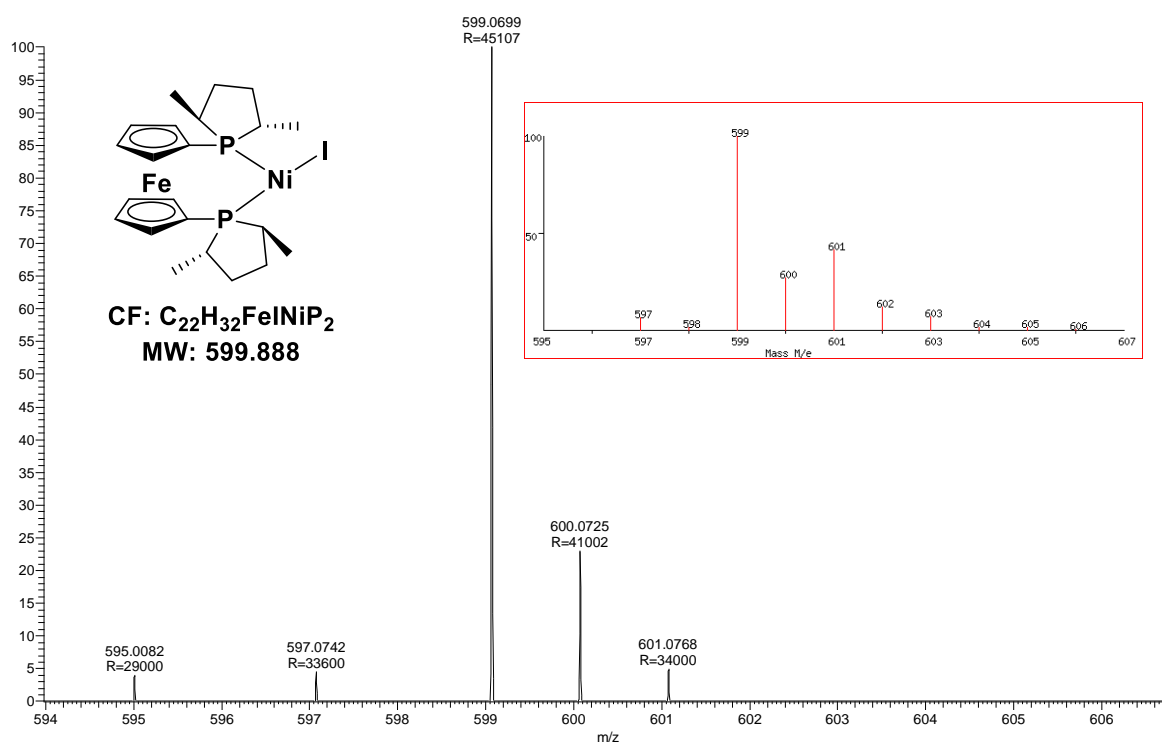
Figure 4.3: ESI-MS(+ve) spectra of [Ni-((S,S)Me-FerroLANE)(phenyl)(I)] complex (Ni-Cat.1) in a DMF.

After having established the existence of **Ni-Cat.1**; we set out to evaluate the performance of **Ni-Cat.1** in catalytic asymmetric C-P coupling (phosphination) reaction. A representation phosphination reaction leading to P-stereogenic phosphine is depicted in Scheme 4.2 and screening of reaction condition is summarized in Table 4.1.
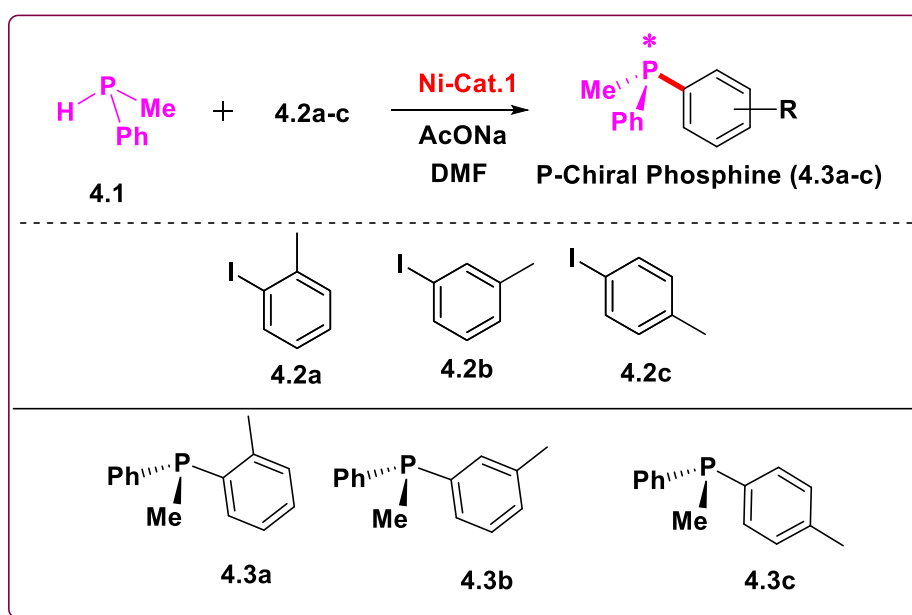
Scheme 4.2: Synthesis of P-chiral phosphine (**4.3a-c**) using a **Ni-Cat.1** catalyst.

P-chiral phosphines were synthesized from racemic methyl(phenyl)phosphine (**4.1**) with iodo-methylbenzene (**4.2a-c**) in presence of **Ni-Cat.1** with base NaOAc at different

temperatures in a DMF solvent. In our previous work, the NaOAc base and DMF solvent were found to be the best elements for P-C coupling reactions (explained in chapter 3). Therefore, we started with DMF as solvent and NaOAc as a base. In a Schlenk tube stoichiometric amount of methyl(phenyl)phosphine (**4.1**), 1-iodo-2-methylbenzene (**4.2a**), was taken and NaOAc and (5 mol %) **Ni-Cat.1** catalyst was added in a DMF (2 ml) solvent at 68 °C. The reaction was monitored by ^{31}P NMR spectroscopy. The **Ni-Cat.1** was found to be active in the asymmetric phosphination reaction and led to >99% conversion to compound **4.3a** (run 1). When the temperature of the reaction mixture was decreased to 40 °C then there was a decrease in the conversion (23% for 192 hr) of compound **4.3c** (run 2). The **Ni-Cat.1** loading was increased to 15 mol % leading to increased conversion to product **4.3c** (run 3). The **Ni-Cat.1** loading was kept constant and the reaction temperature was reduced to 0 °C, leading to reduced conversion (run 4). The scope of P-C coupling reaction was extended and synthesis of **4.3a** (28%) (run 5) and **4.3c** (31%) (run 6) was achieved.

Table 4.1: Nickel-catalyzed asymmetric phosphination.[a]

Sr. No.	Secondary phosphine	IodoAryl (4.2a-c)	Temperature (°C)	Time (hr)	Conversion (%)[b]	ee (%)[d]
1	4.1	4.2a	68	18	99	0
2	4.1	4.2a	40	192	23	0
3 [c]	4.1	4.2a	rt	192	44	0
4 [c]	4.1	4.2a	0	192	34	0
5 [c]	4.1	4.2b	0	192	28	0
6 [c]	4.1	4.2c	0	192	31	0

[a] Conditions: **Ni**-**Cat.1** = 0.005 mmol, **4.1** = 0.1 mmol, **4.2a-d** = 0.1 mmol, NaOAc = 0.1 mmol, in 2 ml DMF; [b] Determined by ^{31}P NMR; [c] **Ni-Cat. 1** = 0.015 mmol; [d] Determined by chiral HPLC after protection with sulfur.

Whereas, when we check the performance of **Ni-Cat.1** in the synthesis of P-chiral supramolecular phosphine then the **Ni-Cat. 1** yielded excellent activity (Scheme 4.3). A stoichiometric reaction between **4.1**, 1-(3-iodophenyl)urea (**4.2d**), NaOAc and **Ni-Cat.1** gives 92% ee and 40% conversion to 1-(3-(methyl(phenyl)phosphanyl)phenyl)urea (**4.3d**) (Table 2, run 1). These results indicate that **Ni-Cat.1** indeed improves the enantiomeric excess. To work on the yield, we have screened the bases. In our attempts to identify optimal organic base, triethylamine (Et$_3$N) was screened but this base affected the enantiomeric excess (0% ee) as well as conversion (4%) (Table 2, run 2). When potassium *tert*-butoxide (KO*t*Bu) was used, then there was no enantiomeric excess (0%) and 14% conversion (run 3) was oberved. Thus, a strong base such as KO*t*Bu and an organic base (Et$_3$N) reduces the enantiomeric excess as well as conversion. When the reaction was performed at room temperature with NaOAc base and

Ni-Cat.1, 43% conversion and 0% ee was observed (run 4). In our attempt to improve the conversion and enantiomeric excess phosphination was performed with 15 mol % **Ni-Cat.1** loading and the conversion was improved to 51% and with enantiomeric excess 99% (run 5).
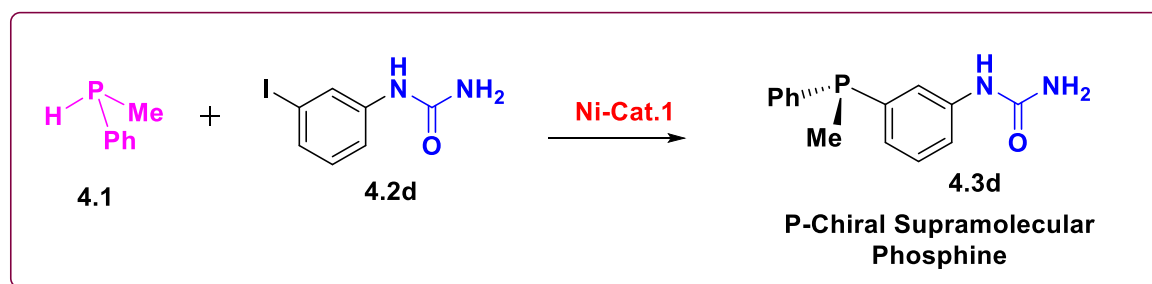
Scheme 4.3. Chiral **Ni-Cat.1** catalyzed synthesis of 1-(3-(methyl(phenyl)phosphanyl)phenyl)urea (**4.3d**).

Table 4.2: Nickel-catalyzed asymmetric phosphination.[a]

Sr. No.	Secondary phosphine	IodoAryl 4.2a-d	Ni-Cat.	Base	Temperature (ºC)	Conversion (%)[b]	ee (%)[c]
1	4.1	4.2a	Ni-Cat.1	NaOAC	-3.5	40	92
2	4.1	4.2a	Ni-Cat.1	NEt$_3$	-3.5	4	0
3	4.1	4.2a	Ni-Cat.1	KOtBu	-3.5	32	0
4	4.1	4.2a	Ni-Cat.1	NaOAC	rt	43	2
5[d]	4.1	4.2a	Ni-Cat.1	NaOAC	-3.5	51	99

[a] Conditions: **Ni-Cat.1** or **Ni-Cat.2** = 0.005 mmol, **4.1** = 0.1 mmol, **4.2a-d** = 0.1 mmol, base = 0.3 mmol; [b] Determined by ^{31}P NMR; [c] Determined by chiral HPLC after protection with sulfur; [d] **Ni-Cat. 1** = 0.015 mmol; in 2 ml DMF, 18 h.

The product 1-(3-(methyl(phenyl)phosphanyl)phenyl)urea (**4.3d**) was purified from reactions run 1-5 by column and preparative TLC but the **4.3d** was found to decompose. Finally **4.3d** was purified by HPLC as white-yellow color solid (4 mg). The proton NMR spectrum of the resultant solid revealed absence of NH$_2$ proton. Instead, unexpected peaks at 9.00 ppm and 8.26 ppm were observed which does not belong to **4.3d**. ESI-MS(+ve) of this compound revealed a molecular ion peak at m/z = 275.09 [M]$^+$ (Fig.4.5). ESI-MS report shows m/z = 275.09 Da molecular weight, which is exactly matching with the molecular weight of *N*-(3-(methyl(phenyl)phosphanyl)phenyl)formamide (**4.3d'**). The ^{1}H NMR spectrum revealed a peak at 9.00 ppm that can be assigned to aldehyde proton and 8.26 ppm peak for NH proton. The existence of compound **4.3d'** was also confirmed by chiral HPLC method. The HPLC spectrum of **4.3d** displayed retention time Rt$_1$ = 33.05 min. for one isomer and Rt$_2$ = 37.05 min. for another isomer (Fig. 4.6). We observed 1-2 min. difference when we measured **Ni-Cat.1** catalyzed compound on HPLC. The HPLC spectrum of **Ni-Cat.1** catalyzed compound displayed retaintion time Rt$_1$ = 37.24min. for one isomer and Rt$_2$ = 40.72 min.(run 5) (Fig. 4.7). It is most likely that during the catalytic reaction, the urea group decomposed to amide. This could be also one of the reasons for less conversion to the product.
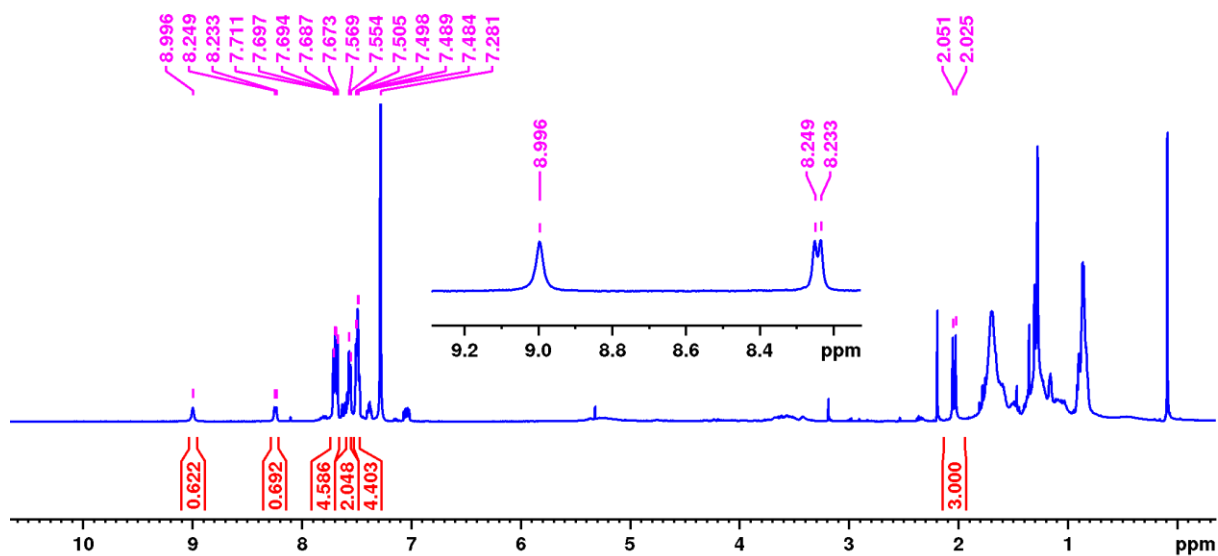
Figure 4.4: ^{1}H NMR spectrum of N-(3-(methyl(phenyl)phosphanyl)phenyl)formamide (**4.3d'**) in a CDCl$_3$.
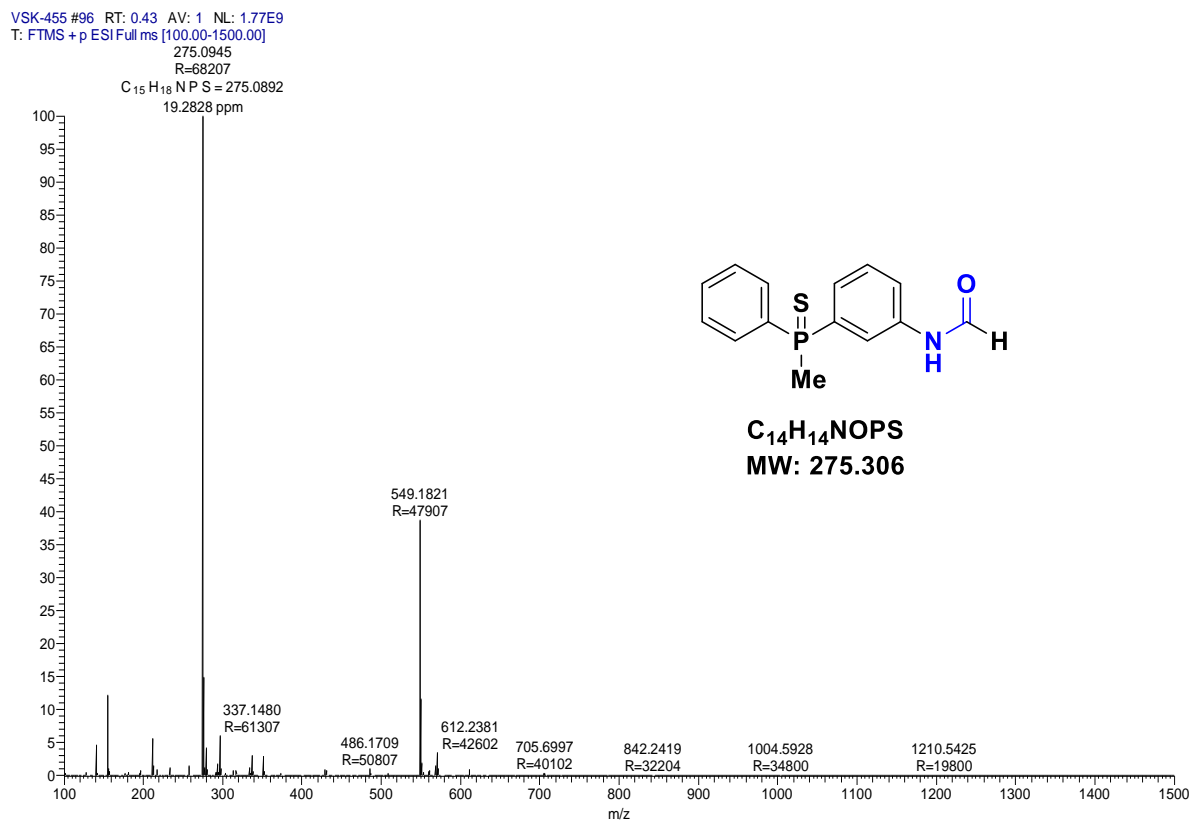
Figure 4.5: ESI-MS (+ve) spectrum of *N*-(3-(methyl(phenyl)phosphanyl)phenyl)formamide (**4.3d'**).
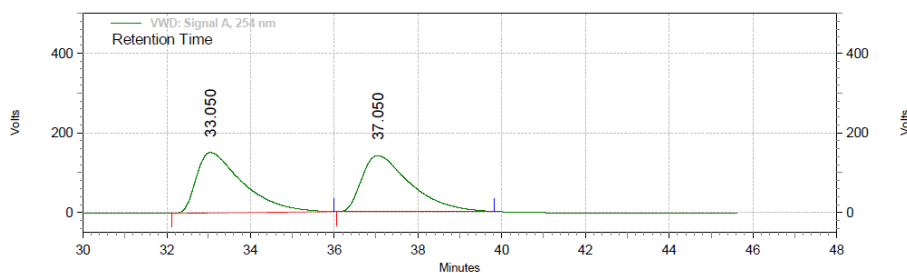
VWD: Signal A, 254 nm Results

Retention Time	Area	Area %
33.050	196419930	50.86
37.050	189797204	49.14

Totals		
	386217134	100.00

Figure 4.6: HPLC chromatogram of racemic **4.3d**.
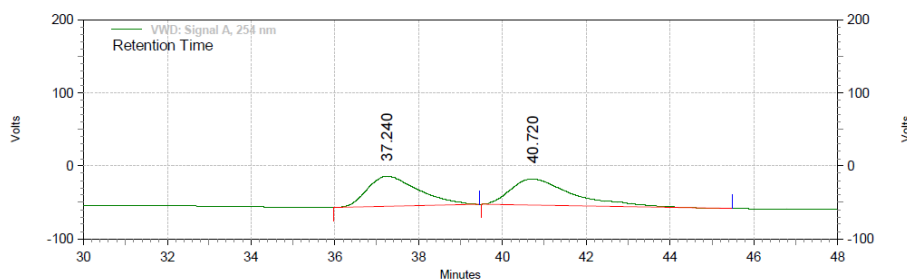
VWD: Signal A, 254 nm Results

Retention Time	Area	Area %
37.240	57667485	48.50
40.720	61228863	51.50

Totals		
	118896348	100.00

Figure 4.7: HPLC chromatogram of racemic **4.3d'**.

4.4. Conclusions

Synthesis of [Ni-((*S,S*)Me-DuPHOS)(phenyl)(I)] catalyst (**Ni-Cat.1**) and [Ni-((*S,S*)Me-FerroLANE)(phenyl)(I)] complex (**Ni-Cat.2**) from ((*S,S*)Me-DuPHOS) and (*(S)*Me-FerroLANE respectively with [Ni-(di(triphenylphosphine))(phenyl)(I)] precursor was achieved. The resultant **Ni-Cat.2** was characterized by ^{1}H, ^{13}C, ^{31}P NMR spectroscopy, and mass spectroscopy, and the identity was fully established. Indeed, the rationally designed **Ni-Cat. 2** was found to accelerate the enantiomeric excess (99%) and moderate conversion (51%) was observed. It is most likely that the electron-rich nature and wide *bite* angle offered by Me-FerroLANE is responsible for the improved performance of **Ni-Cat. 2**. The prepared **Ni-Cat. 2** was screened to optimize reaction conditions. Sodium acetate in a polar solvent (DMF) were found to be efficient.

4.5.   Experimental section

4.5.1.   General methods and materials

All manipulations were carried out under an inert atmosphere using standard Schlenk line techniques or m-Braun glove box. Solvents were dried by standard procedures unless otherwise mentioned.[26] Toluene was distilled from sodium, and THF from sodium/benzophenone under argon atmosphere. DMF was distilled on calcium-hydride tBuOK, (*S, S*)-Me-DuPHOS, sulfur powder, [Pd(dba)$_2$], were purchased from Sigma-Aldrich and 3-iodoaniline, dichlorophenylphosphine was purchased from Alfa-Aesar. All other reagents/chemicals, solvents were purchased from local suppliers (Spectrochem Pvt. Ltd.; Avra Synthesis Pvt. Ltd.; Thomas Baker Pvt. Ltd. etc). Iodophenyl urea (**4.2a**),[23] [Ni-(di(triphenylphosphine))(phenyl)(I)] complex (**3.3**),[20] Methyl(phenyl)phosphine(**3.1a**),[22] were prepared by following known procedures.

Solution NMR spectra were recorded on a Bruker Avance 400 and 500 MHz instruments at 298 K unless mentioned otherwise. Chemical shifts are referenced to external reference TMS (^{1}H and ^{13}C) or 85% H$_3$PO$_4$ ($\Xi = 40.480747$ MHz, ^{31}P). Coupling constants are given as absolute values. Multiplicities are given as follows s: singlet, d: doublet, t: triplet, m: multiplet. Mass spectra were recorded on Thermo Scientific Q-Exactive mass spectrometer, with Hypersil gold C18 column 150 x 4.6 mm diameter 8 µm particle size mobile phase used is 90% methanol + 10 % water + 0.1 % formic acid. The enantiomeric excess of the P-stereogenic phosphines was determined by chiral HPLC on an Agilent Technologies 1260 Infinity instrument with Chiralpak IF column (20 cm).

4.5.2. Synthesis of [Ni-((*S,S*)Me-FerroLANE)(phenyl)(I)] complex (Ni-Cat.1)

A solution of [Ni-(di(triphenylphosphine))(phenyl)(I)] (0.255 mmol) in toluene (20 mL) along

Ni-Cat.1
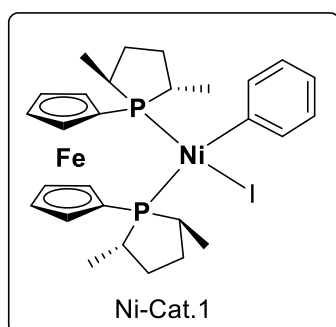
with (*S,S*)Me-FerroLANE (0.255 mmol) was stirred at room temperature and the reaction progress was monitored by ^{31}P NMR spectroscopy. The reaction was complete in 2 hours. After completion of the reaction the volatiles were evaporated to obtain dark gray solid material. The solid was washed with n-hexane (10 mL x 3 times) to yield the desired palladium complex in 65% yield (0.211 mmol).

¹H NMR (500 MHz, CD₃CN, 298 K): δ = 8.75 (s, 1H, Ar), 8.40-7.78 (m, 5H, Ar), 7.37-6.84 (m, 3H, Ar), 5.58 (s, 2H, Ar), 4.63 (s, 4H, C*H*), 3.32 (s, 5H, C*H₂* and C*H₃*), 2.66 (s, 7H, C*H₂* and C*H₃*), 1.88-0.44 (m, 8H, C*H₂* and C*H₃*). **³¹P NMR** (500 MHz, DMSO-d₆, 298 K): δ = 23.25 (s, P). **¹³C NMR** (125 MHz, DMSO-d₆, 298 K): δ = 156.4 (d, J_{C-P} = 32.8 Hz, Ar, quat), 140.7 (d, J_{C-P} = 11.7 Hz, Ar, quat), 135.2 (s, Ar, quat), 134.5 (s, Ar, *C*H), 134.3 (s, Ar, *C*H), 133.7 (s, Ar, *C*H), 132.9 (s, Ar, *C*H), 131.8 (s, Ar, *C*H), 131.2 (s, Ar, *C*H), 130.1 (s, Ar, *C*H), 129.7 (s, Ar, *C*H), 128.5 (s, Ar, *C*H), 119.2 (s, Ar, *C*H), 118.0 (s, Ar, *C*H), 116.5 (s, Ar, *C*H), 115.6 (s, Ar, *C*H), 72.1 (s, *C*H), 70.9 (s, *C*H), 31.8 (s, *C*H₂), 29.5 (s, *C*H₂), 13.9 (s, *C*H₃), 12.9 (s, *C*H₃). **ESI-MS** (+ve): (Cal. For $C_{28}H_{38}FeINiP_2$) m/z = 678.67 [M+H]⁺, 599.06 [M-Ph]⁺.

4.5.3. Synthesis of P-stereogenic supramolecular phosphines (3.5)

4.5.3.1. General procedure for phosphination reaction

A Schenk tube was loaded with catalyst **Ni-Cat.1**, iodotoluene (**4.2a-c**) or iodophenylurea (**4.2d**) racemic secondary phosphine **4.1** in a glove box. The screw-capped Schlenk tube was taken out and after the standard vacuum-argon cycle, NaOAc and 1 ml of DMF were added to the reaction mixture under positive argon flow. The reaction mixture was stirred at the appropriate temperature for desired time. The progress of the reaction was monitored by ³¹P NMR spectroscopy.

4.5.3.2. *Racemic* methyl(phenyl)(o-tolyl)phosphine sulfide (4.3a)

A 1-iodo-2-methylbenzene (**4.2a**) (0.01 mmol) was dissolved in 5 ml of THF, which was
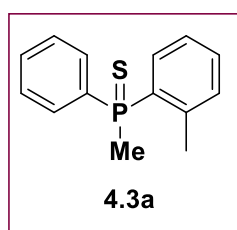
followed by addition of triethylamine (0.03 mmol) and methyl(phenyl)phosphine **4.1** (0.01 mmol). After stirring for 10 minutes, [Ni(OAc)₂] (0.5 mol %) was added and the mixture was refluxed overnight at 68 °C. After completion of the reaction, the sulfur powder was added in the reaction mixture at the same temperature and stirred it

for half an hour. Thus, above mixture was then treated with degassed water and was extracted with ethyl acetate (3 × 10 mL). The combined organic layer was dried on MgSO₄ for 2 hours and the volatiles were evaporated under reduced pressure. The crude **4.3a** was purified by silica gel column chromatography using 99: 1 mixture of petroleum ether:ethyl acetate. The desired product was isolated as a white solid in 87% yield (21 mg, 0.0085 mmol).

¹H NMR (500 MHz, CDCl₃, 298 K): δ = 7.85-7.79 (m, 3H, Ar), 7.74-7.67 (m, 2H, Ar), 7.49-7.48 (m, 4H, Ar), 7.28 (s, 2H, Ar), 2.40 (s, 3H, CH₃), 2.28 (q, J_{H-P} = 13, 9 Hz, 3H, CH₃). **³¹P**

NMR (500 MHz, CDCl$_3$, 298 K): δ = 35.15. **^{13}C NMR** (125 MHz, CDCl$_3$, 298 K): δ = 141.9 (s, Ar, quat.), 134.3 (d, $J_{C\text{-}P}$ = 37 Hz, Ar, quat), 133.5 (d, $J_{C\text{-}P}$ = 37 Hz, Ar, quat.), 131.4 (d, $J_{C\text{-}P}$ = 12.5 Hz, Ar, CH), 130.7 (s, Ar, CH), 130.7 (d, $J_{C\text{-}P}$ = 3.8 Hz, Ar, CH), 130.6 (d, $J_{C\text{-}P}$ = 3.2 Hz, Ar, CH), 130.5 (s, Ar, CH), 129.3 (d, $J_{C\text{-}P}$ = 4.9 Hz, Ar, CH), 129.2 (d, $J_{C\text{-}P}$ = 4.4 Hz, Ar, CH), 128.6 (d, $J_{C\text{-}P}$ = 4.9 Hz, Ar, CH), 128.5 (d, $J_{C\text{-}P}$ = 4.9 Hz, Ar, CH), 21.9 (d, $J_{C\text{-}P}$ = 49 Hz, CH$_3$), 21.3 (s, CH$_3$). **ESI-MS** (+ve): (Cal. For C$_{14}$H$_{15}$NaPS) m/z = 269.05 [M+ Na]$^+$.

3.5.3.3. *Chiral* methyl(phenyl)(o-tolyl)phosphine sulfide (4.3a)

A Schlenk tube was loaded with **Ni-Cat.1** (0.0005 mmol) catalyst, 1-iodo-2-methylbenzene (**4.2a**) (0.01 mmol), methyl(phenyl)phosphine (**4.1**) (0.01 mmol) in a glove box. The screw-

capped Schlenk tube was taken out and appropriate temperature was attained. After the standard vacuum-argon cycle NaOAc (0.03 mmol), 1 ml of DMF was added to the reaction mixture. The progress of the reaction was monitored by ^{31}P NMR spectroscopy. After completion of the reaction, the sulfur powder was added in the reaction mixture at the same temperature and it was stirred for half an hour. The content was treated with degassed water (which was pre-cooled at an appropriate temperature) and extracted with ethyl acetate (10 mL × 3) (which was pre-cooled at an appropriate temperature). The combined organic layer was dried on MgSO$_4$ for half hour at a suitable temperature and the volatiles were evaporated under reduced pressure. The crude mixture was dissolved in DCM and filtered over a plug of silica. The plug was washed with DCM until the impurities were eluted, and then the expected product was pushed through with ethyl acetate. After evaporation of the solvent, the product was obtained as a pale yellow solid **4.3a** which was analyzed by a combination of spectroscopic and analytical tools.

4.5.3.4. *Racemic* methyl(phenyl)(*m*-tolyl)phosphine sulfide (4.3b)
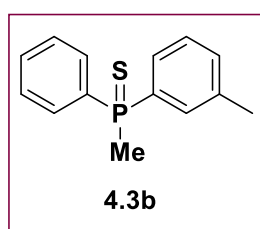
A 1-iodo-3-methylbenzene (**4.2b**) (0.01 mmol) was dissolved in 5 ml of THF, which was followed by addition of triethylamine (0.03 mmol) and methyl(phenyl)phosphine **4.1** (0.01 mmol). After stirring for 10 minutes, [Ni(OAc)$_2$] (0.5 mol %) was added and the mixture was refluxed overnight at 68 °C. After completion of the reaction, the

sulfur powder was added in the reaction mixture at the same temperature and it was stirred for half an hour. Thus, above mixture was then treated with degassed water and was extracted with

ethyl acetate (3×10 mL). The combined organic layer was dried on $MgSO_4$ for 2 hours and the volatiles were evaporated under reduced pressure. The crude **4.3b** was purified by silica gel column chromatography using 98: 2 mixture of petroleum ether:ethyl acetate. The desired product was isolated as a white solid in 83% yield (20 mg, 0.008 mmol).

^{1}H NMR (500 MHz, CDCl$_3$, 298 K): δ = 7.82 (q, J_{H-P} =13.15, 7.6 Hz, 2H, Ar), 7.68 (d, J_{H-P} =14.2 Hz, 1H, Ar), 7.52-7.46 (m, 5H, Ar), 7.34-7.32 (m, 2H, Ar), 2.37 (d, J_{H-P} = 9.3 Hz, 3H, CH$_3$), 2.27 (q, J_{H-P} = 13.16, 4.8 Hz, 3H, CH$_3$). **^{31}P NMR** (500 MHz, CDCl$_3$, 298 K): δ = 35.83. **^{13}C NMR** (125 MHz, CDCl$_3$, 298 K): δ = 138.5 (d, J_{C-P} = 12.0 Hz, Ar, quat), 134.1 (d, J_{C-P} = 42.1 Hz, Ar, quat.), 134.3 (d, J_{C-P} = 42.7 Hz, Ar, quat.), 133.7 (q, J_{C-P} = 92.0, 3.9 Hz, Ar, *C*H), 131.6 (d, J_{C-P} = 91.8 Hz, Ar, *C*H), 131.3 (d, J_{C-P} = 2.8 Hz, Ar, *C*H), 130.6 (d, J_{C-P} = 10.0 Hz, Ar, *C*H), 128.5 (d, J_{C-P} =12.4 Hz, Ar, *C*H), 128.4 (t, J_{C-P} = 13.0 Hz, Ar, *C*H), 127.9 (d, J_{C-P} = 77.5 Hz, Ar, *C*H), 127.6 (s, Ar, *C*H), 21.6 (d, J_{C-P} = 59.4 Hz, CH$_3$), 21.3 (s, *C*H$_3$). **ESI-MS** (+ve): (Cal. For C$_{14}$H$_{15}$PS) m/z = 247.07 [M+ H]$^+$.

3.5.3.5. *Chiral* methyl(phenyl)(*m*-tolyl)phosphine sulfide (4.3b)

A Schlenk tube was loaded with catalyst **Ni-Cat.1** (0.0005 mmol), 1-iodo-3-methylbenzene (**4.2b**) (0.01 mmol) and methyl(phenyl)phosphine (**4.1**) (0.01 mmol) in a glove box. The screw-capped Schlenk tube was taken out and the appropriate temperature was attained. After the standard vacuum-argon cycle NaOAc (0.03 mmol) and 1 ml of DMF were added to the reaction mixture. The progress of the reaction was monitored by ^{31}P NMR spectroscopy. After completion of the reaction, the sulfur powder was added in the reaction mixture at the same temperature and it was stirred for half an hour. The content was treated with degassed water (which was pre-cooled at an appropriate temperature) and extracted with ethyl acetate (10 mL $\times$ 3) (which was pre-cooled at an appropriate temperature). The combined organic layer was dried on $MgSO_4$ for half hour at a suitable temperature and the volatiles were evaporated under reduced pressure. The crude mixture was dissolved in DCM and filtered over a plug of silica. The plug was washed with DCM until the impurities were eluted, and then the expected product was pushed through with ethyl acetate. After evaporation of the solvent, the product was obtained as a pale yellow solid **4.3b** which was analyzed by a combination of spectroscopic and analytical tools.

^{31}P NMR (500 MHz, CDCl$_3$, 298 K) δ = 35.83.

4.5.3.6. *Racemic* methyl(phenyl)(*p*-tolyl)phosphine sulfide (4.3c)

A 1-iodo-4-methylbenzene (**4.2c**) (0.01 mmol) was dissolved in 5 ml of THF, which was followed by addition of triethylamine (0.03 mmol) and methyl(phenyl)phosphine **4.1** (0.01 mmol). After stirring for 10 minutes, [Ni(OAc)$_2$] (0.5 mol %) was added and the mixture was refluxed overnight at 68 °C. After completion of the reaction, the sulfur powder was added i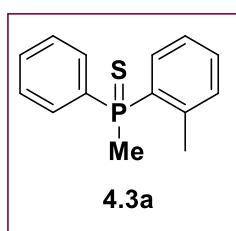n the reaction mixture at the same temperature and stirred for half an hour. The above mixture was then treated with degassed water and was extracted with ethyl acetate (3 × 10 mL). The combined organic layer was dried on MgSO$_4$ for 2 hours and the volatiles were evaporated under reduced pressure. The crude **4.3c** was purified by silica gel column chromatography using 99: 1 mixture of petroleum ether: ethyl acetate. The desired product was isolated as a white solid in 75% yield (18 mg, 0.07 mmol).
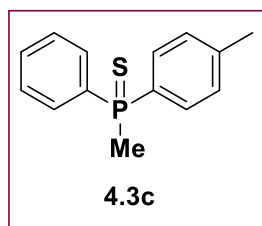
^{1}H NMR (500 MHz, CDCl$_3$, 298 K): δ = 7.85-7.79 (m, 3H, Ar), 7.72-7.69 (m, 1H, Ar), 7.48 (d, J_{H-P} = 2.2 Hz, 2H, Ar), 7.47 (d, J_{H-P} = 7.5 Hz, 2H, Ar), 7.27 (s, 1H, Ar), 2.40 (s, 3H, CH$_3$). 2.27 (q, J_{H-P} = 13.1, 9.1 Hz, 3H, CH$_3$). **^{31}P NMR** (500 MHz, CDCl$_3$, 298 K): δ = 35.51. **^{13}C NMR** (125 MHz, CDCl$_3$, 298 K): δ = 141.9 (d, J_{C-P} = 15.13 Hz, Ar, quat), 134.0 (q, J_{C-P} = 82.5, 37.5 Hz, Ar, quat.), 131.3 (d, J_{C-P} = 2.5 Hz, Ar, *C*H), 131.2 (d, J_{C-P} = 2.5 Hz, Ar, *C*H), 130.6 (dt, J_{C-P} = 24.7, 10.5 Hz, Ar, *C*H), 129.9 (s, Ar, quat.), 129.3 (d, J_{C-P} = 5 Hz, Ar, *C*H), 129.2 (d, J_{C-P} = 5 Hz, Ar, *C*H), 128.6 (d, J_{C-P} = 4.6 Hz, Ar, *C*H), 128.4 (d, J_{C-P} = 4.6 Hz, Ar, *C*H), 21.6 (d, J_{C-P} = 59 Hz, *C*H$_3$), 21.3 (s, *C*H$_3$). **ESI-MS** (+ve): (Cal. For C$_{14}$H$_{15}$NaPS) m/z = 269.05 [M+ Na]$^+$.

### 3.5.3.7. *Chiral* methyl(phenyl)(*p*-tolyl)phosphine sulfide (4.3c)

A Schlenk tube was loaded with catalyst **Ni-Cat.1** (0.0005 mmol), 1-iodo-4-methylbenzene (**4.2c**) (0.01 mmol) and methyl(phenyl)phosphine (**4.1**) (0.01 mmol) in a glove box. The screw-capped Schlenk tube was taken out and the appropriate temperature was attained. After the standard vacuum-argon cycle NaOAc (0.03 mmol) and 1 ml of DMF were added to the reaction mixture. The progress of the reaction was monitored by ^{31}P NMR spectroscopy. After completion of the reaction, the sulfur powder was added in the reaction mixture at the same temperature and it was stirred for half an hour. The content was treated with degassed water (which was pre-cooled at an appropriate temperature) and extracted with ethyl acetate (10 mL × 3) (which was pre-cooled at an appropriate temperature). The combined organic layer was

dried on MgSO$_4$ for half hour at a suitable temperature and the volatiles were evaporated under reduced pressure. The crude mixture was dissolved in DCM and filtered over a plug of silica. The plug was washed with DCM until the impurities were eluted, and then the expected product was pushed through with ethyl acetate. After evaporation of the solvent, the product was obtained as a pale yellow solid **4.3c** which was analyzed by a combination of spectroscopic and analytical tools.

^{31}P NMR (500 MHz, CDCl$_3$, 298 K) δ = 35.51.

4.5.3.8. *Racemic N-(3-(methyl(phenyl)phosphanyl)phenyl)formamide (4.3d')*

A Schlenk tube was loaded with catalyst **Ni-Cat.1** (0.15 mmol), 3-iodophenylurea (**4.2d**) (0.2 mmol), methyl(phenyl)phosphine (**4.1**) (0.2 mmol) in a glove box. The screw-capped Schlenk
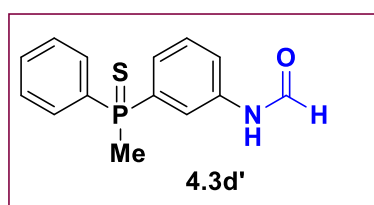
tube was taken out and the room temperature was attained. After the standard vacuum-argon cycle NaOAc (0.6 mmol) and 1 ml of DMF were added to the reaction mixture. The progress of the reaction was monitored by ^{31}P NMR spectroscopy. After completion of the reaction, the sulfur powder was added in the reaction mixture at the same temperature and it was stirred for half an hour. The content was treated with degassed water (which was pre-cooled at an appropriate temperature) and extracted with ethyl acetate (10 mL × 3) (which was pre-cooled at an appropriate temperature). The combined organic layer was dried on MgSO$_4$ for half hour at a suitable temperature and the volatiles were evaporated under reduced pressure. The crude mixture was dissolved in DCM and filtered over a plug of silica. The plug was washed with DCM until the impurities were eluted, and then the expected product was pushed through with ethyl acetate. After evaporation of the solvent, the product was obtained as a pale yellow solid. The solid compound was dissolved in 1 ml of 2-isopropanol and injected in chiral HPLC. The HPLC eluted fraction was 10-12 times in one flask. After evaporation of the solvent, the product was obtained as a pale yellow solid **4.3d'** with (6 mg), 11% yield which was analyzed by a combination of spectroscopic and analytical tools.

^{1}H NMR (500 MHz, CDCl$_3$, 298 K): δ = 9.00 (s, 1H, CHO), 8.24 (d, J_{H-P} = 7.8 Hz, 1H, N*H*), 7.71-7.67 (m, 4H, Ar), 7.56-7.55 (m, 2H, Ar), 7.50-7.48 (m, 4H, Ar), 2.03 (d, J_{H-P} =13.10 Hz, 3H, CH$_3$). **^{31}P NMR** (500 MHz, CDCl$_3$, 298 K): δ = 33.42 (s), 29.18 (s). **ESI-MS** (+ve): (Cal. For C$_{14}$H$_{14}$NOPS) m/z = 275.09 [M]$^+$

3.5.3.9. *Chiral N-(3-(methyl(phenyl)phosphanyl)phenyl)formamide (4.3d')*

A Schlenk tube was loaded with catalyst **Ni-Cat.1** (0.0075 mmol), 3-iodophenylurea (**4.2d**) (0.05 mmol) and methyl(phenyl)phosphine (**4.1**) (0.05 mmol) in a glove box. The screw-capped

4.5d'
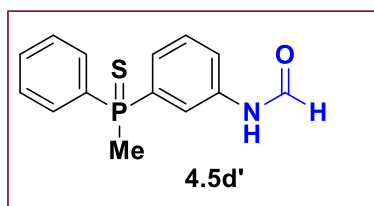
Schlenk tube was taken out and -3.5 °C temperature was attained. After the standard vacuum-argon cycle NaOAc (0.15 mmol) and 1 ml of DMF were added to the reaction mixture. The progress of the reaction was monitored by ^{31}P NMR

spectroscopy. After completion of the reaction, the sulfur powder was added in the reaction mixture at the same temperature and it was stirred for half an hour. The content was treated with degassed water (which was pre-cooled at an appropriate temperature) and extracted with ethyl acetate (10 mL × 3) (which was pre-cooled at an appropriate temperature). The combined organic layer was dried on $MgSO_4$ for half hour at a suitable temperature and the volatiles were evaporated under reduced pressure. The crude mixture was dissolved in DCM and filtered over a plug of silica. The plug was washed with DCM until the impurities were eluted, and then the expected product was pushed through with ethyl acetate. After evaporation of the solvent, the product was obtained as a pale yellow solid. The solid compound was dissolved in 1 ml of 2-isopropanol solvent and injected in chiral HPLC. The HPLC eluted fraction was collected for 10-12 times in one flask. After evaporation of the solvent, the product was obtained as a pale yellow solid **4.3d'** with (4 mg), 29% yield which was analyzed by a combination of spectroscopic and analytical tools.

^{31}**P NMR** (500 MHz, CDCl$_3$, 298 K) δ = 37.34 (s). **HPLC:** Daicel Chiralpak-IF, 1 mL/min, 10:90 (2-PrOH:Hexane), Rt_1 = 37.02 min; Rt_2 = 40.72 min. ee = 92%.

VWD: Signal A, 254 nm Results

Retention Time	Area	Area %
37.240	57667485	48.50
40.720	61228863	51.50
Totals	118896348	100.00
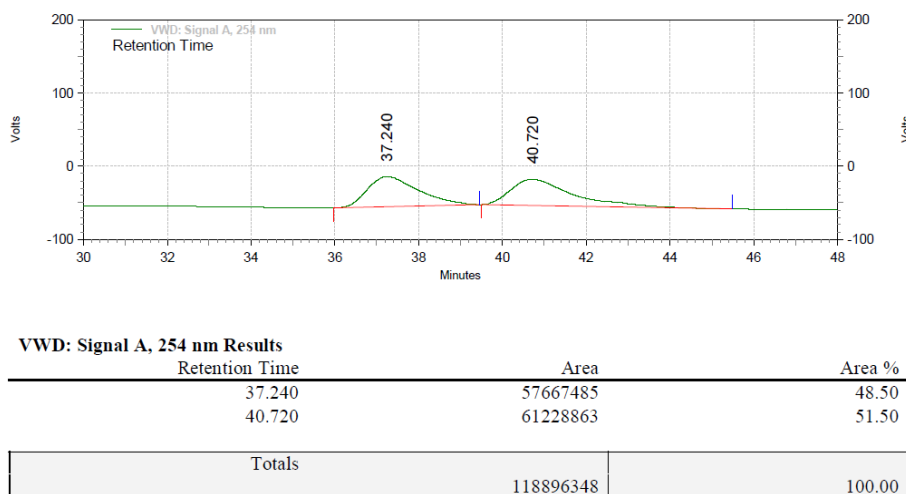
Figure 4.8: Racemic HPLC spectrum of Ni-catalyzed synthesis of racemic **4.3d'** compound.
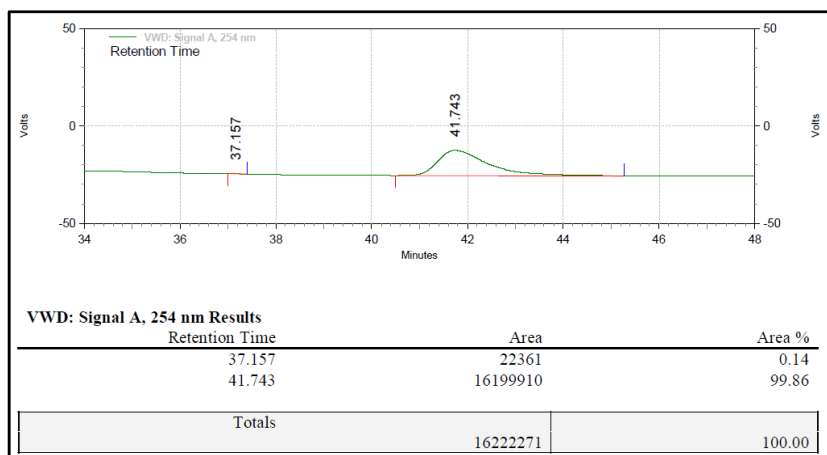
Figure 4.9: Chiral HPLC spectrum of Ni-catalyzed synthesis of chiral **4.3d'** compound.

4.6. Characterization of compounds
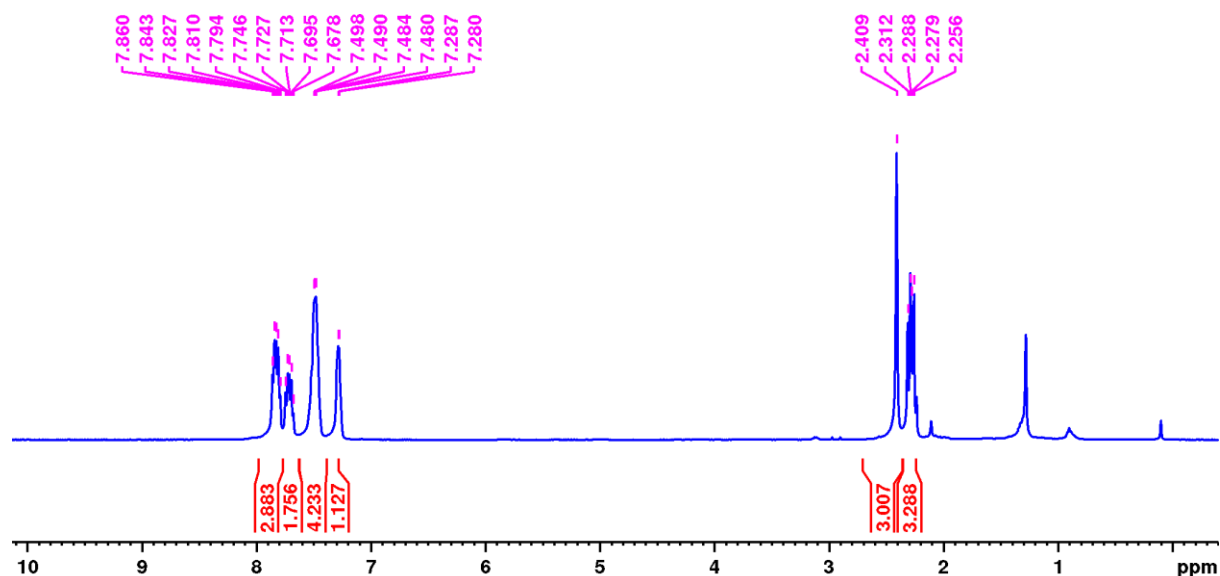
Figure 4.10: ^{1}H NMR spectrum of methyl(phenyl)(*o*-tolyl)phosphine sulfide (**4.3a**) in a CDCl$_3$.
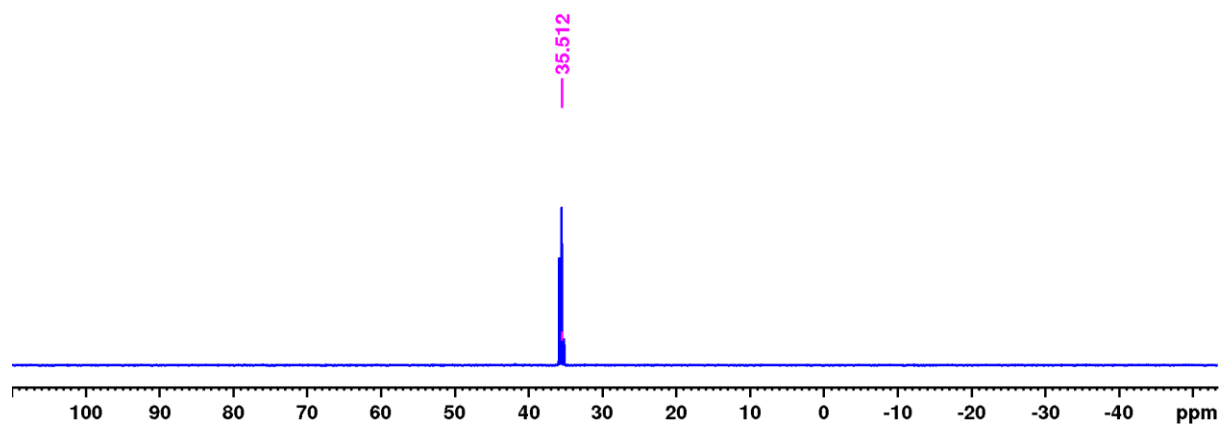
Figure 4.11: ^{31}P NMR spectrum of methyl(phenyl)(*o*-tolyl)phosphine sulfide (**4.3a**) in a CDCl$_3$.
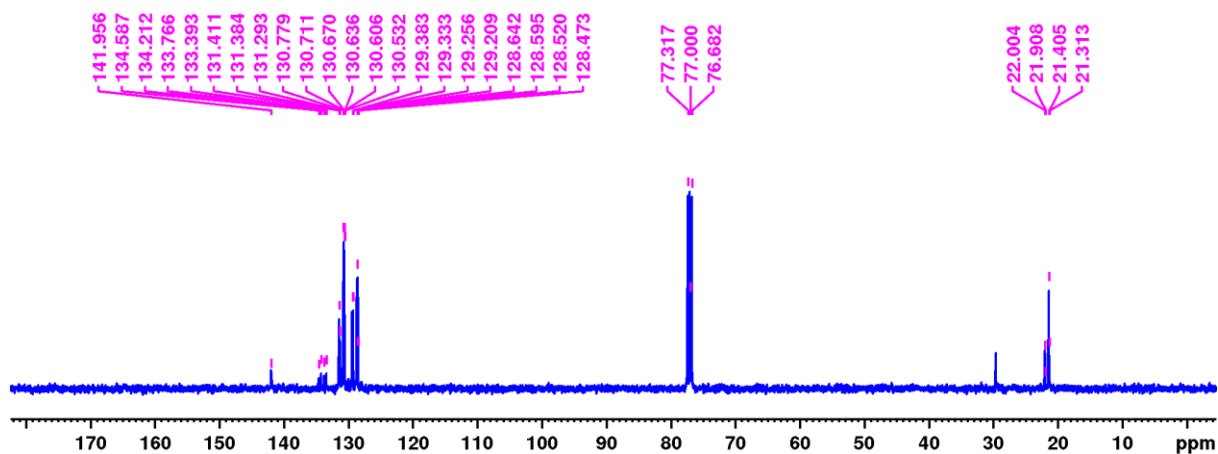
Figure 4.12: ^{13}C NMR spectrum of methyl(phenyl)(*o*-tolyl)phosphine sulfide (**4.3a**) in a CDCl$_3$.
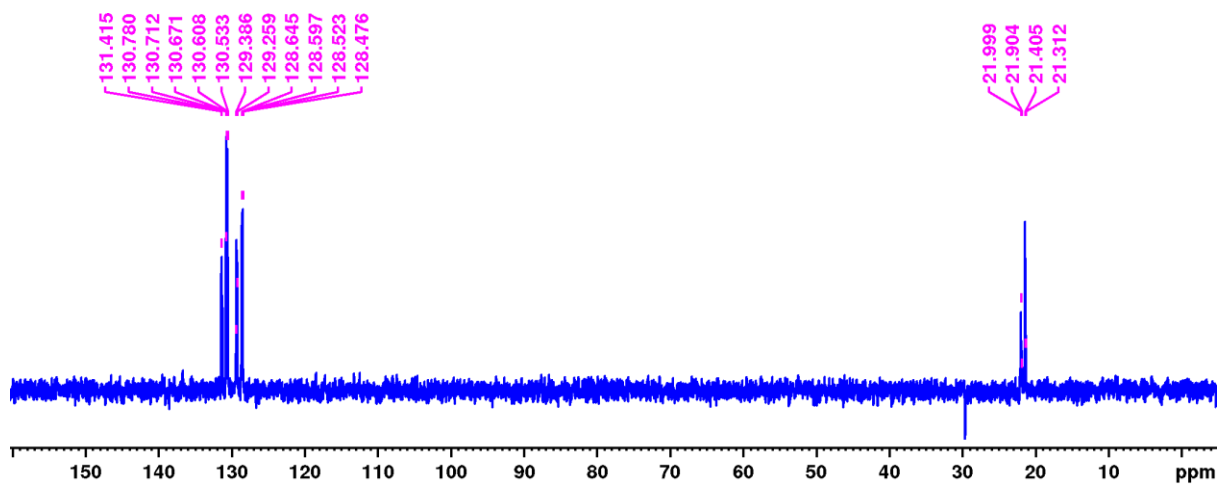
Figure 4.13: ^{13}C (DEPT) NMR spectrum of methyl(phenyl)(*o*-tolyl)phosphine sulfide (**4.3a**) in a CDCl$_3$.
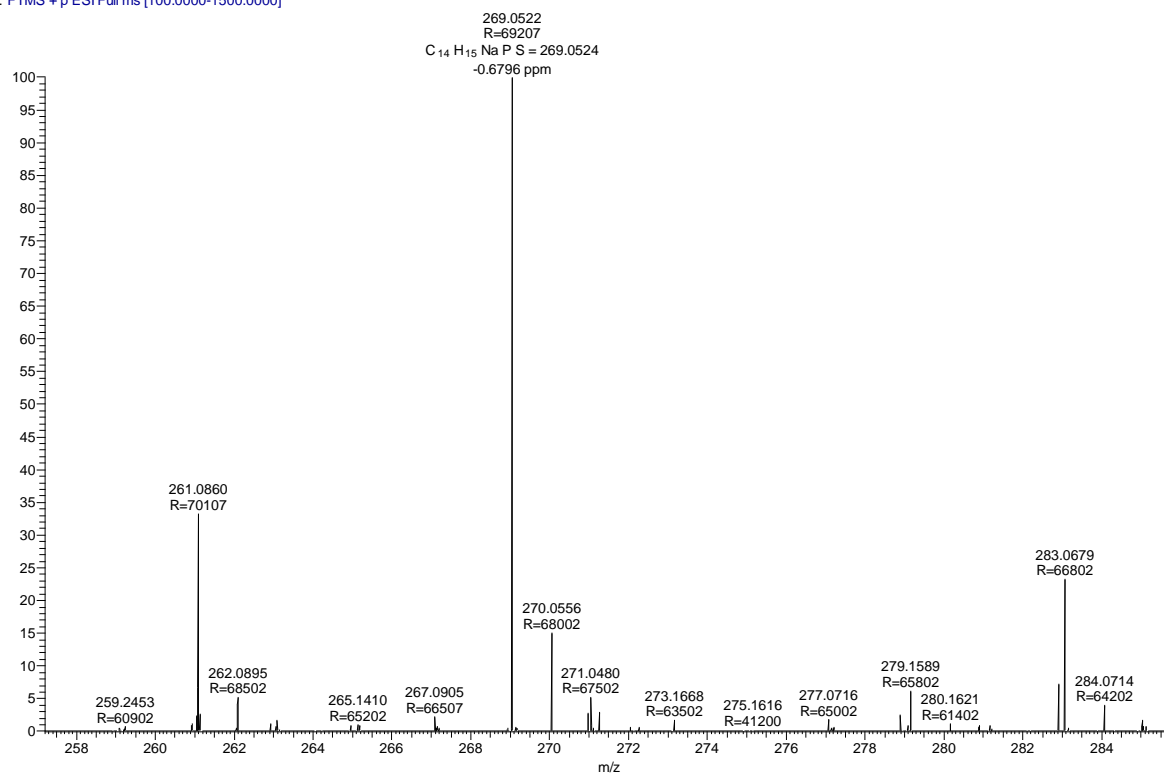
Figure 4.14: ESI-MS(+ve) spectrum of methyl(phenyl)(*o*-tolyl)phosphine sulfide (**4.3a**) in a methanol.
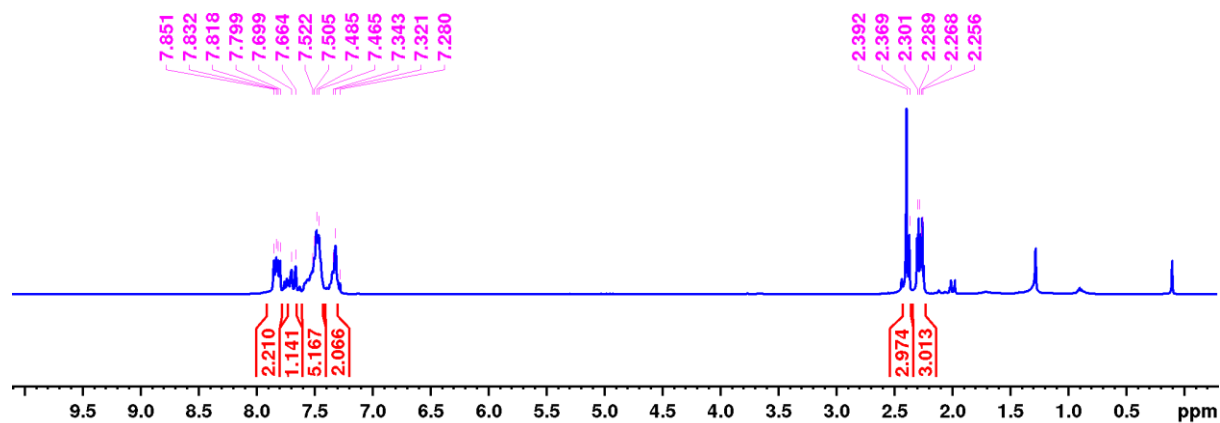
Figure 4.15: ¹H NMR spectrum of methyl(phenyl)(*m*-tolyl)phosphine sulfide (**4.3b**) in a CDCl₃.
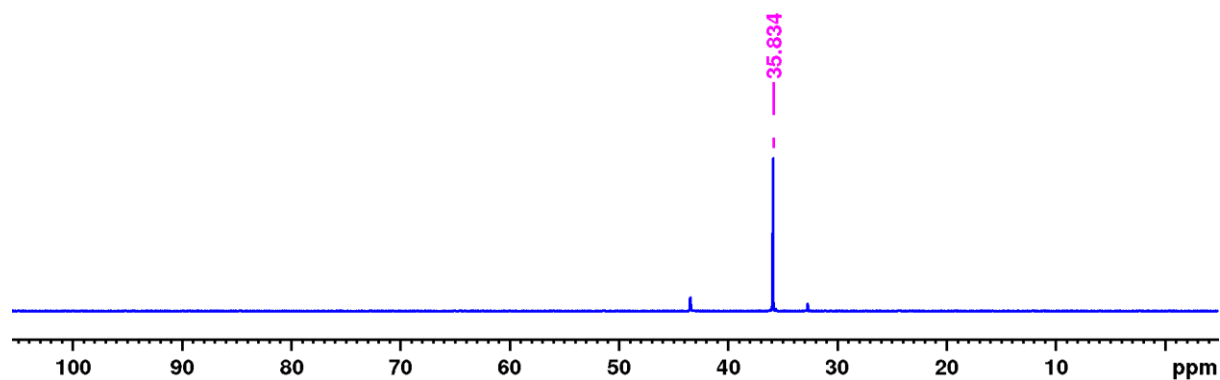
Figure 4.16: ³¹P NMR spectrum of methyl(phenyl)(m-tolyl)phosphine sulfide (**4.3b**) in a CDCl₃.
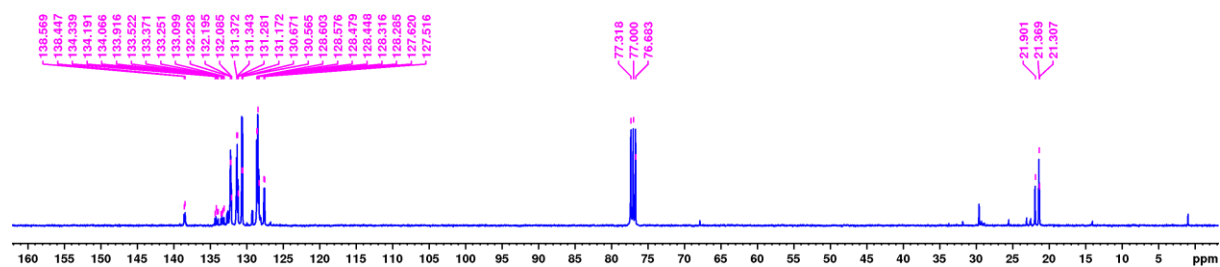
Figure 4.17: ¹³C NMR spectrum of methyl(phenyl)(*m*-tolyl)phosphine sulfide (**4.3b**) in a CDCl₃.
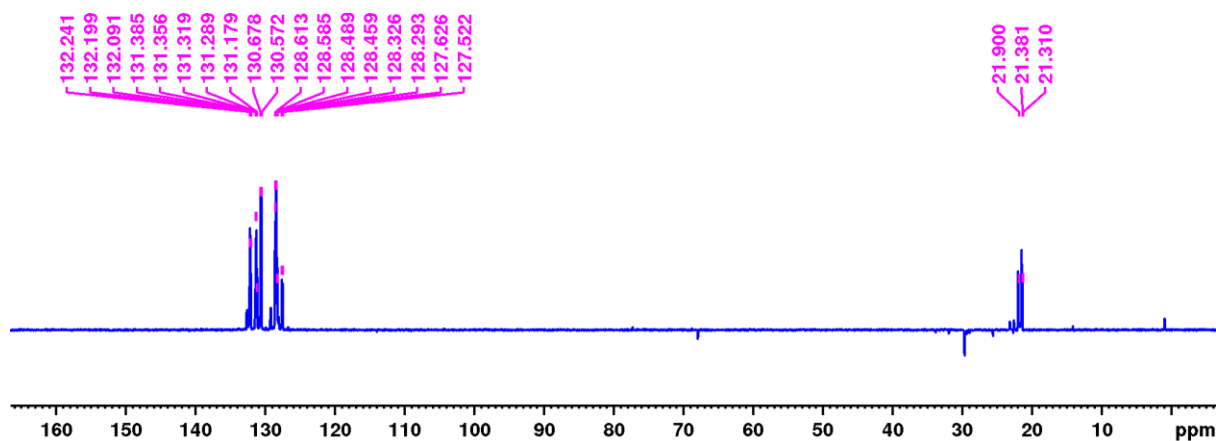
Figure 4.18: ^{13}C (DEPT) NMR spectrum of methyl(phenyl)(*m*-tolyl)phosphine sulfide (**4.3b**) in a CDCl$_3$.

VSK-16_180205155818 #280 RT: 1.25 AV: 1 NL: 4.57E7
T: FTMS + p ESI Full ms [100.0000-1500.0000]

247.0703
R=73007
C $_{14}$ H $_{16}$ P S = 247.0705
-0.8188 ppm
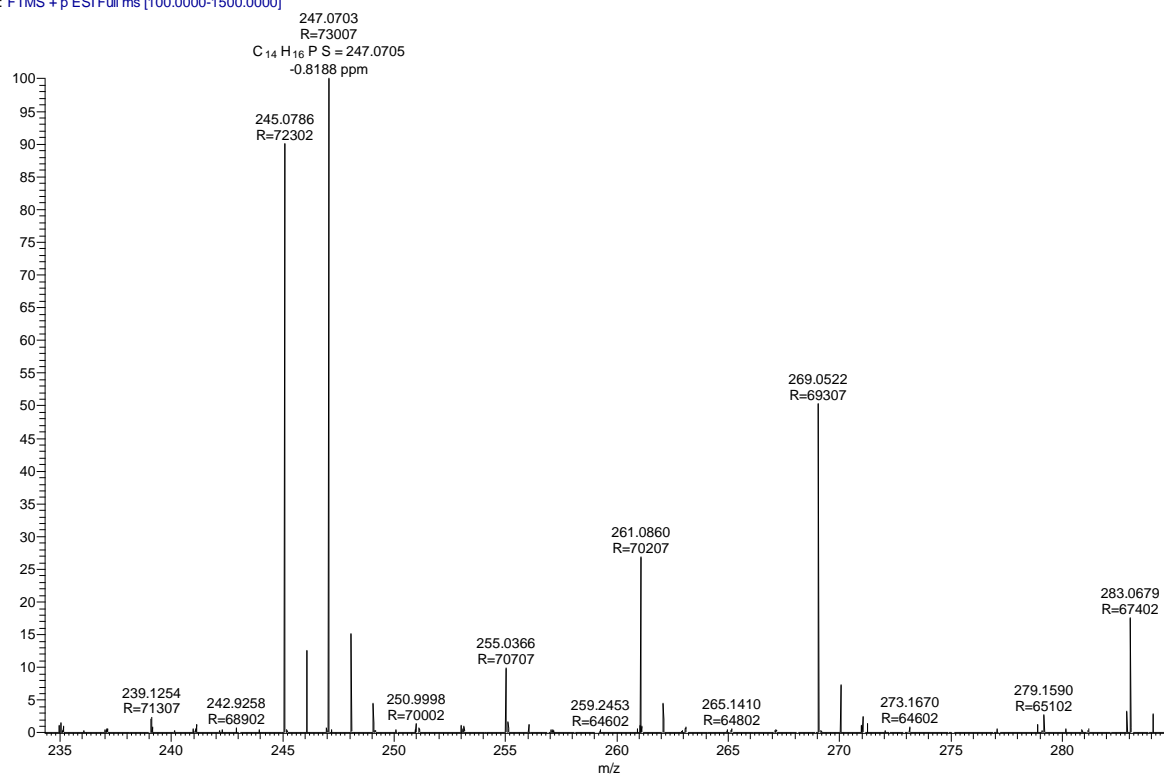
Figure 4.19: ESI-MS(+ve) spectrum of methyl(phenyl)(*m*-tolyl)phosphine sulfide (**4.3b**) in a methanol.
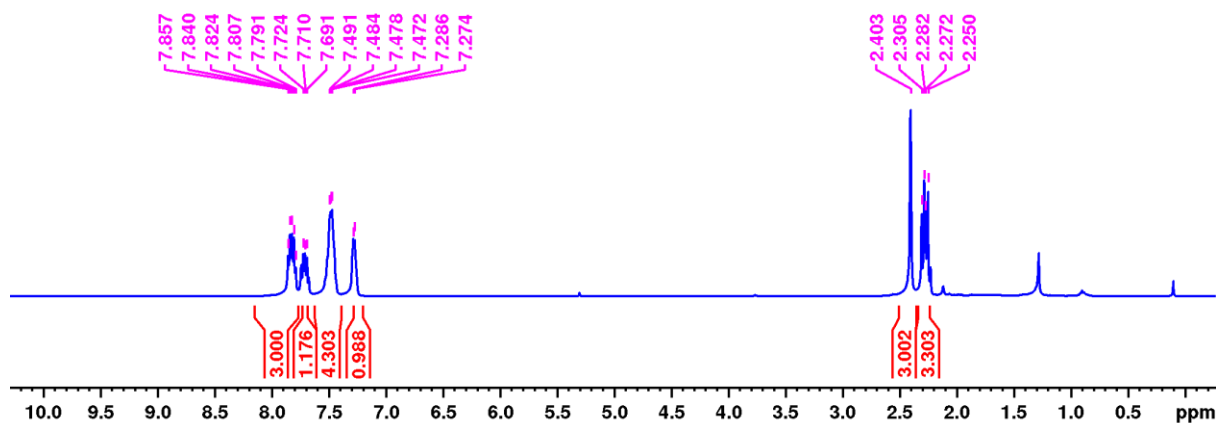
Figure 4.20: ^{1}H NMR spectrum of methyl(phenyl)(*p*-tolyl)phosphine sulfide (**4.3c**) in a CDCl$_3$.
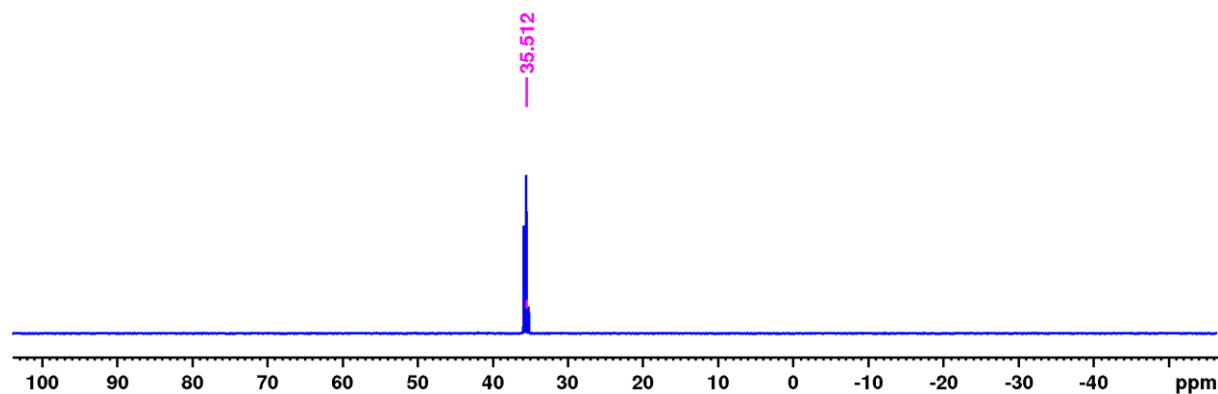
Figure 4.21: ^{31}P NMR spectrum of methyl(phenyl)(*p*-tolyl)phosphine sulfide (**4.3c**) in a CDCl$_3$.
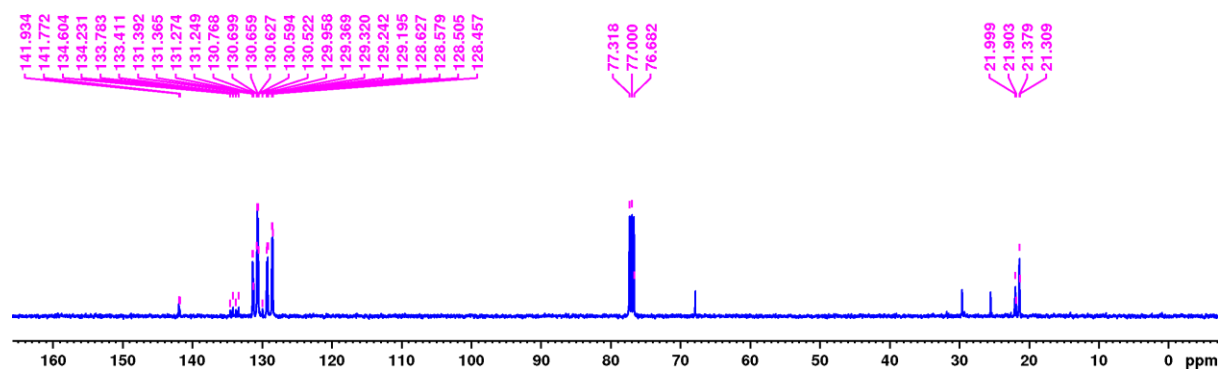
Figure 4.22: ^{13}C NMR spectrum of methyl(phenyl)(*p*-tolyl)phosphine sulfide (**4.3c**) in a CDCl$_3$.
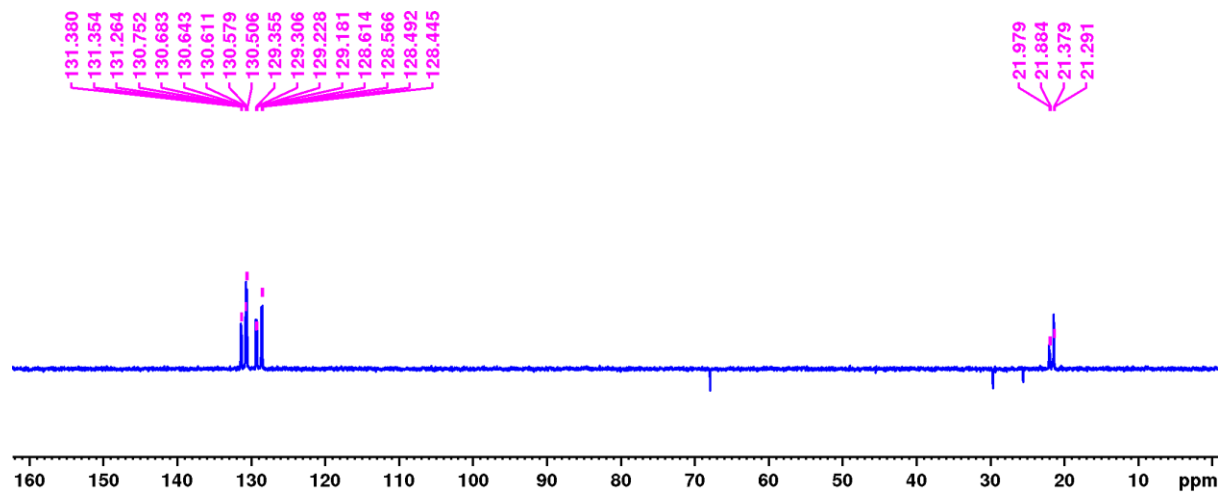
Figure 4.23: ^{13}C (DEPT) NMR spectrum of methyl(phenyl)(*p*-tolyl)phosphine sulfide (**4.3c**) in a CDCl$_3$.
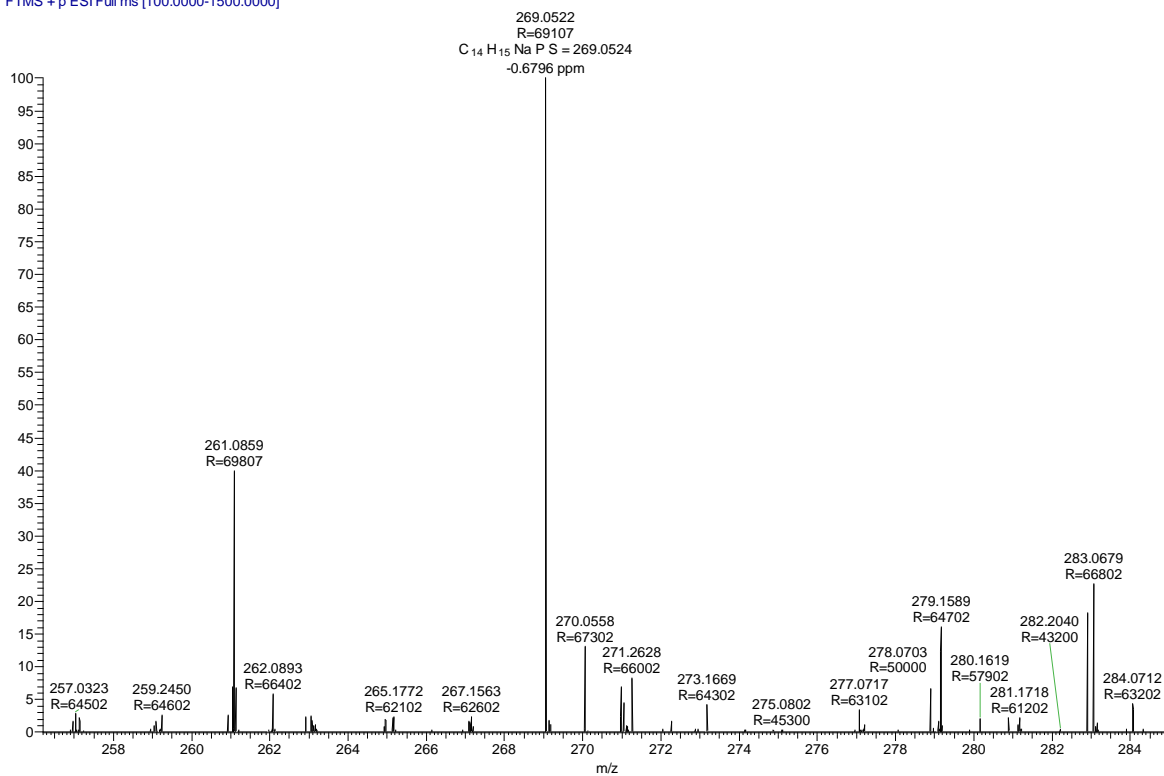
Figure 4.24: ESI-MS(+ve) spectrum of methyl(phenyl)(*p*-tolyl)phosphine sulfide (**4.3c**) in a methanol.
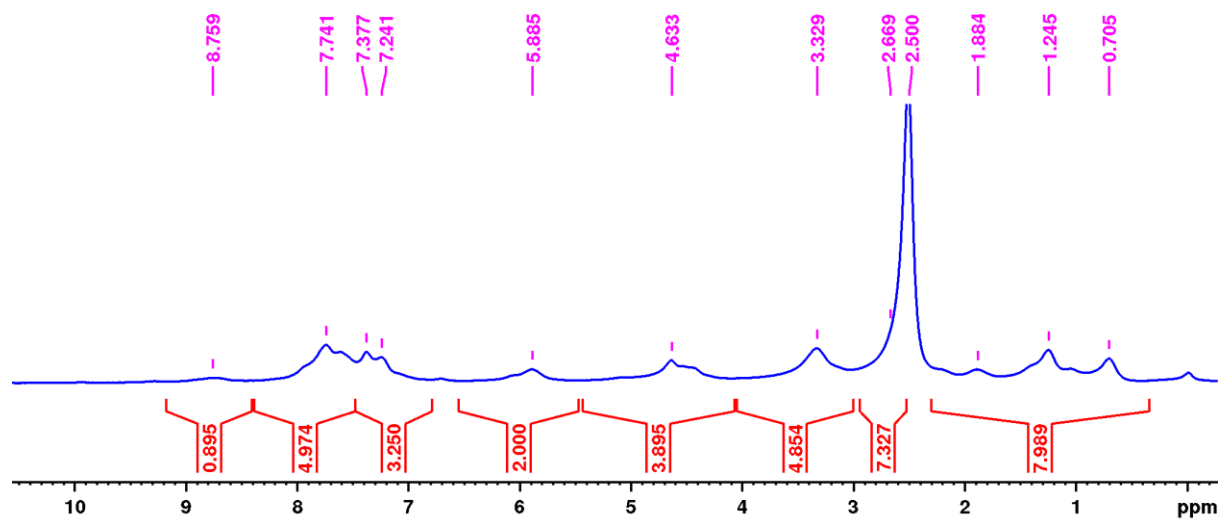
Figure 4.25: ¹H NMR spectrum of [Ni-((*S*,*S*)Me-FerroLANE)(phenyl)(I)] complex (**Ni-Cat.1**) in a DMSO-d₆.
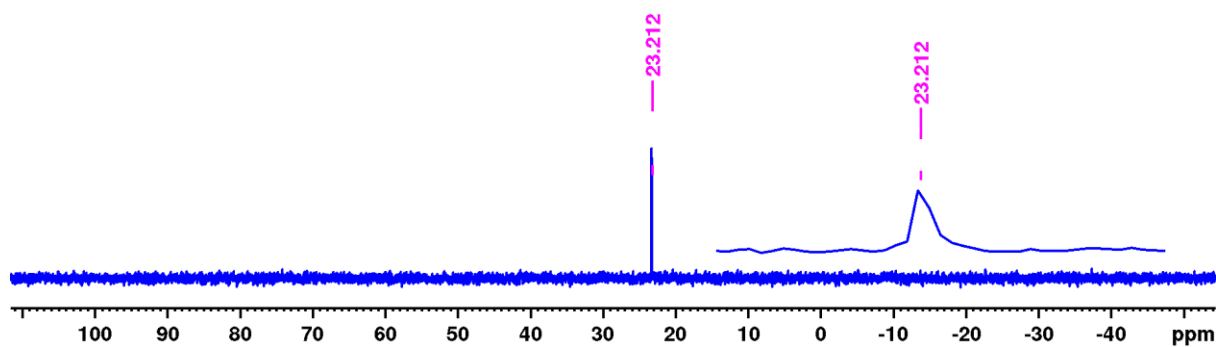
Figure 4.26: ^{31}P NMR spectrum of [Ni-((S,S)Me-FerroLANE)(phenyl)(I)] complex (**Ni-Cat.1**) in a DMSO-d$_6$.
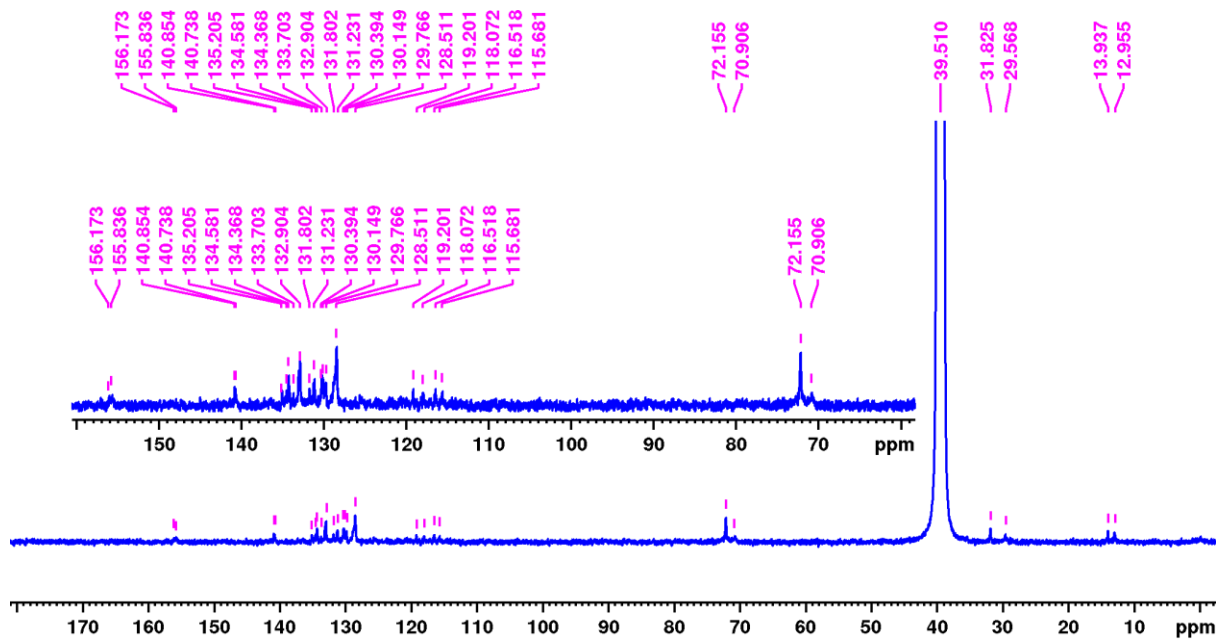
Figure 4.27: ^{13}C NMR spectrum of [Ni-((S,S)Me-FerroLANE)(phenyl)(I)] complex (**Ni-Cat.1**) in a DMSO-d$_6$.
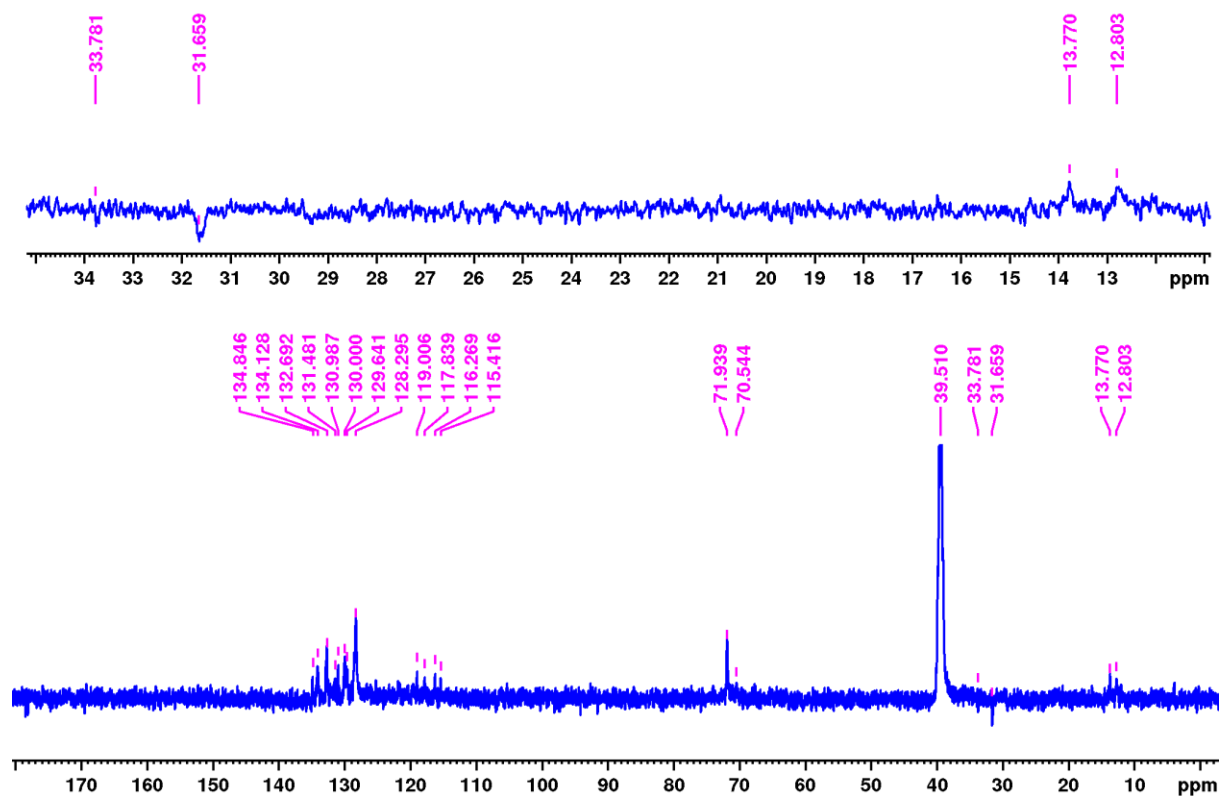
Figure 4.28: ^{13}C (DEPT) NMR spectrum of [Ni-((*S*,*S*)Me-FerroLANE)(phenyl)(I)] complex (**Ni-Cat.1**) in a DMSO-d$_6$.
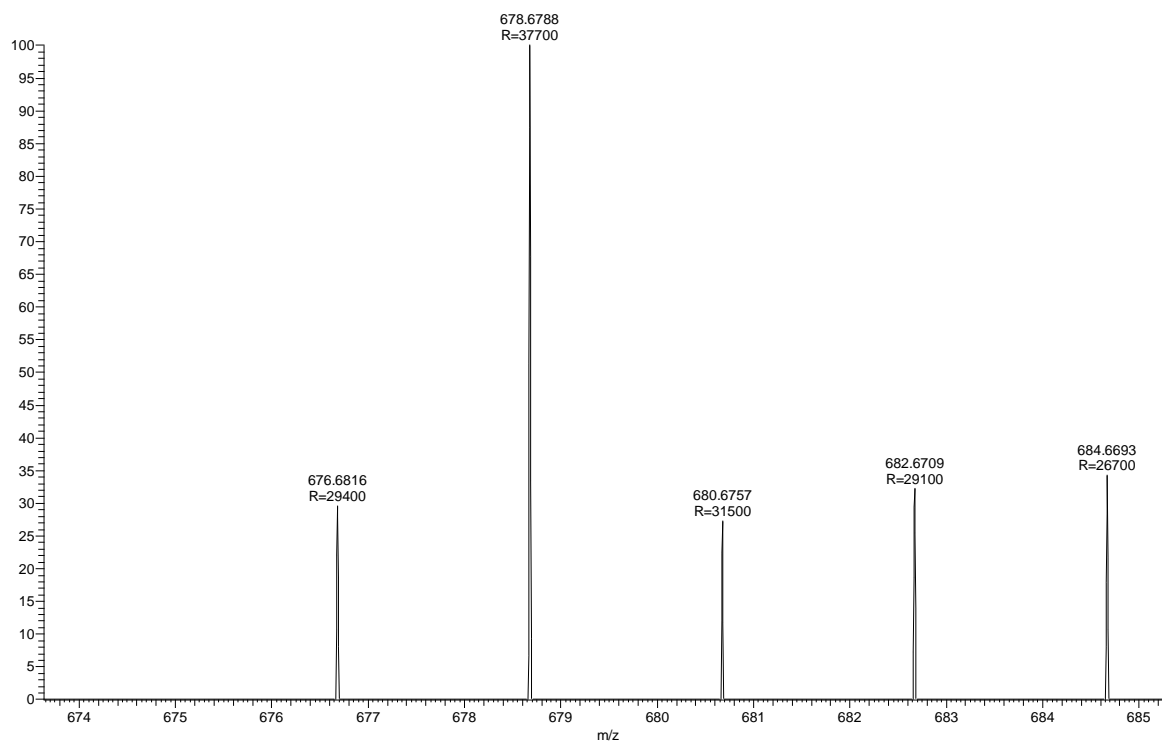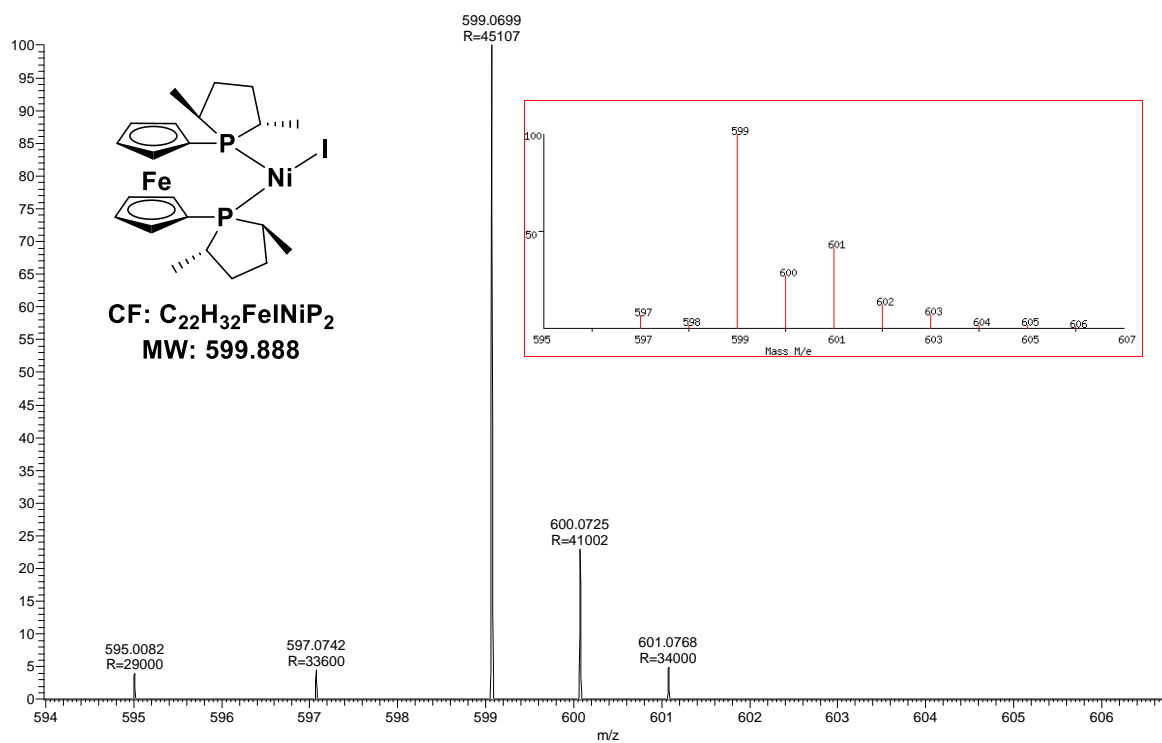
Figure 4.29: ESI-MS(+ve) spectrum of [Ni-((*S,S*)Me-FerroLANE)(phenyl)(I)] complex (**Ni-Cat.1**) in a DMF.
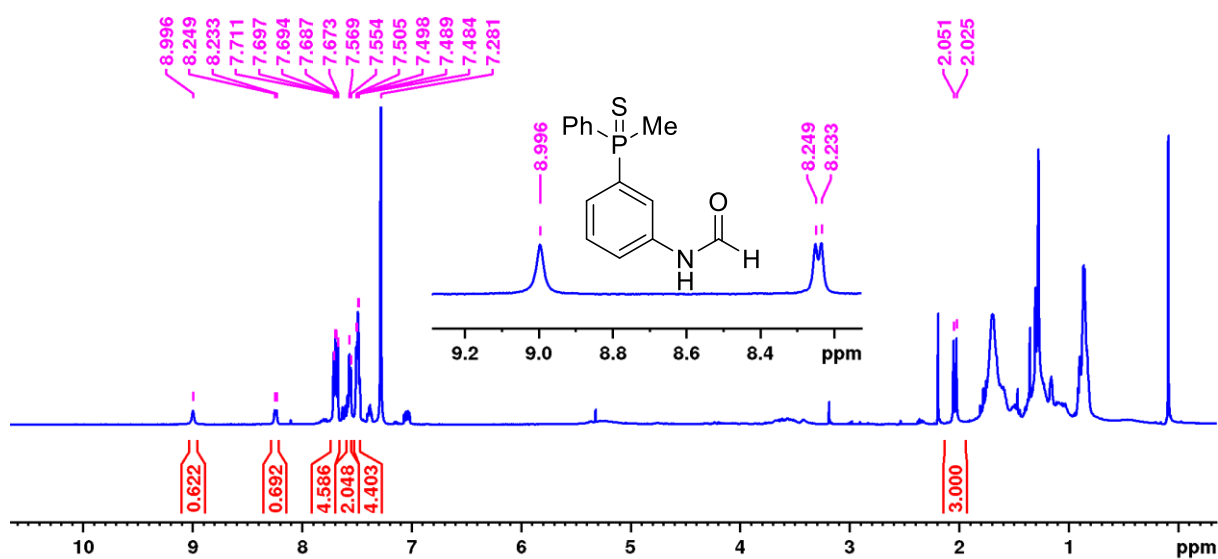
Figure 4.30: ^{1}H NMR spectrum of *N*-(3-(methyl(phenyl)phosphanyl)phenyl)formamide (**4.3d'**) in a CDCl$_3$.
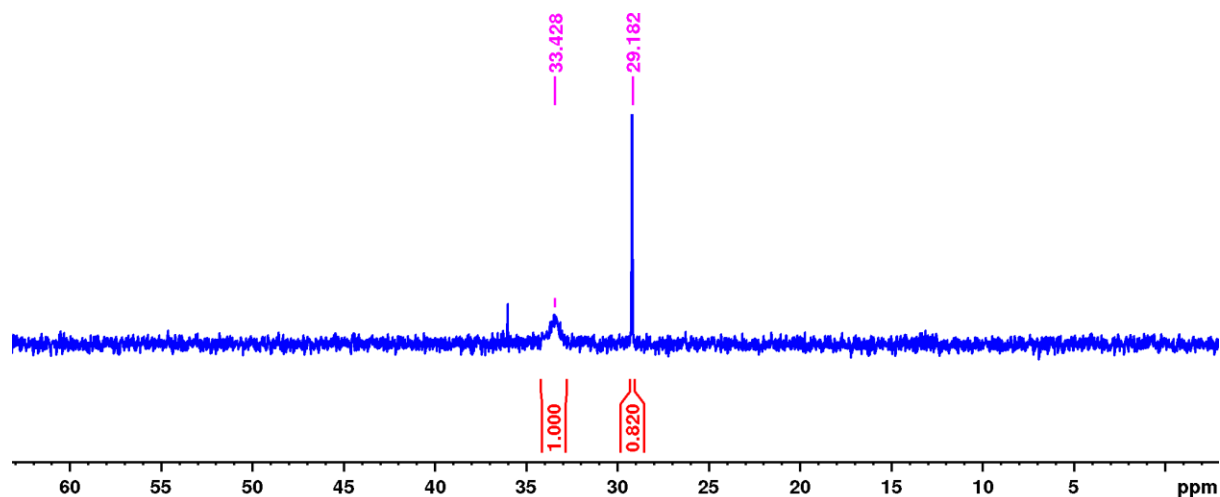
Figure 4.31: ^{31}P NMR spectrum of *N*-(3-(methyl(phenyl)phosphanyl)phenyl)formamide (**4.3d'**) in a CDCl$_3$.
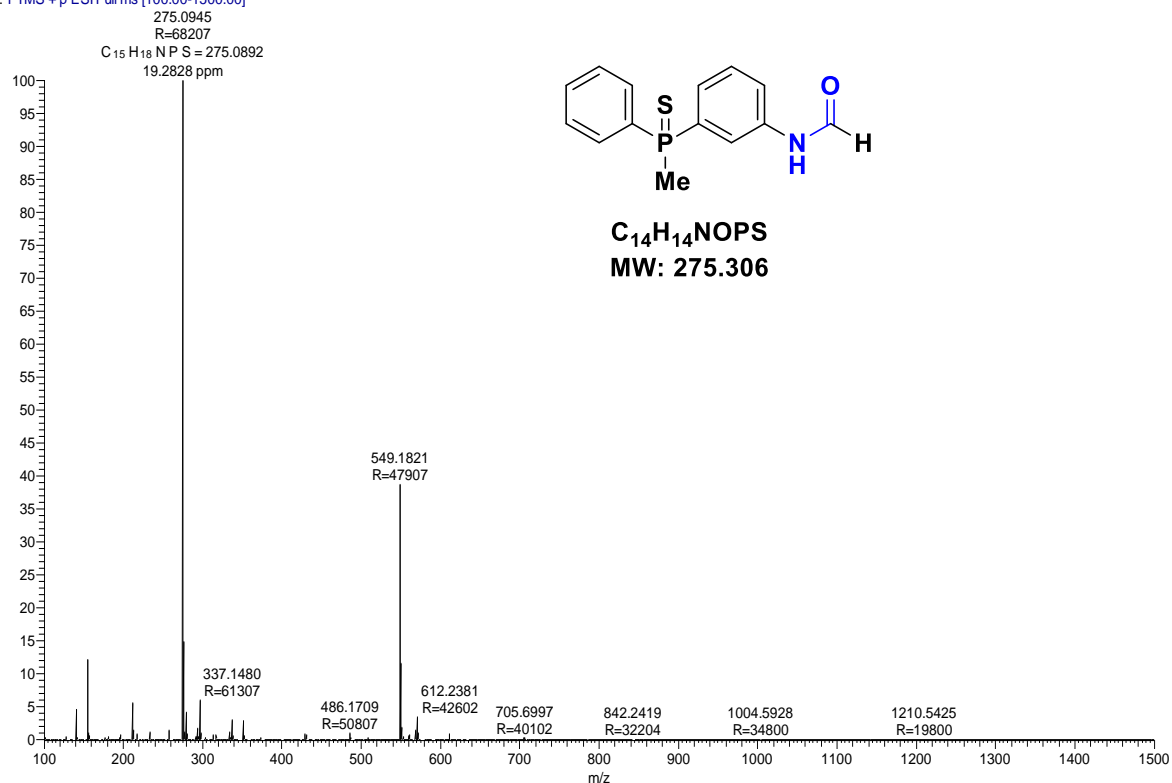
Figure. 4.32: ESI-MS(+ve) spectrum of *N*-(3-(methyl(phenyl)phosphanyl)phenyl)formamide (**4.3d'**) in a DMF.

4.7. Reference

1. A. Börner. *Phosphorus Ligands in Asymmetric Catalysis*, Ed. Wiley-VCH: Weinheim, Vols. *I−III*, 2008.

2. a) R. R. Noyori, *Asymmetric Catalysis in Organic Synthesis,* Wiley-Interscience, New York, 1994; b) W. S. Knowles, *Asymmetric Catalysis on Industrial Scale, Challenges, Approaches, and Solutions* (Eds.: H. U. Blaser and E. Schmidt,), Wiley-VCH, Weinheim, 2004, pp 23-38.

3. L. M. Pignolet, *Homogeneous Catalysis with Metal Phosphine Complexes,* Springer US, 1983.

4. P. W. N. M. Leeuwen, P. C. J. Kamer, J. N. H. Reek and P. Dierkes, *Chem. Rev.,* 2000, **100**, 2741–2770.

5. S. H. Chikkali, J. I. van der Vlugt and J. N. H. Reek, *Coord. Chem. Rev.*, 2014, **262**, 1-15.

6. a) M. L. Clarke and J. J. R. Frew, *Ligand Electronic Effects in Homogeneous Catalysis using Transition Metal Complexes of Phosphine Ligands:* (Eds.: I. J. S. Fairlamb and J. M. Lynam)*, Organomet. Chem.,* **2009**, *35,* pp 19-46.; b) L. A. Adrio and K. K. Hii, *Application of phosphine ligands in organic synthesis,* (Eds.: I. J. S. Fairlamb and J. M. Lynam), *Organomet. Chem.,* 2009, **35***,* pp 62-62.

7. J. Bayardon, S. Juge, *Phosphorus (III) Ligands in Homogeneous Catalysis: Design and Synthesis (*Eds.: P. C. J. Kamer and P. W. N. M. van Leeuwen*)*, Jon Wiley & Sons Ltd., 2012, pp 335.

8. P. A. R. Breuil, F. W. Patureau and J. N. H. Reek, *Angew. Chem. Int. Ed.,* 2009, **48,** 2162-2165.

9. B. Breit and W. Seiche, *J. Am. Chem. Soc.,* 2003, **125**, 6608-6609.

10. M. T. Reetz and S. R. Waldvogel, *Angew. Chem. Int. Ed.,* 1997, **36**, 865-867.

11. For supramolecular phosphines in hydroformylation, see: a) T. Besset, D. W. Norman and J. N. H. Reek, *Adv. Synth. Catal.* 2013*,* **355***,* 348-352; b) P. Dydio, R. J. Detz and J. N. H. Reek, *J. Am. Chem. Soc.,* 2013, **135**, 10817-10828; c) D. Fuchs, G. Rousseau, L. Diab, U. Gellrich and B. Breit, *Angew. Chem. Int. Ed.,* 2012, **51**, 2178-2182; d) U. Gellrich, W. Seiche, M. Keller and B. Breit, *Angew. Chem. Int. Ed.,* 2012, **51**, 11033-11038; e) P. Dydio, C. Rubay, T. Gadzikwa, M. Lutz and J. N. H.Reek, *J. Am. Chem. Soc.,* 2011, **133**, 17176-17179. f) P. Dydio and J. N. H. Reek, *Angew. Chem. Int. Ed.,* 2013, **52**, 3878-3882; g) T. Gadzikwa, R. Bellini, H. L. Dekker and J. N. H. Reek, *J. Am. Chem. Soc.,* **2012**, *134*, 2860-2863; h) R. Bellini, S. H. Chikkali, G. Berthon-Gelloz and J. N. H. Reek, *Angew. Chem. Int. Ed.,* **2011**, *50*, 7342-7345.

12. The p-stereogenic phosphines earned Prof. Knowles the 2001 Nobel Prize, for more details see: a) B. D. Vineyard, W. S. Knowles, M. J. Sabacky, G. L. Bachmann and D. J. Weinkauff, *J. Am. Chem. Soc.,* 1977, **99**, 5946-5952; b) W. S. Knowles, *Angew. Chem. Int. Ed.,* 2002, **41**, 1998-2007; c) D. S. Glueck, *Synlett,* 2007, **17**, 2627–2634.

13. a) S. Jugé, *Phosphorus, Sulfur Silicon,* 2008, **183**, 233; b) A. Grabulosa, J. Granell and G. Muller, *Coord. Chem. Rev.,* 2007, **251**, 25; c) T. Ohkuma, M. Kitamura and R. Noyori, *Catalytic Asymmetric Synthesis*, Wiley-VCH, New York, 1993.

14. Chiral auxiliary based synthesis of P-chiral phosphines is the most established method to prepare P-chiral phosphines on a larger scale; for the synthesis, see: a) K. M. Pietrusiewicz and M. Zablocka, *Chem. Rev.* 1994, **94**, 1375-1411; b) W. Tang and X. Zhang, *Chem. Rev.*, 2003, **103**, 3029-3070; c) T. Imamoto, K. Tamura, Z. Zhang, Y. Horiuchi, M. Sugiya, K. Yoshida, A. Yanagisawa and A. D. Gridnev, *J. Am. Chem. Soc.,* 2012, **134**, 1754-1769; d) T. Imamoto, Y. Saitoh, A. Koide, T. Ogura and K. Yoshida, *Angew.*

Chem. Int. Ed., 2007, **46**, 8636-8639; e) A. Karim, A. Mortreux, F. Petit, G. Buono, V. Peiffer and C. Siv, *J. Organomet. Chem.,* 1986, **317**, 93-104.

15. Palladium-catalyzed the synthesis of P-chiral phosphine, see: J. R. Moncarz, M. F. Laritcheva and D. S. Glueck, *J. Am. Chem. Soc.,* 2002, **124**, 13356−13357.

16. Platinum-catalyzed synthesis of P-chiral phosphine, see: C. Scriban and D. S. Glueck, *J. Am. Chem. Soc.*, 2006, **128**, 2788.

17. Ruthenium-catalyzed synthesis of P-chiral phosphine, see: V. S. Chan, I. C. Stewart, R. G. Bergman and F. D. Toste, *J. Am. Chem. Soc.*, **2006**, *128*, 2786.

18. V. S. Koshti, N. R. Mote, R.G. Gonnade and S. Chikkali, *Organometallics*, 2015, **34**, 4802-4805.

19. B. L. Lei Liu, Y. Fu, S. W. Luo, Q. Chen and Q. X. Guo, *Organometallics*, 2014, **23**, 2114-2123.

20. T. J. Brunker, N. F. Blank, J. R. Moncarz, C. Scriban, B. J. Anderson, D. S. Glueck, L. N. Zakharov, J. A. Golen, R. D. Sommer, C. D. Incarvito and A. L. Rheingold, *Organometallics,* 2005, **24***, 2730-2746.

21. S. Bajo, G. Laidlaw, A. R. Kennedy, S. Sproules and D. J. Nelson, *Organometallics,* 2017, **36***, 1662-1672.

22. Y. Huang, Y. Li, P. H. Leung and T. Hayashi, *J. Am. Chem. Soc.,* 2014, **136**, 4865-4868.

23. V. S. Koshti, S. H. Thorat, R. P. Gote, S. H .Chikkali and R. G. Gonnade, *CrystEngComm*, 2016, **18**, 7078-7094.

Chapter 5

Self-assembly of P-chiral supramolecular phosphine on rhodium and a direct evidence for Rh-catalyst-substrate interaction in asymmetric hydrogenation

5.1. Abstract

Supramolecular catalysts are known to provide high enantioselectivity in asymmetric transformations such as hydrogenation, but direct evidence unraveling the role of secondary interactions are largely missing. Therefore, the role of hydrogen bonding in asymmetric hydrogenation catalyzed by supramolecular catalysts is investigated. To identify the nature of hydrogen bonding in the self-assembled Rh-complex, NMR experiments were performed at different temperatures and concentrations. The NH and NH_2 peaks of 1-(3-(phenyl(o-tolyl)phosphanyl)phenyl)urea (**L1**) shift downfield with increasing temperature. This observation suggested presence of intermolecular hydrogen bonding in **L1**. In addition with decreasing temperature the NH and NH_2 resonances of **L1** were found to shift downfield. The deshielding of NH and NH_2 proton once again indicated existence of intermolecular hydrogen bonding in **L1**. On the other hand, the chemical shift of NH and NH_2 resonances did not change with increasing concentration of the self-assembled Rh-complex (**C1**). No significant change in the chemical shift of NH and NH_2 protons supports existence of intramolecular hydrogen bonding in **C1**. The variable temperature NMR experiments further supported this with decreasing temperature, there was no significant change in the chemical shift of NH_2 protons,
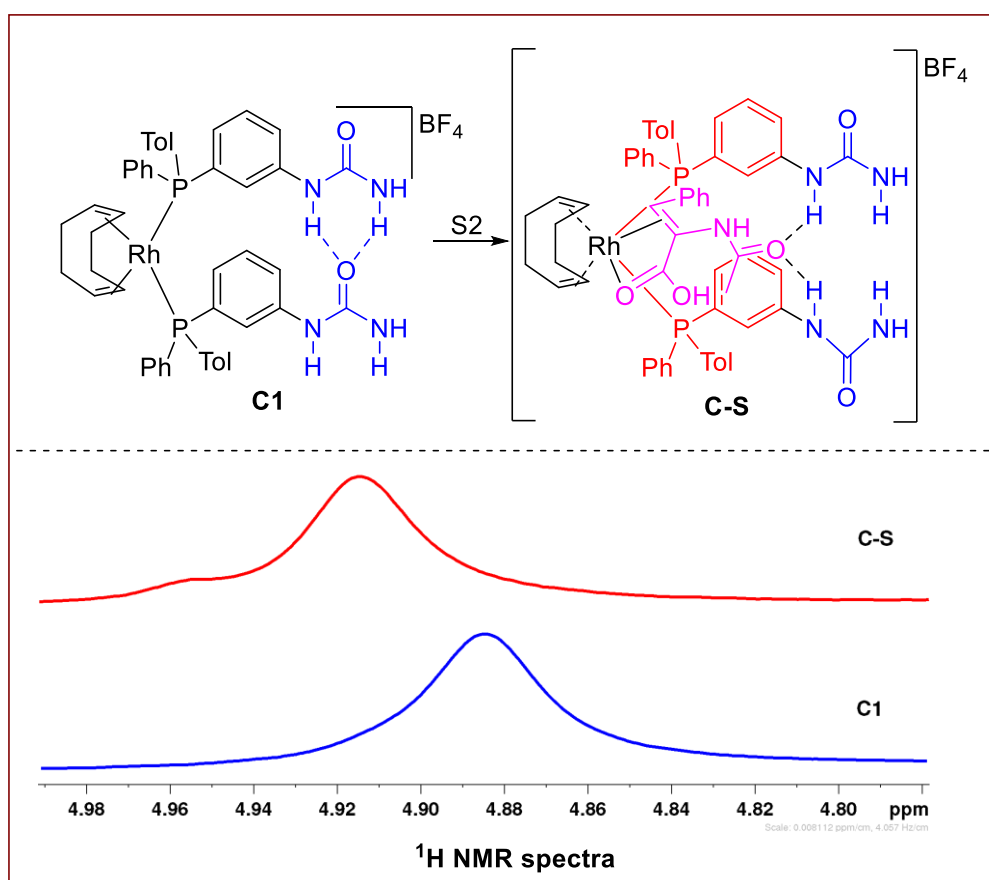
V. S. Koshti, A. Sen, D. Shinde and S. Chikkali, *Dalton Trans*. 2017, *46*, 13966-13973.

indicating intramolecular hydrogen bonding in **C1**. In a stoichiometric experiment, hydrogenation substrate *N*-acetyldehydrophenylalanine (**S2**) was treated with **C1** and proton NMR was recorded. The NH_2 protons of the self-assembled Rh-complex shift downfield, as compared to untreated **C1**. These findings indicated that there is a hydrogen bonding interaction between Rh-complex and the substrate. To further support this hypothesis, NH and NH_2 groups were exchanged to ND and ND_2 groups respectively, and a self-assembled Rh-complex was prepared using the deuterated supramolecular phosphine ligand **L1.D**. When the deuterated Rh-complex (**C1.D**) was treated with substrate **S2**, the ND and ND_2 resonances were found to shift downfield. Thus, the labelling experiment further authenticated the existence of catalyst-substrate interaction. The high enantiomeric excess observed in the asymmetric hydrogenation of **S2** could be due to the catalyst-substrate interaction.

5.2. Introduction
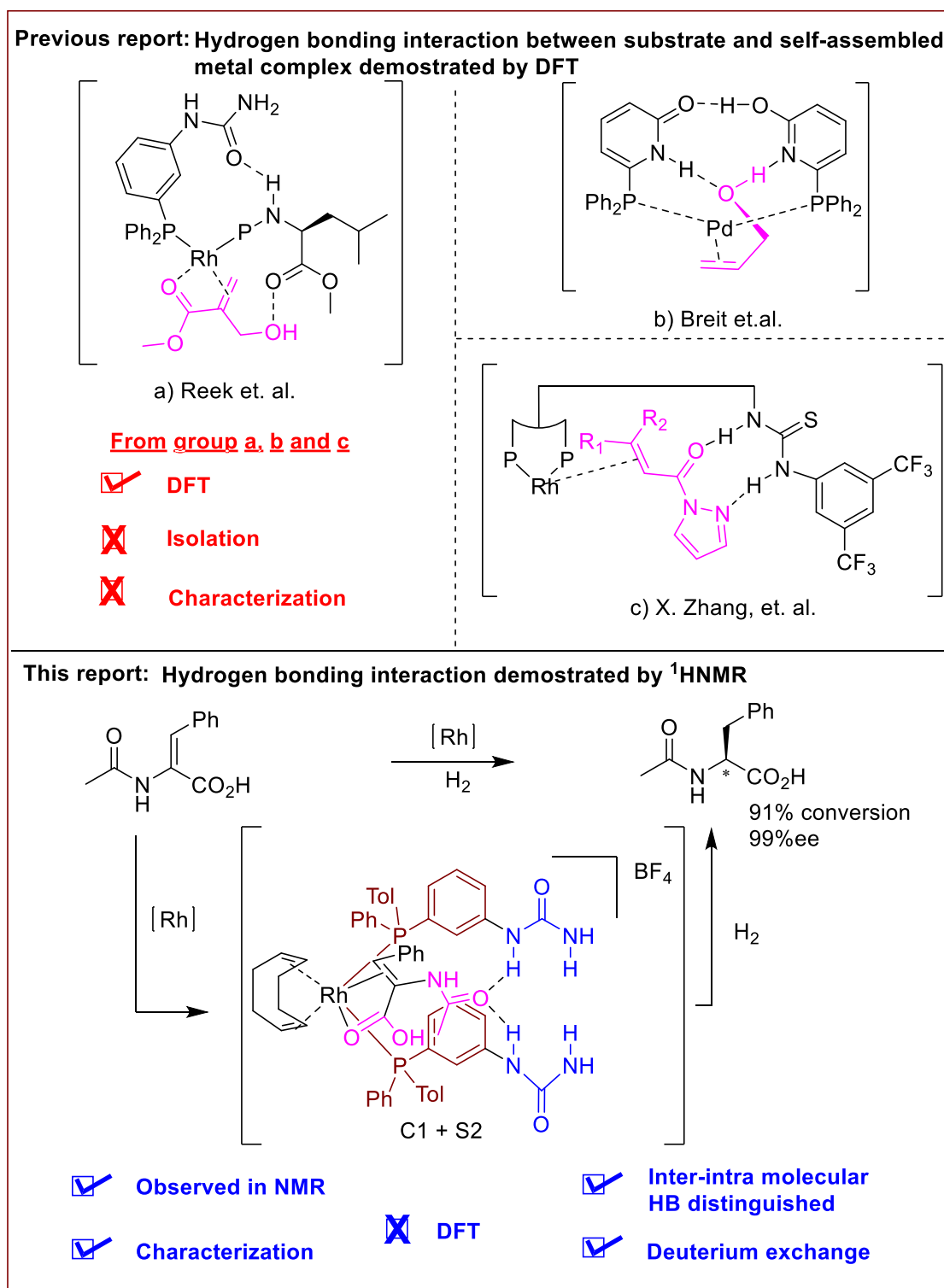
Figure 5.1: Recent reports in the field of supramolecular catalysis (top) and proposed H-bonding interaction between the catalyst and substrate (this work, bottom).

Metal-catalyzed asymmetric hydrogenation is a well-known reaction in the synthesis of chiral compounds, pharmaceuticals, and natural products.[1] Phosphine ligands are known to play

a prominent role in altering the reactivity and selectivity of a hydrogenation catalyst.[2] The classical approach utilizes either monodentate ligands which suffer from limited selectivity or bidentate ligands that are less reactive and require time consuming synthesis.[3,4] A strategy to address this emerged at the beginning of year 2000, which is called "supramolecular ligand designing strategy".[5] Since then the supramolecular metal catalysts are being regularly used in hydrogenation and hydroformylation.[6,7] Due to the weak hydrogen bonding the self-assembled supramolecular catalysts are flexible enough to provide cooperative behaviour during the catalysis[8] and might lower the energy barrier (of the transition state) to accelerate the reaction.[9] Apart from high activity, the supramolecular catalysts tend to provide high enanatioselectivities.[10] There have been constant attempts to understand the origin of the stereo-selectivity.[11] Recently, Reek and co-workers revealed existence of hydrogen bonding interaction between ester functional group of a self-assembled metal catalyst and the hydroxyl group of a substrate using DFT calculation (Fig. 5.1a, top).[12] The computational study demonstrated that the supramolecular motif appended on the catalyst actually aligns the substrate through hydrogen bonding, leading to high enantioselectivities in a asymmetric hydrogenation reaction. In addition, secondary interactions are known to induce selectivity in various cross-coupling reactions,[13] as well as in gold and organo-catalysis.[14] Along the same lines, Breit and co-workers published decarboxylative hydroformylation of α, β-unsaturated carboxylic acids using a supramolecular catalyst.[15]

It was speculated that the interaction between the ligand and the substrate guides the reaction to display excellent selectivity (Fig. 5.1b, top).[16] Thus, computational experiments were utilized to demonstrate the hydrogen bonding interactions between the catalyst and substrate, and it was assumed that these interactions promote stereoselectivity[17] Zhang and co-workers employed a rhodium complex, appended with thiourea units in the asymmetric hydrogenation of H-bond acceptor, *a,β*-unsaturated acylpyrazoles[18] The authors speculated that the donor thiourea unit appended on the catalyst interacts with the *a,β*-unsaturated acylpyrazoles substrate to achieve high enantioselectivity (Fig. 5.1c, top) in a asymmetric hydrogenation reaction. This hypothesis is mainly based on computational investigations, which indicated the presence of hydrogen bonding between the substrate and the supramolecular ligand. It has been also assumed that the hydrogen bonding interaction is the driving force to bring the substrate in the close proximity of the catalytically active metal center[19] Solvent effects in supramolecular catalysis were considered by Börner and co-workers who stated that solvent can potentially alter the reactivity and selectivity of an asymmetric hydrogenation reaction catalyzed by self-assembled metal catalysts[20] Thus, some progress has

been reported to understand the role of secondary interactions in asymmetric reactions and DFT was used as a tool to prove the existence of H-bonding interaction. However, a direct evidence to demonstrate the existence of a hydrogen bonding interaction between self-assembled metal complex and the substrates is largely missing. In our opinion, there are no reports that present any experimental evidence for the role of hydrogen bonding interaction in supramolecular catalysis.

As presented in previous chapter. We have been interested in supramolecular chemistry,[21] P-chiral supramolecular phosphines[22] as well as asymmetric reactions.[23] To mimic the bidentate ligand coordination, synthesis of P-stereogenic ligands equipped with additional supramolecular bonding motif was undertaken and their ability to catalyze asymmetric hydrogenation was elucidated.[22] It was found that *N*-acetyldehydrophenylalanine (**S2**), provided excellent enantiomeric excess (ee), However asymmetric hydrogenation of dimethyl itaconate (**S1**), a bench mark substrate, led to modest ee's. To understand this anomalous behaviour, we investigated catalyst-substrate interactions. In the process, direct experimental evidence for the interaction between the substrate and the supramolecular catalyst was obtained. NMR spectroscopy was used to demonstrate the self-assembly of p-chiral phosphines on a metal to yield supramolecular catalyst. The existence of hydrogen bonding between the supramolecular catalyst and substrate was probed using a combination of NMR spectroscopy, deuterium labelling experiments, and FTIR.

5.3. Results and discussion

In chapter 1, the catalytic synthesis of P-stereogenic supramolecular phosphine ligands and their self- assembled Rh-complexes was reported (Scheme 4.1).[22] To unambiguously establish the existence of inter and intra-molecular hydrogen bonding in the self-assembled complex, the effect of concentration and temperature on hydrogen bonding was investigated.
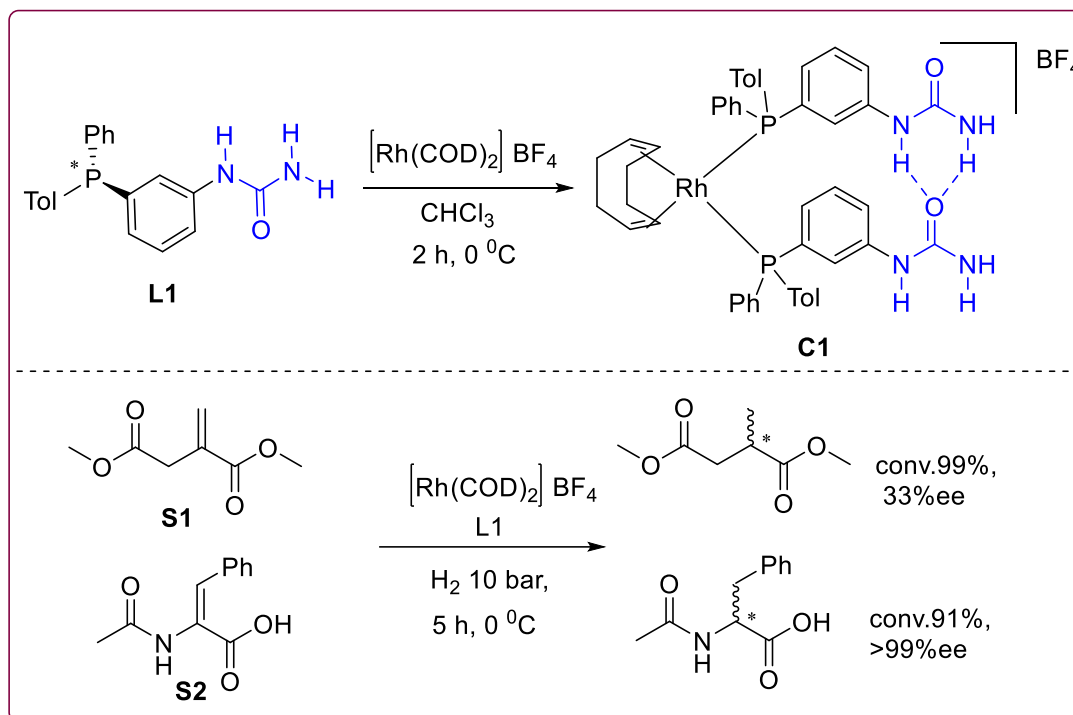
Scheme 5.1: Synthesis of self-assembled Rh-complex (C1) (top) and asymmetric hydrogenation (bottom).

5.3.1. Effect of concentration on hydrogen bonding

The effect of concentration of 1-(3-(phenyl(o-tolyl)phosphanyl)phenyl)urea (**L1**) on the hydrogen bonding of **L1** was investigated using proton NMR spectroscopy. Note that the P-stereogenic supramolecular phosphine ligands are equipped with urea as a hydrogen bonding motif. A proton NMR of 10 mM solution of above ligand **L1** at 25 °C displayed a NH resonance at 6.43 ppm and the NH$_2$ signal at 4.59 ppm (Fig. 5.2, left, Fig 5.12). Next, the concentration of ligand **L1** was increased from 10 mM to 20, 30, 40 and 50 mM (Fig. 5.2, left). It was found that with increasing concentration of **L1**, the NH and NH$_2$ peaks shifted to downfield region. Thus, the NH protons appeared at 6.43 ppm at 10 mM and at 6.85 ppm at 50 mM concentration with an average 0.4 ppm downfield shift (Table 5.1). Similar tendency was observed for NH$_2$ [4.59 ppm (10 mM) to 4.70 ppm (50 mM)] protons with an average 0.11 ppm change in chemical shift. Thus, the downfield shift of the NH and NH$_2$ protons with increasing concentration from 10 mM to 50 mM is a characteristic feature of an intermolecular hydrogen bonding.[24] The NMR findings were further supported by FTIR studies that revealed change in carbonyl band (Fig. 5.3) with increasing concentration. Similar experiments were performed with complex **C1** and ^{1}H NMR was recorded. The NH protons of the **C1** were overlapped by the aromatic protons, and there it was difficult to identify them. At a 10 mM concentration, the NH proton seems to be buried under the aromatic protons and therefore it was difficult to

distinguish NH peak (Fig. 5.2, right, Fig.5.13) from the aromatic protons. But, the NH_2 protons could be identified. With increasing concentration of self-assembled complex, there was no change in the chemical shift of the NH_2 protons (Table 5.2, right). Almost no change in chemical shift of NH_2 protons strongly suggests existence of intramolecular hydrogen bonding interaction in **C1**.[25] The NMR findings were supplimented by IR studies, and no change in carbonyl band was observed with increasing concentration of **C1** (Fig. 5.4). Above assumption was further testified by recording variable temperature proton NMR of **C1**.

Table 5.1: Monitoring the change in chemical shift of NH and NH2 proton as a function of concentration of the L1.

Sr. no.	L1 (g)	L1 conc. (mM)	NH (ppm)	NH$_2$ (ppm)
1	0.0017	10	6.43	4.59
2	0.0017 + 0.0017	20	6.55	4.62
3	0.0034 + 0.0017	30	6.66	4.65
4	0.0050 + 0.0017	40	6.76	4.68
5	0.0067 + 0.0017	50	6.85	4.70

Table 5.2: Monitoring the change in chemical shift of NH$_2$ proton as a function of concentration of the **C1**.

Sr. no.	Self-assembled Rh-complex (g)	C1 conc. (mM)	NH$_2$ (ppm)
1	0.0048	10	5.15
2	0.0048 + 0.0048	20	5.16
3	0.0096 + 0.0048	30	5.17
4	0.0144 + 0.0048	40	5.18 [(5.26+5.11)/2]
5	0.0192 + 0.0048	50	5.19 [(5.28+5.09)/2]
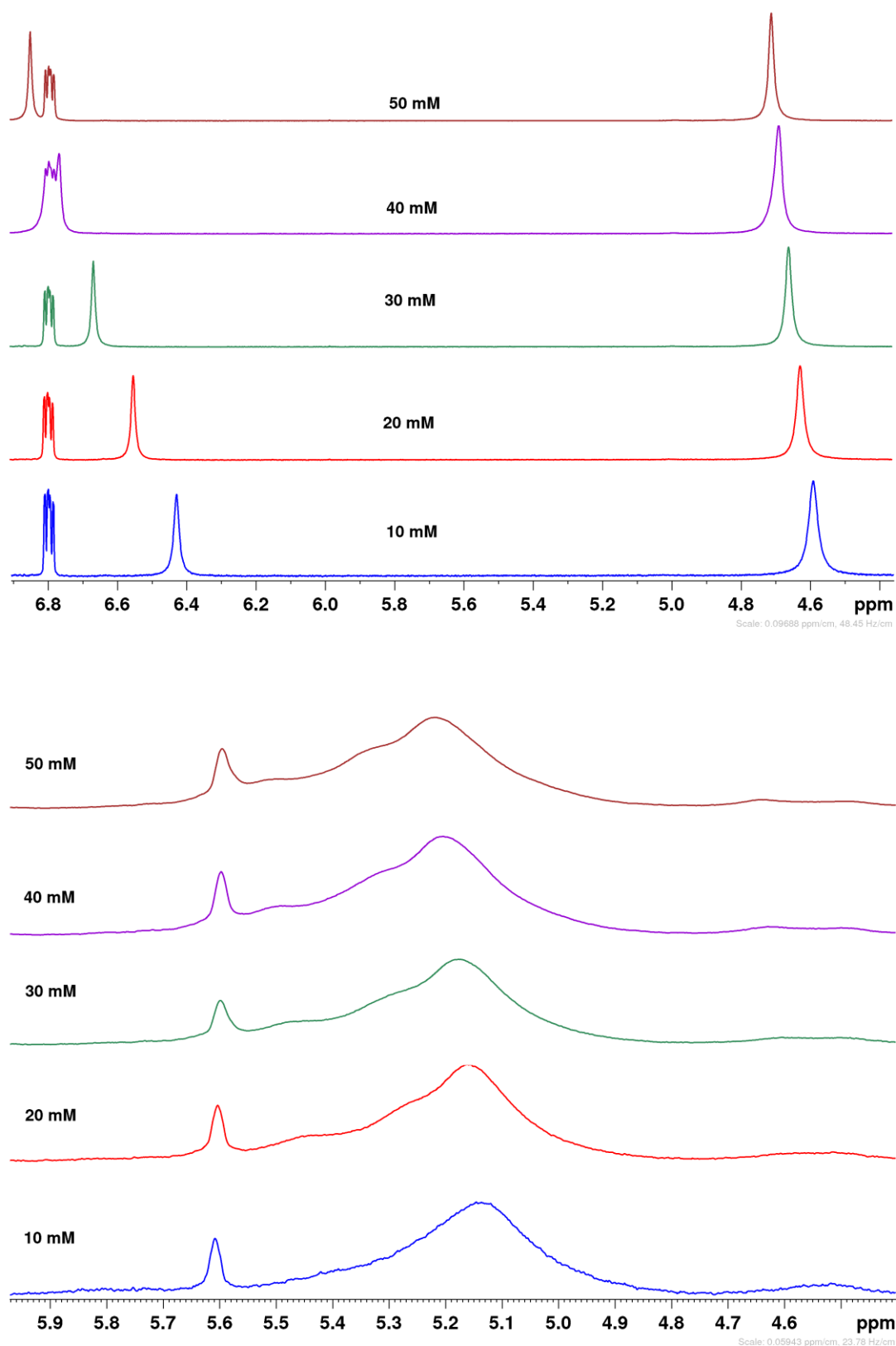
Figure 5.2: Effect of concentration of P-stereogenic supramolecular phosphine (**L1**) (top) and self-assembled Rh-complex (bottom) on hydrogen bonding.
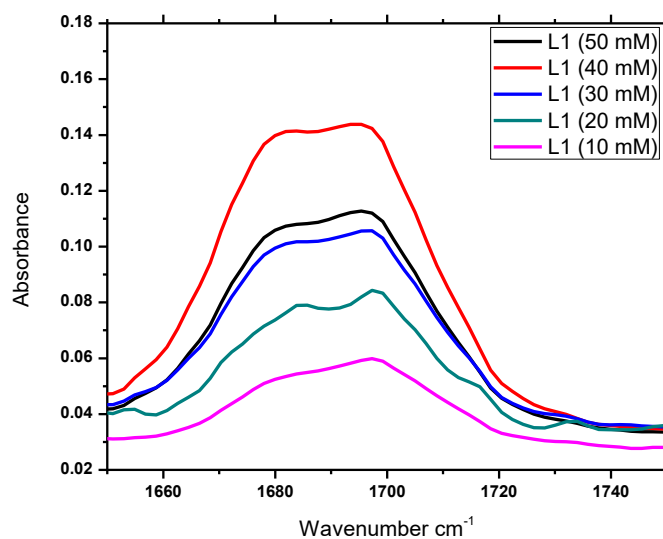
Figure 5.3: IR spectra of P-stereogenic supramolecular phosphine (**L1)** at different concentration.
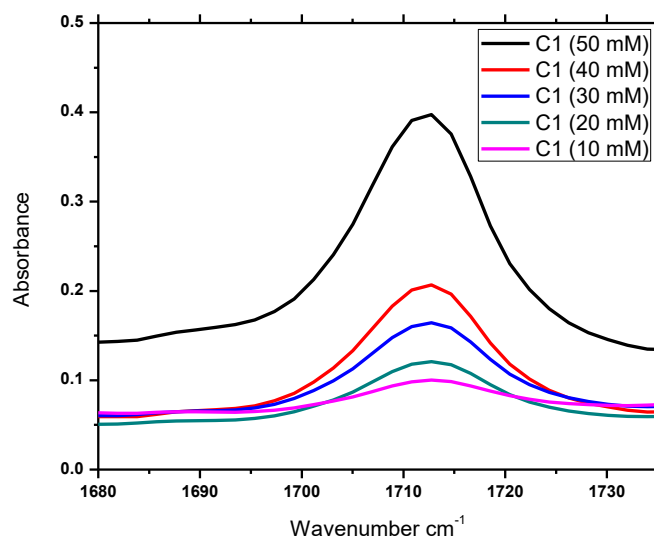
Figure 5.4: IR spectra of **C1** at different concentration.

5.3.2. Effect of temperature on hydrogen bonding

10 mM solution of **L1** was charged to an NMR tube and a ^{1}H NMR spectrum of this solution was collected at different temperatures between 298-263 K. The NH and NH_2 resonances shift downfield with decreasing temperature (Fig. 5.5, left and Fig. 5.14). This finding indicates that with decreasing temperature the intermolecular hydrogen bonding interaction becomes stronger and the NH and NH_2 protons shift downfield. Similarly, proton NMR of supramolecular catalyst at 10 mM concentration was recorded at 298 K to 263 K. As

opposed to the ligand behaviour; with decreasing temperature there was hardly any change in the chemical shift of NH_2 protons (Fig. 5.5, right and Fig. 5.15). This observation directly indicated existence of a stronger hydrogen bonding (i.e. intramolecular hydrogen bonding) in supramolecular catalyst.

Thus, effect of temperature and concentration on the chemical shift of NH and NH_2 protons of the ligand **L1** and NH_2 protons of the catalyst **C1** was investigated, and from these experiments it can be concluded that the P-stereogenic supramolecular phosphine ligand displays an intermolecular hydrogen bonding and the self-assembled complex **C1** reveals an intramolecular hydrogen bonding (Fig. 5.5, and Fig. 5.14-5.15).

Table 5.3: Monitoring the change in chemical shift of NH and NH_2 proton as a function of temperature of the **L1**.

Sr. no.	Temperature (K)	L1 conc. (mM)	NH (ppm)	NH₂ (ppm)
1	298	10	6.37	4.55
2	293	10	6.43	4.58
3	283	10	6.50	4.62
4ᵃ	273	10	6.59	4.66
5ᵃ	263	10	6.69	4.70

Table 5.4: Monitoring the change in chemical shift of NH and NH_2 proton of **C1** as a function of temperature.

Sr. no.	C1 conc. (mM)	Temperature (K)	NH₂ (ppm)
1	10	298	5.12
2	10	293	5.13
3	10	283	5.14
4	10	273	5.18
5	10	263	5.19
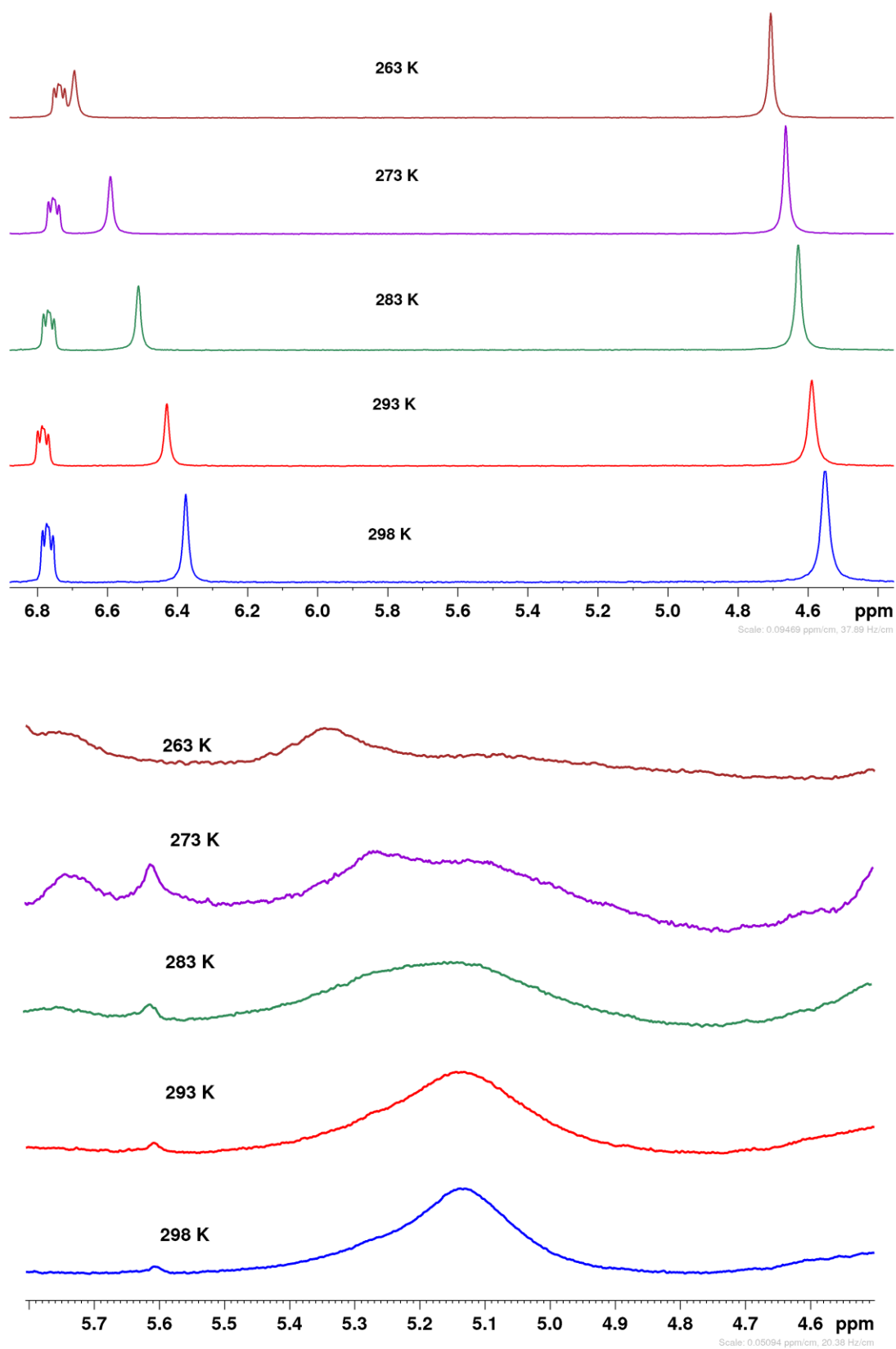
Figure 5.5: Effect of temperature on hydrogen bonding in **L1** (top) and **C1** (bottom).

5.3.3. Evidence for catalyst-substrate interactions

Noted that the self-assembled catalyst **C1** was found to induce high enantioselectivity in the asymmetric hydrogenation of *N*-acetyldehydrophenylalanine (**S2**). In order to understand the origin of the selectivity, stoichiometric reactions between the complex **C1** and substrate *N*-acetyldehydrophenylalanine (**S2**) were performed and the changes were monitored by NMR spectroscopy. Initially, ^{1}H NMR of **C1** in acetonitrile-d$_3$ was recorded which revealed NH$_2$ resonance at 4.88 ppm (Fig. 5.26). When substrate **S2** was added to this NMR tube, the NH$_2$ resonance was found to shift downfield to appear at 4.92 ppm (Fig. 5.27). The change in the chemical shift of NH$_2$ protons indicates presence of hydrogen bonding interaction between the substrate (**S2**) and the **C1** (Fig 5.6). This finding was further supported by IR spectroscopy. The catalyst **C1** at 10 mM (in chloroform solvent) concentration displayed an IR band at 1710 cm^{-1} that can be assigned to the urea carbonyl. A solution of stoichiometric amount of **C1** and substrate (**S2**) in chloroform solvent (10 mM) revealed a carbonyl band at 1700 cm^{-1} (Fig. 5.7). The change in carbonyl stretching frequencies is in line with the reported literature data.[26] The change in the IR frequency after addition of substrate indicates existence of weak interaction between the **C1** and **S2**. In a control experiment, **C1** was treated with dimethyl itaconate (**S1**) and IR was recorded. There was hardly any change in the substrate carbonyl band, indicating very weak **C1**-**S1** interaction, compared to **C1**-**S2** interaction (the substrate carbonyl bands shifts by 8 cm^{-1}) (Fig. 5.8, 5.9).
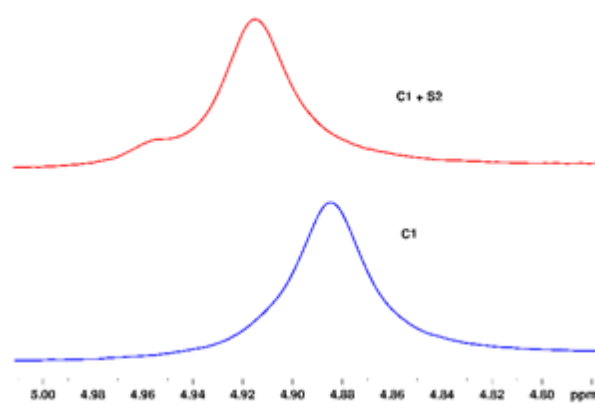
Figure 5.6: ^{1}H NMR of self-assembled complex **C1** (bottom, blue) and complex **C1** + substrate **S2** top (red).
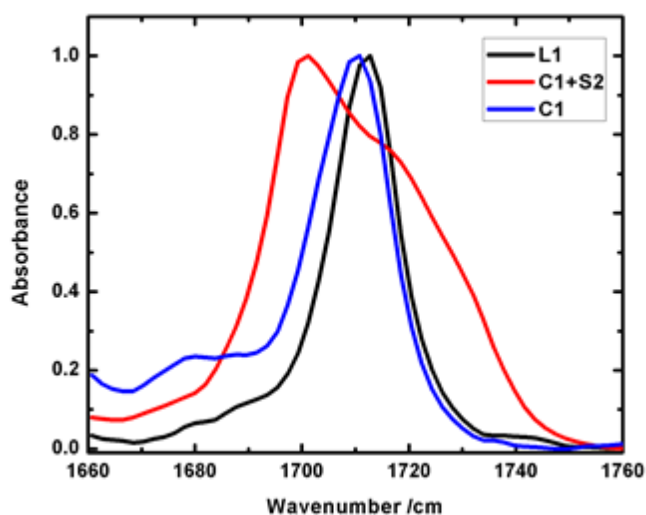
Figure 5.7: IR spectra of ligand **L1** (black), self-assembled complex **C1** (blue) and complex **C1** + substrate **S2** (red).
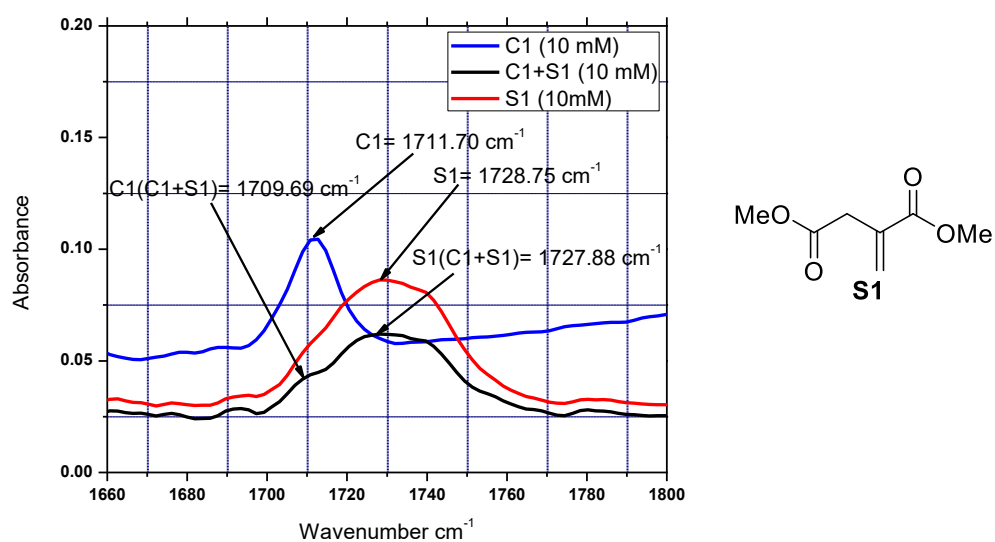
Figure 5.8: IR spectra of neat **C1**, neat **S1** and stoichiometric experiment of **C1**+**S1**.
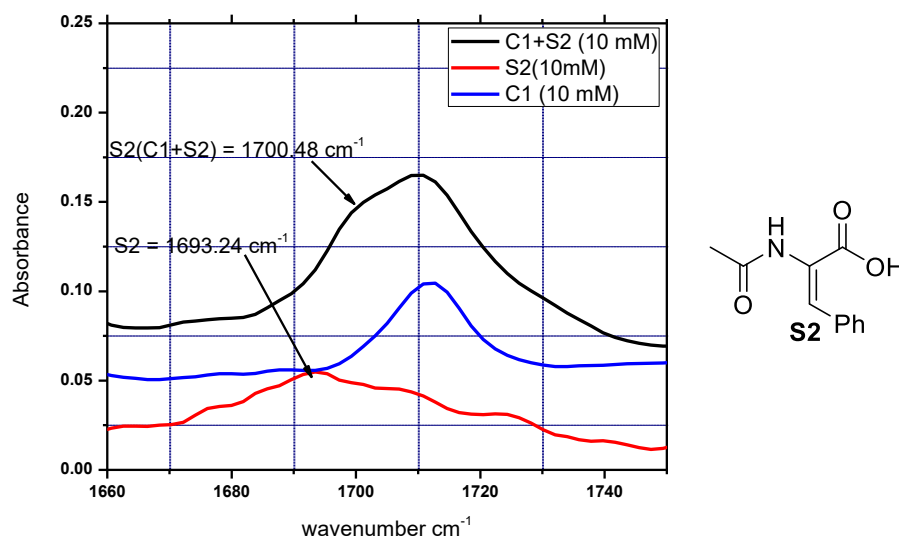
Figure 5.9: IR spectra of neat **C1**, neat **S2** and stoichiometric experiment of **C1**+**S2**.

5.3.4. Isotopic labelling studies

As discussed in the earlier section, NH protons of the self-assembled complex appear in the aromatic region due to which only limited conclusions could be drawn from the proton NMR of the self-assembled complex **C1**. To address this bottle-neck, the p-chiral supramolecular phosphine ligand **L1** was treated with CD_3OD for 3-5 hours, after which volatiles were evaporated to obtain deuterium labelled ligand (**L1.D**).[27] Thus, the NH and NH_2 groups were deuterated to ND and ND_2 respectively. The deuterium labelling was confirmed by recording deuterium NMR for a 10 mM solution of **L1.D**, which revealed a ND_2 resonance at 5.45 ppm and a ND resonance at 7.87 ppm (Fig 5.16). The identy of **L1.D** was fully established using a combination of spectroscopic and analytical methods. 2 equivalent of **L1.D** was treated with rhodium precursor $[Rh(COD)_2BF_4]$ to obtain a deuterium labelled self-assembled Rh-complex (**C1.D**). The ND_2 and ND resonance were observed at 5.56 ppm, 8.29 ppm respectively (Fig 5.21). The NMR results were corroborated by a positive mode ESI-MS of **C1.D** that revealed a $[M]^+$ peak at m/z = 879.24 Da. It is most likely that during the ionization the deuterium is exchanged with protons and therefore, the mass of 879.24 Da corresponds to protonated complex **C1** (Fig 5.25). Next, a stoichiometric reaction was performed between the **C1.D** (10 mM) and **S2** (10 mM) and a deuterium NMR was recorded in THF-d_8. A deuterium NMR of this adduct revealed downfield shifted ND_2 and ND signals which appeared at 5.62 and 8.45 ppm respectively (with THF-d_8 as an internal standard) (Fig. 5.28). The existence of **C1.D**+**S2** adduct was further authenticated by positive mode ESI-MS, which revealed a peak

at m/z = 1116.24 Da (Fig. 5.29). Thus, a direct evidence for the interaction between the **C1.D** and the substrate (**S2)** was obtained, confirming the role of hydrogen bonding in the asymmetric hydrogenation of **S2** (Fig 5.29). Based on above experimental findings, we propose existence of hydrogen bonding interaction between **C1.D+S2** as depicted in Figure 5.11, although other possibilities of hydrogen bonding cannot be fully excluded at this stage.
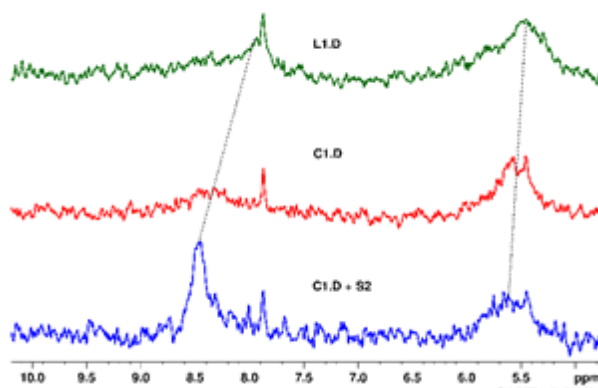
Figure 5.10: ^{2}H NMR of **L1** (green), **C1** (red) and **C1** + substrate **S2** (blue).
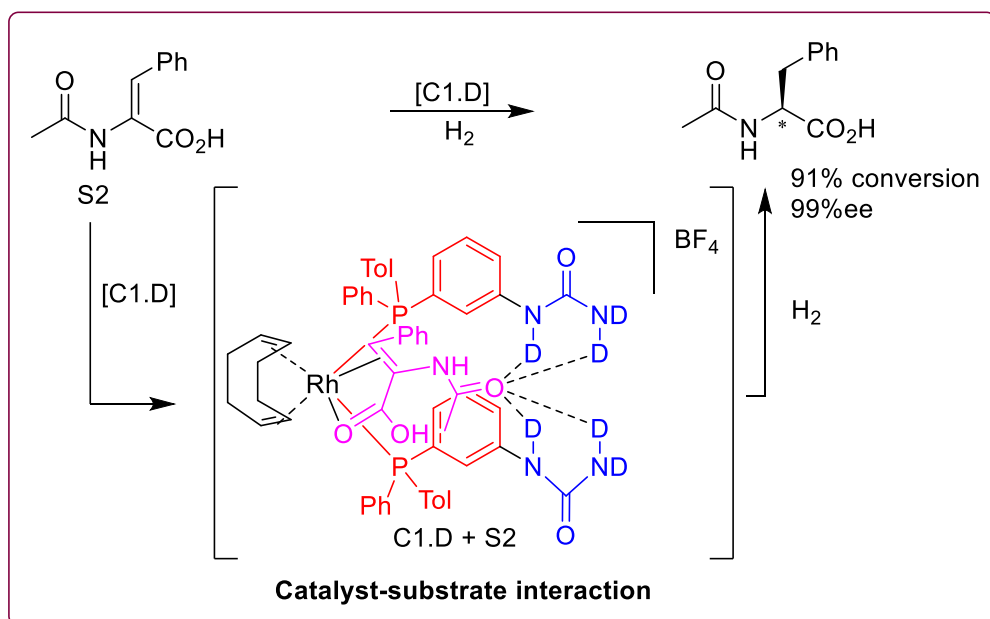
Figure 5.11: Proposed H-bonding interaction between the **C1.D** and **S2**.

5.4. Conclusions

In conclusion, the self-assembly of 1-(3-(phenyl(o-tolyl)phosphanyl)phenyl)urea (**L1**) to form rhodium complex **C1** was unambiguously demonstrated using a combination of temperature and concentration dependent NMR spectroscopy. The NH and NH$_2$ peaks were

found to shift downfield with decreasing temperature or with increasing concentration, in the free ligand **L1**. This observation suggested presence of inter-molecular hydrogen bonding in **L1**. In contrast, no change in chemical shift of the NH_2 proton was observed for **C1** with decreasing temperature or with increasing concentrations. Thus, it appears that there exists a strong intra-molecular hydrogen bonding in **C1**, which is responsible for above findings. The role of catalyst-substrate interactions was investigated by preparing deuterium labeled supramolecular phosphine ligand **L1.D**. Subsequently **L1.D** self-assembles on a rhodium template **C1.D**. The identity of **C1.D** was established from NMR and mass spectroscopy. When the deuterated metal complex **C1.D** was treated with *N*-acetyldehydrophenylalanine (**S2**) further downfield shift of the ND and ND_2 groups was observed. Thus, the change in chemical shift after addition **S2** indicates presence of hydrogen bonding interactions between **C1.D** and **S2**. These investigations allow to conclude that a hydrogen bonding interaction as depicted in Figure 5.11 might be responsible for the high enantioselectivities observed in the asymmetric hydrogenation of **S2**.

5.5. Experimental section

All manipulations were carried out under an inert atmosphere of argon using standard Schlenk line techniques or m-Braun glove box. Solvents were dried by standard procedures.[28] THF was distilled from sodium/benzophenone under argon atmosphere. Acetonitrile and methylene chloride were distilled on calcium-hydride. [$(COD)_2RhBF_4$] and *N*-acetyldehydrophenylalanine were purchased from Sigma-Aldrich. All other reagents/chemicals, solvents were purchased from local suppliers (Spectrochem Pvt. Ltd.; Avra Synthesis Pvt. Ltd.; Thomas Baker Pvt. Ltd. etc.).

Solution NMR spectra were recorded on a Bruker Avance 400 and 500 MHz instruments at 298 K unless mentioned otherwise. Chemical shifts are referenced to external reference TMS (^{1}H and ^{13}C) or 85% H_3PO_4 ($\Xi = 40.480747$ MHz, ^{31}P). Coupling constants are given as absolute values. Multiplicities are given as follows s: singlet, d: doublet, t: triplet, m: multiplet, quat, br: broad, quaternary carbon. FT-IR spectra were recorded on a Bruker α-T spectrophotometer in the range of 4000-400 cm^{-1}. Mass spectra were recorded on Thermo scientific Q-Exactive mass spectrometer. Synthesis of self-assembled Rh-complex was achieved as reported in the literature.[22]

5.5.1. Demonstrating the self-assembly

5.5.1.1. Effect of concentration on H-bonding in L1

In a NMR tube, 0.0017 g (0.005 mmol) of **L1** was dissolved in 0.5 ml of $CDCl_3$ to make 10 mM solution of **L1**. The ^{1}H NMR of 10 mM solution was recorded at 25 ^{o}C and chemical shift of NH and NH_2 protons was identified. Next, in the same NMR tube another 0.0017 g (0.005 mmol) of **L1** (to make 20 mM solution of **L1**) was added and proton NMR was recorded. In similar manner, 30 mM, 40 mM, and 50 mM solution of **L1** was prepared and ^{1}H NMR was measured. Table 5.1. Summarizes the change in chemical shift of NH and NH_2 protons of **L1** with increasing concentrations (Fig 5.12).

5.5.1.2. Effect of concentration on H-bonding in C1

Along the same lines, 0.0048 g (0.005 mmol) of **C1** was dissolved in 0.5 ml of $CDCl_3$ in a NMR tube to make 10 mM solution of **C1**. The ^{1}H NMR of 10 mM solution was recorded at 25 ^{o}C and chemical shift of NH_2 protons was noted. Next, in the same NMR tube, another 0.0048 g (0.005 mmol) of **C1** (to make 20 mM solution of **C1**) was added and proton NMR was recorded. In similar manner, 30 mM, 40 mM, and 50 mM solution of **C1** was prepared and ^{1}H NMR was measured. Table 5.2 summarizes the change in chemical shift of NH and NH_2 protons of **C1** with increasing concentrations (Fig. 5.13).
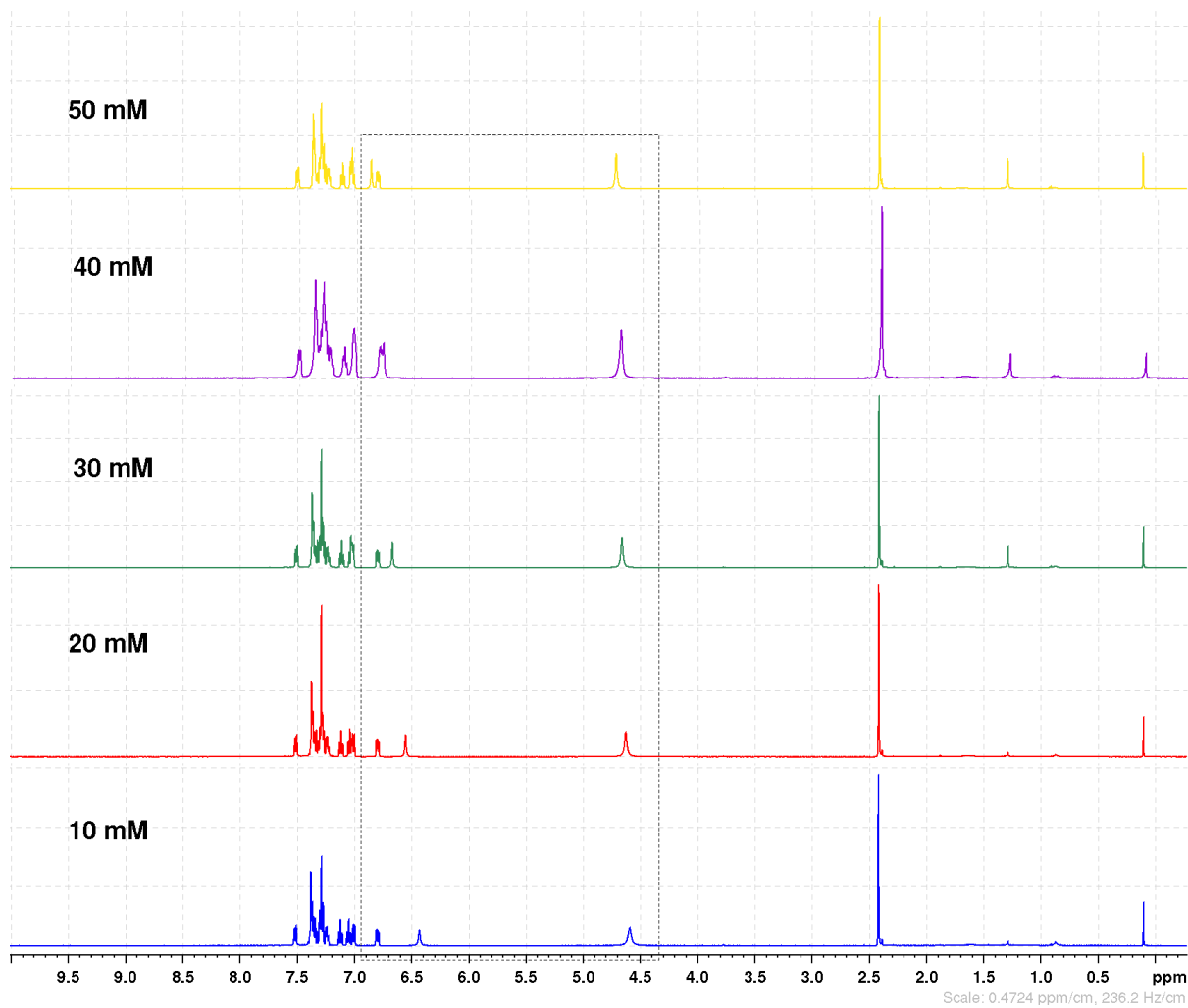
Figure 5.12: [^1]H NMR spectra of P-stereogenic supramolecular phosphine (**L1)** at different concentration.
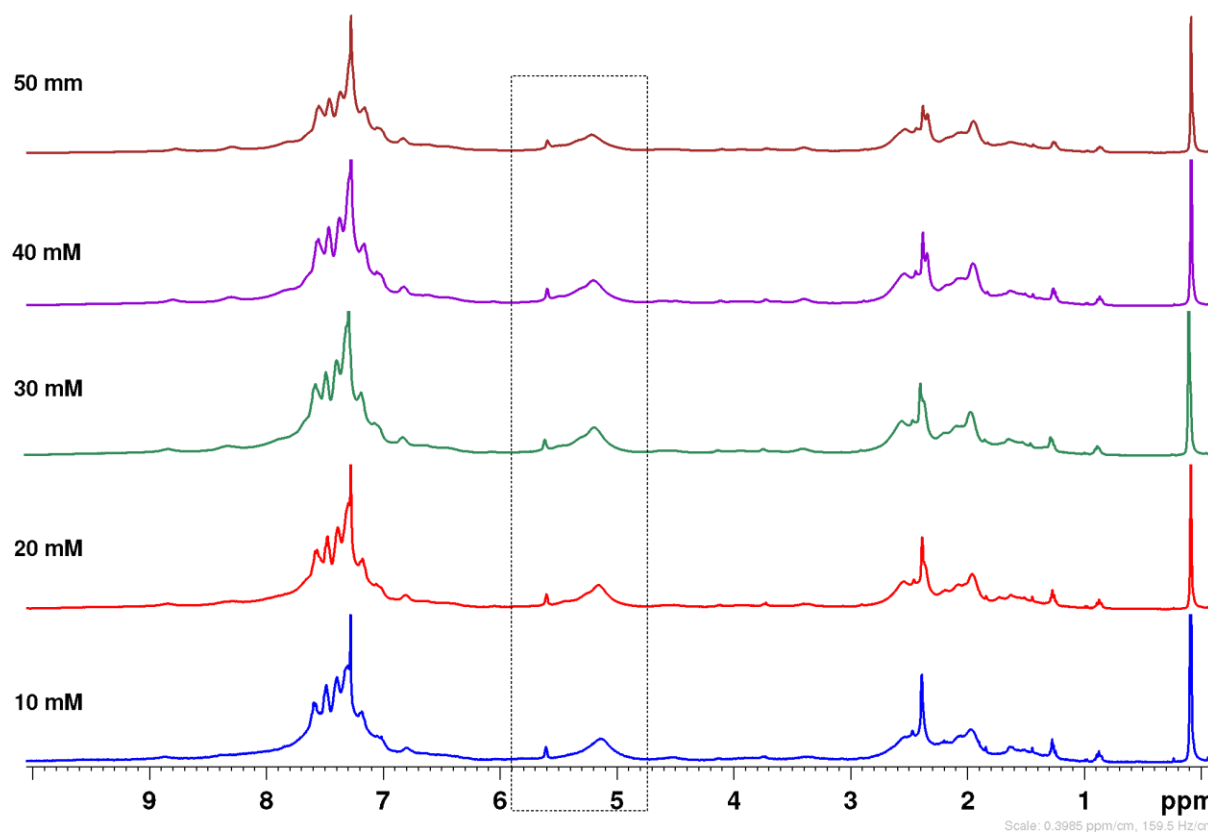
Figure 5.13: ^{1}H NMR spectra of self-assembled Rh-complex (**C1**) at different concentration.

5.5.1.3. Effect of temperature on H-bonding in L1

In a NMR tube, 0.0017 g (0.005 mmol) of **L1** was dissolved in 0.5 ml of $CDCl_3$ to make 10 mM solution. The ^{1}H NMR was measured at different temperature starting from 298 K to 293 K, 283 K, 273 K and 263 K. The change in chemical shift of the NH and NH_2 protons as a function of decreasing temperature is summarized in Table 5.3 (Fig. 5.14).

5.5.1.4. Effect of temperature on H-bonding in C1

Similarly, 0.0048 g (0.005 mmol) of **C1** was charged to the NMR tube which was then dissolved in 0.5 ml of $CDCl_3$ to make a 10 mM solution of **C1**. The ^{1}H NMR of this 10 mM solution was recorded at different temperatures starting from 298 K to 293 K, 283 K, 273 K and 263 K. There was hardly any change in the chemical shift of NH_2 proton as a function of decreasing temperature and Table 5.4 (Fig. 5.15).
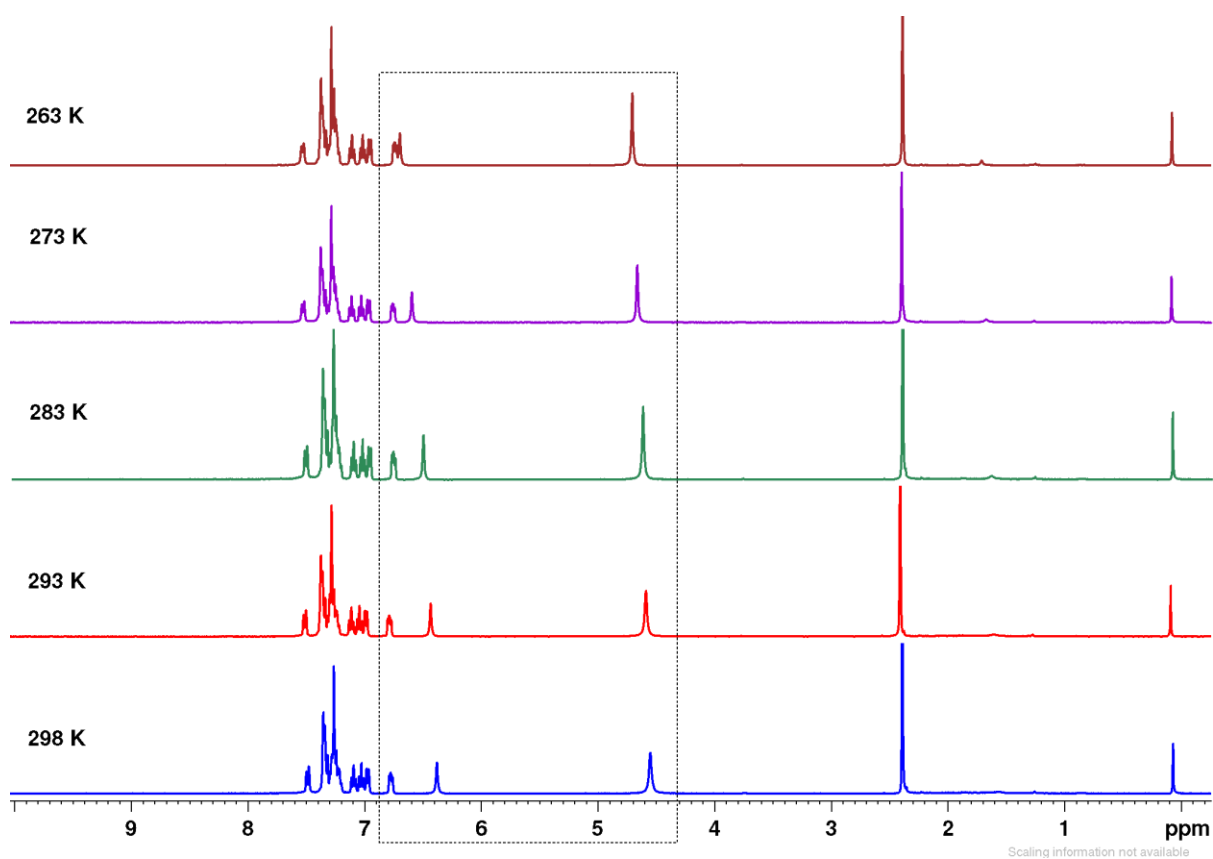
Figure 5.14: ^{1}H NMR spectra of **L1** at different tempreture.
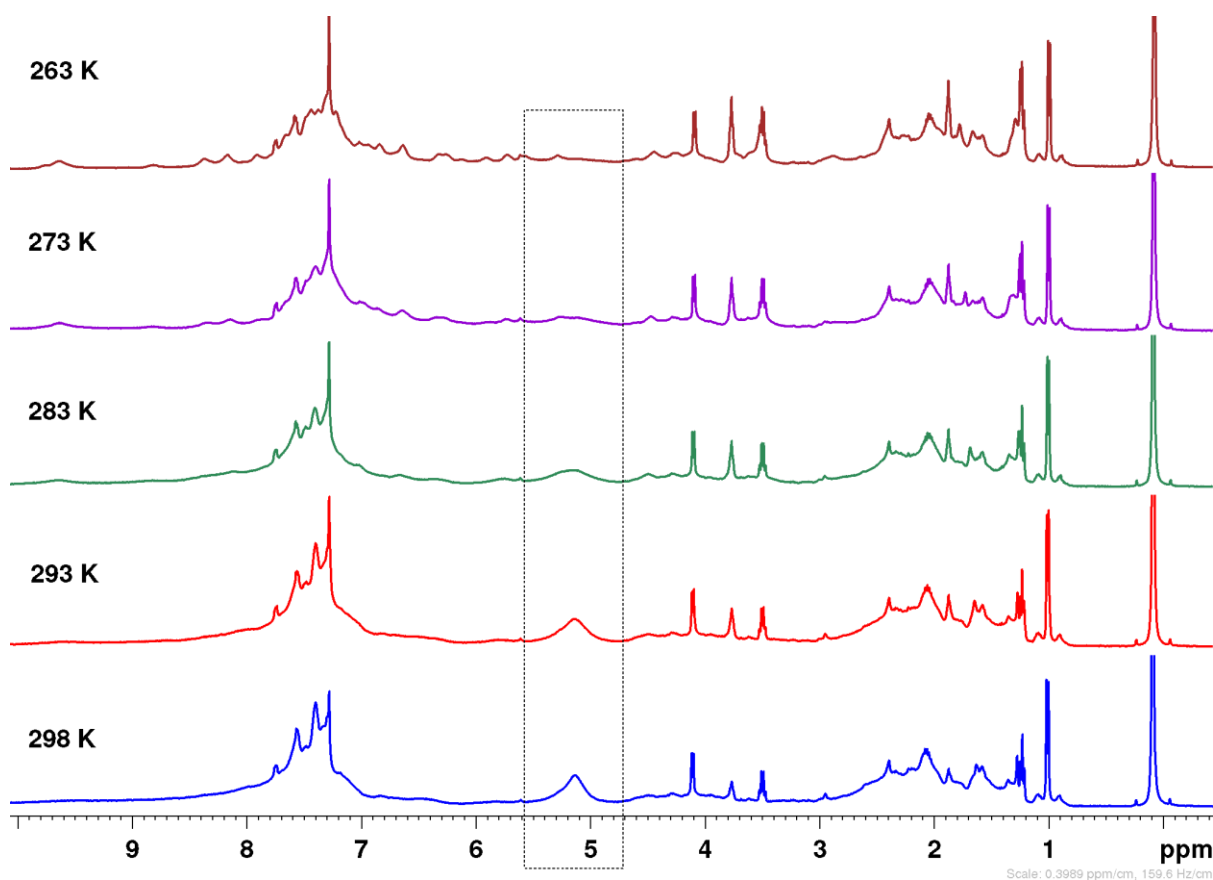
Figure 5.15: ^{1}H NMR spectra of **C1** at different tempreture.

5.5.2. Synthesis of deuterated supramolecular phosphine ligand (L1.D)

In a 50 ml Schlenk flask 0.136 g (0.4 mmol) of ligand **L1** was dissolved in 2 ml CD$_3$OD. The above reaction solution was stirred for 2.5 hours at room temperature. The progress of the exchange reaction was monitored by ^{1}H NMR (Fig. 5.17). After the reaction was complete, volatiles were evaporated under vacuum. The residue was dried under high vacuum and ^{1}H NMR was recorded in CDCl$_3$ (Fig. 5.17-5.19). ^{2}H NMR was recorded in 0.5 ml THF (THF-d$_8$:THF, 0.1:0.4 ml) (Fig. 5.16) and ESI-MS (+ve mode) was measured (Fig. 5.20).
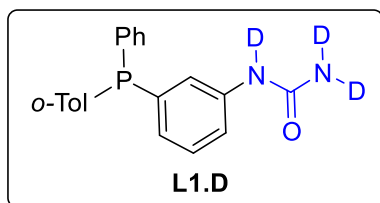
L1.D

^{2}H NMR (500 MHz, THF-d$_8$, 298 K): δ = 7.87 (s, *ND*), 5.45 (s, *ND$_2$*). **^{1}H NMR** (500 MHz, CDCl$_3$, 298 K): δ = 7.45 (d, *J* = 7.25 Hz, 1H, Ar), 7.33 (br. s., 3H, Ar), 7.16 - 7.30 (m, 5H, Ar), 7.04 - 7.14 (m, 2H, Ar), 6.97 (t, *J* = 6.87 Hz, 1H, Ar), 6.74 - 6.84 (m, 1H, Ar), 4.85 (d, *J* = 5.34 Hz, 0.80H, *NH*), 2.39 (s, 3H, *CH$_3$*). **^{13}C NMR** (126 MHz, CDCl$_3$, 298 K): δ = 156.6 (s, *CO*), 142.3 (s, Ar), 142.1 (s, Ar), 138.7 (t, *J* = 7.7 Hz, Ar), 137.7 (d, *J* = 10.5 Hz, Ar), 135.9 (d, *J* = 10.4 Hz, Ar), 135.5 (d, *J* = 11.5 Hz, Ar), 133.5 (d, *J* = 20.1 Hz, Ar), 132.7 (s, Ar), 130.4 (s, Ar), 130.1 (d, *J* = 4.8 Hz, Ar), 129.4 (d, *J* = 7.6 Hz, Ar), 129.2 (d, *J* = 18.2 Hz, Ar), 128.8 (d, *J* = 8.5 Hz, Ar), 128.6 (d, *J* = 6.6 Hz, Ar), 126.0 (s, Ar), 125.4 (d, *J* = 20.9 Hz, Ar), 120.5 (d, *J* = 20.4 Hz, Ar), 21.1 (d, *J* = 21.1 Hz, *CH$_3$*). **^{31}P NMR** (500 MHz, CDCl$_3$, 298 K): δ = -13.00. **ESI-MS** (+ve) (For M = C$_{20}$H$_{19}$N$_2$OP) m/z = 335.13 [M+H]$^+$.
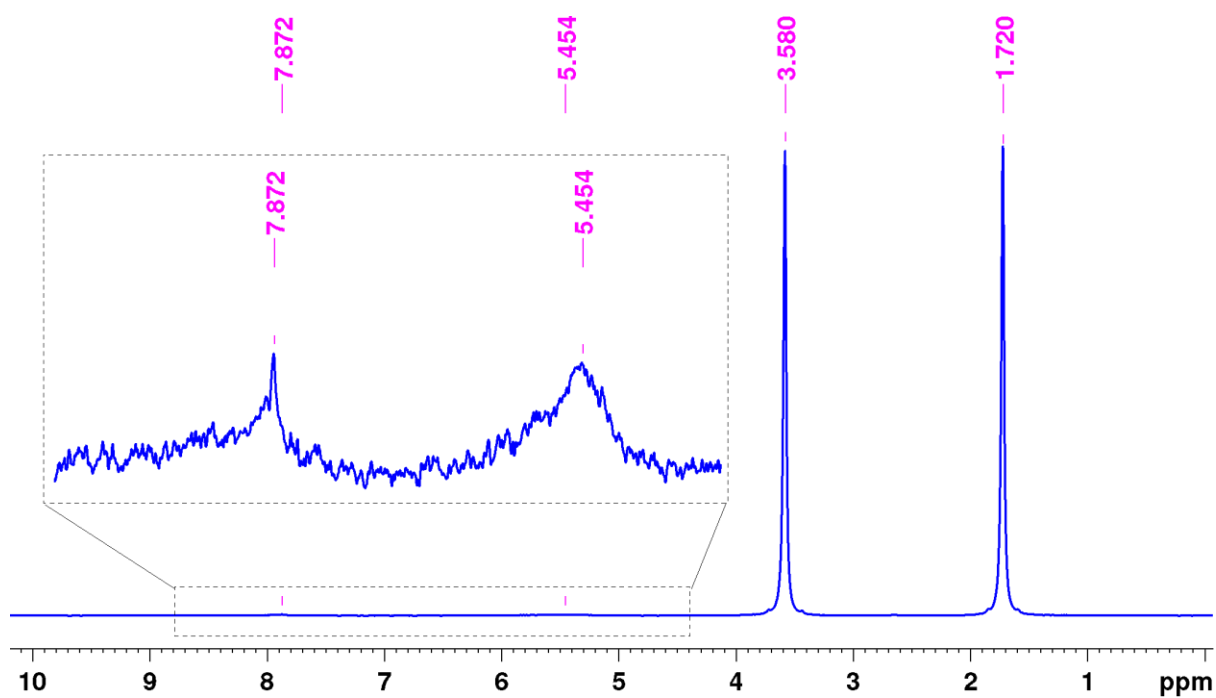
Figure 5.16: ^{2}H NMR spectrum of **L1.D** in THF-D$_8$:THF (0.1:0.4 ml) solvent.
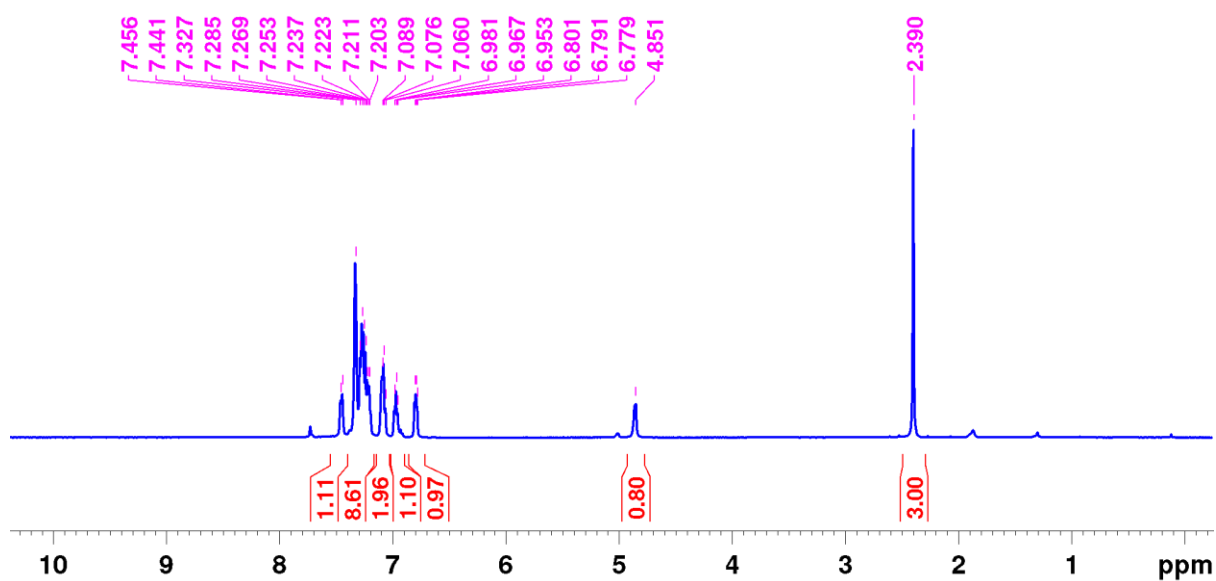
Figure 5.17: ^{1}H NMR spectrum of **L1.D** in CDCl$_3$.
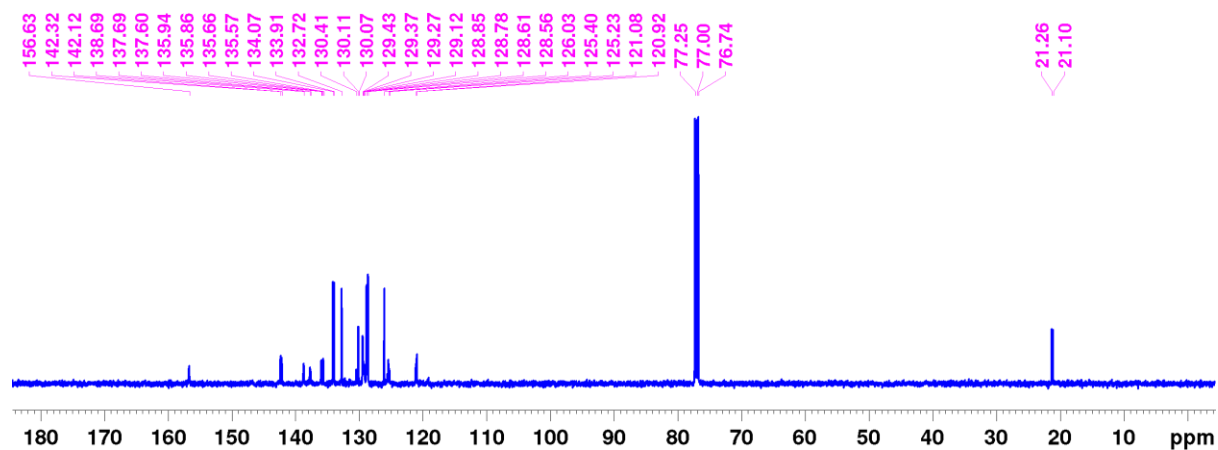
Figure 5.18: ^{13}C NMR spectrum of **L1.D** in CDCl$_3$.
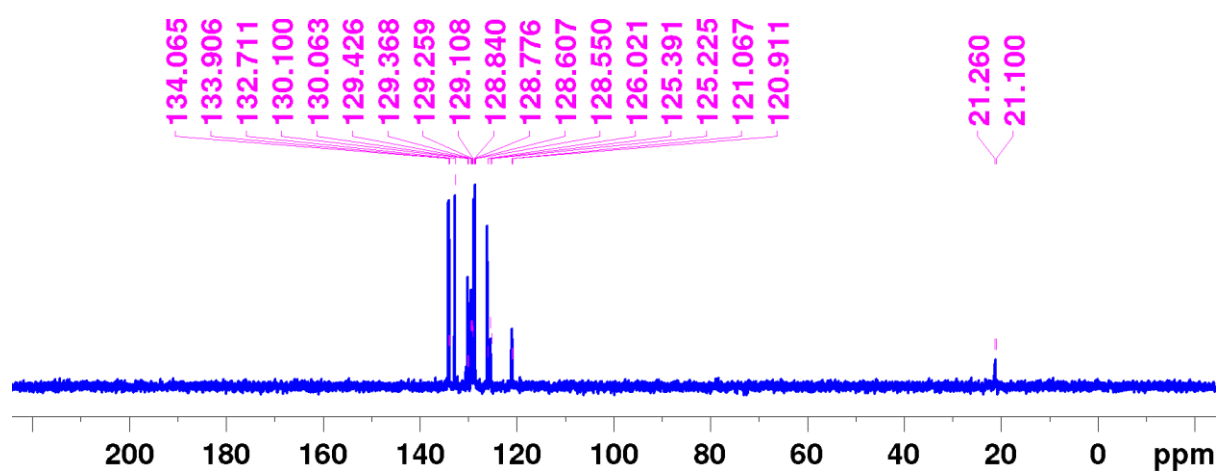
Figure 5.19: ^{13}C NMR (DEPT) spectrum of **L1.D** in CDCl$_3$.
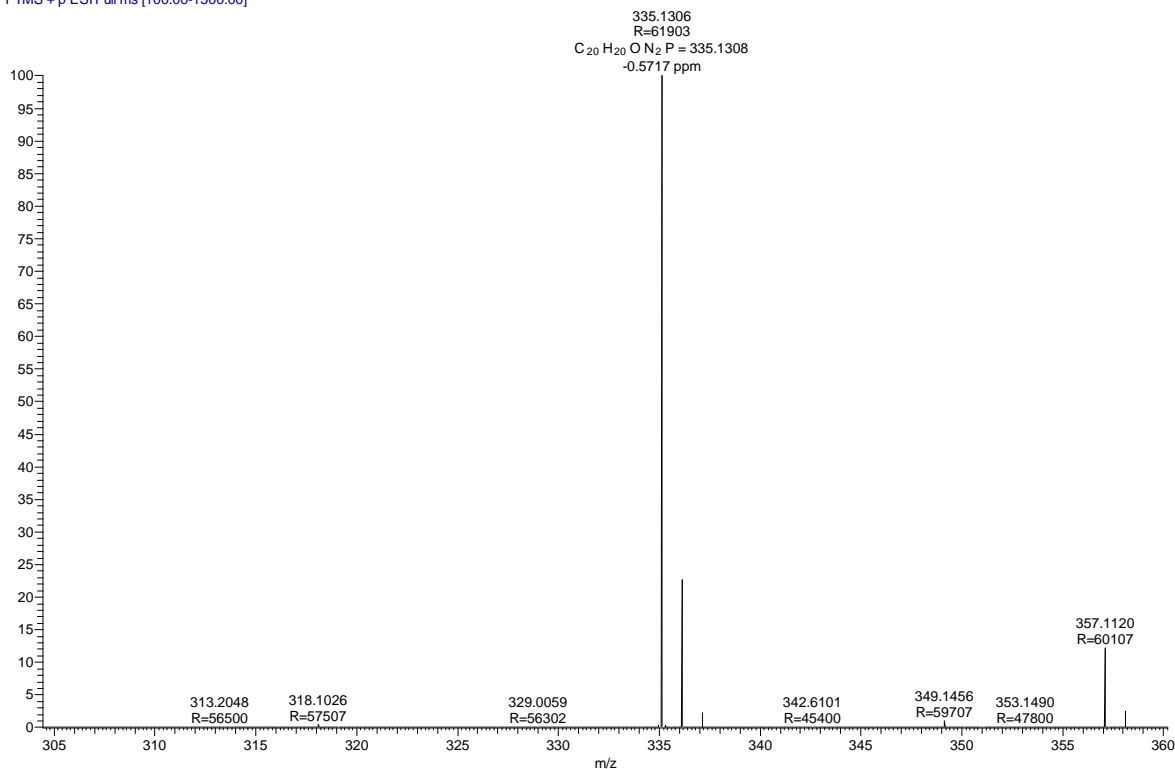
Figure 5.20: ESIMS (+ve mode) spectrum of **L1.D**.

5.5.3. Synthesis of deuterated self-assembled Rh-complex (C1.D)

In a vacuum dried Schlenk flask [Rh(COD)$_2$BF$_4$] (1 eqv., 0.0985 mmol) and phosphine ligand **L1.D** (2 eq., 0.1974 mmol) was taken inside the glove box. The above mixture was dissolved in 8 ml DCM and reaction content was stirred for 2 hours at room temperature. After completion of reaction, the reaction content was evaporated and concentrated to 2 ml. 20 ml diethyl ether was added to above content to obtain yellow coloured precipitate. The resultant solid was separated by cannula filtration, washed with diethyl ether (10 ml x 3 ml) and dried under vacuum. The resultant residue was identified as **C1.D** after complete characterization (Fig 5.21-5.25).

^{2}H NMR (500 MHz, THF-d$_8$, 298 K): δ = 8.29 (s, *ND*), 5.55 (s, *ND$_2$*). **^{1}H NMR** (400 MHz, CDCl$_3$, 298 K): δ = 8.23-6.00 (m 26H, Ar), 5.75-4.95 (m, 5H, *CH*), 2.90-2.14 (m, 8H, *CH$_2$*), 2.14 (m, 6H, *CH$_3$*). **^{13}C NMR** (101 MHz, CDCl$_3$, 298 K): δ = 157.3 (s, *CO*), 156.8 (s, *CO*), 142.8 (s, Ar), 141.7 (s, Ar), 140.1 (s, Ar), 139.6 (s, Ar), 132.6 (s, Ar), 132.2 (s, Ar), 131.7 (s, Ar), 131.6 (s, Ar), 130.5 (s, Ar), 130.0 (s, Ar), 128.6 (s, Ar), 126.0 (s, Ar), 125.6 (s, Ar), 125.4 (s, Ar), 123.0 (s, Ar), 121.6 (s, Ar), 118.7 (s, *CH*), 104.4 (s, *CH*), 65.7 (s, *CH$_2$*), 47.2 (s, *CH$_2$*), 32.6 (s, *CH$_2$*), 27.9 (s, *CH$_2$*), 23.5 (s, *CH$_3$*), 21.5 (s, *CH$_3$*). **^{31}P NMR** (500 MHz, CDCl$_3$,

298 K): δ = 19.04 (d, J_{Rh-P} = 140 Hz). **ESI-MS** (+ve) (For M = $C_{48}H_{50}N_4O_2P_2Rh$) m/z = 879.24 [M]$^+$.
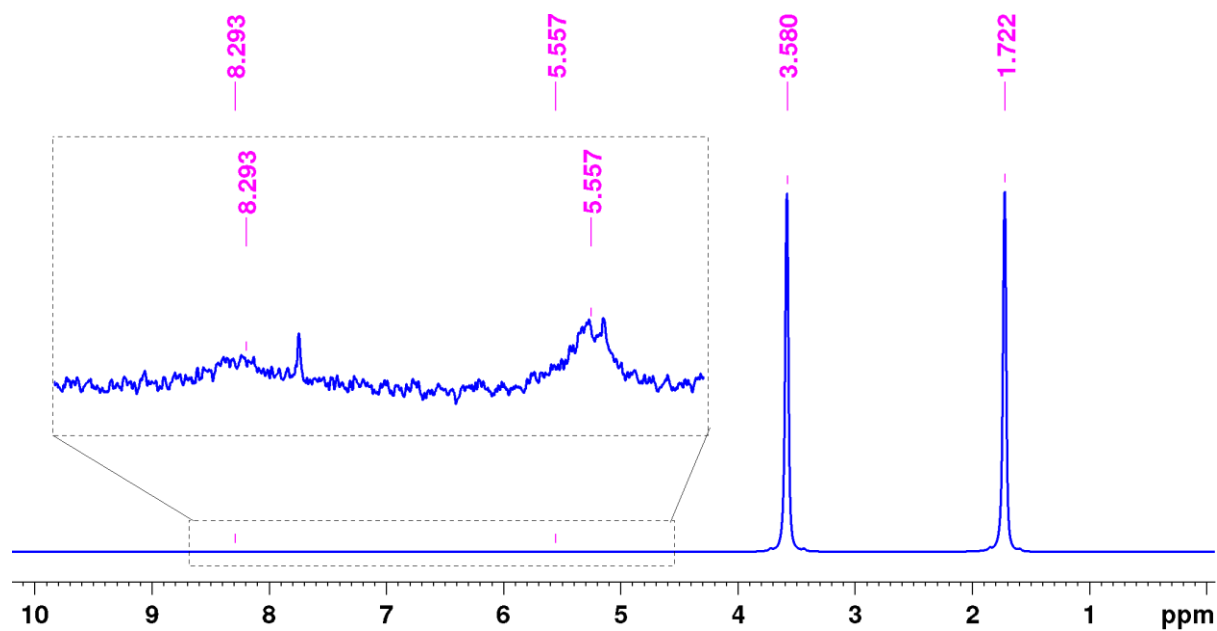
Figure 5.21: ^{2}H NMR spectrum of **C1.D** in THF-D$_8$:THF (0.1:0.4 ml) solvent.
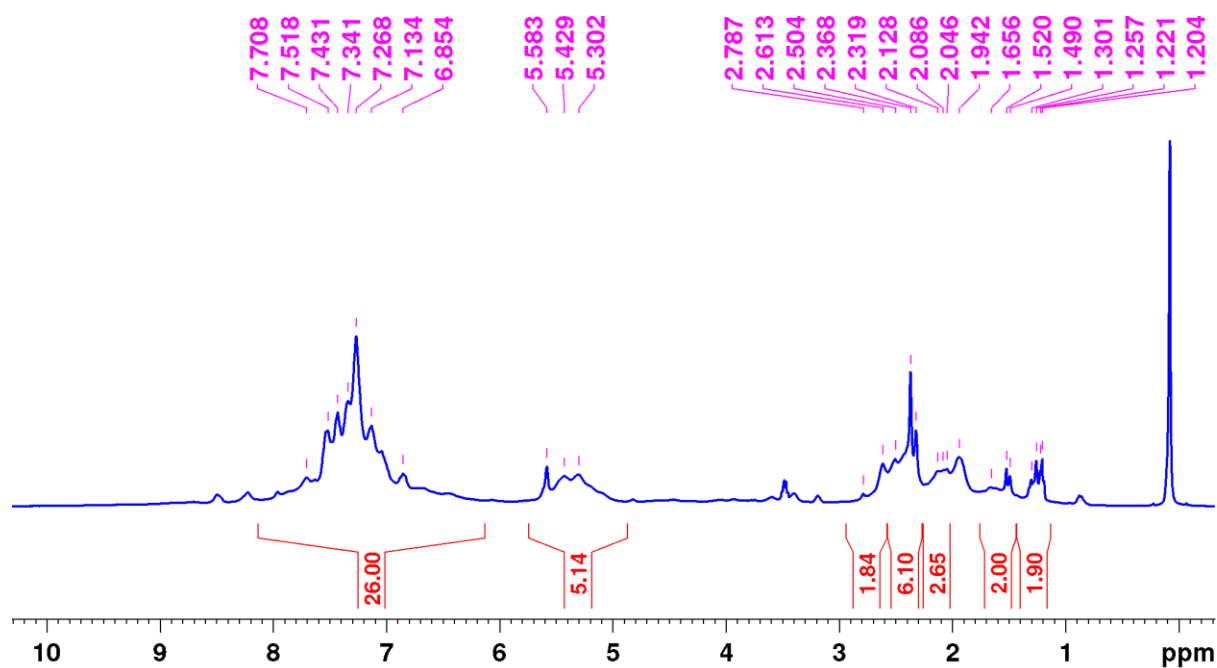
Figure 5.22: ^{1}H NMR spectrum of **C1.D** in CDCl$_3$.
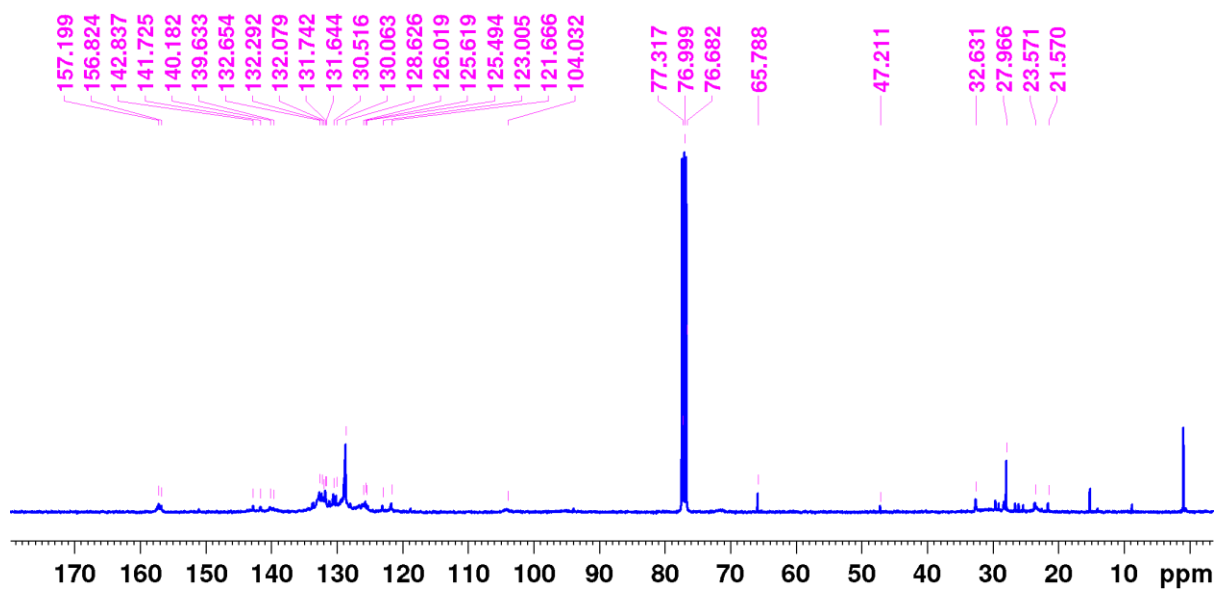
Figure 5.23: ^{13}C NMR spectrum of **C1.D** in CDCl$_3$.
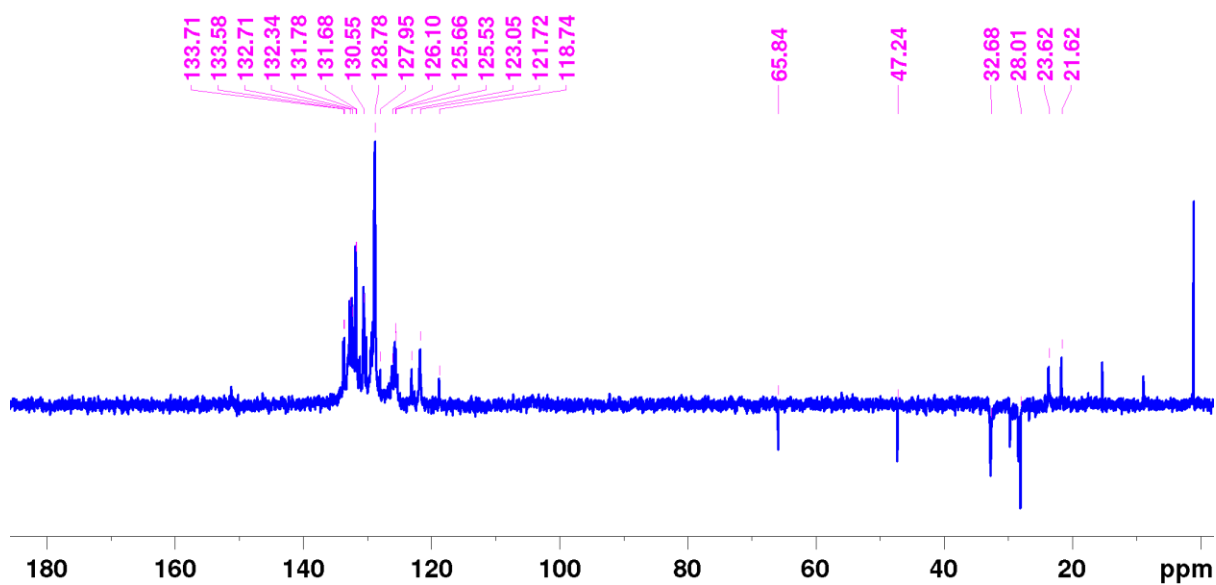
Figure 5.24: ^{13}C NMR (DEPT) spectrum of **C1.D** in CDCl$_3$.
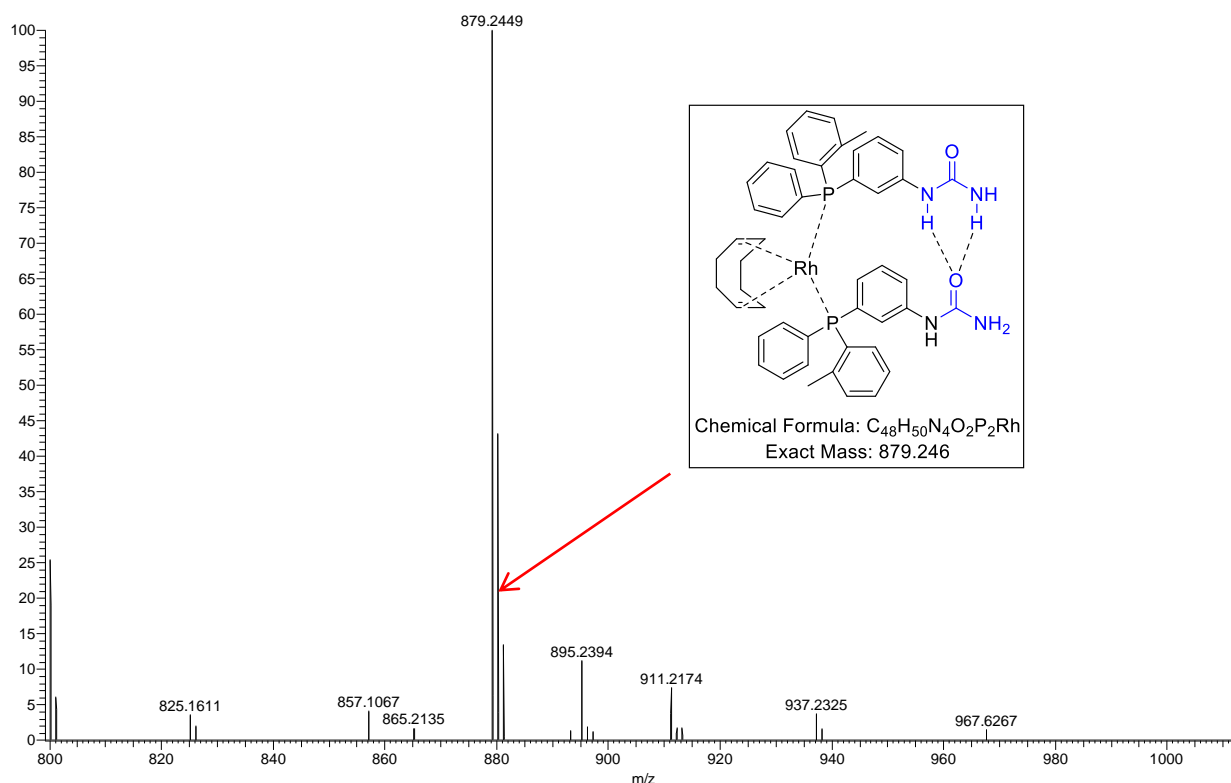
Figure 5.25: ESIMS (+ve mode) spectrum of **C1.D**.

5.5.4. Stoichiometric study of self-assembled Rh-complex and S2

In the NMR tube **C1** (0.0048 g, 0.005 mmol) was dissolved in CD_3CN to make 10 mM solution. The NH_2 proton chemical shift was confirm by ^1H NMR (Fig. 5.26). In the same NMR tube **S2** 0.010 g, 0.005 mmol was added and ^1H NMR was measured (Fig. 5.26). Similar experiment was done with deuterium labelled self-assembled Rh-complex (**C1.D**) and **S2**, and ^2H NMR was recorded in THF-d_8:THF (0.1:0.4 ml) solvent.
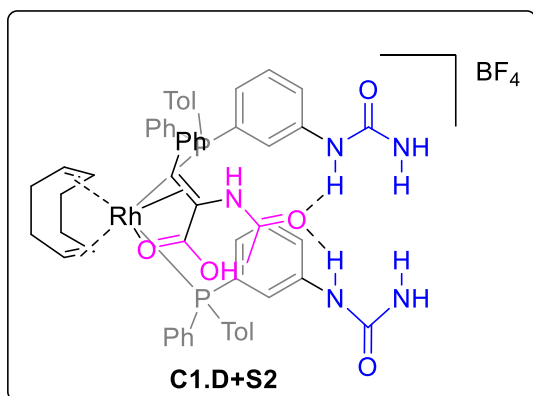
For this experiment deuterium labeled self-assembled Rh-complex **C1.D** (0.0048 g, 0.005 mmol) was dissolved in THF-d_8:THF (0.1:0.4 ml) to prepare 10 mM solution and ^2H NMR was measured to confirm the chemical shift of ND and ND_2 (Fig. 5.21). After that **S2** (0.010 g, 0.005 mmol) was added in the same NMR tube and ^2H NMR was recorded (Fig. 5.28).

^2H **NMR** (500 MHz, THF-d_8, 298 K) δ = 8.45 (s, *ND*), 5.61 (s, *ND$_2$*). ^1H **NMR** (400 MHz, CD$_3$CN, 298 K) δ = 7.81-7.10 (m, 33H, Ar and *NH*), 5.10-4.10 (m, 9H, *CH* and

NH₂), 2.41 (m, 4H, *CH₂*), 2.12 (m, 9H, *CH₃*), 1.53 (m, 2H, *CH₂*), 1.27 (m, 2H, *CH₂*).

ESI-MS (+ve) (For $C_{59}H_{55}D_4LiN_5NaO_5P_2Rh$) m/z = 1116.24 [M]$^+$.
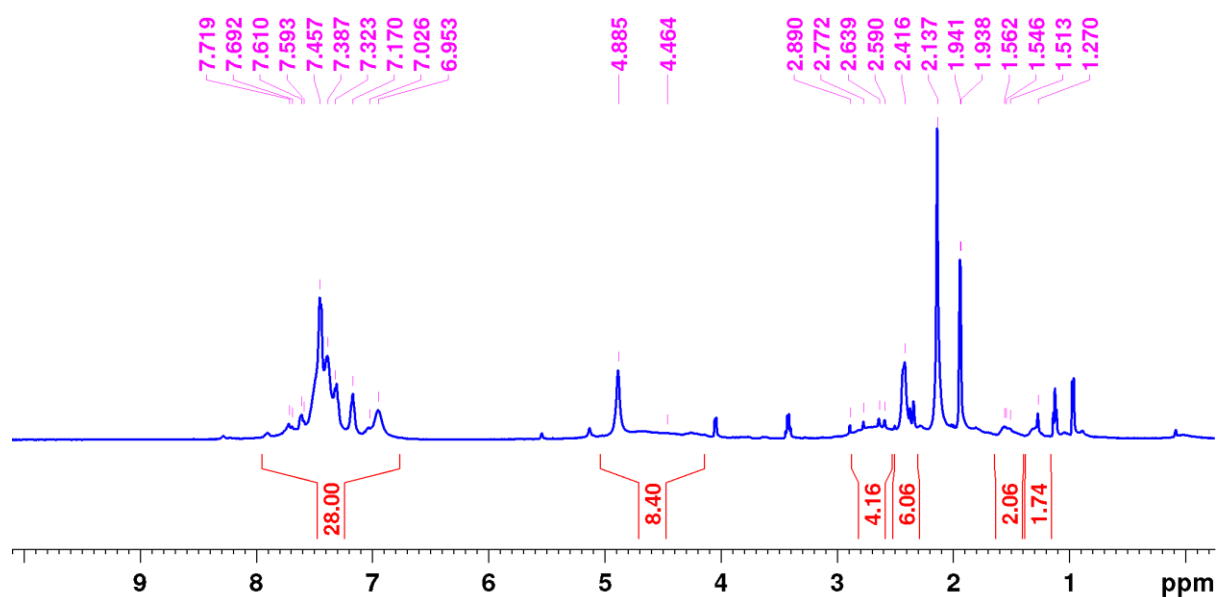
Figure 5.26: ^{1}H NMR spectrum of **C1** in CD$_3$CN.
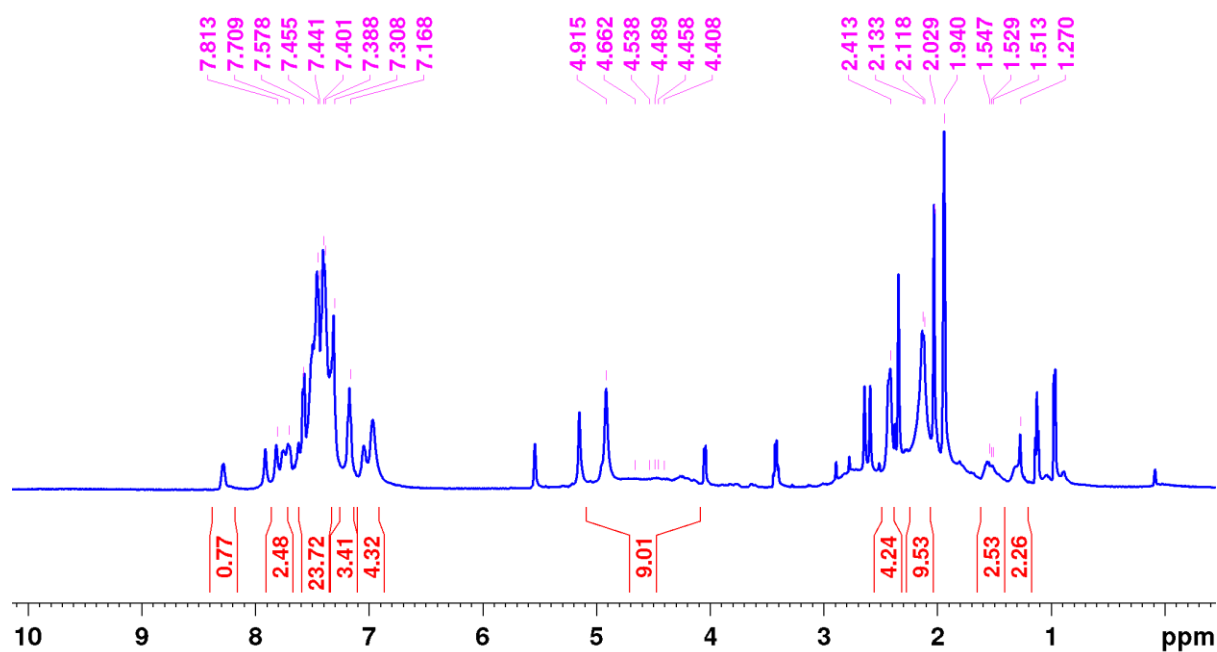
Figure 5.27: ^{1}H NMR spectrum of self-assembled Rh-complex **C1-S2** in CD$_3$CN.
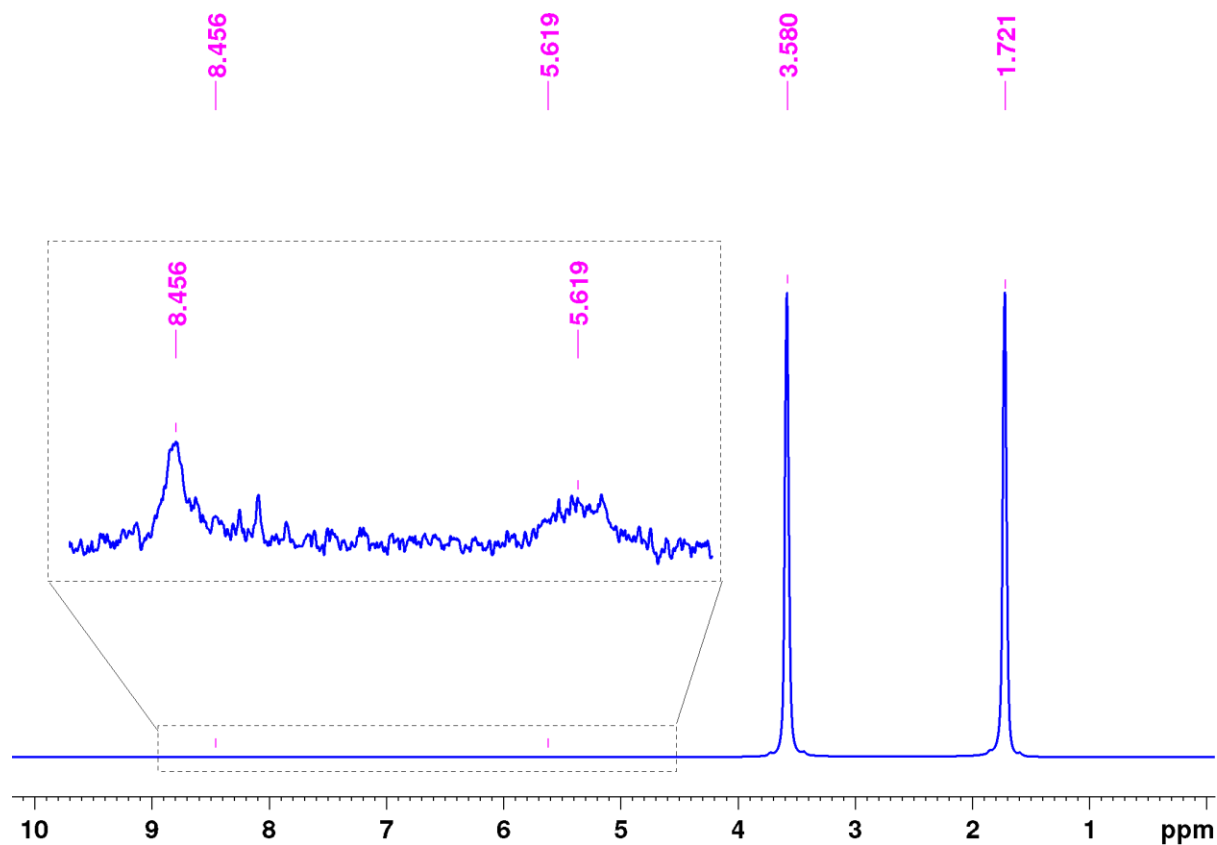
Figure 5.28: ²H NMR spectrum of **C1.D-S2** in THF-D₈:THF (0.1:0.4 ml) solvent.
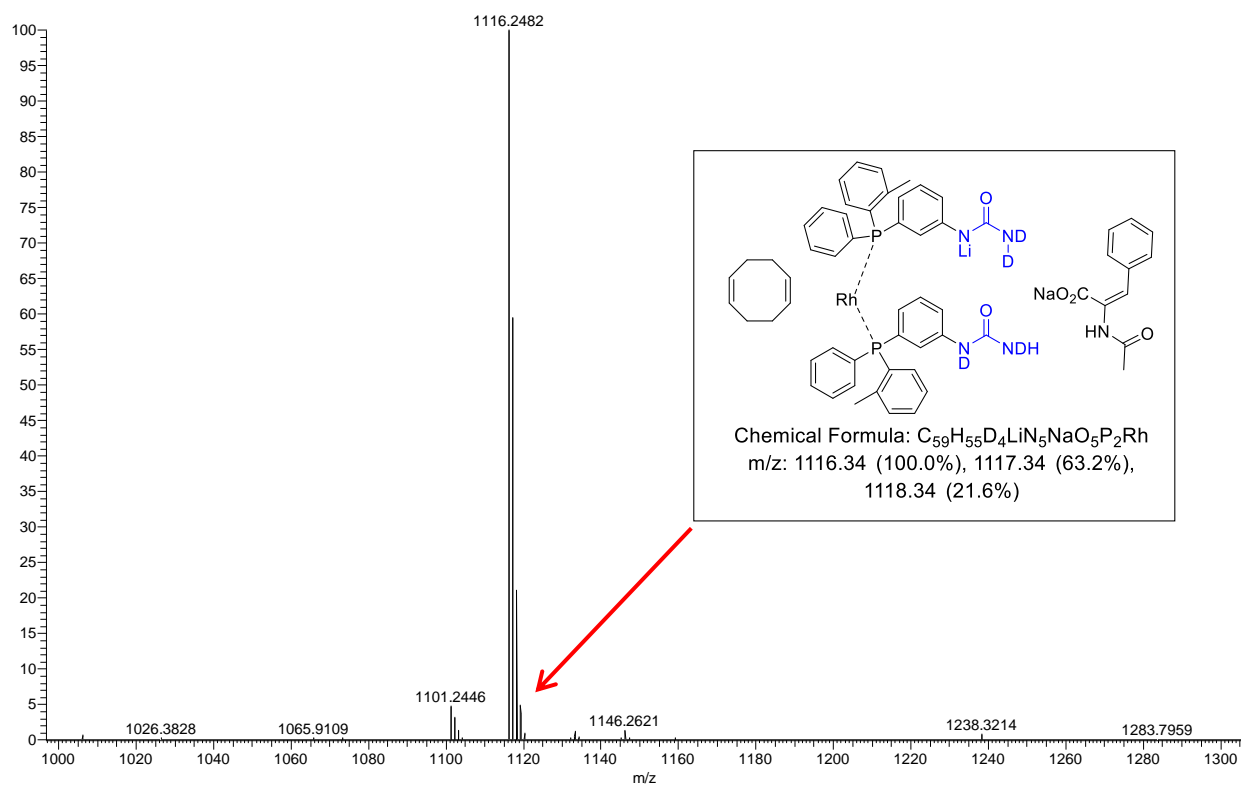
Figure 5.29: ESI-MS (+ve mode) spectrum of **C1.D-S2**.

5.6. References

1 a) T. C. Nugent, *Chiral Amine Synthesis: Methods, Developments and Applications, Wiley-VCH, Weinheim*, 2010; b) W. Zhang and X. Zhang *in Comprehensive Chirality* (Eds.: E. M. Carreira and H. Yamamoto)*, Elsevier, Amsterdam*, 2012, pp. 301– 317; c) J. H. Xie, S. F. Zhu and Q. L. Zhou, *Chem. Rev*. 2011, **111**, 1713–1760; d) T. C. Nugent and M. El-Shazly, *Adv. Synth. Catal*., 2010, **352**, 753–819; e) Z. Yu, W. Jin and Q. Jiang, *Angew. Chem.,* 2012, **124**, 6164–6177; *Angew. Chem. Int. Ed*., 2012, **51**, 6060– 6072.

2 a) W. S. Knowles, *Asymmetric Catalysis in Organic Synthesis; Wiley-Interscience: New York*, 1994; b) H. U. Blaser, E. Schmidt, *In Asymmetric Catalysis on Industrial Scale, Challenges, Approaches, and Solutions; Eds.; Wiley-VCH: Weinheim, Germany,* 2004, pp23−38.

3 P. W. N. M. Van Leeuwen, P. C. J. Kamer, C. Claver, O. Pamies and M. Dieguez, *Chem. Rev*., 2011, **111**, 2077-2118.

4 a) For a review on asymmetric hydrogenation, see: C. Margarita and P. G. Andersson, *J. Am. Chem. Soc.,* 2017, **139**, 1346-1356; b) For a review on asymmetric hydroformylation, see: S. H. Chikkali, J. I. van der Vlugt and J. N. H. Reek, *Coord. Chem. Rev*., 2014, **262**, 1-15; c) for bimetallic catalysts in hydrogenation and hydroformylation, see: D. G. H. Hetterscheid, S. H. Chikkali, B. de Bruin and J. N. H. Reek, *ChemCatChem*, 2013, **5**, 2785-2793.

5 A. J. Sandee and J. N. H. Reek, *Dalton Trans*., 2006, 3385–3391; b) B. Breit, *Angew. Chem. Int. Ed*., 2005, **44**, 6816–6825.

6 M. Weise, C. Waloch, W. Seiche and B. Breit, *J. Am. Chem. Soc*., 2006, **128**, 4188-4189.

7 B. Breit and W. Seiche, *J. Am. Chem. Soc*., 2003, **125**, 6608-6609.

8 P. Dydio and J. N. H. Reek, *Chem. Sci*., 2014, **5**, 2135-2145.

9 P. Dydio, R. J. Detz, B. Bruin and J. N. H. Reek, *J. Am. Chem. Soc.,* 2014, **136**, 8418−8429.

10 a) J. Meeuwissen and J. N. H. Reek, *Nat. Chem*., 2010, **2**, 615-621; b) J. Weiland and B. Breit, *Nat. Chem*., 2010, **2**, 832-837.

11 For a review on introducing selectivity via supramolecular chemistry, see: S. H. A. M. Leenders, R. Gramage-Doria, B. de Bruin and J. N. H. Reek, *Chem. Soc. Rev*., 2015, **44**, 433-448.

12 P. R. Breuil, F. W. Patureau and J. N. H. Reek, *Angew. Chem. Int. Ed*., 2009, **48**, 2162 –2165.

13 a) M. Sawamura and Y. Ito, *Chem. Rev*., 1992, **92**, 857-871; b) Y. Park, K. C. Harper, N. Kuhl, E. E. Kwan, R. Y. Liu and E. N. Jacobsen, *Science*, 2017, **355**, 162-166.

14 S. M. Inamdar, A. Konala and N. T. Patil, *Chem. Commun*., 2014, **50**, 15124-15135.

15 a) T. Smejka and B. Breit, *Angew. Chem. Int. Ed*., 2008, **47**, 3946–3949; b) D. Fuchs, G. Rousseau, L. Diab, U. Gellrich and B. Breit, *Angew. Chem. Int. Ed.,* 2012, **51**, 2178–2182.

16 I. Usui, S. Schmidt, M. Keller and B. Breit, *Org. Lett*., 2008, **10**, 1207-1210.

17 a) U. Gellrich, W. Seiche, M. Keller and B. Breit, *Angew. Chem. Int. Ed.*, 2012, **51**, 11033-11038; b) L. Diab, U. Gellrich and B. Breit, *Chem. Commun*., 2013, **49**, 9737-9739.

18 P. Li, X. Hu, X. Dong and X. Zhang, *Chem. Commun*., 2016, **52**, 11677-11680.

19 U. Gellrich, J. Huang, W. Seiche, M. Keller, M. Meuwly, and B. Breit, *J. Am. Chem. Soc*., 2011, **133**, 964–975.

20 I. A. Shuklov, N. V. Dubrovina, E. Barsch, R. Ludwig, D. Michalika and A. Borner, *Chem. Commun.*, 2009, 1535–1537.

21 a) V. S. Koshti, S. R. Gaikwad and S. H. Chikkali, *Coord. Chem. Rev.*, 2014, **265**, 52−73; b) V. S. Koshti, S. H. Thorat, R. P. Gote, S. H. Chikkali and R. G. Gonnade, *CrystEngComm*, 2016, **18**, 7078-7094; b) K. Patel, S. S. Deshmukh, D. Bodkhe, M. Mane, K. Vanka, D. Shinde, P. R. Rajamohanan, S. Nandi, R. Vaidhyanathan and S. H. Chikkali, *J. Org. Chem.*, 2017, **82**, 4342-4351.

22   V. S. Koshti, N. R. Mote and S. Chikkali, *Organometallics*, 2015, **34**, 4802.

23 a) S. H. Chikkali, R. Bellini, B. de Bruin, J. I. van der Vlugt and J. N. H. Reek, *J. Am. Chem. Soc.*, 2012, **134**, 6607-6616; b) S. H. Chikkali, R. Bellini, G. Berthon-Gelloz, J. I. Van der Vlugt, B. de Bruin and J. N. H. Reek, *Chem. Commun.*, 2010, **46**, 1244-1246.

24 Similar change in chemical shift was encountered by Reek and co-workers, see: A. J. Sandee, A. M. van der Burg and J. N. H. Reek, *Chem. Commun.*, 2007, 864-866.

25 This observation is in line with previous reports, see: J. Meeuwissen, R. Detz, A. J. Sandee, B. de Bruin, M. A. Siegler, A. L. Spek and J. N. H. Reek, *Eur. J. Inorg. Chem.*, 2010, **19**, 2992-2997.

26 a) I. A. Shuklov, N. V. Dubrovina, E. Barsch, R. Ludwig, D. Michalik and A. Boerner, *Chem. Commun.*, 2009, 1535-1537; b) U. Boas, S. H. M. Soentjens, K. J. Jensen, J. B. Christensen and E. W. Meijer, *ChemBioChem*, 2002, **3**, 433-439.

27 CD$_3$OD, CD$_3$COOD, D$_2$O are commonly used for exchanging NH protons to ND, see: a) G. S. Coumbarides, J. Eames, M. J. Suggate and N. Weerasooriya, *J Label Compd Radiopharm*, 2006, **49**, 641-652; b) B. Weber, W. Bauer, T. Pfaffeneder, M. M. Dirtu, A. D. Naik, A. Rotaru and Y. Garcia, *Eur. J. Inorg. Chem.,* 2011, 3193-3206.

28 D. D. Perrin, W. L. Armarego and L. F. Willfred, *Purification of Laboratory Chemicals, Pergamon, Oxford*, 1988.

Chapter 6

Summary and Outlook

6.1. Summary

This Ph.D. thesis entitled as "**Catalytic synthesis of P-chiral supramolecular phosphines, their self-assembled metal complexes and implication in asymmetric catalysis**" consists of five chapters. Over the past five years, we initiated a new research effort to understand the role of bidentate chiral phosphine ligands in metal catalysis. The bidentate phosphine ligands coordinate with metal from two sides to yield stable metal complex. The effect of chelation in metal catalysis plays an important role and governs the activity. Although bidentate ligands play important role in metal catalysis but the synthesis of such type of bidentate phosphine ligands requires 5-7 synthetic steps which is time-consuming and tedious. To overcome this problem monodentate supramolecular phosphine ligands were introduced which require one-two step synthesis (explained in chapter 1). Due to the hydrogen bonding interactions between monodentate supramolecular phosphines ligands, the resultant complex mimics the bidentate ligand coordination. Thus last decade witnessed the emergence of C-chiral and axially chiral supramolecular phosphine ligands and their performance in various asymmetric transformations have been reported. However, synthesis of supramolecular ligands with chirality on phosphorous is a challenge. If P-chiral supramolecular phosphines ligands are made accessible these would address the following challenges.
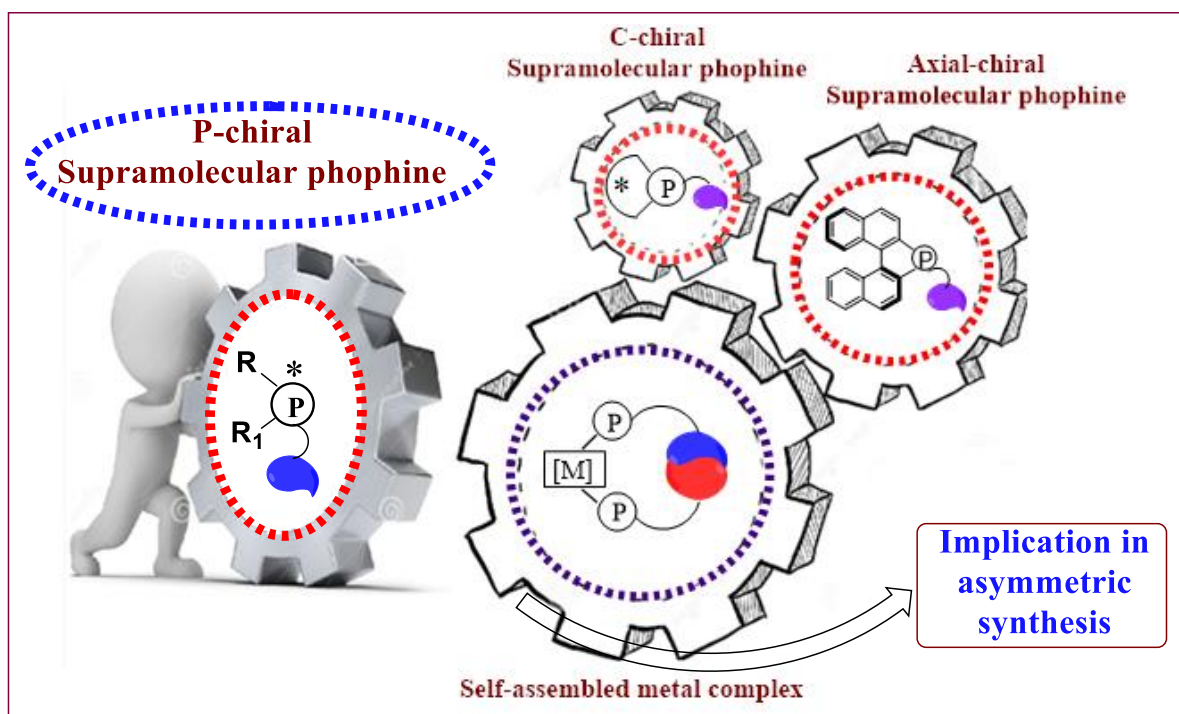
a) The chirality would be just next to the metal center, which can be effectively transferred to the product in catalysis. b) The monodentate P-chiral supramolecular phosphines would self-assemble, circumventing the tedious synthesis. As stated by the Noble laureate Prof. W. S.

Knowles, "*The asymmetry would have to be directly on the phosphorus. That is where the action is.*" Therefore, synthesis of ligands with chirality on phosphorus would be highly desirable. There are challenges such as phosphines are air and moisture sensitive and we wanted hydrogen bonding motif in the same molecule. Secondly, room temperature is enough for inversion of phosphine. So it will difficult to hold chirality on phosphorous while handling at room temperature during the reaction workup and purification. We took up this challenge and put efforts to resolve it by tailoring various reaction parameters.

Chapter 2; we have reported the catalytic asymmetric synthesis of a new class of P-stereogenic supramolecular phosphines for the first time. An isolated Pd-Me-DuPHOS complex catalyzes asymmetric phosphination of urea substituted aryl-halides and secondary phosphines to produce the corresponding C-P coupling products. Judicious selection of substrate and tuning of reaction parameters led to an unprecedented enantioselectivity of 97% in P-chiral supramolecular phosphine; along with significant conversion (65%). Preliminary mechanistic investigations failed to spot Pd(0)-species; whereas spectroscopic observation of a phosphido-intermediate suggests that the phosphination reaction most likely proceeds via oxidative addition step followed by reductive elimination step.

Chapter 3; inspired by our preliminary report, we explored the synthesis of [Pd-((*S,S*)Me-FerroLANE)(*m*-phenylurea)(I)] complex from *(S)*Me-FerroLANE and [Pd-(TMEDA)(*m*-phenylurea)(I)] precursor. Two doublets in ^{31}P NMR and ^{1}H NMR data suggested the formation of [Pd-((*S,S*)Me-FerroLANE)(*m*-phenylurea)(I)] which was isolated in 68% yield. Indeed, the rationally designed [Pd-((*S,S*)Me-FerroLANE)(*m*-phenylurea)(I)] was found to accelerate the reaction to completion within 18 hours. It is most likely that the electron-rich nature and wide *bite* angle offered by Me-FerroLANE is responsible for the improved performance of [Pd-((*S,S*)Me-FerroLANE)(*m*-phenylurea)(I)]. The thus obtained [Pd-((*S,S*)Me-FerroLANE)(*m*-phenylurea)(I)] was screened to optimize reaction conditions for a P-C coupling reaction. Sodium acetate in a polar solvent (DMF) was found to be the optimal combination. A P-C coupling reaction was typically carried out at -3.5 °C for 18 hours. A library of 22 P-stereogenic supramolecular phosphine ligands was synthesized using [Pd-((*S,S*)Me-FerroLANE)(*m*-phenylurea)(I)]. The mesityl phenyl phosphine revealed the highest enantiomeric excess of 58% along with the excellent conversion of 99%.

Chapter 4; we have applied cheap and earth-abundant nickel in the synthesis of P-stereogenic (supramolecular) phosphine. Synthesis of [Ni-((*S,S*)Me-FerroLANE)(phenyl)(I)] from *(S)*Me-FerroLANE with [Ni-(di(triphenylphosphine))(phenyl)(I)] precursor was

achieved. The resultant [Ni-((*S,S*)Me-FerroLANE)(phenyl)(I)] was characterized by ^{1}H, ^{13}C, ^{31}P NMR, and Mass spectroscopy and the identity was fully established. The prepared [Ni-((*S,S*)Me-FerroLANE)(phenyl)(I)] was screened to optimize reaction conditions for the P-C coupling reaction. Indeed, the rationally designed [Ni-((*S,S*)Me-FerroLANE)(phenyl)(I)] was found to accelerate the enantiomeric excess to 99% along with the moderate conversion of 51%.

Chapter 6; the thus prepared enantio-enriched 1-(3-(phenyl(o-tolyl)phosphanyl)phenyl)urea self-assembles upon simple mixing with [Rh(COD)$_2$BF$_4$] to form rhodium complex. When 1-(3-(phenyl(o-tolyl)phosphanyl)phenyl)urea with [Rh(COD)$_2$BF$_4$] was employed in asymmetric hydrogenation of *N*-acetyldehydrophenylalanine, 1-(3-(phenyl(o-tolyl)phosphanyl)phenyl)urea, it displayed an excellent enantiomeric excess of 99%, along with 91% conversion. These findings demonstrate the potential of P-stereogenic supramolecular phosphines in asymmetric catalysis. The role of self-assembled Rh-complex in the asymmetric hydrogenation was investigated by ^{1}H, ^{2}H NMR, and Mass spectroscopy. The self-assembly of rhodium complex was unambiguously demonstrated using a combination of temperature and concentration-dependent NMR experiments. The NH and NH$_2$ peaks were found to shift downfield with decreasing temperature or with increasing concentration, in the free ligand 1-(3-(phenyl(o-tolyl)phosphanyl)phenyl)urea. This observation suggested presence of inter-molecular hydrogen bonding in 1-(3-(phenyl(o-tolyl)phosphanyl)phenyl)urea. In contrast, no change in chemical shift of the NH$_2$ proton was observed for self-assembled Rh-complex with decreasing temperature or with increasing concentrations. Thus, it appears that there exists a strong intra-molecular hydrogen bonding in self-assembled Rh-complex, which is responsible for above findings. The role of catalyst-substrate interactions was investigated by preparing deuterium labeled 1-(3-(phenyl(o-tolyl)phosphanyl)phenyl)urea ligand. Subsequently, deuterium labeled 1-(3-(phenyl(o-tolyl)phosphanyl)phenyl)urea self-assembles on a rhodium template to yield deuterium labeled self-assembled Rh-complex. The identity of deuterium-labeled self-assembled Rh-complex was established by NMR and mass spectroscopy. When the deuterium-labeled self-assembled Rh-complex was treated with *N*-acetyldehydrophenylalanine further downfield shift of the ND and ND$_2$ groups was observed. Thus, the change in chemical shift after addition *N*-acetyldehydrophenylalanine indicates the presence of hydrogen bonding interactions between deuterium labeled self-assembled Rh-complex and *N*-acetyldehydrophenylalanine. These investigations allow concluding that a hydrogen bonding

interaction might be responsible for the high enantioselectivities observed in the asymmetric hydrogenation of *N*-acetyldehydrophenylalanine.

6.2. Outlook

The work described in this thesis contributes to the continuing trend of designing chiral ligands and their chiral metal catalysts for various asymmetric transformations. The supramolecular ligands with chiral phosphorus donor atom can have an extraordinarily broad performance profile. The P-chiral supramolecular phosphine ligands have demonstrated their ability to induce chirality in asymmetric hydrogenation and can be applied in a variety of asymmetric transformations. The newly developed chiral palladium catalysts showed better reactivity or stereoselectivity compared to the state-of-the-art Me-DuPHOS derived complex, probably due to the wide range of electronic properties exhibited by these bidentate ligands. Particularly noteworthy is the [Pd(II)-Me-FerroLANE] complexes, which upon 5 mol% loading gives >99% conversion in P-C coupling reaction and can be used with a low catalyst loading. Further, the beneficial P-stereogenic supramolecular phosphine ligands could be easily prepared without carrying out the tedious and time-consuming resolution. This strategy significantly simplified the preparation of chiral ligands and would make it possible to produce chiral ligands on a large scale. The performance of the monodentate supramolecular phosphine ligands is more or less similar to bidentate ligands in asymmetric reaction. For asymmetric organic transformation, bidentate phosphine ligands can be replaced by monodentate supramolecular phosphine ligands.

The inter-molecular and intra-molecular hydrogen bonding interaction in the phosphine ligands and self-assembled metal complexes respectively was confirmed by different experiments like variable temperature NMR, different concentration, and deuterium exchange study. This study will help to understand the role of intermediate species formed during the supramolecular metal catalysis, supramolecular organocatalysis, and enzymatic reactions. This study also helps to understand the catalyst and substrate interaction during catalysis which can be confirm that the self-assembled metal catalyst interacts with the substrate (functional olefin). This affects the activity of the catalyst, transfer of chirality, and regioselectivity.

Appendix 1

The impact of modular substitution on crystal

packing: The tale of two urea's

A.1. Abstract

A small library of 13 (3a-3m) compounds with modular positioning of iodide and urea/thiourea groups was synthesized in excellent yields in a single step synthetic protocol. The existence of the anticipated (thio)urea derivatives was unambiguously established using a combination of 1-2D NMR spectroscopy, ESI-MS and single crystal X-ray diffraction studies. These (thio)urea compounds were classified into four classes as a) mono-substituted, b) di-substituted, c) di-substituted thiourea and d) electronically tailored di-substituted thiourea. The changes in molecular conformation and crystal packing due to the change in the relative positioning of the iodo group at phenyl ring attached to one of the N atoms and different substituents at other N atoms in urea and thiourea derivatives have been discussed. The urea derivatives in general, display the chain association through one dimensional three centered N-H…O hydrogen bonding interactions due to the *trans-trans* orientation of its both NH protons with respect to the carbonyl group. Whereas, the thiourea compounds exhibit a centrosymmetric dimeric assembly via the complementary N-H…S interactions because of the *trans-cis* arrangement of NH protons with respect to the thiocarbonyl group leading to either a helical or a sheet pattern. The presence of nitro group at *para* position of thiourea derivative leads to *trans-trans* arrangement of both NH protons with respect to the thiocarbonyl groups thus yielding chain assembly through one dimensional three centered N-H…S interactions similar to urea derivatives. Associations of these chain or sheets in urea/thiourea derivatives through halogen bonding interactions (hal…hal, hal…π, hal…S *etc.*) generate 2D assembly.

Supramolecular favoured motifs in thio(urea)
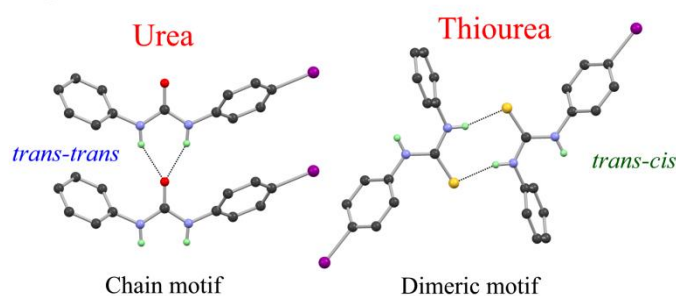
Urea   Thiourea

trans-trans   *trans-cis*

Chain motif   Dimeric motif

A.2. Introduction

Weak chemical interactions are very creatively and effectively used by Mother Nature in the complex process of chemical evolution. For example, many enzymes fold in a particular shape due to weak hydrogen-bonding interactions between the strands and perform a selective reaction that is vital to the survival of that species. Therefore, it is no wonder that inter- and intra- molecular interactions are being increasingly used to design variety of solid state structures such as macrocycles, cryptands, one dimensional wires, two dimensional grids, to name a few.[1] These non-covalent interactions which constitute a supramolecular synthons include hydrogen bonding, halogen-bonding, π-stacking, coordinative interactions *etc*.[2] Taking the motivation from nature, various supramolecular architectures were artificially prepared and their selectivity in various chemical transformations has been tested.[3] For instance, Raymond's a specially designed cage-compound enables acid catalyzed hydrolysis of orthoesters, even in a basic medium,[4] or monoterpene cyclization by exclusion of water,[5] or harnesses aza-Cope reaction.[6] In addition to serving as a structural unit, the non-covalent interactions have started delivering a function. The potential of the non-covalent interaction in tailoring the reactivity or selectivity of a transformation has been lately recognized and last decade has seen a tremendous growth in supramolecular catalysis.[7] For instance, monodentate ligands with hydrogen-bonding start behaving like a bidentate ligand in presence of a metal and render enhanced selectivity as compared to their non-hydrogen-bonding counterparts.[8] This concept has been very innovatively used to generate a large catalyst library from a small set of monodentate ligands.[9] Apart from serving as structural units, the supramolecular motifs can be tuned to serve as directing synthons in supramolecular-catalysis (Fig. A.1). The "directing synthons" can be broadly defined as supramolecular units that engage in non-covalent interactions with the incoming substrate and in turn enhance selectivities. Notable examples of this type include supramolecular hydroformylation,[10] hydrogenation[11] and C-H activation.[12] Amongst such supramolecular synthons, symmetrical or unsymmetrical *N,N'*-di-substitution of urea is known to form persistent and robust one dimensional three centered N-H…O hydrogen-bonded chains in solution, fiber, gel or solid state etc. because of the *trans-trans* arrangement of NH protons with respect to the C=O group.[13] Because of their pronounced directionality and relatively high strength they are utilized as building blocks for designing various crystalline frameworks.
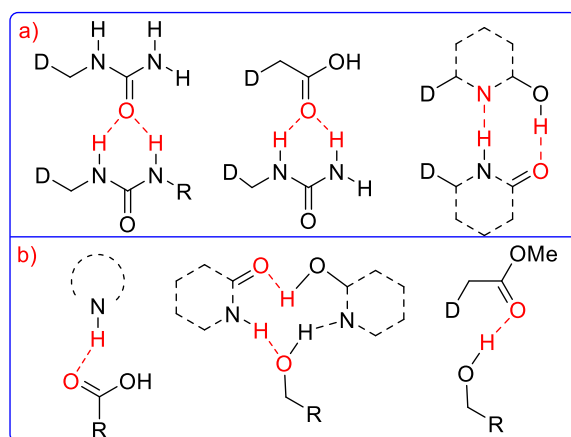
Figure. A.1 Representative synthons in supramolecular catalysis; a) synthons as structural building blocks, b) synthons as functional units

The good complementarity between the donor (two NH protons) and acceptor (C=O) groups generates the predictable self-assembled one-dimensional extended hydrogen bonded chain structure. In contrast, the supramolecular synthons in *N, N*'-di-substituted thiourea's are comparatively less predictable which could be because of the relatively weak acidic nature of C=S group thus making it weak proton acceptor.[13] Cambridge Structural Database (CSD) survey revealed two different self-associative synthons for thiourea's depending on the conformation of the NH protons. The *trans-trans* association leads to hydrogen bonded chain similar to the ureas, whereas *the trans-cis* conformation yields dimeric N-H…S hydrogen bond. Therefore, investigating the effect of substitution patterns on the self-assembly of urea and thiourea derivatives is highly desirable.

In this context, we report the synthesis of various derivatives of urea and thiourea. Further, the effect of modular substitution on the molecular conformation, H-bonding pattern and crystal packing is presented. This investigation reveals that H-bonding chain pattern is dominant in urea derivatives, whereas the dimeric association through N-H…S hydrogen bond is preferred mode of interaction in thioureas.

A.3. Results and discussion

The three centered N-H…O hydrogen bonding synthon in urea is one of the most elegant and robust synthons in supramolecular chemistry. It is mostly utilized for the designing of various crystalline frameworks because of this highly directional and predictable geometry. Further the crystal packing of urea can be readily tuned by substituting the two protons on nitrogen atoms. As indicated in Figure A.2, the resulting 13 compounds have been classified
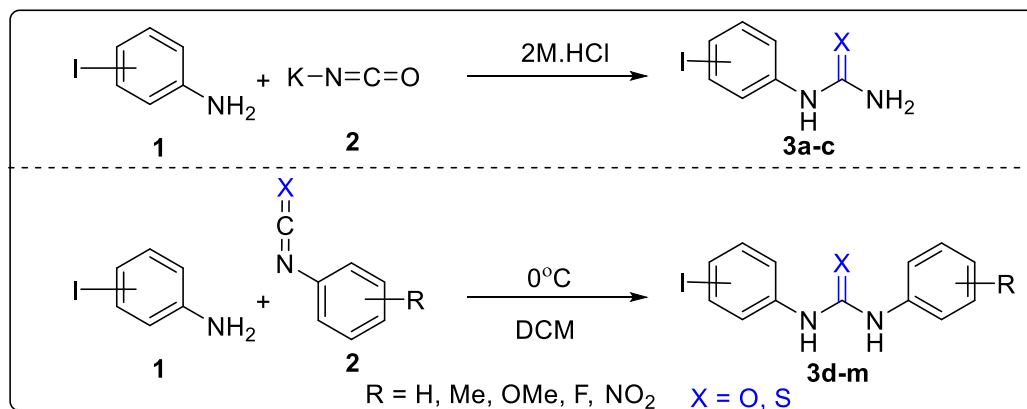
Scheme A.1: General scheme for the synthesis of iodo-phenylurea/thiourea compounds.
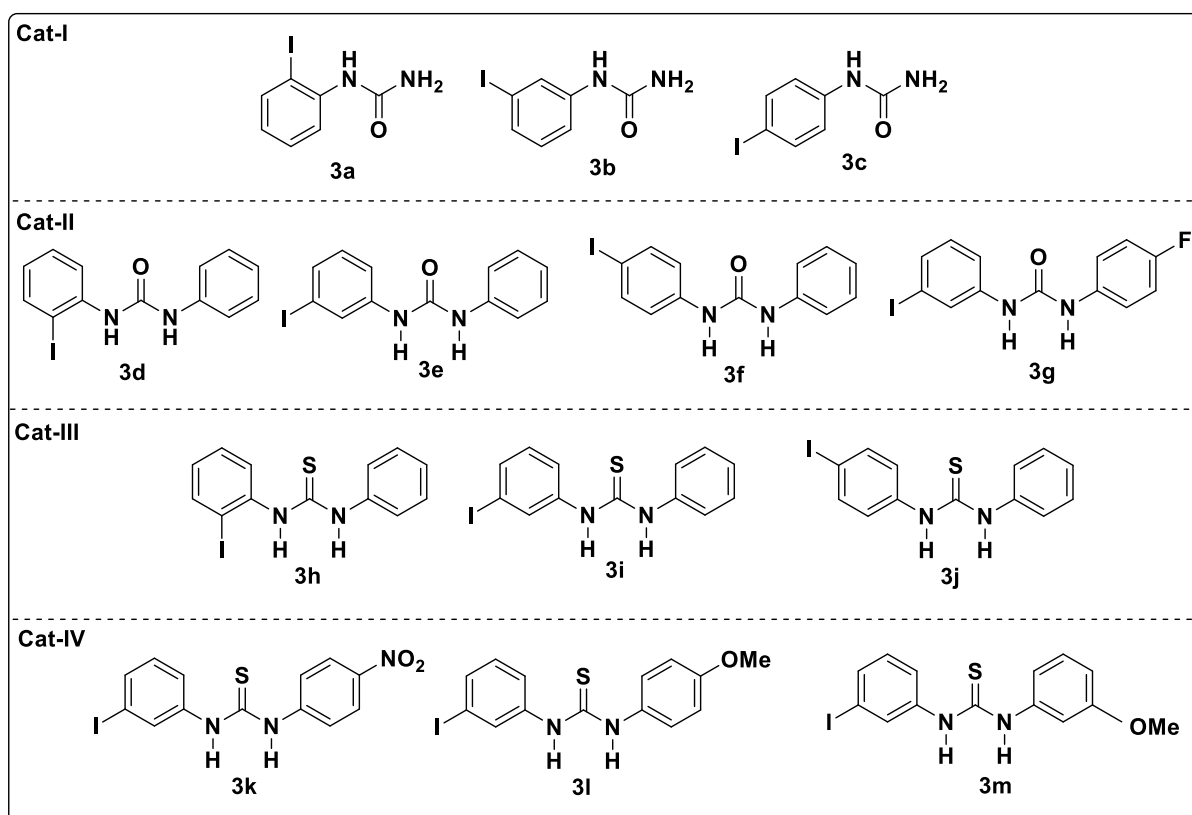
Figure A.2: The three possible isomers of mono-substituted iodo-aryl urea (Cat-I), di-substituted iodo-aryl urea (Cat-II), di-substituted iodo-aryl thiourea (Cat-III) and electronically tailored di-substituted iodo-aryl thiourea (Cat-IV).

according to substitution pattern; mono-substituted urea (category-I), di-substituted urea (category-II), di-substituted thiourea (category-III) and electronically tailored di-substituted thiourea (category-IV). As depicted in scheme A.1, two synthetic strategies were adopted to prepare compounds **3a-m**. Mono-substituted urea compounds were prepared by treating iodoanilines with potassium isocyanate in a 2 molar hydrochloric acid solution. In the second strategy; the di-substituted urea and thiourea derivatives were prepared at 0°C in

dichloromethane. Detailed synthesis and crystal structure analyses of all the compounds has been done. None of the compounds exhibit polymorphism on crystallization from different solvents as well as polymorphic transition during DSC measurements. All the inherent structural features present in these compounds are described below.

A.3.1. Category I: Mono-substituted urea (3a-c)

The 2-iodophenylurea **3a** was prepared by mixing hydrochloric acid solution of 2-iodoaniline with aqueous potassium-isocyanate at room temperature. A white precipitate was observed after 4 hours, which was then washed with water and toluene respectively to obtain pure **3a**. The proton resonances at 7.62 and 6.35 ppm (Figure A.7) and a carbon signal at 155.8 ppm indicated formation of the urea motif (Figure A.8). A CO stretching band at 1698 cm^{-1} (Figure A.10) further confirmed the existence of a carbonyl group. A positive mode electrospray ionization mass spectroscopy (ESI-MS) revealed a molecular ion peak at m/z = 262.96 [M+H]$^{+}$ (Figure A.11), further corroborating the NMR findings. Compound **3a** was crystalized from a 1:1 mixture of ethanol and ethyl acetate in open flask. The structure of **3a** was unambiguously ascertained form a single crystal X-ray diffraction. In our attempts to investigate the impact of positional change on the secondary interaction, we synthesized 3-iodophenylurea by treating 3-iodoaniline with potassium-isocyanate in acidic media to produce **3b** as white solid. The proton resonance at 8.66 and 5.94 ppm (for NH and NH$_2$ groups respectively) and appearance of carbonyl resonance at 157.2 ppm suggested formation of desired 3-iodophenylurea **3b**. Infrared spectroscopy and electrospray ionization mass spectroscopy further confirmed the existence of **3b**. Compound **3b** was crystalized from a mixture of ethanol and ethyl acetate (1:1) solution by slow evaporation. The crystals were analyzed using single crystal X-ray diffraction. Having synthesized the *ortho-* and *meta-*substituted urea derivatives, we investigated the influence of *para-*substitution on the weak interactions. Reaction of 4-iodoaniline with pottasiumisocyanate in acidic media followed by aqueous workup produced the desired 1-(4-iodophenyl)urea (**3c**) in 72% isolated yield. Preliminary spectroscopic and analytical evidences suggested formation of **3c**.

A.3.2. Category II: di-substituted urea (3d-g)

Substitution of terminal N-H proton with a phenyl group might considerably change the course of secondary interactions. To investigate this hypothesis, a small library of 4 molecules was prepared and the crystallographic changes are noted in the following section. Treatment of 2-iodoaniline with phenyl-isocyanate produced **3d** as white solid. Purification by column

chromatography using ethyl acetate and petroleum ether (10:90) as eluent produced **3d** in excellent yield (81%). As compared to **3a**, the urea protons were down field shifted and appeared at 9.44 and 7.90 ppm. Observation of ^{13}C carbonyl carbon at 152.3 ppm in combination with proton resonances supported the formation of **3d**. The existence of **3d** was confirmed by ESI-MS (+ve mode), which revealed a molecular ion peak at m/z = 338.99 [M+H]$^{+}$. Compound **3d** was crystalized from 1:1 mixture of DMF and ethyl acetate at room temperature producing shiny crystals.

Reaction of 3-iodoaniline with phenyl-isocyanate in DCM produced 1-(3-iodophenyl)-3-phenylurea **3e** as a solid melting at 195°C. Close-by appearance of the N*H* protons at 8.75 and 8.67 ppm (as both the N-atoms have very similar substituents), attested the formation of desired compound **3e**, which was further confirmed by ^{13}C NMR. Additionally, the infrared spectroscopy and mass spectroscopy validated the formation of compound **3e**. Suitable crystals were obtained from a saturated solution (1:1 mixture of DMF and ethyl acetate) of compound **3e**.

Along the same line, reaction of 4-iodoaniline with isocyanatobenzene led to the formation of terminal N-H proton substituted product **3f**. The resultant reaction mixture was purified by column chromatography (ethyl acetate and petroleum ether 30:70) to produce **3f** in 90% isolated yields. The relative down field shift and appearance of close-by N-H proton resonances (8.79, 8.70 ppm) indicated formation of compound **3f**. The NMR findings were further supplemented by IR and mass analysis. The unambiguous proof for the existence of **3f** was obtained from a single crystal X-ray diffraction data.

In our endeavor to examine the impact of electron withdrawing groups on the secondary interactions, we prepared 1-(4-fluorophenyl)-3-(3-iodophenyl)urea (**3g**). The desired compound **3g** was isolated in 81% yield after column (ethyl-acetate: petroleum ether; 60:40). Observation of the two NH protons (8.78 and 8.75 ppm) and the urea carbonyl carbon (158.4 ppm) confirmed the formation of compound **3g**. Crystals of suitable quality were obtained from a solution of **3g** in 1:1 DMF and ethyl acetate mixture.

A.3.3. Category III: di-substituted thiourea (3h-j)

The sulfur-analogue of **3d** was obtained by reacting 2-iodoaniline with phenyl-isothiocyanate. Work-up followed by column purification using ethyl acetate and petroleum ether (10:90) produced **3h** in 62% isolated yield. Relatively down field shifted NH proton resonances (9.93 and 9.33 ppm) and a carbon resonance at 180.2 ppm supported formation of **3h**. The NMR findings were further supported by ESI-MS (+ve mode) that disclosed a

molecular ion peak at m/z = 354.97 (M+H)$^+$ and 376.96 (M+Na)$^+$. The molecular crystals of **3h** were obtained from 1:1 mixture of DMF and ethyl acetate.

The sulfur counterpart of **3e** was obtained by treating 3-iodoaniline with isothiocyanatobenzene. Chromatographic purification of the crude produced the desired compound **3i** in 94% isolated yield as a white solid. 1-(3-iodophenyl)-3-phenylthiourea (**3i**) was found to melt at 110°C, which is significantly lower than the corresponding oxygen analogue **3e**. Both the NH protons were down field shifted and appeared at 9.95 and 9.86 ppm and the sulfur substituted carbon appeared at 179.5 ppm confirming the formation of **3i**. The infrared spectrum revealed a single NH stretching band at 3323 cm^{-1} and the CS band at 1577 cm^{-1} attesting the formation of **3i**. The mass-spectroscopic evidences also indicated formation of **3i**. Crystals of suitable quality were grown from a 1:1 solution of THF and ethyl acetate at 25°C and were subjected to X-ray diffraction analysis.

Similarly, the sulfur analogue of **3f** was prepared by treating 4-iodoaniline with isothiocyanatobenzene in DCM at 0°C to yield **3j**. The crude 1-(4-iodophenyl)-3-phenylthiourea was purified by passing it through column (ethyl acetate and petroleum ether 30:70) to obtain **3j** as white solid in 90% yield. As anticipated, the N-H protons appeared down field (8.78 and 8.69 ppm) compared to the parent urea **3c** and confirmed the formation of **3j**. Further, the C=S carbon appeared at 179.4 ppm and the electrospray ionization mass spectrum revealed molecular ion peak at m/z = 354.97 [M+H]$^+$, 376.95 [M+Na]$^+$. Above spectroscopic and analytical data attested the formation of desired compound **3j**. The ultimate proof for the existence of the 1-(4-iodophenyl)-3-phenylthiourea came from the single crystal X-ray diffraction data.

A.3.4. Category IV: Electronically tailored di-substituted thiourea (3k-m)

Secondary interactions are known to be influenced by electron donating and electron withdrawing groups. To investigate the effect of electron withdrawing groups on the secondary interaction, we prepared 1-(3-iodophenyl)-3-(4-nitrophenyl)thiourea **(3k)** by treating 3-iodoaniline with 1-isothiocyanato-4-nitrobenzene. Indeed, the effect of installing an electron withdrawing group at *para*-position was very significant. As compared to parent compound **3i**, the urea protons in **3k** appeared further down field at 10.50 and 10.30 ppm (almost 1.00 ppm shift), whereas the thio-bound carbon remained undisturbed at 179.3 ppm. The NMR findings were further corroborated by IR and ESI-MS and the existence of **3k** was confirmed.

We anticipated that installing an electron donating substitute at *para*-position to the thiourea nitrogen might display the opposite behavior to that of **3k**. Reaction of 3-iodoaniline

with 1-isothiocyanato-4-methoxybenzene led to the production of yellow powder in 94% isolated yield after column chromatographic separation. The 1-(3-iodophenyl)-3-(4-methoxyphenyl)thiourea **(3l)** melted at 105°C, which is significantly lower than the nitro-analogue **3k** (150°C). Furthermore, the substitution effect was apparent in proton NMR; the two NH protons were up-field shifted to 9.76 and 9.68 ppm. However, as anticipated, the thio-bound carbon (C=S) remained unaffected at 179.7 ppm. Slow evaporation of the solution of **3l** (in 1:1 mixture of DMF, ethyl acetate) produced crystals of suitable size and the existence of **3l** was established from X-ray diffraction analysis. A detailed account of these interactions in a solid state is presented in the next section. Even the relative position of a substituent on the N'-substituted phenyl ring seems to challenge the secondary interactions. For example, *meta*-substituted, 1-(3-iodophenyl)-3-(3-methoxyphenyl)thiourea **(3m)** behaves very differently. Compared to the *para*-methoxy**3l**, the thiourea protons in **3m** are relatively down field shifted to 9.95, 9.04 ppm, whereas the C=S carbon remains unaltered at 179.3 ppm.

A.3.5. X-ray crystallography

A.3.5.1. Category I: mono-substituted urea (3a-c)

The Crystals of **3a**, **3c** and **3b** belongs to monoclinic space group *P*21/*c*, orthorhombic space group *Pccn* and monoclinic chiral space group *P*21 respectively. Crystals structures of all these compounds contain one molecule in the asymmetric unit (Z'=1). Iodo-phenyl ring in these compounds showed significant deviation from the planarity of urea moiety. In **3a** it is almost perpendicular to the basal plane of urea (difference, 74.19°) while in both **3b** and **3c** compounds it Table A.1 Geometrical parameters deviate by almost 50° from the planarity of urea moiety (Figure A.3, left side). The NH protons in all the three derivatives took an anti-orientation with respect to the carbonyl group. In the one dimensional three centered N-H…O hydrogen bonding chain formation these *trans* protons act as donor and the C=O proton as the acceptor with graph set notations $C(4)[R_2^1(6)]$, wherein $C(4)$ denotes a chain motif with 4 atoms in the repeat unit, and $[R_2^1(6)]$ denotes a hydrogen-bonded ring motif consisting of 6 atoms, with 2 donors groups and 1 acceptor group. Crystal structure of **3a** and **3b** are grossly isostructural whereas that of **3c** differs slightly. Neighboring molecules having *c*-glide relationship in **3a** and **3b** form a bifurcated N-H…O hydrogen bonding chain whereas in **3c** unit-translated molecules generate the linear chain.
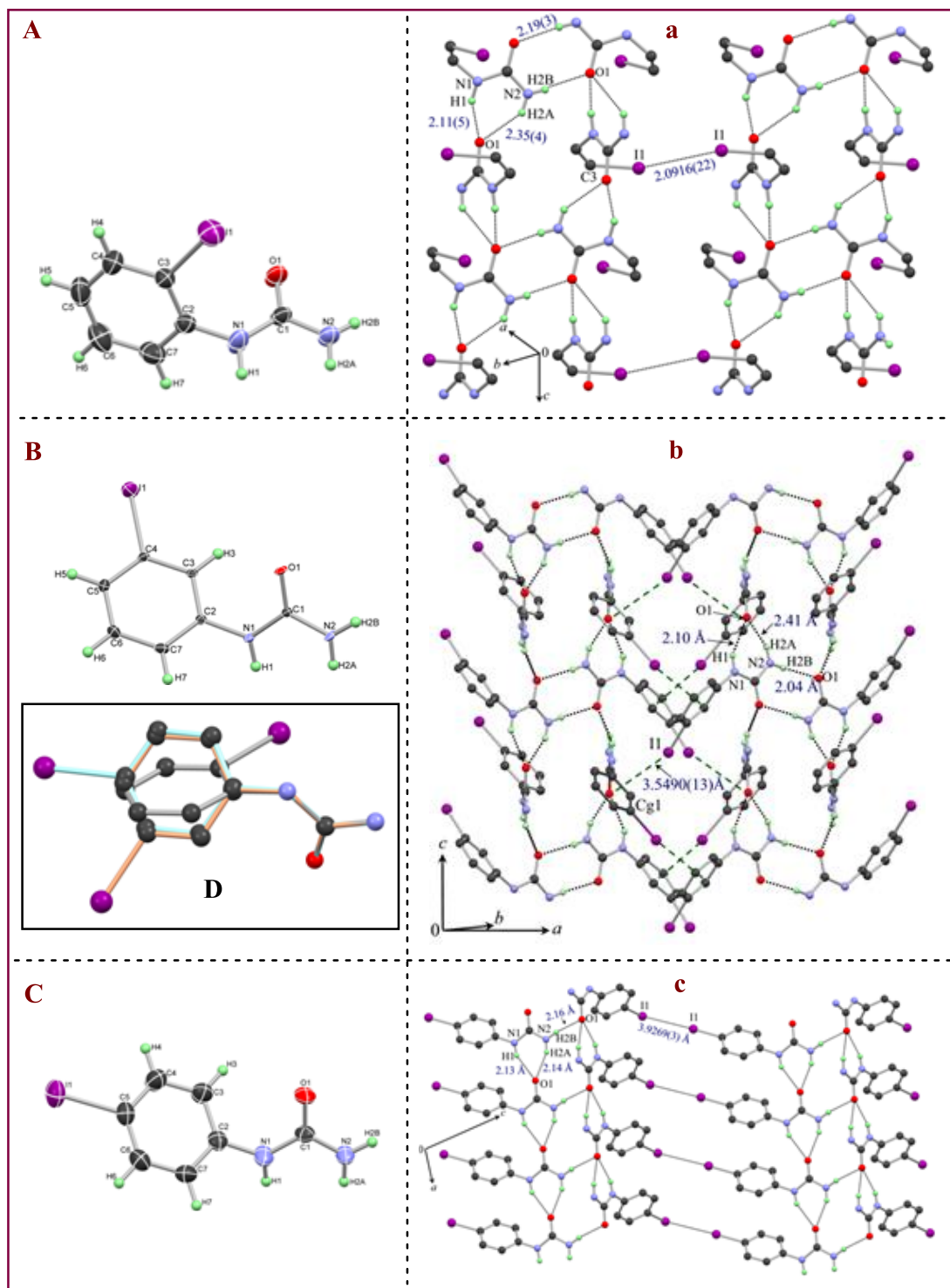
Figure A.3: (A) (B) and (C) ORTEPs of **3a**, **3b** and **3c** respectively are showing the atom numbering scheme. The displacements ellipsoids are drawn at the 50% probability level and H atoms are shown as small spheres with arbitrary radii. (D) Overlay of structures of **3a** (gray), **3b** (orange) and **3c** (cyan) (left side). View of molecular packing in crystals of (a) **3a**, (b) **3b** and (c) **3c**. Some of the atoms in the packing are omitted for clarity. All the distances are in Å unit (right side).

Table A.1: Geometrical parameters of intermolecular interactions

Entry	Interactions	D-H (Å)	H···A (Å)	D···A (Å)	D-H···A/α (°)	Symmetry codes
			3a			
1	N1-H1···O1	0.91(4)	2.10(5)	2.914(2)	150(4)	*x*, 1/2-*y*, 1/2+*z*
2	N2-H2A···O1	0.86(4)	2.34(4)	3.050(3)	141(3)	*x*, 1/2-*y*, 1/2+*z*
3	N2-H2B···O1	0.77(3)	2.19(3)	2.940(3)	168(4)	*-x*, *-y*, *-z*
4	C3-I1...I1	2.092(2)	3.8557(4)	-	157.93(6)	1-*x*, -*y*, -*z*
			3b			
5	N1-H1···O1	0.88	2.10	2.895(2)	150	*x*, 1/2-*y*, -1/2+*z*
6	N2-H2A···O1	0.88	2.41	3.136(3)	140	*x*, 1/2-*y*, -1/2+*z*
7	N2-H2B···O1	0.88	2.04	2.907(3)	167	1-*x*, 1-*y*, 1-*z*
8	C4-I1··· Cg1 Cg1= C2 – C7	2.009(3)	3.5483(9)	5.402(2)	151.8.6(7)	1/2-*x*, *y*, 1/2+*y*
			3c			
9	N1-H1···O1	0.88	2.09	2.900(2)	152	1+*x*, *y*, *z*
10	N2-H2A···O1	0.88	2.11	2.970(3)	167	1-*x*, 1/2+*y*, 1-*z*
11	N2-H2B···O1	0.88	2.10	2.896(3)	159	1+*x*,*y*,*z*
12	C5-I1...I1	2.101(3)	3.8793(8)		170.61(7)	-*x*, -1/2+*y*, -*z*
			3d			
13	N1-H1···O1	0.79(5)	2.19(5)	2.925(4)	156(4)	*x*, -1+*y*, *z*
14	N2-H2···O1	0.81(4)	2.09(4)	2.866(4)	159(4)	*x*, -1+*y*, *z*
15	C3-I1...Cg1	2.095(4)	3.7401(16)	3.890(4)	78.06(10)	*x*, -1+*y*, *z*
16	C7-H7... Cg2	0.96(4)	3.202	4.100	161	*x*, ½-*y*, -1/2+*z*
Centroid of the phenyl ring, α is the dihedral angle between planes of phenyl rings.Cg1 = C2 – C7, Cg2 = C8 – C13.					
			3e			
17	N1-H1···O1	0.88	2.08	2.895(6)	154	*x*, 1+*y*, *z*
18	N2-H2···O1	0.88	2.12	2.924(6)	152	*x*, 1+*y*, *z*
19	C4-I1...I1	2.105(5)	3.9473(11)		158.98(17)	2-*x*, -1/2+*y*, 3/2-*z*
			3f			
20	N1-H1···O1	0.88	2.05	2.870(4)	155	*x*, 1+*y*, *z*
21	N2-H2···O1	0.88	2.11	2.917(4)	151	*x*, 1+*y*, *z*
22	C5-I1...I1	2.101(3)	3.8808(6)		164.04(10)	-*x*, -1/2+*y*, 2.5-*z*
			3g			
23	N1-H1···O1	0.88	2.08	2.881(2)	151	*x*, 1+*y*, *z*
24	N2-H2···O1	0.88	2.09	2.893(2)	152	*x*, 1+*y*, *z*
25	C4-I1...I1	2.0997(18)	3.9168(11)		158.39(5)	1-*x*, 1/2+*y*, 1/2-*z*
26	C11-F1...F1	1.359(3)	2.880(2)		153.80(13)	-*x*, -*y*, 1-*z*
			3h			
27	N1-H1···I1	0.88	2.95	3.618(5)	135	*x*,-1+*y*, *z*
28	N2-H2···S1	0.88	2.47	3.319(5)	162	-*x*, 1-*y*, 1-*z*
29	C7-H7...S1	0.95	2.88	3.710	147	*x*,-1+*y*, *z*
30	C3-I1...I1	2.073(3)	3.839(2)		164.70(17)	1.5-*x*, -1/2+*y*, 1.5-*z*
			3i			
31	N1-H1···I1	0.88	2.99	3.795(3)	153	3/2-*x*, -1/2+*y*, 1/2-*z*
32	N2-H2···S1	0.88	2.49	3.292(4)	152	2-*x*, 2-*y*, -*z*
33	C7-H7...S1	0.95	2.90	3.631	135	*x*, -1+*y*, *z*
34	C4-I1...Cg2 Cg2 = C8 -C13	2.093(4)	3.684(2)	5.712(4)	162.08(11)	3/2-*x*, 1/2+*y*, 1/2-*z*
			3j			
35	N2-H2···S1	0.88	2.48	3.323(3)	161	2-*x*, -*y*, 1-*z*
36	C7-H7...S1	0.95	2.93	3.791	151	*x*, 1+*y*, *z*
37	C3-H3...I1	0.95	3.08	3.925	150	3/2-*x*, -1/2+*y*, 3/2-*z*
38	C5-I1...Cg2 Cg2 = C8 -C13	2.101(3)	4.063	6.061	157.26	3/2-*x*,-1/2+*y*, 3/2-*z*

			3k			
39	N1-H1···S1	0.88	2.43	3.292(5)	168	2-*x*, -*y*, -1/2+*z*
40	N2-H2···S1	0.88	2.59	3.428(5)	160	2-*x*, -*y*, -1/2+*z*
41	C9-H9···O2	0.95	2.51	3.241(6)	133	1/2+*x*, 1/2-*y*,*z*
42	C6-H6…S1	0.95	2.93	3.671	136	-1/2+*x*, 1/2-*y*,*z*
43	C10-H10···I1	0.95	3.12	4.029	162	*x*, -1+*y*,*z*
44	C4-I1...O1	2.097	3.135(4)		168.65(17)	*x*, 1+*y*,*z*
45	Cg1...Cg2		3.728(4)		3.2(3)	2-*x*, -*y*,-1/2+*z*
46	Cg1...Cg2		3.763(4)		3.2(3)	2-*x*, -*y*,1/2+*z*
			3l			
47	N1-H1···O1'	0.88	2.29	3.069(4)	148.0	*x, y,z*
48	N1'-H1'···O1	0.88	2.17	2.894(5)	140	*x, y,z*
49	N2-H2···S1'	0.88	2.48	3.321(3)	161.0	-1+*x, y, z*
50	N2'-H2'···S1	0.88	2.52	3.329(4)	153	1+*x, y, z*
51	C10'-H10'···S1	0.95	2.83	3.687(5)	150.3	1-*x*, 2-*y*, 1-*z*
52	C6-H6···S1'	0.95	2.91	3.526(6)	123.7	2-*x*, 2-*y*, 1-*z*
53	C9'-H9'···I1'	0.95	3.18	3.989(5)	144.4	2-*x*, 1/2+*y*, 1/2-*z*
54	C4-I1...S1'	2.107	3.4534(12)		168.41(11)	-1+*x*, 3/2-*y*, 1/2+*z*
55	C4'-I1'...S1	2.105	3.7058(12)		166.58	1+*x*, 3/2-*y*,-1/2+*z*
56	C9-H9···Cg1 Cg1 = C2 – C7	0.95	2.82	3.605(4)	140	1-*x*, 2-*y*,1-*z*
			3m			
57	N1-H1N···O1	0.85(3)	2.18(3)	3.002(2)	161	1-*x*, 1-*y*, 1-*z*
58	N2-H2N···I1	0.788	3.078	3.77	149.23	2-*x*, 1-*y*, 2-*z*
59	C9-H9···S1	0.95	2.966	3.909	172.09	1-*x*, 1-*y*, 2-*z*
60	C6-H6···S1	0.95	2.877	3.753	153.83	*x*, 1.5-*y*, -1/2+*z*
61	C4-I1···S1	2.105	3.607		158.42	1+*x, y, z*
62	Cg2··· Cg2		3.7764(11)		0	1-*x*, 1-*y*, 1-*z*
63	C5-H5··· Cg2	0.93	2.76	3.526(2)	138	2-*x*, -1/2+*y*, 3/2-*z*
[a] Cg-centered of the phenyl ring, α is the dihedral angle between planes of phenyl rings; Cg2 = C8 – C13.						

The geometry of bifurcated N-H…O interactions differs in crystals of **3a** and **3b** whereas it is similar in crystals of **3c** (entries 1, 2, 5, 6, 9, 10, Table A. 1). The H…O distance involving unsubstituted N-H group (N2) is longer and the angle N-H…O deviate from the linearity in crystals of **3a** and **3b** while the H…O distance involving substituted NH group (N1) is shorter and the angular approach is moderate. The neighboring antiparallel chains are stitched centrosymmetrically in **3a** and **3b** through dimeric N-H…O interactions whereas in **3c** the 2_1-screw axis neighboring chains are linked via monomeric N-H…O hydrogen bond engaging *cis* N-H proton and carbonyl oxygen (Figure A.3, right side). The geometry of this N-H…O interaction is stronger compared to bifurcated N-H…O interactions (Entry 3, 7, 11, Table A.1). This shows that the carbonyl oxygen is acting as a trifurcated proton acceptor for all the NH protons to generate the monolayer in all the structures (Figure A.3, right side). All the structures differ in the weaving of these monolayers to generate bilayer structure. In **3a**, the adjacent monolayers interact *via* centrosymmetric I…I halogen bonding interaction of type I category,

in **3b** the bilayers are generated by joining of the *c*-glide related neighboring monolayers through C-I…π interactions whereas in **3c** the 2₁-screw axis related neighboring monolayers are linked via I…I halogen bonding interaction[14] of type II category[15] (entries 4, 8, 12, Table A.1).

A.3.5.2. Category II: di-substituted urea (3d-g)

Crystals of **3d**, **3e**, **3f** and **3g** belong to monoclinic space group *P*21/*c* containing one molecule in the asymmetric unit. Structure overlay reveals similar conformation of molecule in crystals of **3f** and **3g** suggested isostructurality in their molecular organization. Whereas significant difference in the orientations of substituents (phenyl rings) with respect to the central urea moiety was observed in other derivatives. The iodophenyl rings of compounds **3d** and **3f** have similar orientations however the N2-substituent phenyl ring displayed marked difference in orientation (79°) (Figure A.4, left side). Conversely, the iodophenyl rings of compounds **3d** and **3e** showed significant difference in orientations (71.5°) whereas the orientation of other phenyl ring is almost the same (Figure A.4, left side). Crystal structures of **3e**, **3f** and **3g** are grossly isostructural whereas that of **3d** differs (Figure A.4, left side). Molecules in all these four compounds form unit-translated one dimensional three centered N-H…O hydrogen bonding chain along the b-axis (similar to compounds **3a**, **3b** and **3c**) employing their two NH proton donors and the C=O proton acceptor in bifurcated hydrogen bonds with graph set notations C(4)[R$_2^1$(6)], where C(4) denotes a chain with 4 atoms, and [R$_2^1$(6)] denotes a hydrogen-bonded ring motif containing of 6 atoms, with 2 donors groups and 1 acceptor group. The geometry of these bifurcated N-H…O interactions in all the compounds is comparable, the distance is short and the angle is moderate (entries 13, 14, 17, 18, 20, 21, 23, 24, Table A.1). Neighboring c-glide symmetry related one dimensional chains in compound **3d** are networked through off-centered C-I…π interactions (entry 15 Table A.1) involving iodophenyl rings along the *c*-axis to generate the bilayer structure (Figure A.4, right side) whereas in compounds **3e**, **3f** and **3g** the adjacent crystallographic 21-screw axis related one hydrogen bonded chains linked through I…I halogen bonding (entries 19, 22, 25 Table A.1) interactions of type II category to generate the flat helical structure. The rather long but linear C7-H7…π (Cg1) interaction (entry 16, Table A.1) also supplements the helical assembly in crystals of **3d**. The crystallographic 21-screw related adjoining chains joined loosely through hydrophobic forces to generate a bilayer structure in crystals of **3d**, **3e** and **3f**. However, the

Figure A.4: (A) (B) (C) and (D) ORTEPs of **3d**, **3e**, **3f** and **3g** respectively are showing the atom numbering scheme (left side). The displacements ellipsoids are drawn at the 50% probability level and H atoms are shown as small spheres with arbitrary radii. View of molecular packing in crystals of (a) **3d**, (b) **3e**, (c) **3f** and (d) **3g** (right side).

neighboring helices in **3g** are connected centrosymmetrically along the *a*-axis through F…F[16] short (entry 26, Table A.1) contact of type I category to create a 2-dimensional way packing on the ab plane (Figure A.4, right side).

A.3.5.3. Category III: mono-substituted thiourea (3h-j)

Crystals of **3h**, **3i** and **3j** belongs to monoclinic $P2_1/n$ space group containing one molecule in the asymmetric unit. Structure overlay reveals difference in the orientations of iodo-phenyl and other phenyl ring with respect to the central thiourea moiety due to the free rotation along N-C bond. The orientation of phenyl rings of compounds **3h** and **3j** differ by 79° while that of **3h** and **3i** differ by 60°. The conformation of phenyl ring in compounds **3j** and **3i** differ slightly by ~7°. Similarly, conformation of iodophenyl ring showed noticeable difference. The conformation of iodophenyl ring in **3h** and **3j** differ by ~30°, that of **3h** and **3i** by ~36° whereas compounds **3j** and **3i** displayed significant orientation difference (~66°) (Figure A.5, left side).

Unlike, crystals of substituted urea which form one dimensional three centered N-H…O hydrogen bonding chain structure, thiourea compounds preferred dimeric association. This is because of the *trans-cis* arrangement of NH protons with respect to the thiocarbonyl group.[13] The *trans-cis* arrangement of N-H protons leads to dimeric self-assembly through N-H…S hydrogen bond. There is also equal probability of both NH protons adopting anti conformation depending on the substituents. The trans-trans orientation leads to generation of one-dimensional H-bonding chain structure similar to that seen urea derivatives. In crystal structures of **3h, 3i** and **3j**, H-atoms have acquired *trans-cis* orientations resulting in the formation of dimeric N-H…S hydrogen bond between the neighboring molecules involving *cis* H-atom and C=S group (Figure A.5, left side). The geometry of N-H…S hydrogen bond in all the compounds is comparable (entries 28, 32, 35, Table A.1). The adjacent dimers generate extended ribbon structure through N-H…I hydrogen bond involving *trans* H-atom and iodo group in **3h** (entry 27, Table A.1). The ribbon structure is also supported by moderate C7-H7…S1 interaction (Figure A.5a right side, entry 29, Table A.1) engaging *ortho* C-H of the iodophenyl ring and thiocarbonyl group. In crystals of **3i** and **3j** the *trans* NH atom do not participate in any interaction within the chain and the ribbon structure is solely stabilized by centrosymmetric C7-H7…S1 hydrogen bond (Figure A.5b and c right side, entries 33, 36, Table A.1). The geometrical parameters of C-H…S interaction are similar. The adjoining parallel ribbons are stitched differently in three structures. The adjacent ribbons are linked

through type II category, I…I halogen bonding interaction in **3h** (entry 30, Table A.1), in **3i** the ribbons are connected *via* N-H…I interactions engaging *trans* N-H proton and off-centered C-I…π halogen bonding interactions (entries 31, 34, Table A.1) whereas in **3j** the ribbons are joined through only off-centered C-I…π halogen bonding interactions (entry 38, Table A.1).
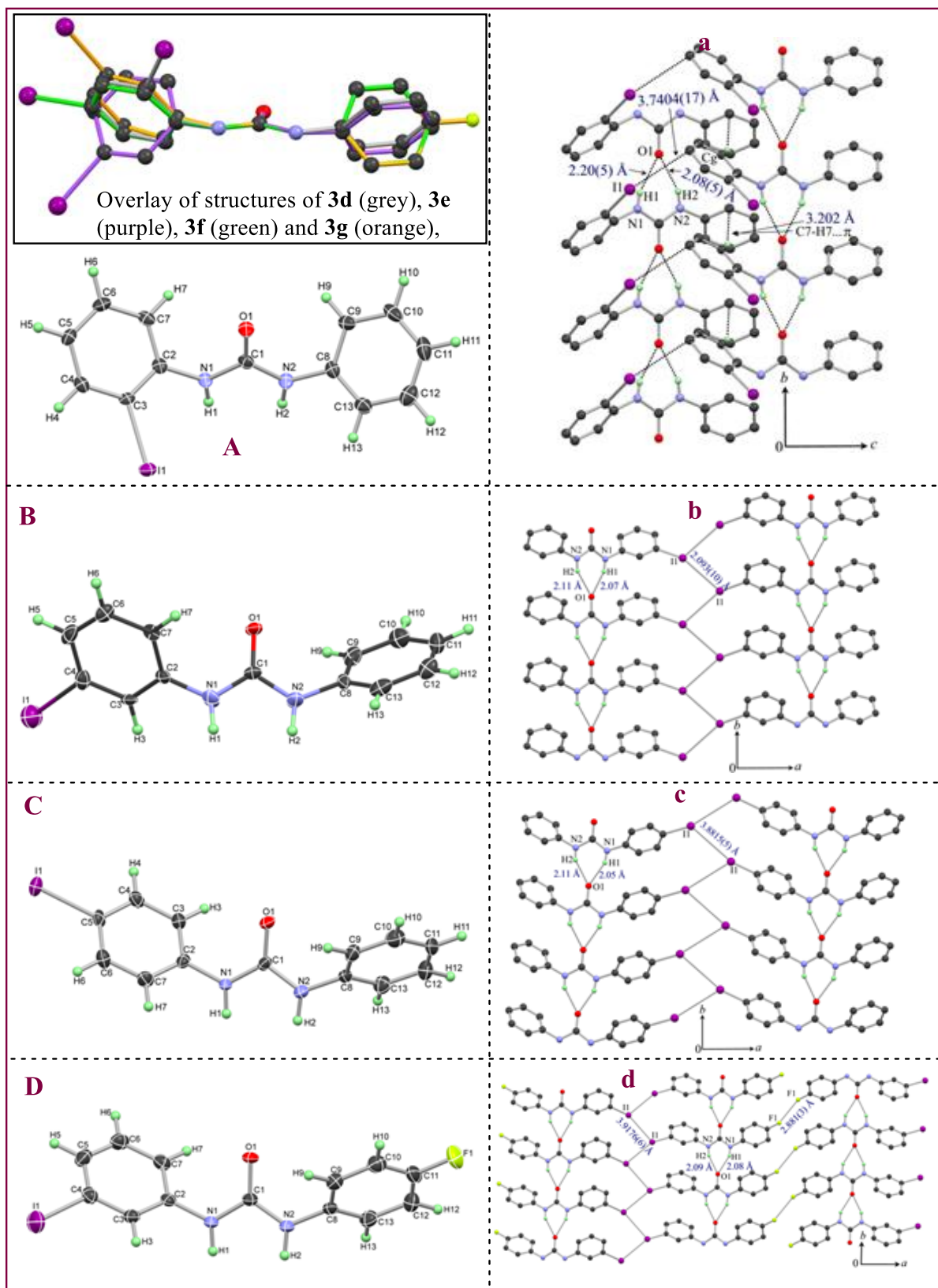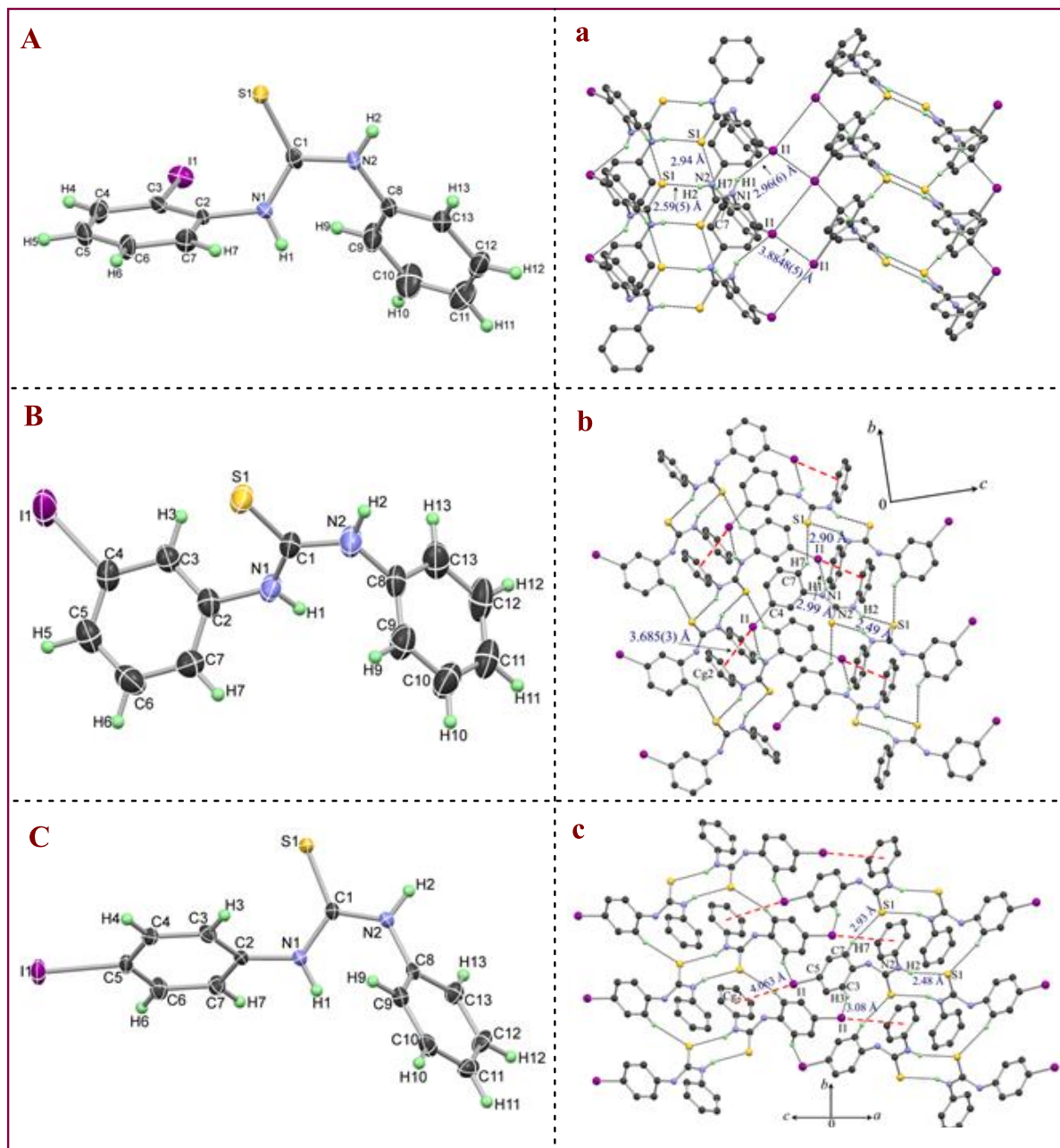

Figure A.5: (A) (B) and (C) ORTEPs of **3h**, **3i**, and **3j** respectively are showing the atom numbering scheme (left side). The displacements ellipsoids are drawn at the 50% probability level and H atoms are shown as small spheres with arbitrary radii. View of molecular packing in crystals of (a) **3h**, (b) **3i**, and (c) **3j** (right side).

A.3.5.4. Category IV: Electronically tailored di-substituted thiourea (3k-m)

In compounds **3k, 3l**, and **3m**, the N2-phenyl ring is substituted with electron withdrawing (NO₂) and electron donor (OMe) groups to investigate the electronic effect on the orientations of N-H atoms with respect to the thiocarbonyl group. Compound **3k** (NO₂ substituted) crystallized in orthorhombic space group *Pna*2₁, whereas compounds **3l** and **3m** (OMe substituted) crystallized in monoclinic space group *P*2₁/*c*. Compound **3l** contains two molecules in the asymmetric unit whereas **3k** and **3m** contained one molecule each. Structure overlay revealed marked difference in the orientations of iodophenyl ring in crystals of **3l** and **3m**(~88°) compared to the difference between the conformations of methoxy substituted phenyl ring (~31°). Orientations of iodophenyl ring in **3k** and **3l** also showed considerable difference (~70°), this also reveals the difference in the orientation of iodophenyl ring in compounds **3k** and **3m** is ~18°. Similar to compounds **3h**, **3i** and **3j**, the N-H moiety adopts *trans-cis* orientations in methoxy substituted compounds **3l** and **3m** irrespective of the position of methoxy group on the phenyl ring. However, the substitution of electron withdrawing NO₂ group at *para*-position of benzene ring in compound **3k** alters the N-H conformation to *trans-trans* geometry similar to urea derivatives (Figure A.6a, left side),

The *trans-trans* conformation of N-H atoms in compounds **3k** resulted in the generation of helical H-bonding chain employing its two NH proton as donors and the C=S as proton acceptor in bifurcated (three centered) N-H…S hydrogen bonding synthon across the crystallographic 2₁-screw axis (Figure A.6a right side,). The geometry of both N-H…S interaction is comparable (entries 39-40, Table A.1). The graph set notations of this synthon is similar to three centered N-H…O hydrogen bonding motif observed in urea moiety. However, there is significant difference from urea derivatives with respect to the approach of two NH protons towards thiocarbonyl group. Although the thiourea derivative **3k** having *trans-trans* orientations of NH protons forms hydrogen bonding chain similar to those formed by urea moiety. However, the two NH protons and the thiocarbonyl group take almost perpendicular orientation with respect to each other due to the sideway approach of the NH donors to the thiocarbonyl acceptor. The orthogonal approach of *trans* NH protons towards C=S group generate a *zig-zag* pattern in contrast to the linear chain formed by urea derivatives. This difference in the H-bonding pattern of urea and thiourea moiety could be because of the differences in the charge distribution around (thio)carbonyl group. The electron density in thioureas is delocalized on the surface of C=S bond leading to the generation *zig-zag* pattern.
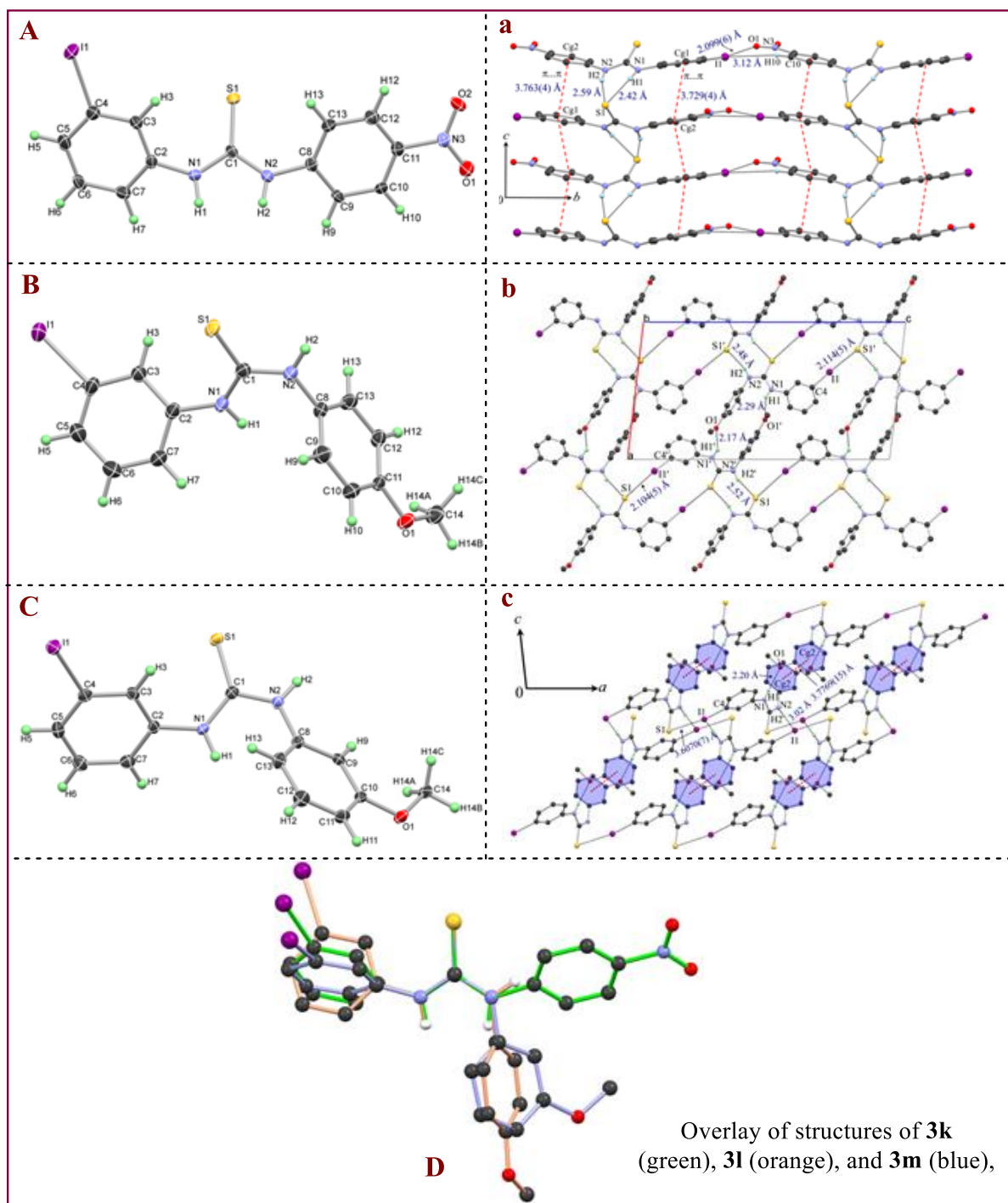
Figure A.6: (A) (B) and (C) ORTEPs of **3k**, **3l**, and **3m** respectively are showing the atom numbering scheme (left side). The displacements ellipsoids are drawn at the 50% probability level and H atoms are shown as small spheres with arbitrary radii. View of molecular packing in crystals of (a) **3k**, (b) **3l**, and (c) **3m** (right side).

In crystals of **3k** the perpendicular approach of the thiocarbonyl groups along the helical chain places the phenyl rings at both ends in stacking mode to generate the extended π-stacking chain along the direction of *c*-axis. Along the chain neighboring molecules are stacked through off-centered π…π aromatic stacking interactions engaging phenyl rings of methoxy benzene

and iodobenzene groups with the centroid-centroid distances being ~3.7 Å (entries 45-46, Table A.1). These neighboring 2_1-screw related helical chains along the *b*-axis are stitched through mono-coordinated I…NO$_2$ halogen bonding interaction[17] supplemented by C-H…I interactions between C-H of the nitrobenzene group and I atom (Figure A.6A, left side, entries 43-44, Table A.1). Along the *a*-axis the adjacent helical chains are related by *a*-glide symmetry and are linked through short and non-linear C-H…O and C-H…S interactions (entries 41-42, Table A.1) to generate the 2D assembly on the *ac* plane.

The *trans-cis* conformation of N-H atoms with respect to the thiocarbonyl group in compound **3l** led to the formation of dimeric N-H…S=C hydrogen bonding synthon between the symmetrically independent neighboring molecules involving *cis* N-H and C=S group. The geometries of both these interactions are comparable (entries 49-50, Table A.1). The adjacent dimeric synthons generate extended ribbon structure through dimeric C-I…S halogen bonding interactions along the *c*-axis.[14] The strength of both these halogen bonding interactions is similar (entries 54-55, Table A.1). The neighboring ribbons along the *a*-axis weaved through dimeric N-H…O hydrogen bond between *trans* N-H and methoxy O atom (entries 47-48, Table A.1) of symmetry independent molecules to generate the bilayer structure on the *ac* plane (Figure A.6b right side). The neighboring bilayers along the *b*-axis are linked via C-H…S, C-H…I and C-H…π interaction (entries 51, 52, 53 and 56, Table A.1).

The change of methoxy position from *para* (**3l**) to *meta* (**3m**) has altered the molecular packing significantly. Although the conformation of N-H hydrogens with respect to the thiocarbonyl group is *trans-cis* in compound **3m**, molecules do not associate in dimeric fashion through N-H…S=C hydrogen bond as observed in other thio derivatives having similar conformation of N-H protons with respect to the thiocarbonyl group. Instead, unit-translated molecules in **3m** generate an extended chain through C-I…S halogen bond running parallel to the *a*-axis (entry 61, Table A.1, Figure A.6c right side). The approach of iodine atom to thiocarbonyl group is perpendicular similar to the approach of N-H hydrogens towards thiocarbonyl group in **3k** (Figure A.6a right side). The adjacent antiparallel chains stitched centro-symmetrically through dimeric N-H…O hydrogen bonding interaction engaging *trans* N-H and oxygen of the methoxy group to generate the one dimensional ribbon along the *a*-axis (Figure A6c (right side), entry 57, Table A.1). The dimeric association of molecules through N-H…O hydrogen bond also places the phenyl rings of the methoxy benzene group in stacking mode to generate intermolecular π-stacking interaction with a Cg⋯Cg distance of 3.7769 (15) Å (Cg…Cg is the distance between ring centroids, entry 62, Table A.1). The adjacent ribbons

are stitched centrosymmetrically through N-H…I interactions engaging *cis* N-H proton and I atom and C-H…S interactions (entries 58-60, Table A.1) roughly along *a*-axis and to create a compact packing on the *ac* plane.

A.3.5.5. Cambridge Structural Database (CSD) Survey

Cambridge Structural Database Survey on the preference mode of association of molecules in ureas and thioureas has already been reported earlier.[13] The study reveals that molecules prefer to associate via chain structure in urea due to *trans-trans* conformation of NH protons. However, in thioureas two modes of association of molecules were observed i.e. dimeric motif through N-H…S hydrogen bonding interaction with *trans-cis* conformation of NH protons and the second mode is the formation of *zig-zag* chain through three centered N-H…S interactions similar to those found in ureas because of the trans-trans conformation of N-H protons. CSD survey revealed equal probabilities for both type of association in thioureas whereas in case of ureas the chain association was dominant. In order to further investigate the current trend in the favored mode of association of molecules in ureas and thioureas and the effect of substituents on their association, a survey of the recent version of Cambridge Structural Database (CSD, Version 5.37, November 2015) was carried out. All the searches were carried out for the organic molecules with no restriction on R-factor, 3D coordinates determined, error-free coordinates and restricted entries of disordered, ionic, polymeric and X-ray powder diffraction structures. Out of 1616 (1072) structures containing urea (thiourea) moiety, 773 (258) hits were excluded in which urea (thiourea) moieties were involved in cyclic structure having *cis-cis* orientation of NH protons (only one example of *cis-cis* acyclic thiourea was found, refcode: ELOPOK).Similar searches with thioureas led to 1072 hits, of which 258 hits were involved in ring formation and therefore excluded. The remaining hits were segregated based on the conformation of NH protons (*trans-cis* or *trans-trans*) using O(S)=C-N-H dihedral angle criterion. The dihedral angle is close to 0° for *trans-cis* conformation and around 180° for *trans-trans* geometry of NH protons related to O(S)=C group. The dihedral angle criterion for *trans-cis* conformation were 130° to 230° (*trans*) and -50° to +50° (*cis*) whereas for *trans-trans* geometry they were 130° to 230°. Interestingly, the considerable number of hits 171was found for *trans-cis* and maximum number of hits (604) was found for *trans-trans* conformation in ureas. In contrast maximum number of hits (700) was observed for *trans-cis* conformation and relatively fewer hits (114) could be found for *trans-trans* geometry in thioureas. This reveals that *trans-trans* conformation of NH protons is the most preferred

motif in ureas whereas the trend is reverse for the thioureas. Custelcean et al. reported that either of these motifs can be manipulated by the bulkiness[13] of the substituents on the thiourea group whereas no such tendency was observed in ureas. The presence of electron withdrawing group (e.g. NO_2, F, Cl or Br) on aromatic ring attached to thioureas also favored *trans-trans* geometry of NH protons leading to hydrogen bonding chain formation. The electron withdrawing group (EWG) increases the acidity of NH protons which then act a good hydrogen bond donor and seems to be favoring the formation of one dimensional bifurcated N-H…S hydrogen bonded chain. The presence and positions of other stronger proton accepting groups such as C=O, N in thioureas containing EWG also influence the conformation of NH protons considerably. Proximity of such hydrogen atom acceptor atoms and NH protons in thioureas facilitate the formation of intramolecular N-H…O/N-H…N hydrogen bonds and this could be the reason for *trans-cis* geometry for NH protons. However, if the proton accepting groups are at a remote distance that prevents the formation of intramolecular N-H…O/N-H…N hydrogen bonds, in such cases intermolecular N-H…O/N-H…N hydrogen bonds formation is favored resulting in the *trans-trans* conformation of NH protons. In case of ureas, the presence of other strong proton accepting groups C=O, N (e.g. acyl or pyridine groups) also influence the conformation of NH protons considerably. Proximity of such hydrogen atom acceptor atoms and NH protons in ureas also facilitate the formation of intramolecular N-H…O/N-H…N hydrogen bonds and this could be the reason for *trans-cis* geometry for NH protons.

A.4. Conclusion

In conclusion, a small library of 13 (**3a**-**3m**) compounds with modular positioning of Iodide and urea/thiourea groups was synthesized in excellent yields in a single step synthetic protocol. The existence of the anticipated (thio)urea derivatives was unambiguously established using a combination of 1-2D NMR spectroscopy, ESI-MS and single crystal X-ray diffraction. These (thio)urea compounds have been classified into four classes; a) mono-substituted, b) di-substituted, c) di-substituted thiourea and d) electronically tailored di-substituted thiourea. The crystal structures of all the derivatives were influenced by conformation of N-H protons with respect to the thio(carbonyl) group. Both N-H protons in urea compounds (**3a**-**3g**) adopt *trans-trans* conformation with respect to the carbonyl group which resulted in the formation three centered N-H…O hydrogen bonding motif leading to the generation of one-dimensional hydrogen bonding chain. These neighbouring chains are linked via either I…I or C-I…π halogen bonding interactions to construct two dimensional networks. However, in thiourea

derivatives both N-H protons take most preferred *trans-cis* orientations with respect to the thiocarbonyl group leading to dimeric association of molecules through N-H…S hydrogen bonding synthon. These dimeirc synthons generate the extended chain structure through C-H…S interactions and the neighbouring chains are connected through either I…I or C-I…π halogen bonding interactions to make two dimensional packing. The effect of substitution of electron withdrawing or donating groups at the phenyl ring on the conformation of two NH protons and its influence on the molecular packing has also been investigated. The presence of electron donating group (OMe) do not change the orientations of the NH atoms however it changes the molecular packing depending on its position on the phenyl ring. In **3l** molecules form dimeric synthon through N-H…S hydrogen bonding interactions (as observed in earlier thio urea derivatives), the successive association of which through N-H…O and I…S interactions generate the 2D structure. However, the installation of OMe group at *meta* position (**3m**) rules out the dimeric association of molecules through N-H…S interactions. Instead, molecule create dimeric structure via centrosymmetric N-H…O interactions engaging *trans* NH proton and methoxy oxygen. The neighboring dimers are further linked through dimeric N-H…I interactions employing *cis* NH proton and I atom to generate an extended chain. The centrosymmetric short I…S contact linked these adjoining chains along the direction of *a*-axis. The preference for the dimeric association of molecules through N-H…S hydrogen bonds over three centered N-H…S linked *zig-zag* chains is also supplemented by CSD survey. Above studies and CSD survey clearly indicates that it is also possible to design the desired supramolecular network using thioureas akin to ureas by manipulating the positions and the nature of the substituents on thioureas. The newly prepared iodophenyl (thio)ureas can be installed on a phosphorus atom to fabricate supramolecular phosphines, and the resultant supramolecular phosphines can be used as ligands in various organometallic transformation such as asymmetric hydrogenation.[18]

A.5. Experimental

A.5.1. Methods and materials

All manipulations were carried out under an inert atmosphere using standard Schlenk technique or m-Braun glove box, excluding **3a-c**. Solvents were dried by standard procedures unless otherwise mentioned, THF from sodium/benzophenone and DCM from calcium hydride under argon atmosphere. Phenylisothicyantes derivatives were purchased from Sigma-Aldrich. Iodoanilines were procured from Alfa-Aesar. All other reagents/chemicals, solvents were

purchased from local suppliers (Spectrochem Pvt. Ltd.; Avra Synthesis Pvt. Ltd.; Thomas Baker Pvt. Ltd. etc). Solution NMR spectra were recorded on a Bruker Avance 200, 400 and 500 MHz instruments at 298K unless mentioned otherwise. Chemical shifts are referenced to external reference TMS (^{1}H and ^{13}C). Coupling constants are given as absolute values. Multiplicities are given as follows s: singlet, d: doublet, t: triplet, m: multiplet, quat: quaternary carbon. The single crystal data was collected using Bruker SMART APEX II single crystal X-ray CCD diffractometer with graphite-monochromatised (Mo-kα = 0.71073 A^o) radiation. Melting point was determined in an open capillary on Bio Technics India melting point apparatus.

A.5.2. Synthesis of ureas and thiourea

A.5.2.1. General procedure for synthesis of compounds 3a-c

3a-c: The iodophenyl-urea compounds were prepared by modified literature procedure.[18] In a 1L flask, iodoaniline (50 mmol) was dissolved in25 mL of aqueous hydrochloric acid (2M). 200 mL of water was added to dissolve the solid. In another beaker KNCO (65 mmol) was dissolved in a minimum volume of water and was dropwise added to the above solution. The reaction mixture was stirred for 4hours at room temperature; after which the white precipitate was filtered and washed with water (20 ml × 3 times). The compound was dried under vacuum, washed with toluene (20 ml × 3 times) and dried under vacuum to get the iodophenyl-urea **3a**-**c**.

A.5.2.2. General procedure for synthesis of compounds 3d-m

3d-m: The phenylisocyanates or isothiocyanates (1 eq.) or the derivatives of these, were dissolved in dichloromethane (5 mL) at 0°C. Subsequently, iodoanilines (1.4 eq.), were added drop wise with constant stirring. The progress of the reaction was monitored by TLC. After completion of reaction, solvent was evaporated from the reaction mixture and the product was purified by column chromatography in excellent yield.

3a:^{1}H NMR (500 MHz, DMSO-d$_6$, 298K) δ = 7.78 (ddd, J_{H-H} = 12.3 Hz, 8.3 Hz, 1.4 Hz, 2H, Ar, C*H*), 7.62 (s, 1H, N*H*), 7.28 (t, J_{H-H} = 7.8 Hz, 1H, Ar, C*H*), 6.76 (t, J_{H-H} = 7.5 Hz, 1H, Ar, C*H*), 6.35 (s, 2H, N*H*$_2$). **^{13}C NMR** (125 MHz, DMSO-d$_6$, 298K) δ = 155.8 (s, *C*O), 140.6 (s, Ar, quat-*C*H), 138.7 (s, Ar, *C*H), 128.4 (s, Ar, *C*H), 124.4 (s, Ar, *C*H), 122.8 (s, Ar, *C*H), 90.8 (s, Ar-I). **IR** (cm^{-1}): 3430 (NH$_2$), 3298 (NH$_2$), 3200 (NH), 1698 (C=O). **ESI-MS** (+ve) (For C$_7$H$_7$IN$_2$O) m/z = 262.96 [M+H]$^+$, 284.94 [M+Na]$^+$. **Mp** = 140°C.

3b:^{1}**H NMR** (500 MHz, DMSO-d$_6$, 298K) δ = 8.66 (s, 1H, N*H*), 7.98 (s, 1H, Ar, C*H*), 7.24 (q, J_{H-H} = 6.7 Hz, 2H, Ar, C*H*), 6.99 (t, J_{H-H} = 8.00 Hz, 1H, Ar, C*H*), 5.94 (s, 2H, N*H$_2$*). ^{13}**C NMR** (125 MHz, THF-d$_8$, 298K) δ = 157.2 (s, *C*O), 143.3 (s, Ar, quat-*C*H), 131.2 (s, Ar, *C*H), 131.0 (s, Ar, *C*H), 127.8 (s, Ar, *C*H), 118.3 (s, Ar, *C*H), 94.8 (s, Ar-I). **IR** (cm^{-1}): 3429 (NH$_2$), 3295 (NH$_2$), 3203 (NH), 1698 (C=O). **ESI-MS** (+ve) (For C$_7$H$_7$IN$_2$O) m/z = 262.96 [M+H]$^+$, 284.94 [M+Na]$^+$. **Mp** = 165°C.

3c:^{1}**H NMR** (500 MHz, DMSO-d$_6$, 298K) δ = 8.7 (s, 1H, N*H*), 7.52 (s, 2H, Ar, C*H*), 7.26 (s, 2H, Ar, C*H*), 5.93 (s, 2H, N*H$_2$*). ^{13}**C NMR** (125 MHz, DMSO-d$_6$, 298K) δ = 155.8 (s, *C*O), 140.5 (s, Ar, quat-*C*H), 137.1 (s, Ar, *C*H), 120.0 (s, Ar, *C*H), 83.6 (s, Ar-I). **IR** (cm^{-1}): 3423 (NH$_2$), 3303 (NH$_2$), 3259 (NH), 1654 (C=O). **ESI-MS** (+ve) (For C$_7$H$_7$IN$_2$O) m/z = 262.96 [M+H]$^+$, 284.94 [M+Na]$^+$. **Mp** = 220°C.

3d:^{1}**H NMR** (500 MHz, DMSO-d$_6$, 298K) δ = 9.44 (s, 1H, N*H*), 7.90 (s, 1H, N*H*), 7.86 (dd, J_{H-H} = 7.95 Hz, 1.14Hz, 1H, Ar, C*H*), 7.83 (dd, J_{H-H} = 7.92 Hz, 1.12Hz, 1H, Ar, C*H*), 7.50 (s, 1H, Ar,C*H*), 7.48 (s, 1H, Ar, C*H*),7.34 (s, 1H, Ar, C*H*), 7.30 (td, 8.6Hz, 1.3Hz, 2H, Ar, C*H*), 6.98 (t, J_{H-H} = 7.28 Hz, 1H, Ar, C*H*), 6.83 (td, 7.65Hz, 1.2Hz, 1H, Ar, C*H*). ^{13}**C NMR** (125 MHz, DMSO-d$_6$, 298K) δ = 152.3 (s, quat, C=O), 139.8 (s, quat, Ar), 139.6 (s, quat, Ar), 138.9 (s, Ar), 128.8 (s, Ar), 128.5(s, Ar), 125.0 (s, Ar), 123.0(s, Ar), 122.0 (s, Ar), 118.2 (s, Ar), 91.3 (s, quat, Ar, C-*I*). **IR** (cm^{-1}): 3284 (NH), 1644 (C=O). **ESI-MS** (+ve) (Cal. For C$_{13}$H$_{11}$N$_2$OI) m/z = 338.99[M+H]$^+$, 360.98[M+Na]$^+$. **Mp**= 190°C.

3e:^{1}**H NMR** (200 MHz, DMSO-d$_6$298K) δ = 8.75 (s, 1H, N*H*), 8.67 (s, 1H, N*H*), 7.97 (d, 1.8Hz, 1H, C*H*), 7.42 (s, 1H, Ar, C*H*), 7.39 (s, 1H, Ar, C*H*), 7.27-7.22 (m, 4H, Ar, C*H*), 7.03 (t, J_{H-H} = 8.32 Hz 1H, Ar, C*H*), 6.94 (t, J_{H-H} = 7.33 Hz, 1H, Ar, C*H*). ^{13}**C NMR** (100 MHz, DMSO-d$_6$,298K) δ = 152.4 (s, quat, C=O), 141.2 (s, quat, Ar), 139.4 (s, quat, Ar), 130.8 (s, Ar), 130.3(s, Ar), 128.8 (s, Ar), 126.3 (s, Ar), 122.1 (s, Ar), 118.4 (s, Ar), 117.5 (s, Ar), 94.8 (s, quat, Ar).**IR**(cm^{-1}): 3295 (NH), 1631 (C=O). **ESI-MS** (+ve) (Cal. For C$_{13}$H$_{11}$N$_2$OI) m/z = 338.99[M+H]$^+$, 360.98[M+Na]$^+$. **Mp** = 195°C.

3f:^{1}**H NMR** (400MHz, DMSO-d$_6$, 298K) δ =8.79 (s, 1H, N*H*), 8.70 (s, 1H, N*H*), 7.60 (d, J_{H-H} = 8.66 Hz, 2H, C*H*), 7.46 (d, J_{H-H} = 7.66Hz, 2H, C*H*), 7.33 (d, J_{H-H} = 8.66 Hz, 2H, C*H*), 7.28 (t, J_{H-H} = 7.66 Hz, 2H, C*H*), 6.98 (t, J_{H-H} = 7.34 Hz, 1H, C*H*). ^{13}**C NMR** (100 MHz, DMSO-d$_6$, 298K)δ = 152.3 (s, quat, C=O), 139.6 (s, quat, Ar), 139.5 (s, quat, Ar), 137.3 (s, Ar, *C*H), 128.3 (s, Ar, *C*H), 121.8 (s, Ar, *C*H), 120.4 (s, Ar, *C*H), 118.3 (s, Ar, *C*H), 84.6 (s, quat, Ar). **IR** (cm^{-1}): 3300 (NH), 1632 (C=O). **ESI-MS** (+ve) (Cal. For C$_{13}$H$_{11}$N$_2$OI) m/z = 338.99[M+H]$^+$, 360.98[M+Na]$^+$. **Mp**= 150°C.

3g:[1]**H NMR** (500 MHz, DMSO-d$_6$, 298K): δ = 8.78 (s, 1H, N*H*), 8.75(s, 1H, N*H*), 8.01 (s, 1H, Ar, C*H*), 7.46 (q, J_{H-H} = 7.26 Hz, 2H, Ar, C*H*), 7.32 (q, J_{H-H} = 8.98 Hz, 2H, Ar, C*H*), 7.12 (t, J_{H-H} = 7.10 Hz, 2H, Ar, C*H*), 7.06 (t, J_{H-H} = 7.05 Hz, 1H, Ar, C*H*). **^{13}C NMR** (125 MHz, DMSO-d$_6$, 298K): δ = 158.4 (s, quat, C=S), 152.4 (s, quat, Ar), 141.2 (s, quat, Ar), 135.7(s, quat, Ar), 130.7 (s, Ar, CH), 130.3 (s, Ar, CH), 126.3 (s, Ar, CH), 120.2 (d, Ar, CH), 117.5 (s, Ar, CH), 115.2 (s, Ar, CH), 94.7 (s, quat, Ar, C-I).**IR (cm^{-1}):** 3300 (NH), 1632 (C=O). **ESI-MS** (+ve) (Cal. For C$_{13}$H$_{11}$N$_2$OFI) m/z = 356.98 [M+H]$^+$, 378.97 [M+Na]$^+$.**Mp**= 210°C.

3h:[1]**H NMR** (400MHz, DMSO-d$_6$, 298K) δ =9.93 (s, 1H, N*H*), 9.33 (s, 1H, N*H*), 7.88 (d, $^J_{H-H}$ = 7.96 Hz, 1H, Ar, C*H*), 7.56 (d, J_{H-H} = 7.71Hz, 2H, Ar, C*H*), 7.33-7.44 (m, 4H, Ar, C*H*), 7.15 (t, J_{H-H} = 7.20 Hz, 1H, Ar, C*H*), 7.02 (t, J_{H-H} = 6.57 Hz, 1H, Ar, C*H*). **^{13}C NMR**(100MHz, DMSO-d$_6$, 298K) δ = 180.2 (s, quat, C=S), 141.1 (s, quat, Ar), 139.7 (s, quat, Ar), 138.9 (s, Ar), 128.9 (s, Ar), 128.5 (s, Ar), 128.5 (s, Ar), 128.2 (s, Ar), 124.6 (s, Ar), 123.8 (s, Ar), 99.6 (s, quat, Ar, C-*I*). **IR** (cm^{-1}): 3289 (NH), 1588 (C=S). **ESI-MS** (+ve) (Cal. For C$_{13}$H$_{11}$N$_2$SI) m/z = 354.97[M+H]$^+$, 376.95[M+Na]$^+$. **Mp**= 160°C.

3i:[1]**H NMR** (400 MHz, DMSO-d$_6$, 298K) δ = 9.95 (s, 1H, N*H*), 9.86 (s, 1H, N*H*), 7.97 (s, 1H, Ar, C*H*), 7.48 (d, J_{H-H} = 7.57 Hz, 4H, Ar, C*H*), 7.35 (t, J_{H-H} = 7.58, 2H, Ar, C*H*), 7.14 (q, J_{H-H} = 7.34 Hz, 2H, Ar, C*H*). **^{13}C NMR** (100 MHz, DMSO-d$_6$, 298K) δ = 179.5 (s, quat, C=S), 141.0 (s, quat, Ar), 139.1 (s, quat, Ar), 132.7 (s, Ar), 131.7 (s, Ar), 130.3 (s, Ar), 128.5 (s, Ar), 124.6 (s, Ar), 123.3 (s, Ar), 122.9 (s, Ar), 93.8 (s, quat, Ar). **IR** (cm^{-1}): 3323 (NH), 1577 (C=S). **ESI-MS** (+ve) (Cal. For C$_{13}$H$_{11}$N$_2$SI) m/z = 354.97[M+H]$^+$, 376.95[M+Na]$^+$. **Mp**=110°C.

3j:[1]**H NMR** (500 MHz, DMSO-d$_6$, 298K) δ = 8.78 (s, 1H, N*H*), 8.69 (s, 1H, N*H*), 7.61 (d, 2H, J_{H-H} = 8.31 Hz, 2H, Ar, C*H*), 7.45 (d, J_{H-H} = 7.99 Hz, 2H, Ar, C*H*), 7.27-7.33 (m, 4H, Ar, C*H*), 6.98 (t, J_{H-H} = 7.20 Hz, 1H, Ar, C*H*). **^{13}C NMR** (50 MHz, DMSO-d$_6$, 298K) δ = 179.4 (s, quat, C=S), 139.4 (s, quat, Ar), 139.3 (s, quat, Ar), 137.0 (s, Ar), 128.5 (s, Ar), 125.7 (s, Ar), 124.6 (s, Ar), 123.7 (s, Ar), 88.5 (s, quat, Ar, C-*I*). **IR**(cm^{-1}): 3199 (NH), 1587 (C=S). **ESI-MS**(+ve) (Cal. For C$_{13}$H$_{11}$N$_2$SI) m/z = 354.97[M+H]$^+$, 376.95[M+Na]$^+$. **Mp**= 140°C.

3k:[1]**H NMR** (500 MHz, , DMSO-d$_6$, 298K): δ = 10.50 (s, 1H, N*H*), 10.30 (s, 1H, N*H*), 8.23 (d, 2H, J_{H-H} = 9.16 Hz, Ar, C*H*), 7.95 (s, 1H, Ar, C*H*), 7.83 (d, J_{H-H} = 9.16 Hz, 2H, Ar, C*H*), 7.52 (d, J_{H-H} = 7.60 Hz, 1H, Ar, C*H*), 7.50 (d, J_{H-H} = 7.85 Hz, 1H, Ar, C*H*), 7.17 (t, J_{H-H} = 7.93 Hz, 1H, Ar, C*H*). **^{13}C NMR** (125 MHz, DMSO-d$_6$, 298K): δ = 179.3 (s, quat, C=S), 145.9 (s, quat, Ar), 142.4 (s, quat, Ar), 140.4 (s, quat, Ar), 133.4 (s, Ar, CH), 131.8 (s, Ar, CH), 130.5 (s, Ar, CH), 124.4 (s, Ar, CH), 123.0 (s, Ar, *CH*), 121.7 (s, Ar, CH), 93.9 (s, quat, Ar, C-

I). **IR** (cm^{-1}): 3216 (NH), 3154 (NH), 1576 (C=S). **ESI-MS** (+ve) (Cal. For C$_{13}$H$_{10}$N$_3$O$_2$SI) m/z = 399.96[M+H]$^+$. **Mp**= 150°C.

3l:^{1}**H NMR** (500 MHz, DMSO-d$_6$, 298K) δ = 9.76 (s, 1H, N*H*), 9.68 (s, 1H, N*H*), 7.95 (s, 1H, Ar, C*H*), 7.46 (d, J_{H-H} = 7.6 Hz, 2H Ar, C*H*), 7.32 (d, J_{H-H} = 9.0 Hz, 2H, Ar, C*H*), 7.11 (t, J_{H-H} = 7.6 Hz, 1H, Ar, C*H*), 6.92 (d, J_{H-H} = 8.5 Hz, 2H, C*H*), 3.75 (s, 3H, OC*H$_3$*). ^{13}**C NMR** (125 MHz, DMSO-d$_6$, 298K): δ = 179.7 (s, quat, C=S), 156.7 (s, quat, Ar, *C-OMe*), 141.1 (s, quat, Ar), 132.6 (s, Ar, CH), 131.6 (s, Ar, CH), 131.7 (s, Ar, CH), 130.2(s, Ar, CH), 126.1 (s, Ar, CH), 122.9 (s, Ar, *CH*), 113.7 (s, quat, Ar), 93.8 (s, quat, Ar, C-I), 55.2 (s, *OCH$_3$*). **IR** (cm^{-1}): 3199 (NH), 1587 (C=S). **ESI-MS** (+ve) (Cal. For C$_{14}$H$_{13}$N$_2$OSI) m/z = 384.98[M+H]$^+$, 406.96[M+Na]$^+$. **Mp**= 105°C.

3m:^{1}**H NMR** (400 MHz, DMSO-d$_6$, 298K) δ = 9.95 (s, 1H, N*H*), 9.04 (s, 1H, N*H*), 7.95 (s, 1H, Ar, C*H*), 7.48 (d, 2H, J_{H-H} = 8.07 Hz, Ar, C*H*), 7.25 (t, J_{H-H} = 8.07 Hz, 1H, Ar, C*H*), 7.16 (s, 1H, Ar, C*H*), 7.13 (t, J_{H-H} = 8.32 Hz, 1H, Ar, C*H*), 7.02 (d, J_{H-H} = 8.00 Hz, 1H, Ar, C*H*), 6.73 (d, J_{H-H} = 7.68 Hz, 1H, Ar, C*H*), 3.75 (s, 3H, *OCH$_3$*). ^{13}**C NMR** (100 MHz, DMSO-d$_6$, 298K) δ = 179.3 (s, quat, C=S), 159.3 (s, quat, Ar, *C-OMe*), 140.9 (s, quat, Ar), 140.2 (s, quat, Ar), 132.8 (s, Ar), 131.7 (s, Ar), 130.3 (s, Ar), 129.3 (s, Ar), 122.9 (s, Ar), 115.6 (s, Ar), 110.0 (s, Ar), 109.3 (s, Ar), 93.8 (s, quat, Ar, *C-I*), 55.1 (s, Ar, *OCH$_3$*). **IR** (cm^{-1}): 3190 (NH), 1580 (C=S). **ESI-MS** (+ve) (Cal. For C$_{14}$H$_{13}$N$_2$OSI) m/z = 384.98 [M+H]$^+$, 406.96 [M+Na]$^+$. **Mp**= 115°C.

A.5.3. Crystallization

Crystallization of compounds **3a**-**3c** was attempted from the mixture of ethanol-ethyl acetate (1:1, v:v) solvents while that of **3i** from THF-ethyl acetate (1:1, v:v) whereas other compounds **3d**-**3h** and **3j**-**3m** crystallized from DMF-ethyl acetate solvent mixture (1:1, v:v) at ambient temperature. A clear solution was obtained by vigorous shaking and/or warming of the compound in the solvent and the solution was allowed to evaporate at room temperature over 1-2 days to yield good quality crystals. Crystallization from other solvents like methanol, ethanol, ethyl acetate, THF, acetonitrile, DMF and DMSO also was also attempted, however, we failed to obtain X-ray quality crystals from these solvents. Crystallization from other solvents like chloroform, dichloromethane, toluene, diethyl ether, *n*-hexane could not be carried out because of the solubility issue.

A.5.3.1. Differential Scanning Calorimetry (DSC) Studies

The thermal behavior of all the urea and thioureas derivatives was investigated by measuring the enthalpy change on a MettlerToledo differential scanning calorimeter (DSC 822^e). Crystals obtained from crystallization were first air-dried before they were used for DSC analysis. Crystals (~ 3-5 mg) were placed in a sealed aluminum pan (40 μL) with crimped pan closure and heated at a rate of 5 °C min^{-1} and dry nitrogen gas was used for purging. Crystals were analyzed from room temperature (30°C) to 250 °C using an empty aluminum pan as reference. DSC profiles of all the compounds revealed single endotherm attributed to their melting. No other endothermic/exothermic peak was observed before the melting endotherm thus ruled out any phase transition before melting.

A.5.3.2. Crystallographic details

Good quality single crystals of all the derivatives were selected using Leica polarizing microscope MZ75 for the single crystal X-ray diffraction studies. The diffraction data measurements were carried out on a Bruker SMART APEX CCD diffractometer with graphite-monochromatized (Mo Kα = 0.71073Å) radiation. The X-ray generator was operated at 50 kV and 30 mA. A preliminary set of cell constants and an orientation matrix were calculated from total 36 frames. The optimized strategy used for data collection consisted different sets of φ and ω scans with 0.5° steps in φ/ω. Data were collected keeping the sample-to-detector distance fixed at 5.00 cm. The X-ray data acquisition was monitored by APEX2 program suit. All the data were corrected for Lorentz-polarization and absorption effects using SAINT and SADABS programs integrated in APEX2 package. The structures were solved by direct methods and refinedby full matrix least squares, based on F^2, using SHELX-97.[19] Molecular diagrams were generated using Mercury programs.[20] Geometrical calculations were performed using SHELX-97[19] and PLATON.[21]

Hydrogen atoms bound to N-atoms in compounds **3a**, **3d** and **3h** were located in the difference Fourier and refined isotropically. The remaining H-atoms for all the compounds were placed in geometrically idealized positions (C-H = 0.95 and N-H = 0.88 Å for the phenyl and N-H atoms for compounds **3e, 3j, 3f, 3i, 3l, 3m,** fluoro and C-H = 0.93 and N-H = 0.86 Å for compounds **3b, 3c, 3k;** C-H = 0.96 and 0.98 for the methyl H-atoms of compounds **3k** and **3m** respectively) and constrained to ride on their parent atoms {[U$_{iso}$(H) = 1.2 U$_{eq}$(C) and U$_{eq}$(N) for phenyl and N-H atoms and [U$_{iso}$(H) = 1.5 U$_{eq}$(C)] form methyl H-atoms}.

Table A.2 Crystallographic data and structure refinement parameters for **3a**-**m**.

	3a	3b	3c	3d	3e
Mol. Formula	$C_7H_7IN_2O$	$C_7H_7IN_2O$	$C_7H_7IN_2O$	$C_{13}H_{11}IN_2O$	$C_{13}H_{11}IN_2O$
Mr	262.05	262.05	262.05	338.14	338.14
Temp. (K)	296(2)	100(2)	150(2)	150(2)	150(2)
Crystal System	Monoclinic	Orthorhombic	Monoclinic	Monoclinic	Monoclinic
Space group	*P2₁/c*	*Pccn*	*P2₁*	*P2₁/c*	*P2₁/c*
a/Å	11.8183(6)	21.4515(4)	4.6211(7)	21.0485(13)	27.253(5)
b/Å	7.9251(4)	8.44460(10)	5.2775(8)	4.6303(3)	4.6408(9)
c/Å	8.9570(5)	8.99770(10)	16.932(3)	12.8294(7)	9.8532(18)
α/°	90	90	90	90	90
β/°	90.047(3)	90	96.344(2)	102.835(4)	91.991(6)
γ/°	90	90	90	90	90
V/Å³	838.92(8)	1629.93(4)	410.40(11)	1219.12(13)	1245.5(4)
Z,D$_{calc}$/g cm⁻³	4, 2.075	8, 2.136	2, 2.121	4, 1.842	4,1.803
μ/mm⁻¹	3.760	3.871	3.843	2.611	20.081
F (000)	496	992	248	656	656
θ max/°	34.78	43.946	31.586	30.753	68.388
Absor. Correction	multi-scan	multi-scan	multi-scan	multi-scan	multi-scan
Refln. Collected	13070	57286	6434	11390	11283
Unique Refln	3612	5815	2567	3066	2158
Observed Refln.	2976	4231	2544	2743	1859
R$_{int}$	0.0471	0.0447	0.0194	0.0307	0.0555
No. of parameter	112	101	100	198	154
*R₁*_obs, *R₁*_all	0.0369,0.0461	0.0465, 0.0710	0.0148, 0.0150	0.0411,0.0492	0.0570,0.0717
*wR₂*_obs, *wR₂*_all	0.0872,0.0922	0.1360, 0.1520	0.0358, 0.0359	0.0692,0.0713	0.1608,0.1728
GoF	1.052	1.024	1.103	1.257	1.150
Δρ_{max},Δρ_{min}/eÅ⁻³	1.391, -0.986	1.579, -2.587	0.534 ,-0.761	1.110, -1.830	0.659, -0.744
CCDC No.	1046367	1046368	1046369	1483979	1484013

Table A.2: Continue

	3f	3g	3h	3i	3j
Mol. Formula	$C_{13}H_{11}IN_2O$	$C_{13}H_{10}FIN_2O$	$C_{13}H_{11}IN_2S$	$C_{13}H_{11}IN_2S$	$C_{13}H_{11}IN_2S$
Mr	338.14	356.13	354.20	354.20	354.20
Temp. (K)	200(2)	200(2)	150(2)	200(2)	150(2)
Crystal System	Monoclinic	Monoclinic	Monoclinic	Monoclinic	Monoclinic
Space group	*P2₁/c*	*P2₁/c*	*P2₁/n*	*P2₁/n*	*P2₁/n*
a/Å	26.1800(17)	27.607(6)	12.683(8)	12.6626(17)	15.3895(12)
b/Å	4.6273(3)	4.6224(11)	5.065(3)	7.0591(10)	5.4985(5)
c/Å	9.9779(7)	9.750(2)	20.530(12)	15.395(2)	17.1612(15)
α/°	90	90	90	90	90
β/°	91.646(3)	93.235(3)	98.948(8)	94.006(2)	116.180(4)
γ/°	90	90	90	90	90
V/Å³	1208.25(14)	1242.3(5)	1302.8(14)	1372.7(3)	1303.2(2)
Z,D$_{calc}$/g cm⁻³	4, 1.859	4,1.904	4, 1.806	4,1.714	4, 1.805
μ/mm⁻¹	2.635	2.579	2.597	2.464	2.596
F (000)	656	688	688	688	688
θ max/°	28.728	31.636	31.684	31.568	40.969
Absor. Correction	multi-scan	Multi-scan	multi-scan	Multi-scan	multi-scan
Refln. Collected	8397	18098	18315	19962	33486
Unique Refln	2899	3985	4189	4367	5966
Observed Refln.	2485	3323	3554	3650	5352
R$_{int}$	0.0320	0.0411	0.0741	0.0465	0.0357
No. of parameter	154	163	154	154	154
*R₁*_obs, *R₁*_all	0.0310, 0.0448	0.0316,0.0409	0.0717, 0.0907	0.0484,0.0568	0.0549, 0.0639

*wR₂*_obs, *wR₂*_all	0.1004, 0.1446	0.0792,0.0834	0.1404, 0.1474	0.1309,0.1354	0.1094, 0.1126
GoF	1.057	1.040	1.217	1.054	1.240
$\Delta\rho_{max},\Delta\rho_{min}/e\text{Å}^{-3}$	1.302, -1.206	1.378 ,-0.593	2.857, -2.746	2.441, -1.578	2.651 , -1.510
CCDC No.	1483987	1483981	1483978	1483980	1483986

Table A.2 Continued.

	3k	3l	3m
Mol. Formula	$C_{13}H_{10}IN_3O_2S$	$C_{14}H_{13}IN_2OS$	$C_{14}H_{13}IN_2OS$
Mr	399.20	384.22	384.22
Temp. (K)	150(2)	150(2)	150 (2)
Crystal System	Orthorhombic	Monoclinic	Monoclinic
Space group	*Pna*2₁	*P*2₁/*c*	P2₁/*c*
a/Å	14.2167(19)	12.481(2)	8.1518(6)
b/Å	14.5308(18)	9.9446(16)	18.2688(13)
c/Å	6.8955(10)	23.867(4)	9.5334(7)
α/°	90	90	90
β/°	90	96.736(2)	93.6720(10)
γ/°	90	90	90
V/Å³	1424.5(3)	2941.9(8)	1416.83(18)
Z,D_calc/g cm⁻³	4, 1.861	8,1.735	4, 1.801
µ/mm⁻¹	2.399	2.312	2.401
F (000)	776	1504	752
θ max/°	31.147	31.578	31.753
Absor. Correction	multi-scan	Multi-scan	multi-scan
Refln. Collected	18112	43395	22086
Unique Refln	4003	9334	4463
Observed Refln.	3411	8270	4335
R_int	0.0328	0.0513	0.0203
No. of parameter	181	345	181
*R₁*_obs, *R₁* _all	0.0424, 0.0540	0.0567,0.0643	0.0257, 0.0267
*wR₂*_obs, *wR₂*_all	0.0835, 0.0870	0.1265,0.1300	0.0579, 0.0583
GoF	1.088	1.181	1.228
$\Delta\rho_{max},\Delta\rho_{min}/e\text{Å}^{-3}$	1.431 , -0.817	3.494, -1.133	0.808, -0.830
CCDC No.	1483985	1483982	1483984

A.6. Characterization

Figure 7. ^{1}H-NMR spectrum of 1-(2-iodophenyl)-3-phenylurea (**3a**) in DMSO-d$_6$.

Figure 8. ^{13}C-NMR spectrum of 1-(2-iodophenyl)-3-phenylurea (**3a**) in DMSO-d$_6$.
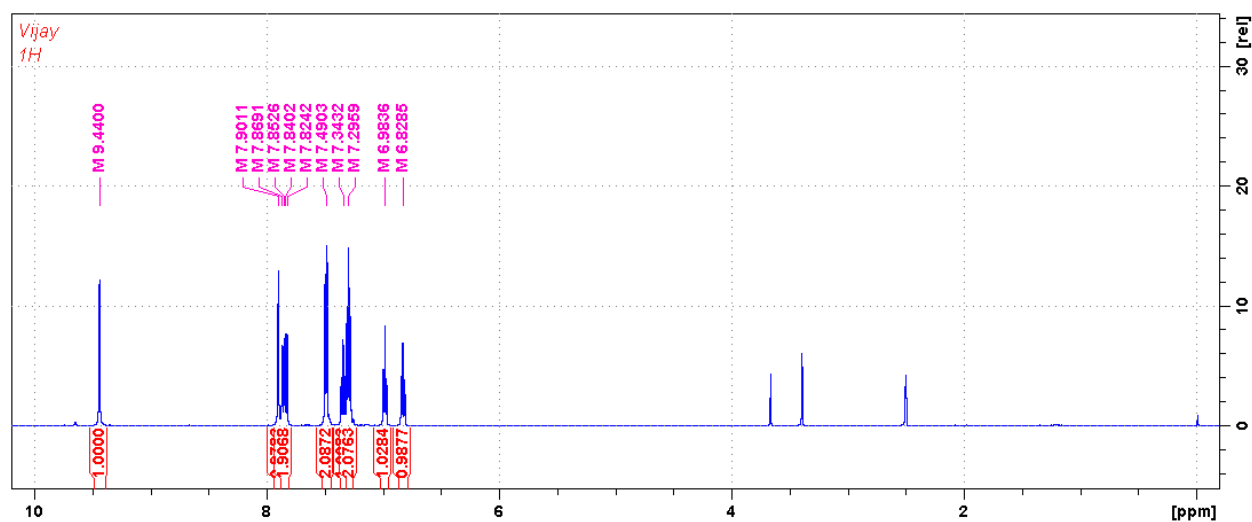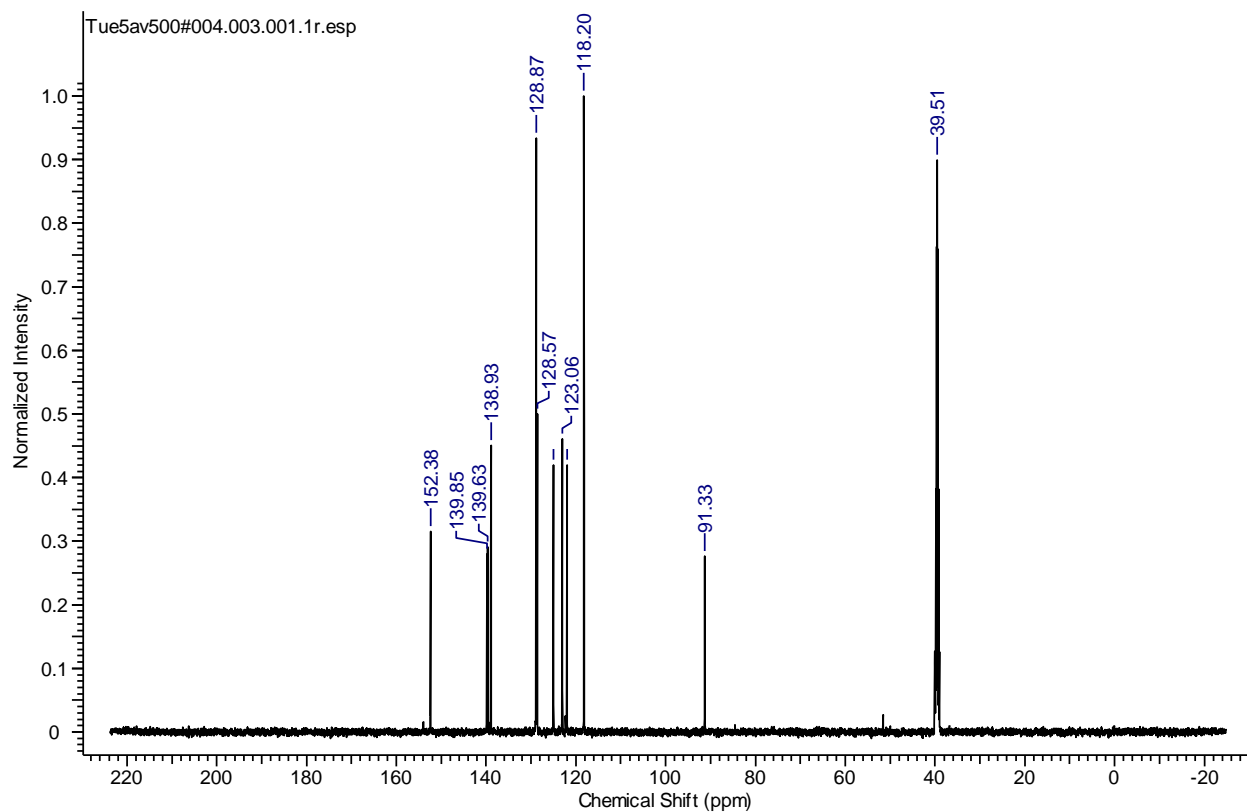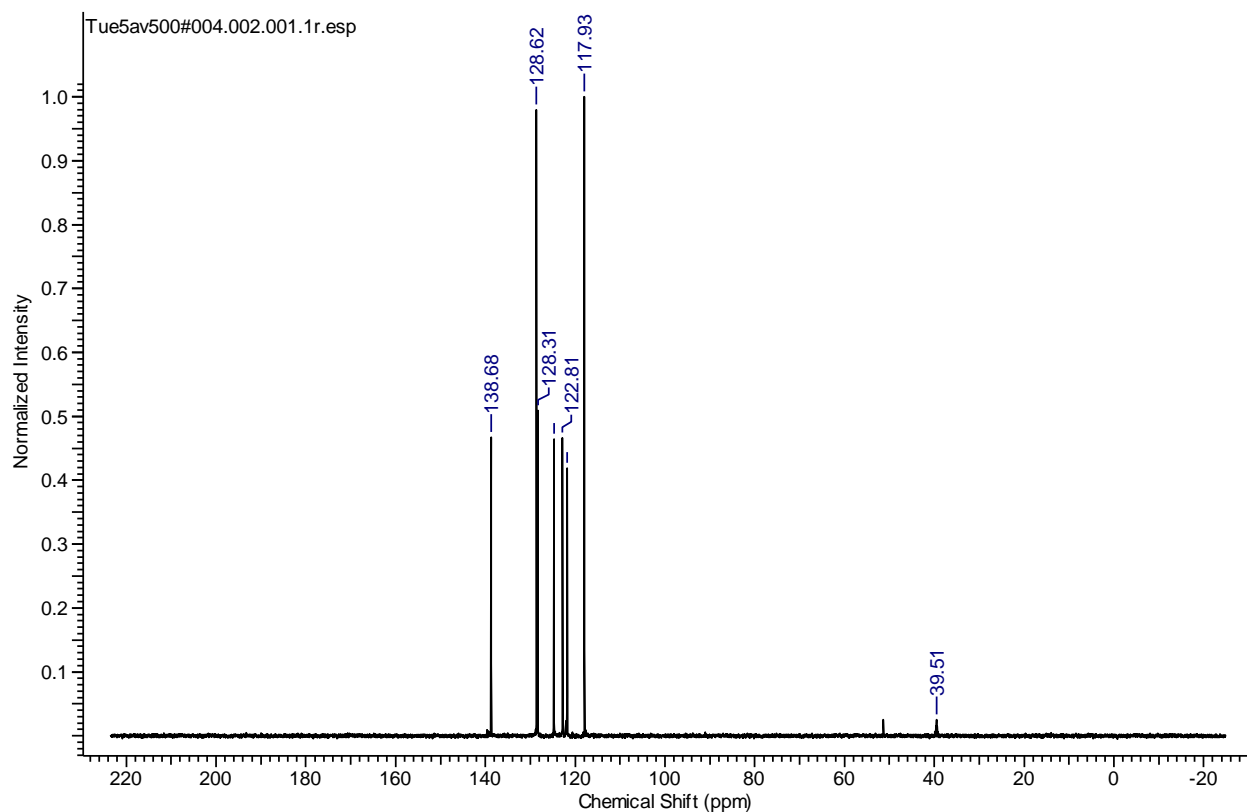

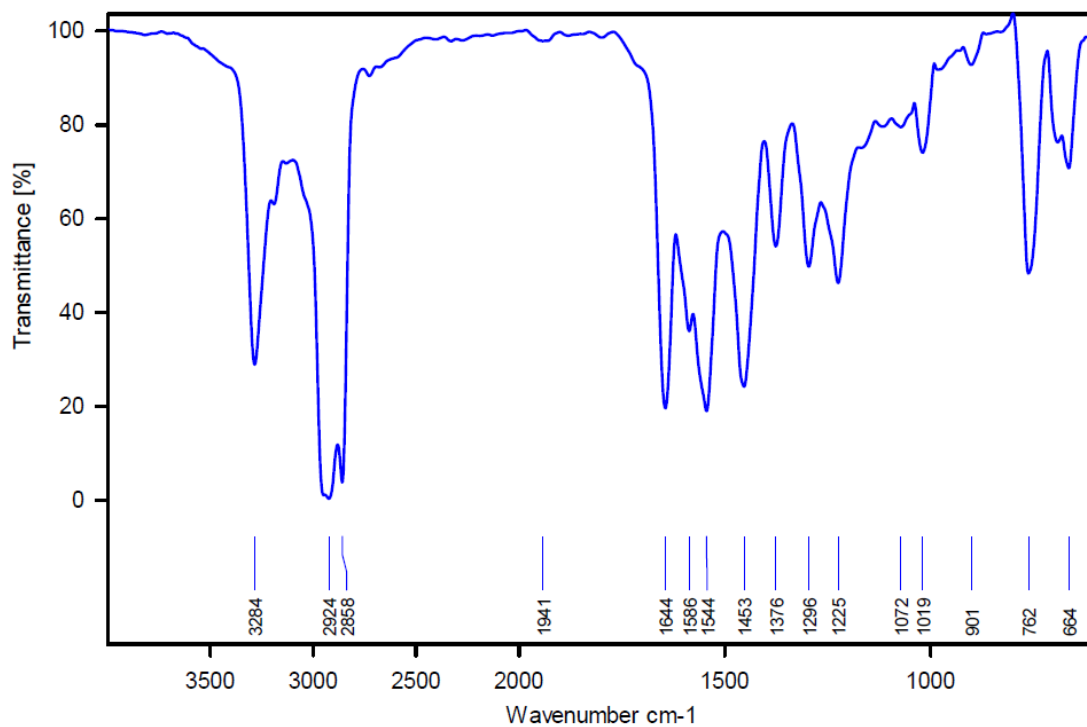**Figure 9.** ^{13}C-NMR spectrum of 1-(2-iodophenyl)-3-phenylurea (**3a**) in DMSO-d$_6$.

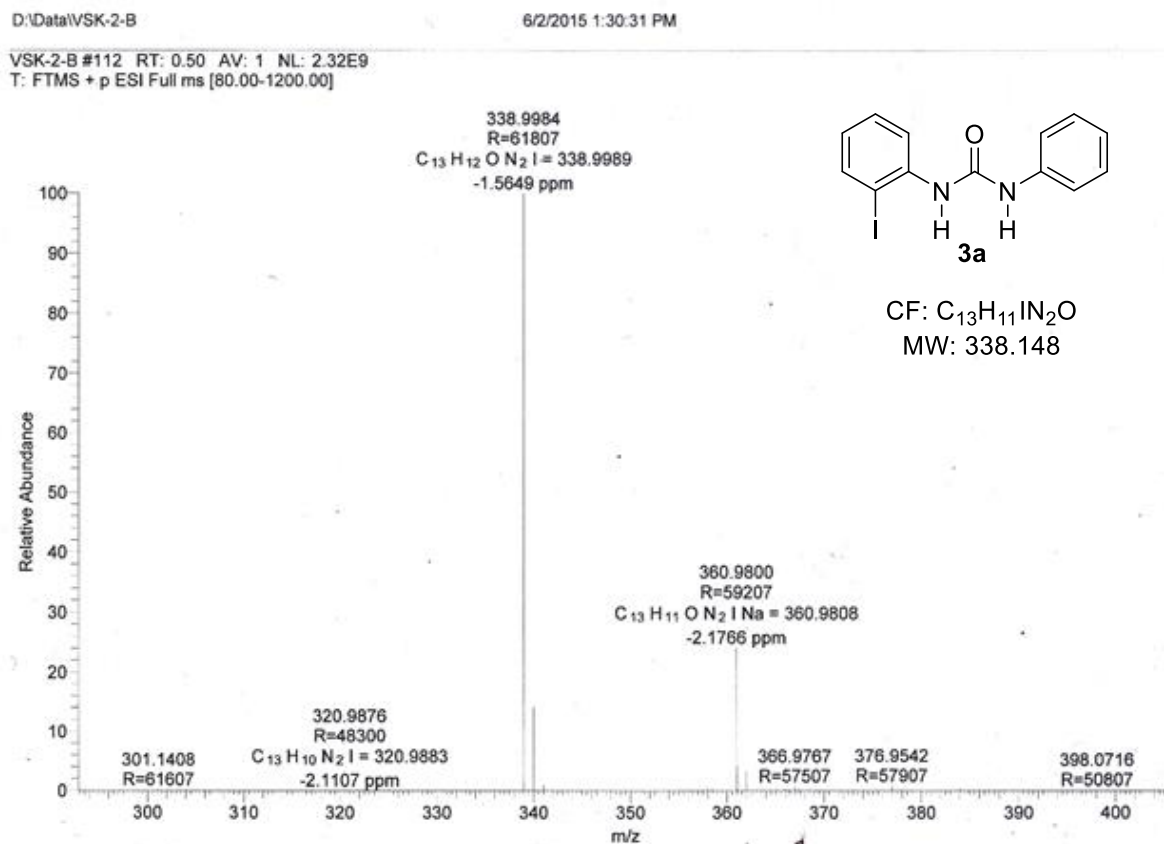**Figure 10.** IR spectrum of 1-(2-iodophenyl)-3-phenylurea (**3a**).

Figure 11. ESIMS (+ve mode) spectrum of 1-(2-iodophenyl)-3-phenylurea (**3a**).

A.7. References

1   J. M. Lehn, in *Supramolecular Chemistry: Concepts and Perspectives*, VCH, Weinheim, 1995.

2   G. R.Desiraju, in *Crystal Engineering in organic solids*, Elsevier, 1989.

3   Reactivity in confined self-assembled nanospaces is detailed in the following review, see: T. S. Koblenz, J.Wassenaar and J. N. H. Reek, *Chem. Soc., Rev.,* 2008, **37**, 247-262.

4   M. D.Pluth, R. G. Bergman and K. N. Raymond, *Science*, 2007, **316**, 85-88.

5   W. M. Hart-Cooper, K. N. Clary, F. D.Toste, R. G. Bergman and K. N. Raymond, *J. Am. Chem. Soc.,* 2012, **134**,17873-17876.

6   D. Fiedler, H. van Halbeek, R. G. Bergman and K. N. Raymond, *J. Am. Chem. Soc.,* 2006, **128**, 10240-10252.

7   *(a)* B. Breit and W.Seiche, *J. Am. Chem. Soc.,* 2003, **125**, 6608-6609; *(b)* V. F. Slagt, P. W. N. M. van Leeuwen and J. N. H. Reek, *Angew. Chem. Int. Ed.,* 2003, **42**, 5619-5623.

8   *(a)* U. Gellrich, W. Seiche, M. Keller and B. Breit, *Angew. Chem. Int. Ed.,* 2012, **51**, 11033-11038; *(b)* A. J. Sandee, A. M. van der Burg and J. N. H. Reek, *Chem. Commun.,* 2007, 864-866; *(c)* M. Weis, C. Waloch, W. Seiche and B.Breit, *J. Am. Chem. Soc.,* 2006, **128**, 4188-4189.

9   For reviews on this topic see: *(a)* J. Meeuwissen and J. N. H. Reek, *Nat. Chem.,* 2010, **2**, 615-621; *(b)* J. Wieland and B. Breit, *Nat. Chem.,* 2010, **2**, 832-837; *(c)* A. J. Sandee and J. N. H. Reek, *Dalton Trans.,* 2006, 3385-339; *(d)* B. Breit, *Angew. Chem. Int. Ed.,* 2005, **44**, 6816-6825.

10 *(a)* P. Dydio, R. J. Detz, B. de Bruin and J. N. H. Reek, *J. Am. Chem. Soc.,* 2014, **136**, 8418-8429; *(b)* P. Dydio, R. Detz and J. N. H. Reek, *J. Am. Chem. Soc.,* 2013, **135**, 10817-10828; *(c)* P. Dydio and J. N. H. Reek, *Angew. Chem. Int. Ed.,* 2013, **52**, 3878-3882; *(d)* J. Meeuwissen, A. Sandee, B. de Bruin, M. A. Siegler, A. L. Spek and J. N. H. Reek, *Organometallics*, 2010, **29**, 2413-2421; *(e)* L. Diab, T. Smejkal, J. Geier and B. Breit, *Angew. Chem. Int. Ed.,* 2009, **48**, 8022-8026.

11 *(a)* P.Dydio, C. Rubay, T. Gadzikwa, M. Lutz and J. N. H. Reek, *J. Am. Chem. Soc.,* 2011, **133**, 17176-17179; *(b)* P. A. R. Breuil, F. W. Patureau and J. N. H. Reek, *Angew. Chem. Int. Ed.,* 2009, **48**, 2162-2165; *(c)* P. E. Goudriaan, M. Kuil, X. B. Jiang, P. W. N. M. van Leeuwen and J. N. H. Reek, *Dalton Trans.,* 2009, 1801-1805.

12 Y. Kuninobu, H. Ida, M. Nishi, M.Kanai, *Nat. Chem.,* 2015, **7**, 712-717.

13 *(a)* R. Custelcean, *Chem. Commun.,* 2008, 295-307. (b) K. Paisner, L. N. Zakharov and K. M. Doxsee, *Cryst. Growth Des.,* 2010, **10**, 3757-3762.

14 *(a)* P. Metrangola and G. Resnati, in *Halogen bonding: Fundamentals and applications,* Springer Verlag, Berlin, Heidelberg, 2008; *(b)* P. Metrangolo and G. Resnati, *Chem.–Eur. J.,* 2001, **7**, 2511; *(c)* R. G. Gonnade, M. S. Shashidhar and M. M. Bhadbhade, *J. Indian Inst. Sci.,* 2007, **87**, 149-165; *(d)* P. Metrangolo, F. Meyer, T. Pilati, G. Resnati and G. Terraneo, *Angew. Chem. Int. Ed.,* 2008, **47**, 6114-6127; *(e)* G. Cavallo, P. Metrangolo, T. Pilati, G. Resnati, M. Sansotera and G. Terraneo, *Chem. Soc. Rev.,* 2010, **39**, 3772-3783.

15 *(a)* G. R. DesirajuR. Parthasarathi, *J. Am. Chem. Soc*., 1989, **111**, 8725-8726; *(b)* N. Ramasubbu, R. Parthasarathy, P. Murray-Rust, *J . Am. Chem. Soc.* 1986, **108**, 4308-4314.

16 D. Chopra, T. S. Cameron, J. D. Ferrara and T. N. Guru Row, *J. Phys. Chem. A,* 2006, **110**, 10465-10477.

17 *(a)* G. R. Desiraju and V. R. Pedireddi, *J. Chem. Soc. Chem. Commun.,* 1989, 1112-1113; *(b)* V. R. Pedireddi, J. A. R. P. Sarma and G. R. Desiraju, *J. Chem. Soc. Perkin Trans.* 1992, **2**,311-320; *(c)* G. R. Desiraju, V. R. Pedireddi, J. A. R. P. Sarma and D. E. Zacharias, *ActaChim. Hung.* 1993, 451-465.

18 V. S. Koshti, N. R. Mote, R. G. Gonnade and S. H. Chikkali, *Organometallics*, 2015, **34**, 4802-4805.

19 G. M. Sheldrick, *ActaCryst*., 2008, **A64**, 112-122.

20 C. F. Macrae, I. J. Bruno, J. A. Chisholm, P. R. Edgington, P. McCabe E. Pidcock, L. Rodriguez Monge, R. Taylor, J. van de Streek and P. A. Wood, *J. Appl. Crystallogr*., 2008, **41**, 466-470.

21 A. L. Spek, *ActaCryst.,* 2009, **D65**, 148-155.

1. "Contemporary avenues in catalytic P-H bond addition reaction: A case study of hydrophosphination,"

   V. S. Koshti, S. R. Gaikwad and S. H. Chikkali,* *Coord. Chem. Rev.,* 2014, **265**, 52−73.

2. "Highly enantioselective Pd-catalyzed synthesis of p-stereogenic supramolecular phosphines, self-assembly, and implication,"

   V. S. Koshti, N. R. Mote, R. G. Gonnade and S. Chikkali,* *Organometallics*, 2015, **34**, 4802-4805.

3. "The impact of modular substitution on crystal packing: the tale of two ureas",

   V. S. Koshti, S. H. Thorat, R. P. Gote, S. H. Chikkali* and R. G. Gonnade,* *CrystEngComm*, 2016, **18**, 7078-7094.

4. "Self-assembly of P-chiral supramolecular phosphines on rhodium and direct evidence for Rh-catalyst-substrate interactions",

   V. S. Koshti, A. Sen, D. Shinde and S. Chikkali,* *Dalton Trans.,* 2017, **46**, 13966-13973.

5. "H-Bonding assisted self-assembly of anionic and neutral ligand on metal: A comprehensive strategy to mimic ditopic ligands in olefin polymerization",

   N. R. Mote, K. Patel, D. R. Shinde, S. R. Gaikwad, **V. S. Koshti**, R. G. Gonnade, and S. H. Chikkali,* *Inorg. Chem.*, 2017, **56**, 12448–12456.

6. "Reactivity of difunctional polar monomers and ethylene copolymerization: A comprehensive account",

   S. Gaikwad, S. Deshmukh, **V. S. Koshti**, S. Poddar, R. G. Gonnade, P. R. Rajamohanan and S. Chikkali,* *Macromolecules*, 2017, **50**, 5748–5758.

7. "Enhancing the rate of enantioselective P-C coupling reaction through rational Pd-catalyst selection",

   V. S. Koshti, R. P. Gote and S. H. Chikkali,* (Manuscript under preparation)

8. "Ni-catalyst for enantioselective synthesis of P-stereogenic (supramolecular) phosphines"

   V. S. Koshti, S. H. Chikkali,* (Manuscript under preparation)